

***R*-PARITY-VIOLATING SUPERSYMMETRY**

**R. Barbier¹, C. Bérat², M. Besançon³, M. Chemtob⁴,
A. Deandrea¹, E. Dudas^{5,6}, P. Fayet⁷, S. Lavignac^{4,8},
G. Moreau⁹, E. Perez³ and Y. Sirois¹⁰**

¹ *IPNL, Université Claude Bernard, IN2P3-CNRS, 69622 Villeurbanne, France*

² *LPSC, Université de Grenoble 1, IN2P3-CNRS, 38026 Grenoble, France*

³ *DAPNIA/Service de Physique des Particules, CEA-Saclay, 91191 Gif-sur-Yvette, France*

⁴ *Service de Physique Théorique, CEA-Saclay, 91191 Gif-sur-Yvette, France*

⁵ *Laboratoire de Physique Théorique, Université de Paris-Sud, 91405 Orsay, France*

⁶ *Centre de Physique Théorique, Ecole Polytechnique, 91128 Palaiseau, France*

⁷ *Laboratoire de Physique Théorique, Ecole Normale Supérieure, 75005 Paris, France*

⁸ *CERN Theory Division, CH-1211 Genève, Suisse*

⁹ *Service de Physique Théorique, Université Libre de Bruxelles, 1050 Brussels, Belgium*

¹⁰ *Laboratoire Leprince-Ringuet, Ecole Polytechnique, IN2P3-CNRS, 91128 Palaiseau, France*

Abstract

Theoretical and phenomenological implications of R -parity violation in supersymmetric theories are discussed in the context of particle physics and cosmology. Fundamental aspects include the relation with continuous and discrete symmetries and the various allowed patterns of R -parity breaking. Recent developments on the generation of neutrino masses and mixings within different scenarios of R -parity violation are discussed. The possible contribution of R -parity-violating Yukawa couplings in processes involving virtual supersymmetric particles and the resulting constraints are reviewed. Finally, direct production of supersymmetric particles and their decays in the presence of R -parity-violating couplings is discussed together with a survey of existing constraints from collider experiments.

To be submitted to Physics Reports

Contents

INTRODUCTORY REMARKS	5
1 WHAT IS R-PARITY ?	7
1.1 What Is R -Parity, and How Was It Introduced ?	7
1.2 Nature Does Not Seem To Be Supersymmetric !	11
1.3 Continuous R -Invariance, and Electroweak Breaking	14
1.4 R -Invariance and R -Parity in the Supersymmetric Standard Model	15
1.5 Gravitino and Gluino Masses: From R -Invariance to R -Parity	19
2 HOW CAN R-PARITY BE VIOLATED?	22
2.1 R -Parity-Violating Couplings	22
2.1.1 Superpotential Couplings	23
2.1.2 Lagrangian Terms Associated with the Superpotential Couplings	24
2.1.3 Soft Supersymmetry-Breaking Terms	26
2.1.4 Choice of the Weak Interaction Basis	27
2.1.5 Constraints on the Size of \mathcal{R}_p Couplings	28
2.2 Patterns of R -Parity Breaking	29
2.3 Effects of Bilinear R -Parity violation	31
2.3.1 Distinguishing Between Higgs and Lepton Doublet Superfields	32
2.3.2 Trilinear Couplings Induced by Bilinear \mathcal{R}_p Terms	35
2.3.3 Higgsino-Lepton Mixing	36
2.3.4 Experimental Signatures of Bilinear R -Parity Violation	38
2.4 Spontaneous Breaking of R -Parity	39
2.5 Constraining \mathcal{R}_p Couplings from Flavour Symmetries	41
2.6 R -Parity Violation in Grand Unified Theories	44
2.7 Restrictions on R -Parity Violations from Generalized Matter, Baryon or Lepton Parities	46

3	RENORMALIZATION GROUP SCALE EVOLUTION OF \mathcal{R}_p COUPLINGS	51
3.1	Renormalization Group Equations	52
3.1.1	Evolution of the Bilinear μ Terms	52
3.1.2	Evolution of the Trilinear \mathcal{R}_p Yukawa Couplings	54
3.1.3	Evolution of the Gauge Couplings	55
3.2	Perturbative Unitarity Constraints	56
3.3	Quasi-fixed points analysis for \mathcal{R}_p couplings	56
3.4	Supersymmetry Breaking	59
4	COSMOLOGY AND ASTROPHYSICS	60
4.1	Constraints from the lifetime of the Lightest Supersymmetric Particle	61
4.1.1	Decays of the Lightest Supersymmetric Particle	61
4.1.2	Gravitino Relics	63
4.2	Cosmological Baryon Asymmetry	65
4.2.1	Baryogenesis from \mathcal{R} -Parity-Violating Interactions	65
4.2.2	Survival of a Baryon Asymmetry in the Presence of \mathcal{R}_p Interactions	68
5	NEUTRINO MASSES AND MIXINGS	72
5.1	\mathcal{R}_p Contributions to Neutrino Masses and Mixings	72
5.1.1	\mathcal{R} -Parity Violation as a Source of Neutrino Masses	72
5.1.2	Tree-Level Contribution Generated by Neutrino-Neutralino Mixing	73
5.1.3	One-Loop Contributions Generated by Trilinear \mathcal{R}_p Couplings	75
5.1.4	One-Loop Contributions Generated by both Bilinear and Trilinear \mathcal{R}_p Couplings	77
5.2	Explicit Models of Neutrino Masses	80
5.2.1	Experimental Constraints on Neutrino Masses and Mixings	80
5.2.2	Classification of Models	81
	a) Models with Trilinear Couplings only	81
	b) Models with both Bilinear and Trilinear Couplings	82
	c) Models with Bilinear Couplings only	83
5.3	Neutrino Transition Magnetic Moments	85
5.4	Neutrino Flavour Transitions in Matter Induced by \mathcal{R}_p Interactions	86
5.5	$\Delta L = 2$ Sneutrino Masses and Sneutrino-Antisneutrino Mixing	87

6	INDIRECT BOUNDS ON R-parity ODD INTERACTIONS	89
6.1	Assumptions and Framework	90
6.1.1	The Single Coupling Dominance Hypothesis	90
6.1.2	Choice of the Lepton and Quark Superfield Bases	90
6.1.3	A Basis-Independent Parametrization of R -Parity Violation	92
6.1.4	Specific Conventions Used in this Chapter	93
6.2	Constraints on Bilinear \mathcal{R}_p Terms and on Spontaneously Broken R -Parity . . .	94
6.2.1	Models with Explicit R -Parity Breaking	94
6.2.2	Models with Spontaneous R -Parity Breaking	95
6.3	Constraints on the Trilinear \mathcal{R}_p Interactions	97
6.3.1	Charged Current Interactions	97
6.3.2	Neutral Current Interactions	102
6.3.3	Anomalous Magnetic Dipole Moments	109
6.3.4	CP Violation	110
6.4	Trilinear \mathcal{R}_p Interactions in Flavour Violating Processes and in \mathcal{B} and \mathcal{L} Processes	120
6.4.1	Hadron Flavour Violating Processes	121
6.4.2	Lepton Flavour Violating Processes	129
6.4.3	Lepton Number Non-Conserving Processes	132
6.4.4	Baryon Number Non-Conserving Processes	135
6.5	General Discussion of Indirect Trilinear Bounds	140
6.5.1	Summary of Main Experimental Bounds	140
6.5.2	Observations on the Bound Robustness and Validity	147
	a) Natural Order of Magnitude for \mathcal{R}_p Couplings	147
	b) Impact of the SUSY Masses on the Bounds	147
	c) Validity of the Assumption of one or two Dominant Couplings	148
	d) Bound Robustness in Regards to Model Dependence	149
6.5.3	Phenomenological Implications of Bounds	149

7	PHENOMENOLOGY AND SEARCHES AT COLLIDERS	152
7.1	Introduction	152
7.2	Interaction Strength and Search Strategies	153
7.3	Decay of Sparticles Involving \mathcal{R}_p Couplings	155
7.3.1	Direct \mathcal{R}_p Decays of Sfermions	155
7.3.2	Direct \mathcal{R}_p Decays of Gauginos-Higgsinos	156
7.3.3	Cascade Decays Initiated by Gauge Couplings	159
7.3.4	Decays Through Mixing Involving Bilinear Interactions	161
7.4	\mathcal{R}_p Phenomenology from Pair Produced Sparticles	162
7.4.1	Gaugino-Higgsino Pair Production	162
	a) Production and Final States	162
	b) Searches for Gaugino Pair Production at e^+e^- Colliders	164
	c) Searches for Gaugino Pair Production at Hadron Colliders	168
7.4.2	Sfermion Pair Production	168
	a) Production and final states	168
	b) Results on Slepton Searches	169
	c) Results on Squark Searches	176
	d) Sfermion and Gluino Pair Production at Hadron Colliders	178
7.4.3	Effects of Bilinear \mathcal{R}_p Interactions	181
7.5	Single Sparticle Production	183
7.5.1	Single Sparticle Production at Leptonic Colliders	184
7.5.2	Single Sparticle Production at Lepton-Hadron Colliders	190
7.5.3	Single Sparticle Production at Hadron-Hadron Colliders	194
7.6	Virtual Effects involving \mathcal{R}_p Couplings	204
7.6.1	Fermion Pair Production	205
7.6.2	\mathcal{R}_p Contributions to FCNC	212
7.6.3	\mathcal{R}_p Contributions to CP Violation	216
8	CONCLUSIONS AND PROSPECTS	219
A	Notations and Conventions	225
B	Yukawa-like \mathcal{R}_p Interactions Associated with the Trilinear \mathcal{R}_p Superpotential	228
C	Production and Decay Formulae	230
C.1	Sfermions	231
C.2	Neutralinos	233
C.3	Charginos	235

INTRODUCTORY REMARKS

The possible appearance of R -parity-violating couplings, and hence the question of the conservation or non-conservation of baryon and lepton numbers (B and L) in supersymmetric theories, has been emphasized for a long time. The rich phenomenology implied by R -parity violation has gained full attention in the search for supersymmetry. We shall discuss here the theoretical as well as phenomenological aspects of R_p supersymmetry in particle and astroparticle physics.

In chapter 1 we introduce fundamental aspects of supersymmetry, having in mind the question of the definition of conserved baryon and lepton numbers in supersymmetric theories. In supersymmetric extensions of the Standard Model R -parity has emerged as a discrete remnant of a group of continuous $U(1)$ R -symmetry transformations acting on the supersymmetry generator. R -parity is intimately connected with baryon and lepton numbers, its conservation naturally allowing for conserved baryon and lepton numbers in supersymmetric theories. Conversely, the violation of R -parity requires violations of B and/or L conservation laws. This generally leads to important phenomenological difficulties, unless R -parity-violating interactions are sufficiently small. How small they have to be, and how these difficulties may be turned into opportunities in some specific cases, concerning for example neutrino masses and mixings, constitute important aspects of this review.

Chapter 2 is devoted to the discussion of *how R -parity may be broken*. The corresponding superpotential couplings (and resulting Lagrangian terms) and soft supersymmetry-breaking terms are recalled. Various possible patterns of R -parity breaking are discussed, including bilinear breaking as well as spontaneous breaking. Further theoretical insights on the possible origin of such terms violating B and/or L as well as the R -parity symmetry are reviewed. This includes more recent developments on abelian family symmetries, grand-unified gauge symmetries, and other discrete symmetries, and what they could tell us about possible R_p terms.

The high-energy convergence of the gauge couplings obtained by renormalization-group evolution of low-energy measurements gets remarkably improved once supersymmetry is introduced. More generally, the renormalization group equations governing the evolutions of the coupling and mass parameters between two energy scales provide a way to test, at lower energies, physical assumptions postulated at a much higher energy scale; or conversely to translate available experimental data into quantities at a higher energy scale. In chapter 3 we consider *the effects of the renormalization group equations*, in the presence of R -parity-violating interactions. We focus in particular, within the supergravity framework, on the evolution of the constraints associated with perturbative unitarity, the existence of infrared fixed points and the tests of grand-unification schemes. The additional effects of the new soft supersymmetry-breaking terms associated with R_p -violations are also discussed.

Supersymmetric theories with conserved R -parity naturally provide a (color and electrically neutral) stable lightest supersymmetric particle (LSP), i.e. a weakly-interacting massive particle which turns out to be a very good Dark Matter candidate. In contrast, one of the most striking features of supersymmetric theories with R -parity-violating interactions stems from the fact that *the LSP can now decay into Standard Model particles only*. We discuss in chapter 4 how such an unstable LSP might still remain (if its lifetime is sufficiently long) a possible Dark Matter candidate. We also discuss the gravitino relic issue, and the origin of the cosmological baryon asymmetry, reviewing several attempts at generating this asymmetry, as well as how it could survive in the presence of R -parity-violating interactions.

The most dramatic implication of L -violating interactions from R -parity violations is the automatic generation of *neutrino masses and mixings*. The possibility that the results of atmospheric and solar neutrino experiments be explained by neutrino masses and mixings originating from R -parity-violating interactions has motivated a large number of studies and models. R -parity violation in the lepton sector also leads to many new phenomena related to neutrino and sneutrino physics. These aspects of neutrino physics related to L -violating interactions are reviewed in chapter 5.

In chapter 6 we discuss the possible contribution of R -parity violating couplings to processes involving the *virtual effects* of supersymmetric particles. Indeed R -parity-violating couplings in the Supersymmetric Standard Model introduce new interactions between ordinary and supersymmetric particles which can contribute to a large variety of low, intermediate and high-energy processes, not involving the direct production of supersymmetric particles in the final state. The requirement that the R -parity-violating contribution to a given observable avoids conflicting with actual experimental measurements, leads to upper bounds on the R -parity-violating couplings possibly involved. These bounds are extensively discussed, the main ones being summarized at the end of the chapter, in section 6.5. Their robustness as well as phenomenological implications are also discussed at the end of this chapter.

The search for \mathcal{R}_p -supersymmetry processes has been a major analysis activity at high-energy colliders over the past 15 years, and is likely to be pursued at existing and future colliders. Chapter 7.1 is dedicated to the phenomenology and *direct searches*, at colliders, for supersymmetric particles involving R -parity-violating couplings. The essential ingredients of the corresponding phenomenology at colliders, including discussions on the magnitude of R -parity-violating couplings and the subsequent decay of supersymmetric particles, are reviewed.

We then discuss the main and generic features of the R -parity-violating phenomenology for *gaugino-higgsino pair production* and *sfermion pair production*, both at leptonic and hadronic colliders. Furthermore, a remarkable specificity of the phenomenology of \mathcal{R}_p at colliders comes from possibility of producing *a single supersymmetric particle*. (This is also discussed in chapter 7 for leptonic, lepton-hadron and hadronic colliders.) The phenomenology of \mathcal{R}_p at colliders also covers virtual effects such as those concerning fermion pair production, contributions to flavor-changing neutral currents and to CP violation. These aspects are also met in chapter 7.1.

Altogether, many direct experimental limits have accumulated during the last 15 years of searches for \mathcal{R}_p processes at colliders. We do not aim here at an exhaustive (and possibly tedious) catalog of all these searches with the corresponding limits. We rather choose to refer the reader interested in specific limits and details of experimental analyses to the relevant literature and emphasize only the description of generic features of the phenomenology of R -parity-violating processes at colliders, illustrated by examples from the literature.

Conclusions and prospects for supersymmetry with R_p -violating couplings are given in chapter 8. Finally, notations and conventions are summarized in appendix A. The Yukawa-like \mathcal{R}_p interactions associated with the trilinear \mathcal{R}_p superpotential couplings (given in appendix A) are derived in appendix B. Useful formulae for the production and decays of sfermions, neutralinos and charginos are given in appendix C.

Chapter 1

WHAT IS R -PARITY ?

In this chapter, we recall how R -parity emerged, in supersymmetric extensions of the Standard Model, as a discrete remnant of a continuous $U(1)$ R -symmetry group acting on the supersymmetry generator, necessarily broken so as to allow for the gravitino and gluinos to acquire masses. R -parity naturally forbids unwanted squark and slepton exchanges, allowing for conserved baryon (B) and lepton (L) numbers in supersymmetric theories. It guarantees the stability of the “Lightest Supersymmetric Particle”, which is, also, a very good candidate for the non-baryonic Dark Matter of the universe. *A contrario*, R -parity violations are necessarily accompanied by B and/or L violations. This is, usually, a source of phenomenological difficulties, unless R -parity-violating (R_p) interactions are sufficiently small, as we shall discuss in this review article. R -parity violations, on the other hand, could also appear as a desired feature, since they may provide a source of Majorana masses for neutrinos. Whether R -parity turns out to be absolutely conserved, or not, it plays an essential rôle in the phenomenology of supersymmetric theories, and the experimental searches for the new sparticles.

1.1 What Is R -Parity, and How Was It Introduced ?

Among the problems one had to solve before thinking of applying supersymmetry to the real world, was the question of the definition of conserved quantum numbers, like baryon number B and lepton number L . These are carried by Dirac fermions, the spin- $\frac{1}{2}$ quarks and leptons. But supersymmetric theories make a systematic use of *Majorana* fermions, in particular the fermionic partners of the spin-1 gauge bosons (now called gauginos). This makes it very difficult, even in general practically impossible, for them to carry additive conserved quantum numbers like B and L , in a supersymmetric theory.

Still, even Majorana fermions may be arranged into (chiral or non-chiral) Dirac fermions so as to carry non-zero values of a new additive quantum number, called R . In an early $SU(2) \times U(1)$ supersymmetric electroweak model with two chiral doublet Higgs superfields, now called H_d and H_u (or H_1 and H_2), the definition of a continuous R -symmetry acting on the supersymmetry generator allowed for an additive conserved quantum number, R , one unit of which is carried by the supersymmetry generator [1]. The values of R for bosons and fermions differ by ± 1 unit inside the multiplets of supersymmetry, the photon, for example, having $R = 0$ while its spin- $\frac{1}{2}$ partner, constrained from the continuous R -invariance to remain massless, carries $R = \pm 1$. Such a quantum number might tentatively have been identified as

a lepton number, despite the Majorana nature of the spin- $\frac{1}{2}$ partner of the photon, if the latter could have been identified as one of the neutrinos. This, however, is not the case. The fermionic partner of the photon should be considered as a neutrino of a new type, a “photonic neutrino”, called in 1977 the *photino*.

This still leaves us with the question of how to define, in such theories, Dirac spinors carrying conserved quantum numbers like B and L . Furthermore, these quantum numbers, presently known to be carried by fundamental fermions only, not by bosons, seem to appear as *intrinsically-fermionic* numbers. Such a feature cannot be maintained in a supersymmetric theory (in the usual framework of the “linear realizations” of supersymmetry), and one had to accept the (then rather heretic) idea of attributing baryon and lepton numbers to fundamental bosons, as well as to fermions. These new bosons carrying B or L are the superpartners of the spin- $\frac{1}{2}$ quarks and leptons, namely the now-familiar, although still unobserved, spin-0 *squarks* and *sleptons*. Altogether, all known particles should be associated with new *superpartners* [2].

This introduction of squarks and sleptons now makes the definition of baryon and lepton numbers in supersymmetric theories a quasi-triviality – these new spin-0 particles carrying B and L , respectively, almost by definition – to the point that this old problem is now hardly remembered, since we are so used to its solution. This does not mean, however, that these newly-defined B and L should *necessarily* be conserved, since new interactions that could be present in supersymmetric theories might spoil our familiar baryon and lepton-number conservation laws, even without taking into account the possibility of Grand Unification!

In fact the introduction of a large number of new bosons has a price, and carries with it the risk of potential difficulties. Could these new bosons be exchanged between ordinary particles, concurrently with the gauge bosons of electroweak and strong interactions? But known interactions are due to the exchanges of spin-1 gauge bosons, not spin-0 particles! Can we then construct supersymmetric theories of weak, electromagnetic and strong interactions, which would be free of this potential problem posed by unwanted interactions mediated by spin-0 particles? Fortunately, the answer is yes. As a matter of fact the above problem, related with the conservation or non-conservation of B and L , comes with its own natural solution, namely R -invariance or, more precisely, a discrete version of it, known as R -parity. This one is closely related, of course, with the definitions of B and L , once we have decided, and accepted, to attribute B and L to the new squarks and sleptons, as well as to the ordinary quarks and leptons.

R -parity is associated with a Z_2 subgroup of the group of continuous $U(1)$ R -symmetry transformations – often referred to as $U(1)_R$ – acting on the gauge superfields and the two chiral doublet Higgs superfields H_d and H_u responsible for electroweak symmetry breaking [1], with their definition extended to quark and lepton superfields so that quarks and leptons carry $R = 0$, and squarks and sleptons, $R = \pm 1$ [2]. As we shall see later, R -parity appears in fact as the discrete remnant of this continuous $U(1)$ R -invariance when gravitational interactions are introduced [3], in the framework of local supersymmetry (supergravity), in which the gravitino must at some point acquire a mass $m_{3/2}$ (which breaks the continuous R -invariance). In addition, either the continuous R -invariance, or simply its discrete version of R -parity, if imposed, naturally forbid the unwanted direct exchanges of the new squarks and sleptons between ordinary quarks and leptons. It is, therefore, no surprise if the re-introduction of (unnecessary) R_p terms in the Lagrangian density generally introduces again, most of the time, the problems that were elegantly solved by R -parity.

The precise definition of R -invariance, which acts chirally on the anticommuting Grassmann coordinate θ appearing in the definition of superspace and superfields, will be given later

(see Table 1.3 in subsection 1.4). R -transformations are defined so as not to act on ordinary particles, which all have $R = 0$, their superpartners having, therefore, $R = \pm 1$. This allows one to distinguish between two separate sectors of R -even and R -odd particles. R -even particles (having R -parity $R_p = +1$) include the gluons, the photon, the W^\pm and Z gauge bosons, the quarks and leptons, the Higgs bosons originating from the two Higgs doublets (required in supersymmetry to trigger the electroweak breaking and to generate quark and lepton masses) – and the graviton. R -odd particles (having R -parity $R_p = -1$) include their superpartners, i.e. the gluinos and the various neutralinos and charginos, squarks and sleptons – and the gravitino. According to this first definition, R -parity simply corresponds to the parity of the additive quantum number R associated with the above continuous $U(1)$ R -invariance, as given by the expression [4]:

$$R\text{-parity } R_p = (-1)^R = \begin{cases} +1 & \text{for ordinary particles,} \\ -1 & \text{for their superpartners.} \end{cases} \quad (1.1)$$

But should we limit ourselves to the discrete R -parity symmetry, rather than considering its full continuous parent R -invariance? This *continuous* $U(1)$ R -invariance, from which R -parity has emerged, is indeed a symmetry of all four necessary basic building blocks of the Supersymmetric Standard Model [2]:

- 1) the Lagrangian density for the $SU(3) \times SU(2) \times U(1)$ gauge superfields responsible for strong and electroweak interactions;
- 2) the $SU(3) \times SU(2) \times U(1)$ gauge interactions of the quark and lepton superfields;
- 3) the $SU(2) \times U(1)$ gauge interactions of the two chiral doublet Higgs superfields H_d and H_u responsible for the electroweak breaking;
- 4) and the “super-Yukawa” interactions responsible for quark and lepton masses, through the trilinear superpotential couplings of quark and lepton superfields with the Higgs superfields H_d and H_u ,

$$W = \lambda_{ij}^e H_d L_i E_j^c + \lambda_{ij}^d H_d Q_i D_j^c - \lambda_{ij}^u H_u Q_i U_j^c, \quad (1.2)$$

in which chiral quark and lepton superfields are all taken as left-handed and denoted by Q_i, U_i^c, D_i^c and L_i, E_i^c respectively (with $i = 1, 2$ or 3 being the generation index).

Since all the corresponding contributions to the Lagrangian density are invariant under this continuous R -symmetry, why not simply keep it instead of abandoning it in favour of its discrete version, R -parity? But an unbroken continuous R -invariance, which acts chirally on *gluinos*, would constrain them to remain massless, even after a spontaneous breaking of the supersymmetry. We would then expect the existence of relatively light “ R -hadrons” [5, 6] made of quarks, antiquarks and gluinos, which have not been observed. Once the continuous R -invariance is abandoned, and supersymmetry is spontaneously broken, radiative corrections do indeed allow for the generation of gluino masses [7], a point to which we shall return later. Furthermore, the necessity of generating a mass for the Majorana spin- $\frac{3}{2}$ *gravitino*, once *local* supersymmetry is spontaneously broken, also forces us to abandon the continuous R -invariance in favour of the discrete R -parity symmetry, thereby automatically allowing for gravitino, gluino, and other gaugino masses [3].

Once we drop the continuous R -invariance in favour of its discrete R -parity version, it is legitimate to look back and ask: how general is this notion of R -parity, and, correlatively, are we *forced* to have this R -parity conserved? As a matter of fact, there is from the beginning a close

connection between R -parity and baryon and lepton-number conservation laws, which has its origin in our desire to get supersymmetric theories in which B and L could be conserved, and, at the same time, to avoid unwanted exchanges of spin-0 particles.

Actually the superpotential of the supersymmetric extensions of the Standard Model discussed in Ref. [2] was constrained from the beginning, for that purpose, to be an *even* function of the quark and lepton superfields. In other terms, *odd* gauge-invariant superpotential terms (W' , also denoted W_{R_p}), which would have violated the “matter-parity” symmetry $(-1)^{(3B+L)}$, were then excluded from the beginning, to be able to recover B and L conservation laws, and avoid direct Yukawa exchanges of spin-0 squarks and sleptons between ordinary quarks and leptons.

Tolerating unnecessary superpotential terms which are *odd* functions of the quark and lepton superfields (i.e. R_p terms, precisely those that we are going to discuss in this review), does indeed create, in general, immediate problems with baryon- and lepton-number conservation laws [8]. Most notably, a squark-induced proton instability with a much too fast decay rate, if both B and L violations are simultaneously allowed; or neutrino masses (and other effects) that could be too large, if L violations are allowed so that ordinary neutrinos can mix with neutral higgsinos and gauginos. The aim of this review is to discuss in detail how much of these R_p contributions – parametrized by sets of coefficients λ_{ijk} , λ'_{ijk} , λ''_{ijk} (and possibly μ_i , etc.) – may be tolerated in the superpotential and in the various supersymmetry-breaking terms.

The above intimate connection between R -parity and B and L conservation laws can be made explicit by re-expressing the R -parity (1.1) in terms of the spin S and a matter-parity $(-1)^{3B+L}$, as follows [5]:

$$\boxed{R\text{-parity} = (-1)^{2S} (-1)^{3B+L} .} \quad (1.3)$$

To understand the origin of this formula we note that, for all ordinary particles, $(-1)^{2S}$ coincides with $(-1)^{3B+L}$, expressing that among Standard Model fundamental particles, *leptons and quarks, and only them, are fermions*, i.e. that B and L normally appear as intrinsically-fermionic numbers. The quantity $(-1)^{2S} (-1)^{3B+L}$ is always, trivially, identical to unity for all known particles (whether fundamental or composite) and for Higgs bosons as well, all of them previously defined as having R -parity $+1$. (Indeed expression (1.1) of R -parity comes from the fact that the (additive) quantum number R was defined so as to vanish for ordinary particles, which then have R -parity $+1$, their superpartners having, therefore, R -parity -1 .) This immediately translates into the equivalent expression (1.3) of R -parity.

R -parity may also be rewritten as $(-1)^{2S} (-1)^{3(B-L)}$, showing that this discrete symmetry (now allowing for gravitino and gluino masses) may still be conserved even if baryon and lepton numbers are separately violated, as long as their difference ($B - L$) remains conserved, even only modulo 2. Again, it should be emphasized that the conservation (or non-conservation) of R -parity is closely related with the conservation (or non-conservation) of baryon and lepton numbers, B and L . Abandoning R -parity by tolerating both B and L violations, simultaneously, would allow for the proton to decay, with a very short lifetime !

The R -parity operator plays an essential rôle in the construction of supersymmetric theories of interactions, and the discussion of the experimental signatures of the new particles. R -invariance, or simply its discrete version of R -parity, guarantees that *the new spin-0 squarks and sleptons cannot be directly exchanged* between ordinary quarks and leptons. It ensures that

the new R -odd sparticles can only be pair-produced, and that the decay of an R -odd sparticle should always lead to another one (or an odd number of them). Conserved R -parity also ensures the stability of the “Lightest Supersymmetric Particle” (or LSP), a neutralino for example (or conceivably a sneutrino, or gravitino)¹, which appears as an almost ideal candidate to constitute the non-baryonic Dark Matter that seems to be present in our universe.

Expression (1.3) of R -parity in terms of B and L makes very apparent that imposing R -parity is equivalent to imposing a matter-parity symmetry. Still the definition of R -parity offers the additional advantage of identifying the two separate sectors of $R_p = +1$ particles and $R_p = -1$ sparticles, making apparent the pair-production law of the new R -odd sparticles, and the stability of the LSP, if R -parity is conserved. Considering “matter-parity” alone would only imply directly the stability of the lightest “matter-odd” particle, not a very useful result !

Obviously, in the presence of R -parity violations, the LSP is no longer required to be stable, superpartners being allowed to decay into ordinary particles.

1.2 Nature Does Not Seem To Be Supersymmetric !

The algebraic structure of supersymmetry involves a spin- $\frac{1}{2}$ fermionic symmetry generator Q satisfying the (anti) commutation relations in four dimensions [9, 10, 11]:

$$\left\{ \begin{array}{l} \{Q, \bar{Q}\} = -2 \gamma_\mu P^\mu \quad , \\ [Q, P^\mu] = 0 \quad . \end{array} \right. \quad (1.4)$$

This spin- $\frac{1}{2}$ supersymmetry generator Q , here written as a 4-component Majorana spinor, was originally introduced as relating fermionic with bosonic fields, in relativistic quantum field theories. The presence of the generator of space-time translations P^μ on the right-hand side of the anticommutation relations (1.4) is at the origin of the relation of supersymmetry with general relativity and gravitation, since a locally supersymmetric theory must be invariant under local coordinate transformations [12].

The supersymmetry algebra (1.4) was introduced with quite different motivations: in connection with parity violation, with the hope of understanding parity violation in weak interactions as a consequence of a (misidentified) intrinsically parity-violating nature of the supersymmetry algebra [9]; in an attempt to explain the masslessness of the neutrino from a possible interpretation as a spin- $\frac{1}{2}$ Goldstone particle [10]; or by extending to four dimensions the supersymmetry transformations acting on the two-dimensional string worldsheet [11]. However, the mathematical existence of an algebraic structure does not mean that it could play a rôle as an invariance of the fundamental laws of Nature².

Indeed many obstacles seemed, long ago, to prevent supersymmetry from possibly being a fundamental symmetry of Nature. Is spontaneous supersymmetry breaking possible at all ? Where is the spin- $\frac{1}{2}$ Goldstone fermion of supersymmetry, if not a neutrino ? Can we use

¹The possibility of a *charged* or *colored* LSP may also be considered, although it seems rather strongly disfavoured, as it could lead to new heavy isotopes of hydrogen and other elements, which have not been observed (cf. subsection 4.1.1 in chapter 4).

²Incidentally while supersymmetry is commonly referred to as “relating fermions with bosons”, its algebra (1.4) does not even require the existence of fundamental bosons ! With non-linear realizations of supersymmetry a fermionic field can be transformed into a *composite* bosonic field made of fermionic ones [10].

supersymmetry to relate directly known bosons and fermions? And, if not, why? If known bosons and fermions cannot be directly related by supersymmetry, do we have to accept this as the sign that supersymmetry is *not* a symmetry of the fundamental laws of Nature? Can one define conserved baryon and lepton numbers in such theories, although they systematically involve *self-conjugate* Majorana fermions, (so far) unknown in Nature? And finally, if we have to postulate the existence of new bosons carrying B and L – the new spin-0 squarks and sleptons – can we prevent them from mediating new unwanted interactions?

While bosons and fermions should have equal masses in a supersymmetric theory, this is certainly not the case in Nature. Supersymmetry should clearly be broken. But it is a special symmetry, since the Hamiltonian, which appears on the right-hand side of the anticommutation relations (1.4), can be expressed proportionally to the sum of the squares of the components of the supersymmetry generator, as $H = \frac{1}{4} \sum_{\alpha} Q_{\alpha}^2$. This implies that a supersymmetry-preserving vacuum state must have vanishing energy, while a state which is not invariant under supersymmetry could naïvely be expected to have a larger, positive, energy. As a result, potential candidates for supersymmetry-breaking vacuum states seemed to be necessarily unstable. This led to the question

Q1 : *Is spontaneous supersymmetry breaking possible at all?* (1.5)

As it turned out, and despite the above argument, several ways of breaking spontaneously global or local supersymmetry have been found [13, 14]. But spontaneous supersymmetry breaking remains in general rather difficult to obtain, at least in global supersymmetry (and even without addressing yet the issue of how this breaking could lead to a realistic theory), since theories tend to prefer systematically, for energy reasons, supersymmetric vacuum states. Only in very exceptional situations can the existence of such states be avoided! In local supersymmetry, which includes gravity, one also has to arrange, at the price of a very severe fine-tuning, for the energy density of the vacuum to vanish exactly, or almost exactly, to an extremely good accuracy, so as not to generate an unacceptably large value of the cosmological constant Λ .

We still have to break supersymmetry in an acceptable way, so as to get – if this is indeed possible – a physical world which looks like the one we know! Of course just accepting explicit supersymmetry-breaking terms without worrying too much about their possible origin would make things much easier (unfortunately also at the price of introducing a large number of arbitrary parameters). But such terms must have their origin in a spontaneous supersymmetry-breaking mechanism, if we want supersymmetry to play a fundamental rôle, especially if it is to be realized as a local fermionic gauge symmetry, as it should in the framework of supergravity theories.

But the spontaneous breaking of the global supersymmetry must generate a massless spin- $\frac{1}{2}$ Goldstone particle, leading to the next question,

Q2 : *Where is the spin- $\frac{1}{2}$ Goldstone fermion of supersymmetry?* (1.6)

Could it be one of the neutrinos [10]? A first attempt at implementing this idea within a $SU(2) \times U(1)$ electroweak model of “leptons” [1] quickly illustrated that it could not be pursued very far. The “leptons” of this model were soon to be reinterpreted as the “charginos” and “neutralinos” of the Supersymmetric Standard Model.

If the Goldstone fermion of supersymmetry is not one of the neutrinos, why hasn’t it been observed? Today we tend not to think at all about the question, since: 1) the generalized use

of soft terms breaking *explicitly* the supersymmetry seems to render this question irrelevant; 2) since supersymmetry has to be realized locally anyway, within the framework of supergravity [12], the massless spin- $\frac{1}{2}$ Goldstone fermion (“goldstino”) should in any case be eliminated in favour of extra degrees of freedom for a massive spin- $\frac{3}{2}$ gravitino [3, 14].

But where is the gravitino, and why has no one ever seen a fundamental spin- $\frac{3}{2}$ particle? To discuss this properly we need to know which bosons and fermions could be associated under supersymmetry. Still, even before addressing this crucial question we might already anticipate that the interactions of the gravitino, with amplitudes proportional to the square root of the Newton constant $\sqrt{G_N} \simeq 10^{-19} \text{ GeV}^{-1}$, should in any case be absolutely negligible in particle physics experiments, so that we don’t have to worry about the fact that no gravitino has been observed.

This simple but naïve answer is, however, not true in all circumstances! It could be that the gravitino is light, possibly even extremely light, so that it would still interact very much like the massless Goldstone fermion of global supersymmetry, according to the “equivalence theorem” of supersymmetry [3]. Its interaction amplitudes are then determined by the ratio $\sqrt{G_N}/m_{3/2}$ (i.e. are inversely proportional to the square of the “supersymmetry-breaking scale” Λ_{ss}). As a result a sufficiently light gravitino could have non-negligible interactions, which might even make it observable in particle physics experiments, provided that the supersymmetry-breaking scale parameter fixing the value of its mass $m_{3/2}$ is not too large [3, 15]! Because of the conservation of R -parity, at least to a good approximation, in the Supersymmetric Standard Model, the R -odd gravitino should normally be produced in association with another R -odd superpartner, provided the available energy is sufficient. Gravitinos could also be pair-produced, although these processes are normally suppressed at lower energies. But they would remain essentially “invisible” in particle physics, as soon as the supersymmetry-breaking scale is large enough (compared to the electroweak scale), which is in fact the most plausible and widely considered situation.

In any case, much before getting to the Supersymmetric Standard Model, the crucial question to ask, if supersymmetry is to be relevant in particle physics, is:

$$\text{Q3 : } \textit{Which bosons and fermions could be related by supersymmetry ?} \quad (1.7)$$

But there seems to be no answer since known bosons and fermions do not appear to have much in common (excepted, maybe, for the photon and the neutrino). In addition the number of (known) degrees of freedom is significantly larger for fermions than for bosons. And these fermions and bosons have very different gauge symmetry properties! Furthermore, as discussed in subsection 1.1, the question

$$\text{Q4 : } \textit{How could one define (conserved) baryon and lepton numbers, in a supersymmetric theory ?} \quad (1.8)$$

once appeared as a serious difficulty, owing in particular to the presence of *self-conjugate* Majorana fermions in supersymmetric theories. Of course nowadays we are so used to dealing with spin-0 squarks and sleptons, carrying baryon and lepton numbers almost by definition, that we can hardly imagine this could once have appeared as a problem. Its solution required accepting the idea of attributing baryon or lepton numbers to a large number of new fundamental bosons. Even then, if such new spin-0 squarks and sleptons are introduced, their direct (Yukawa) exchanges between ordinary quarks and leptons, if allowed, could lead to an immediate disaster, preventing us from getting a theory of electroweak and strong interactions mediated by spin-1

gauge bosons, and not spin-0 particles, with conserved B and L quantum numbers ! This may be expressed by the question

$$\text{Q5 : } \quad \begin{array}{l} \textit{How can we avoid unwanted interactions} \\ \textit{mediated by spin-0 squark and slepton exchanges ?} \end{array} \quad (1.9)$$

Fortunately, we can naturally avoid such unwanted interactions, thanks to R -parity, which, if present, guarantees that squarks and sleptons can *not* be directly exchanged between ordinary quarks and leptons, allowing for conserved baryon and lepton numbers in supersymmetric theories.

1.3 Continuous R -Invariance, and Electroweak Breaking

The definition of the continuous R -invariance we are using arose from an early attempt at relating known bosons and fermions together, in particular the spin-1 photon with a spin- $\frac{1}{2}$ neutrino. If we want to try to identify the companion of the photon as being a “neutrino”, although it initially appears as a self-conjugate Majorana fermion, we need to understand how it could carry a conserved quantum number that we might attempt to interpret as a “lepton” number. This led to the definition of *a continuous $U(1)$ R -invariance* [1], which also guaranteed the masslessness of this “neutrino” (“ ν_L ”, carrying $+1$ unit of R), by acting chirally on the Grassmann coordinate θ which appears in the expression of the various gauge and chiral superfields³.

Attempting to relate the photon with one of the neutrinos could only be an exercise of limited validity. The would-be “neutrino”, in particular, while having in this model a $V - A$ coupling to its associated “lepton” and the charged W^\pm boson, was in fact what we would now call a “photino”, not directly coupled to the Z ! Still this first attempt, which became a part of the Supersymmetric Standard Model, illustrated how one can break spontaneously a $SU(2) \times U(1)$ electroweak gauge symmetry in a supersymmetric theory, using *a pair of chiral doublet Higgs superfields*, now known as H_d and H_u ! Using only a single doublet Higgs superfield would have left us with *a massless charged chiral fermion*, which is, evidently, unacceptable. Our previous charged “leptons” were in fact what we now call two winos, or charginos, obtained from the mixing of charged gaugino and higgsino components, as given by the mass matrix

$$M_C = \begin{pmatrix} (M_2 = 0) & \frac{g v_u}{\sqrt{2}} = M_W \sqrt{2} \sin \beta \\ \frac{g v_d}{\sqrt{2}} = M_W \sqrt{2} \cos \beta & \mu = 0 \end{pmatrix} \quad (1.10)$$

in the absence of a direct higgsino mass originating from a $\mu H_u H_d$ mass term in the superpotential⁴. The whole construction showed that one could deal elegantly with elementary spin-0

³This R -invariance itself originates from an analogous Q -invariance used, in a two-Higgs-doublet presupersymmetry model, to restrict the allowed Yukawa and φ^4 interactions, in a way which prepared for the two Higgs doublets and chiral fermion doublets to be related by supersymmetry [16]. Q -transformations were then modified into R -symmetry transformations, which survive the electroweak breaking and allow for massive Dirac fermions carrying the new quantum number R . Transformations similar to R -transformations were also considered in [17], but acted differently on two disconnected sets of chiral superfields ϕ_+ and ϕ_- , with no mutual interactions; i.e. they acted differently on the Grassmann coordinate θ , depending on whether the superfields considered belonged to the first or second set.

⁴This μ term initially written in [1] (which would have broken explicitly the continuous $U(1)$ R -invariance) was immediately replaced by a $\lambda H_u H_d N$ trilinear coupling involving an *extra neutral singlet chiral superfield* N : $\mu H_u H_d \longmapsto \lambda H_u H_d N$, as in the so-called Next-to-Minimal Supersymmetric Standard Model (NMSSM).

Higgs fields (not a very popular ingredient at the time), in the framework of spontaneously-broken supersymmetric theories. Quartic Higgs couplings are no longer completely arbitrary, but fixed by the values of the electroweak gauge couplings g and g' through the following “ D -terms” in the scalar potential given ⁵ in [1]:

$$\begin{aligned} V_{\text{Higgs}} &= \frac{g^2}{8} (h_d^\dagger \vec{\tau} h_d + h_u^\dagger \vec{\tau} h_u)^2 + \frac{g'^2}{8} (h_d^\dagger h_d - h_u^\dagger h_u)^2 + \dots \\ &= \frac{g^2 + g'^2}{8} (h_d^\dagger h_d - h_u^\dagger h_u)^2 + \frac{g^2}{2} |h_d^\dagger h_u|^2 + \dots \end{aligned} \quad (1.11)$$

This is precisely the quartic Higgs potential of the “minimal” version of the Supersymmetric Standard Model, the so-called Minimal Supersymmetric Standard Model (MSSM). Further contributions to this quartic Higgs potential also appear in the presence of additional superfields, such as the neutral singlet chiral superfield N already introduced in the previous model, which plays an important rôle in the NMSSM, i.e. in “next-to-minimal” or “non-minimal” versions of the Supersymmetric Standard Model. Charged Higgs bosons (called H^\pm) are always present in this framework, as well as several neutral ones, three of them at least. Their mass spectrum depends on the details of the supersymmetry-breaking mechanism considered: soft-breaking terms, possibly “derived from supergravity”, presence or absence of extra $U(1)$ gauge fields and/or additional chiral superfields, rôle of radiative corrections, etc..

1.4 R -Invariance and R -Parity in the Supersymmetric Standard Model

These two Higgs doublets H_d and H_u are precisely those used to generate the masses of charged leptons and down quarks, and of up quarks, in supersymmetric extensions of the Standard Model [2]. Note that at the time having to introduce Higgs fields was generally considered as rather unpleasant. While one Higgs doublet was taken as probably unavoidable to get to the Standard Model or at least simulate the effects of the spontaneous breaking of the electroweak symmetry, having to consider two doublets, necessitating charged Higgs bosons as well as several neutral ones, in addition to the “doubling of the number of particles”, was usually considered as further indication of the irrelevance of supersymmetry. As a matter of fact, considerable work was devoted for a while on attempts to avoid fundamental spin-0 Higgs fields (and extra sparticles), before returning to fundamental Higgs bosons, precisely in this framework of supersymmetry.

In the previous $SU(2) \times U(1)$ model [1], it was impossible to view seriously for very long “gaugino” and “higgsino” fields as possible building blocks for our familiar lepton fields. This led to consider that all quarks, and leptons, ought to be associated with new bosonic partners, the *spin-0 squarks and sleptons*. Gauginos and higgsinos, mixed together by the spontaneous breaking of the electroweak symmetry, correspond to a new class of fermions, now known as “charginos” and “neutralinos”. In particular, the partner of the photon under supersymmetry, which cannot be identified with any of the known neutrinos, should be viewed as a new “photonic neutrino”, the *photino*; the fermionic partner of the gluon octet is an octet of self-conjugate Majorana fermions called *gluinos* (although at the time *colored fermions* belonging

⁵With a different denomination for the two Higgs doublets, such that $\varphi'' \mapsto$ Higgs doublet h_d , $(\varphi')^c \mapsto$ Higgs doublet h_u , $\tan \delta = v'/v'' \mapsto \tan \beta = v_u/v_d$.

- | |
|---|
| <ol style="list-style-type: none"> 1) the three $SU(3) \times SU(2) \times U(1)$ gauge superfields; 2) chiral superfields for the three quark and lepton families; 3) the two doublet Higgs superfields H_d and H_u responsible for the spontaneous electroweak breaking, and the generation of quark and lepton masses; 4) the trilinear superpotential of Eq. (1.2). |
|---|

Table 1.1: *The basic ingredients of the Supersymmetric Standard Model.*

to *octet* representations of the colour $SU(3)$ gauge group were generally believed not to exist), etc..

The two doublet Higgs superfields ⁶ H_d and H_u generate quark and lepton masses [2], in the usual way, through the familiar trilinear superpotential of Eq. (1.2). The vacuum expectation values of the two corresponding spin-0 Higgs doublets h_d and h_u generate charged-lepton and down-quark masses, and up-quark masses, with mass matrices given by $m_{ij}^e = \lambda_{ij}^e v_d/\sqrt{2}$, $m_{ij}^d = \lambda_{ij}^d v_d/\sqrt{2}$, and $m_{ij}^u = \lambda_{ij}^u v_u/\sqrt{2}$, respectively. This constitutes the basic structure of the **Supersymmetric Standard Model**, which involves, at least, the basic ingredients shown in Table 1.1. Other ingredients, such as a $\mu H_u H_d$ direct Higgs superfield mass term in the superpotential, or an extra singlet chiral superfield N with a trilinear superpotential coupling $\lambda H_u H_d N + \dots$ possibly acting as a replacement for a direct $\mu H_u H_d$ mass term [1], and/or extra $U(1)$ factors in the gauge group, may or may not be present, depending on the particular version of the Supersymmetric Standard Model considered.

In any case, independently of the details of the supersymmetry-breaking mechanism ultimately considered and of the absence or presence of R_p interactions, we obtain the following minimal particle content of the Supersymmetric Standard Model, as summarized in Table 1.2. Each spin- $\frac{1}{2}$ quark q or charged lepton l^- is associated with *two* spin-0 partners collectively denoted by \tilde{q} or \tilde{l}^- , while a left-handed neutrino ν_L is associated with a *single* spin-0 sneutrino $\tilde{\nu}_L$. We have ignored for simplicity, in this table, further mixing between the various “neutralinos” described by neutral gaugino and higgsino fields, schematically denoted by $\tilde{\gamma}$, $\tilde{Z}_{1,2}$, and \tilde{h}^0 . More precisely, all such models include four neutral Majorana fermions at least, mixings of the fermionic partners of the two neutral $SU(2) \times U(1)$ gauge bosons (usually denoted by \tilde{Z} and $\tilde{\gamma}$, or \tilde{W}_3 and \tilde{B}) and of the two neutral higgsino components (\tilde{h}_d^0 and \tilde{h}_u^0). Non-minimal models also involve additional gauginos and/or higgsinos.

Let us return to the definition of the continuous $U(1)$ R -symmetry, and discrete R -parity, transformations. As explained earlier, the new *additive* quantum number R associated with this continuous $U(1)$ R -symmetry is carried by the supersymmetry generator, and distinguishes between bosons and fermions within the multiplets of supersymmetry [1]. Gauge bosons and

⁶The correspondence between earlier notations and modern ones is as follows:

$$\begin{array}{ccc}
 S = \begin{pmatrix} S^0 \\ S^- \end{pmatrix} & \text{and } T = \begin{pmatrix} T^0 \\ T^- \end{pmatrix} & \mapsto & H_d = \begin{pmatrix} H_d^0 \\ H_d^- \end{pmatrix} & \text{and } H_u = \begin{pmatrix} H_u^+ \\ H_u^0 \end{pmatrix} \\
 \text{(left-handed)} & \text{(right-handed)} & & \text{(both left-handed)} &
 \end{array}$$

Spin 1	Spin 1/2	Spin 0
gluons g photon γ	gluinos \tilde{g} photino $\tilde{\gamma}$	
W^\pm Z	winos $\tilde{W}_{1,2}^\pm$ zinos $\tilde{Z}_{1,2}$ higgsino \tilde{h}^0	H^\pm H h, A } Higgs bosons
	leptons l quarks q	sleptons \tilde{l} squarks \tilde{q}

Table 1.2: Minimal particle content of the Supersymmetric Standard Model.

$V(x, \theta, \bar{\theta})$	\rightarrow	$V(x, \theta e^{-i\alpha}, \bar{\theta} e^{i\alpha})$	for the $SU(3) \times SU(2) \times U(1)$ gauge superfields
$H_{d,u}(x, \theta)$	\rightarrow	$H_{d,u}(x, \theta e^{-i\alpha})$	for the left-handed doublet Higgs superfields H_d and H_u
$S(x, \theta)$	\rightarrow	$e^{i\alpha} S(x, \theta e^{-i\alpha})$	for the left-handed (anti)quark and (anti)lepton superfields $Q_i, U_i^c, D_i^c, L_i, E_i^c$

Table 1.3: Action of a continuous $U(1)$ R -symmetry transformation on the gauge and chiral superfields of the Supersymmetric Standard Model.

Higgs bosons have $R = 0$ while their partners under supersymmetry, now interpreted as gauginos and higgsinos, have $R = \pm 1$. This definition is extended to the chiral quark and lepton superfields, spin- $\frac{1}{2}$ quarks and leptons having $R = 0$, and their spin-0 superpartners, $R = +1$ (for \tilde{q}_L, \tilde{l}_L) or $R = -1$ (for \tilde{q}_R, \tilde{l}_R) [2]. The action of these R -symmetry transformations, which survive the spontaneous breaking of the electroweak symmetry (see also footnote 3 in section 1.3), is given in Table 1.3.

This continuous $U(1)$ R -symmetry ($U(1)_R$) is indeed a symmetry of the four basic building blocks of the Supersymmetric Standard Model (cf. Table 1.1). This includes the self-interactions of the $SU(3) \times SU(2) \times U(1)$ gauge superfields, and their interactions with the chiral quark and lepton superfields, and the two doublet Higgs superfields H_d and H_u . Also invariant under the continuous $U(1)$ R -symmetry are the super-Yukawa interactions of H_d and H_u , responsible for the generation of quark and lepton masses through the superpotential (1.2). Indeed it follows from Table 1.3 that this trilinear superpotential W transforms under the continuous R -symmetry with “ R -weight” $n_W = \sum_i n_i = 2$, i.e. according to

$$W(x, \theta) \rightarrow e^{2i\alpha} W(x, \theta e^{-i\alpha}) . \quad (1.12)$$

Bosons	Fermions
gauge and Higgs bosons graviton $(R = 0)$ R -parity +	gauginos and higgsinos gravitino $(R = \pm 1)$ R -parity -
sleptons and squarks $(R = \pm 1)$ R -parity -	leptons and quarks $(R = 0)$ R -parity +

Table 1.4: R -parities in the Supersymmetric Standard Model.

Its auxiliary “ F -component”, obtained from the coefficient of the bilinear $\theta\theta$ term in the expansion of this superpotential W , is therefore R -invariant, generating R -invariant interaction terms in the Lagrangian density. Note, however, that a direct Higgs superfield mass term $\mu H_u H_d$ in the superpotential, which has R -weight $n = 0$, does *not* lead to interactions invariant under the continuous R -symmetry (see also footnote 4 in section 1.3 and [1] for a replacement of the μ term by a trilinear coupling with an extra singlet chiral superfield, as in the NMSSM). But it gets in general re-allowed as soon as the continuous R -symmetry gets reduced to its discrete version of R -parity.

This R -invariance led us to distinguish between a sector of R -even particles, which includes all those of the Standard Model, with $R = 0$ (and therefore $R_p = (-1)^R = +1$); and their R -odd superpartners, gauginos and higgsinos, sleptons and squarks, with $R = \pm 1$ (and $R_p = -1$), as indicated in Table 1.4.

More precisely the necessity of generating masses for the (Majorana) spin- $\frac{3}{2}$ gravitino [3] and the spin- $\frac{1}{2}$ gluinos did not allow us to keep a distinction between $R = +1$ and $R = -1$ particles, forcing us to abandon the continuous R -invariance in favour of its discrete version, R -parity. The – even or odd – parity character of the (additive) R quantum number corresponds to the well-known R -parity, first defined as $+1$ for the ordinary particles and -1 for their superpartners, simply written as $(-1)^R$ in (1.1) [4], then re-expressed as $(-1)^{2S}(-1)^{3B+L}$ in (1.3) as an effect of the close connection between R -parity and baryon and lepton-number conservation laws.

This R -parity symmetry operator may also be viewed as a non-trivial geometrical discrete symmetry associated with a reflection of the anticommuting fermionic Grassmann coordinate, $\theta \rightarrow -\theta$, in superspace [18]. This R -parity operator plays an essential rôle in the construction of supersymmetric theories of interactions, and in the discussion of the experimental signatures of the new particles. A conserved R -parity guarantees that *the new spin-0 squarks and sleptons cannot be directly exchanged* between ordinary quarks and leptons, as well as the absolute stability of the LSP. But let us discuss more precisely the reasons which led to discarding the continuous R -invariance in favour of its discrete version, R -parity.

1.5 Gravitino and Gluino Masses: From R -Invariance to R -Parity

There are two strong reasons, at least, to abandon the continuous R -invariance in favour of its discrete Z_2 subgroup generated by the R -parity transformation. One is theoretical, the necessity – once gravitation is introduced – of generating a mass for the (Majorana) spin- $\frac{3}{2}$ *gravitino* in the framework of spontaneously-broken locally supersymmetric theories [3]. The other is phenomenological, the non-observation of massless (or even light) *gluinos*. Both particles would have to stay massless in the absence of a breaking of the continuous $U(1)$ R -invariance, thereby preventing, in the case of the gravitino, supersymmetry from being spontaneously broken. (A third reason could now be the non-observation at LEP of a charged *wino* – also called *chargino* – lighter than the W^\pm , that would exist in the case of a continuous $U(1)$ R -invariance [1, 2], as shown by the mass matrix M_C given in Eq.(1.10).)

All this is, therefore, also connected with the mechanism by which the supersymmetry should get spontaneously broken, in the Supersymmetric Standard Model. The question has not received a definitive answer yet. The inclusion of universal soft supersymmetry-breaking terms for all squarks and sleptons,

$$- \sum_{\tilde{q}, \tilde{l}} m_0^2 (\tilde{q}^\dagger \tilde{q} + \tilde{l}^\dagger \tilde{l}) , \quad (1.13)$$

was already considered in 1976, for lack of a better solution. But such terms should in fact be generated by some spontaneous supersymmetry-breaking mechanism, if supersymmetry is to be realized locally. In any case one now considers in general all soft supersymmetry-breaking terms [19] (possibly “induced by supergravity”), which essentially serve as a parametrisation of our ignorance about the true mechanism of supersymmetry breaking chosen by Nature to make superpartners heavy.

But let us return to gluino masses. Since R -transformations act *chirally* on the Majorana octet of gluinos,

$$\tilde{g} \rightarrow e^{\gamma_5 \alpha} \tilde{g} \quad (1.14)$$

a continuous R -invariance would require the gluinos to remain massless, even after a spontaneous breaking of the supersymmetry ! As mentioned before (see section 1.1), one would then expect the existence of “ R -hadrons” which have not been observed [5, 6]. Present experimental constraints indicate that gluinos, if they exist, must be very massive [20], requiring a significant breaking of the continuous R -invariance, in addition to the necessary breaking of the supersymmetry.

In the framework of global supersymmetry it is not so easy to generate large gluino masses. Even if global supersymmetry is spontaneously broken, and if the continuous R -symmetry is not present, it is still in general rather difficult to obtain large masses for gluinos, since: i) no direct gluino mass term is present in the Lagrangian density; and ii) no such term may be generated spontaneously, at the tree approximation, via gluino couplings involving *coloured* spin-0 fields.

A gluino mass may then be generated by radiative corrections involving a new sector of quarks sensitive to the source of supersymmetry breaking, that would now be called “messenger quarks” [7], but iii) this can only be through diagrams which “know” both about: a) the spontaneous breaking of the global supersymmetry, through some appropriately generated

VEVs for auxiliary gauge or chiral components, $\langle D \rangle$, $\langle F \rangle$ or $\langle G \rangle$'s; b) the existence of superpotential interactions which do not preserve the continuous $U(1)$ R -symmetry. Such radiatively generated gluino masses, however, generally tend to be rather small, unless one introduces, in some often rather complicated “hidden sector”, very large mass scales $\gg M_W$.

Fortunately gluino masses may also result directly from supergravity, as observed long ago [3]. Gravitational interactions require, within local supersymmetry, that the spin-2 graviton be associated with a spin-3/2 partner [12], the gravitino. Since the gravitino is the fermionic gauge particle of supersymmetry it must acquire a mass $m_{3/2}$ as soon as the local supersymmetry gets spontaneously broken⁷. Since the gravitino is a self-conjugate Majorana fermion its mass breaks the continuous R -invariance which acts chirally on it, just as for the gluinos, forcing us to abandon the continuous $U(1)$ R -invariance, in favour of its discrete Z_2 subgroup generated by the R -parity transformation. We can no longer distinguish between the values $+1$ and -1 of the (*additive*) quantum number R ; but only between “ R -odd” particles (having $R = \pm 1$) and “ R -even” ones, i.e. between particles having R -parities $R_p = (-1)^R = -1$, and $+1$, respectively (cf. Table 1.4).

In particular, when the spin- $\frac{3}{2}$ gravitino mass term $m_{3/2}$, which corresponds to a change in R $\Delta R = \pm 2$, is introduced, the “left-handed sfermions” \tilde{f}_L , which carry $R = +1$, can mix with the “right-handed” ones \tilde{f}_R , carrying $R = -1$, through mixing terms having $\Delta R = \pm 2$, which may naturally (but not necessarily) be of order $m_{3/2} m_f$ (so that the lightest of the squarks and sleptons may well turn out to be one of the two stop quarks \tilde{t}). Supergravity theories offer a natural framework in which to include, in addition, direct gaugino Majorana mass terms

$$-\frac{1}{2} M_3 \tilde{g}^a \tilde{g}^a - \frac{1}{2} M_2 \tilde{W}^i \tilde{W}^i - \frac{1}{2} M_1 \tilde{B} \tilde{B} , \quad (1.15)$$

which also correspond to $\Delta R = \pm 2$, just as for the gravitino mass itself. The mass parameters M_3 , M_2 and M_1 associated with the $SU(3) \times SU(2) \times U(1)$ gauginos may then naturally (but not necessarily) be of the same order as the gravitino mass $m_{3/2}$.

Furthermore, once the continuous R -invariance is reduced to its discrete R -parity subgroup, a direct Higgs superfield mass term $\mu H_u H_d$ which was not allowed by the continuous $U(1)$ R -symmetry (but could be replaced by a trilinear $\lambda H_u H_d N$ superpotential term), gets reallocated in the superpotential, as for example in the MSSM. The size of this supersymmetric μ parameter might conceivably have been a source of difficulty, in case this parameter, present even if there is no supersymmetry breaking, turned out to be large. But since the μ term breaks explicitly the continuous R -invariance of Table 1.3 (and, also, another “extra $U(1)$ ” symmetry acting axially on quark and lepton superfields [2]), its size may be controlled by considering one or the other of these two symmetries. Even better, since μ got reallocated just as we abandoned the continuous R -invariance so as to allow for gluino and gravitino masses, the size of μ may naturally be of the same order as the supersymmetry-breaking gaugino mass parameters M_i , or the gravitino mass $m_{3/2}$, since they all appear in violation of the continuous R -symmetry of Table 1.3 [21]. Altogether there is here no specific hierarchy problem associated with the size of μ .

In general, irrespective of the supersymmetry-breaking mechanism considered, still unknown (and parametrized using a variety of possible soft supersymmetry-breaking terms), one

⁷Depending on the notation this mass may be expressed as $m_{3/2} = \kappa d/\sqrt{6}$, or $m_{3/2} = \kappa F_S/\sqrt{3} = \sqrt{8\pi/3} F_S/M_P$, where F_S (or d) is the supersymmetry-breaking scale parameter, $\kappa^2 = 8\pi G_N$, and M_P is the Planck mass. Supersymmetry is often said to be broken “at the scale” $\sqrt{F_S}$ (or \sqrt{d}) $= \Lambda_{ss} \approx \sqrt{m_{3/2} M_P}$.

normally expects the various superpartners not to be too heavy. Otherwise the corresponding new mass scale introduced in the game would tend to contaminate the electroweak scale, thereby *creating* a hierarchy problem in the Supersymmetric Standard Model. Superpartner masses are then normally expected to be naturally of the order of M_W , or at most in the \sim TeV range.

Beyond that, in a more ambitious framework involving extra spacetime dimensions, R -parity may also be responsible for an elegant way of implementing supersymmetry breaking by dimensional reduction, by demanding *discrete* – periodic or antiperiodic – boundary conditions for ordinary R -even particles and their R -odd superpartners, respectively. The masses of the lowest-lying superpartners would now get fixed by the compactification scale – e.g. in the simplest case and up to radiative correction effects, by

$$m_{3/2} = M_i = \frac{\pi \hbar}{L c} = \frac{\hbar}{2 R c} , \quad (1.16)$$

in terms of the size L of the extra dimension responsible for the supersymmetry breaking [22]. This led to consider, already a long time ago, the possibility of relatively “large” extra dimensions (as compared for example to the Planck length of 10^{-33} cm), associated with a compactification scale that could then be as “low” as \sim TeV scale. If this is true, the discovery of superpartners in the \lesssim TeV scale should be followed by the discovery of series of heavy copies for all particles, corresponding to the Kaluza-Klein excitations of the extra dimensions – quite a spectacular discovery !

Landing back on four dimensions, the Supersymmetric Standard Model (whether “minimal” or not), with its R -parity symmetry (whether it turns out to be absolutely conserved or not), provided the basis for the experimental searches for the new superpartners and Higgs bosons, starting with the first searches for gluinos and photinos, selectrons and smuons, in 1978-1980. But how the supersymmetry should actually be broken – if indeed it is a symmetry of Nature ! – is not known yet, and this concentrates a large part of the remaining uncertainties in the Supersymmetric Standard Model. Furthermore, it is worth to discuss more precisely the question of the conservation, or non-conservation, of R -parity. In other terms, how much violation of the R -parity symmetry may be tolerated, without running in conflict with existing experimental results on proton decay, neutrino masses, and various accelerator or astrophysical data ? Or, conversely, could R_p effects be responsible for the generation of small Majorana masses for neutrinos ? This is the subject of the present review article.

Chapter 2

HOW CAN R -PARITY BE VIOLATED?

The non-conservation of baryon (B) and lepton (L) numbers is a generic feature of numerous extensions of the Standard Model. In theories involving new symmetries valid at some high energy scale such as Grand Unified Theories (GUTs), such B - and L -violating effects are usually suppressed by powers of the high scale, and therefore generally small - even though some of them, like proton decay, may be observable. By contrast, in supersymmetric extensions of the Standard Model, the scale of possible baryon and lepton-number violations is associated with the masses of the superpartners (squarks and leptons) responsible for the violations, which may lead to unacceptably large effects. Avoiding this, was the main interest of the introduction of R -parity, as discussed in the previous chapter. In view of the important phenomenological differences between supersymmetric models with and without R -parity, it is worth studying the extent to which R -parity can be broken. Furthermore, there are in principle other symmetries (discrete or continuous, global or local) that can forbid proton decay while still allowing for the presence of some R -parity-violating couplings. Their classification will allow to explore which kind of R -parity-violating terms can possibly appear.

2.1 R -Parity-Violating Couplings

In the Standard Model (assuming two-component, massless neutrino fields) it is impossible to write down renormalizable, gauge-invariant interactions that violate baryon or lepton numbers. This is no longer the case in supersymmetric extensions of the Standard Model where, for each ordinary fermion (boson), the introduction of a scalar (fermionic) partner allows for new interactions that do not preserve baryon or lepton number. As explained in chapter 1, these interactions can be forbidden by introducing R -parity. This leads in particular to the popular “Minimal Supersymmetric Standard Model” (MSSM), the supersymmetric extension of the Standard Model with gauge symmetry $SU(3)_C \times SU(2)_L \times U(1)_Y$, with minimal particle content and for which R -parity invariance is generally assumed. Throughout most of this review, the MSSM will normally be our reference model, although the discussion of R -parity violation does not in general depend much on the specific version of the Supersymmetric Standard Model which is considered.

R_p couplings originate either from the superpotential itself, or from soft supersymmetry-breaking terms. There are various kinds of such couplings, of dimensions 4, 3 or 2 only, with a potentially rich flavour structure. In this section, we shall write down explicitly all possible R_p

terms in the framework of the MSSM, assuming the most general breaking of R -parity. We shall then consider particular scenarios which allow to reduce the number of independent couplings used to parametrize R -parity violation.

2.1.1 Superpotential Couplings

Assuming R -parity invariance, the superpotential of the Supersymmetric Standard Model with minimal particle content contains only one supersymmetric Higgs mass term, the μ -term, and the supersymmetric Yukawa interactions generating masses for the quarks and charged leptons (see section 1.1, and Appendix A for the definition of superfields),

$$W_{R_p} \equiv W_{MSSM} = \mu H_u H_d + \lambda_{ij}^e H_d L_i E_j^c + \lambda_{ij}^d H_d Q_i D_j^c - \lambda_{ij}^u H_u Q_i U_j^c. \quad (2.1)$$

Other versions of the Supersymmetric Standard Model, with an extended Higgs sector and/or additional $U(1)$ gauge factors, may have a slightly different R -parity conserving superpotential, especially since they involve in general additional chiral superfields. This is for instance the case in the NMSSM where an extra neutral singlet is coupled to the two doublet Higgs superfields H_d and H_u .

In the absence of R -parity, however, R -parity odd terms allowed by renormalizability and gauge invariance must also, in principle, be included in the superpotential. The ones that violate lepton-number conservation can be easily found by noting that the lepton superfields L_i and the Higgs superfield H_d have exactly the same gauge quantum numbers. Thus, gauge invariance allows for bilinear and trilinear lepton-number-violating superpotential couplings obtained by replacing H_d by L_i in Eq. (2.1). The only other renormalizable \mathcal{R}_p superpotential term allowed by gauge invariance, $U_i^c D_j^c D_k^c$, breaks baryon-number conservation. Therefore the most general renormalizable, R -parity odd superpotential consistent with the gauge symmetry and field content of the MSSM is¹ [8] (see also [23]),

$$W_{\mathcal{R}_p} = \mu_i H_u L_i + \frac{1}{2} \lambda_{ijk} L_i L_j E_k^c + \lambda'_{ijk} L_i Q_j D_k^c + \frac{1}{2} \lambda''_{ijk} U_i^c D_j^c D_k^c, \quad (2.2)$$

where, like in Eq. (2.1), there is a summation over the generation indices $i, j, k = 1, 2, 3$, and summation over gauge indices is understood. One has for example $L_i L_j E_k^c \equiv (\epsilon_{ab} L_i^a L_j^b) E_k^c = (N_i E_j - E_i N_j) E_k^c$ and $U_i^c D_j^c D_k^c \equiv \epsilon^{\alpha\beta\gamma} U_{i\alpha}^c D_{j\beta}^c D_{k\gamma}^c$, where $a, b = 1, 2$ are $SU(2)_L$ indices, $\alpha, \beta, \gamma = 1, 2, 3$ are $SU(3)_C$ indices, and ϵ_{ab} and $\epsilon_{\alpha\beta\gamma}$ are totally antisymmetric tensors. Gauge invariance enforces antisymmetry of the λ_{ijk} couplings with respect to their first two indices. As a matter of fact, one has

$$\lambda_{ijk} L_i L_j E_k^c = \lambda_{ijk} \epsilon_{ab} L_i^a L_j^b E_k^c = -\lambda_{jik} \epsilon_{ba} L_j^a L_i^b E_k^c = -\lambda_{jik} L_i L_j E_k^c, \quad (2.3)$$

which leads to

$$\lambda_{ijk} = -\lambda_{jik}. \quad (2.4)$$

Gauge invariance also enforces antisymmetry of the λ''_{ijk} couplings with respect to their last two indices:

$$\lambda''_{ijk} = -\lambda''_{ikj}. \quad (2.5)$$

At this point one should make a comment on the bilinear \mathcal{R}_p superpotential terms $\mu_i H_u L_i$. These terms can be rotated away from the superpotential upon suitably redefining the lepton

¹Other versions of the Supersymmetric Standard Model may allow for additional \mathcal{R}_p superpotential terms.

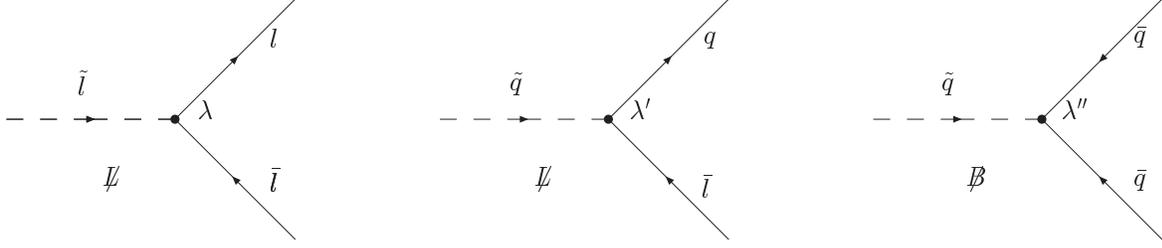


Figure 2.1: Basic tree diagrams associated with the trilinear \mathcal{R}_p superpotential interactions involving the Yukawa couplings λ or λ' (Ψ), or λ'' (\mathcal{B}). q (\bar{q}) and l (\bar{l}) denote (s)quarks and (s)leptons. The arrows on the (s)quark and (s)lepton lines indicate the flow of the baryon (resp. lepton) number.

and Higgs superfields (with $H_d \rightarrow H'_d \propto \mu H_d + \mu_i L_i$) [24]. However, this rotation will generate \mathcal{R}_p scalar mass terms (see subsection 2.1.3) from the ordinary, R -parity conserving soft supersymmetry-breaking terms of dimension 2, so that bilinear R -parity-violating terms will then reappear in the scalar potential. The fact that one can make $\mu_i = 0$ in Eq. (2.2) does not mean that the Higgs-lepton mixing associated with bilinear R -parity breaking is unphysical, but rather that there is no unique way of parametrizing it, as will be discussed in subsection 2.1.4.

Altogether, Eq. (2.2) involves 48 (*a priori* complex) parameters: 3 dimensionful parameters μ_i mixing the charged lepton and down-type Higgs superfields, and 45 dimensionless Yukawa-like couplings divided into 9 λ_{ijk} and 27 λ'_{ijk} couplings which break lepton-number conservation, and 9 λ''_{ijk} couplings which break baryon-number conservation.

2.1.2 Lagrangian Terms Associated with the Superpotential Couplings

We now derive the interaction terms in the Lagrangian density generated from the R -parity odd superpotential of Eq. (2.2).

i) \mathcal{R}_p Yukawa couplings

Let us first consider the terms involving fermions. They consist of fermion bilinears associated with the bilinear superpotential terms $\mu_i H_u L_i$, and of trilinear, Yukawa-like interactions associated with the superpotential couplings λ , λ' and λ'' . In two-component notation for spinors, the fermion bilinears read (see Appendix A for the definition of fields, and Ref. [25] for the two-component notation):

$$\mathcal{L}_{H_u L_i} = \mu_i \left(\tilde{h}_u^0 \nu_i - \tilde{h}_u^+ l_i^- \right) + \text{h.c.} . \quad (2.6)$$

These terms, which mix lepton with higgsino fields, will be discussed in section 2.3. Expanded in standard four-component Dirac notation, the trilinear interaction terms associated with the λ , λ' and λ'' couplings read, respectively (see Appendix A for the definition of fields, and Appendix B for the derivation of this Lagrangian density):

$$\mathcal{L}_{L_i L_j E_k^c} = -\frac{1}{2} \lambda_{ijk} \left(\tilde{\nu}_{iL} \bar{l}_{kR} l_{jL} + \tilde{l}_{jL} \bar{l}_{kR} \nu_{iL} + \tilde{l}_{kR}^* \bar{\nu}_{iR}^c l_{jL} - (i \leftrightarrow j) \right) + \text{h.c.} , \quad (2.7)$$

$$\begin{aligned} \mathcal{L}_{L_i Q_j D_k^c} = & -\lambda'_{ijk} \left(\tilde{\nu}_{iL} \bar{d}_{kR} d_{jL} + \tilde{d}_{jL} \bar{d}_{kR} \nu_{iL} + \tilde{d}_{kR}^* \bar{\nu}_{iR}^c d_{jL} \right. \\ & \left. - \tilde{l}_{iL} \bar{d}_{kR} u_{jL} - \tilde{u}_{jL} \bar{d}_{kR} l_{iL} - \tilde{d}_{kR}^* \bar{l}_{iR}^c u_{jL} \right) + \text{h.c.} , \end{aligned} \quad (2.8)$$

and²

$$\mathcal{L}_{U_i^c D_j^c D_k^c} = -\frac{1}{2} \lambda''_{ijk} \left(\tilde{u}_{iR}^* \bar{d}_{jR} d_{kL}^c + \tilde{d}_{kR}^* \bar{u}_{iR} d_{jL}^c + \tilde{d}_{jR}^* \bar{u}_{iR} d_{kL}^c \right) + \text{h.c.} . \quad (2.9)$$

In these equations, the superscript c denotes the charge conjugate of a spinor (for instance $\bar{\nu}_{iR}^c = (\nu_i^c)_R$ is the adjoint of the charge conjugate of ν_{iL}), the superscript $*$ the complex conjugate of a scalar field, and the R and L chirality indices on scalar fields distinguish between independent fields corresponding to the superpartners of right- and left-handed fermion fields, respectively. Like in Eq. (2.2), an implicit sum runs freely over the quark and lepton generations labelled by the indices i, j, k , and summation over gauge indices is understood. The trilinear interactions of Eqs. (2.7), (2.8) and (2.9) couple a scalar field and two fermionic fields (see Fig. 2.1), and are indeed forbidden by the R -parity symmetry defined by Eq. (1.3).

ii) \mathcal{R}_p scalar interactions

Let us now consider the \mathcal{R}_p scalar interactions associated with the \mathcal{R}_p superpotential couplings (2.2). The bilinear superpotential terms induce dimension-2 and -3 terms,

$$V_{\mathcal{R}_p}^{\mu_i} = \mu^* \mu_i h_d^\dagger \tilde{L}_i - \mu_i^* \lambda_{jk}^u (\tilde{L}_i^\dagger \tilde{Q}_j) \tilde{u}_k^c + \sum_l \mu_l^* \lambda_{li}^e (h_u^\dagger h_d) \tilde{l}_i^c + \text{h.c.} , \quad (2.10)$$

while the trilinear superpotential couplings induce dimension-4 terms,

$$\begin{aligned} V_{\mathcal{R}_p}^{\lambda, \lambda', \lambda''} = & -\sum_l \lambda_{lj}^{e*} \lambda_{lik} (h_d^\dagger \tilde{L}_i) \tilde{l}_j^{c*} \tilde{l}_k^c + \frac{1}{2} \sum_l \lambda_{il}^{e*} \lambda_{jkl} (h_d \tilde{L}_i)^* (\tilde{L}_j \tilde{L}_k) \\ & - \sum_l \lambda_{lj}^{e*} \lambda'_{lik} (h_d^\dagger \tilde{Q}_i) \tilde{l}_j^{c*} \tilde{d}_k^c + \sum_l \lambda_{lj}^{d*} \lambda'_{ilk} (h_d \tilde{L}_i) \tilde{d}_j^{c*} \tilde{d}_k^c \\ & - \sum_l \lambda_{lj}^{u*} \lambda'_{ilk} (h_u^\dagger \tilde{L}_i) \tilde{u}_j^{c*} \tilde{d}_k^c + \sum_l \lambda_{il}^{d*} \lambda'_{jkl} (h_d \tilde{Q}_i)^* (\tilde{L}_j \tilde{Q}_k) \\ & + \sum_l \lambda_{il}^{d*} \lambda''_{jkl} (h_d \tilde{Q}_i)^* \tilde{u}_j^c \tilde{d}_k^c - \frac{1}{2} \sum_l \lambda_{il}^{u*} \lambda''_{ljk} (h_u \tilde{Q}_i)^* \tilde{d}_j^c \tilde{d}_k^c + \text{h.c.} . \end{aligned} \quad (2.11)$$

iii) Additional \mathcal{R}_p conserving scalar couplings

The superpotential (2.2) also yields scalar couplings that depend quadratically on the \mathcal{R}_p couplings. Since R -parity acts as a Z_2 symmetry, these terms correspond in fact to R -parity conserving interactions, even if they vanish in the limit of exact R -parity,

$$V_{\mathcal{R}_p}^{\mu_i} = \sum_i |\mu_i|^2 \left(h_u^\dagger h_u + \tilde{L}_i^\dagger \tilde{L}_i \right) , \quad (2.12)$$

²Due to the antisymmetry property of the λ''_{ijk} couplings and to $SU(3)_C$ invariance, the second and third terms in Eq. (2.9) are actually identical.

$$\begin{aligned}
V_{R_p}^{\lambda, \lambda', \lambda''} &= \sum_m \lambda_{mik}^* \lambda_{mjl} (\tilde{L}_i^\dagger \tilde{L}_j) \tilde{l}_k^{c*} \tilde{l}_l^c + \frac{1}{4} \sum_m \lambda_{ijm}^* \lambda_{klm} (\tilde{L}_i \tilde{L}_j)^* (\tilde{L}_k \tilde{L}_l) \\
&+ \sum_m \left(\lambda_{mik}^* \lambda'_{mjl} (\tilde{L}_i^\dagger \tilde{Q}_j) \tilde{l}_k^{c*} \tilde{d}_l^c + \text{h.c.} \right) + \sum_m \lambda_{mik}^* \lambda'_{mjl} (\tilde{Q}_i^\dagger \tilde{Q}_j) \tilde{d}_k^{c*} \tilde{d}_l^c \\
&+ \sum_m \lambda_{imk}^* \lambda'_{jml} (\tilde{L}_i^\dagger \tilde{L}_j) \tilde{d}_k^{c*} \tilde{d}_l^c + \sum_m \lambda_{ijm}^* \lambda'_{klm} (\tilde{L}_i \tilde{Q}_j)^* (\tilde{L}_k \tilde{Q}_l) \\
&+ \sum_m \left(\lambda_{ijm}^* \lambda''_{klm} (\tilde{L}_i \tilde{Q}_j)^* \tilde{u}_k^c \tilde{d}_l^c + \text{h.c.} \right) + \frac{1}{2} \sum_m \lambda_{mik}^* \lambda''_{mjl} (\tilde{d}_i^{c*} \tilde{d}_j^c) (\tilde{d}_k^{c*} \tilde{d}_l^c) \\
&+ \sum_m \lambda_{ikm}^* \lambda''_{jlm} \left[(\tilde{u}_i^{c*} \tilde{u}_j^c) (\tilde{d}_k^{c*} \tilde{d}_l^c) - (\tilde{u}_i^c \tilde{d}_l^c) (\tilde{d}_k^{c*} \tilde{u}_j^c) \right], \tag{2.13}
\end{aligned}$$

and

$$V_{R_p}^{\mu_i, \lambda, \lambda'} = - \sum_l \mu_l^* \lambda_{lij} (h_u^\dagger \tilde{L}_i) \tilde{l}_j^c - \sum_l \mu_l^* \lambda'_{lij} (h_u^\dagger \tilde{Q}_i) \tilde{d}_j^c + \text{h.c.} \tag{2.14}$$

2.1.3 Soft Supersymmetry-Breaking Terms

Since supersymmetry is necessarily broken, a proper treatment of R -parity violation must also include \mathcal{R}_p soft terms. In the Supersymmetric Standard Model, we parametrize our ignorance about the mechanism responsible for supersymmetry breaking by introducing the most general terms that break supersymmetry in a soft way, i.e. without reintroducing quadratic divergences. The possible soft terms were classified by Girardello and Grisaru [19]. They consist of mass terms for the gauginos ($M\lambda\lambda$), analytic³ couplings for the scalar fields known as ‘‘A-terms’’ ($A_{ijk} \phi_i \phi_j \phi_k$), analytic scalar mass terms known as ‘‘B-terms’’ ($B_{ij} \phi_i \phi_j$), and scalar mass terms ($m_{ij}^2 \phi_i^\dagger \phi_j$). This leads to the following soft supersymmetry-breaking Lagrangian density for the Supersymmetric Standard Model (see Appendix A), given by:

$$\begin{aligned}
- \mathcal{L}_{R_p}^{soft} &= (m_{\tilde{Q}}^2)_{ij} \tilde{Q}_i^\dagger \tilde{Q}_j + (m_{\tilde{u}^c}^2)_{ij} \tilde{u}_i^{c\dagger} \tilde{u}_j^c + (m_{\tilde{d}^c}^2)_{ij} \tilde{d}_i^{c\dagger} \tilde{d}_j^c + (m_{\tilde{L}}^2)_{ij} \tilde{L}_i^\dagger \tilde{L}_j + (m_{\tilde{l}^c}^2)_{ij} \tilde{l}_i^{c\dagger} \tilde{l}_j^c \\
&+ \left(A_{ij}^e h_d \tilde{L}_i \tilde{l}_j^c + A_{ij}^d h_d \tilde{Q}_i \tilde{d}_j^c - A_{ij}^u h_u \tilde{Q}_i \tilde{u}_j^c + \text{h.c.} \right) \\
&+ \tilde{m}_d^2 h_d^\dagger h_d + \tilde{m}_u^2 h_u^\dagger h_u + (B h_u h_d + \text{h.c.}) \\
&+ \frac{1}{2} M_1 \tilde{B} \tilde{B} + \frac{1}{2} M_2 \tilde{W}^3 \tilde{W}^3 + M_2 \tilde{W}^+ \tilde{W}^+ + \frac{1}{2} M_3 \tilde{g}^a \tilde{g}^a. \tag{2.15}
\end{aligned}$$

In the absence of R -parity, one must in principle also consider the most general soft terms associated with W_{R_p} :

$$\begin{aligned}
V_{R_p}^{soft} &= \frac{1}{2} A_{ijk} \tilde{L}_i \tilde{L}_j \tilde{l}_k^c + A'_{ijk} \tilde{L}_i \tilde{Q}_j \tilde{d}_k^c + \frac{1}{2} A''_{ijk} \tilde{u}_i^c \tilde{d}_j^c \tilde{d}_k^c \\
&+ B_i h_u \tilde{L}_i + \tilde{m}_{di}^2 h_d^\dagger \tilde{L}_i + \text{h.c.} \tag{2.16}
\end{aligned}$$

Again Eqs. (2.15) and (2.16) assume the particle content of the MSSM; more general versions of the Supersymmetric Standard Model may allow for additional soft terms, both R -parity even and R -parity odd.

The soft potential (2.16) introduces 51 new (*a priori* complex) \mathcal{R}_p parameters: $9 + 27 + 9 = 45$ \mathcal{R}_p A-terms with the same antisymmetry properties as the corresponding trilinear

³‘‘Analytic’’ means here that these couplings involve only products of the scalar components of the (left-handed) chiral superfields, and not their complex conjugates.

superpotential couplings, 3 B_i associated with the bilinear superpotential terms, and 3 \mathcal{R}_p soft mass parameters \tilde{m}_{di}^2 mixing the down-type Higgs boson with the slepton fields. In the presence of the bilinear \mathcal{R}_p soft terms, the radiative electroweak symmetry breaking generally leads to non-vanishing sneutrino vacuum expectation values $\langle \tilde{\nu}_i \rangle \equiv v_i/\sqrt{2}$, together with the familiar Higgs VEVs $\langle h_d^0 \rangle \equiv v_d/\sqrt{2}$ and $\langle h_u^0 \rangle \equiv v_u/\sqrt{2}$. Indeed, the bilinear terms in Eq. (2.16) yield linear terms in the $\tilde{\nu}_i$ fields after translation of the Higgs fields, $h_d^0 \rightarrow h_d^0 + v_d/\sqrt{2}$ and $h_u^0 \rightarrow h_u^0 + v_u/\sqrt{2}$, which destabilizes the scalar potential and leads to $\langle \tilde{\nu}_i \rangle \neq 0$ – unless particular conditions are satisfied by the bilinear soft terms.

Since the sneutrino fields correspond to R -parity odd particles, these VEVs in turn induce new \mathcal{R}_p terms in the Lagrangian. In particular new mixing terms between lepton and chargino/neutralino fields (resp. between slepton and Higgs boson fields) are generated from the gauge and R -parity conserving Yukawa couplings (resp. from the R -parity conserving A -terms). It is important to keep in mind, however, that the slepton VEVs are not independent \mathcal{R}_p parameters, since they are functions of the \mathcal{R}_p couplings; as we shall see below it is always possible to find a weak eigenstate basis in which $v_i = 0$.

2.1.4 Choice of the Weak Interaction Basis

In the absence of R -parity and lepton-number conservation, there is no *a priori* distinction between the $Y = -1$ Higgs (H_d) and the lepton (L_i) superfields, which have the same gauge interactions. One can therefore freely rotate the weak eigenstate basis by a unitary transformation [24]:

$$\begin{pmatrix} H_d \\ L_i \end{pmatrix} \rightarrow \begin{pmatrix} H'_d \\ L'_i \end{pmatrix} = U \begin{pmatrix} H_d \\ L_i \end{pmatrix}, \quad (2.17)$$

where U is an $SU(4)$ matrix with entries $U_{\alpha\beta}$, $\alpha \equiv (0, i) = (0, 1, 2, 3)$, $\beta \equiv (0, j) = (0, 1, 2, 3)$. Under (2.17), \mathcal{R}_p couplings and slepton VEVs transform as follows (we use the notation \tilde{m}_{ij}^2 instead of $(m_{\tilde{L}}^2)_{ij}$):

$$\mu'_i = U_{i0}^* \mu + \sum_j U_{ij}^* \mu_j, \quad (2.18)$$

$$\tilde{m}'^2_{di} = U_{00} U_{i0}^* \tilde{m}_d^2 + \sum_{l,m} U_{0l} U_{im}^* \tilde{m}_{lm}^2 + \sum_l (U_{00} U_{il}^* \tilde{m}_{dl}^2 + U_{0l} U_{i0}^* (\tilde{m}_{dl}^2)^*), \quad (2.19)$$

$$B'_i = U_{i0}^* B + \sum_j U_{ij}^* B_j, \quad v'_i = U_{i0} v_d + \sum_j U_{ij} v_j, \quad (2.20)$$

$$(\lambda_{ijk})' = \sum_l (U_{i0}^* U_{jl}^* - U_{il}^* U_{j0}^*) \lambda_{lk}^e + \sum_{l,m} U_{il}^* U_{jm}^* \lambda_{lmk}, \quad (2.21)$$

$$(\lambda'_{ijk})' = U_{i0}^* \lambda_{jk}^d + \sum_l U_{il}^* \lambda'_{ljk}, \quad (\lambda''_{ijk})' = \lambda''_{ijk}. \quad (2.22)$$

Since the A -terms transform exactly in the same way as the trilinear superpotential couplings, we do not write explicitly the corresponding transformation for A_{ijk} , A'_{ijk} and A''_{ijk} .

From the above equations it is clear that the values of the lepton-number-violating couplings are basis-dependent. There is also a redundancy between the bilinear and trilinear \mathcal{R}_p parameters, as can be seen from the fact that 3 among the 9 bilinear \mathcal{R}_p parameters μ_i , B_i and \tilde{m}_{di}^2 can be rotated away upon a suitable superfield redefinition, as expressed by Eq. (2.17). This leaves us with $48 + 51 - 3 = 96$ physically meaningful (in general complex) parameters.

As already noticed, it is always possible to choose a basis in which $\mu'_i = 0$, eliminating all bilinear R -parity violation from the superpotential; but then in general non-vanishing slepton VEVs are induced by the presence of the bilinear \mathcal{R}_p soft terms. Alternatively, one can choose a basis in which all slepton VEVs vanish⁴, $v'_i = 0$, but then in general $\mu'_i \neq 0$. It is therefore crucial, when discussing \mathcal{R}_p effects, to specify in which basis one is working. A particular choice of basis, in which the Higgs-lepton mixing induced by bilinear R -parity violation is parametrized in an economical and physically sensible way, will be presented in section 2.3. Another option (to be discussed in subsection 6.1.3) is to define a complete set of basis-independent quantities parametrizing \mathcal{R}_p effects [26, 27, 28].

Before closing this subsection, let us write down explicitly the infinitesimal $SU(4)$ transformation that rotates away small bilinear \mathcal{R}_p terms from the superpotential (2.2), $\mu_i \ll \mu$. Defining $\epsilon_i \equiv \frac{\mu_i}{\mu}$, we can write the corresponding unitary matrix U , up to $\mathcal{O}(\epsilon^2)$ terms, as⁵ [24]:

$$U = \begin{pmatrix} 1 & -\epsilon_i \\ \epsilon_i^* & 1_{3 \times 3} \end{pmatrix}. \quad (2.23)$$

In the new basis $\mu'_i = 0$, and the trilinear \mathcal{R}_p superpotential couplings are modified to $(\lambda'_{ijk})' = \lambda_{ijk} + (\epsilon_i \lambda_{jk}^e - \epsilon_j \lambda_{ik}^e)$ and $(\lambda'_{ijk})' = \lambda'_{ijk} + \epsilon_i \lambda_{jk}^d$, where λ_{jk}^e and λ_{jk}^d are the Yukawa couplings in the initial basis. In the supersymmetry-breaking sector, the mass parameters transform (omitting $\mathcal{O}(\epsilon^2)$ terms) as:

$$B' = B - \sum_i \epsilon_i^* B_i, \quad B'_i = B_i + \epsilon_i B, \quad (2.24)$$

$$\tilde{m}_d'^2 = \tilde{m}_d^2 - (\sum_i \epsilon_i^* \tilde{m}_{di}^2 + \text{h.c.}), \quad \tilde{m}_{ij}'^2 = \tilde{m}_{ij}^2 + (\epsilon_i^* \tilde{m}_{dj}^2 + \text{h.c.}), \quad (2.25)$$

$$\tilde{m}_{di}'^2 = \tilde{m}_{di}^2 + \epsilon_i \tilde{m}_d^2 - \sum_j \epsilon_j \tilde{m}_{ji}^2. \quad (2.26)$$

As stressed above, such a pattern of soft mass parameters generally induces non-vanishing slepton vacuum expectation values, unless some very particular constraints, that shall be discussed in section 2.3, are satisfied.

2.1.5 Constraints on the Size of \mathcal{R}_p Couplings

Being renormalizable, the \mathcal{R}_p couplings of Eqs. (2.2) and (2.16) are not expected to be suppressed by any large mass scale, and may thus induce excessively large baryon and lepton-number-violating effects. In particular, the combination of couplings $\lambda'_{imk} \lambda''_{11k}^*$ ($i = 1, 2, 3$, $m = 1, 2$) would lead to proton decay via tree-level down squark exchange at an unacceptable rate, unless $|\lambda'_{imk} \lambda''_{11k}^*|$ is smaller than about 10^{-26} for a typical squark mass in the 300 GeV range, smaller by more than twelve orders of magnitude than a typical GUT scale (see Section 6.4.4 for a discussion of this bound). There are many other constraints, both theoretical and phenomenological, on the superpotential and soft supersymmetry-breaking \mathcal{R}_p parameters. Bounds on the \mathcal{R}_p superpotential couplings coming from the non-observation of baryon and lepton-number-violating processes and from direct searches at colliders are reviewed in chapters 6 and 7 respectively. Astrophysical and cosmological bounds are presented in chapter 4, and constraints associated with the effects of the renormalization group evolution (perturbative unitarity bounds and unification constraints), in chapter 3.

⁴This does not mean, however, that the scalar potential is free from any term mixing the slepton and Higgs fields in this basis. Instead B_i and \tilde{m}_{di}^2 satisfy a particular relation that prevents the slepton fields from acquiring a VEV (see the discussion at the end of subsection 2.3.1).

⁵For $\mu_i \sim \mu$, Eq. (2.23) is no longer a good approximation. The explicit form of a unitary matrix U that rotates away arbitrarily large bilinear \mathcal{R}_p parameters from the superpotential can be found in Ref. [29].

2.2 Patterns of R -Parity Breaking

Several patterns of R -parity breaking can be considered, depending on whether the breaking is explicit or spontaneous – and, in the case of an explicit breaking, on which type of couplings, bilinear, trilinear, or both, are present. Before classifying the various patterns considered in the literature, let us make some general comments on subtleties associated with the lepton-number-violating couplings.

First of all, if lepton-number conservation is not associated with a symmetry of the theory, there is in general no preferred (H_d, L_i) basis, as was seen in the previous section, and the statement that only a certain class of lepton-number-violating \mathcal{R}_p couplings are present is basis-dependent.

Still it is not an empty statement, especially if one thinks in terms of the number of independent parameters. Indeed, if there is a basis in which all λ_{ijk} and λ'_{ijk} superpotential couplings as well as their associated soft terms vanish, lepton-number violation can be parametrized by 9 parameters only (3 μ_i and 6 bilinear soft terms). In a different basis the λ_{ijk} and λ'_{ijk} couplings do not vanish, but their values are determined, through the rotation (2.17), from the original down quark and charged lepton R_p -conserving Yukawa couplings.

Secondly, in a consistent quantum field theory, all operators breaking a symmetry up to some dimension d must normally be included in the Lagrangian density, since if some of them are absent at tree level they are in general expected to be generated by radiative corrections. A well-known manifestation of this effect is the generation of bilinear \mathcal{R}_p terms through one-loop diagrams involving lepton-number-violating trilinear \mathcal{R}_p interactions [30, 31] (see also Ref. [32]). For example, the $d = 4$ couplings (2.7) induce the $d = 3$ higgsino-lepton mixing terms $\mu_i \tilde{h}_u L_i$ as well as the $d = 2$ Higgs-slepton mixing mass terms $B_i h_u \tilde{L}_i$ and $\tilde{m}_{di}^2 h_d^\dagger \tilde{L}_i$ (where L_i and \tilde{L}_i denote the fermionic and scalar components of the lepton doublet superfields L_i , respectively). This provides at least three consistent patterns of R -parity violation in the lepton sector at the quantum level⁶:

- (a) **R -parity violation through $d = 2$, $d = 3$ and $d = 4$ terms:** this corresponds to the most general explicit breaking of R -parity, with all superpotential and soft \mathcal{R}_p terms allowed by gauge invariance and renormalizability present in the Lagrangian density. In this case one has to deal with 99 new (in general complex) parameters beyond the (R_p -conserving) MSSM: 3 bilinear (μ_i) and 45 trilinear (9 λ_{ijk} , 27 λ'_{ijk} , 9 λ''_{ijk}) couplings in the superpotential, together with their associated B -terms (3 B_i) and A -terms (9 A_{ijk} , 27 A'_{ijk} , 9 A''_{ijk}), and 3 additional \mathcal{R}_p soft masses (\tilde{m}_{di}^2) in the scalar potential. (The 3 slepton VEVs v_i are not independent \mathcal{R}_p parameters, since they can be expressed in terms of the MSSM parameters and \mathcal{R}_p couplings.) Due to the ambiguity in the choice of the (H_d, L_i) basis, however, only 6 among the 9 bilinear \mathcal{R}_p parameters are physical, thus reducing the number of physically meaningful \mathcal{R}_p parameters to 96.
- (b) **R -parity violation through $d = 2$ and $d = 3$ terms:** in this case all soft \mathcal{R}_p terms are present in the scalar potential (both the bilinear terms $B_i h_u \tilde{L}_i$ and $\tilde{m}_{di}^2 h_d^\dagger \tilde{L}_i$ and the triscalar couplings A_{ijk} , A'_{ijk} and A''_{ijk}), while the superpotential contains only the bilinear \mathcal{R}_p terms $\mu_i H_u L_i$, which corresponds to both $d = 2$ and $d = 3$ terms in the Lagrangian

⁶We do not assume the conservation of lepton or baryon number *a priori*. Of course, if lepton-number conservation (resp. baryon-number conservation) were assumed, \mathcal{L} couplings (resp. \mathcal{B} couplings) would never be generated by radiative corrections.

density. We are thus left with 54 \mathcal{R}_p parameters (3 μ_i in the superpotential; 3 B_i , 3 \tilde{m}_{di}^2 , 9 A_{ijk} , 27 A'_{ijk} and 9 A''_{ijk} in the scalar potential), all of them physically meaningful.

- (c) **R -parity violation through $d = 2$ terms:** in this case, R -parity violation originates solely from the soft terms $B_i h_u \tilde{L}_i$ and $\tilde{m}_{di}^2 h_d^\dagger \tilde{L}_i$, and can therefore be parametrized by 6 parameters only.

A closer look at the renormalization group equations (see chapter 3) shows that there actually exist other consistent patterns of R -parity violation. In particular the popular “bilinear R -parity breaking” scenario, in which R -parity is explicitly broken by bilinear (superpotential and soft) terms only, is perfectly consistent at the quantum level since \mathcal{R}_p dimension-3 A -terms are not generated from the bilinear superpotential μ_i terms, also of dimension 3. On the other hand another popular scenario in which R -parity is broken solely by trilinear terms is not consistent since, as already mentioned, bilinear \mathcal{R}_p terms are then generated from quantum corrections. The absence of bilinear \mathcal{R}_p terms can only be assumed, strictly speaking, at the level of the classical Lagrangian.

With the above remarks in mind, we can now comment on the scenarios of R -parity violation that have received most attention in the literature: explicit \mathcal{R}_p by trilinear terms, explicit \mathcal{R}_p by bilinear terms (“bilinear R -parity breaking”) and spontaneous R -parity violation.

- (i) *explicit \mathcal{R}_p by trilinear terms:* in this case one assumes that all bilinear \mathcal{R}_p terms are absent from the tree-level Lagrangian. One is then left with 45 trilinear \mathcal{R}_p couplings in the superpotential, and their associated A -terms. This is the situation considered in most phenomenological studies of R -parity violation, and in the major part of this review. The absence of bilinear couplings and sneutrino VEVs also has the practical advantage of removing the ambiguity associated with the choice of the weak interaction basis (cf. subsection 2.1.4). One must keep in mind, however, that bilinear \mathcal{R}_p cannot be completely absent. Indeed, if only trilinear couplings are present at some energy scale, they will generate bilinear couplings at some other energy scale through renormalisation group evolution⁷ [30, 31] (see chapter 3 for details). Thus, in a consistent quantum field theory, one must include bilinear \mathcal{R}_p terms as soon as trilinear terms are present. Still, since the experimental and cosmological bounds on neutrino masses put strong constraints on the tolerable amount of bilinear R -parity violation (see next section), it makes sense to consider a situation in which the phenomenology of trilinear \mathcal{R}_p interactions is not affected by the presence of bilinear \mathcal{R}_p terms – except for some specific phenomena such as neutrino oscillations.
- (ii) *explicit \mathcal{R}_p by bilinear terms:* assuming that, in an appropriately chosen basis, R -parity is broken solely by bilinear terms, the number of independent \mathcal{R}_p parameters reduces to 9 (3 μ_i or ν_i , 3 B_i and 3 \tilde{m}_{di}^2). Since bilinear \mathcal{R}_p terms mix leptons with Higgs fields, however, trilinear \mathcal{R}_p interactions of the λ and λ' type (both triscalar and Yukawa-like interactions) are generated upon rotating the initial weak eigenstate basis to the mass eigenstate basis. Still those couplings can be expressed in terms of the initial bilinear \mathcal{R}_p couplings and of the down-type Yukawa couplings, and are not independent \mathcal{R}_p parameters. Note that, due

⁷This is in fact a consequence of supersymmetry breaking. In the limit of exact supersymmetry, the $\mu_i H_u L_i$ terms generated radiatively can be removed from the superpotential by a rotation (2.17), eliminating any bilinear \mathcal{R}_p term from the Lagrangian. In the presence of soft supersymmetry-breaking terms, however, the bilinear \mathcal{R}_p terms generated in the superpotential and in the scalar potential cannot be rotated away simultaneously.

to the fact that R -parity breaking originates here from L -number-violating interactions, no B -violating λ' -type interactions are generated, thus avoiding the problem of a too fast proton decay. The advantage of such a scenario resides in its predictivity (albeit it is difficult to motivate the absence of trilinear couplings by other considerations than simplicity or predictivity); the main difficulty lies in suppressing the neutrino masses induced by bilinear \mathcal{R}_p terms to an acceptable level without fine-tuning (see chapter 5). A detailed discussion of bilinear R -parity breaking is given in section 2.3.

- (iii) *spontaneous \mathcal{R}_p* : a completely different option is the spontaneous breaking of R -parity induced by the vacuum expectation value of an R -parity odd scalar (i.e. necessarily a scalar neutrino in the Minimal Supersymmetric Standard Model). Such a scenario can be implemented in various ways. Common features of the models are a constrained pattern of \mathcal{R}_p couplings, showing some analogy with the bilinear \mathcal{R}_p case, and - with the exception of the models where lepton number is gauged - a variety of new interactions involving a massless Goldstone boson (or a massive pseudo-Goldstone boson in the presence of a small amount of explicit lepton-number violation) associated with the breaking of the lepton number. Spontaneous R -parity breaking is addressed in section 2.4.

Even within a restricted pattern of R -parity violation like (i) or (ii), one is generally left with a very large number of arbitrary \mathcal{R}_p parameters. For this reason, it is often necessary to make some assumptions on their flavour structure; for example, the bounds coming from particular processes are generally derived under the assumption that a single coupling or combination of couplings gives the dominant contribution (see chapter 6). From a more theoretical perspective it is interesting to study models that can constrain the flavour structure of the \mathcal{R}_p couplings. In particular, the case of an abelian flavour symmetry is addressed in section 2.5. Furthermore, extensions of the Supersymmetric Standard Model with an enlarged gauge structure may have a more restricted pattern of \mathcal{R}_p couplings than the Supersymmetric Standard Model itself. R -parity violation in the context of Grand Unified Theories is discussed in section 2.6.

Finally, it should be kept in mind that despite its simplicity, R -parity may be viewed as having no clear theoretical origin, at least at this level. Thus, in the absence of R -parity, it is a valid option to consider other discrete or continuous symmetries sharing with R -parity the capability of protecting proton decay from renormalizable operators, while allowing some baryon or lepton-number-violating couplings. Well-known examples of such symmetries are “baryon parities”, which allow only for lepton-number violation, and “lepton parities”, which allow only for baryon-number violation. Some of these symmetries are even more efficient than R -parity in suppressing proton decay from non-renormalizable operators which may be generated from some fundamental theory beyond the Supersymmetric Standard Model. These other symmetries (“alternatives” to R -parity) are discussed in section 2.7.

2.3 Effects of Bilinear R -Parity violation

As already argued in the previous section, bilinear \mathcal{R}_p terms are present in any consistent pattern of R -parity violation, although they have often been neglected in the literature; most of the studies assume R -parity breaking by trilinear terms only. The purpose of this section is to describe the effects associated with the presence of bilinear \mathcal{R}_p terms. The effects of trilinear \mathcal{R}_p terms will be discussed in chapters 6 and 7. Let us stress that the following discussion does not only apply to the bilinear and spontaneous R_p -breaking scenarios, but also to the most general

scenario in which both bilinear and trilinear \mathcal{R}_p couplings are present. The phenomenology of bilinear R -parity violation has been first investigated in Refs. [24, 33, 34].

2.3.1 Distinguishing Between Higgs and Lepton Doublet Superfields

As we have already said, in the limit of unbroken supersymmetry, the bilinear \mathcal{R}_p superpotential terms $H_u L_i$ can always be rotated away by a suitable redefinition, as expressed by Eq. (2.17) of the four superfields $(H_d, L_{i=1,2,3})$. This redefinition leaves a single bilinear term in the superpotential, the μ -term $\mu H_u H_d$, but generates new contributions to the $\lambda_{ijk} L_i L_j E_k^c$ and $\lambda'_{ijk} L_i Q_j D_k^c$ terms from the charged lepton and down quark Yukawa couplings. So, as long as supersymmetry is unbroken, R -parity violation can be parametrized by trilinear couplings only. In the presence of soft terms, however, the scalar potential and the superpotential provide *two independent sources of bilinear R -parity violation that cannot be simultaneously rotated away* [24], unless some very particular conditions to be discussed below are satisfied. Furthermore these conditions are not renormalization group invariant. Therefore bilinear \mathcal{R}_p terms, if absent at some energy scale, are always regenerated at other energy scales. One is then left with a physically relevant mixing between the Higgs and lepton superfields, which leads to specific signatures, as discussed in the next subsections.

The Higgs-lepton mixing associated with bilinear R -parity violation results in an ambiguity in the definition of the H_d and L_i superfields, which carry the same gauge charges. The values of the lepton-number-violating couplings, in particular, depend on the choice of the (H_d, L_i) basis (see subsection 2.1.4). It is therefore crucial, in phenomenological studies of R -parity violation, to specify in which basis one is working. Of course any physical quantity one may compute will not depend on the choice of basis made; but the formula that expresses this quantity as a function of the lepton-number-violating couplings will. In this subsection, we shall introduce two basis-independent quantities $\sin \xi$ and $\sin \zeta$ that control the size of the effects of bilinear R -parity violation in the fermion and in the sfermion sectors, respectively.

Before doing so, let us rewrite the most general superpotential and soft scalar potential, Eqs. (2.1) – (2.2) and (2.15) – (2.16), in a form that makes apparent the freedom of rotating the H_d and L_i superfields. For this purpose we group them into a 4-vector \hat{L}_α , $\alpha = 0, 1, 2, 3$ [35]. The renormalizable superpotential, including all possible R -parity-preserving and -violating terms, then reads:

$$\begin{aligned} W = & \mu_\alpha H_u \hat{L}_\alpha + \frac{1}{2} \lambda_{\alpha\beta k}^e \hat{L}_\alpha \hat{L}_\beta E_k^c + \lambda_{\alpha j k}^d \hat{L}_\alpha Q_j D_k^c \\ & - \lambda_{j k}^u H_u Q_j U_k^c + \frac{1}{2} \lambda''_{i j k} U_i^c D_j^c D_k^c, \end{aligned} \quad (2.27)$$

and the soft supersymmetry-breaking terms in the scalar sector read:

$$\begin{aligned} V_{\text{soft}} = & \left(B_\alpha h_u \hat{L}_\alpha + \text{h.c.} \right) + \tilde{m}_{\alpha\beta}^2 \hat{L}_\alpha^\dagger \hat{L}_\beta + \tilde{m}_u^2 h_u^\dagger h_u + \dots \\ & + \left(\frac{1}{2} A_{\alpha\beta k}^e \tilde{L}_\alpha \tilde{L}_\beta \tilde{l}_k^c + A_{\alpha j k}^d \tilde{L}_\alpha \tilde{Q}_j \tilde{d}_k^c + \frac{1}{2} A''_{i j k} \tilde{u}_i^c \tilde{d}_j^c \tilde{d}_k^c + \text{h.c.} \right), \end{aligned} \quad (2.28)$$

where the dots stand for the other soft (squark and "right-handed" slepton) scalar mass terms. In the presence of the bilinear soft terms in Eq. (2.28), the radiative breaking of the electroweak symmetry leads to a vacuum expectation value for each of the neutral scalar components of the \hat{L}_α doublet superfields, $\langle \hat{\nu}_\alpha \rangle \equiv v_\alpha / \sqrt{2}$. The covariance of Eqs. (2.27) and (2.28) under

$SU(4)$ rotations of the \hat{L}_α superfields, $\hat{L}_\alpha \rightarrow U_{\alpha\beta} \hat{L}_\alpha$, dictates the transformation laws for the parameters μ_α , $\lambda_{\alpha\beta k}^e$, $\lambda_{\alpha j k}^d$, B_α , $\tilde{m}_{\alpha\beta}^2$, $A_{\alpha\beta k}^e$ and $A_{\alpha j k}^d$.

Up to now, we have not chosen a specific basis for the \hat{L}_α superfields. Several bases have been considered in the literature. A first possibility [24] is to define the down-type Higgs superfield H_d as the combination of the \hat{L}_α superfields that couples to H_u in the superpotential. This choice implies $\mu_i = 0$ for the orthogonal combinations L_i , i.e. all bilinear \mathcal{R}_p terms are contained in the soft supersymmetry-breaking contribution to the scalar potential, but the lepton scalars have in general non-vanishing VEVs, $v_i \neq 0$. A second, more physical possibility is to define H_d as the combination of the \hat{L}_α superfields whose vacuum expectation value breaks the weak hypercharge [35], implying $v_i = 0$ for all three sneutrino fields. In the following, we choose the latter option and define

$$H_d = \frac{1}{v_d} \sum_{\alpha} v_{\alpha} \hat{L}_{\alpha}, \quad (2.29)$$

where $v_d \equiv (\sum_{\alpha} v_{\alpha}^2)^{1/2}$ (here and in the following, we neglect phases for simplicity, since taking them into account is straightforward). The orthogonal combinations L_i , $i = 1, 2, 3$ correspond to the usual slepton fields with vanishing VEVs:

$$\hat{L}_{\alpha} = \frac{v_{\alpha}}{v_d} H_d + \sum_i e_{\alpha i} L_i, \quad (2.30)$$

where the 4-vectors $\vec{e}_i \equiv \{e_{\alpha i}\}_{\alpha=0\dots 3}$ satisfy $\vec{v} \cdot \vec{e}_i = 0$ and $\vec{e}_i \cdot \vec{e}_j = \delta_{ij}$. At this point one can still rotate freely the L_i superfields. This freedom can be removed by diagonalizing the charged lepton Yukawa couplings [36]. The advantage of this choice is that, in the physically relevant limit $\sin \xi \ll 1$, to be discussed below, the charged leptons almost coincide with their mass eigenstates, and the lepton flavour composition of the massive neutrino (see below) can be parametrized in terms of the μ_i . Alternatively, one may require that a single lepton doublet superfield, say L_3 , couples to H_u in the superpotential, i.e. $\vec{\mu} \cdot \vec{e}_1 = \vec{\mu} \cdot \vec{e}_2 = 0$. [37]. The latter choice allows one to rewrite the superpotential as (leaving aside the last two terms in Eq. (2.27), which are not modified):

$$W = \lambda_{ik}^e H_d L_i E_k^c + \lambda_{ik}^d H_d Q_i D_k^c + \frac{1}{2} \lambda_{ijk} L_i L_j E_k^c + \lambda'_{ijk} L_i Q_j D_k^c + \mu \cos \xi H_u H_d + \mu \sin \xi H_u L_3, \quad (2.31)$$

where $\mu \equiv (\sum_{\alpha} \mu_{\alpha}^2)^{1/2}$, ξ is the angle between the 4-vectors $\vec{\mu}$ and \vec{v} , given by [35]

$$\cos \xi \equiv \frac{1}{\mu v_d} \sum_{\alpha} \mu_{\alpha} v_{\alpha}, \quad (2.32)$$

and the physical Yukawa and trilinear \mathcal{R}_p couplings are given by:

$$\lambda_{ik}^e = \sum_{\alpha, \beta} \frac{v_{\alpha}}{v_d} e_{\beta i} \lambda_{\alpha\beta k}^e, \quad \lambda_{ik}^d = \sum_{\alpha} \frac{v_{\alpha}}{v_d} \lambda_{\alpha i k}^d, \quad (2.33)$$

$$\lambda_{ijk} = \sum_{\alpha, \beta} e_{\alpha i} e_{\beta j} \lambda_{\alpha\beta k}^e, \quad \lambda'_{ijk} = \sum_{\alpha} e_{\alpha i} \lambda_{\alpha j k}^d \quad (2.34)$$

(similar relations hold for the associated A -terms A_{ij}^e , A_{ij}^d , A_{ijk} and A'_{ijk}). The residual term $H_u L_3$ in Eq. (2.31) corresponds to a physical higgsino-lepton mixing that cannot be removed

by a field redefinition, unless the vacuum expectation values v_α are proportional to the μ_α , so that $\sin \xi = 0$. Indeed, contrary to the μ_α and v_α which are basis-dependent quantities and do not have any intrinsic physical meaning, their relative angle ξ does not depend on the choice of basis for the \hat{L}_α superfields. *This angle controls the size of the effects of bilinear R -parity violation in the fermion sector* (see section 2.3).

Similarly, the amount of bilinear R -parity violation in the scalar sector is measured by the angle ζ formed by the 4-vectors \vec{B} and \vec{v} [38],

$$\cos \zeta \equiv \frac{1}{B v_d} \sum_{\alpha} B_{\alpha} v_{\alpha}, \quad (2.35)$$

where $B \equiv (\sum_{\alpha} B_{\alpha}^2)^{1/2}$. Indeed, in the $v_i = 0$ basis, the \mathcal{R}_p scalar potential reduces to:

$$\begin{aligned} V_{\mathcal{R}_p}^{(2)} &= \mu^* \mu_i h_d^\dagger \tilde{L}_i + B_i h_u \tilde{L}_i + \tilde{m}_{di}^2 h_d^\dagger \tilde{L}_i + \text{h.c.} \\ &= B_i \left(h_u - \tan \beta h_d^\dagger \right) \tilde{L}_i + \text{h.c.}, \end{aligned} \quad (2.36)$$

where $\tan \beta \equiv v_u/v_d$, $B_i = \sum_{\alpha} B_{\alpha} e_{\alpha i}$, and we have used the minimization condition $\tilde{m}_{di}^2 + \mu^* \mu_i + B_i \tan \beta = 0$ to derive the last equality. This condition ensures that the \tilde{L}_i fields only couple to the combination of h_u and h_d that does not acquire a VEV, thus allowing for vanishing v_i 's. Since $\sum_i B_i^2 = B^2 \sin^2 \zeta$, Eq. (2.36) tells us that *the overall amount of physical Higgs-slepton mixing is controlled by the angle ζ* ; in particular, it vanishes if and only if the vacuum expectation values v_α are proportional to the soft parameters B_α , so that $\sin \zeta = 0$. In this case all bilinear soft terms are R -parity conserving in the $v_i = 0$ basis, i.e. $V_{\text{soft}}^{(2)} = (B h_u h_d + \text{h.c.}) + \tilde{m}_d^2 h_d^\dagger h_d + \tilde{m}_u^2 h_u^\dagger h_u + \tilde{m}_{ij}^2 \tilde{L}_i^\dagger \tilde{L}_j + \dots$. Some phenomenological consequences of the Higgs-slepton mixing are discussed at the end of subsection 2.3.4 and later in section 5.5.

In general the vacuum expectation values v_α are neither aligned with the superpotential masses μ_α nor with the soft parameters B_α . This results in a physical Higgs/lepton mixing both in the fermion and in the scalar sectors, characterized by the two misalignment angles ξ and ζ , respectively. The case $\sin \xi = 0$ corresponds to the absence of mixing in the fermion sector: $\mu_i = v_i = 0$ in the same basis, and all effects of bilinear R -parity violation come from the Higgs-slepton mixing, Eq. (2.36). Conversely, the case $\sin \zeta = 0$ corresponds to the absence of mixing in the scalar sector: $B_i = v_i = 0$ in the same basis, and all effects of bilinear R -parity violation come from the higgsino-lepton mixing, Eq. (2.31). Finally, in the case where $\sin \xi = \sin \zeta = 0$, all bilinear \mathcal{R}_p terms can be simultaneously rotated away from the Lagrangian, and R -parity violation is purely of the trilinear type. Again, the statement that $\sin \xi$ or $\sin \zeta$ vanishes is scale-dependent [30, 31].

As we shall discuss in subsection 2.3.3, there are particularly strong constraints on $\sin \xi$ coming from neutrino masses. Therefore, it is legitimate to ask under which circumstances $\sin \xi$ vanishes. To achieve this situation, it is sufficient (but not necessary) to impose the following two conditions on the \mathcal{R}_p soft terms [35]: (i) the B terms are proportional to the μ -terms, $B_\alpha \propto \mu_\alpha$ [24]; (ii) $\vec{\mu}$ is an eigenvector of the scalar mass-squared matrix, $\tilde{m}_{\alpha\beta}^2 \mu_\beta = \tilde{m}_d^2 \mu_\alpha$. Although these relations are not likely to hold exactly at the weak scale, a strong correlation between the soft parameters and the μ_α may result from a flavour symmetry [35] or from some universality assumption at the GUT scale [39, 40], leading to an approximate alignment between the 4-vectors $\vec{\mu}$ and \vec{v} , so that $\sin \xi \ll 1$ (see chapter 3 for more details). Actually conditions (i) and (ii) do not only imply $\sin \xi = 0$, but also $\sin \zeta = 0$; therefore they are sufficient to ensure

the absence of bilinear R -parity violation at the scale at which they are satisfied. Finally, when only condition (i) holds, one has $\sin \xi = \sin \zeta$, hence bilinear R -parity violation is parametrized by a single physical parameter ξ (with $B_i = B \sin \xi \delta_{i3}$ in the basis where $\mu_i = \mu \sin \xi \delta_{i3}$).

2.3.2 Trilinear Couplings Induced by Bilinear \mathcal{R}_p Terms

Let us now comment on an interesting consequence of Eqs. (2.33)–(2.34) in scenarios where, in some particular basis \hat{L}_α , the trilinear \mathcal{R}_p couplings vanish (i.e. $\lambda_{ijk}^e = \lambda_{ijk}^d = 0$, while $\lambda_{0jk}^e = -\lambda_{j0k}^e$ and λ_{0jk}^d are non-vanishing). This is the case, in particular, in the “bilinear” and spontaneous R_p -breaking scenarios. Then, in the (H_d, L_i) basis defined by Eq. (2.30), the trilinear \mathcal{R}_p couplings are related to the ordinary Yukawa couplings λ_{ij}^e and λ_{ij}^d by

$$\lambda_{ijk} = \frac{v_d}{v_0} (e_{0i} \lambda_{jk}^e - e_{0j} \lambda_{ik}^e) , \quad \lambda'_{ijk} = \frac{v_d}{v_0} e_{0i} \lambda_{jk}^d , \quad (2.37)$$

where v_0 and e_{0i} are the $\alpha = 0$ components of the 4-vectors v_α and $e_{\alpha i}$ that define the (H_d, L_i) basis. The flavour dependence of the λ_{ijk} and λ'_{ijk} is then determined by the charged lepton and down quark Yukawa couplings, respectively.

Eq. (2.37) has two obvious consequences. First, unless there is a hierarchy of VEVs $v_0 \ll v_i$ in the initial basis, the trilinear \mathcal{R}_p couplings are at most of the same order of magnitude as the down-type Yukawa couplings. This suppression, which is stronger for smaller values of $\tan \beta$, allows them to evade most of the direct and indirect bounds that shall be discussed in chapters 6 and 7 (some particularly severe bounds require an additional suppression of the rotation parameters e_{0i}). Second, the contributions of the trilinear \mathcal{R}_p couplings (2.37) to flavour-changing neutral current (FCNC) processes either vanish or are strongly suppressed [37]. Indeed, the $\lambda'_{ijk} L_i Q_j D_k^c$ terms read, in the mass eigenstate basis of the quarks (we put a bar on the trilinear \mathcal{R}_p couplings when they are defined in the mass eigenstate basis for fermions):

$$\bar{\lambda}'_{ijk} \left(N_i D_j - E_i V_{jp}^\dagger U_p \right) D_k^c \quad \text{with} \quad \bar{\lambda}'_{ijk} = e_{0i} \frac{\sqrt{2} m_{d_j}}{v_0} \delta_{jk} , \quad (2.38)$$

where V is the CKM matrix. It follows that the λ' couplings induced by bilinear \mathcal{R}_p vanish for quark-flavour-changing transitions $d_j \rightarrow d_k$, while $u_j \rightarrow d_k$ transitions are suppressed by the CKM angles. Thus most of the constraints on λ' couplings due to quark-flavour-violating processes (see chapter 6) are trivially satisfied.

The case of lepton-flavour violation is more subtle, both because the relation between the λ_{ijk} and λ_{ij}^e couplings is not an exact proportionality relation, and because the charged lepton masses are not given by the eigenvalues of the Yukawa matrix, due to the lepton-higgsino mixing (see discussion below). However, for small mixing ($\sin \xi \ll 1$), one can write, in the mass eigenstate basis of the charged leptons:

$$\bar{\lambda}_{ijk} N_i E_j E_k^c \quad \text{with} \quad \bar{\lambda}_{ijk} \simeq \frac{\sqrt{2}}{v_0} \left(R_{Lil}^{e*} e_{0l} m_{e_j} \delta_{jk} - R_{Ljl}^{e*} e_{0l} m_{e_i} \delta_{ik} \right) , \quad (2.39)$$

where the matrix R_L^e rotates the left-handed charged leptons fields to their corresponding mass eigenstates⁸. These couplings violate lepton flavour, but there is a restricted number of them,

⁸Strictly speaking, the couplings $\bar{\lambda}_{ijk}$ are defined in the basis in which the charged lepton Yukawa couplings are diagonal, i.e. R_L^e is defined by $R_L^e \lambda^e R_R^{e\dagger} = \text{Diag}(\lambda_{e_1}, \lambda_{e_2}, \lambda_{e_3})$. However, for $\sin \xi \ll 1$ this basis approximately coincides with the mass eigenstate basis, and therefore $\lambda_{e_i} v_d \simeq \sqrt{2} m_{e_i}$. In the limit $\sin \xi = 0$, both bases coincide and Eq. (2.39) is exact.

since $\bar{\lambda}_{ijk} \neq 0$ only if $i = k$ or $j = k$. Furthermore, the non-vanishing couplings are suppressed by the small lepton Yukawa couplings. This significantly reduces their contributions to lepton-flavour-violating processes, especially in the small $\tan\beta$ case.

The above conclusions hold when the trilinear \mathcal{R}_p couplings vanish in the original \hat{L}_α basis, i.e. $\lambda_{ijk}^e = \lambda_{ijk}^d = 0$. If this is not the case, the physical trilinear \mathcal{R}_p couplings λ_{ijk} and λ'_{ijk} (defined in the (H_d, L_i) basis) receive an additional contribution from the initial λ_{ijk}^e and λ_{ijk}^d couplings, which modifies Eqs. (2.37), (2.38) and (2.39) as well as the resulting conclusions for FCNC processes.

2.3.3 Higgsino-Lepton Mixing

As already mentioned, the main effect of bilinear R -parity violation is a physical mixing between sleptons and Higgs bosons in the scalar sector, and between leptons and neutralinos/charginos in the fermion sector. We do not discuss the details of the mixing in the scalar sector here, and refer the interested reader to the literature (see e.g. Refs. [41, 42, 43, 44, 45]). In the fermion sector, in an arbitrary basis \hat{L}_α , the superpotential mass parameters μ_α mix the fermionic components of the \hat{L}_α and H_u superfields (i.e. the neutrino fields $\hat{\nu}_\alpha$ with the neutral higgsino field \tilde{h}_u^0 , and the charged lepton fields \hat{l}_α^- with the conjugate of the charged higgsino field \tilde{h}_u^+), and the VEVs v_α mix the neutrino fields $\hat{\nu}_\alpha$ with the gaugino associated with the Z gauge boson.

As a result the 4×4 neutralino mass matrix (resp. the 2×2 chargino mass matrix) of the MSSM becomes a 7×7 neutralino-neutrino mass matrix (resp. a 5×5 chargino-charged lepton mass matrix). With the notation $\mathcal{L}_{\text{mass}} = -\frac{1}{2} \psi^{0T} M_N \psi^0 + \text{h.c.}$, the 7×7 neutralino-neutrino mass matrix M_N reads, in the $\psi^0 = (-i\lambda_\gamma, -i\lambda_Z, \tilde{h}_u^0, \hat{\nu}_\alpha)_{\alpha=0\dots3}$ basis⁹ [35]:

$$M_N = \begin{pmatrix} M_1 c_W^2 + M_2 s_W^2 & (M_2 - M_1) s_W c_W & 0 & 0_{1 \times 4} \\ (M_2 - M_1) s_W c_W & M_1 s_W^2 + M_2 c_W^2 & \frac{g}{2c_W} v_u & -\frac{g}{2c_W} v_\alpha \\ 0 & \frac{g}{2c_W} v_u & 0 & -\mu_\alpha \\ 0_{4 \times 1} & -\frac{g}{2c_W} v_\alpha & -\mu_\alpha & 0_{4 \times 4} \end{pmatrix}, \quad (2.40)$$

where M_1 and M_2 are the $U(1)_Y$ and $SU(2)_L$ gaugino masses, g is the $SU(2)_L$ gauge coupling, $c_W = \cos\theta_W$ and $s_W = \sin\theta_W$.

The 5×5 chargino-charged lepton mass matrix, defined by $\mathcal{L}_{\text{mass}} = -\psi^{-T} M_C \psi^+ + \text{h.c.}$, reads, in the $\psi^- = (-i\lambda^-, \hat{l}_\alpha^-)_{\alpha=0\dots3}$ and $\psi^+ = (-i\lambda^+, \tilde{h}_u^+, l_k^c)_{k=1\dots3}$ basis [35]:

$$M_C = \begin{pmatrix} M_2 & gv_u/\sqrt{2} & 0_{1 \times 3} \\ gv_\alpha/\sqrt{2} & \mu_\alpha & \lambda_{\alpha\beta k} v_\beta \end{pmatrix}, \quad (2.41)$$

or, in a more explicit form:

$$M_C = \begin{pmatrix} M_2 & gv_u/\sqrt{2} & 0_{1 \times 3} \\ gv_0/\sqrt{2} & \mu_0 & \lambda_{0\beta k} v_\beta \\ gv_i/\sqrt{2} & \mu_i & \lambda_{i\beta k} v_\beta \end{pmatrix}. \quad (2.42)$$

⁹We use here a two-component notation for spinors. With the conventions of Ref. [25], the two-component spinors λ_γ and λ_Z are related to the four-component Majorana spinors $\tilde{\gamma}$ and \tilde{Z} by $\tilde{\gamma} = (-i\lambda_\gamma, i\bar{\lambda}_\gamma)^T$ and $\tilde{Z} = (-i\lambda_Z, i\bar{\lambda}_Z)^T$. Similarly, the two-component spinors λ^+ and λ^- are related to the Dirac spinor \tilde{W}^+ by $\tilde{W}^+ = (-i\lambda^+, i\bar{\lambda}^-)^T$.

In the R -parity conserving case, it is possible to find a (H_d, L_i) basis in which $\mu_\alpha \equiv (\mu, 0, 0, 0)$ and $v_\alpha \equiv (v_d, 0, 0, 0)$. Then Eqs. (2.40) and (2.41) reduce in the “ino” sector to the well-known (4×4) neutralino and (2×2) chargino mass matrices of the MSSM with R -parity conservation (cf. Eq. (1.10)).

In order to discuss the physical implications of the neutrino-neutralino and charged lepton-chargino mixings caused by bilinear R -parity violation, we now turn to the basis defined by Eqs. (2.29) and (2.31), in which $\mu_\alpha \equiv (\mu \cos \xi, 0, 0, \mu \sin \xi)$ and $v_\alpha \equiv (v_d, 0, 0, 0)$. This choice of basis leaves only a physical mixing in M_N and M_C , proportional to the misalignment parameter $\sin \xi$. The structure of both matrices is schematically:

$$\left(\begin{array}{c|c} \text{MSSM} & \\ \text{neutralino (chargino)} & R_p \text{ terms} \\ \text{mass matrix} & \\ \hline R_p \text{ terms} & \text{neutrino} \\ & \text{(charged lepton)} \\ & \text{mass matrix} \end{array} \right). \quad (2.43)$$

More precisely, M_N reads:

$$M_N = \left(\begin{array}{cc|cc|c} M_1 c_W^2 + M_2 s_W^2 & (M_2 - M_1) s_W c_W & 0 & 0 & 0 \\ (M_2 - M_1) s_W c_W & M_1 s_W^2 + M_2 c_W^2 & M_Z \sin \beta & -M_Z \cos \beta & 0 \\ 0 & M_Z \sin \beta & 0 & -\mu \cos \xi & -\mu \sin \xi \\ 0 & -M_Z \cos \beta & -\mu \cos \xi & 0 & 0 \\ \hline 0 & 0 & -\mu \sin \xi & 0 & 0 \end{array} \right), \quad (2.44)$$

where $\tan \beta \equiv v_u/v_d$. As can also be seen from Eq. (2.31), ν_1 and ν_2 decouple from the tree-level neutrino-neutralino mass matrix, and only the mixing between ν_3 and the neutralinos remains (this is no longer the case at the one-loop level, where all three neutrinos mix with the neutralinos, see chapter 5). As for the chargino-charged lepton mass matrix, it reads:

$$M_C = \left(\begin{array}{cc|c} M_2 & gv_u/\sqrt{2} & 0_{1 \times 3} \\ gv_d/\sqrt{2} & \mu \cos \xi & 0_{1 \times 3} \\ \hline 0_{3 \times 1} & \mu \delta_{i3} \sin \xi & \lambda_{ik}^e v_d/\sqrt{2} \end{array} \right). \quad (2.45)$$

As already mentioned above, the mixing in M_N and M_C , proportional to $\sin \xi$, is suppressed when the VEVs v_α are approximately aligned with the μ_α ; we shall see below that experimental constraints on neutrino masses actually require a strong alignment, i.e. a very small value of $\sin \xi$. The matrix M_C has five mass eigenstates; the three lightest ones are identified with the charged leptons l_i^- (which, due to the higgsino-lepton mixing, do not exactly coincide with the eigenstates of the Yukawa matrix λ_{ik}^e , although this mismatch can be neglected when $\sin \xi \ll 1$), and the two heaviest ones with the charginos $\tilde{\chi}_1^-$ and $\tilde{\chi}_2^-$. In addition to its two massless eigenstates ν_1 and ν_2 , the matrix M_N has five massive eigenstates; the four heaviest ones are the neutralinos $\tilde{\chi}_i^0$, $i = 1 \dots 4$; the lightest one, which is mainly ν_3 in the $\sin \xi \ll 1$ case, can be identified with a Majorana neutrino with a mass [35]

$$m_{\nu_3} = m_0 \tan^2 \xi, \quad (2.46)$$

where m_0 is given, in the case $\sin \xi \ll 1$, by the following expression [39]:

$$m_0 \simeq \frac{M_Z^2 \cos^2 \beta (M_1 c_W^2 + M_2 s_W^2)}{M_1 M_2 \mu \cos \xi - M_Z^2 \sin 2\beta (M_1 c_W^2 + M_2 s_W^2)} \mu \cos \xi. \quad (2.47)$$

For a rough estimate, we can take:

$$m_0 \sim (100 \text{ GeV}) \cos^2 \beta \left(\frac{100 \text{ GeV}}{M_2} \right). \quad (2.48)$$

The exact value of m_0 depends on the gaugino masses, μ and $\tan \beta$, but Eq. (2.48) becomes a good approximation for a heavy supersymmetric spectrum or for large values of $\tan \beta$. Thus we see that the neutrino mass is proportional to the square of the \mathcal{R}_p angle ξ (it could not have been linear in $\tan \xi$, since the neutrino mass term is R -parity even), and therefore roughly measures the overall amount of bilinear R -parity violation in the fermion sector. The other two neutrinos remain massless at tree-level, but acquire masses at the one-loop level (see chapter 5).

Since m_{ν_3} is proportional to $\tan^2 \xi$, with a natural scale in the (1 – 100) GeV range depending on the value of $\tan \beta$, the known experimental and cosmological upper bounds on the heaviest neutrino mass provide strong constraints on bilinear R -parity violation. Indeed, the cosmological bound on neutrino masses inferred from CMB [46] and large scale structure data [47] ($\sum_i m_{\nu_i} \lesssim 1 \text{ eV}$, where the sum runs over all neutrino species) imposes a strong alignment of the v_α with the μ_α , typically¹⁰ $\sin \xi \lesssim 3 \times 10^{-6} \sqrt{1 + \tan^2 \beta}$.

We see that the presence of bilinear \mathcal{R}_p terms can only be tolerated at the expense of some significant amount of tuning in the parameters so as to keep neutrinos sufficiently light. It is important to keep in mind that the values of μ_i and v_i by themselves are not a good measurement of this tuning, since in an arbitrary weak eigenstate basis, large values of the μ_i and v_i can be compatible with a strong alignment. However in the $v_i = 0$ basis (resp. $\mu_i = 0$ basis), the μ_i (resp. v_i) are constrained to be small, according to the estimate $\mu_i \sim \mu \sin \xi$ (resp. $v_i \sim v_d \sin \xi$).

Finally, let us mention the fact that the neutrino sector also constrains the tolerable amount of bilinear R -parity violation in the scalar sector, yielding $\sin \zeta \lesssim (10^{-4} - 10^{-3})$ for the cosmological bound (see section 5.1).

2.3.4 Experimental Signatures of Bilinear R -Parity Violation

The mixing of ordinary leptons with charginos and neutralinos also leads to interactions that are characteristic of bilinear R -parity violation. These are: (i) \mathcal{R}_p gauge interactions, (ii) lepton-flavour-violating Z couplings, and (iii) trilinear \mathcal{R}_p interactions distinct from those generated from the superpotential λ and λ' terms. These interactions are suppressed by at least one power of $\sin \xi$, and are therefore very difficult to observe experimentally, with however a few exceptions. We give a brief description of them below:

- (i) Non-diagonal couplings of the Z and W bosons to a lepton and a supersymmetric fermion (chargino or neutralino) appear when the currents are written in terms of the mass eigenstates: $Z \tilde{\chi}_i^\pm l_j^\mp$, $Z \tilde{\chi}_i^0 \nu_3$, $W^- \tilde{\chi}_i^+ \nu_j$, $W^- \tilde{\chi}_i^0 l_j^+$. These \mathcal{R}_p gauge couplings are proportional to $\sin \xi$, and therefore correlated to the heaviest neutrino mass, m_{ν_3} . They give rise to \mathcal{R}_p processes such as single production of charginos and neutralinos (e.g. through the decays $Z \rightarrow \tilde{\chi}_i^\pm l_j^\mp$ and $Z \rightarrow \tilde{\chi}_i^0 \nu_3$ at LEP) and decays of the lightest neutralino into three standard fermions ($\tilde{\chi}_1^0 \rightarrow \nu_3 f \bar{f}'$ or $\tilde{\chi}_1^0 \rightarrow l_i f \bar{f}'$) or, if it is heavier than the gauge bosons,

¹⁰Some scenarios in which the heaviest neutrino has rapid enough decay modes could in principle evade this bound, but this possibility looks rather unnatural in view of the experimental evidence for neutrino oscillations (see e.g. the discussion at the end of section 2.4).

into $l_i W$ or $\nu_3 Z$. Since the cross-section goes as $\sin^2 \xi$, single production is unobservable in practice. The two-body decays are characteristic of bilinear R -parity violation, while the three-body decays are also induced by the trilinear \mathcal{R}_p couplings (except however for $\tilde{\chi}_1^0 \rightarrow \nu_3 \nu \bar{\nu}$). Studies of the corresponding signals at LEP and at hadron colliders can be found in Refs. [48] and [49, 50], respectively. More recently, the \mathcal{R}_p decays of a neutralino LSP have been discussed in Refs. [50, 51]. See also Ref. [52] for the \mathcal{R}_p decays of a chargino LSP.

- (ii) Together with the previous \mathcal{R}_p gauge interactions, bilinear \mathcal{R}_p also gives rise to flavour-violating couplings of the Z boson to the leptons, $Z l_i^- l_j^+$. These couplings, which contribute to FCNC processes such as $\mu \rightarrow 3e$ [36], are proportional to $\sin^2 \xi$, and their effects are therefore extremely difficult to observe experimentally. In particular, the flavour-violating Z -boson decays $Z \rightarrow l_i^+ l_j^-$ are suppressed by $\sin^4 \xi$, well below the experimental upper limits, $\text{BR}(Z \rightarrow l_i^+ l_j^-) < (10^{-6} - 10^{-5})$ [20].
- (iii) Finally, the couplings of neutralinos and charginos to matter fields give rise, when written in terms of mass eigenstates, to \mathcal{R}_p trilinear interactions proportional to $\sin \xi$ [53]. The ones that originate from down-type higgsino couplings are similar to interactions generated from the superpotential λ and λ' couplings; they are suppressed both by the smallness of the Yukawa couplings and by $\sin \xi$. The ones that originate from up-type higgsino or gaugino couplings, on the other hand, cannot arise from superpotential λ or λ' couplings. Examples of such interactions are $\bar{l}_R d_L \tilde{u}_R^*$ and $\bar{\nu}_R^c u_L \tilde{u}_R^*$.

Since all the above couplings are suppressed by at least one power of $\sin \xi$, which is constrained to be very small by the cosmological bound on neutrino masses, the corresponding experimental signatures are very difficult to observe in practice, with a few exceptions like the decays $\tilde{\chi}_1^0 \rightarrow l_i f \bar{f}'$ when the lightest neutralino $\tilde{\chi}_1^0$ is the LSP.

Finally, bilinear R -parity violation introduces a mixing in the scalar sector between the Higgs bosons and the sleptons, which leads to \mathcal{R}_p decay modes of these scalars, such as $h, H \rightarrow \tilde{\chi}^0 \nu, \chi^+ l^-$ for neutral CP -even Higgs bosons [26, 41, 42], or $\tilde{\tau}_1 \rightarrow l^- \nu, q \bar{q}'$ for the lightest stau [54].

2.4 Spontaneous Breaking of R -Parity

Spontaneous breaking of R -parity has been considered as an interesting alternative to explicit R -parity breaking, because of its predictivity and potentially rich phenomenology. Also, if spontaneous R -parity breaking occurs below a few TeV, the strong cosmological bounds on trilinear \mathcal{R}_p couplings associated with the requirement that \mathcal{R}_p interactions do not erase any primordial baryon asymmetry (see section 4.2.2) can be evaded.

The simplest possibility to break R -parity spontaneously is to give a vacuum expectation value to a sneutrino field [55, 56, 57], e.g. $\langle \tilde{\nu}_\tau \rangle \neq 0$ (i.e. $v_3 \neq 0$ with our previous notations). This may occur since the squared masses of the sneutrinos receive negative contributions both at tree-level from the D -terms and from radiative corrections. Due to the larger third family Yukawa couplings, radiative corrections are expected to generate a VEV for the tau sneutrino only. However, since the conservation of lepton number is associated with a global symmetry, its spontaneous breaking would give rise to a massless Goldstone boson J , called the Majoron [58,

59], together with a scalar ρ having a mass of the order of $\langle \tilde{\nu}_\tau \rangle$. The decay mode¹¹ $Z \rightarrow J \rho$ would then contribute to the invisible decay width of the Z boson like half a neutrino flavour, which is excluded by experimental data. There are several ways out: (i) introduce some amount of explicit lepton number breaking into the MSSM, so as to give to the pseudo-Majoron a mass $m_J > M_Z$ [61]; (ii) enlarge the gauge group to include lepton number, so that the would-be Majoron becomes the longitudinal degree of freedom of a new gauge boson [62]; (iii) break R -parity through the VEV of a right-handed sneutrino, $\langle \tilde{\nu}_\tau^c \rangle \neq 0$, so that the Majoron is mainly an electroweak singlet, and does not contribute sizeably to the Z decay width [63, 64, 65].

Let us illustrate approach (iii) by giving the main features of the model of Ref. [63]. The model contains, beyond the MSSM superfields, the following $SU(2) \times U(1)$ singlets: three right-handed neutrinos N_i^c , three singlets S_i with lepton number $L = 1$, and an additional singlet Φ whose rôle is to generate the μ -term – as in the “NMSSM” (Next to Minimal Supersymmetric Standard Model). The superpotential contains, beyond the quark and charged lepton Yukawa couplings, the following cubic terms [66]:

$$W = h_0 H_u H_d \Phi + \lambda_\Phi \Phi^3 + h_{\nu ij} H_u L_i N_j^c + h_{ij} S_i N_j^c \Phi \quad (2.49)$$

This superpotential preserves both R -parity and total lepton number. R -parity is spontaneously broken provided that the lepton singlets acquire vacuum expectation values (in the following, we restrict ourselves to the one-family case):

$$\langle \tilde{\nu}_{R\tau} \rangle \equiv \frac{v_R}{\sqrt{2}}, \quad \langle \tilde{S}_\tau \rangle \equiv \frac{v_S}{\sqrt{2}}. \quad (2.50)$$

The most general minimum also involves, together with the Higgs VEVs $v_u/\sqrt{2}$ and $v_d/\sqrt{2}$ required to break the electroweak symmetry, a sneutrino VEV $\langle \tilde{\nu}_{L\tau} \rangle \equiv v_L/\sqrt{2}$, assumed to be small. The Majoron J is given by the imaginary part of the linear combination:

$$\frac{1}{\sqrt{v_R^2 + v_S^2}} \left[\frac{v_L^2}{v^2} (v_u h_u - v_d h_d) + v_L \tilde{\nu}_\tau + v_R \tilde{\nu}_\tau^c + v_S \tilde{S}_\tau \right]. \quad (2.51)$$

The most stringent constraint on J comes from astrophysics: in order to avoid a too large stellar energy loss via Majoron emission, one must impose [63] $v_L^2/v_R m_W \lesssim 10^{-7}$, i.e. $v_L \lesssim 100$ MeV for $v_R \sim 1$ TeV. This small value of v_L ensures that J couples only very weakly to the Z boson, and therefore does not affect its invisible decay width. Typical values for a viable R_p -breaking minimum of the scalar potential are 10 GeV $\lesssim v_R, v_S, v_\Phi \lesssim 1$ TeV and $v_L \lesssim (10 - 100)$ MeV. The hierarchy $v_L \ll v_R$ can be understood in terms of small Yukawa couplings, since v_L is found to be proportional to the neutrino Yukawa coupling constants $h_{\nu ij}$.

As can be seen from Eq. (2.49), a nonzero v_R generates effective superpotential bilinear terms, $\mu_i = h_{\nu i3} v_R / \sqrt{2}$. As a result, upon a redefinition of the Higgs superfield H_d , small trilinear couplings λ and λ' are generated with the same flavour structure as in the previous section, and R_p effects are induced in gauge and matter interactions of neutralinos and charginos, as well as in slepton and Higgs decays. The magnitude of these effects is related to the value of the heaviest neutrino mass. However, there is a noticeable difference with the explicit bilinear R -parity breaking discussed in the previous section, due to the presence of the Majoron. This

¹¹Several constraints on $\langle \tilde{\nu}_\tau \rangle$, e.g. the LEP limit on the tau neutrino mass which requires $\langle \tilde{\nu}_\tau \rangle \lesssim 2$ GeV (as can be seen by adapting formulae (2.46) and (2.47) to the case $\mu_i = 0, v_3 \neq 0$), or the even stronger bound $\langle \tilde{\nu}_\tau \rangle \lesssim 100$ keV coming from stellar energy loss through Majoron emission in Compton scattering processes $e\gamma \rightarrow eJ$ [60], ensure that $m_\rho < M_Z$, so that this decay mode is indeed kinematically allowed.

results in new interactions, such as chargino and (invisible) neutralino decays $\tilde{\chi}^\pm \rightarrow \tau^\pm J$ and $\tilde{\chi}^0 \rightarrow \nu_i J$, invisible decay of the lightest Higgs boson $h \rightarrow JJ$ (which may be sizeable [67]), flavour-violating decays of charged leptons $e_i \rightarrow e_j J$, and tau neutrino annihilation $\nu_\tau \nu_\tau \rightarrow JJ$ and decay $\nu_\tau \rightarrow \nu_\mu J$. It has been argued that the latter processes could be large enough to relax the energy density and nucleosynthesis constraints on the tau neutrino mass, and allow it to be as large as the LEP limit of 18.2 MeV [68]. However such a possibility, quite popular at a time where atmospheric neutrino oscillations were not established on a very solid basis, does not look very appealing today since it fails to accommodate both solar and atmospheric neutrino oscillations.

The feasibility of spontaneous \mathcal{R}_p along the lines of Ref. [63] has been investigated by several authors; it has in particular been shown that spontaneous R -parity breaking could be induced radiatively together with electroweak symmetry breaking [66]. Numerous studies of the experimental signatures of spontaneous \mathcal{R}_p can be found in the literature, see e.g. Refs. [67, 69, 70].

2.5 Constraining \mathcal{R}_p Couplings from Flavour Symmetries

The trilinear terms in the \mathcal{R}_p superpotential of Eq. (2.2) are very similar to those associated with the quark and charged lepton Yukawa couplings in Eq. (2.1), known from the pattern of fermion masses and mixing angles to have a rather hierarchical structure. It is conceivable that the mechanism at the origin of this hierarchy also provides a hierarchical structure for \mathcal{R}_p couplings.

A possible simple explanation for the fermion mass hierarchy has been provided long ago by Froggatt and Nielsen, who postulated the existence of a spontaneously broken, flavour-dependent abelian symmetry. In this section, we show that such a symmetry may also naturally generate a flavour hierarchy between \mathcal{R}_p couplings [29, 35, 37, 71, 72, 73, 74]. For the case of a non-abelian flavour symmetry, see e.g. Ref. [75].

Let us first explain how a family-dependent symmetry $U(1)_X$ constrains the Yukawa sector [73, 76]. Consider a Yukawa coupling $H_u Q_i U_j^c$ and let us denote generically the X -charge of a superfield Φ_i by the corresponding small letter ϕ_i . Invariance under $U(1)_X$ implies that $H_u Q_i U_j^c$ appears in the superpotential only if its X -charge vanishes, i.e. $q_i + u_j + h_u = 0$. To account for the large top quark mass, one assumes that this happens only for the Yukawa coupling $H_u Q_3 U_3^c$; thus all fermions but the top quark are massless before the breaking of this symmetry. One further assumes that the flavour symmetry is broken by the VEV of a Standard Model singlet θ with X -charge -1 , and that the other Yukawa couplings are generated from (gauge-invariant) interactions of the form

$$y_{ij}^u H_u Q_i U_j^c \left(\frac{\theta}{M} \right)^{q_i + u_j + h_u}, \quad (2.52)$$

where M is a mass scale, y_{ij}^u is an unconstrained coupling of order one, and $q_i + u_j + h_u > 0$. Such non-renormalizable terms typically appear in the low-energy effective field theory of a fundamental theory with heavy fermions of mass M (one may also think of a string theory, in which case $M \sim M_P$). If $U(1)_X$ is indeed broken below the scale M , $\epsilon = \langle \theta \rangle / M$ is a small parameter, and (2.52) generates an effective Yukawa coupling

$$\lambda_{ij}^u = y_{ij}^u \epsilon^{q_i + u_j + h_u}, \quad (2.53)$$

whose order of magnitude is fixed by the values of the X -charges. Similarly one has, for down quarks and charged leptons:

$$\lambda_{ij}^d \sim \epsilon^{q_i+d_j+h_d}, \quad \lambda_{ij}^e \sim \epsilon^{l_i+e_j+h_d}. \quad (2.54)$$

Such a family-dependent symmetry thus naturally yields a hierarchy between Yukawa couplings, and therefore fermion masses.

For example, the charge assignment $q_1 - q_3 = 3$, $q_2 - q_3 = 2$, $u_1 - u_3 = 5$, $u_2 - u_3 = 2$, $d_1 - d_3 = 1$, $d_2 - d_3 = 0$ yields quark Yukawa matrices of the form:

$$\lambda^u \sim \begin{pmatrix} \epsilon^8 & \epsilon^5 & \epsilon^3 \\ \epsilon^7 & \epsilon^4 & \epsilon^2 \\ \epsilon^5 & \epsilon^2 & 1 \end{pmatrix}, \quad \lambda^d \sim \epsilon^{q_3+d_3+h_d} \begin{pmatrix} \epsilon^4 & \epsilon^3 & \epsilon^3 \\ \epsilon^3 & \epsilon^2 & \epsilon^2 \\ \epsilon & 1 & 1 \end{pmatrix}, \quad (2.55)$$

where the symbol \sim indicates that the entries are known up to factors of order one only. Eq. (2.55) holds at the scale at which the abelian symmetry is spontaneously broken, usually taken to be close to the Planck scale. With renormalisation group effects down to the weak scale taken into account, these Yukawa matrices can accommodate the observed quark masses and mixings if the small number ϵ is of the order of the Cabibbo angle, i.e. $\epsilon \approx V_{us} \simeq 0.22$. More generally, assuming that the X -charge associated with each Yukawa coupling is positive, only a few structures for λ^u and λ^d , which differ from Eq. (2.55) by a ± 1 change in the powers of ϵ , are allowed by the data. In the lepton sector there is more freedom, as long as a mechanism for generating neutrino masses is not specified. The combination of X -charges $q_3 + d_3 + h_d$, related to the value of $\tan \beta$ by $m_t/m_b \sim \tan \beta \epsilon^{-(q_3+d_3+h_d)}$, is actually constrained if one imposes gauge anomaly cancellation conditions.

\mathcal{R}_p couplings are then constrained by $U(1)_X$ exactly as for Yukawa couplings. They are generated from the following non-renormalizable superpotential terms:

$$L_i L_j E_k^c \left(\frac{\theta}{M} \right)^{l_i+l_j+e_k}, \quad L_i Q_j D_k^c \left(\frac{\theta}{M} \right)^{l_i+q_j+d_k}. \quad (2.56)$$

To avoid unnaturally large values of the quark X -charges, we have assumed a baryon parity that forbids the baryon-number-violating superpotential terms $U^c D^c D^c$ as well as the dangerous dimension-5 operators discussed in Section 2.7, thus preventing proton decay. One can see from Eq. (2.56) that abelian flavour symmetries yield a hierarchy between \mathcal{R}_p couplings that mimics (in order of magnitude) the down quark and charged lepton mass hierarchies. Indeed, one has:

$$\lambda_{ijk} \sim \epsilon^{l_i-h_d} \lambda_{jk}^e, \quad \lambda'_{ijk} \sim \epsilon^{l_i-h_d} \lambda_{jk}^d. \quad (2.57)$$

Provided that the Yukawa matrices λ^d and λ^e are known, experimental limits on λ and λ' can be translated into a constraint on $l_i - h_d$. We shall assume here that the X -charge carried by each operator is positive, and take for λ^d the structure of Eq. (2.55). In the lepton sector, the λ_{ij}^e are less constrained; however, it is possible to derive upper bounds on the λ_{ijk} couplings from the three charged lepton masses. Assuming a small value of $\tan \beta$ (corresponding to $q_3 + d_3 + h_d = 3$), one finds that the experimental bounds on coupling products (including the limit coming from ϵ_K , $|\Im(\lambda'_{i12} \lambda_{i21}^*)| \leq 8 \times 10^{-12}$) are satisfied as soon as [77]:

$$l_i - h_d \geq 2 - 3. \quad (2.58)$$

For moderate or large values of $\tan \beta$, larger values of the X -charges would be required.

The condition (2.58) can now be used, together with Eq. (2.57), to derive, in the framework considered, $\tan\beta$ -independent upper bounds on the individual couplings λ and λ' . All of them are well below the experimental limits. Thus, if abelian flavour symmetries are responsible for the observed fermion mass spectrum along the lines discussed above, one expects the first signals for broken R -parity to come from FCNC processes [77]. These conclusions, however, are not completely generic for abelian flavour symmetries: they would be modified if $U(1)_X$ were broken by a vector-like pair of singlets [74], or if we gave up the assumption that the X -charge associated with each operator is positive.

Let us now consider the most general scenario of R -parity violation, with both bilinear and trilinear \mathcal{R}_p couplings (see section 2.3 for the notations used in the following, where we closely follow the discussion of Ref. [37]). Assuming that the bilinear terms are generated through supersymmetry breaking [78] (which ensures that the μ_α are of the order of the weak scale, as required by electroweak symmetry breaking), one finds:

$$\mu_\alpha \sim \tilde{m} \epsilon^{\tilde{l}_\alpha}, \quad v_\alpha \sim v_d \epsilon^{\tilde{l}_\alpha - \tilde{l}_0}, \quad (2.59)$$

where \tilde{m} is the typical mass scale associated with the soft supersymmetry-breaking terms, $\tilde{l}_\alpha \equiv |l_\alpha + h_u|$, and the above estimates are valid for $0 \leq \tilde{l}_0 < \tilde{l}_i$, $i = 1, 2, 3$. Thus the v_α are approximatively aligned along the μ_α by the flavour symmetry [35], which implies (assuming with no loss of generality $\tilde{l}_3 \leq \tilde{l}_{1,2}$):

$$\sin^2 \xi \sim \epsilon^{2(\tilde{l}_3 - \tilde{l}_0)}. \quad (2.60)$$

Furthermore, the redefinition (2.30) is completely fixed by requiring $L_1 \simeq \hat{L}_1$ and $L_2 \simeq \hat{L}_2$, with

$$\frac{v_\alpha}{v_d} \sim \epsilon^{\tilde{l}_\alpha - \tilde{l}_0}, \quad e_{\alpha i} \sim \epsilon^{|\tilde{l}_\alpha - \tilde{l}_i|}. \quad (2.61)$$

Note that $H_d \simeq \hat{L}_0$, which allows us to define $h_d \equiv l_0$.

The low-energy \mathcal{R}_p couplings depend on the signs of the charges $l_\alpha + h_u$. In all phenomenologically viable cases, the order of magnitude relations (2.57) are modified to:

$$\lambda_{ijk} \sim \epsilon^{\tilde{l}_i - \tilde{l}_0} \lambda_{jk}^e, \quad \lambda'_{ijk} \sim \epsilon^{\tilde{l}_i - \tilde{l}_0} \lambda_{jk}^d. \quad (2.62)$$

By combining Eqs. (2.46), (2.60) and (2.62), we can write down a relation between the mass of the tau neutrino, the \mathcal{R}_p couplings λ'_{3jk} and the down quark Yukawa couplings (m_0 is defined in Eq. (2.48)),

$$m_{\nu_3} \sim m_0 \left(\frac{\lambda'_{3jk}}{\lambda_{jk}^d} \right)^2, \quad (2.63)$$

which is a generic prediction of this class of models. Let us stress however that, in Eqs. (2.60) and (2.63), we have assumed that the suppression of the misalignment angle ξ is only due to the abelian flavour symmetry. In this case the cosmological bound on neutrino masses, $m_\nu \leq \mathcal{O}(1 \text{ eV})$, requires very large values of the \tilde{l}_α , so that R -parity violation should be very suppressed and in practice unobservable. This conclusion can be evaded only if some other mechanism provides the required alignment between the v_α and the μ_α , in which case Eqs. (2.60) and (2.63) are no longer valid.

Let us now concentrate on the case $l_i + h_u \geq 0 > l_0 + h_u$, which leads to an enhancement of flavour-diagonal couplings relative to off-diagonal couplings. Indeed, the dominant terms in

Eq. (2.34) correspond to $\alpha = 0$ or $\beta = 0$, which provides an alignment of the \mathcal{R}_p couplings along the Yukawa couplings:

$$\lambda_{ijk} \simeq (e_{0i} \lambda_{jk}^e - e_{0j} \lambda_{ik}^e), \quad \lambda'_{ijk} \simeq e_{0i} \lambda_{jk}^d. \quad (2.64)$$

As a consequence, \mathcal{R}_p couplings are almost diagonal in the basis of fermion mass eigenstates. Furthermore, they undergo an enhancement relative to the naive power counting, since e.g.

$$\lambda'_{ijk} \sim \epsilon^{\tilde{l}_i - \tilde{l}_0} \lambda_{jk}^d \sim \epsilon^{-2\tilde{l}_0} \epsilon^{l_i + q_j + d_k}. \quad (2.65)$$

This opens the phenomenologically interesting possibility that R -parity violation be sizeable while its contribution to FCNC processes is suppressed, as required by experimental data – provided however that the misalignment angle ξ is reduced to phenomenologically acceptable values by some other mechanism than the suppression by large lepton X -charges.

Abelian flavour symmetries can also play a useful rôle in controlling the proton decay rate in supersymmetric theories with unbroken R -parity. Indeed, they can suppress the coefficients of the dangerous dimension-5 operators¹² $QQQL$ and $U^c U^c D^c E^c$ [72, 79], which preserve R -parity but violate baryon number and lepton number, and are expected to be generated from unknown Planck-scale physics (see Section 2.7). Flavour symmetry models that explain the fermion mass hierarchy and are compatible with the experimental lower limit on the proton lifetime generally predict proton decay close to the present experimental sensitivity [29, 79, 80].

2.6 R -Parity Violation in Grand Unified Theories

Up to now we discussed R -Parity Violation in the framework of the Supersymmetric Standard Model (possibly augmented by some flavour symmetries). More sophisticated supersymmetric extensions of the Standard Model may lead to a different structure of \mathcal{R}_p couplings. In particular, nontrivial constraints on the allowed \mathcal{R}_p couplings generally result from an enlarged gauge structure, as in Grand Unified Theories (see e.g. Refs. [24, 39, 81, 23, 82, 83, 84, 85]).

In Grand Unified Theories based on the $SU(5)$ gauge group, all trilinear \mathcal{R}_p superpotential couplings originate, at the renormalizable level, from the same operator [23]

$$\frac{1}{2} \Lambda_{ijk} \bar{\mathbf{5}}_i \bar{\mathbf{5}}_j \mathbf{10}_k, \quad (2.66)$$

antisymmetric under the exchange of $\bar{\mathbf{5}}_i$ and $\bar{\mathbf{5}}_j$, where the antifundamental representation $\bar{\mathbf{5}}_i$ contains the L_i and D_i^c superfields, while the antisymmetric representation $\mathbf{10}_i$ contains the Q_i , U_i^c and E_i^c superfields¹³. As a result, all three types of trilinear \mathcal{R}_p couplings are simultaneously present or absent, and related by

$$\lambda_{ijk} = \frac{1}{2} \lambda'_{ikj} = \lambda''_{kij}, \quad (2.67)$$

¹²Of course, this statement also holds in supersymmetric theories without R -parity [72], but in this case one may find more appealing to invoke a discrete symmetry forbidding baryon number violation from both dimension-4 and dimension-5 operators (see Section 2.7), as we did in the above discussion.

¹³Ordinary quark and charged lepton Yukawa couplings are generated, at the renormalizable level, from the superpotential terms $\Lambda_{ij}^d \mathbf{10}_i \bar{\mathbf{5}}_j \bar{\mathbf{5}}_d + \Lambda_{ij}^u \mathbf{10}_i \mathbf{10}_j \mathbf{5}_u$, where the representations $\bar{\mathbf{5}}_d$ and $\mathbf{5}_u$ contain the doublet Higgs superfields H_d and H_u , respectively. The first term leads to the relation $\lambda_{ij}^d = \lambda_{ji}^e$, which even after taking into account the renormalization effects is in gross contradiction with the measured fermion masses, and must be corrected by terms (renormalizable or not) involving higher-dimensional Higgs representations.

with the resulting antisymmetry of the λ' couplings, $\lambda'_{ijk} = -\lambda'_{kji}$. We are then left with 9 superpotential couplings, as well as the 9 corresponding A -terms satisfying the same relation. Since both λ' and λ'' couplings are simultaneously present, the experimental bound on the proton lifetime severely constrains these couplings, with $|\Lambda_{ij1}|, |\Lambda_{123}| \lesssim 2 \times 10^{-13}$ at M_{GUT} [81], where the constraint on the Λ_{ij1} comes from the familiar $(B - L)$ -conserving operators, while the constraint on Λ_{123} comes from $(B + L)$ -conserving operators generated by diagrams involving a left-right mixing mass insertion of third generation squarks [33]. The other Λ_{ijk} couplings do not induce proton decay at tree level, but can contribute at the one-loop level, and must therefore satisfy $|\Lambda_{ijk}(M_{GUT})| \lesssim 3 \times 10^{-9}$ [81].

However Eq. (2.67) only applies when the $\bar{\mathbf{5}}_i \bar{\mathbf{5}}_j \mathbf{10}_k$ operator arises at the renormalizable level, i.e. when the Λ_{ijk} are field independent. On the contrary when these couplings are induced by VEVs responsible for GUT symmetry breaking, a different pattern for trilinear R -parity breaking can be obtained (see e.g. Ref. [83] for a model leading to λ''_{ijk} couplings only, and Refs. [84, 85] for models leading to λ'_{ijk} couplings only). $SU(5)$ Grand Unified Theories also potentially contain a bilinear \mathcal{R}_p superpotential operator

$$M_i \mathbf{5}_u \bar{\mathbf{5}}_i, \quad (2.68)$$

where $\mathbf{5}_u$ contains both the usual doublet Higgs superfield H_u and a (superheavy) Higgs colour triplet T_u . This yields, together with the usual $H_u L_i$ terms, a baryon-number-violating term $T_u D_i^c$. While the former is a source for λ and λ' couplings, the latter is a source for λ'' couplings, which are the only surviving \mathcal{B} couplings at low energy. However these are small if the ‘‘doublet-triplet splitting problem’’ is solved (with $m_{H_u} \sim M_{weak} \ll m_{T_u} \sim M_{GUT}$) and $M_i \lesssim M_{weak}$ [24]. Then the effective low energy \mathcal{B} couplings are suppressed relative to \mathcal{L} couplings by a typical factor of M_{weak}/M_{GUT} , and one ends up with an approximate conservation of baryon number.

It is natural to ask whether one can avoid the generation of \mathcal{R}_p couplings – without imposing R -parity or any other global symmetry – by considering a unification group larger than $SU(5)$. It is well known that one of the generators of the $SO(10)$ group acts as $B - L$ on the Supersymmetric Standard Model fields, with the matter superfields embedded into the spinorial representation $\mathbf{16}_i$ (which decomposes under $SU(5)$ as $\mathbf{16}_i = \mathbf{10}_i \oplus \bar{\mathbf{5}}_i \oplus \mathbf{1}_i$, where $\mathbf{1}_i$ corresponds to a right-handed neutrino), and the Higgs doublet superfields embedded into the representation $\mathbf{10} = \mathbf{5} \oplus \bar{\mathbf{5}}$. Since R -parity can be rewritten as $(-)^{2S+3(B-L)}$, it follows that \mathcal{R}_p operators are forbidden by the $SO(10)$ gauge symmetry (at least as long as it is unbroken). For instance, with the above field content, the only cubic operator compatible with the $SO(10)$ gauge symmetry takes the form $\mathbf{10} \mathbf{16} \mathbf{16}$ and preserves R -parity.

Still the process of gauge symmetry breaking down to $SU(3)_C \times SU(2)_L \times U(1)_Y$ may lead to a theory that does not conserve R -parity. The question of whether R -parity remains exact or not and of what types of \mathcal{R}_p couplings are generated crucially depends on the breaking scheme (for a discussion, see e.g. [86]). If the $B - L$ symmetry is spontaneously broken by the VEV of (the right-handed neutrino-like component of) a Higgs boson in the spinorial representation $\mathbf{16}_H$, then R -parity gets broken in the low-energy effective theory. More precisely, the renormalizable operator

$$\mathbf{10}_u \mathbf{16}_H \mathbf{16}_i, \quad (2.69)$$

gives rise, through $\langle \mathbf{16}_H \rangle \neq 0$, to both baryon number and lepton-number-violating bilinear terms, contained in the $SU(5)$ \mathcal{R}_p operator $\mathbf{5}_u \bar{\mathbf{5}}_i$. These are especially dangerous since

$\langle \mathbf{16}_H \rangle$ is generally much larger than M_{weak} . Trilinear \mathcal{R}_p couplings are generated from higher-dimensional operators like

$$\mathbf{16}_i \mathbf{16}_j \mathbf{16}_k \mathbf{16}_H . \quad (2.70)$$

If present, these operators generate trilinear \mathcal{R}_p couplings λ , λ' and λ'' satisfying the $SU(5)$ relations (2.67). Alternatively, the $B - L$ symmetry can be broken by the VEV of a Higgs boson in the $\mathbf{126}$ representation. In this case the selection rule $\Delta(B - L) = 2$ holds, and R -parity is automatically conserved.

The breaking of $SO(10)$ into an intermediate $SU(5)$ requires a $\mathbf{16}_H$, while if $SO(10)$ first breaks into a left-right symmetric gauge group $SU(4)_C \times SU(2)_L \times SU(2)_R$ or $SU(3)_C \times SU(2)_L \times SU(2)_R \times U(1)_{B-L}$, the breaking of the $B - L$ gauge symmetry involves either a $\mathbf{16}_H$ or a $\mathbf{126}_H$. (Actually supersymmetry demands a vector-like pair of Higgs representations, e.g. $\mathbf{16}_H \oplus \overline{\mathbf{16}}_H$.) We conclude that the $SO(10)$ breaking chain with an intermediate $SU(5)$ gauge symmetry, or with an intermediate left-right symmetry spontaneously broken by a $\mathbf{16}_H$, leads to unacceptably large \mathcal{R}_p couplings, unless the dangerous operators (2.69) and (2.70) are forbidden by some symmetry or strongly suppressed by some mechanism.

2.7 Restrictions on R -Parity Violations from Generalized Matter, Baryon or Lepton Parities

As already alluded to before in this chapter, there exist discrete symmetries that can protect proton decay from renormalizable operators as efficiently as R -parity, while allowing for some \mathcal{R}_p couplings. Such symmetries therefore provide viable patterns of R -parity violations, and it is useful to classify them, as we do in this section, following the discussion of Ref. [87].

Let us first note that R -parity actually does not forbid all dangerous baryon-number- and lepton-number-violating couplings. Indeed, it is highly probable that the Supersymmetric Standard Model is just an effective theory, to be embedded in a more fundamental theory including quantum gravity at some high energy scale Λ . Gauge-invariant, higher-dimensional non-renormalizable operators are then generated in the low-energy theory by integrating out massive particles. In particular the effective superpotential is expected to contain the following quartic terms:

$$\begin{aligned} W_{n.r.} \ni & \frac{(\kappa_1)_{ijkl}}{\Lambda} (Q_i Q_j) (Q_k L_l) + \frac{(\kappa_2)_{ijkl}}{\Lambda} (U_i^c U_j^c D_k^c) E_l^c + \frac{(\kappa_3)_{ijk}}{\Lambda} (Q_i Q_j) (Q_k H_d) \\ & + \frac{(\kappa_4)_{ijk}}{\Lambda} (Q_i H_d) (U_j^c E_k^c) + \frac{(\kappa_5)_{ij}}{\Lambda} (L_i H_u) (L_j H_u) + \frac{(\kappa_6)_i}{\Lambda} (L_i H_u) (H_d H_u) , \end{aligned} \quad (2.71)$$

where Λ can be viewed as parametrizing the scale of new physics (e.g. the string scale, the Planck scale or the GUT scale) beyond the Supersymmetric Standard Model. Other non-renormalizable \mathcal{B} and \mathcal{L} operators can be present in the Kähler potential K , the function that defines the matter kinetic terms in a non-renormalizable supersymmetric theory (for example, the kinetic terms for complex scalar fields ϕ_i read $\mathcal{L}_{kin} = (\partial^2 K / \partial \phi_i \partial \bar{\phi}_j) \partial_\mu \phi_i \partial^\mu \bar{\phi}_j$) [87, 88]:

$$\begin{aligned} K_{n.r.} \ni & \frac{(\kappa_7)_{ijk}}{\Lambda} (Q_i Q_j) D_k^{c\dagger} + \frac{(\kappa_8)_i}{\Lambda} (H_u^\dagger H_d) E_i^c \\ & + \frac{(\kappa_9)_{ijk}}{\Lambda} (Q_i L_j^\dagger) U_k^c + \frac{(\kappa_{10})_{ijk}}{\Lambda} (U_i^c D_j^{c\dagger}) E_k^c , \end{aligned} \quad (2.72)$$

where we have kept only the trilinear terms, which correspond to dimension-5 operators in the Lagrangian density.

In Eqs. (2.71) and (2.72), we assumed the particle content of the MSSM; other versions of the Supersymmetric Standard Model may allow for additional terms. It is easy to see that the operators parametrized by κ_1 , κ_2 and κ_5 , while compatible with R -parity, still violate the baryon number and lepton number symmetries. The operator LH_uLH_u generates Majorana masses for the neutrinos; as long as $\Lambda \gtrsim 5 \times 10^{13}$ GeV, its contribution is compatible with the experimental constraints on neutrino masses, and the $(\kappa_5)_{ij}$ are not required to be small. The operators $QQQL$ and $U^cU^cD^cE^c$, on the other hand, induce proton decay and their coefficients κ_1 and κ_2 are therefore constrained to be small, even if the cutoff scale Λ is taken to be as large as the Planck mass (i.e. $\Lambda \sim 10^{19}$ GeV). In particular, $(\kappa_1)_{112l} \leq \mathcal{O}(10^{-7})$ for typical superpartner masses in the TeV range. Other operators in Eqs. (2.71) and (2.72) induce proton decay in conjunction with the dimension-4 \mathcal{R}_p operators of Eq. (2.2), implying severe bounds on the products $\kappa_4\lambda''$, $\kappa_9\lambda''$ and $\kappa_{10}\lambda''$. This provides an additional motivation for searching for discrete symmetries protecting proton decay from renormalizable operators, while allowing for some of the \mathcal{R}_p terms in Eq. (2.2). Some of these symmetries will eventually turn out to be more efficient than R -parity in forbidding the dangerous \mathcal{B} and \mathcal{L} nonrenormalizable operators in Eqs. (2.71) and (2.72).

We are interested in discrete symmetries of the R -parity conserving superpotential of Eq. (2.1) (i.e. symmetries compatible with the presence of the μ -term and of quark and lepton Yukawa couplings) protecting proton decay from renormalizable operators. These symmetries, which are either commuting with supersymmetry or R -symmetries also acting on the supersymmetry generator, can be divided into three general classes [87]:

i) *Generalized matter (R -)parities (GMP)* : discrete (R -)symmetries protecting both baryon and lepton number from dimension-4 operators, i.e. enforcing $\lambda = \lambda' = \lambda'' = 0$;

ii) *Generalized baryon (R -)parities (GBP)* : discrete (R -)symmetries protecting baryon number from dimension-4 operators and allowing for lepton-number violations, i.e. enforcing $\lambda'' = 0$;

iii) *Generalized lepton (R -)parities (GLP)* : discrete (R -) symmetries protecting lepton number from dimension-4 operators and allowing for baryon-number violations, i.e. enforcing $\lambda = \lambda' = 0$.

For simplicity, we restrict our discussion to flavour-blind symmetries (the case of flavour-dependent symmetries has been illustrated in section 2.5), and we assume the particle content of the MSSM. To start with, let us consider discrete Z_N symmetries commuting with supersymmetry, which act on the chiral superfields as ($k = 0 \cdots N - 1$):

$$\begin{aligned} Q &\rightarrow e^{2k\pi i q/N} Q \quad , \quad U^c \rightarrow e^{2k\pi i u/N} U^c \quad , \quad D^c \rightarrow e^{2k\pi i d/N} D^c \quad , \\ L &\rightarrow e^{2k\pi i l/N} L \quad , \quad E^c \rightarrow e^{2k\pi i e/N} E^c \quad , \quad H_{u,d} \rightarrow e^{2k\pi i h_{u,d}/N} H_{u,d} \quad , \end{aligned} \quad (2.73)$$

where q, \dots, h_d, h_u denote here the Z_N charges of the MSSM superfields, defined modulo N . Restricting the scan to Z_2 and Z_3 symmetries, one finds the generalized parities listed in Table 2.1 [87].

The Z_2 GMP (Z_2^M) is actually equivalent, after a weak hypercharge rotation, to a symmetry X acting on MSSM superfields as $X(Q_i, U_i^c, D_i^c, L_i, E_i^c) = -(Q_i, U_i^c, D_i^c, L_i, E_i^c)$, $X(H_d, H_u) = +(H_d, H_u)$. This symmetry is identical to the matter parity symmetry already considered in

Generalized parities	q	u	d	l	e	h_d	h_u
Z_2^M, Z_3^M	0	-1	1	0	1	-1	1
Z_3^M	0	-1	1	1	0	-1	1
Z_2^L, Z_3^L	0	0	0	-1	1	0	0
Z_2^B	0	-1	1	-1	0	-1	1
Z_3^B	0	-1	1	-1	-1	-1	1

Table 2.1: Matter, lepton and baryon generalized parities in the MSSM. Superscript indices distinguish between matter (M), baryon (B) and lepton (L) generalized parities. The letters q, u, d, \dots denote the Z_N charges referring to the action of the generalized parities as expressed in Eq. (2.73).

chapter 1, and is therefore equivalent to R -parity. Contrary to the other generalized parities listed in Table 2.1, the Z_2 and Z_3 GBP's do not forbid the bilinear lepton number violating operators $L_i H_u$. Some of the symmetries listed in Table 2.1 are actually not better than R -parity in forbidding the dangerous non-renormalizable dimension-5 operators in Eqs. (2.71) and (2.72). Indeed, the first two GMP's (including the usual matter parity) allow for such terms.

A similar analysis can be done for discrete R -symmetries, i.e. discrete versions of the continuous R -symmetries discussed in chapter 1. Since R -symmetries do not commute with supersymmetry, the transformations (2.73) must be supplemented with a corresponding action on Grassmann variables θ , which defines also the total charge of the superpotential (see Eq. (1.12)),

$$W(x, \theta) \rightarrow e^{-2k\pi i/N} W(x, e^{k\pi i/N} \theta). \quad (2.74)$$

Scanning over all flavour-blind Z_2 and Z_3 discrete R -symmetries, one finds the generalized R -parities [87] listed in Table 2.2. Like the generalized parities of Table 2.1, the generalized R -parities do not necessarily forbid all dangerous dimension-5 operators. Actually only one generalized matter R -parity satisfies the requirement of forbidding all operators in Eqs. (2.71) and (2.72) but $LH_u LH_u$, the second Z_3^M symmetry listed in Table 2.2. The baryon and lepton R -parities listed in Table 2.2 are at this stage all safe, since they forbid at least one dangerous coupling appearing in experimentally constrained products of couplings.

One may wonder whether the discrete symmetries considered above are likely to be exact at low energy. Indeed, any global symmetry, continuous or discrete, might be broken by quantum gravity effects. Even if this happens only at the Planck scale, as noticed above, the strong constraints coming from proton decay rule out the corresponding symmetry [89]. It is however well known that a discrete symmetry originating from the spontaneous breaking of some continuous gauge symmetry is protected against quantum-gravity violations. The original gauge quantum numbers are of course very constrained by cancellation of triangle gauge anomalies, as well as by mixed gauge-gravitational anomalies. As noticed in [87, 90], there are remnants of these conditions, called ‘‘discrete gauge anomaly cancellation conditions’’ in the low-energy theory after spontaneous symmetry breaking. Discrete symmetries that respect these conditions are therefore safe with respect to anomalies. Among the generalized parities of Table 2.1, only two are discrete anomaly free in the MSSM, namely the standard Z_2 matter parity (Z_2^M), actually equivalent to R -parity, and the Z_3 generalized baryon parity (Z_3^B). If in addition we require the absence of the dimension-5 operators of Eqs. (2.71) and (2.72), we are left with the Z_3 generalized baryon parity only, a remarkable degree of uniqueness.

Let us finally note that the standard matter parity X could also originate from a spontaneously broken anomalous $U(1)_X$ gauge symmetry under which all matter superfields have charge one

Generalized R -parities	q	u	d	l	e	h_d	h_u
Z_2^M	0	0	1	1	0	0	1
Z_3^M	0	0	-1	-1	0	0	-1
Z_3^M	0	1	1	0	1	1	1
Z_3^M	0	1	1	-1	-1	1	1
Z_2^L	0	-1	0	0	0	-1	0
Z_3^L	0	-1	0	1	-1	-1	0
Z_3^L	0	-1	0	0	0	-1	0
Z_2^B	0	0	1	0	1	0	1
Z_3^B	0	1	1	1	0	1	1
Z_3^B	0	0	-1	0	-1	0	-1

Table 2.2: Matter, lepton and baryon generalized R -parities in the MSSM. Superscript indices distinguish between matter (M), baryon (B) and lepton (L) generalized R -parities. The letters q, u, d, \dots denote the Z_N charges referring to the action of the generalized R -parities as expressed in Eq. (2.73).

and the two Higgs superfields have charge zero (however the Yukawa couplings are not invariant under this symmetry, and should therefore be generated by a Froggatt-Nielsen mechanism, as in section 2.5). Indeed, compactifications of the heterotic string often contain a seemingly anomalous abelian gauge symmetry, whose mixed gauge anomalies are compensated for by the Green-Schwarz mechanism [91]. For this mechanism to work, the following condition must be satisfied: $A'g'^2 = Ag^2 = A_3g_3^2$, where A', A, A_3 are the coefficients of the mixed gauge anomalies $[U(1)_Y]^2U(1)_X$, $[SU(2)_L]^2U(1)_X$ and $[SU(3)_C]^2U(1)_X$, and g', g, g_3 are the coupling constants of the gauge groups $U(1)_Y$, $SU(2)_L$ and $SU(3)_C$. This condition can be understood as a relation determining the relative normalization of the generators associated with different gauge groups in terms of the anomaly coefficients. Now the above charge assignment yields $A_3 = A = -12$ and $A' = -20$, implying $g'^2/g^2 = A/A' = 3/5$ (or simply $g_1 = g = g_3$ with $g_1 = \sqrt{5/3}g'$) and therefore [92]

$$\sin^2 \theta_W = \frac{g'^2}{g'^2 + g^2} = \frac{3}{8}, \quad (2.75)$$

a relation known to be successful at the grand unification scale. We conclude that a gauge continuous version of the standard matter parity discussed in chapter 1, which is equivalent to the Z_2 matter parity of Table 2.1 and has the same effect as R -parity, may be a good string symmetry. This provides a further motivation for R -parity conservation. Still the arguments developed earlier in this section as well as in section 2.5 motivate possible violations of the R -parity symmetry, with a hierarchy of \mathcal{R}_p couplings that could make them well compatible with experimental data.

In this chapter, we studied from a theoretical point of view the possible violations of the R -parity symmetry introduced in chapter 1 in connection with baryon and lepton-number conservation. We first gave the most general form of the \mathcal{R}_p terms that may be present in the superpotential and in the soft supersymmetry-breaking scalar potential, and addressed issues associated with the choice of a basis for the Higgs and lepton superfields H_d and L_i , in the presence of bilinear R -parity violation.

Then we classified the patterns of R -parity breaking that are consistent at the quantum level, according to which types of \mathcal{R}_p terms are present in the Lagrangian density. We also discussed three scenarios of R -parity violation often considered in the literature, namely explicit \mathcal{R}_p by trilinear terms, explicit \mathcal{R}_p by bilinear terms and spontaneous R -parity breaking. We then discussed the effects of the Higgs-lepton mixing associated with the presence of bilinear \mathcal{R}_p terms, which leads to a potentially very large (order M_Z) neutrino mass and to specific \mathcal{R}_p signatures at colliders. To suppress the neutrino mass to a phenomenologically acceptable value, either a strong fine-tuning of bilinear \mathcal{R}_p parameters or an “alignment” mechanism is required. We also presented a scenario of spontaneous R -parity breaking involving a singlet Majoron, thus avoiding conflict with the measured invisible decay width of the Z boson.

Finally, we discussed possible microscopic origins for terms violating lepton and baryon numbers. We focussed essentially on abelian flavour symmetries, Grand Unified gauge symmetries and discrete symmetries generalizing R -parity. The latter appear for example in string theories. The phenomenological constraints on the lepton- and baryon-number violations, which are crucial tests of any extension of the Standard Model, become therefore a window into the structure of the underlying high energy theory.

Chapter 3

RENORMALIZATION GROUP SCALE EVOLUTION OF \mathcal{R}_p COUPLINGS

One of the most interesting indications for supersymmetry is the unification of gauge couplings at a high scale, obtained by renormalization group evolution of the measurements done by LEP at the “low” scale of M_Z [93]. The renormalization group allows one to evolve couplings and mass parameters between two energy scales, thus providing a way to test at the available energies physical assumptions postulated at a higher scale, or vice-versa to translate available experimental data into quantities at high energy.

In this chapter, we shall focus on the renormalization group evolution of constraints for the \mathcal{R}_p interactions and cover in particular those associated with the perturbative unitarity or the so-called “triviality bounds”, the infrared fixed points and the tests of grand unification schemes. The rôle of supersymmetry-breaking effects will also be discussed. In the limit of unbroken supersymmetry the bilinear \mathcal{R}_p interactions can be recast only in terms of the μ -term by a suitable redefinition of the four superfields $\hat{L}_\alpha \equiv (H_d, L_1, L_2, L_3)$, therefore R -parity violation can be parametrized by trilinear couplings only. In the presence of soft terms, as explained in chapter 2, the superpotential and the scalar potential contain two independent sources of bilinear R -parity violation which, in general, cannot be simultaneously rotated away by field redefinitions. In turn, the Higgs-lepton mixing due to bilinear R -parity violation leaves an arbitrariness in the choice of the \hat{L}_α basis. It is therefore crucial, when dealing with numerical results, to specify the choice of basis. A detailed discussion is given in section 2.3.1. In the following we shall keep the discussion general, and, when referring to numerical results, the reader will be guided to cited papers for the choice of basis and detailed assumptions.

Our discussion of renormalization group studies in presence of \mathcal{R}_p will mostly concern the so-called supergravity framework. In this framework, the soft supersymmetry-breaking terms are supposed to be generated through gravity in the limit in which the gravitational coupling constant ($\kappa = \sqrt{8\pi G_N}$) is taken to be small. Since this is closely tied with a grand unified theory approach, one is led to consider the scale evolution of parameters up to large energy scales of the order of the grand unification scale M_X (or the compactified string theory scale M_C , or the Planck scale M_P). Conversely to this bottom-up type scale evolution, one may also envisage a top-down type scale evolution, by assigning boundary condition values for the (fewer in number) unified parameters at the large scale and using the renormalization group equations (RGEs) to evolve the entire set of Minimal Supersymmetric Standard Model parameters values down to the electroweak symmetry breaking mass scale.

3.1 Renormalization Group Equations

As remarked in chapter 2, in the absence of R -parity and lepton-number conservation laws, there is no *a priori* distinction between the H_d Higgs and L_i lepton superfields, as they have the same gauge quantum numbers. Only after electroweak symmetry breaking, the mass eigenstate basis defines which combinations of the H_d and L_i component fields correspond to the physical leptons and sleptons. The magnitude of \hat{R}_p couplings depends in particular on which direction in the space of weak doublet superfields with weak hypercharge -1 ultimately corresponds to the Higgs. One possible strategy consists in constructing combinations of coupling constants that are invariant under these basis redefinitions [26, 27, 28], and parametrize the \hat{R}_p content of the Lagrangian density in a way similar to the Jarlskog invariants for CP violations [94].

In order to express the superpotential and the renormalization group equations (RGEs) in a compact way, we rewrite Eqs. (2.1) and (2.2) of section 2.1.1 in the form of Eq. (2.27):

$$W_{R_p} + W_{\hat{R}_p} = \mu_\alpha H_u \hat{L}_\alpha + \frac{1}{2} \lambda_{\alpha\beta k}^e \hat{L}_\alpha \hat{L}_\beta E_k^c + \lambda_{\alpha j k}^d \hat{L}_\alpha Q_j D_k^c + \lambda'' \text{ and } \lambda_{ij}^u \text{ terms,} \quad (3.1)$$

where $\alpha \equiv (0, i) = (0, 1, 2, 3)$, $\beta \equiv (0, j) = (0, 1, 2, 3)$. Here we use the following notation:

$$H_d \equiv \hat{L}_0, \quad \mu \equiv \mu_0, \quad (3.2)$$

$$\lambda_{0jk}^e \equiv \lambda_{jk}^e, \quad \lambda_{0jk}^d \equiv \lambda_{jk}^d. \quad (3.3)$$

This allows us to write the $SU(4)$ transformation of Eq. (2.17) and following equations as:

$$\hat{L}_\alpha \rightarrow U_{\alpha\beta} \hat{L}_\beta, \quad (3.4)$$

$$\mu_\alpha \rightarrow U_{\alpha\beta}^* \mu_\beta, \quad (3.5)$$

$$\lambda_{\alpha\beta k}^e \rightarrow U_{\alpha\gamma}^* U_{\beta\delta}^* \lambda_{\gamma\delta k}^e, \quad (3.6)$$

$$\lambda_{\alpha j k}^d \rightarrow U_{\alpha\beta}^* \lambda_{\beta j k}^d, \quad (3.7)$$

where U is the $SU(4)$ matrix with entries $U_{\alpha\beta}$ associated with the basis rotation. It is clear from the above equations that the lepton-number-violating couplings are basis-dependent. For a detailed discussion see chapter 2.

In the following, explicit expressions for the \hat{R}_p RGEs up to the two loop order will be written using the above notations. To facilitate a comparison with the existing literature we give in Table 3.1 the correspondence between our notations and the ones of [95].

3.1.1 Evolution of the Bilinear μ Terms

Following the general equations given in [96] the RGEs for the bilinear μ terms including all \hat{R}_p effects can be written as:

$$\frac{d}{dt} \mu_\alpha = \mu_\alpha \Gamma_{uu} + \mu_\beta \Gamma_{\alpha\beta}, \quad (3.8)$$

where $t = \log q^2$ and Γ are the anomalous dimensions. The index α is defined as in the previous section ($\alpha \equiv (0, i)$). The notation Γ_{uu} is a shorthand for the anomalous dimension $\Gamma_{H_u H_u}$ for

Our Notation	Notation of [95]
H_d	H_1
H_u	H_2
λ_{ijk}^e	$(\Lambda_{E^k})_{ij}$
$\lambda_{jk}^e \equiv \lambda_{0jk}^e$	$-(Y_E)_{jk}$
λ_{ijk}^d	$(\Lambda_{D^k})_{ij}$
$\lambda_{jk}^d \equiv \lambda_{0jk}^d$	$-(Y_D)_{jk}$
λ_{ijk}''	$(\Lambda_{U^k})_{ij}$
λ_{jk}^u	$(Y_U)_{jk}$

Table 3.1: Correspondence among our notation and the one of [95].

the H_u superfield. In a similar way Γ_{00} stands for $\Gamma_{H_d H_d}$ and Γ_{ij} means $\Gamma_{L_i L_j}$. Expanding Eq. (3.8) into its components one obtains

$$\frac{d}{dt}\mu_0 = \mu_0 \Gamma_{uu} + \mu_0 \Gamma_{00} + \mu_i \Gamma_{0i}, \quad (3.9)$$

$$\frac{d}{dt}\mu_i = \mu_i \Gamma_{uu} + \mu_0 \Gamma_{i0} + \mu_j \Gamma_{ij}. \quad (3.10)$$

This set of equations implies that even if we start with all $\mu_i = 0$, non-zero μ_i will be generated through the RGEs via a non-zero μ_0 and vice-versa.

The bilinear terms do not appear in the equations for the evolution of the Yukawa couplings or the gauge couplings. Thus, they do not directly affect the unification of the latter. The anomalous dimensions Γ transform as follows under the $SU(4)$ rotation of the fields:

$$\Gamma_{uu} \rightarrow \Gamma_{uu}, \quad (3.11)$$

$$\Gamma_{\alpha\beta} \rightarrow U_{\beta\gamma} U_{\alpha\tau}^* \Gamma_{\tau\gamma}. \quad (3.12)$$

The anomalous dimensions are given by

$$\Gamma_{ij} = \frac{1}{16\pi^2} \gamma_{ij}^{(1)} + \frac{1}{(16\pi^2)^2} \gamma_{ij}^{(2)} + \dots \quad (3.13)$$

where $\gamma^{(1)}, \gamma^{(2)}, \dots$ are 1-loop, 2-loop, ... contributions:

$$\gamma_{ij}^{(1)} = \frac{1}{2} Y_{imn} Y_{jmn}^* - 2 \delta_{ij} \sum_a g_a^2 C_a(i), \quad (3.14)$$

$$\begin{aligned} \gamma_{ij}^{(2)} = & -\frac{1}{2} Y_{imn} Y_{npq}^* Y_{pqr} Y_{mrj}^* + Y_{imn} Y_{jmn}^* \sum_a g_a^2 [2C_a(p) - C_a(i)] \\ & + 2 \delta_{ij} \sum_a g_a^2 \left[g_a^2 C_a(i) S_a(R) + 2 \sum_b g_b^2 C_a(i) C_b(i) - 3g_a^2 C_a(i) C(G_a) \right]. \end{aligned} \quad (3.15)$$

Y_{ijk} is a generic Yukawa coupling (it stands for λ^e , λ^d or λ''), $C_a(f)$ is the quadratic Casimir of the representation f of the gauge group G_a . $C(G)$ is an invariant of the adjoint representation of the gauge group G and $S_a(R)$ is the second invariant of the representation R in the gauge group G_a . Explicitly if t^A are the representation matrices of a group G one has:

$$(t^A t^A)_{ij} = C(R) \delta_{ij}, \quad (3.16)$$

for $SU(3)$ triplets Q and $SU(2)$ doublets L :

$$C_{SU(3)}(Q) = \frac{4}{3}, \quad C_{SU(2)}(L) = \frac{3}{4}, \quad (3.17)$$

and for the $U(1)$ weak hypercharge embedded in $SU(5)$:

$$C(\phi) = \frac{3}{5}y^2(\phi), \quad (3.18)$$

where $y(\phi)$ is the weak hypercharge of the field ϕ . The factor $3/5$ comes from the $SU(5)$ grand unified normalisation of the weak hypercharge generator. For the adjoint representation:

$$C(G) \delta^{AB} = f^{ACD} f^{BCD}, \quad (3.19)$$

where f^{ABC} are the structure constants. For the groups under study:

$$C(SU(3)_C) = 3, \quad C(SU(2)_L) = 2, \quad C(U(1)_Y) = 0, \quad C(SU(N)) = N. \quad (3.20)$$

The Dynkin index is defined by

$$\text{Tr}_R(t^A t^B) = S(R) \delta^{AB}. \quad (3.21)$$

For the fundamental representations f we have

$$SU(3), SU(2) \rightarrow S(f) = \frac{1}{2}, \quad (3.22)$$

$$U(1)_Y \rightarrow S(f) = \frac{3}{5}y^2(f). \quad (3.23)$$

3.1.2 Evolution of the Trilinear \mathcal{R}_p Yukawa Couplings

As already stated in chapter 2, scenarios in which R -parity is broken only by trilinear interaction terms are in general not consistent since bilinear \mathcal{R}_p terms are generated by quantum corrections and cannot be rotated away through a $SU(4)$ redefinition of the superfields, due to the presence of soft supersymmetry-breaking terms. One has therefore to consider all the couplings when studying the renormalization group evolution. The general RGEs for the Yukawa couplings Y_{ijk} (where Y stands for $\lambda_{\alpha\beta k}^e$, or $\lambda_{\alpha j k}^d$, $\lambda_{i k}^u$ or $\lambda''_{i j k}$ of Eq. (3.1)) are given by [96]:

$$\frac{d}{dt}Y_{ijk} = Y_{ijl} \Gamma_{lk} + (k \leftrightarrow j) + (k \leftrightarrow i). \quad (3.24)$$

For the Yukawa couplings $\lambda_{\alpha\beta k}^e$ and $\lambda_{\alpha j k}^d$ this gives

$$\frac{d}{dt}\lambda_{\alpha\beta k}^e = \lambda_{\alpha\beta l}^e \Gamma_{E_l E_k} + \lambda_{\alpha\delta k}^e \Gamma_{\delta\beta} + \lambda_{\gamma\beta k}^e \Gamma_{\gamma\alpha}, \quad (3.25)$$

$$\frac{d}{dt}\lambda_{\alpha j k}^d = \lambda_{\alpha j l}^d \Gamma_{D_l D_k} + \lambda_{\alpha l k}^d \Gamma_{Q_l Q_j} + \lambda_{\gamma j k}^d \Gamma_{\gamma\alpha}, \quad (3.26)$$

while for the Yukawa couplings $\lambda''_{i j k}$ and $\lambda_{i k}^u$ we have

$$\frac{d}{dt}\lambda_{i j}^u = \lambda_{i k}^u \Gamma_{U_j U_k} + \lambda_{i j}^u \Gamma_{uu} + \lambda_{k j}^u \Gamma_{Q_i Q_k}, \quad (3.27)$$

$$\frac{d}{dt}\lambda''_{i j k} = \lambda''_{i l k} \Gamma_{D_j D_l} + \lambda''_{l j k} \Gamma_{U_i U_l} + \lambda''_{i j l} \Gamma_{D_k D_l}. \quad (3.28)$$

Of course the two-loop RGEs for the Yukawa couplings preserve $\lambda''_{ijk} = 0$ (for all i, j, k) at all scales if they are zero at some scale (i.e. baryon parity is conserved). The same is true if lepton parity is imposed at some scale for λ_{ijk}^e and λ_{ijk}^d . If however one imposes only one coupling to be non-zero at some scale, this remains in general not true at all scales. Take for example only $\lambda_{111}^d \neq 0$ at some scale. Then through the CKM mixing the other terms λ_{1ij}^d will be generated by the RGEs.

3.1.3 Evolution of the Gauge Couplings

The RGEs for the Standard Model gauge couplings g_1 [for $U(1)_Y$, with $g_1 = \sqrt{5/3} g'$ using for example the $SU(5)$ GUT normalisation], g_2 [for $SU(2)_L$] and g_3 [for $SU(3)_c$] can be written:

$$\begin{aligned} \frac{d}{dt}g_a = & \frac{g_a^3}{16\pi^2}B_a^{(1)} + \frac{g_a^3}{(16\pi^2)^2} \left[\sum_{b=1}^3 B_{ab}^{(2)} g_b^2 - C_a^e \text{Tr}(\lambda_{jk}^{e\dagger} \lambda_{jk}^e) - C_a^d \text{Tr}(\lambda_{jk}^{d\dagger} \lambda_{jk}^d) \right. \\ & \left. - C_a^u \text{Tr}(\lambda_{jk}^{u\dagger} \lambda_{jk}^u) + A_a^e \sum_{k=1}^3 \text{Tr}(\lambda_{ijk}^{e\dagger} \lambda_{ijk}^e) + A_a^d \sum_{k=1}^3 \text{Tr}(\lambda_{ijk}^{d\dagger} \lambda_{ijk}^d) + A_a^u \sum_{k=1}^3 \text{Tr}(\lambda_{ijk}^{u\dagger} \lambda_{ijk}^u) \right]. \end{aligned} \quad (3.29)$$

In the evolution equation for the gauge couplings, the equations are coupled only starting with the two-loop term, while up to one loop each coupling has an independent evolution.

The coefficients B_a , B_{ab} , and C_a^x are calculated in [97]:

$$B_a^{(1)} = \left(\frac{33}{5}, 1, -3 \right), \quad (3.30)$$

$$B_{ab}^{(2)} = \begin{pmatrix} 199/25 & 27/5 & 88/5 \\ 9/5 & 25 & 24 \\ 11/5 & 9 & 14 \end{pmatrix}, \quad (3.31)$$

$$C_a^{u,d,e} = \begin{pmatrix} 26/5 & 14/5 & 18/5 \\ 6 & 6 & 2 \\ 4 & 4 & 0 \end{pmatrix}, \quad (3.32)$$

where the index u, d, e refers to the lines of the matrix. The \mathcal{R}_p contributions to the running of the gauge couplings appear only at two-loops. They are given in [95]:

$$A_a^{u,d,e} = \begin{pmatrix} 12/5 & 14/5 & 9/5 \\ 0 & 6 & 1 \\ 3 & 4 & 0 \end{pmatrix}. \quad (3.33)$$

In the Minimal Supersymmetric Standard Model there is a relation between the running of the top-quark mass and the ratio of VEVs of the two Higgs doublets, $\tan \beta$. Given the measure of the top-quark mass there is a restriction for the allowed $\tan \beta$ range. In the presence of \mathcal{R}_p , however, there is no such a restrictive prediction. Furthermore, allowing the bilinear lepton-number-violating terms [106, 95, 40, 98, 42], bottom-tau Yukawa unification can occur for any value of $\tan \beta$.

3.2 Perturbative Unitarity Constraints

It is possible to derive upper bounds on the \mathcal{R}_p coupling constants, without the need of specifying further input boundary conditions, simply by imposing the requirement that the ultraviolet scale evolution remains perturbative up to the large unification scale,

$$\frac{Y_{ijk}^2(M_X)}{(4\pi)^2} < 1, \quad (3.34)$$

where Y_{ijk} is a generic trilinear \mathcal{R}_p coupling constant. In more general terms, the unitarity limits concern the upper bound constraints on the coupling constants imposed by the condition of a scale evolution between the electroweak and the unification scales, free of divergences or Landau poles for the entire set of coupling constants. The principal inputs here are the Standard Model gauge coupling constants, the superpartner spectrum together with the ratio of Higgs bosons VEVs parameter, $\tan \beta = v_u/v_d$, and the quark and lepton mass spectra, as described by the Yukawa coupling constants, $\lambda_{ij}^{u,d,e}$. Since the third generation Yukawa coupling constants, $\lambda_t = \lambda_{33}^u$, $\lambda_b = \lambda_{33}^d$, $\lambda_\tau = \lambda_{33}^e$, are predominant, the influential \mathcal{R}_p coupling constants are expected to be those containing the maximal number of third generation indices, namely λ_{233}^e , λ_{333}^d , λ_{313}'' , λ_{323}'' .

The first study developing perturbative unitarity bounds is due to Brahmachari and Roy [99]. The derived bounds for the baryon-number-violating interactions, $[\lambda_{313}'', \lambda_{323}''] < 1.12$, turn out to be very weakly dependent on the input value for $\tan \beta$. These bounds increase smoothly with the input value of m_t , diverging at $m_t \approx 185$ GeV. Bounds for the other configurations of the generation indices of λ_{ijk}'' have been obtained on the same basis by Goity and Sher [100], $\lambda_{mjk}'' < 1.25$, $[m = 1, 2]$. Allanach et al. [95] carry out a systematic analysis of the renormalization flow equations, up to the two-loop order, for the lepton and baryon-number-violating interactions λ_{ijk}^e , λ_{ijk}^d and λ_{ijk}'' . The resulting coupling constant bounds read $\lambda_{323}^e(m_t) < 0.93$, $\lambda_{333}^d(m_t) < 1.06$, $\lambda_{323}''(m_t) < 1.07$, at $\tan \beta = 5$. Choosing a higher $\tan \beta$ lowers these bounds slightly.

3.3 Quasi-fixed points analysis for \mathcal{R}_p couplings

The RGEs describing the evolution of the Yukawa couplings down from a large scale M_X may have fixed points which give information on the couplings. The existence of infrared fixed points (IRFP) for the third generation Yukawa coupling constants and the relevant \mathcal{R}_p coupling constants, is signalled by vanishing solutions for the beta-functions describing the scale evolution for the ratios of the above Yukawa coupling constants to the gauge interaction coupling constants. In principle, one seeks fixed point solutions [101] characterized by the exact absence in the infrared regime of a renormalization group flow for ratios such as, for instance, λ_t^2/g_3^2 or λ_{323}^e/g_3^2 . In practice however, this fixed point regime may be inaccessible since it would set in at a scale much lower than the electroweak scale, making it irrelevant. In that case the values of the Yukawa couplings are determined by quasi-fixed points (QFP) [102] describing the actual asymptotic behaviour of the couplings. In such a case, the values at the weak scale are essentially independent of their values at the large scale, provided the initial values are large. For an analytical study see [103].

As an example let us consider a simplified renormalization group equation for the top-quark Yukawa coupling λ_t at one loop in the Standard Model:

$$16\pi^2 \frac{d\lambda_t}{dt} = \frac{\lambda_t}{2} (9\lambda_t^2 - 16g_3^2), \quad (3.35)$$

where $t = \log q^2$ and we have neglected the contributions from the lighter quarks and the electroweak contributions. By forming the difference of the previous equation with the one for the evolution of the QCD strong interaction coupling:

$$16\pi^2 \frac{dg_3}{dt} = g_3^3 \left(\frac{2}{3}N_f - 11 \right) \quad (3.36)$$

where N_f is the number of flavours, one obtains:

$$16\pi^2 \frac{d}{dt} \log(\lambda_t/g_3) = \frac{9}{2}\lambda_t^2 + g_3^2 \left(3 - \frac{2}{3}N_f \right) . \quad (3.37)$$

When the value

$$\lambda_t^2 = \frac{2}{9}g_3^2 \left(\frac{2}{3}N_f - 3 \right) \quad (3.38)$$

is reached, Eq. (3.37) has zero on the right-hand side which implies a constant ratio of the two couplings for subsequent decreasing values of the scale t . This is the Pendleton-Ross fixed point. However this behaviour would only set in at a very low scale, of the order of 1 GeV, while the region of interest is the one in which the scale is around m_t . The reason why the fixed point is important only at a very low scale is that in Eq. (3.35) the strong coupling constant g_3 becomes large only below 1 GeV. In the intermediate region λ_t evolves with the lowering of the mass scale until the g_3 coupling becomes of the same order, i.e. :

$$\frac{9}{2}\lambda_t^2 \simeq 8g_3^2 . \quad (3.39)$$

In this intermediate region the right-hand side of equation (3.35) is close to zero, which in turn implies that λ_t must remain relatively constant. The previous argument can be made more precise by a detailed calculation or a graph of $\lambda_t(q)$ versus $\lambda_t(M_X)$ where M_X is the high scale and q is in the intermediate range. In both cases the asymptotic behaviour is ascribed to the condition (3.39) which is termed a quasi-fixed point.

Before considering the effect of \mathcal{R}_p , let us consider the quasi-fixed point regime for the Minimal Supersymmetric Standard Model. In this case the renormalization group flow points towards the value of the top quark coupling constant $\lambda_t(m_t) \simeq 1.1$, which establishes a correlation between the top mass and $\tan \beta$, described by the relation

$$m_t(\text{pole}) = \frac{v \sin \beta}{\sqrt{2}} \lambda_t(\text{pole}) . \quad (3.40)$$

Substitution of the physical top mass m_t as an input value singles out a discrete range for $\tan \beta$.

When the third generation \mathcal{R}_p interactions are switched on, individually or collectively, solutions of the quasi-fixed point type continue to exist. These fixed point values of the coupling constants provide theoretical bounds under the assumption that the theory remains perturbative. By requiring a lower bound on the top mass, say, $m_t > 150$ GeV, they would lead to excluded domains in the parameter space of λ_t and the \mathcal{R}_p Yukawa coupling constants [99]. Looking for a simultaneous quasi-fixed point in λ_t and/or λ_b and in the \mathcal{R}_p coupling constants one at a time, one obtains [104, 105]: $\lambda_t \simeq 0.94$, $\lambda_{323}'' \simeq 1.18$, $\lambda_{333}^d \simeq 1.07$, and $\lambda_t \simeq 1.16$, $\lambda_{233}^e \simeq 0.64$, at small $\tan \beta$ and $\lambda_t \simeq 0.92$, $\lambda_b \simeq 0.92$, $\lambda_{323}'' \simeq 1.08$, at large $\tan \beta$. As the \mathcal{R}_p couplings λ^e , λ^d , λ'' are successively switched on, the regular top Yukawa coupling varies as, $\lambda_t \simeq 1.06 \rightarrow 1.06 \rightarrow 0.99$, respectively in the small $\tan \beta$ regime. In the large $\tan \beta \simeq m_t/m_b \approx 35$ regime, the solution

for the quasi-fixed point predictions are modified as, $\lambda_t \simeq 1.00 \rightarrow 1.01 \rightarrow 0.87$, respectively and $\lambda_b \simeq 0.92 \rightarrow 0.78 \rightarrow 0.85$, respectively, the corresponding fixed point values for the \tilde{R}_p coupling constants being $\lambda_{333}^d \simeq 0.71$, $\lambda_{323}'' \simeq 0.92$ [104, 105]. Further discussions of the fixed point physics in connection with \tilde{R}_p can be found in [106].

The stability condition with respect to small variations of the parameters for a renormalization group fixed point requires that the matrix of derivatives of the beta-functions with respect to the coupling constants has all its eigenvalues of the same fixed (positive in our conventions) sign. Discussion of the stability issue motivated by the supersymmetric models can be found in [107, 108, 109]. The above stability condition is actually never satisfied in the Minimal Supersymmetric Standard Model even for the trivial fixed point at which the \tilde{R}_p coupling constants tend to zero. Once one includes the \tilde{R}_p interactions, a stable infrared quasi-fixed point does exist, but only if one considers simultaneously the third generation regular Yukawa coupling constants, λ_t , λ_b , along with λ_{332}'' [110]. In particular there is no simultaneous B - and L -violating infrared fixed point. Note that the validity of these results is based on the extent of what variation of the parameters is considered “small”.

The quasi-fixed points are reached for large initial values of the couplings at the GUT scale, therefore they reflect the assumption of perturbative unitarity of the corresponding couplings. Under this assumption, the quasi-fixed points provide upper bounds on the relevant Yukawa couplings, especially the B -violating coupling λ_{332}'' [111].

In the Minimal Supersymmetric Standard Model the coupling constants g_1 , g_2 and g_3 unify at a certain scale M_{GUT} thanks to R -parity conservation. The scale evolution of the gauge couplings leads to a successful unification with the values of the unified coupling constant and the unification scale given by, $\alpha_X(M_X) \simeq 1/24.5 = 0.041$, $[g_X(M_X) \simeq 0.72]$, $M_X \simeq 2.3 \times 10^{16}$ GeV. Besides gauge coupling unification, GUT theories reduce the number of free parameters in the Yukawa sector. \tilde{R}_p affects this picture: the feed-back effects of the \tilde{R}_p trilinear interactions on the regular Yukawa interactions may have significant implications for the constraints set by grand unification on the Minimal Supersymmetric Standard Model parameters.

In the context of Grand Unified Theories one could consider a unification of the \tilde{R}_p parameters. However, if the \tilde{R}_p interactions arise from a $SU(5)$ invariant term there would be a relation between B - and L -violating terms and this in turn would imply non-zero contributions to the proton decay, either directly or at one-loop level through flavour mixing, therefore limiting the \tilde{R}_p couplings to very small values as already discussed in section 2. The situation for the widely used hypothesis of Yukawa coupling unification $\lambda_b = \lambda_\tau$ is analogous, even if there is no direct link between the two sorts of coupling unification. Analyses avoiding the assumption of $\lambda_b = \lambda_\tau$ unification have been performed and the quasi-fixed point values for the \tilde{R}_p coupling constants are found as [104, 105], $\lambda_{233}^e = 0.90$, $\lambda_{333}^d = 1.01$, $\lambda_{323}'' = 1.02$, for $\tan \beta < 30$.

As a simplifying assumption one can take a hierarchy similar to the one between Standard Model Yukawa couplings, and therefore consider only one coupling at a time. Solving the two-loop RGEs, Allanach et al. [95] find that by turning on any one of the three relevant \tilde{R}_p third generation related coupling constants, from zero to their maximally allowed values, the unification coupling constant, α_X , is insignificantly affected by less than 5%, while the unification scale, M_X , can be reduced by up to 20%. Note also that for large values of the R -parity violating coupling, the value of $\alpha_s(M_Z)$ predicted from unification can be reduced by 5% with respect to the R -parity conserving case.

3.4 Supersymmetry Breaking

The renormalization group studies in the presence of the soft supersymmetry-breaking become far less tractable. A proper treatment of R -parity violation must also include \mathcal{R}_p soft terms, therefore a large number of additional parameters arise which all have a mutual influence on one another. Within the MSSM, these additional terms are given in Eq. (2.16) and introduce 51 new \mathcal{R}_p parameters: 3 B_i associated with the bilinear superpotential terms, 45 \mathcal{R}_p A -terms with the same antisymmetry properties as the corresponding trilinear superpotential couplings, and 3 \mathcal{R}_p soft mass terms \tilde{m}_{di}^2 mixing the down-type Higgs boson and slepton fields.

The inclusion of R -parity violation in the superpotential allows the generation of lepton-Higgs mixing which leads to sneutrino VEVs and hence neutrino masses as discussed in chapter 2. The indirect generation of sneutrino VEVs through the running of the RGEs for the soft terms can lead to large effects. They induce finite sneutrino VEVs v_i , via the renormalization group evolution of the \mathcal{R}_p trilinear interactions from the grand unification scale to the electroweak scale, as discussed in [30]. A renormalization group analysis, including the soft supersymmetry-breaking parameters, is developed within a supergravity framework [88], where the \mathcal{R}_p trilinear interactions are specified at the grand unification scale, $\lambda_{ijk}^e(M_X)$, and one performs at each energy scale the requisite field transformation aimed at removing away the bilinear interactions in the superpotential, $\mu_i(q) = 0$. Since finite v_i contribute, via the mixing with neutralinos, to the neutrino Majorana masses (see chapter 5), the condition that the experimental limits on these masses are satisfied leads to the following qualitative bounds at the unification scale, $\lambda_{i33}^e < (10^{-2} - 10^{-3})$ and $\lambda_{i33}^d < (10^{-2} - 10^{-3})$. The \mathcal{R}_p interactions also initiate, through the renormalization group evolution, indirect contributions to flavour changing soft mass and \mathcal{R}_p parameters. An application to the prototype process $\mu \rightarrow e + \gamma$ indicates that these indirect effects turn out to dominate over the direct effects associated with the explicit contributions from the one-loop diagrams discussed in chapter 6. However, the situation cannot be described in terms of quantitative predictions, owing to the large number of free parameters and the occurrence of strong cancellations amongst contributions from different sources.

In another study [112] the rôle of the \mathcal{R}_p interactions in driving certain superpartner mass squared to negative values is examined. The sneutrinos are most sensitive to this vacuum stability constraint because of the weaker experimental bounds on their masses. The attractive contribution from the \mathcal{R}_p interactions reads $\delta m_{\tilde{\nu}}^2 \simeq -|\lambda_{ijk}^d(M_X)|^2(13m_0^2 + 49M_{\frac{1}{2}}^2 - 1.5M_{\frac{1}{2}}A - 12A^2)$, where m_0 , $M_{\frac{1}{2}}$ and A stand for the unification values of the soft scalar masses, the gaugino masses and the A -terms respectively, assumed to be universal. Invoking the experimental constraint on $m_{\tilde{\nu}}$ from LEP, one may derive bounds on the \mathcal{R}_p coupling constants at the unification scale, valid for all flavour configurations, such as $\lambda_{ijk}^d(M_X) < 0.15$, which translate into bounds at the electroweak scale, of the form $\lambda_{ijk}^d \approx \lambda_{ijk}^d(M_Z) < 0.3$. The indirect effects of the \mathcal{R}_p interactions on the flavour changing parameters are also examined for the process $b \rightarrow s + \gamma$. These contributions appear to dominate over the direct perturbative contributions from the one-loop diagrams. However, because of the large number of relevant parameters and the complicated dependence on the observables, one can again only infer conclusions of a qualitative nature.

In conclusion, the renormalization group evolution is a powerful tool to link theoretical hypotheses and experimental data, by allowing the comparison of quantities such as coupling constants at different scales. It is however difficult to draw general conclusions on the bounds that one can obtain as they may strongly depend on assumptions, in a range of energy that is still to be explored. Nonetheless if one allows to include the general picture of grand unification and supersymmetry a number of interesting results can be obtained.

Chapter 4

COSMOLOGY AND ASTROPHYSICS

One of the first merit of a conserved R -parity is to provide, naturally, a stable lightest supersymmetric particle (LSP). If R -parity is absolutely conserved, the LSP is absolutely stable – none of its possible decay channels being kinematically allowed – and therefore it constitutes a possible dark matter candidate.

A broken R -parity supersymmetry could have important implications on this issue of the dark matter of the universe. The LSP can then decay through \mathcal{R}_p interactions into Standard Model particles only. Such an unstable LSP can still remain, however, a possible dark matter candidate, provided its lifetime is sufficiently long; the corresponding \mathcal{R}_p couplings are then required to be extremely small. On the other hand a short-lived LSP, irrelevant to the dark matter problem, is required to decay sufficiently quickly so as not to affect the successful predictions of Big Bang nucleosynthesis.

A second important issue concerns the cosmological baryon asymmetry, i.e. the fact that there is no significant amount of antibaryons in the universe. Understanding the origin of the observed baryon-to-photon ratio $n_B/n_\gamma = (6.1_{-0.2}^{+0.3}) \times 10^{-10}$ [46], or in other terms of the cosmological baryon asymmetry $\eta_B \equiv (n_B - n_{\bar{B}})/n_\gamma$, raises the question of how and when this baryon-antibaryon asymmetry was generated, and what the protection of this asymmetry against subsequent dilution by baryon-number-violating interactions over the history of the universe requires. Different solutions for the creation of the cosmological baryon asymmetry have been proposed in the literature, either directly through B -violating interactions, or indirectly through L -violating interactions (the resulting lepton number asymmetry being turned into a baryon asymmetry through $B - L$ conserving but $B + L$ violating processes known as sphalerons). This also requires that the corresponding interactions should violate, in addition to baryon and/or lepton number, the C and CP symmetries between particles and antiparticles.

Supersymmetric theories with broken R -parity have the interesting feature of providing the baryon and/or lepton-number non-conservation needed for baryogenesis. However, while these \mathcal{R}_p interactions may generate a baryon or lepton asymmetry all by themselves, in reverse, they might also dilute a pre-existing baryon asymmetry.

4.1 Constraints from the lifetime of the Lightest Supersymmetric Particle

4.1.1 Decays of the Lightest Supersymmetric Particle

In supersymmetric extensions of the Standard Model with unbroken R -parity, the LSP plays a fundamental rôle as the sole supersymmetric relic from the Big Bang, and may then provide the non-baryonic component of the dark matter of the universe.

In principle the LSP could be any supersymmetric particle, such as the lightest neutralino or chargino, a sneutrino, a charged slepton, a squark or a gluino. There are however strong arguments in favour of an electrically neutral and uncoloured (stable) LSP [113]. Stable, electrically charged and uncoloured particles would combine with electrons (if they have charge +1) or with protons or nuclei (if they have charge -1) to form superheavy isotopes of the hydrogen or of other elements. Stable coloured particles would first bind into new hadrons (such as $(\tilde{t}ud)^+$ or $(\tilde{t}dd)^0$ in the case of a stop LSP), which would then combine with electrons (in the case of a stable, charge +1 heavy hadron) or with nuclei to form superheavy isotopes of the hydrogen or of other elements. The relic number densities of such massive stable particles have been evaluated to be $n_X/n_B \simeq 10^{-6} (m_X/1 \text{ GeV})$ for an electrically charged, uncoloured particle [114] such as a charged slepton LSP, and $n_X/n_B \simeq 10^{-10}$, independently of the hadron mass, for a coloured particle [114, 115], such as a squark or a gluino LSP. However, terrestrial experiments searching for anomalously heavy protons or superheavy isotopes have placed stringent upper limits on the relic abundances of electrically charged or coloured stable particles (for a review see Ref. [116]). For example “heavy proton” experimental searches yield the limit $n_X/n_B < 10^{-21}$ for $m_X < 350 \text{ GeV}$ [117]; heavy isotopes searches, $n_X/n_B < (2 \times 10^{-16} - 7 \times 10^{-9})$, depending on the element, for $10^2 \text{ GeV} < m_X < 10^4 \text{ GeV}$ [118]; and searches for superheavy isotopes of hydrogen in water, $n_X/n_B < 10^{-28}$ [119], 3×10^{-20} [118] and 6×10^{-15} [120] in the mass ranges $(10 - 10^3) \text{ GeV}$, $(10^2 - 10^4) \text{ GeV}$ and $(10^4 - 10^8) \text{ GeV}$, respectively. The comparison of these negative experimental results with the above predicted relic abundances almost certainly rules out charged or coloured superparticles as suitable (stable) LSP candidates.

Among the possible electrically neutral and uncoloured LSPs, the lightest neutralino $\tilde{\chi}_1^0$ appears to be the best candidate for the non-baryonic dark matter of the universe. The gravitino remains a possible dark matter candidate, but it generally suffers from an abundance excess problem, while the possibility of a sneutrino LSP has been excluded, in the Minimal Supersymmetric Standard Model, by direct dark matter searches in underground experiments [121, 122]. The requirement that the relic density of the lightest neutralino falls within the range allowed by observations, $\Omega_{CDM} = 0.23 \pm 0.04$ [46], where $\Omega_{CDM} \equiv \rho_{CDM}/\rho_c$ is the ratio of the present cold dark matter (CDM) energy density to the critical energy density, puts strong constraints on the parameters of the Supersymmetric Standard Model. But the fact that satisfactory values of the relic abundance can be obtained constitutes one of the important motivations for R -parity conservation in supersymmetric extensions of the Standard Model¹.

The above state of affairs gets drastically modified in the case of a broken R -parity. The most important effect of R_p interactions is the resulting instability of the LSP. An unstable LSP

¹If the strong CP problem is solved by the Peccei-Quinn mechanism [123], the supersymmetric partner of the axion, the axino, could also be a viable dark matter candidate (see e.g. Ref. [124], assuming primordial axinos to have been diluted by inflation).

can still be a dark matter component of the universe provided it is sufficiently long-lived, so as to retain most of its primordial abundance until the present time – but this requires extremely small values of the \mathcal{R}_p couplings. A LSP with lifetime shorter than a fraction of the age of the universe, on the other hand, would now have disappeared almost completely and can no longer play a rôle as a dark matter component of the universe. In this case however, the constraints associated with experimental searches for anomalously heavy protons or superheavy isotopes no longer apply, and the LSP can be any superpartner – not necessarily an electrically neutral and uncoloured particle. We shall though restrict ourselves to the case of a neutralino LSP in the following.

Depending on the lifetime $\tau_{\tilde{\chi}}^0$ of the LSP (i.e. depending on the strength of the \mathcal{R}_p couplings responsible for its decay), different types of cosmological constraints apply. The decays of a long-lived LSP, with a lifetime comparable to, or slightly larger than, the present age t_0 of the universe, $\tau_{\tilde{\chi}}^0 \gtrsim t_0$, can produce an excess of particles such as antiprotons or positrons in our galaxy at a level incompatible with observations. To avoid this problem, one must require $\tau_{\tilde{\chi}}^0 \gg t_0$, i.e. extremely small values of the trilinear \mathcal{R}_p couplings, at the level of $\mathcal{O}(10^{-20})$ or below. These very strong constraints do not apply, of course, when the LSP lifetime is shorter than the age of the universe. In this case, the LSP must decay sufficiently quickly so that its late decays do not modify the light element abundances successfully predicted by Big-Bang nucleosynthesis. This constraint results in an upper bound on $\tau_{\tilde{\chi}}^0$, or equivalently on a lower bound on trilinear \mathcal{R}_p couplings of the order of $\mathcal{O}(10^{-12})$ [126]. For comparison, these couplings are required to be larger than $\mathcal{O}(10^{-8})$ for the LSP to decay inside a laboratory detector.

We now present a more detailed discussion of the constraints originating from nucleosynthesis. The decay of an unstable relic particle after the nucleosynthesis epoch would have produced electromagnetic and/or hadronic showers that could have either dissociated or created light nuclei [125]. Hence, in order not to destroy the predictions of Big-Bang nucleosynthesis, the LSP lifetime, if not greater than the age of the universe, must not exceed some upper limit. Focusing on the constraints arising from deuterium photo-dissociation, Kim et al. [126] estimate the maximal allowed lifetime to be $(\tau_{\tilde{\chi}^0})_{max} \simeq 2.24 \times 10^7 \text{ s} / [4.92 + \ln(m_{\tilde{\chi}^0}/1 \text{ GeV}) - \ln(n_B/n_\gamma)]$. Imposing that the neutralino LSP lifetime associated to its decays via trilinear \mathcal{R}_p couplings is shorter than the above value leads to a lower bound of the order of 10^{-12} on a weighted sum of squared couplings. As an example, for a 60 GeV photino-like neutralino, assuming a universal sfermion mass of 1 TeV, the constraint reads:

$$0.12 \sum_{i,j,k} |\lambda_{ijk}|^2 + 0.31 \sum_{i,j \neq 3,k} |\lambda'_{ijk}|^2 + 0.04 \sum_{i,k} |\lambda'_{i3k}|^2 + 0.23 \sum_{i < j, k \neq 3} |\lambda''_{ijk}|^2 > 7.7 \times 10^{-24} . \quad (4.1)$$

Let us now discuss the constraints applying to a neutralino LSP with a lifetime greater than the age of the universe ($\tau_{\tilde{\chi}}^0 > t_0$). A first set of constraints comes from the production of antiprotons through LSP decays mediated by the λ'_{ijk} and λ''_{ijk} couplings [127]. The observed flux of cosmic rays antiprotons places a strong bound on such decays, resulting in stringent upper limits on the corresponding \mathcal{R}_p couplings:

$$\lambda'_{ijk}, \lambda''_{ijk} < (10^{-24} - 10^{-19}) , \quad (4.2)$$

for all generation indices, exclusive of λ''_{3jk} in the case where the LSP is lighter than the top quark. The upper bound on a given coupling strongly depends on the model parameters (especially on the neutralino and squark masses), but is always smaller by some 3 orders of magnitude

than the upper bound corresponding to the condition that the LSP lifetime is greater than the age of the universe, $\tau_{\tilde{\chi}^0}^0 > t_0$ (see Ref. [127] for details).

A very long-lived LSP neutralino can also produce positrons through the three-body decays $\tilde{\chi}^0 \rightarrow e^+ + 2 \text{ fermions}$, which can be induced both by trilinear and bilinear \mathcal{R}_p interactions. The experimentally measured positron flux in our galaxy imposes the following bound on the corresponding partial lifetime of the neutralino [128]: $\tau(\tilde{\chi}^0 \rightarrow e^+ + 2 \text{ fermions})/t_0 > 6 \times 10^{10} h (m_{\tilde{\chi}^0}/100 \text{ GeV})^{\frac{1}{2}} (\tilde{m}/100 \text{ GeV})^{\frac{1}{2}}$, where all sfermion masses have been set to \tilde{m} , and h is the reduced Hubble parameter defined by $H_0 = 100 h \text{ km/s/Mpc}$. This leads to stringent upper bounds on all trilinear and bilinear \mathcal{R}_p superpotential couplings [129]:

$$\begin{aligned} \lambda_{ijk}, \lambda'_{ijk}, \lambda''_{ijk} &< 4 \times 10^{-23} N_{1l}^{-1} \left(\frac{m_{\tilde{f}}}{100 \text{ GeV}} \right)^2 \left(\frac{m_{\tilde{\chi}^0}}{100 \text{ GeV}} \right)^{-9/8} \left(\frac{1 \text{ GeV}}{m_f} \right)^{1/2}, \\ \mu_i &< 6 \times 10^{-23} N_{1l}^{-1} \left(\frac{m_{\tilde{\chi}^0}}{100 \text{ GeV}} \right) \left(\frac{\tilde{m}}{100 \text{ GeV}} \right)^{-7/4} \text{ GeV}, \end{aligned} \quad (4.3)$$

where m_f is the emitted fermion mass and the N_{1l} [$l = 3, 4$] parametrize the amount of the higgsino components in the neutralino.

4.1.2 Gravitino Relics

It is well known that supergravity theories are plagued with a cosmological gravitino problem. Indeed, since the gravitino interacts only gravitationally, it has a very small annihilation cross-section and tends to overclose the universe; or, if it is unstable, to destroy the successful predictions of Big-Bang nucleosynthesis through its late decays. In the case of a stable gravitino (or a quasi-stable one with a lifetime longer than the age of the universe), the annihilation rate is too weak to prevent the relic energy density of heavy gravitinos from exceeding the critical energy density [130, 131]. Then gravitinos must be very light, $m_{3/2} \lesssim 1 \text{ keV}$ [132], in order for their relic abundance not to overclose the universe². In the case of an unstable gravitino, its decay must occur sufficiently early so as not to affect nucleosynthesis. Indeed, if the gravitino decays after nucleosynthesis, its decay products will either dissociate or create light nuclei and modify their relative abundances, thus destroying the agreement between Big-Bang nucleosynthesis predictions and observations. Furthermore the entropy release subsequent to gravitino decays will wash out the baryon asymmetry and spoil the concordance between the observed baryon-to-photon ratio and the light nuclei abundances. The second problem can be evaded if the gravitino is heavier than about 10^4 GeV [130]. This lower bound assumes that the gravitino is not the LSP, so that it can decay to lighter supersymmetric partners; if the gravitino is the LSP and decays via \mathcal{R}_p channels, it should be even heavier – but then all superpartners should be extremely heavy. To summarize, there is no cosmological gravitino problem if $m_{3/2} \lesssim 1 \text{ keV}$, or if the gravitino is unstable and heavy ($m_{3/2} \gtrsim 10 \text{ TeV}$ if it is not the LSP).

The above constraints, however, were derived within standard cosmology (without inflation), and can be relaxed if there is an inflationary phase which dilutes the gravitino abundance

²Because the effective strength of its couplings are fixed by the ratio $G_N/m_{3/2}^2$, a gravitino heavier than a few eV would have extremely small interaction cross-sections and decouple very early, allowing for its residual abundance to be higher than that of a neutrino with the same mass [133, 134]. The upper limit on the mass of such a light gravitino, obtained by demanding that its relic energy density be less than the critical density, is then increased (as compared to the corresponding limit for neutrinos), up to $\sim 1 \text{ keV}$ [132] – its precise value depending on the number of particle species in thermal equilibrium at the gravitino decoupling time.

[135, 136, 137]. In this case one still has to face a cosmological gravitino problem associated with the gravitinos produced during the reheating phase after inflation, whose abundance is essentially proportional to the reheating temperature T_R . If the gravitino is stable, requiring that its relic energy density is less than the critical density therefore results in an upper bound on T_R . If it is unstable, its decays should not affect the light nuclei abundances successfully predicted by Big-Bang nucleosynthesis, which requires values of T_R lower than in the case of a stable gravitino. One typically finds $T_R \lesssim 10^7$ GeV for $m_{3/2} \sim 100$ GeV if the gravitino is not the LSP [138]. Such a stringent upper bound is problematic for standard inflationary models [139, 140], which generally predict much higher values of the reheating temperature.

Let us consider in greater detail the case of an unstable gravitino. All decay rates of the gravitino are proportional to Newton's constant $G_N = 1/M_P^2$, and may be expressed as $\Gamma_{\tilde{G}} \approx \alpha_{\tilde{G}} m_{3/2}^3/M_P^2$, where $\alpha_{\tilde{G}}$ is a dimensionless coefficient. The fastest possible decay modes, for which the coefficient $\alpha_{\tilde{G}}$ is of order one, are the R -parity conserving two-body decay modes, such as $\tilde{G} \rightarrow \tilde{\chi}^\mp + W^\pm$, $\tilde{G} \rightarrow \tilde{\chi}^0 + \gamma(Z)$ and $\tilde{G} \rightarrow \tilde{l}^\mp + l^\pm$. These are allowed only if the gravitino is not the LSP. In the presence of \mathcal{R}_p interactions, the gravitino can also decay into channels solely comprising the ordinary (R -even) particles [141], but with much smaller rates than the R -parity conserving modes ($\alpha_{\tilde{G}} \ll 1$) due to the smallness of the \mathcal{R}_p couplings. As a result, the \mathcal{R}_p decay channels are relevant only for the case of a gravitino LSP, on which we shall concentrate now.

The case of bilinear R -parity violation has been discussed in Ref. [142]. Assuming that the lightest neutralino is essentially bino-like, the dominant decay mode of the gravitino LSP is $\tilde{G} \rightarrow \nu\gamma$, for which $\alpha_{\tilde{G}} \simeq \frac{1}{32\pi} \cos^2 \theta_W m_\nu / m_{\tilde{\chi}_1^0}$, where m_ν is the neutrino mass generated at tree level by the bilinear \mathcal{R}_p terms (see chapter 5). The experimental and cosmological constraints on neutrino masses then imply that the gravitino lifetime is much longer than the age of the universe, even for a gravitino mass as high as 100 GeV. The gravitino relic abundance and mass are further constrained by the requirement that the photon flux produced in gravitino decays does not exceed the observed diffuse photon background; for a relic abundance in the relevant range for dark matter and $m_\nu \sim 0.07$ eV, this implies $m_{3/2} \lesssim 1$ GeV. Thus, in the presence of bilinear R -parity violation (at the level required to explain atmospheric neutrino data), a gravitino LSP can constitute the dark matter of the universe only if it is lighter than about 1 GeV, assuming in addition that the reheating temperature is low enough for the gravitino relic density to fall in the range relevant for dark matter. The case of trilinear R -parity violation has been discussed in Ref. [143]. Assuming standard cosmology (without an inflationary phase), a gravitino LSP which decays via trilinear \mathcal{R}_p couplings λ_{ijk} , λ'_{ijk} or λ''_{ijk} can evade the relic abundance problem, but it is excluded by nucleosynthesis constraints, unless the gravitino mass is unnaturally large. This abundance problem, however, can be solved by inflation. To conclude, R -parity violation does not seem to provide a natural solution to the cosmological gravitino problem.

Still a gravitino with \mathcal{R}_p decay can have interesting implications in astrophysics and cosmology. As mentioned above, nucleosynthesis severely constrains the possibility of a late decaying massive particle, and the constraint is particularly strong for an unstable gravitino. However one can consider an alternative scenario to Big-Bang nucleosynthesis which relies on such a particle [144]. In this scenario, light element production takes place when the hadronic decay products interact with the ambient protons and ${}^4\text{He}$. In order to reproduce the observed abundances, very specific properties of the decaying particle are required; it must in particular decay after nucleosynthesis and have a small baryonic branching ratio, $r_B \sim 10^{-2}$. The candidate proposed in Ref. [145] is a massive, not LSP gravitino decaying to hadrons predominantly via

the L -violating trilinear \mathcal{R}_p couplings. One can arrange for the required small baryonic branching ratio in gravitino decays by considering a sneutrino LSP and assuming non-vanishing \mathcal{R}_p couplings λ_{131} , λ_{232} and λ'_{3jk} with $\lambda'_{3jk}/\lambda_{131} \sim 0.1$ and $\lambda'_{3jk}/\lambda_{232} \sim 0.1$. The gravitino then undergoes the following cascade decays: $\tilde{G} \rightarrow \nu\bar{\nu}$, $\tilde{\nu} \rightarrow (e\bar{e}, \mu\bar{\mu}, \dots) + (q\bar{q})$. The predicted abundances of D , ${}^4\text{He}$ and ${}^7\text{Li}$ can be made to match the observations even for a universe closed by baryons [144, 146] (i.e. with $\Omega_B \simeq 1$), but the scenario overproduces ${}^6\text{Li}$ and is therefore disfavoured [147].

4.2 Cosmological Baryon Asymmetry

4.2.1 Baryogenesis from R -Parity-Violating Interactions

Generating the observed baryon asymmetry of the universe is one of the challenges of particle physics. In order for a baryon-antibaryon asymmetry to be dynamically generated in an expanding universe, three necessary conditions, known as Sakharov's conditions [148], must be met: (i) baryon-number violation; (ii) C and CP violation; (iii) departure from thermal equilibrium. In principle, all three ingredients are already present in the Standard Model, where baryon number is violated by nonperturbative processes known as sphalerons [149, 150, 151] (which violate $B + L$ but preserve $B - L$ and are in thermal equilibrium above the electroweak scale), and the departure from thermal equilibrium could be due to the electroweak phase transition. This leads to the standard electroweak baryogenesis scenario, which however has been excluded as a viable mechanism in the Standard Model [152], and works only in a restricted portion of the Minimal Supersymmetric Standard Model parameter space [153]. Other mechanisms, such as leptogenesis [154], in which a lepton asymmetry is generated by out-of-equilibrium decays of heavy Majorana neutrinos and then partially converted into a baryon asymmetry by sphaleron transitions, or Affleck-Dine baryogenesis [155], offer possible alternatives to the standard scenario. In this section, we review several attempts to generate the observed baryon asymmetry from R_p -violating interactions.

A first class of scenarios uses the trilinear \mathcal{R}_p couplings λ''_{ijk} and their associated A -terms A''_{ijk} as the source of baryon-number violation. The λ''_{ijk} couplings induce decays of a squark (resp. an antisquark) into two antiquarks (resp. two quarks), which violate baryon number by one unit. The differences between the various scenarios that rely on this process reside in the way departure from equilibrium is realized, and in the mechanism that produces squarks.

In the scenario proposed by Dimopoulos and Hall [156], squarks are produced far from thermal equilibrium at the end of inflation as decay products of the inflaton field. Their subsequent decays into quarks and antiquarks induced by the \mathcal{R}_p couplings λ''_{ijk} generate a baryon asymmetry directly proportional to the CP asymmetry in these decays, $\Delta\Gamma_{\tilde{q}} = (\Gamma(\tilde{q}_R \rightarrow \bar{q}_R\bar{q}_R) - \Gamma(\tilde{q}_L^c \rightarrow q_R q_R))/(\Gamma_{\tilde{q}_R} + \Gamma_{\tilde{q}_L^c})$. The dominant contribution to this CP asymmetry comes from the interference between tree-level and two-loop diagrams involving the CP -violating phases present in the A -terms (in the convention in which gaugino mass parameters are real). In order for this scenario to work, the reheating temperature T_R must be extremely low (typically $T_R \lesssim 1$ GeV) so that scattering processes induced by the λ''_{ijk} couplings, which could dilute the baryon asymmetry created in squark decays, are suppressed.

In the scenario considered by Cline and Raby [157], the departure from thermal equilibrium is provided by the late decays of the gravitino, and the baryon asymmetry is produced in two

steps. First an asymmetry in the number densities of squarks and antisquarks is produced by CP -violating decays of the neutral gauginos produced in the out-of equilibrium decays of the gravitino, or by CP -violating decays of the gravitino itself, but the total baryon number remains conserved due to an opposite asymmetry in the number densities of quarks and antiquarks. As in the previous model, the source of CP violation is the relative phase between the gaugino mass parameters and the A -terms, but now the CP asymmetry arises from the interference between tree-level and one-loop diagrams. In the case of gluons, the asymmetry induced by non-vanishing λ''_{323} and A''_{323} couplings reads:

$$\Delta\Gamma_{\tilde{g}} \equiv \frac{\Gamma(\tilde{g} \rightarrow t\tilde{t}^c) - \Gamma(\tilde{g} \rightarrow \bar{t}\tilde{t})}{\Gamma_{\tilde{g}}} \approx \frac{\lambda''_{323}}{16\pi} \frac{\Im(A''_{323} m_{\tilde{g}})}{|m_{\tilde{g}}|^2}, \quad (4.4)$$

where \Im denotes the imaginary part. In the second step, this asymmetry gets partially converted into a baryon asymmetry by the B -violating decays of the (anti)squarks induced by the λ''_{ijk} couplings – it is assumed here that the squarks are lighter than the gauginos, so that their only relevant tree-level decay mode is into two quarks. At the time where the squark decays occur, the scattering processes that could erase the CP asymmetry are highly suppressed by low particle densities. For this scenario to work, the reheating temperature must be high enough for the required gravitino abundance to be regenerated after inflation, i.e. typically $T_R \gtrsim 10^{15}$ GeV. In addition, the gravitino should be heavy enough ($m_{3/2} \gtrsim 50$ TeV) so that its decay products do not affect nucleosynthesis.

To generate the observed baryon asymmetry, the previous two scenarios require the CP asymmetry to be close to its maximal allowed value, i.e. the CP -violating phase should be close to the upper bound associated with the electric dipole moment of the neutron, and the dominant B -violating coupling should be of order one. The source of baryon-number violation must then be a coupling that is not constrained by $\Delta B = 2$ processes such as neutron-antineutron oscillations and heavy nuclei decays (see chapter 6), e.g. λ''_{323} .

A variant of the scenario considered by Cline and Raby, which also works for smaller values of the CP asymmetry and for lower reheating temperatures, has been proposed by Mollerach and Roulet [158]. In this scenario, a large, out-of-equilibrium population of gluinos is created in the decays of heavy axinos (\tilde{a}) and/or saxinos (s), the fermionic superpartners and scalar partners of the pseudoscalar axions, respectively. This requires $m_{\tilde{a}} > m_{\tilde{g}}$ ($m_s > 2m_{\tilde{g}}$), so that the decay channel $\tilde{a} \rightarrow g\tilde{g}$ ($s \rightarrow \tilde{g}\tilde{g}$) be kinematically allowed. The axinos (saxinos) decay at a temperature around 1 GeV and thus do not interfere with nucleosynthesis. The baryon asymmetry is then generated in two steps from gluino decays, like in the scenario of Cline and Raby, but the present scenario is much more efficient and the CP asymmetry is not required to be close to its maximal value. The CP -violating phase can thus be small, and the B -violating coupling can be smaller than one. In the presence of an inflationary phase, the observed amount of baryon asymmetry can be obtained for reheating temperatures as low as 10^4 GeV (in the case of a large CP asymmetry), due to the fact that (s)axinos are regenerated much more efficiently than gravitinos.

In another scenario studied by Adhikari and Sarkar [159], the baryon asymmetry is generated in out-of-equilibrium decays of the lightest neutralino induced by the λ''_{ijk} couplings, $\tilde{\chi}_1^0 \rightarrow u_{iR} d_{jR} d_{kR}$, rather than in squark decays. The CP asymmetry in these decays arises at the one-loop level, and can be large even for small values of the B -violating couplings, which are required by the out-of-equilibrium condition. Unlike in the previous scenarios, CP violation is due to the complexity of the λ''_{ijk} couplings. The sfermions are assumed to be much heavier than the lightest neutralino, so that the former have already decayed at the time where

the latter decays, and their \tilde{R}_p decay modes do not erase the generated baryon asymmetry. The other processes that could dilute the baryon asymmetry, such as the $\Delta B = 1$ scattering processes $u_{iR} d_{jR} \rightarrow \bar{d}_{kR} \tilde{\chi}_1^0$, must be out of equilibrium. This requires rather small values of the λ''_{ijk} couplings; still Adhikari and Sarkar estimate that it is possible to generate the observed baryon asymmetry of the universe for values of the λ'_{ijk} couplings in the $10^{-4} - 10^{-3}$ range (see however the footnote below).

In a second class of scenarios, the \tilde{R}_p couplings λ_{ijk} and λ'_{ijk} , which violate lepton number, are used to create a lepton asymmetry at the electroweak scale. This one is then partially converted into a baryon asymmetry by the sphaleron processes³.

In the scenario considered by Masiero and Riotto [161], the lepton asymmetry is generated through the \tilde{R}_p (and CP -violating) decays of the LSP, which is produced out of equilibrium in bubble collisions during the electroweak phase transition. The origin of CP violation is simply the presence of phases in the \tilde{R}_p couplings λ_{ijk} and λ'_{ijk} . Assuming that the LSP is the lightest neutralino, the dominant decay channel is expected to be $\tilde{\chi}_1^0 \rightarrow l_i^- \bar{t} d_k$ ($l_i^+ \bar{t} d_k$), and the CP asymmetry is given by:

$$\epsilon = \frac{\Gamma(\tilde{\chi}_1^0 \rightarrow l^- \bar{t} d) - \Gamma(\tilde{\chi}_1^0 \rightarrow l^+ \bar{t} d)}{\Gamma(\tilde{\chi}_1^0 \rightarrow l^- \bar{t} d) + \Gamma(\tilde{\chi}_1^0 \rightarrow l^+ \bar{t} d)} \simeq \frac{1}{16\pi} \frac{\sum_{i,k,l,m,n} \Im(\lambda_{inl}^* \lambda'_{mnl} \lambda_{m3k}^* \lambda'_{i3k})}{\sum_{i,k} |\lambda'_{i3k}|^2}. \quad (4.5)$$

For this mechanism to work, the phase transition must be first order, i.e. it must proceed by nucleation of bubbles of true vacuum in the unbroken phase. Furthermore, contrary to what is required in the standard electroweak baryogenesis scenario, the sphaleron processes must remain in equilibrium until the temperature drops below the critical temperature. This can indeed be the case if the Higgs sector of the Supersymmetric Standard Model is extended by the addition of one or more singlet superfields. Finally, the \tilde{R}_p interactions responsible for the generation of the lepton asymmetry must be in equilibrium at the electroweak scale, while the $\Delta L = 1$ scattering processes $l_{iL} \bar{d}_{kR} \rightleftharpoons \tilde{\chi}_1^0 \bar{t}$, which could wash it out, must be out of equilibrium. The first condition turns into a lower bound on the λ'_{i3k} couplings:

$$|\lambda'_{i3k}| \gtrsim 5.3 \times 10^{-5} \left(\frac{500 \text{ GeV}}{m_{\tilde{\chi}_1^0}} \right) \left(\frac{T_0}{150 \text{ GeV}} \right) \left(\frac{m_{\tilde{t}_L}}{1 \text{ TeV}} \right)^2, \quad (4.6)$$

and the second one into an upper bound on the same couplings:

$$|\lambda'_{i3k}| \lesssim 2.4 \times 10^{-4} \left(\frac{500 \text{ GeV}}{m_{\tilde{\chi}_1^0}} \right) \left(\frac{150 \text{ GeV}}{T_0} \right)^{1/2} \left(\frac{m_{\tilde{t}_L}}{1 \text{ TeV}} \right)^2. \quad (4.7)$$

where T_0 is the critical temperature of the electroweak phase transition. For values of the \tilde{R}_p couplings in the range delimited by Eqs. (4.6) and (4.7), this scenario can generate the observed baryon asymmetry, provided that the top squark is heavy. Indeed, relatively high values of λ'_{i3k} are needed to provide a large enough CP asymmetry (typically $|\lambda'_{i3k}| \sim 10^{-2}$, which requires $m_{\tilde{t}_L} \gtrsim 6$ (3) TeV if $m_{\tilde{\chi}_1^0} \simeq 500$ (100) GeV).

Adhikari and Sarkar [162] noticed that, in the presence of flavour-violating couplings of the neutralinos, the generation of the lepton asymmetry can be much more efficient. This is

³It has been noted in Ref. [160] that the lepton or baryon asymmetry generated at the electroweak scale from the decay of gauge non-singlet particles can be strongly suppressed due to the efficiency of the annihilation of these particles into two gauge bosons. This effect had been overlooked or underestimated in the scenarios discussed below, as well as in the scenario of Ref. [159].

especially so if some sfermions are not much heavier than the lightest neutralino, so that they can be produced in bubble collisions and contribute to the lepton asymmetry through their \tilde{R}_p decays $\tilde{\nu}_{iL} \rightarrow d_{kR} \bar{d}_{jL}, \bar{d}_{jL} \rightarrow d_{kR} \bar{\nu}_{iL}, \bar{d}_{kR} \rightarrow d_{jL} \bar{\nu}_{iL}, \dots$

Hambye, Ma and Sarkar [163] consider another scenario in which a lepton asymmetry is created in out-of-equilibrium decays of the lightest neutralino into a charged Higgs boson and a lepton singlet, $\tilde{\chi}_1^0 \rightarrow l_R^\pm h^\mp$. The CP asymmetry is proportional to the square of the parameter ξ that accounts for the mixing between the slepton singlets and the charged Higgs boson, and the CP -violating phase comes from the neutralino mass matrix. The same parameter ξ controls the out-of-equilibrium condition for $\Delta L = 2$ processes that could erase the generated lepton asymmetry. For this mechanism to produce enough baryon asymmetry, ξ must be close to the upper bound associated with this condition. This can be achieved by introducing non-holomorphic \tilde{R}_p soft terms of the form $H_u^+ H_d \tilde{l}^c$, which contrary to the standard \tilde{R}_p soft terms are not constrained by experimental data.

4.2.2 Survival of a Baryon Asymmetry in the Presence of \tilde{R}_p Interactions

We have seen in the previous subsection that R -parity violation may be at the origin of the baryon asymmetry of the universe. In general, however, \tilde{R}_p interactions are considered as a danger since they can erase a baryon asymmetry that would be present before the electroweak phase transition. In order to avoid this, one requires \tilde{R}_p interactions to be out of equilibrium above the critical temperature of the electroweak phase transition, which results in strong upper bounds on the \tilde{R}_p couplings.

Let us first review the standard conditions for a baryon asymmetry generated during the thermal history of the universe to be preserved until today, in the absence of B - and L -violating interactions. Above the critical temperature $T_c \sim 100$ GeV and up to temperatures of the order of 10^{12} GeV, nonperturbative processes which violate $B + L$ but preserve $B - L$ are in thermal equilibrium [150, 151]. These processes, known as sphalerons, tend to erase any $B + L$ asymmetry present in the high temperature phase, in such a way that a baryon asymmetry can persist only if it corresponds to a $B - L$ asymmetry. More precisely, the existence of sphaleron processes in thermal equilibrium with the interactions of the Standard Model (or of the Minimal Supersymmetric Standard Model) leads to the following proportionality relation between the B and $B - L$ asymmetries [164, 165]:

$$Y_B = \frac{24 + 4N_H}{66 + 13N_H} Y_{B-L}, \quad (4.8)$$

where $Y_B \equiv (n_B - n_{\bar{B}})/s$ ($Y_L \equiv (n_L - n_{\bar{L}})/s$), with n_B (n_L) the baryon (lepton) number density and s the entropy density of the universe, and N_H is the number of Higgs doublets. For the Standard Model with one Higgs doublet, one has $Y_B/Y_{B-L} = 28/79$, while for the Minimal Supersymmetric Standard Model one has $Y_B/Y_{B-L} = 8/23$. As a result, there are only two viable possibilities for generating the baryon asymmetry of the universe: one can generate it at or after the electroweak phase transition (when sphaleron transitions are suppressed), or above the electroweak phase transition in the form of a $B - L$ asymmetry.

The above discussion must be modified in the presence of interactions that violate $B - L$, such as \tilde{R}_p interactions [166, 167, 168, 169, 170, 171]. Assuming that a $B - L$ asymmetry is generated by some mechanism above the electroweak phase transition, the only possibility for it to be preserved is that the $B - L$ -violating interactions be out of equilibrium, i.e. that their

characteristic timescale be longer than the age of the universe. This condition can be written as $\Gamma_{B-L} < H$, where Γ_{B-L} is the rate of a typical $B - L$ -violating process, and H is the Hubble parameter. In the case of R -parity violation, this yields strong upper bounds on \mathcal{R}_p parameters. For the trilinear couplings, the processes that yield the best bounds are the decays of squarks and sleptons into two fermions or sfermions, and the corresponding rates are given by [167, 169]:

$$\Gamma_{\hat{\lambda}} \simeq 1.4 \times 10^{-2} |\hat{\lambda}|^2 \frac{m_{\Phi}^2}{T}, \quad \Gamma_{\hat{A}} \simeq 1.4 \times 10^{-2} \frac{|\hat{A}|^2}{T}, \quad (4.9)$$

where m_{Φ} is the mass of the decaying sfermion, $\hat{\lambda}$ stands for any of the couplings λ_{ijk} , λ'_{ijk} or λ''_{ijk} , and \hat{A} for A_{ijk} , A'_{ijk} or A''_{ijk} . Since the temperature dependence of the Hubble parameter is given by $H \simeq 1.66 g_*^{1/2} T^2 / M_P$ (where g_* is the number of effectively massless degrees of freedom at the temperature T), the out-of equilibrium condition $\Gamma < H$ is more easily satisfied at high temperature, and the best bounds are obtained for $T \sim T_c$. Assuming $m_{\Phi} \sim T_c \sim 100$ GeV, one obtains [169]:

$$|\lambda_{ijk}|, |\lambda'_{ijk}|, |\lambda''_{ijk}| \lesssim 10^{-7}, \quad (4.10)$$

$$|A_{ijk}|, |A'_{ijk}|, |A''_{ijk}| \lesssim 10^{-5} \text{ GeV}. \quad (4.11)$$

For heavier sfermions, these constraints are slightly weakened, e.g. for $T \sim m_{\Phi} \sim 1$ TeV the upper bounds (4.10) are increased by a factor of 3. Also, the bounds (4.10) and (4.11) were derived under the assumption that the decays are kinematically allowed, which is not necessarily the case for the decays induced by A -terms. The bounds on the \mathcal{R}_p A -terms associated with scattering processes can be estimated to be one order of magnitude weaker [172].

For bilinear \mathcal{R}_p couplings, the relevant interaction rates are [169]:

$$\Gamma_{\mu_i} \simeq 1.4 \times 10^{-2} g^2 \frac{|\mu_i|^2}{\tilde{m}^2} T, \quad \Gamma_{B_i} \simeq 1.4 \times 10^{-2} g^2 \frac{|B_i|^2}{\tilde{m}^4} T, \\ \Gamma_{\tilde{m}_{di}^2} \simeq 1.4 \times 10^{-2} g^2 \frac{|\tilde{m}_{di}^2|^2}{\tilde{m}^4} T, \quad (4.12)$$

where \tilde{m} stands for the relevant scalar or supersymmetric fermion mass. As usual, the bilinear \mathcal{R}_p parameters μ_i , B_i and \tilde{m}_{di}^2 are expressed in the (H_d, L_i) basis in which the sneutrino VEVs $\langle \tilde{\nu}_i \rangle$ vanish and the charged lepton Yukawa couplings are diagonal (see subsection 2.3.1). Assuming $\tilde{m} \sim T_c \sim 100$ GeV, one obtains the bounds:

$$|\mu_i| \lesssim 2 \times 10^{-5} \text{ GeV}, \quad |B_i|, |\tilde{m}_{di}^2| \lesssim 2 \times 10^{-3} \text{ GeV}^2. \quad (4.13)$$

There is however a little subtlety in deriving these bounds, due to the fact that the thermal mass eigenstate basis for the H_d and L_i fields above the electroweak phase transition is not the same as the zero temperature mass eigenstate basis [26, 27]. For a discussion of the cosmological bounds on \mathcal{R}_p couplings in terms of basis-independent quantities, see Ref. [27].

As discussed in section 2.7, baryon- and lepton-number violation may also proceed through non-renormalizable operators, which are expected to be generated from some more fundamental theory than the Supersymmetric Standard Model. Writing a generic non-renormalizable operator of dimension $4 + n$ as $\mathcal{O}_{4+n} / M_{4+n}^n$, where all couplings have been absorbed in the definition of the mass scale M_{4+n} , one can estimate the rate of the $B - L$ -violating processes induced by this operator to be $\Gamma \sim 10^{-3} T^{2n+1} / M_{4+n}^{2n}$. The requirement that these processes are out of thermal equilibrium at the temperature T yields a lower bound on the mass scale M_{4+n} :

$$M_{4+n} \gtrsim 10^{2+\frac{6}{n}} \text{ GeV} \left(\frac{T}{100 \text{ GeV}} \right)^{1-\frac{1}{2n}}. \quad (4.14)$$

The interaction rates for non-renormalizable operators increase faster with temperature than the Hubble parameter; therefore, the strongest bounds on M_{4+n} are obtained at high temperature. In principle⁴, the bound (4.14) should be applied at the temperature at which the baryon asymmetry has been created, but it is no longer valid above $T \sim 10^{12}$ GeV, where sphaleron processes are out of equilibrium. It should be noted that the bound (4.14) applies not only to \mathcal{R}_p operators, but also to the R -parity conserving operators which violate $B - L$, such as the superpotential term $\frac{1}{M_5} L H_u L H_u$, which induces Majorana masses for the neutrinos. The bound on M_5 is $M_5 \gtrsim 10^8 \text{ GeV} (T/100 \text{ GeV})^{1/2}$, which is compatible with the cosmological bound on neutrino masses $\sum_i m_{\nu_i} \lesssim 1 \text{ eV}$ [46], even if the bound on M_5 applies up to $T \sim 10^{12}$ GeV.

In the above, we did not make any distinction between couplings which violate different lepton flavours. However, since the sphaleron processes preserve each one of the three combinations $B/3 - L_i$, $i = 1, 2, 3$, a $B - L$ asymmetry generated before the electroweak phase transition will survive as soon as the processes violating one of the $B/3 - L_i$ are out of equilibrium, even if the other two are violated by processes in thermal equilibrium. This means that the bounds (4.10) to (4.14) must be satisfied by all baryon-number-violating couplings and by the couplings that violate, say L_e , while the \mathcal{R}_p couplings that violate L_μ or L_τ can be arbitrarily large – provided however that the sources of lepton-flavour violation are out of equilibrium [170]. Explicitly, the conditions for preserving a $B/3 - L_e$ asymmetry generated before the electroweak phase transition read (for superpartner masses of the order of $T_c \sim 100$ GeV):

$$|\lambda_{1jk}|, |\lambda_{ij1}|, |\lambda'_{1pq}|, |\lambda''_{npq}| \lesssim 10^{-7}, \quad (4.15)$$

$$|A_{1jk}|, |A_{ij1}|, |A'_{1pq}|, |A''_{npq}| \lesssim 10^{-5} \text{ GeV}, \quad (4.16)$$

$$|\mu_1| \lesssim 2 \times 10^{-5} \text{ GeV}, \quad |B_1|, |\tilde{m}_{d1}^2| \lesssim 2 \times 10^{-3} \text{ GeV}^2, \quad (4.17)$$

where $i, j, k \neq 1$. The \mathcal{R}_p couplings that violate L_μ or L_τ can be much larger if the off-diagonal slepton soft terms are small enough, so that they do not induce lepton-flavour-violating processes at thermal equilibrium [170, 172]:

$$\left| \frac{(m_{\tilde{L}}^2)_{1j}}{(m_{\tilde{L}}^2)_{11}} \right|, \left| \frac{(m_{\tilde{L}^c}^2)_{1j}}{(m_{\tilde{L}^c}^2)_{11}} \right| \lesssim 5 \times 10^{-2}, \quad |A_{1j}^e| \lesssim 10^{-5} \text{ GeV}, \quad (4.18)$$

where $j = 2$ or 3 . The constraints (4.15) to (4.17) can be summarized by saying that baryon-number violation, as well as lepton-number violation in at least one generation, must be strongly suppressed.

The constraints presented in this subsection should be regarded as sufficient conditions for the baryon asymmetry of the universe not to be erased by \mathcal{R}_p interactions, rather than strict bounds. First of all, they do not apply if the baryon asymmetry of the universe is generated at or after the electroweak phase transition, like in the standard electroweak baryogenesis scenario, or in all baryogenesis scenarios discussed in the previous subsection, where the \mathcal{R}_p interactions act as the source of the baryon asymmetry. Indeed, the sphaleron processes come out of equilibrium just below the critical temperature, so that they can no longer erase a $B + L$ asymmetry. Furthermore, there are several loopholes in the cosmological arguments used to derive

⁴For operators that do not involve the right-handed electron field, it may be enough to require that the corresponding interactions are out of equilibrium up to $T_{e_R} \sim (10^4 - 10^5) \text{ GeV}$ [173, 174]. Indeed, above T_{e_R} , the electron Yukawa coupling is out of equilibrium, so that an asymmetry stored in e_R cannot be transferred to other particle species. In baryogenesis scenarios that generate an e_R asymmetry, this can protect the baryon asymmetry down to the temperature T_{e_R} .

the bounds on \overline{R}_p couplings displayed above, and these (or some of them) can be evaded in several baryogenesis scenarios, even if the baryon asymmetry is generated above the electroweak phase transition (see e.g. Refs. [170, 175]).

In this chapter, we studied the implications of a broken R -parity in cosmology and astrophysics. The most dramatic change with respect to the R -parity conserving Supersymmetric Standard Model is the instability of the LSP, which rules it out as a natural candidate for the non-baryonic dark matter of the universe, unless \overline{R}_p couplings are unrealistically small. An even more damaging effect of R -parity violation is the potential erasure of the baryon asymmetry of the universe by \overline{R}_p interactions, if it has been generated before the electroweak phase transition. These could be two good reasons to stick to a conserved R -parity. On the other hand, R -parity violation can help solving the cosmological gravitino problem, although with some difficulty, and provide new mechanisms for generating the baryon asymmetry of the universe at or after the electroweak phase transition.

Chapter 5

NEUTRINO MASSES AND MIXINGS

R -parity forbids lepton-number (L) violation from renormalizable interactions. Allowing for violation of L -conservation law has several important effects in the neutrino sector. The most dramatic implication of non-vanishing couplings λ_{ijk} , λ'_{ijk} and/or bilinear \mathcal{R}_p parameters is the automatic generation of neutrino masses and mixings. As a consequence, the possibility that the atmospheric and solar neutrino data, now interpreted in terms of neutrino oscillations, be explained by \mathcal{R}_p interactions has motivated a large number of studies and models. Besides neutrino masses, R -parity violation in the lepton sector leads to neutrino transition magnetic moments, new contributions to neutrinoless double beta decays, neutrino-flavour transitions in matter and sneutrino-antisneutrino oscillations. In this chapter, we shall concentrate on the question of neutrino masses and mixings in supersymmetric models without R -parity, and on the related issues of neutrino transition magnetic moments, \mathcal{R}_p -induced neutrino-flavour transitions in matter and sneutrino-antisneutrino mixing. Neutrinoless double beta decay will be discussed in Chapter 6.

5.1 \mathcal{R}_p Contributions to Neutrino Masses and Mixings

5.1.1 R -Parity Violation as a Source of Neutrino Masses

In order to account for nonzero neutrino masses and mixings, the Standard Model (with two-component, left-handed neutrino fields) has to be supplemented with additional particles. The simplest possibility is to add right-handed neutrinos, which either leads to Dirac neutrinos or, if the right-handed neutrinos have heavy Majorana masses, to Majorana neutrinos through the well-known seesaw mechanism [176]. Other mechanisms, which directly generate a Majorana mass term for the standard two-component neutrino fields, do not involve right-handed neutrinos but require an enlarged Higgs sector, involving additional $SU(2)_L$ triplet [59] or singlet and doublet [177, 178] Higgs fields.

A new possibility arises in the Supersymmetric Standard Model. Indeed, in the absence of R -parity, lepton-number-violating couplings induce Majorana masses for neutrinos without the need of right-handed neutrinos or exotic Higgs fields. In other words, *supersymmetry without R -parity automatically incorporates massive neutrinos*. This may be regarded both as an appealing feature of \mathcal{R}_p models and as a potential problem, since the contribution of \mathcal{R}_p couplings may exceed by several orders of magnitude the experimental bounds on neutrino masses.

One can distinguish between two types of contributions to neutrino masses and mixings in supersymmetric models without R -parity¹ [24]: (i) a tree-level contribution arising from the neutrino-neutralino mixing due to bilinear R -parity violation; (ii) loop contributions induced by the trilinear \tilde{R}_p couplings λ_{ijk} and λ'_{ijk} and/or bilinear \tilde{R}_p parameters. These contributions, if present, are generally expected to be large and potentially in conflict with the experimental limits on neutrino masses [20],

$$m_{\nu_e} < 3 \text{ eV} , \quad m_{\nu_\mu} < 190 \text{ keV} , \quad m_{\nu_\tau} < 18.2 \text{ MeV} , \quad (5.1)$$

and with the cosmological bound on stable neutrinos, $\sum_i m_{\nu_i} \lesssim 1 \text{ eV}$ [46]. The effective Majorana masses generated through mechanisms (i) and (ii) can be written as (with the neutral gauginos and higgsinos integrated out)

$$-\frac{1}{2} M_{ij}^\nu \bar{\nu}_{Li} \nu_{Rj}^c + \text{h.c.} , \quad (5.2)$$

where $i, j = 1, 2, 3$ are generation indices, and the 3×3 matrix M^ν is symmetric by virtue of the properties of the charge conjugation matrix. The relative rotation between charged lepton and neutrino mass eigenstates defines a lepton mixing matrix U , 3×3 and unitary, the Pontecorvo-Maki-Nakagawa-Sakata (PMNS) matrix [179, 180], responsible for neutrino oscillations. With the conventions $R_L^e M^e R_R^{e+} = \text{Diag}(m_{e1}, m_{e2}, m_{e3})$ and $M^\nu = R^\nu \text{Diag}(m_{\nu_1}, m_{\nu_2}, m_{\nu_3}) R^{\nu T}$, the lepton mixing matrix reads $U = R_L^e R^\nu$, and the weak eigenstate neutrinos $\nu_{\alpha=e,\mu,\tau}$ – i.e. the $SU(2)_L$ partners of the mass eigenstate charged leptons – are related to the mass eigenstate neutrinos $\nu_{i=1,2,3}$ by $\nu_\alpha = \sum_i U_{\alpha i} \nu_i$. Here M^e is an effective mass matrix obtained after integrating out the charged gauginos and higgsinos, which mix with charged leptons through bilinear R -parity violation (see subsection 2.3.3). In general it is not simply proportional to the charged lepton Yukawa matrix, although $M^e = \lambda^e v_d / \sqrt{2}$ remains a good approximation in the phenomenologically relevant limit of small bilinear R -parity violation.

In the following, we shall neglect CP violation in the lepton sector, and therefore assume the charged lepton Yukawa couplings λ_{ij}^e and the \tilde{R}_p couplings μ_i , λ_{ijk} and λ'_{ijk} to be real. The MNS matrix is then real and can be parametrized by three angles θ_{12} , θ_{13} and θ_{23} , responsible for solar, reactor and atmospheric neutrino oscillations respectively:

$$U = \begin{pmatrix} c_{13}c_{12} & c_{13}s_{12} & s_{13} \\ -c_{23}s_{12} - s_{13}s_{23}c_{12} & c_{23}c_{12} - s_{13}s_{23}s_{12} & c_{13}s_{23} \\ s_{23}s_{12} - s_{13}c_{23}c_{12} & -s_{23}c_{12} - s_{13}c_{23}s_{12} & c_{13}c_{23} \end{pmatrix}. \quad (5.3)$$

Let us finally notice that since we are assuming non-vanishing L -violating couplings, we should make sure that the B -violating couplings λ''_{ijk} are absent from the theory – otherwise the proton would decay at a much too rapid rate. This can be ensured by imposing, instead of R -parity, the Z_3 baryon parity discussed in section 2.7. The advantage of this symmetry, which is discrete anomaly free in the MSSM, is that it forbids not only the λ'' couplings, but also the dangerous dimension-5 operators leading to proton decay.

5.1.2 Tree-Level Contribution Generated by Neutrino-Neutralino Mixing

Let us first consider the tree-level contributions. As discussed in section 2.3.3, bilinear R -parity violation induces a mixing between neutrinos and neutralinos, which yields a single massive

¹For early discussions on neutrino masses in supersymmetric models with explicitly or spontaneously broken R -parity, see Refs. [24, 33, 34, 55, 56].

neutrino state at tree level. This can be understood as a kind of seesaw mechanism, in which the neutral gauginos and higgsinos play the rôle of the right-handed neutrinos. Indeed, in the limit of a small neutrino-neutralino mixing, the 7×7 neutrino-neutralino mass matrix M_N has a “seesaw” structure, with a strong hierarchy² between the gaugino-higgsino diagonal 4×4 block M_χ and the off-diagonal 3×4 block m :

$$M_N|_{tree} = \begin{pmatrix} M_\chi & m^T \\ m & 0_{3 \times 3} \end{pmatrix}. \quad (5.4)$$

The effective mass matrix obtained by integrating out the neutralinos, which yields the neutrino mass and mixing angles, is given by $M_{tree}^\nu \simeq -m M_\chi^{-1} m^T$. The fact that only one neutrino becomes massive is most easily seen in a basis in which the superpotential \mathcal{R}_p mass parameters μ_1 and μ_2 (together with the sneutrino VEVs v_i) vanish; then both L_1^0 and L_2^0 decouple from $M_N|_{tree}$, as can be seen from Eq. (2.44). Of course, when quantum corrections are included, all three neutrinos acquire a mass, as explained in the next sections.

In order to determine the flavour composition of the single neutrino that acquires a mass at this level, one has in principle to diagonalize the chargino mass matrix. Indeed, since bilinear R -parity violation mixes charged leptons with charginos, the physical charged leptons are the three lightest eigenstates of the 5×5 charged lepton-chargino mass matrix M_C , Eq. (2.45). In general these do not coincide with the eigenstates of the Yukawa matrix λ_{ij}^e . However, in the limit of a small charged lepton-chargino mixing we are interested in, one can identify the two bases to a good approximation. We therefore choose to write M_N and M_C in the basis in which the sneutrino VEVs v_i vanish and the charged lepton Yukawa couplings λ_{ij}^e are diagonal. In this basis, the effective neutrino mass matrix reads [181]:

$$M_{tree}^\nu \simeq -m M_\chi^{-1} m^T = -\frac{m_{\nu_{tree}}}{\sum_i \mu_i^2} \begin{pmatrix} \mu_1^2 & \mu_1 \mu_2 & \mu_1 \mu_3 \\ \mu_1 \mu_2 & \mu_2^2 & \mu_2 \mu_3 \\ \mu_1 \mu_3 & \mu_2 \mu_3 & \mu_3^2 \end{pmatrix}, \quad (5.5)$$

where $m_{\nu_{tree}}$ is given by Eqs. (2.46) and (2.47),

$$m_{\nu_{tree}} \simeq \frac{M_Z^2 \cos^2 \beta (M_1 c_W^2 + M_2 s_W^2) \mu \cos \xi}{M_1 M_2 \mu \cos \xi - M_Z^2 \sin 2\beta (M_1 c_W^2 + M_2 s_W^2)} \tan^2 \xi. \quad (5.6)$$

The misalignment angle ξ , defined in subsection 2.3.1, is a basis-independent quantity that controls the size of the bilinear \mathcal{R}_p effects in the fermion sector (in particular, assuming small neutrino-neutralino and charged lepton-chargino mixings amounts to require $\sin \xi \ll 1$). In the basis in which we are working, it is given by $\sin \xi = \sqrt{\sum_i \mu_i^2} / \mu$. As already noticed in section 2.3.3, phenomenologically relevant values of $m_{\nu_{tree}}$ require a strong alignment between the 4-vectors $\mu_\alpha \equiv (\mu_0, \mu_i)$ and $v_\alpha \equiv (v_0, v_i)$, $\sin \xi \sim 3 \times 10^{-6} \sqrt{1 + \tan^2 \beta} \sqrt{m_{\nu_{tree}} / 1 \text{ eV}}$. Several authors [39, 40] have studied the possibility of obtaining the desired amount of alignment from GUT-scale universality in the soft terms. With this assumption the LEP bound on the tauneutrino mass can be satisfied in a relatively large region of the parameterspace, but a significant amount of fine-tuning in the bilinear \mathcal{R}_p parameters is necessary in order to reach the eV region (one would typically need $\mu_i / \mu \sim 10^{-4}$ at the GUT scale). Another possibility is to invoke an abelian flavour symmetry [35]; however rather large values of the associated charges are necessary to yield the desired alignment (see section 2.5).

²As in section 2.3, we are working in a (H_d, L_i) basis in which the sneutrino VEVs vanish, $v_i = 0$. The seesaw structure may be less obvious in an arbitrary basis where both $\mu_i \neq 0$ and $v_i \neq 0$, since large values of μ_i and v_i are in principle compatible with a small physical neutrino-neutralino mixing (see subsection 2.3.3).

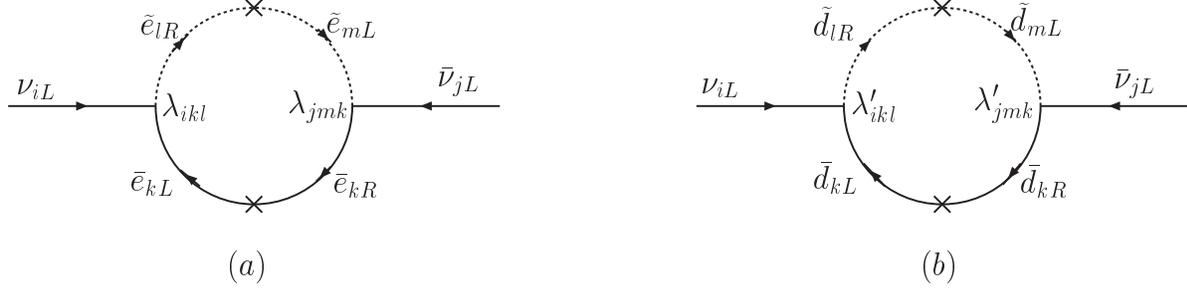


Figure 5.1: One-loop contributions to neutrino masses and mixings induced by the trilinear \mathcal{R}_p couplings λ_{ijk} (a) and λ'_{ijk} (b). The cross on the sfermion line indicates the insertion of a left-right mixing mass term. The arrows on external legs follow the flow of the lepton number.

The massive neutrino is mainly a superposition of the electroweak neutrino eigenstates, and its flavour composition is given, in the basis we are considering, by the superpotential \mathcal{R}_p mass parameters μ_i [181]:

$$\nu_3 \simeq \frac{1}{\sqrt{\sum_i \mu_i^2}} (\mu_1 \nu_e + \mu_2 \nu_\mu + \mu_3 \nu_\tau) . \quad (5.7)$$

In terms of mixing angles, this gives the relations

$$\sin \theta_{13} = \frac{\mu_1}{\sqrt{\sum_i \mu_i^2}} , \quad \sin \theta_{23} = \frac{\mu_2}{\sqrt{\mu_2^2 + \mu_3^2}} , \quad (5.8)$$

while $\sin \theta_{12}$ is undetermined.

5.1.3 One-Loop Contributions Generated by Trilinear \mathcal{R}_p Couplings

At the one-loop level, a variety of diagrams involving the trilinear \mathcal{R}_p couplings λ and λ' and/or insertions of bilinear \mathcal{R}_p masses contribute to the neutralino-neutrino mass matrix, thus correcting Eq. (5.5). In this subsection, we concentrate on the diagrams involving trilinear \mathcal{R}_p couplings only. These diagrams represent the dominant one-loop contribution to neutrino masses and mixings when bilinear R -parity violation is strongly suppressed (i.e. when $\sin \xi \simeq 0$ and $\sin \zeta \simeq 0$ in the language of subsection 2.3.1, where the angle ζ formed by the 4-vectors $B_\alpha \equiv (B_0, B_i)$ and $v_\alpha \equiv (v_0, v_i)$ controls the Higgs-slepton mixing). The one-loop diagrams involving bilinear \mathcal{R}_p masses will be discussed in the next subsection.

The trilinear \mathcal{R}_p couplings λ_{ijk} and λ'_{ijk} contribute to each entry of the neutrino mass matrix through the lepton-slepton and quark-squark loops of Fig. 5.1, yielding [24, 182]

$$M_{ij}^\nu|_\lambda = \frac{1}{16\pi^2} \sum_{k,l,m} \lambda_{ikl} \lambda_{jmk} m_{e_k} \frac{(\tilde{m}_{LR}^{e2})_{ml}}{m_{\tilde{e}_{Rl}}^2 - m_{\tilde{e}_{Lm}}^2} \ln \left(\frac{m_{\tilde{e}_{Rl}}^2}{m_{\tilde{e}_{Lm}}^2} \right) + (i \leftrightarrow j) , \quad (5.9)$$

$$M_{ij}^\nu|_{\lambda'} = \frac{3}{16\pi^2} \sum_{k,l,m} \lambda'_{ikl} \lambda'_{jmk} m_{d_k} \frac{(\tilde{m}_{LR}^{d2})_{ml}}{m_{\tilde{d}_{Rl}}^2 - m_{\tilde{d}_{Lm}}^2} \ln \left(\frac{m_{\tilde{d}_{Rl}}^2}{m_{\tilde{d}_{Lm}}^2} \right) + (i \leftrightarrow j) , \quad (5.10)$$

Here the couplings λ_{ijk} (resp. λ'_{ijk}) and the left-right slepton mixing matrix $\tilde{m}_{LR}^{e2} = (A_{ij}^e - \mu \tan \beta \lambda_{ij}^e) v_d / \sqrt{2}$ (resp. the left-right squark mixing matrix $\tilde{m}_{LR}^{d2} = (A_{ij}^d - \mu \tan \beta \lambda_{ij}^d) v_d / \sqrt{2}$) are expressed in the basis in which the charged lepton masses (resp. the down quark masses) as

well as the mass matrices for the associated doublet and singlet scalars are diagonal. The above expressions simplify if, as is customary, one assumes that the sfermion masses are approximately degenerate, and that the A -terms are proportional to the Yukawa couplings, $A_{ij}^e = A^e \lambda_{ij}^e$ and $A_{ij}^d = A^d \lambda_{ij}^d$. Then Eqs. (5.9) and (5.10) reduce to:

$$M_{ij}^\nu|_\lambda \simeq \frac{1}{8\pi^2} \frac{A^e - \mu \tan \beta}{\bar{m}_e^2} \sum_{k,l} \lambda_{ikl} \lambda_{jlk} m_{e_k} m_{e_l}, \quad (5.11)$$

$$M_{ij}^\nu|_{\lambda'} \simeq \frac{3}{8\pi^2} \frac{A^d - \mu \tan \beta}{\bar{m}_d^2} \sum_{k,l} \lambda'_{ikl} \lambda'_{jlk} m_{d_k} m_{d_l}, \quad (5.12)$$

where \bar{m}_e (resp. \bar{m}_d) is an averaged scalar mass parameter, and the couplings λ_{ijk} (resp. λ'_{ijk}) are now expressed in the superfield basis corresponding to the charged lepton (resp. down quark) mass eigenstate basis. Even after those approximations, the neutrino mass matrix still depends on a large number of trilinear \mathcal{R}_p couplings (9 λ_{ijk} and 27 λ'_{ijk}). To obtain a more predictive scheme, one has to make assumptions on the generational structure of the trilinear \mathcal{R}_p couplings.

One may for instance assume that, for a given generation index i , there is no strong hierarchy among the couplings λ_{ijk} and λ'_{ijk} , or that their flavour structure in the indices j and k is linked to the fermion mass hierarchy [35, 71, 37]. The second assumption is natural in models where the fermion mass hierarchy is explained by flavour symmetries (see section 2.5). In both cases the contributions with $k, l = 2$ or 3 dominate in Eqs. (5.11) and (5.12), and one obtains

$$M_{ij}^\nu|_\lambda \simeq \frac{1}{8\pi^2} \left\{ \lambda_{i33} \lambda_{j33} \frac{m_\tau^2}{\tilde{m}} + (\lambda_{i23} \lambda_{j32} + \lambda_{i32} \lambda_{j23}) \frac{m_\mu m_\tau}{\tilde{m}} + \lambda_{i22} \lambda_{j22} \frac{m_\mu^2}{\tilde{m}} \right\}, \quad (5.13)$$

$$M_{ij}^\nu|_{\lambda'} \simeq \frac{3}{8\pi^2} \left\{ \lambda'_{i33} \lambda'_{j33} \frac{m_b^2}{\tilde{m}} + (\lambda'_{i23} \lambda'_{j32} + \lambda'_{i32} \lambda'_{j23}) \frac{m_s m_b}{\tilde{m}} + \lambda'_{i22} \lambda'_{j22} \frac{m_s^2}{\tilde{m}} \right\}, \quad (5.14)$$

where we have set all sfermion mass parameters equal to \tilde{m} . The term proportional to m_τ^2 in Eq. (5.13) comes from the tau-stau loop and gives $M_{ij}^\nu|_\lambda \sim \lambda_{i33} \lambda_{j33} (4 \times 10^5 \text{ eV}) (100 \text{ GeV}/\tilde{m})$; similarly, the term proportional to m_b^2 in Eq. (5.14) comes from the bottom-sbottom loop and gives $M_{ij}^\nu|_{\lambda'} \sim \lambda'_{i33} \lambda'_{j33} (7.7 \times 10^6 \text{ eV}) (m_b/4.5 \text{ GeV})^2 (100 \text{ GeV}/\tilde{m})$.

This shows that trilinear \mathcal{R}_p couplings of order 1 would lead to large entries in the neutrino mass matrix, grossly conflicting with experimental data. This in turn puts strong constraints on the trilinear \mathcal{R}_p couplings. The most stringent upper bound comes from the non-observation of neutrinoless double beta decay, whose rate is directly related to the $(i, j) = (11)$ element of M^ν [183]:

$$|\lambda_{133}| \leq 9.4 \times 10^{-4} \left(\frac{\langle m_\nu \rangle}{0.35 \text{ eV}} \right)^{\frac{1}{2}} \left(\frac{\tilde{m}}{100 \text{ GeV}} \right)^{\frac{1}{2}}, \quad (5.15)$$

$$|\lambda'_{133}| \leq 2.1 \times 10^{-4} \left(\frac{\langle m_\nu \rangle}{0.35 \text{ eV}} \right)^{\frac{1}{2}} \left(\frac{4.5 \text{ GeV}}{m_b} \right) \left(\frac{\tilde{m}}{100 \text{ GeV}} \right)^{\frac{1}{2}}, \quad (5.16)$$

where $\langle m_\nu \rangle$ is the effective neutrino mass, bounded by neutrinoless double beta decay experiments. From the other terms in Eqs. (5.13) and (5.14) one can also extract (weaker) bounds on the couplings λ_{1kl} and λ'_{1kl} , $(k, l) \neq (3, 3)$. From a different perspective it is quite remarkable that a small amount of R -parity violation through trilinear couplings, with λ_{ijk} and λ'_{ijk} comparable in strength with the charged lepton and down quark Yukawa couplings, can induce neutrino masses in the phenomenologically interesting range, namely $10^{-3} \text{ eV} \lesssim m_\nu \lesssim 1 \text{ eV}$.

Let us now discuss the flavour structure of the neutrino mass matrix. Assuming further that the λ -type couplings are not greater than the λ' -type couplings, the leading contribution to $M_{loop}^\nu \equiv M^\nu|_\lambda + M^\nu|_{\lambda'}$ comes from the bottom-sbottom loop. Then

$$M_{loop}^\nu = \frac{m_{\nu_{loop}}}{\sum_i \lambda_{i33}'^2} \begin{pmatrix} \lambda_{133}'^2 & \lambda_{133}' \lambda_{233}' & \lambda_{133}' \lambda_{333}' \\ \lambda_{133}' \lambda_{233}' & \lambda_{233}'^2 & \lambda_{233}' \lambda_{333}' \\ \lambda_{133}' \lambda_{333}' & \lambda_{233}' \lambda_{333}' & \lambda_{333}'^2 \end{pmatrix} + \dots, \quad (5.17)$$

where

$$m_{\nu_{loop}} = \frac{3m_b^2}{8\pi^2 \tilde{m}} \sum_i \lambda_{i33}'^2 \quad (5.18)$$

and the dots stand for corrections of order

$$\frac{m_\tau^2}{8\pi^2 \tilde{m}} \lambda_{i33} \lambda_{j33}, \quad \frac{3m_b m_s}{8\pi^2 \tilde{m}} (\lambda_{i23}' \lambda_{j32}' + \lambda_{i32}' \lambda_{j23}'), \quad \frac{m_\mu m_\tau}{8\pi^2 \tilde{m}} (\lambda_{i23} \lambda_{j32} + \lambda_{i32} \lambda_{j23}) \dots$$

(with $i, j \neq 3$ for the m_τ^2 corrections, and $(i, j) \neq (2, 2), (3, 3)$ for the $m_\mu m_\tau$ corrections). The structure (5.17) generally leads to a hierarchical mass spectrum. Indeed, only one neutrino becomes massive at leading order, with a mass $m_{\nu_3} = m_{\nu_{loop}}$ and a flavour composition given by the mixing angles $\sin \theta_{13} = \lambda_{133}' / \sqrt{\sum_i \lambda_{i33}'^2}$ and $\sin \theta_{23} = \lambda_{233}' / \sqrt{\lambda_{233}'^2 + \lambda_{333}'^2}$ (θ_{12} remains undetermined at dominant order). Once sub-dominant contributions to M^ν are included, all three neutrinos become massive. Let us stress again that the above discussion does not take into account the contributions of bilinear \mathcal{R}_p parameters to the neutrino mass matrix.

5.1.4 One-Loop Contributions Generated by both Bilinear and Trilinear \mathcal{R}_p Couplings

In the above, we discussed one-loop contributions to neutrino masses in the limit where bilinear R -parity violation can be neglected. However this is generally not a valid approximation, since bilinear \mathcal{R}_p terms are always generated radiatively from trilinear \mathcal{R}_p interactions, and the presence of bilinear \mathcal{R}_p terms drastically changes the discussion of one-loop neutrino masses. First of all, the neutrino mass matrix receives contributions already at tree level, as discussed in section 5.1.2. Secondly, in addition to the lepton-slepton and quark-squark loops already encountered, one-loop diagrams involving insertions of bilinear \mathcal{R}_p masses or slepton VEVs must be considered [24, 39, 184, 38, 185, 186, 187, 188, 189, 190, 191, 192]. Here we shall only present briefly the main classes of loop contributions, and comment on the level of suppression of bilinear \mathcal{R}_p parameters required by neutrino mass constraints. We refer the interested reader to Ref. [191] for a detailed classification and evaluation of the various diagrams.

Let us first notice that there are two ways of computing the one-loop neutrino masses and mixing angles. The first one is to compute one-loop corrections to the full 7×7 neutralino-neutrino mass matrix, Eq. (5.4) [39, 186, 189]. The second one is to compute one-loop corrections to the tree-level effective 3×3 neutrino mass matrix, Eq. (5.5) [190, 191]; in this case the Feynman rules are written in terms of tree-level MSSM mass eigenstates (i.e. the tree-level mass matrices are diagonalized neglecting R -parity violation) and the bilinear \mathcal{R}_p masses are included in the diagrams as mass insertions, both on internal and external lines. The second approach is more suitable for a discussion of the various contributions to neutrino masses and mixings. Leaving aside gauge boson loops and diagrams with two \mathcal{R}_p mass insertions on the

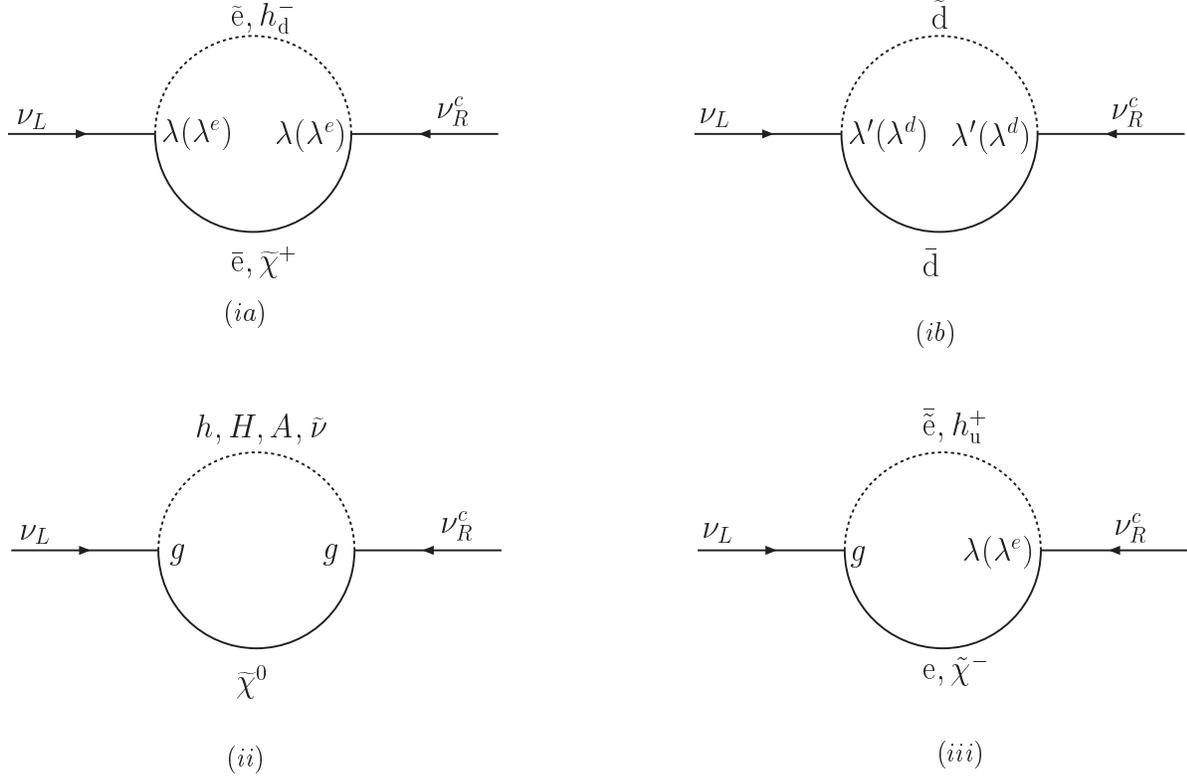


Figure 5.2: Schematic description of the one-loop diagrams contributing to neutrino masses and mixings, divided into three classes as described in the text. \mathcal{R}_p mass insertions on internal and/or external lines are not shown. The arrows on external legs follow the flow of the lepton number.

external legs, which renormalize the tree-level neutrino mass, one can divide the one-loop contributions to the neutrino mass matrix into three classes (see Fig. 5.2), depending on which couplings appear at the two vertices (a diagram with two couplings λ_1 and λ_2 at the vertices will be denoted by (λ_1, λ_2)) [191]:

- (i) diagrams involving trilinear \mathcal{R}_p couplings and/or Yukawa couplings at the vertices, with charged fermions and scalars in the loop; in addition to the (λ, λ) and (λ', λ') diagrams discussed above, there are (λ, λ^e) and (λ', λ^d) diagrams with one \mathcal{R}_p mass insertion, and (λ^e, λ^e) and (λ^d, λ^d) diagrams with two \mathcal{R}_p mass insertions;
- (ii) diagrams involving two gauge couplings, with a neutralino and neutral scalars in the loop [184, 38]; these diagrams have two \mathcal{R}_p mass insertions;
- (iii) diagrams involving a trilinear \mathcal{R}_p coupling or a Yukawa coupling at one vertex and a gauge coupling at the other vertex, with a chargino and charged fermions and scalars in the loop; the (g, λ) and (g, λ') diagrams have one \mathcal{R}_p mass insertion, while the (g, λ^e) and (g, λ^d) diagrams have two \mathcal{R}_p mass insertions.

Each of these diagrams contains two \mathcal{R}_p interactions, which can be trilinear (λ and λ' couplings), mass insertions on lepton or higgsino lines (μ_i mixing parameters or slepton VEVs v_i), LR mixing mass insertions on scalar lines (slepton VEVs v_i) or soft \mathcal{R}_p mass insertions on scalar lines (B_i and $\tilde{m}_{\tilde{d}_i}^2$ parameters). Note that the mass insertion approximation is valid only in a

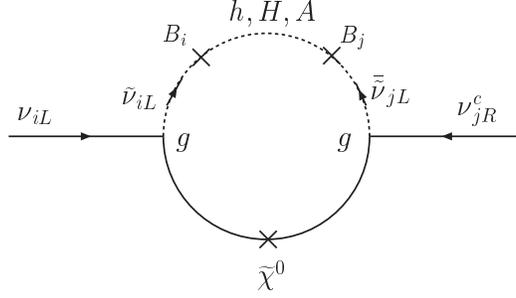


Figure 5.3: Neutral loop with gauge couplings at the vertices and two \mathcal{R}_p mass insertions on the scalar line. The cross on the neutralino line indicates a Majorana mass insertion. The arrows on external legs follow the flow of the lepton number.

basis in which \mathcal{R}_p masses are indeed small, e.g. in the $v_i = 0$ basis. We adopt this basis for the rest of the section.

Depending on the relative size of the various \mathcal{R}_p parameters, some diagrams can be neglected. For example, assuming that the trilinear couplings always give a significant contribution, one can consider three representative cases [191] (it may also happen that the contribution of the bilinear terms in the loops dominates over the contribution of the trilinear couplings, see Ref. [193]):

- (a) the contribution of bilinear terms in the loops is negligible. This is the situation discussed in the previous subsection, where only the (λ, λ) and (λ', λ') diagrams were considered;
- (b) the bilinear soft terms, but not the bilinear superpotential masses, induce sizeable loop contributions. In addition to the previous diagrams, the neutral loop from class (ii) with two \mathcal{R}_p soft mass insertions on the scalar line (see Fig. 5.3) must be taken into account;
- (c) both the bilinear soft terms and the bilinear superpotential masses induce sizeable loop contributions. In this case, all diagrams listed above must be considered a priori.

The contribution of the diagrams of Fig. 5.3 can be estimated to be [191],

$$\Delta M_{ij}^\nu \sim \frac{g^2}{64\pi^2} \frac{B_i B_j}{\tilde{m}^3} \frac{\epsilon_H}{\cos^2 \beta}, \quad (5.19)$$

where \tilde{m} is the typical mass of the particles in the loop, and ϵ_H takes into account the cancellation between the h , A and H loops. As noticed in Ref. [193], the different Higgs loops tend to cancel partially, and the cancellation becomes stronger when the pseudoscalar Higgs boson becomes heavier ($\epsilon_H \rightarrow 0$ in the decoupling limit $M_A \rightarrow \infty$). Furthermore, ϵ_H decreases when $\tan \beta$ increases, which softens the dependence of Eq. (5.19) on $\tan \beta$. Assuming $\tilde{m} \sim 100$ GeV and $\epsilon_H / \cos^2 \beta \sim 0.1$, one can see from Eq. (5.19) that soft \mathcal{R}_p masses $\sqrt{B_i} \sim 1$ GeV are enough to generate neutrino mass matrix entries of the order of the cosmological bound ($\Delta M_{ij}^\nu \sim 1$ eV). Thus, neutrino masses do not only constrain the misalignment angle in the fermion sector ($\sin \xi \lesssim 3 \times 10^{-6} \sqrt{1 + \tan^2 \beta}$ for $m_\nu \leq 1$ eV), but also the misalignment angle in the scalar sector. Namely, one has $\sin \zeta \lesssim (10^{-4} - 10^{-3}) (\tilde{m}/100 \text{ GeV})^{3/2} (100 \text{ GeV}/\sqrt{B})^2$ for $m_\nu \leq 1$ eV, assuming a partial cancellation between the different Higgs loops in the range $\epsilon_H / \cos^2 \beta = 0.01 - 1$.

5.2 Explicit Models of Neutrino Masses

We have seen in the previous section how the violation of R -parity improves our understanding of the generation of neutrino masses. The questions that immediately arise is how well \mathcal{R}_p models can account for the observed neutrino oscillation parameters, and whether these models lead to specific experimental signatures that could allow to test them. Numerous studies have been devoted to these questions, and we shall not attempt to give an exhaustive account of the existing literature on the subject. Rather we would like to stress the main characteristics of \mathcal{R}_p models of neutrino masses through a detailed discussion of some representative examples.

Before doing so, let us summarize the experimental status of neutrino masses and mixings.

5.2.1 Experimental Constraints on Neutrino Masses and Mixings

Atmospheric neutrino data [194, 195, 196] strongly suggest oscillations of atmospheric ν_μ 's into ν_τ 's, with a squared mass difference $\Delta m_{atm}^2 \equiv m_{\nu_3}^2 - m_{\nu_2}^2 \simeq (1.5 - 3.9) \times 10^{-3} \text{ eV}^2$, and a large-to-maximal mixing angle, $\tan^2 \theta_{23} = (0.45 - 2.3)$, both at the 3σ level [198]. The results of the K2K long-baseline neutrino oscillation experiment [197] are consistent with these oscillation parameters.

Solar neutrino data [199, 200, 201, 202, 203] combined with the results of the KamLAND experiment [204] provide evidence for oscillations of solar ν_e 's into ν_μ 's and ν_τ 's. Before the SNO and KamLAND results, four different solutions to the solar neutrino deficit were allowed, out of which three are now excluded. We nevertheless list them for future reference (the following pre-SNO allowed ranges of parameters are taken from Ref. [205]): (i) a small mixing angle solution (SMA) in the MSW regime, in which neutrino oscillations inside the sun are enhanced by matter effects (known as the Mikheev-Smirnov-Wolfenstein, or MSW effect [206, 207]), with a squared mass difference $\Delta m_\odot^2 \equiv m_{\nu_2}^2 - m_{\nu_1}^2 \simeq (4 \times 10^{-6} - 10^{-5}) \text{ eV}^2$ and a mixing angle $\tan^2 \theta_{12} \simeq (10^{-4} - 2 \times 10^{-3})$; (ii) a large mixing angle MSW solution (LMA) with $\Delta m_\odot^2 = (10^{-5} - 5 \times 10^{-4}) \text{ eV}^2$ and $\tan^2 \theta_{12} \simeq (0.2 - 1.)$; (iii) a solution with low squared mass difference (LOW), which extends to quasi-vacuum oscillations, with $\Delta m_\odot^2 = (4 \times 10^{-10} - 4 \times 10^{-7}) \text{ eV}^2$ and $\tan^2 \theta_{12} \simeq (0.2 - 4.)$; (iv) a tower of regions in the vacuum oscillation regime (VO), in which the oscillations occur during the propagation of the neutrinos from the sun to the Earth, with $\Delta m_\odot^2 \sim (10^{-11} - 5 \times 10^{-10}) \text{ eV}^2$ and a large mixing angle. After the results from the SNO and KamLAND collaborations, LMA is the only allowed solution (see e.g. Refs. [208, 209, 210, 211]), with smaller allowed regions in the oscillation parameter space: $\Delta m_\odot^2 \simeq (5.4 - 10.) \times 10^{-5} \text{ eV}^2$ and $\Delta m_\odot^2 \simeq (14. - 19.) \times 10^{-5} \text{ eV}^2$ (high-LMA region), $\tan^2 \theta_{12} \simeq (0.29 - 0.82)$ at the 3σ level [198].

The CHOOZ reactor experiment [212] provides an upper limit on the mixing angle θ_{13} that connects the solar and atmospheric neutrino sectors, $|U_{e3}| = |\sin \theta_{13}| < 0.2$ (90% CL).

One should also mention the LSND experiment [213], which claims evidence for $\nu_\mu \leftrightarrow \nu_e$ oscillations with parameters $\Delta m^2 = (0.2 - 2) \text{ eV}^2$ and $\sin^2 2\theta = (3 \times 10^{-3} - 3 \times 10^{-2})$. However this result, which cannot be accounted for together with the other neutrino oscillation data within the standard scheme of three-neutrino oscillation, is still controversial.

Finally, upper bounds on the absolute neutrino mass come from direct mass measurements, $m_{\nu_e} < 3 \text{ eV}$ [20]; CMB [46] and large scale structure data [47], $\sum_i m_{\nu_i} \lesssim 1 \text{ eV}$; and from neutrinoless double beta decay experiments which are sensitive to the effective neutrino mass $\langle m_\nu \rangle \equiv \sum_i m_{\nu_i} U_{ei}^2$, found to verify $\langle m_\nu \rangle \leq (0.35 - 1.05) \text{ eV}$ (90% CL) [214].

5.2.2 Classification of Models

One can classify the \mathcal{R}_p neutrino mass models according to the pattern of R -parity violation that they assume. We shall distinguish between models with trilinear couplings only, models with both bilinear and trilinear couplings, and models with bilinear couplings only. In the first class of models, bilinear R -parity violation is neglected, and neutrino masses and mixings arise at the one-loop level. A more realistic variant assumes the absence of bilinear R -parity violation at the GUT scale, and takes into account the tree-level contribution of the bilinear \mathcal{R}_p terms generated from the renormalization group evolution. In the second class of models, both bilinear and trilinear \mathcal{R}_p terms are present, and the neutrino mass matrix receives both tree-level and loop contributions. In the third class of models, R -parity violation can be parametrized in terms of bilinear \mathcal{R}_p couplings only. The neutrino mass matrix receives both tree-level and loop contributions, as in the second class of models.

5.2.2 a) Models with Trilinear Couplings only

In the limit where bilinear R -parity violation can be neglected, the only contributions to the neutrino mass matrix come from the (λ, λ) , or lepton-slepton, and (λ', λ') , or quark-squark loop diagrams, and are given by Eqs. (5.9) and (5.10) (cf. subsections 5.1.3 and 5.1.4). These expressions simplify to Eqs. (5.11) and (5.12) under the (very common) assumptions of proportionality of the A -terms to the Yukawa couplings and flavour-independence of sfermion masses. Despite the large number of arbitrary parameters involved in those formulae, trilinear R -parity violation leads to an interesting structure for the neutrino mass matrix, given by Eq. (5.17), when the hierarchy among trilinear couplings is mild or linked to the fermion mass hierarchy, and the λ -type couplings are not greater than the λ' -type couplings. Indeed the structure (5.17) can account for both the large atmospheric mixing angle (with $\lambda'_{233} \approx \lambda'_{333}$) and the hierarchy of oscillation frequencies $\Delta m_{\odot}^2 \ll \Delta m_{atm}^2$ (with Δm_{\odot}^2 determined by the subdominant contributions to M'_{loop} , governed by the charged lepton and down quark mass hierarchies). The correct scale of atmospheric neutrino oscillations is obtained for values of the \mathcal{R}_p couplings that could give rise to FCNC processes (see chapter 6) and to observable signals at colliders (see chapter 7).

As a prototype of model trying to explain atmospheric and solar neutrino oscillations in terms of trilinear \mathcal{R}_p couplings, let us discuss a model by Drees et al. [215]. Besides the standard assumptions on soft terms, the authors require that all \mathcal{R}_p trilinear couplings that are not forbidden by a symmetry be of comparable magnitude. While theoretically not well motivated, this hypothesis gives them some control on the subdominant contributions to the neutrino mass matrix. Note that the only way to account for the smallness of $|U_{e3}|$ consistently with their hypothesis is to set $\lambda'_{133} = 0$. Then, leaving aside the contribution of λ couplings, one obtains at leading order:

$$M'_{loop} \sim \frac{3m_b^2}{8\pi^2\tilde{m}} \lambda_{333}^2 \begin{pmatrix} \frac{m_s}{m_b} & \frac{m_s}{m_b} & \frac{m_s}{m_b} \\ \frac{m_s}{m_b} & 1 & 1 \\ \frac{m_s}{m_b} & 1 & 1 \end{pmatrix}, \quad (5.20)$$

where each entry in Eq. (5.20) should be multiplied by an arbitrary factor of order one, and the determinant of the lower right 2×2 sub-matrix is of order m_s/m_b . This structure is not altered when the contribution of λ -type couplings, which involves the charged lepton masses, is included. One typically obtains $m_{\nu_2}/m_{\nu_3} \sim m_s/m_b \sim 0.04$ (taking $m_s = 200$ MeV and $m_b = 5$ GeV), yielding a Δm_{\odot}^2 roughly in the MSW range, and a moderate to large solar mixing angle. This points towards the large mixing angle solution, which is precisely the only allowed

solution to the solar neutrino problem after the KamLAND results. Such a scenario would require λ' couplings in the $(5 \times 10^{-5} - 10^{-4}) (\tilde{m}/100 \text{ GeV})^{1/2}$ range, in order for $\Delta m_{atm}^2 \simeq m_{\nu_3}^2$ to fall in the allowed interval. Due to the hierarchy $m_{\nu_2} \ll m_{\nu_3}$ (a frequent feature of \mathcal{R}_p neutrino mass models), no measurable signal is expected for neutrinoless double beta decay. The required value of \mathcal{R}_p trilinear couplings, on the other hand, may give rise to sizeable FCNC decays such as $\mu \rightarrow e\gamma$ and $K^0 \rightarrow \mu e$, depending on the model. Signals at colliders are also expected, due to the decay of the LSP inside the detector – probably without an observable displaced vertex (see also Ref. [216]). In order to motivate the structure of Eq. (5.20), the authors of Ref. [215] try to find a discrete flavour symmetry allowing for the desired couplings, while forbidding λ'_{133} as well as the B -violating couplings λ''_{ijk} and the bilinear \mathcal{R}_p parameters μ_i . They are able to identify such a Z_3 symmetry, which however must be explicitly broken by the strange quark Yukawa coupling. This problem is generic for abelian discrete symmetries and makes their model less natural.

As discussed in sections 2.2 and 3.4, neglecting bilinear R -parity violation in the presence of trilinear \mathcal{R}_p couplings is not always a valid assumption, since the latter induce all types of bilinear \mathcal{R}_p parameters at the one-loop level [30, 31]. In particular, even if only trilinear \mathcal{R}_p couplings are present at the GUT scale, the renormalization group induced bilinear \mathcal{R}_p terms generally give the dominant contribution to the heaviest neutrino mass. This is the situation studied by Joshipura and Vempati in Ref. [217]. For simplicity only the λ'_{ijk} couplings and their associated A -terms are considered, and universality among soft terms is assumed at the GUT scale. At the weak scale, bilinear \mathcal{R}_p terms are generated and give a tree-level contribution to the neutrino mass matrix, which upon neglecting the scale-dependence of the soft parameters in the renormalization group evolution takes the form $(M_{tree}^\nu)_{ij} = m_0 a_i a_j$, where $a_i \equiv \sum_k \lambda'_{ikk} m_{d_k} / v_d$ in the $\mu_i = 0$ basis, and m_0 is determined by solving the renormalization group equations. At the one-loop level, the trilinear couplings give an additional contribution $(\Delta M_{loop}^\nu)_{ij} = m_1 \sum_{k,l} \lambda'_{ikl} \lambda'_{jlk} m_{d_k} m_{d_l} / v_d^2$, see Eq. (5.12) (other loop contributions are neglected). Depending on the MSSM parameters, the ratio m_1/m_0 varies between typical values of 10^{-3} and 10^{-1} ; in some regions of the parameter space cancellations in m_0 can lead to $m_1/m_0 > 1$. For $m_1/m_0 \sim (10^{-2} - 10^{-1})$ and $\lambda'_{ijk} \sim 10^{-4}$ (for small values of $\tan \beta$), one naturally obtains a neutrino mass spectrum compatible with both atmospheric neutrino data and the – now excluded – vacuum oscillation solution of the solar neutrino problem. MSW solutions can also be obtained provided $m_1/m_0 \sim 1$, which happens in a particular region of the MSSM parameter space.

Other examples of neutrino mass models based on trilinear R -parity breaking can be found in Refs. [186, 218, 219, 220]. The last reference also discusses two-loop contributions induced by both superpotential and soft trilinear \mathcal{R}_p couplings.

5.2.2 b) Models with both Bilinear and Trilinear Couplings

In the presence of all types of \mathcal{R}_p couplings, the neutrino mass matrix receives a tree-level contribution from bilinear \mathcal{R}_p terms, Eq. (5.5), and one-loop corrections involving both bilinear and trilinear \mathcal{R}_p couplings, as explained in section 5.1.3. In practice however most studies have omitted the loop diagrams containing bilinear \mathcal{R}_p mass insertions (such as the neutral loop diagrams of Fig. 5.3), thus keeping only the (λ, λ) and (λ', λ') loop contributions, Eqs. (5.9) and (5.10) (see however Ref. [187]).

Since flavour symmetries can constrain \mathcal{R}_p couplings, it is interesting to study their predictions for \mathcal{R}_p models of neutrino masses. The case of a $U(1)_X$ flavour symmetry has been

considered by Borzumati et al. [71] and by several other authors (see e.g. Refs. [37, 193, 221]). In this framework the order of magnitude of each \tilde{R}_p coupling is determined by the X -charge of the corresponding operator (see section 2.5 for details and notations): $\lambda_{ijk} \sim \epsilon^{\tilde{l}_i - \tilde{l}_0} \lambda_{jk}^e$, $\lambda'_{ijk} \sim \epsilon^{\tilde{l}_i - \tilde{l}_0} \lambda_{jk}^d$, $\tilde{m}_{\alpha\beta}^2 \sim \tilde{m}^2 \epsilon^{|\tilde{l}_\alpha - \tilde{l}_\beta|}$ and $B_\alpha/\tilde{m} \sim \mu_\alpha \sim \tilde{m} \epsilon^{\tilde{l}_\alpha}$, where \tilde{m} is the typical scale associated with the soft supersymmetry-breaking terms, $\epsilon \simeq V_{us} = 0.22$, $\tilde{l}_\alpha \equiv |l_\alpha + h_u|$, and the generations of leptons are labelled in such a way that $\tilde{l}_0 < \tilde{l}_3 \leq \tilde{l}_{1,2}$. The flavour symmetry ensures an approximate alignment of the doublet VEVs v_α along the superpotential mass parameters μ_α , resulting in a misalignment angle $\sin^2 \xi \sim \epsilon^{2(\tilde{l}_3 - \tilde{l}_0)}$; still large lepton X -charges are necessary in order for neutrino masses to reach the phenomenologically interesting range. Keeping only the (λ, λ) and (λ', λ') diagrams at the one-loop level, one finds the following structure for the neutrino mass matrix,

$$M_{ij}^\nu \sim (m_0 \delta_{i3} \delta_{j3} + m_1) \epsilon^{\tilde{l}_i + \tilde{l}_j - 2\tilde{l}_0}, \quad (5.21)$$

where $m_0 \sim (100 \text{ GeV}) (100 \text{ GeV}/\tilde{m}) \epsilon^{2\tilde{l}_0}$ is associated with the tree-level contribution, and $m_1 \sim (5 \text{ keV}) (m_b/4.5 \text{ GeV})^4 (100 \text{ GeV}/\tilde{m}) \epsilon^{-2\tilde{l}_0}$ with the one-loop contribution. The neutrino masses and mixing angles are then given by $m_{\nu_3} \sim m_0 \epsilon^{2(\tilde{l}_3 - \tilde{l}_0)}$, $m_{\nu_2} \sim m_1 \epsilon^{2(\tilde{l}_2 - \tilde{l}_0)}$, $m_{\nu_1} \sim m_1 \epsilon^{2(\tilde{l}_1 - \tilde{l}_0)}$ and $\sin \theta_{ij} \sim \epsilon^{|\tilde{l}_i - \tilde{l}_j|}$ ($i \neq j$). The mass spectrum is characterized by a large hierarchy $m_{\nu_2} \ll m_{\nu_3}$. For this model to account for atmospheric and solar neutrino oscillations, one would need both large values of the lepton charges, with $\tilde{l}_3 = 9$ or 10 , and $\tilde{l}_0 \geq 2$, which corresponds to $\tan \beta \gtrsim 20$ (indeed $\tan \beta \sim \epsilon^{-\tilde{l}_0}$). Since the large atmospheric mixing angle favours $\tilde{l}_2 = \tilde{l}_3$, the – now excluded – low Δm_\odot^2 solution is selected for $\tilde{l}_0 = 2$. Then, in order to account for the large solar mixing angle, $|U_{e3}|$ should be close to its present limit. The large mixing angle solution can be accommodated for $\tilde{l}_2 = \tilde{l}_3 + 1$, which is marginally compatible with the large atmospheric mixing angle, and $\tilde{l}_0 = 3$. This discussion neglects the contribution of the diagrams with \tilde{R}_p mass insertions, however. As noticed in Ref. [193], the diagrams of Fig. 5.3 dominate over the (λ', λ') diagrams in a large portion of the parameter space. If one assumes a moderate cancellation between the different Higgs loops, it becomes possible to accommodate the large mixing angle solution to the solar neutrino problem together with the large atmospheric mixing angle.

Other examples of neutrino mass models based on both trilinear and bilinear R -parity breaking can be found in Refs. [187, 222, 223, 224, 225].

5.2.2 c) Models with Bilinear Couplings only

The above discussion clearly shows that models of neutrino masses based on the most general \tilde{R}_p mass terms and couplings suffer from a lack of predictivity. This led several authors [39, 40, 185, 186, 189, 226, 227, 228, 229] to consider the so-called “bilinear R -parity breaking” scenario, in which one assumes that the only seed of R -parity violation resides in the bilinear superpotential and soft terms (see section 2.2). This scenario yields only one massive neutrino at tree level with the flavour composition of Eq. (5.7). Radiative corrections to the neutralino-neutrino mass matrix then generate the other two masses and the solar mixing angle, while slightly modifying the heaviest neutrino state. In order to accommodate the atmospheric neutrino mass scale, these studies generally assume universality of the soft terms at the GUT scale [39, 40, 189] (or at the messenger scale in the context of gauge-mediated supersymmetry breaking [185, 186]) together with the smallness of the \tilde{R}_p parameters, with typically $\mu_i/\mu (M_{GUT}) \leq 10^{-3}$. The second assumption is crucial for obtaining $m_{\nu_{tree}} = \sqrt{\Delta m_{atm}^2} \sim 0.05 \text{ eV}$. Indeed, while the universality conditions lead to an

exact alignment between the superpotential mass parameters μ_α and the doublet VEVs v_α at the GUT scale, radiative corrections induce some amount of non-universality among the soft terms at the weak scale, which spoils this alignment and induces a nonzero neutrino mass. For $\mu_i(M_{GUT}) \sim \mu(M_{GUT})$, however, the resulting neutrino mass would lie in the range $100 \text{ eV} \leq m_{\nu_{tree}} \leq 100 \text{ MeV}$ [39, 40], well above the atmospheric neutrino scale. This is the reason why $\mu_i \ll \mu$ is required at M_{GUT} . Note that the universality assumption reduces the number of independent \tilde{R}_p parameters to only 3, which one can choose to be the three \tilde{R}_p supersymmetric masses at the GUT scale, $\epsilon_i \equiv \mu_i(M_{GUT})$.

A detailed study of this model has been presented in Ref. [189]. The authors define an alignment vector $\Lambda_i \equiv (\mu v_i - v_d \mu_i)|_{M_{weak}}$, which parametrizes the misalignment induced at the weak scale by the renormalization group evolution of the soft terms (in the $\epsilon_i \ll \mu$ limit that we are considering, this alignment vector is related to the misalignment angle ξ defined in subsection 2.3.1 by $\sum_i \Lambda_i^2 \simeq \mu^2 v_d^2 \sin^2 \xi$). The tree-level neutrino mass matrix is given by Eq. (5.5), with the replacement $\mu_i \rightarrow \Lambda_i$. In the regime where $\sum_i \epsilon_i^2 \ll \sqrt{\sum_i \Lambda_i^2}$ and $\epsilon_2 \Lambda_2 / \epsilon_3 \Lambda_3 < 0$, the one-loop corrections are small and do not spoil the structure of the tree-level neutrino mass matrix. Thus the atmospheric neutrino parameters are essentially determined by the Λ_i , with $m_{\nu_3} \sim \sum_i \Lambda_i^2 / \mu^2 M_2$, $\tan \theta_{23} \approx \Lambda_2 / \Lambda_3$ and $|U_{e3}| = \sin \theta_{13} \approx \Lambda_1 / \sqrt{\sum_i \Lambda_i^2}$. Consistency with experimental data requires $\Lambda_1 \ll \Lambda_2 \approx \Lambda_3$ and $\sqrt{\sum_i \Lambda_i^2} \sim 0.1 \text{ GeV}^2$ (the second constraint depends on the values of the supersymmetry parameters). As for the solar neutrino parameters, they are determined by the one-loop corrections to the neutralino-neutrino mass matrix, controlled by the ratios ϵ_i / μ : Δm_{21}^2 is a function of $\sqrt{\sum_i \epsilon_i^2} / \mu$, while θ_{12} depends on $\epsilon_1 / \sqrt{\epsilon_2^2 + \epsilon_3^2}$. In the case of universal boundary conditions at M_{GUT} , the Λ_i / Λ_j are correlated with the ϵ_i / ϵ_j , so that the CHOOZ limit on $|U_{e3}|$ constrains the solar mixing angle to be small. A departure from the universality hypothesis is therefore necessary to accommodate the large mixing angle solution (see Ref. [230] for a more recent analysis of this model).

Interestingly, this scenario can be checked at colliders such as the LHC or a future linear collider [50, 51, 189]. Indeed, for the required values of the ϵ_i , the lightest neutralino (assumed to be the LSP) should decay within the detector. Furthermore, the ratios of branching ratios for semi-leptonic decays into different charged leptons show some correlation with the lepton mixing angles. In particular, $\text{BR}(\tilde{\chi}_1^0 \rightarrow \mu q \bar{q}') / \text{BR}(\tilde{\chi}_1^0 \rightarrow \tau q \bar{q}')$ is strongly correlated with $\tan \theta_{23}$, irrespective of the lightest neutralino mass [50, 189]. The experimentally allowed range for the atmospheric mixing angle indicate that this ratio should be of order one. Similarly, $\text{BR}(\tilde{\chi}_1^0 \rightarrow e q \bar{q}') / \text{BR}(\tilde{\chi}_1^0 \rightarrow \tau q \bar{q}')$ and to a smaller extent $\text{BR}(\tilde{\chi}_1^0 \rightarrow e \tau \nu_i) / \text{BR}(\tilde{\chi}_1^0 \rightarrow \mu \tau \nu_i)$ are correlated with $|U_{e3}|$ and $\tan \theta_{12}$, respectively [51]. Since the solar mixing angle is large, $\text{BR}(\tilde{\chi}_1^0 \rightarrow e \tau \nu_i) / \text{BR}(\tilde{\chi}_1^0 \rightarrow \mu \tau \nu_i)$ should be of order one. All above branching ratios, except $\text{BR}(\tilde{\chi}_1^0 \rightarrow e q \bar{q}')$, are larger than $(10^{-4} - 10^{-3})$ and it should be possible to measure them. Other collider signatures of this scenario are discussed in Refs. [52, 54, 231].

The weakness of this scenario is that there is no a priori reason for the absence of trilinear \tilde{R}_p couplings, nor for the smallness of the ϵ_i . To cure this problem, one may invoke spontaneous R -parity breaking, or an abelian flavour symmetry [232].

A model with soft bilinear couplings only

In Ref. [233], another option has been explored, namely the possibility that R -parity is broken by soft bilinear terms only. This scenario has 6 parameters (3 B_i and 3 \tilde{m}_{di}^2 , or equivalently 3 B_i and 3 v_i) but does not assume anything about the structure of the soft terms, contrary to the previous ‘‘bilinear R -parity breaking’’ scenario, whose predictivity relies on the universality assumption at the GUT scale. In addition to the tree-level contribution, the neutrino mass

matrix receives contributions from the neutral loop diagrams from class (ii), in the classification of subsection 5.1.4. The other loop contributions, class (i) and class (iii), are negligible for low values of $\tan\beta$. The tree-level and loop contributions are governed by the quantities $\delta_\mu^i \equiv v_i/v_d$ and $\delta_B^i \equiv (Bv_i - B_i v_d)/v_d \sqrt{B^2 + \sum_i B_i^2}$, respectively. To make the connection with the misalignment angles ξ and ζ defined in subsection 2.3.3, note that $\sum_i (\delta_\mu^i)^2 = \sin^2 \xi$ and $\sum_i (\delta_B^i)^2 = \sin^2 \zeta$.

In the limit where the subleading loop diagrams are neglected, only two neutrinos are massive. Depending on the values of the various parameters, the heaviest neutrino mass is determined either by the tree-level or the loop contribution. Both atmospheric and solar neutrino data can be accommodated, but the required values of the soft bilinear \tilde{R}_p parameters are very small, with $|\delta_\mu^i| \leq 8 \times 10^{-7}$ and $|\delta_B^i| \leq 3 \times 10^{-5}$. In the absence of a specific mechanism that would explain the weakness of R -parity violation in the soft terms, it is difficult to motivate such small values.

5.3 Neutrino Transition Magnetic Moments

Massive neutrinos can have magnetic dipole moments (and also electric dipole moments if CP is violated). Since the magnetic moment of a neutrino is induced by loop diagrams involving a chirality flip, it is generally proportional to its mass and therefore very tiny. For instance, a Dirac neutrino with no interaction beyond the Standard Model has $\mu_\nu = 3eG_F m_\nu / 8\sqrt{2}\pi^2 \simeq 3.2 \times 10^{-19} (m_\nu / \text{eV}) \mu_B$ [234, 235], where $\mu_B \equiv e/2m_e$ is the Bohr magneton, to be compared with a laboratory limit of $\mu_\nu < 1.0 \times 10^{-10} \mu_B$ at 90% C.L. [20]. In the case of Majorana neutrinos – relevant for supersymmetry without R -parity – only transition dipole moments $\mu_{\nu_i \nu_j}$, $i \neq j$ are allowed (the coefficients $\mu_{\nu_i \nu_j}$ of the effective operators $\bar{\nu}_i \sigma^{\mu\nu} \nu_j F_{\mu\nu}$ are antisymmetric in (i, j) due to the Majorana nature of the neutrino). These correspond to transitions between a left-handed neutrino and a right-handed (anti)neutrino with different flavours, and mediate radiative neutrino decays $\nu_i \rightarrow \nu_j \gamma$. Neutrino transition magnetic moments have several implications in astrophysics; in particular, they can induce spin-flavour transitions such as $\nu_{eL} \rightarrow \nu_{\mu R}^c$ or $\nu_{\mu L} \rightarrow \nu_{eR}^c$ in the solar magnetic field [236, 237]. However this possibility is strongly constrained by solar neutrino and KamLAND data, from which the bound $\mu_\nu \lesssim (10^{-12} - 10^{-11}) \mu_B$, similar to other astrophysical bounds, has been derived [238]. Still obtaining such a large value for μ_ν while keeping small neutrino masses in explicit models is a theoretical challenge.

In \tilde{R}_p models, transition magnetic moments are generated from the trilinear couplings λ_{ijk} and λ'_{ijk} via lepton-slepton and quark-squark loops [182, 239]. The corresponding diagrams only differ from the ones responsible for neutrino masses by an additional photon vertex attached to an internal line. As a consequence, an upper bound on $\mu_{\nu_i \nu_j}$ depending on the neutrino masses can be derived. Barring accidental cancellations between different contributions to the neutrino mass matrix, and assuming a conservative upper bound of 10 eV for each M_{ij}^ν , one finds [239] $|\mu_{\nu_e \nu_\mu}| \leq \mathcal{O}(10^{-13} \mu_B)$ for light sleptons (squarks), much above the Standard Model value. This bound can be saturated only if the mass scales involved in atmospheric and solar neutrino oscillations result from accurate degeneracies among neutrino masses.

An interesting mechanism for avoiding the constraining proportionality between the mass and magnetic moment of a Dirac neutrino is to postulate an approximate $SU(2)_\nu$ symmetry under which ν_L and ν_L^c (the CP conjugate of ν_R) form a doublet [240]. The Lorentz structure of interaction terms is then such that the electromagnetic dipole moment operator $\nu_L^T C \sigma^{\mu\nu} \nu_L^c$ is antisymmetric under $\nu_L \leftrightarrow \nu_L^c$ and transforms as a singlet of $SU(2)_\nu$, while the Dirac mass

operator $\nu_L^T C \nu_L^c$ is symmetric and transforms as a triplet. Thus, in the $SU(2)_\nu$ symmetric limit, μ_ν can be nonzero while m_ν vanishes.

Babu and Mohapatra [241] have generalized this mechanism to Majorana neutrinos by replacing $SU(2)_\nu$ with an horizontal $SU(2)_H$ flavour symmetry acting on the first two generations of leptons. In a \mathcal{R}_p model [182], they consider a discrete version of this symmetry, namely the Z_2 flavour group acting on the electroweak doublet and singlet lepton fields of the first two generations as $(L_e, L_\mu) \rightarrow (L_\mu, -L_e)$, $(e_L^c, \mu_L^c) \rightarrow (\mu_L^c, -e_L^c)$, with all other fields left invariant. In combination with the assumption of conservation of the lepton number difference $L_e - L_\mu$, this leads to a large transition magnetic moment $\mu_{\nu_e \nu_\mu}$ together with vanishing masses for the first two generation neutrinos. At the same time, however, the Z_2 symmetry yields $m_e = m_\mu$. This can be cured by assuming a soft breaking of Z_2 in the slepton sector. Then a contribution to the transition moment as large as $\mu_{\nu_e \nu_\mu} \approx (10^{-11} - 10^{-10}) \mu_B$, consistent with light neutrino masses, $m_{\nu_e}, m_{\nu_\mu} < 10$ eV, and with the observed value of the splitting between the electron and muon masses, $m_\mu - m_e$, can be achieved at the price of a fine-tuning in the slepton mass matrices.

Motivated by the desire of avoiding an unnatural fine-tuning, Barbieri et al. [239] consider the continuous $SU(2)_H$ flavour symmetry to be broken solely by the Yukawa couplings of the electron and the muon. The mismatch $\lambda_{11}^e \neq \lambda_{22}^e$ results in the splitting $(\tilde{m}_{LR}^{e2})_{11} - (\tilde{m}_{LR}^{e2})_{22} \neq 0$ necessary to generate masses for the first two generation neutrinos, while a large transition magnetic moment $\mu_{\nu_e \nu_\mu}$ can be obtained by requiring $(\tilde{m}_{LR}^{e2})_{11} \simeq (\tilde{m}_{LR}^{e2})_{22} \gg |(\tilde{m}_{LR}^{e2})_{11} - (\tilde{m}_{LR}^{e2})_{22}|$. However $(\tilde{m}_{LR}^{e2})_{11}$ is bounded by its contribution to the one-loop corrections to the electron mass, resulting in the upper bound $\mu_{\nu_e \nu_\mu} \leq \mathcal{O}(10^{-12} \mu_B)$. Therefore, even with the help of suitable symmetries, the neutrino transition magnetic moment generated by \mathcal{R}_p couplings happens to be at least 2 orders of magnitude smaller than the present laboratory upper bound.

5.4 Neutrino Flavour Transitions in Matter Induced by \mathcal{R}_p Interactions

The oscillations of neutrinos in matter are affected by their interactions with the medium. The most familiar illustration of this phenomenon is the Mikheev-Smirnov-Wolfenstein (MSW) mechanism [206, 207], i.e. the enhancement of neutrino oscillations inside the sun due to their coherent forward scatterings on electrons and nucleons. Since the charged current interactions only contribute to scatterings of electron neutrinos, the electron neutrinos on one side, and the muon and tau neutrinos on the other side have different scattering amplitudes on electrons, which results in oscillation parameters in matter different from the oscillation parameters in vacuum.

Similarly, any non-standard interaction of neutrinos with the charged leptons and down quarks, such as \mathcal{R}_p interactions [242, 243], modifies neutrino oscillations in matter. For instance the couplings λ'_{131} and λ'_{331} contribute to the scattering processes $\nu_e d \rightarrow \nu_e d$ and $\nu_\tau d \rightarrow \nu_\tau d$, respectively, and the corresponding amplitudes are different as soon as $\lambda'_{131} \neq \lambda'_{331}$. Moreover these couplings, if both present, induce the flavour-changing scatterings $\nu_e d \rightarrow \nu_\tau d$. It follows that \mathcal{R}_p interactions can induce flavour transitions of neutrinos inside the sun or the Earth, even if neutrinos are massless and do not oscillate in vacuum.

Several authors have studied the possibility of accounting for the solar and atmospheric neutrino data with \mathcal{R}_p -induced flavour transitions, or more generally with non-standard neutrino interactions. While flavour-changing non-standard neutrino interactions can only play a

subleading rôle with respect to oscillations in the atmospheric neutrino sector [244], several authors have found that they could be responsible for the solar neutrino deficit (for recent studies, see Refs. [245, 246, 247, 248, 249]), although the case of pure \mathcal{R}_p -induced flavour transitions is strongly disfavoured by the SNO data [249]. However, the KamLAND results have showed that neutrinos in the solar neutrino energy range oscillate in vacuum with parameters consistent with the large mixing angle MSW solution, leaving only the possibility that \mathcal{R}_p -induced flavour transitions contribute as a subdominant effect.

5.5 $\Delta L = 2$ Sneutrino Masses and Sneutrino-Antisneutrino Mixing

Supersymmetry breaking $\Delta L = 2$ sneutrino mass terms, parametrized by the Lagrangian terms $-\frac{1}{2}(\tilde{m}_{\Delta L=2}^2)_{ij}\tilde{\nu}_i\tilde{\nu}_j + \text{h.c.}$ [184, 250], are expected in any supersymmetric model with nonzero neutrino Majorana masses. These terms induce a mass splitting and a mixing between the sneutrino and the antisneutrino of a same generation, which gives rise to characteristic experimental signatures such as sneutrino-antisneutrino oscillations. In the one-generation case, the sneutrino mass splitting is given by $\Delta m_{\tilde{\nu}}^2 \equiv m_{\tilde{\nu}_2}^2 - m_{\tilde{\nu}_1}^2 = 2\tilde{m}_{\Delta L=2}^2$, where the mass eigenstates $\tilde{\nu}_1$ and $\tilde{\nu}_2$ are linear combinations of $\tilde{\nu}$ and $\tilde{\nu}^c$.

In supersymmetric models with bilinear R -parity violation, the sneutrinos mix with the neutral Higgs bosons, which leads to \not{R} sneutrino-antisneutrino mixing at the tree level. Under the assumption of CP conservation, it is convenient to deal with the sneutrino CP eigenstates rather than with the lepton number eigenstates $\tilde{\nu}$ and $\tilde{\nu}^c$. The CP -even sneutrinos $\nu_{+i} \equiv (\tilde{\nu}_i + \tilde{\nu}_i^c)/\sqrt{2}$ mix with the CP -even Higgs bosons h and H , and the CP -odd sneutrinos $\nu_{-i} \equiv -i(\tilde{\nu}_i - \tilde{\nu}_i^c)/\sqrt{2}$ with the CP -odd Higgs boson A and with the Goldstone boson that in the absence of R -parity violation is absorbed by the Z boson. As a result the mass degeneracy between the CP -even and CP -odd sneutrinos of each generation is broken. The sneutrino mass splitting within each generation reads, if one neglects flavour mixing [38]:

$$\Delta m_{\tilde{\nu}_i}^2 \equiv m_{\tilde{\nu}_{+i}}^2 - m_{\tilde{\nu}_{-i}}^2 = \frac{4B_i^2 M_Z^2 m_{\tilde{\nu}_i}^2 \sin^2 \beta}{(m_{\tilde{\nu}_i}^2 - m_H^2)(m_{\tilde{\nu}_i}^2 - m_h^2)(m_{\tilde{\nu}_i}^2 - m_A^2)}, \quad (5.22)$$

where $m_{\tilde{\nu}_i}^2 = (M_L^2)_{ii} + \mu_i^2 - \frac{1}{8}(g^2 + g'^2)(v_u^2 - v_d^2)$, and as usual we are working in a (H_d, L_i) basis in which the sneutrino VEVs v_i vanish. In this basis $\Delta m_{\tilde{\nu}_i}^2$ is proportional to the square of the \mathcal{R}_p soft terms B_i ; therefore the contribution of bilinear R -parity violation to the sneutrino-antisneutrino mixing is controlled by the misalignment between the 4-vectors $B_\alpha \equiv (B_0, B_i)$ and $v_\alpha \equiv (v_0, v_i)$ (see subsection 2.3.1). At the one-loop level, $\Delta m_{\tilde{\nu}_i}^2$ receives additional contributions from the trilinear \mathcal{R}_p couplings λ and λ' and from their associated soft parameters A and A' . In practice $\Delta m_{\tilde{\nu}_i}^2 \ll m_{\tilde{\nu}_i}^2$ and one can write $\Delta m_{\tilde{\nu}_i} \equiv m_{\tilde{\nu}_{+i}} - m_{\tilde{\nu}_{-i}} \simeq \Delta m_{\tilde{\nu}_i}^2 / 2m_{\tilde{\nu}_i}$.

Sneutrino-antisneutrino mixing and neutrino masses are closely linked at the one-loop order. A Majorana neutrino mass term induces radiatively a sneutrino mass splitting term and vice-versa. Taking these effects into account, one finds [38] that for generic model parameters the sneutrino mass splitting to neutrino mass ratio $\frac{\Delta m_{\tilde{\nu}}}{m_\nu}$ falls in the interval

$$10^{-3} \lesssim \frac{\Delta m_{\tilde{\nu}}}{m_\nu} \lesssim 10^3. \quad (5.23)$$

Cancellations between the tree-level and one-loop contributions to m_ν may enhance this ratio, thus allowing for larger sneutrino mass splittings at the price of a fine-tuning. Furthermore there arise strong pairwise correlations, of nearly linear character, between the contributions to the Majorana neutrino masses, the $\Delta L = 2$ sneutrino masses and the neutrinoless double beta decay amplitudes. Hirsch et al. [251] find in the framework of the R -parity conserving Supersymmetric Standard Model that the induced effect of $\tilde{m}_{\Delta L=2}$ on neutrinoless double beta decay imposes the bound $\tilde{m}_{\Delta L=2} < 2 \text{ GeV} (\tilde{m}/100 \text{ GeV})^{3/2}$, resp. $\tilde{m}_{\Delta L=2} < 11 \text{ GeV} (\tilde{m}/100 \text{ GeV})^{7/2}$, in the extreme case where the lightest neutralino is a pure bino, resp. a pure higgsino (all superpartner masses assumed equal to \tilde{m}). Another bound, $\tilde{m}_{\Delta L=2} < (60 - 125) \text{ MeV} (m_\nu/1 \text{ eV})^{1/2}$, is associated with the one-loop contribution to the neutrino mass induced by $\tilde{m}_{\Delta L=2}$. These bounds, which can be converted into bounds on $\Delta m_{\tilde{\nu}}$ via $\Delta m_{\tilde{\nu}} \simeq \tilde{m}_{\Delta L=2}/m_{\tilde{\nu}}$, also apply in the \mathcal{R}_p case.

The phenomenological implications of the sneutrino-antisneutrino mass splittings and mixings have been examined in recent works [184, 38, 250]. For large mass splittings, $\Delta m_{\tilde{\nu}} > 1 \text{ GeV}$, the sneutrino pair production at colliders could be tagged through the leptonic decays of the sneutrinos resulting in characteristic charged dilepton final states [184] through the decay modes $\tilde{\nu} \rightarrow e^\pm \tilde{\chi}^\mp$. Interesting signals could also arise from the resonant sneutrino or antisneutrino production [252] in e^+e^- or $q\bar{q}$ collisions. The corresponding off-shell sneutrino or antisneutrino exchange processes could also be observed via the fermion-antifermion pair production reactions, $e^+e^- \rightarrow \tilde{\nu}, \tilde{\nu}^c \rightarrow f\bar{f}$, at high energy lepton colliders and similarly at hadron colliders [38, 253].

For small mass splittings, $\Delta m_{\tilde{\nu}} \ll 1 \text{ GeV}$, sneutrino-antisneutrino oscillations could rise to a measurable level provided that the oscillation time is shorter than the sneutrino lifetime, corresponding to $x_\nu \equiv \frac{\Delta m_{\tilde{\nu}}}{\Gamma_{\tilde{\nu}}} > 1$. By analogy with the $B - \bar{B}$ system, the production of a sneutrino-antisneutrino pair would be signaled by characteristic like-sign dileptons, provided that the branching ratios of the decay modes $\tilde{\nu} \rightarrow e^\pm \tilde{\chi}^\mp$ are appreciable [184].

Bar-Shalom et al. [253] have developed an interesting test for the \mathcal{R}_p -induced resonant production of sneutrinos at leptonic and hadronic colliders. Based on the current sensitivity reaches, a mere observation of deviations with respect to the Standard Model predictions for the tau-antitau lepton pair production reactions $e^+e^- \rightarrow \tilde{\nu} \rightarrow \tau^+\tau^-$, resp. $p\bar{p} \rightarrow \tilde{\nu} \rightarrow \tau^+\tau^- + X$, would lead to bounds on coupling products of the form $\lambda_{232}\lambda'_{311} < 0.003$, resp. $\lambda_{232}\lambda'_{322} < 0.011$. In the presence of CP violation among \mathcal{R}_p couplings, the $\tilde{\nu}-\tilde{\nu}^c$ mixing could contribute to the CP -odd double spin correlation observables associated with the spin polarisation of the $\tau^+\tau^-$ pair. Nonzero and large contributions arise already at the tree level, thanks to the complex phase dependence provided by the spatial azimuthal angle. Analogous CP -even double spin correlation observables may also be induced through the same type of \mathcal{R}_p interactions.

Altogether, we have seen how the violation of R -parity in supersymmetric theories naturally leads to massive neutrinos. The fact that \mathcal{R}_p models automatically incorporate massive neutrinos, while allowing for observable signals at colliders for the values of \mathcal{R}_p couplings suggested by neutrino data, is certainly an appealing feature of R -parity violation. However, the smallness of neutrino masses dictates strong constraints on \mathcal{R}_p couplings, especially on bilinear \mathcal{R}_p couplings, while \mathcal{R}_p supersymmetric models also suffer from a lack of predictivity in the neutrino sector. This motivates the study of restricted scenarios such as the “bilinear R -parity breaking” scenario, which are more predictive. We have also seen that, given the acceptable neutrino masses, the neutrino transition magnetic moments generated from \mathcal{R}_p couplings generally lie well below the current laboratory upper limit. Finally, \mathcal{R}_p couplings induce $\Delta L = 2$ sneutrino mass terms, which leads to mass splittings and mixings between sneutrinos and antisneutrinos and gives rise to sneutrino-antisneutrino oscillations.

Chapter 6

INDIRECT BOUNDS ON R -parity ODD INTERACTIONS

The assumption of a broken R -parity introduces in the Supersymmetric Standard Model new interactions between ordinary particles and supersymmetric particles, which can contribute to a variety of low, intermediate and high energy processes that do not involve the production of superpartners in the final state. Requiring that the \mathcal{R}_p contribution to a given observable does not exceed the limit imposed by the precision of the experimental measurement and by the theoretical uncertainties on the Standard Model prediction (or, for a process that has not been observed, that it does not exceed the experimental upper limit), yields upper bounds on the \mathcal{R}_p couplings involved. In addition to the bounds associated with renormalization group effects and with astrophysics and cosmology, discussed in chapters 3 and 4, and with the direct limits extracted from supersymmetry searches at colliders, to be discussed in chapter 7, these indirect bounds provide useful information on the possible patterns of R -parity violation.

In this chapter, we give a comprehensive review of the indirect bounds on \mathcal{R}_p interactions coming from low, intermediate and high energy particle phenomenology, as well as from nuclear and atomic physics observables. This complements and updates other existing reviews, e.g. Refs. [254, 255, 256, 257, 258, 259, 260].

The chapter is organised in five main sections. In section 6.1, the assumptions under which the bounds on \mathcal{R}_p couplings have been extracted are presented, and issues concerning quark and lepton superfield bases are addressed, in particular in connection with the single coupling dominance hypothesis. A basis-independent parametrization of R -parity violation is also presented, as an alternative to the choice made in this review. Section 6.2 deals with the constraints on bilinear \mathcal{R}_p parameters, both for an explicit breaking and in the case of a spontaneous R -parity breaking. Section 6.3 reviews the indirect bounds on trilinear \mathcal{R}_p couplings associated with fundamental tests of the Standard Model in charged current and neutral current interactions, with CP violation and with high precision measurements of electroweak observables. In section 6.4 the constraints on trilinear \mathcal{R}_p interactions coming from a variety of hadron flavour or lepton flavour violating processes, and B or L violating processes are presented. Finally, section 6.5 provides a list of the indirect bounds on trilinear \mathcal{R}_p couplings presented in chapters 3 and 5 and in this chapter. The robustness and significance of these bounds are discussed.

6.1 Assumptions and Framework

Our main focus in this chapter will be on the R -parity odd renormalizable superpotential couplings μ_i , λ_{ijk} , λ'_{ijk} and λ''_{ijk} , defined in Eq. (2.2). The simultaneous presence of bilinear and trilinear \mathcal{R}_p terms results in an ambiguity in the choice of a basis for the down-type Higgs and lepton doublet superfields (H_d , L_i), an issue already addressed in subsections 2.1.4 and 2.3.1. In this chapter we adopt a superfield basis in which the VEVs of the sneutrino fields vanish and, unless otherwise stated, the charged lepton Yukawa couplings are diagonal (see the discussion at the beginning of subsection 6.2.1).

6.1.1 The Single Coupling Dominance Hypothesis

Most of established indirect bounds on the trilinear couplings λ_{ijk} , λ'_{ijk} and λ''_{ijk} have been derived under the so-called single coupling dominance hypothesis, where a single \mathcal{R}_p coupling is assumed to dominate over all the others. This useful working hypothesis can be rephrased by saying that each of the \mathcal{R}_p couplings contributes one at a time [254, 261]. The perturbative constraints arising from contributions at loop order l then involve upper bounds on combinations of \mathcal{R}_p couplings and superpartner masses of the form $\frac{\hat{\lambda}^p}{\tilde{m}^q} (\frac{\hat{e}^2}{(4\pi)^2})^l$, where $\hat{\lambda}$, \hat{e} , \tilde{m} are generic symbols for \mathcal{R}_p couplings, gauge couplings and superpartner masses, and the power indices $p \geq 2$, $q \geq 2$ depend on the underlying mechanism. Apart from a few isolated cases, the bounds derived under the single coupling dominance hypothesis are in general moderately strong. The typical orders of magnitude are $\lambda, \lambda', \lambda'' < (10^{-2} - 10^{-1}) \frac{\tilde{m}}{100 \text{ GeV}}$, involving generically a linear dependence on the superpartner mass.

The constraints based on the single coupling dominance hypothesis deal with a somewhat restricted set of applications, such as charged current or neutral current gauge interactions, neutrinoless double beta decay and neutron-antineutron oscillation. By contrast, a much larger fraction of the current constraints on \mathcal{R}_p interactions are derived from extended hypotheses where the dominance is postulated for quadratic or quartic products of couplings. The literature abounds with bounds involving a large variety of flavour configurations for quadratic products of the coupling constants. The processes that yield constraints on products of \mathcal{R}_p couplings can be divided into four main classes: (i) hadron flavour changing processes, such as oscillations of neutral flavoured mesons, and leptonic or semileptonic decays of K or B mesons like $K \rightarrow e_i \bar{e}_j$ and $K \rightarrow \pi \nu \bar{\nu}$; (ii) lepton flavour changing processes, such as $\mu^- \rightarrow e^-$ conversion in nuclei, or radiative decays of charged leptons; (iii) L -violating processes, such as neutrinoless double beta decay, neutrino Majorana masses and mixings (cf. chapter 5), or three-body decays of charged leptons, $l_l^\pm \rightarrow l_n^\pm l_p^\pm$; (iv) B -violating processes, such as nucleon decay, neutron-antineutron oscillations, double nucleon decay or some rare decays of heavy mesons.

6.1.2 Choice of the Lepton and Quark Superfield Bases

When discussing specific bounds on coupling constants, it is necessary to choose a definite basis for quark and lepton superfields, especially if the single coupling dominance hypothesis is used. Two obvious basis choices can be made for quark superfields: the current (or weak eigenstate) basis, in which left-handed quarks have flavour diagonal couplings to the W gauge boson, and the “super-CKM” basis, in which quark mass matrices are diagonal. A similar distinction between weak eigenstate basis and mass eigenstate (or “super-MNS”) basis exists for leptons

when neutrino masses are taken into account. In most studies, it is tacitly understood that the single coupling dominance hypothesis applies in the mass eigenstate basis. It may appear more natural, however, to apply this hypothesis in the weak eigenstate basis when dealing with models in which the hierarchy among (weak-eigenstate-basis) couplings originates from some flavour theory. In this case, a single process may allow to constrain several couplings, provided one has some knowledge of the rotations linking the weak eigenstate and mass eigenstate bases [262].

It is useful to write down the trilinear \mathcal{R}_p superpotential terms in the two superfield bases. Let us first consider the LQD^c terms. We denote by $\hat{\lambda}'_{ijk}$ the corresponding couplings expressed in the weak eigenstate basis, and by λ'^A_{ijk} and λ'^B_{ijk} the same couplings in two useful representations of the mass eigenstate basis:

$$\begin{aligned} W^{(\lambda')} &= \hat{\lambda}'_{ijk}(\hat{N}_i\hat{D}_j - \hat{E}_i\hat{U}_j)\hat{D}_k^c = \lambda'^A_{ijk}(\hat{N}_iD'_j - \hat{E}_iU_j)D_k^c = \lambda'^B_{ijk}(\hat{N}_iD_j - \hat{E}_iU'_j)D_k^c, \\ \lambda'^A_{ijk} &= \hat{\lambda}'_{imn}(V_L^{u\dagger})_{mj}(V_R^{dT})_{nk}, \quad D'_j = V_{jl}D_l, \\ \lambda'^B_{ijk} &= \hat{\lambda}'_{imn}(V_L^{d\dagger})_{mj}(V_R^{dT})_{nk}, \quad U'_j = V_{jl}^\dagger U_l. \end{aligned} \quad (6.1)$$

In (6.1), hatted superfields are in the weak eigenstate basis and unhatted superfields in the mass eigenstate basis; V_L^u , V_L^d and V_R^d are the matrices that rotate, respectively, the left-handed up quarks, the left-handed down quarks and the right-handed down quarks to their mass eigenstate basis (one has e.g. $U_i = \sum_j (V_L^u)_{ij}\hat{U}_j$); and $V = V_{CKM} = V_L^u V_L^{d\dagger}$ is the Cabibbo-Kobayashi-Maskawa (CKM) matrix. Since the three sets of couplings λ'^A , λ'^B and $\hat{\lambda}'$ are related by unitary matrices, the following sum rules hold: $\sum_{jk} |\lambda'^A_{ijk}|^2 = \sum_{jk} |\lambda'^B_{ijk}|^2 = \sum_{jk} |\hat{\lambda}'_{ijk}|^2$. The hypothesis of a single dominant \mathcal{R}_p coupling, when applied to the coupling sets $\{\lambda'^A_{ijk}\}$ or $\{\lambda'^B_{ijk}\}$, may allow for flavour changing transitions in the down quark or up quark sectors, respectively, but not in both simultaneously. The flavour mixing may be formally obtained by replacements of the form $b \rightarrow b' = V_{33}b + V_{32}s + V_{31}d$ in the former case, and $t \rightarrow t' = V_{33}^\dagger t + V_{32}^\dagger c + V_{31}^\dagger u$ in the latter case (with similar relations for the first two generations).

Analogous expressions can be written for the LLE^c interaction terms:

$$\begin{aligned} W^{(\lambda)} &= \frac{1}{2}\hat{\lambda}_{ijk}(\hat{N}_i\hat{E}_j - \hat{E}_i\hat{N}_j)\hat{E}_k^c = \frac{1}{2}\lambda_{ijk}^A(N_iE'_j - E'_iN_j)E_k^c = \frac{1}{2}\lambda_{ijk}^B(N'_iE_j - E_iN'_j)E_k^c, \\ \lambda_{ijk}^A &= \hat{\lambda}_{lmn}(V_L^{\nu\dagger})_{li}(V_L^{\nu\dagger})_{mj}(V_R^{eT})_{nk}, \quad E'_j = V'_{jm}E_m, \\ \lambda_{ijk}^B &= \hat{\lambda}_{lmn}(V_L^{e\dagger})_{li}(V_L^{e\dagger})_{mj}(V_R^{eT})_{nk}, \quad N'_i = V_{il}^\dagger N_l, \end{aligned} \quad (6.2)$$

where V_L^ν , V_L^e and V_R^e are the rotation matrices for left-handed neutrinos, left-handed charged leptons and right-handed charged leptons, respectively, and the Maki-Nakagawa-Sakata matrix is $U_{MNS} = V'^\dagger = V_L^e V_L^{\nu\dagger}$. For the $U^c D^c D^c$ interactions, the mass eigenstate basis couplings λ''_{ijk} are related to the current basis couplings $\hat{\lambda}''_{ijk}$ by $\lambda''_{ijk} = \hat{\lambda}''_{lmn}(V_R^{uT})_{li}(V_R^{dT})_{mj}(V_R^{dT})_{nk}$.

As mentioned above, if the single coupling dominance hypothesis applies in the weak eigenstate basis, several bounds may be derived from a single process. Indeed, let us assume that, in the weak eigenstate basis, the single \mathcal{R}_p coupling $\hat{\lambda}'_{IJK}$ is dominant. Then, in the mass eigenstate basis, this coupling generates the operator $\lambda'^A_{IJK}E_I U_J D_K^c$ and, due to the flavour mixing, subdominant operators $\lambda'^A_{ijk}E_i U_j D_k^c$, $(i, j, k) \neq (I, J, K)$, with couplings λ'^A_{ijk} suppressed relative to λ'^A_{IJK} by fermion mixing angles. Explicitly, we have $\hat{\lambda}'_{IJK}\hat{E}_I\hat{U}_J\hat{D}_K^c \simeq \hat{\lambda}'_{IJK}E_I U_J D_K^c + \sum_{i \neq I} (V_L^{e*})_{iI}\hat{\lambda}'_{IJK}E_i U_J D_K^c + \sum_{j \neq J} (V_L^{u*})_{jJ}\hat{\lambda}'_{IJK}E_I U_j D_K^c + \sum_{k \neq K} (V_R^d)_{kK}\hat{\lambda}'_{IJK}E_I U_J D_k^c + \dots$, where we have assumed that the rotation matrices $V_{L,R}^{(e,u,d)}$ are close to the unit matrix. Since $\lambda'^A_{IJK} \simeq \hat{\lambda}'_{IJK}$, the following relations among couplings in the mass eigenstate basis hold (from now on, we drop the upper index A in the mass eigenstate basis couplings λ'^A_{ijk}):

$\lambda'_{iJK} \simeq (V_L^{e*})_{iI} \lambda'_{IJK}$, $\lambda'_{Ijk} \simeq (V_L^{u*})_{jJ} \lambda'_{IJK}$, $\lambda'_{IJk} \simeq (V_R^d)_{kK} \lambda'_{IJK}$, etc. It may then happen that the most severe bound on the dominant coupling λ'_{IJK} comes from a process involving a subdominant operator $E_i U_j D_k^c$. For instance an upper bound on the coupling λ'_{IJK} , $|\lambda'_{IJK}| < |\lambda'_{IJK}|_{upper}$, yields $|\lambda'_{IJk}| < |\lambda'_{IJK}|_{upper} / |(V_L^{u*})_{jJ}|$. This constraint may be stronger than bounds extracted from processes involving the dominant operator $E_I U_J D_K^c$.

More generally, one can derive a sequence of bounds on \mathcal{R}_p couplings from a single process without any reference to the single coupling dominance hypothesis, provided that one has some knowledge of the rotation matrices $V_{L,R}^{(e,u,d)}$. For instance, in the model of Ref. [74], in which the quark rotation matrices are controlled by an abelian flavour symmetry, the constraints $\lambda'_{111} < 0.002$ and $\lambda'_{133} < 0.001$ (associated with the non-observation of neutrinoless double beta decay and with the upper limit on the electron neutrino mass, respectively, and derived assuming superpartner masses of 200 GeV) are used to derive upper bounds on all λ'_{1jk} couplings. Combining the latter with the bounds extracted from other observables, one obtains $\lambda'_{1jk} < (10^{-3} - 2 \times 10^{-2})$, depending on the coupling. Such bounds obtained from flavour mixing arguments, however, are model-dependent. In Ref. [88], upper bounds on the λ'_{ijk} couplings are derived from the cosmological neutrino mass bound under various assumptions regarding the quark rotation matrices and $(V_{L,R}^e)_{ij} = \delta_{ij}$.

The same arguments allow to transform a bound on a product of \mathcal{R}_p couplings into a bound on a single coupling. For instance, in the model of Ref. [74], the constraint $|\lambda'_{i13} \lambda'_{i31}| < 3.2 \times 10^{-7}$, associated with $B - \bar{B}$ mixing, yields $|\lambda'_{i13}| < 6 \times 10^{-4}$ (again for sfermion masses of 200 GeV).

6.1.3 A Basis-Independent Parametrization of R -Parity Violation

As explained in subsection 2.1.4, there is no a priori distinction between the ($Y = -1$) Higgs superfield and the lepton superfields in the absence of R -parity and lepton number. The choice of a basis for H_d and the L_i becomes even a delicate task if bilinear \mathcal{R}_p terms and/or sneutrino VEVs are present. As a result, the definition of the \mathcal{R}_p parameters is ambiguous (except for the baryon number violating couplings λ''_{ijk} , which are not discussed here). This ambiguity is removed either by choosing a definite (H_d, L_i) basis, as explained in subsection 2.3.1, or by parametrizing R -parity violation by a complete set of basis-invariant quantities instead of the original \mathcal{R}_p Lagrangian parameters.

In this subsection, we briefly present the second approach, as an alternative to the choice made in this review ¹. We use the notations of subsection 2.3.1, with the 4 doublet superfields H_d and L_i grouped into a 4-vector \hat{L}_α , $\alpha = 0, 1, 2, 3$. The renormalizable, baryon number conserving superpotential then reads $W = \mu_\alpha H_u \hat{L}_\alpha + \frac{1}{2} \lambda_{\alpha\beta k}^e \hat{L}_\alpha \hat{L}_\beta E_k^c + \lambda_{\alpha pq}^d \hat{L}_\alpha Q_p D_q^c + \lambda_{pq}^u Q_p U_q^c H_u$. The couplings $\lambda_{\alpha\beta k}^e = (\lambda_e^k)_{\alpha\beta}$, $\lambda_{\alpha pq}^d = (\lambda_d^{pq})_\alpha$ and μ_α define 3 matrices and 10 vectors in the \hat{L}_α field space (each value of k defines a 4×4 matrix, and each value of (p, q) a 4-vector). In addition, the \mathcal{R}_p soft terms B_α , $\tilde{m}_{\alpha\beta}^2$, $A_{\alpha\beta k}^e = (A_e^k)_{\alpha\beta}$ and $A_{\alpha pq}^d = (A_e^{pq})_\alpha$ define 4 matrices and 10 vectors. At this stage the ‘‘ordinary’’ Yukawa couplings and the trilinear \mathcal{R}_p interactions cannot be disentangled; the distinction between lepton number conserving and lepton number violating interactions arises once a direction in the \hat{L}_α field space has been chosen for the Higgs superfield.

¹Although we frequently use the basis-independent quantities $\sin \xi$ and $\sin \zeta$ to measure the total amount of bilinear R -parity violation in the fermion and scalar sector, respectively (cf. subsection 2.3.1), we do not make a systematic use of invariants to parametrize R -parity violation.

However, an intrinsic definition of R -parity violation is possible with the help of basis-invariant products of the \mathbb{R}_p parameters [26, 27]. These invariants, being independent of the basis choice in the \hat{L}_α field space, can be defined in a geometrical way. Let us give an example of an invariant involving only superpotential parameters, together with its geometrical interpretation. We first notice that each of the 10 vectors $(\lambda_d^{pq})_\alpha$ and μ_α defines a (would-be) Higgs direction in the \hat{L}_α field space (if $(H_d)_\alpha \propto (\lambda_d^{pq})_\alpha$, all λ'_{ijk} vanish, and if $(H_d)_\alpha \propto \mu_\alpha$, all μ_i vanish). If the directions defined by μ_α and one of the $(\lambda_d^{pq})_\alpha$ differ, R -parity is violated. Another, slightly different criterion for R -parity violation is when one of the $(\lambda_d^{pq})_\alpha$ has a nonzero component along one of the vectors $\sum_\beta \mu_\beta^* (\lambda_e^k)_{\beta\alpha}$ (to be interpreted as the three lepton directions, labeled by the flavour index k , the direction for the Higgs superfield being defined by μ_α). The projection of the vector $(\lambda_d^{pq})_\alpha$ on the direction $\sum_\beta \mu_\beta^* (\lambda_e^k)_{\beta\alpha}$ is then a measure of R -parity violation in the k^{th} lepton number. The corresponding invariant can be defined as [26]:

$$\delta_1^{kpq} = \frac{|\mu^\dagger \lambda_e^k \lambda_d^{pq*}|^2}{|\mu|^2 |\lambda_e^k|^2 |\lambda_d^{pq}|^2}, \quad (6.3)$$

where $\mu^\dagger \lambda_e^k \lambda_d^{pq*} \equiv \sum_{\alpha,\beta} \mu_\alpha^* (\lambda_e^k)_{\alpha\beta} (\lambda_d^{pq})_{\beta\alpha}^*$, $|\mu|^2 \equiv \sum_\alpha |\mu_\alpha|^2$, $|\lambda_e^k|^2 \equiv \sum_{\alpha,\beta} |(\lambda_e^k)_{\alpha\beta}|^2$ and $|\lambda_d^{pq}|^2 \equiv \sum_\alpha |(\lambda_d^{pq})_\alpha|^2$. If $\delta_1^{kpq} \neq 0$ for some (p, q) , R -parity and the k^{th} lepton number are violated (summing δ_1^{kpq} over the right-handed lepton index k provides a measure of the breaking of total lepton number). However, $\delta_1^{kpq} = 0$ for all (k, p, q) does not imply the absence of R -parity violation from the superpotential, since other invariants involving the \mathbb{R}_p parameters $(\lambda_e^k)_{\alpha\beta}$, $(\lambda_d^{pq})_\alpha$ and μ_α can be constructed.

The invariants that may be constructed out of the \mathbb{R}_p Lagrangian parameters are much more numerous than the \mathbb{R}_p parameters themselves, but not all of them are independent. After removing the redundancies, one finds a set of 36 independent invariants parametrizing R -parity violation from the superpotential. Once soft supersymmetry breaking terms are included, one obtains a total number of 78 independent invariants, in agreement with the counting of independent \mathbb{R}_p parameters that do not break baryon number (3 μ_i , 9 λ_{ijk} and 27 λ'_{ijk} in the superpotential; 3 B_i , 3 \tilde{m}_{di}^2 , 9 A_{ijk} and 27 A'_{ijk} in the scalar potential; but due to the freedom of redefining the (H_d, L_i) basis, only 6 among the 9 bilinear \mathbb{R}_p parameters are physical).

The basis-independent approach has been used for the derivation of cosmological bounds on R -parity violation [26, 27] and for the computation of neutrino masses and mixings in \mathbb{R}_p models [190, 191, 233].

6.1.4 Specific Conventions Used in this Chapter

In presenting numerical results for coupling constants, we need at times to distinguish between the first two families and the third. For this purpose, when quoting numerical bounds only, we assume the following conventions for the alphabetical indices: $l, m, n \in [1, 2]$ and $i, j, k \in [1, 2, 3]$. The mass of superpartners are fixed at the reference value of $\tilde{m} = 100$ GeV unless otherwise stated. A notation like \tilde{d}_{kR}^p in a numerical relationship, such as $\lambda'_{ijk} < 0.21 \tilde{d}_{kR}^p$, stands for the expression, $\lambda'_{ijk} < 0.21 \left(\frac{m_{\tilde{k}R}}{100\text{GeV}}\right)^p$.

The following auxiliary parameters for the \mathbb{R}_p coupling constants arise in the main body of the text [254]:

$$r_{ijk}(\tilde{l}) = \frac{M_W^2}{g_2^2 m_{\tilde{l}}^2} |\lambda_{ijk}|^2, \quad r'_{ijk}(\tilde{q}) = \frac{M_W^2}{g_2^2 m_{\tilde{q}}^2} |\lambda'_{ijk}|^2. \quad (6.4)$$

Finally, unless otherwise stated, we also rely on the Review of Particle Physics from the Particle Data Group [20] as a source for the experimental data information as well as for short reviews on the main particle physics subjects. Our notations and conventions are given in appendix A. We also assume familiarity with the standard textbooks and reviews, such as [263] for general theory and [25, 264, 265] for phenomenology.

6.2 Constraints on Bilinear \mathcal{R}_p Terms and on Spontaneously Broken R -Parity

In this section, we summarize the main constraints on bilinear \mathcal{R}_p parameters, both for an explicit breaking (cf. section 2.3) and for a spontaneous breaking of R -parity (cf. section 2.4). The spontaneous breaking of R -parity is characterised by an R -parity invariant Lagrangian leading to non-vanishing VEVs for some R -parity odd scalar field, which in turn generates \mathcal{R}_p terms. Since such a spontaneous breakdown of R -parity generally also entails the breaking of the global continuous symmetry associated lepton number conservation, this scenario is distinguished by a non-trivial scalar sector including a massless Goldstone boson, the Majoron, and a light scalar field, partner of the pseudo-scalar Majoron. Some scenarios of spontaneous R -parity breaking also involve a small amount of explicit lepton number breaking, in which case the Majoron becomes a massive pseudo-Goldstone boson. By contrast, the explicit R -parity breaking case may lead to finite sneutrino VEVs $\langle \tilde{\nu}_i \rangle \equiv v_i/\sqrt{2}$, but the Lagrangian density always includes terms that violate R -parity intrinsically.

6.2.1 Models with Explicit R -Parity Breaking

The bilinear \mathcal{R}_p parameters consist of 3 \mathcal{R}_p superpotential masses μ_i and 6 soft supersymmetry breaking parameters mixing the Higgs bosons with the sleptons (3 \mathcal{R}_p B -terms B_i associated with the μ_i , and 3 \mathcal{R}_p soft mass parameters \tilde{m}_{di}^2). In the presence of these parameters, the sneutrinos generally acquire VEVs v_i , which in turn induce new bilinear \mathcal{R}_p interactions. However the v_i are not independent parameters, since they can be expressed in terms of the Lagrangian parameters – or, alternatively, they can be chosen as input parameters, while 3 among the 9 bilinear \mathcal{R}_p parameters μ_i , B_i and \tilde{m}_{di}^2 are functions of the v_i and of the remaining \mathcal{R}_p parameters.

As explained in subsection 2.3.1, in the presence of bilinear R -parity violation, the (H_d, L_i) superfield basis in which the Lagrangian parameters are defined must be carefully specified. Indeed, due to the higgsino-lepton and Higgs-slepton mixings induced by the bilinear \mathcal{R}_p terms, there is no preferred basis for the H_d and L_i superfields, and a change in basis modifies the values of all lepton number violating parameters, including the trilinear couplings λ_{ijk} and λ'_{ijk} (cf. subsection 2.1.4). In practice the most convenient choice is the basis in which the VEVs of the sneutrino fields vanish and the Yukawa couplings of the charged leptons are diagonal. In the (phenomenologically relevant) limit of small bilinear R -parity violation, this superfield basis is very close to the fermion mass eigenstate basis, and therefore allows for comparison with the indirect bounds on trilinear \mathcal{R}_p couplings derived later in section 6.3. From now on we shall assume that this choice of basis has been made. Therefore:

$$v_i = 0 \quad \text{and} \quad \lambda^e = \text{Diag}(m_e, m_\mu, m_\tau), \quad (6.5)$$

and the bilinear \mathcal{R}_p parameters μ_i , B_i and \tilde{m}_{di}^2 , as well as the trilinear \mathcal{R}_p couplings λ_{ijk} , λ'_{ijk} and their associated A -terms, are unambiguously defined.

Let us now turn to the bounds that can be put on bilinear \mathcal{R}_p parameters, or equivalently on the induced mixings between leptons and neutralinos/charginos, and between sleptons and Higgs bosons.

In the fermion sector, the neutralino-neutrino and chargino-charged lepton mixings lead to a variety of characteristic signatures (cf. subsection 2.3.4) which in principle can be used to constrain the superpotential \mathcal{R}_p masses μ_i . In practice however, the strongest bounds on these parameters come from the neutrino sector. Indeed, the neutralino-neutrino mixing induces a tree-level neutrino mass, given by Eqs. (2.46) and (2.47). In the absence of a fast decay mode of the corresponding neutrino, this mass is subject to the cosmological bound $m_\nu \lesssim 1$ eV [46], which in turn requires a strong suppression of bilinear R -parity violation in the fermion sector:

$$\sin \xi \lesssim 3 \times 10^{-6} \sqrt{1 + \tan^2 \beta}, \quad (6.6)$$

where ξ is the misalignment angle introduced in subsection 2.3.1 to quantify in a basis-independent way the size of the neutralino-neutrino and chargino-charged lepton mixings. Since we are working in a basis where $v_i = 0$, $\sin \xi$ is related to the \mathcal{R}_p superpotential mass parameters μ_i by $\sin^2 \xi = \sum_i \mu_i^2 / \mu^2$. The bound (6.6) is strong enough to suppress the experimental signatures of bilinear \mathcal{R}_p violation in the fermion sector below observational limits ².

In the scalar sector, the strongest constraints on the Higgs-slepton mixing comes again from the neutrino sector. Indeed the \mathcal{R}_p soft masses contribute to the neutrino mass matrix at the one-loop level, through the diagrams discussed in subsection 5.1.4. According to Eq. (5.19), the cosmological bound on neutrino masses yields the following upper limit on bilinear \mathcal{R}_p in the scalar sector:

$$\sin \zeta \lesssim 10^{-4}, \quad (6.7)$$

where ζ is the misalignment angle in the scalar sector introduced in Eq. (2.35) of subsection 2.3.1. Since we are working in a basis where $v_i = 0$, $\sin \zeta$ is related to the \mathcal{R}_p B -terms B_i by $\sin^2 \zeta = \sum_i B_i^2 / B^2$.

Finally, one should mention that some physical quantities receive contributions involving simultaneously bilinear and trilinear \mathcal{R}_p parameters, especially in the neutrino sector (cf. subsections 5.1.4 and 6.4.3). This results in upper bounds on products of \mathcal{R}_p parameters like $\lambda_{ijk} \mu_i$ or $\lambda'_{ijk} \mu_i$.

6.2.2 Models with Spontaneous R -Parity Breaking

The main constraints on models of spontaneously broken R -parity are essentially due to the existence of a Goldstone boson (or, in the presence of interactions breaking explicitly lepton number, of a pseudo-Goldstone boson) associated with the breakdown of lepton number, the Majoron J . The first constraint comes from the invisible decay width of the Z boson, which

²This conclusion would have been different if the heaviest neutrino mass could have been as large as the ν_τ LEP limit of 18.2 MeV [20], as was often assumed in the early literature on bilinear \mathcal{R}_p . Indeed, in most models of spontaneous \mathcal{R}_p the tau neutrino was unstable enough to evade the cosmological energy density bound. Since then many of these models have been excluded by the invisible decay width of the Z boson, and the scenario of a heavy decaying neutrino has become less attractive after the discovery of atmospheric and solar neutrino oscillations (see also subsection 6.2.2).

excludes a massless doublet or triplet Majoron. In viable models, the Majoron must be either mainly an electroweak singlet (i.e. it contains only a very small doublet or triplet component) like in the model of Ref. [63], or a massive pseudo-Goldstone boson like in the model of Ref. [61]. In the second case, m_J should be large enough for the decay $Z \rightarrow J\rho$, where ρ is the scalar partner of the Majoron, to be kinematically forbidden; in practice $m_J \gtrsim M_Z$ is required. A third option, not discussed here, is to gauge the lepton number, in which case the Majoron disappears from the mass spectrum by virtue of the Higgs mechanism.

Due to its electroweak non-singlet components, the Majoron possesses interactions with quarks and leptons of the form $\mathcal{L}_{ffJ} = g_{ffJ} \bar{f} \gamma_5 f J + \text{h.c.}$, where the coupling g_{ffJ} is model-dependent but related to the electroweak non-singlet VEV v_L involved in the breaking of lepton number – generally the VEV of a sneutrino field. In the case of a light Majoron, these couplings induce physical processes that can be used to put upper bounds on v_L , such as exotic semileptonic decay modes of K and π mesons, like $K^+ \rightarrow l^+ \bar{\nu} J$ [266]; neutrino-hadron deep inelastic scattering with Majoron emission initiated by the subprocess $\nu_\mu u \rightarrow l^+ d J$ [266]; or lepton flavour violating decays of charged leptons, like $e \rightarrow \mu J$. In practice however, the strongest constraints on v_L come from astrophysical considerations. Indeed light Majorons can be produced inside the stars via processes such as the Compton scattering $e + \gamma \rightarrow e + J$ [60]. Being weakly coupled, Majorons, once produced, escape from the star, carrying some energy out. The requirement that the corresponding energy loss rate should not modify stellar dynamics beyond observational limits puts a severe bound on the couplings g_{ffJ} , therefore on v_L . The strongest bounds come from red giant stars:

$$g_{eeJ} \lesssim 5 \times 10^{-13}, \quad (6.8)$$

if the Majoron mass does not exceed a few times the characteristic temperature of the process, $m_J \lesssim 10$ keV [267]. In the model of Ref. [63], where J is mainly an electroweak singlet, this bound translates into

$$\frac{v_L^2}{v_R M_W} \lesssim 10^{-7}, \quad (6.9)$$

where $\langle \tilde{\nu}_\tau \rangle \equiv v_L/\sqrt{2}$, and $\langle \tilde{\nu}_{R\tau} \rangle \equiv v_R/\sqrt{2}$ is the VEV of the right-handed sneutrino field involved in the spontaneous breaking of R -parity (cf. section 2.4 for details). For $v_R \sim 1$ TeV, this is satisfied as soon as $v_L \lesssim 100$ MeV. Models involving a doublet or triplet (pseudo-)Majoron are not subject to the constraint (6.8), since such Majorons are too heavy to be produced in stars.

Finally, since spontaneous R -parity breaking involves the VEV of a left-handed sneutrino field and/or generates bilinear \tilde{R}_p terms through the VEV of a right-handed sneutrino field, the constraints on models with explicit bilinear R -parity breaking also apply here. In particular, a single neutrino becomes massive at tree level. This neutrino, if cosmologically stable, is subject to the bound $m_\nu \lesssim 1$ eV [46], which in turn requires a strong suppression of the misalignment angle ξ as expressed by Eq. (6.6). The misalignment angle ξ , defined by Eq. (2.32), can be expressed in terms of the parameters of the model. In the model of Ref. [61], $\sin \xi = v_L/v_d$ and the constraint (6.6) translates into

$$\langle \tilde{\nu}_\tau \rangle \equiv \frac{v_L}{\sqrt{2}} \lesssim 500 \text{ keV}. \quad (6.10)$$

This bound is independent³ of $\tan \beta$, due to the fact that $v_d = v \cos \beta$, which turns out to be a strong constraint on such models.

³In principle models with a massless or light Majoron can evade such a cosmological bound, hence the con-

6.3 Constraints on the Trilinear \mathcal{R}_p Interactions

In this section we discuss the subset of the charged and neutral electroweak current phenomena which forms the basis for the high precision measurements. We also consider applications at the interface of CP violation and R -parity violation and review some miscellaneous topics associated with high precision observables (anomalous magnetic moments or electric dipole moments). Unless otherwise stated, the various numerical results quoted in this section employ Standard Model predictions which include either tree and/or one-loop level contributions. The limits on the \mathcal{R}_p coupling constants quoted in this section are 2σ bounds unless otherwise stated.

6.3.1 Charged Current Interactions

Two important issues associated with the Standard Model charged current interactions are: (1) the universality with respect to the W^\pm gauge boson couplings to quarks and leptons, and between the couplings of different lepton families; (2) the relations linking the independent renormalised physical parameters of the Standard Model at the quantum level.

Charged Current Universality in Lepton Decays

The presence of a $L_1 L_2 E_k^c$ operator leads to the additional contribution to the muon decay shown in Fig. 6.1b. The effective tree-level Fermi coupling G_F which determines the μ lifetime

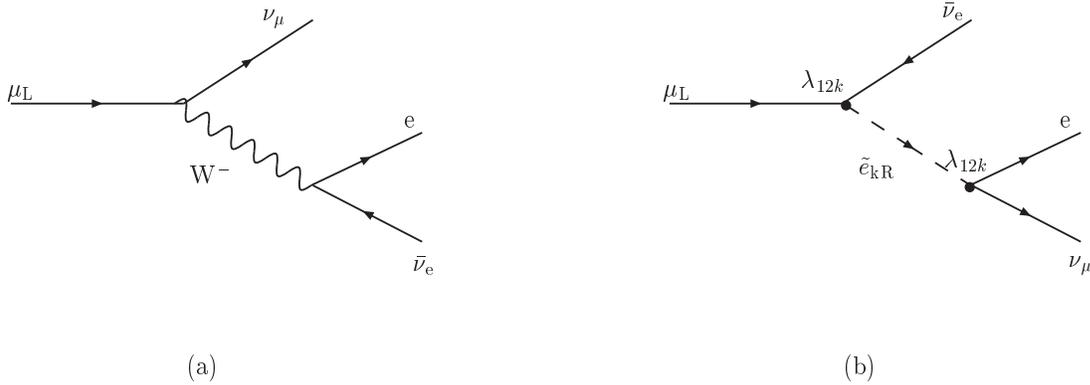


Figure 6.1: Contributions to G_F from (a) the standard model and (b) an \mathcal{R}_p operator $L_1 L_2 E_k^c$.

becomes:

$$\frac{G_F}{\sqrt{2}} = \frac{g^2}{8M_W^2} (1 + r_{12k}(\tilde{e}_{kR})), \quad (6.11)$$

the auxiliary parameter r_{ijk} being defined in section 6.1.4. The direct measurement of G_F together with the tree-level relation (6.11) cannot be used, however, to set conservative constraints

straint (6.6), since the heavy neutrino can decay into a lighter one plus a Majoron, as originally suggested in Ref. [63]. However such a scenario, quite popular at a time where oscillations of atmospheric neutrinos were not established on a firm basis, no longer appears to be very appealing, since it cannot be reconciled with both solar and atmospheric neutrino oscillations.

on λ_{12k} , due to the large effects induced by radiative corrections. A study of the one-loop quantum relations linking the basic set of renormalized input parameters α , G_F , M_Z , with the weak angle and/or the W boson mass parameter m_W has to be performed. For an estimate see [261]. We shall examine here two different versions associated with the off-shell \overline{MS} and on-shell regularization schemes, respectively [268]:

$$\begin{aligned} \text{off-shell } (\overline{MS}) : M_W^2 &= \frac{\pi\alpha(1 + r_{12k}(\tilde{e}_{kR}))}{\sqrt{2}G_F \sin^2 \theta_W(M_Z)|_{\overline{MS}}(1 - \Delta r(M_Z)|_{\overline{MS}})}, \\ \text{on-shell} : \sin^2 \theta_W &\equiv 1 - \left(\frac{M_W}{M_Z}\right)^2 = \frac{\pi\alpha(1 + r_{12k}(\tilde{e}_{kR}))}{\sqrt{2}G_F M_W^2(1 - \Delta r)}. \end{aligned} \quad (6.12)$$

The quantities labeled by \overline{MS} refer to the modified minimal subtraction scheme and those without a label refer to the on-shell renormalization scheme. The off-shell scheme relation can be interpreted as a prediction for the W boson mass m_W depending on the weak interaction parameter $\sin^2 \theta_W(M_Z)|_{\overline{MS}}$, and the on-shell scheme relation as a prediction for this weak interaction parameter, linked to the W mass to all orders of perturbation theory by $\sin^2 \theta_W = 1 - M_W^2/M_Z^2$. The auxiliary parameters in these two schemes, Δr , $\Delta r(M_Z)|_{\overline{MS}}$ are calculable renormalization scheme dependent functions which depend on the basic input parameters and the Standard Model mass spectrum.

We evaluate both relations by using the experimental values for the input parameters [269]. The parameters common to both relations are set as:

$$\begin{aligned} \alpha &= 1/137.035, \quad G_F = 1.16639 \times 10^{-5} \text{ GeV}^{-2}, \\ M_Z &= 91.1867 \pm 0.0020 \text{ GeV}, \quad M_W = 80.405 \pm 0.089 \text{ GeV} \end{aligned} \quad (6.13)$$

. The weak angle in the off-shell \overline{MS} relation is set as $\sin^2 \theta_W(M_Z)|_{\overline{MS}} = 0.23124 \pm 0.00017$, while in the on-shell it is in principle determined in terms of the W mass by $\sin^2 \theta_W = 1 - M_W^2/M_Z^2$. For the auxiliary parameters, we use the values: $\Delta r = 0.0349 \pm 0.0019 \pm 0.0007$, and $\Delta r(M_Z)|_{\overline{MS}} = 0.0706 \pm 0.0011$.

Let us now quote the results of the calculations. We find that the off-shell scheme relation tends to rule out the existence of λ_{12k} . However, taking into account the uncertainties on the input parameters leaves still the possibility of inferring bounds on the \mathcal{R}_p coupling constants. The uncertainty in M_W dominates by far all the other uncertainties. A calculation at the 1 σ level leads to the coupling constant bound $\lambda_{12k} < 0.038 \tilde{e}_{kR}$.

For the on-shell scheme relation, we still find that this tends to rule out λ_{12k} , but yields the 1 σ level bound $\lambda_{12k} < 0.046 \tilde{e}_{kR}$. To illustrate the importance of the uncertainties in the W boson mass in this context, we consider the alternative calculation in the on-shell scheme where we use the experimental value for the on-shell renormalized weak angle $\sin^2 \theta_W = 0.2260 \pm 0.0039$ and evaluate the W mass from the relation $M_W^2 = M_Z^2(1 - \sin^2 \theta_W)$. This prescription is now found to yield definite values for the \mathcal{R}_p coupling constants given by $\lambda_{12k} = 0.081 \tilde{e}_{kR}$.

The main conclusion here is that the constraints for the coupling constants λ_{12k} extracted from the \mathcal{R}_p correction to G_F depend sensitively on the input value of the W boson mass. The comparison of results obtained with the off-shell and on-shell regularization schemes serves, however, as a useful consistency check.

New contributions to the μ decay can be probed by comparing the measurement of the ratio of rates:

$$R_{\tau\mu} = \Gamma(\tau \rightarrow \mu\nu\bar{\nu})/\Gamma(\mu \rightarrow e\nu\bar{\nu})$$

to its SM expectation $R_{\tau\mu}^{SM}$. This was first considered in [254] where it was shown that the small experimental value for $R_{\tau\mu}$ reported in [270] could be accounted for by \mathcal{R}_p muon decays for coupling values $\lambda_{12k} \sim 0.15$. An updated analysis [271] using more precise measurements of $R_{\tau\mu}$ [272] and $O(\alpha)$ values for $R_{\tau\mu}^{SM}$ now yields the bound

$$\lambda_{12k} < 0.07 \tilde{e}_{kR}. \quad (6.14)$$

More generally, the ratio $R_{\tau\mu}$ can also be affected by $L_2 L_3 E_k^c$ operators modifying the τ leptonic decays via \tilde{e}_{kR} exchanges, similarly to the process shown in Fig. 6.1b. The expression of $R_{\tau\mu}$ reads as:

$$R_{\tau\mu} \simeq R_{\tau\mu}^{SM} [1 + 2(r_{23k}(\tilde{e}_{kR}) - r_{12k}(\tilde{e}_{kR}))], \quad (6.15)$$

while the ratio of both leptonic τ decay widths is:

$$R_\tau = \frac{\Gamma(\tau \rightarrow e \bar{\nu}_e \nu_\tau)}{\Gamma(\tau \rightarrow \mu \bar{\nu}_\mu \nu_\tau)} \simeq R_\tau^{SM} [1 + 2(r_{13k}(\tilde{e}_{kR}) - r_{23k}(\tilde{e}_{kR}))]. \quad (6.16)$$

The comparison of the experimental measurements with the SM values yields the following bounds [271] on the coupling constants λ_{i3k} :

$$\lambda_{13k} < 0.07 \tilde{e}_{kR} [R_\tau]; \quad \lambda_{23k} < 0.07 \tilde{e}_{kR} [R_\tau]; \quad \lambda_{23k} < 0.07 \tilde{e}_{kR} [R_{\tau\mu}]. \quad (6.17)$$

Aside from the muon lifetime, the energy and angular distributions of the charged lepton emitted in muon decay offer useful observables in order to test the Lorentz covariant structure of the charged current interactions, through the presence of either non $V - A$ couplings or tensorial couplings. The information is encoded in terms of the Michel parameter ρ and the analogous parameters, η , ξ , δ , functions of the independent Fermi S, V, T invariant couplings, which enter the differential (energy and angle) muon decay distributions [273]. The \tilde{e}_{kR} exchange depicted in Fig. 6.1b and induced by the λ_{12k} coupling alone initiates \mathcal{R}_p contributions to the Lorentz vector and axial vector couplings. However the corresponding corrections in this case are masked by a predominant Standard Model contribution of the same structure, so that no useful constraints can be inferred. In contrast, the tree level exchange of a stau $\tilde{\tau}_L$ initiates corrections to the scalar Lorentz coupling, yielding the bound: $|\lambda_{232}^* \lambda_{131}| < 0.022 \tilde{\tau}_L^2$ [274]. While the above quadratic bound actually turns out to be weaker than those deduced by combining tentatively the individual bounds on the coupling constants λ_{13k} and λ_{23k} given in equation (6.17), it has the advantage of providing a more robust bound, not exposed to invalidating cancellations.

Charged Current Universality in π and τ Decays

Leptonic decays of the π as well as $\tau^- \rightarrow \pi^- \nu_\tau$ can be mediated at the tree level by \mathcal{R}_p interactions, as shown by the diagrams of Fig. 6.2. At low energies, these \mathcal{R}_p contributions can be represented by four fermion interactions between pairs of quarks and leptons, $(\bar{l}\Gamma l)(\bar{q}\Gamma q)$. Writing the effective interactions in this form allows a systematic calculation of the \mathcal{R}_p induced meson leptonic decays and τ semi-hadronic decays. For a general and complete study of bounds from meson decays we refer to [275]. In comparing with the experimental data for the π -meson decay width $\Gamma(\pi^- \rightarrow \mu^- \bar{\nu}_\mu)$, it is advantageous to eliminate the dependence on the pion decay coupling constant, F_π , by considering the ratio [254]:

$$R_\pi = \frac{\Gamma(\pi^- \rightarrow e^- \bar{\nu}_e)}{\Gamma(\pi^- \rightarrow \mu^- \bar{\nu}_\mu)} = R_\pi^{SM} [1 + \frac{2}{V_{ud}} (r'_{11k}(\tilde{d}_{kR}) - r'_{21k}(\tilde{d}_{kR}))], \quad (6.18)$$

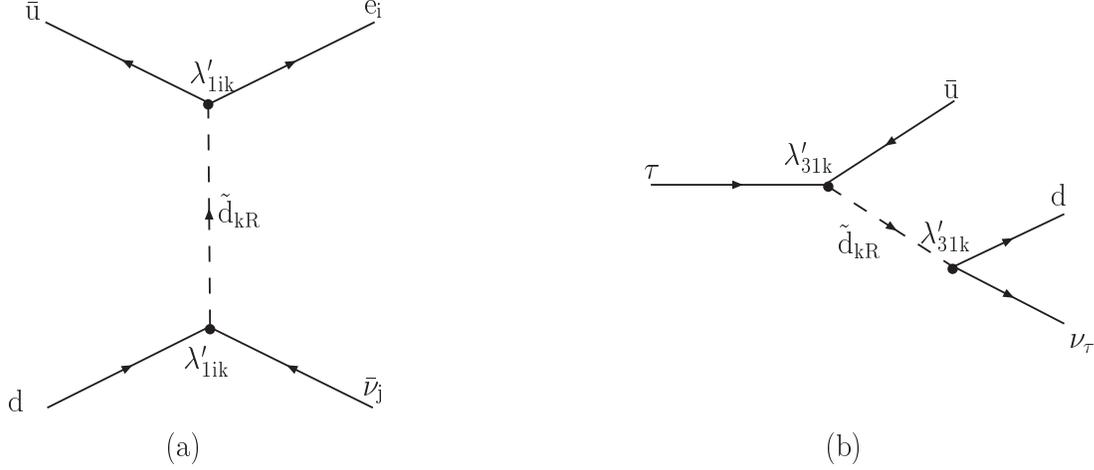


Figure 6.2: Contributions of \mathcal{R}_p interactions to (a) the leptonic π decays and (b) the $\tau \rightarrow \pi \nu_\tau$ decay.

where the auxiliary parameters r'_{ijk} are defined in section 6.1.4. The inferred coupling constant bounds are [275]:

$$\lambda'_{21k} < 0.059 \tilde{d}_{kR}, \quad \lambda'_{11k} < 0.026 \tilde{d}_{kR}. \quad (6.19)$$

The closely related two-body decay $\tau^- \rightarrow \pi^- \nu_\tau$ also offers an additional useful test of the lepton universality [276]. A model-independent analysis based on a comparison with the experimental results for the ratio of τ lepton and π meson decay widths,

$$R_{\tau\pi} = \frac{\Gamma(\tau^- \rightarrow \pi^- \nu_\tau)}{\Gamma(\pi^- \rightarrow \mu^- \nu_\mu)} = R_{\tau\pi}^{SM} \frac{|V_{ud} + r'_{31k}(\tilde{d}_{kR})|^2}{|V_{ud} + r'_{21k}(\tilde{d}_{kR})|^2} \quad (6.20)$$

yields the coupling constant bound:

$$\lambda'_{31k} < 0.12 \tilde{d}_{kR} \quad , \quad \lambda'_{21k} < 0.08 \tilde{d}_{kR} \quad . \quad (6.21)$$

Charged Current Universality in the Quark Sector

In the quark sector, the presence of a $LQ\bar{D}$ operator leads to additional contributions to quark semileptonic decays, via processes similar to that shown in Fig. 6.2 where the incoming anti-quark line is reversed. The experimental value of the CKM matrix element V_{ud} , determined by comparing the nuclear β decay to the muon decay, is then modified according to:

$$|V_{ud}|^2 = \frac{|V_{ud}^{SM} + r'_{11k}(\tilde{d}_{kR})|^2}{|1 + r_{12k}(\tilde{e}_{kR})|^2} \quad . \quad (6.22)$$

Similarly, the rates for $s \rightarrow ul\bar{\nu}_l$ and $b \rightarrow ul\bar{\nu}_l$, measured in K and charmless B decays respectively, are affected by \mathcal{R}_p corrections induced by λ' couplings. The values of V_{us} and V_{ub} extracted from these rates depend again on r_{12k} via the effect of λ_{12k} couplings on G_F . Summing over the down quark generations yields [254]:

$$\sum_{j=1}^3 |V_{ud_j}|^2 = \frac{1}{|1 + r_{12k}(\tilde{e}_R)|^2} [|V_{ud}^{SM} + r'_{11k}(\tilde{d}_{kR})|^2$$

$$\begin{aligned}
& + |V_{us}^{SM} + [r'_{11k}(\tilde{d}_{kR})r'_{12k}(\tilde{d}_{kR})]^{\frac{1}{2}}|^2 \\
& + |V_{ub}^{SM} + [r'_{11k}(\tilde{d}_{kR})r'_{13k}(\tilde{d}_{kR})]^{\frac{1}{2}}|^2] \quad (6.23)
\end{aligned}$$

$$\begin{aligned}
& = 1 - 2r_{12k}(\tilde{e}_{kR})V_{ud}^{SM} + 2r'_{11k}(\tilde{d}_{kR})V_{ud}^{SM} \\
& + 2[r'_{11k}(\tilde{d}_{kR})r'_{12k}(\tilde{d}_{kR})]^{\frac{1}{2}}V_{us}^{SM} + 2[r'_{11k}(\tilde{d}_{kR})r'_{13k}(\tilde{d}_{kR})]^{\frac{1}{2}}V_{ub}^{SM}, \quad (6.24)
\end{aligned}$$

the last equality resulting from the unitarity of the CKM matrix ⁴. At the lowest order in the \mathcal{R}_p corrections into which we specialize, it is consistent to identify the flavour mixing matrix elements appearing in the right-hand side with the measured CKM matrix elements, $V_{ud_j}^{SM} \simeq V_{ud_j}$. Setting the various CKM matrix elements V_{ud_j} and in the sum $\sum_j |V_{ud_j}|^2$ at their measured values [272], the following bounds are obtained in the single and quadratic coupling constant dominance hypothesis, respectively:

$$\begin{aligned}
\lambda_{12k} < 0.05 \tilde{e}_{kR}, \quad \lambda'_{11k} < 0.02 \tilde{d}_{kR}, \\
(\lambda'_{11k} \lambda'_{12k})^{1/2} < 0.04 \tilde{d}_{kR}, \quad (\lambda'_{11k} \lambda'_{13k})^{1/2} < 0.37 \tilde{d}_{kR}. \quad (6.25)
\end{aligned}$$

For more bounds on leptonic meson decays see [360]. A consideration of the unitarity constraints on the other sums of CKM matrix elements, $\sum_{j=1,2,3} |V_{cd_j}|^2$ and $\sum_{j=1,2,3} |V_{cd_j}|^2$, could also be used with the same prescriptions as in the above comparison, to derive bounds on the single coupling constants λ_{i2k} and λ_{i3k} , respectively.

Semileptonic and Leptonic Decays of Heavy Quark Hadrons

An experimental information on the three-body decay channels of charmed mesons is available for the following three classes of semileptonic processes, differing in the final state by the lepton generation or the strange meson type: $D^+ \rightarrow \bar{K}^0 l_i^+ \nu_i$, $D^+ \rightarrow \bar{K}^{0*} l_i^+ \nu_i$, $D^0 \rightarrow K^- l_i^+ \nu_i$, [$l_i = e, \mu$; $\nu_i = \nu_e, \nu_\mu$]. These decays could be enhanced by \mathcal{R}_p contributions involving a λ'_{i2k} coupling as shown in Fig. 6.3. Denoting the branching fraction ratios $B(D \rightarrow \mu \nu_\mu K^{(*)}) / B(D \rightarrow$

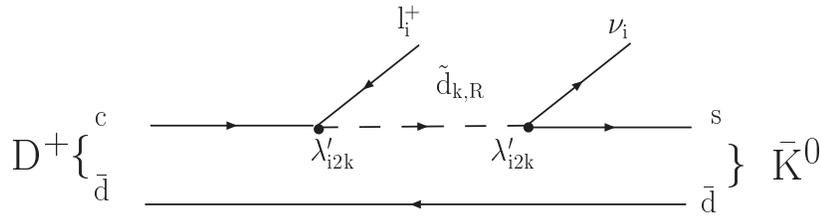


Figure 6.3: \mathcal{R}_p contributions to the semileptonic decay of a charmed meson.

$e \nu_e K^{(*)}$) by $R_{D^+}^{(*)}$, R_{D^0} respectively, one can write the \mathcal{R}_p corrections as [277]:

$$\frac{R_{D^+}}{(R_{D^+})^{SM}} = \frac{R_{D^+}^*}{(R_{D^+}^*)^{SM}} = \frac{R_{D^0}}{(R_{D^0})^{SM}} = \frac{|1 + r'_{22k}(\tilde{d}_{kR})|^2}{|1 + r'_{12k}(\tilde{d}_{kR})|^2}. \quad (6.26)$$

Following [277], we use $(R_D^{(*)})^{SM} = 1/1.03$ to account for the phase space suppression in the muon channel. From the experimental values of $R_D^{(*)}$ given in [272], one deduces the following

⁴We have corrected the formula for the unitarity constraint used in the work by Ledroit and Sajot [271] by noting that the \mathcal{R}_p corrections to the flavour mixing matrix elements V_{us} and V_{ub} are given by quadratic products of the coupling constants.

2σ coupling constant bounds:

$$\begin{aligned} |\lambda'_{12k}| &< 0.44 \tilde{d}_{kR}, & |\lambda'_{22k}| &< 0.61 \tilde{d}_{kR} & [R_{D^+}]; \\ |\lambda'_{12k}| &< 0.23 \tilde{d}_{kR}, & |\lambda'_{22k}| &< 0.38 \tilde{d}_{kR} & [R_{D^+}^*]; \\ |\lambda'_{12k}| &< 0.27 \tilde{d}_{kR}, & |\lambda'_{22k}| &< 0.21 \tilde{d}_{kR} & [R_{D^0}]. \end{aligned} \quad (6.27)$$

By invoking the existence of a flavour mixing in the up-quark sector, within the current basis single coupling constant dominance hypothesis, the \mathcal{R}_p contribution to the inclusive semileptonic B meson inclusive decay process, $B^- \rightarrow X_q \tau^- \bar{\nu}$, may be expressed solely in terms of the single coupling constant λ'_{333} . The comparison with experiment yields the following estimate for the bound [278]:

$$|\lambda'_{333}| < 0.12 \tilde{b}_R. \quad (6.28)$$

The same process as considered in [279] leading to $\lambda'_{333} < 0.32 \tilde{b}_R$. The different predictions furnish an indication of the dependence on the input hadronic parameters.

The two-body leptonic decay channels of the charmed quark mesons, $D_s^- \rightarrow l^- \nu$, also serve a good use in testing the lepton universality. A comparison with the experimental results for the ratios of τ to μ emission,

$$R_{D_s}(\tau\mu) = \frac{B(D_s \rightarrow \tau\nu_\tau)}{B(D_s \rightarrow \mu\nu_\mu)} = \frac{|V_{cs} + r'_{32k}(\tilde{d}_{kR})|^2}{|V_{cs} + r'_{22k}(\tilde{d}_{kR})|^2}, \quad (6.29)$$

yields the coupling constant bounds [271]:

$$|\lambda'_{22k}| < 0.65 \tilde{d}_{kR}, \quad |\lambda'_{32k}| < 0.52 \tilde{d}_{kR} \quad . \quad (6.30)$$

The $\Delta S = 1$ decays of strange baryons, e.g. $\Lambda \rightarrow pl^- \bar{\nu}_e, \dots$ [$l = e, \mu$], provide bounds on quadratic products of the λ' interactions. We quote the 2σ bounds obtained by Tahir et al. [280]:

$$\begin{aligned} |\lambda'_{11k} \lambda'_{12k}| &< 1.3 \times 10^{-1} (5.3 \times 10^{-3}) \tilde{d}_{kR}^2 & [\Lambda \rightarrow pl^- \bar{\nu}_l] & ; \\ |\lambda'_{11k} \lambda'_{12k}| &< 8.5 \times 10^{-2} (1.6 \times 10^{-2}) \tilde{d}_{kR}^2 & [\Sigma^- \rightarrow nl^- \bar{\nu}_l] & ; \\ |\lambda'_{11k} \lambda'_{12k}| &< 1.2 \times 10^{-1} (5.0 \times 10^{-2}) \tilde{d}_{kR}^2 & [\Xi^- \rightarrow \Lambda l^- \bar{\nu}_l] & , \end{aligned} \quad (6.31)$$

from the upper limits on the branching ratios of the indicated decays with $l = e$ ($l = \mu$).

6.3.2 Neutral Current Interactions

Neutrino-Lepton Elastic Scattering and Neutrino-Nucleon Deep Inelastic Scattering

Most of the experimental information on neutrino interactions with hadron targets or with leptons is accessed via experiments using ν_μ and $\bar{\nu}_\mu$ beams. One may consult [281, 282] for reviews. The elastic scattering $\nu_\mu e \rightarrow \nu_\mu e$, $\bar{\nu}_\mu e \rightarrow \bar{\nu}_\mu e$ has been studied by the CHARM II experiment, which provides measurements for the ratio $R = \sigma(\nu_\mu)/\sigma(\bar{\nu}_\mu)$, where $\sigma(\nu_\mu(\bar{\nu}_\mu))$ denotes the cross-section $\sigma(\nu_\mu(\bar{\nu}_\mu)e \rightarrow \nu_\mu(\bar{\nu}_\mu)e)$. Neutral current (NC) and charged current (CC) deep inelastic scattering on nucleons or nuclei, $\nu_\mu N(A) \rightarrow \nu_\mu X$ and $\bar{\nu}_\mu N(A) \rightarrow \bar{\nu}_\mu X$, has been

studied by the CDHS and CHARM experiments at CERN, and by the CCFR Collaboration at Fermilab. These experiments measure the following rates:

$$R_\nu = \frac{\langle \sigma(\nu N)^{NC} \rangle}{\langle \sigma(\nu N)^{CC} \rangle}, \quad R_{\bar{\nu}} = \frac{\langle \sigma(\bar{\nu} N)^{NC} \rangle}{\langle \sigma(\bar{\nu} N)^{CC} \rangle}, \quad (6.32)$$

where the brackets stand for an average over the neutrino beam energy flux distribution. Useful information is also collected through the elastic scattering of neutrinos on a proton target [283]. Each of these observables presents its own specific advantages by providing highly sensitive measurements of the Standard Model parameters.

The neutrino ν_μ scattering on quarks and charged leptons is described by the s -channel Z boson exchange diagram. At energies well below M_Z , the relevant neutral current couplings are encoded in the parameters $g_{L,R}^{\nu f}$ for charged leptons, and $\epsilon_{L,R}(f)$ for quarks, as defined in terms of the effective Lagrangian density,

$$\begin{aligned} \mathcal{L} = & -\frac{4G_F}{\sqrt{2}}(\bar{\nu}_L\gamma_\mu\nu_L)\left[\sum_{l=e,\mu} g_L^{\nu f}(\bar{l}_L\gamma^\mu l_L) + g_R^{\nu l}(\bar{l}_R\gamma^\mu l_R)\right] \\ & + \sum_{q=u,d} \epsilon_L(f)(\bar{q}_L\gamma^\mu q_L) + \epsilon_R(f)(\bar{q}_R\gamma^\mu q_R)]. \end{aligned} \quad (6.33)$$

The \mathcal{R}_p contributions to neutrino elastic scattering arise at the tree level order. Examples are shown in Fig. 6.4 in the case of $\nu_\mu e$ and $\bar{\nu}_\mu e$ scattering. Similar contributions induced by a λ'_{21k} (λ'_{2j1}) coupling affect the $\nu_\mu d$ ($\bar{\nu}_\mu d$) scattering via the exchange of a \tilde{d}_{kR} (\tilde{d}_{jL}) squark. The

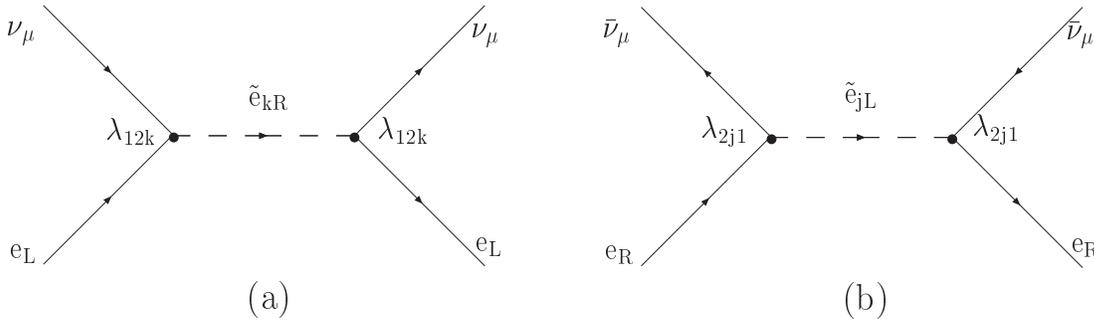


Figure 6.4: Examples of \mathcal{R}_p contributions to (a) $\nu - e$ and (b) $\bar{\nu}_\mu - e$ scattering. Other contributions, as coming from the t -channel exchange of a selectron, are not represented.

results for the combined Standard Model and \mathcal{R}_p contributions read [254]:

$$\begin{aligned} g_L^{\nu e} &= \left(-\frac{1}{2} + x_W\right)(1 - r_{12k}(\tilde{e}_{kR})) - r_{12k}(\tilde{e}_{kR}), \\ g_R^{\nu e} &= x_W(1 - r_{12k}(\tilde{e}_{kR})) + r_{211}(\tilde{e}_L) + r_{231}(\tilde{\tau}_L), \\ \epsilon_L(d) &= \left(-\frac{1}{2} + \frac{1}{3}x_W\right)(1 - r_{12k}(\tilde{e}_{kR})) - r'_{21k}(\tilde{d}_{kR}), \\ \epsilon_R(d) &= \frac{x_W}{3}(1 - r_{12k}(\tilde{e}_{kR})) + r'_{2j1}(\tilde{d}_{jL}), \end{aligned} \quad (6.34)$$

with $x_W = \sin^2 \theta_W$. Note that although a λ_{12k} coupling does not lead to sfermion exchange contributing to $\nu q \rightarrow \nu q$ scattering, it affects ϵ_R and ϵ_L via its effects on G_F (see equation (6.11)). From these relations and using the experimental values for $g_L^{\nu e}$ and $g_R^{\nu e}$ given in [272], which

rely on the $\sigma(\nu_\mu(\bar{\nu}_\mu))$ measurements from the CHARM II experiment [284], one obtains the bounds:

$$\lambda_{12k} < 0.14 \tilde{e}_{kR}, \quad \lambda_{231} < 0.11 \tilde{\tau}_L, \quad \lambda_{121} < 0.13 \tilde{e}_L \quad . \quad (6.35)$$

The fits to the current data from the CDHS and CCFR Collaborations [285] determine the numerical values for the parameters $\epsilon_{L,R}$ [272]. Comparing with the Standard Model values, suitably including the radiative corrections, yields the following limits on the \mathcal{R}_p coupling constants [271]:

$$\lambda_{12k} < 0.13 \tilde{e}_{kR}, \quad \lambda'_{21k} < 0.15 \tilde{d}_{kR}, \quad \lambda'_{2j1} < 0.18 \tilde{d}_{jL} \quad . \quad (6.36)$$

The elastic scattering of ν_μ and $\bar{\nu}_\mu$ on a proton target is known to furnish an independent sensitive means to measure the weak angle, $\sin^2 \theta_W$ [283]. Although this case has been included in the global studies of the electron quark four fermion contact interactions [286], the present experimental accuracy and the theoretical uncertainties on the nucleon weak form factors do not warrant a detailed study of the constraints on the \mathcal{R}_p interactions.

Fermion-Antifermion Pair Production and Z -Boson Pole Observables

The fermion pair production reactions, $e^+e^- \rightarrow f\bar{f}$, [$f = l, q$] have been studied over a wide range of incident energies at the existing leptonic colliders, PEP, PETRA, TRISTAN, LEP and SLC. These reactions provide sensitive tests of the Standard Model [281]. For the high energy regime, the data for the Z boson pole resonant production, $e^+e^- \rightarrow Z^0 \rightarrow f\bar{f}$, as collected at the CERN LEP and the SLC colliders, have provided a wealth of experimental measurements of the Standard Model parameters.

At low energies, the basic parameters are conventionally defined in terms of the following parametrisation for the effective Lagrangian density,

$$\mathcal{L} = -\frac{4G_F}{\sqrt{2}} \sum_{f=l,q} \bar{e}\gamma^\mu (g_L^e P_L + g_R^e P_R) e \bar{f}\gamma^\mu (g_L^f P_L + g_R^f P_R) f. \quad (6.37)$$

The high energy scattering regime, $\sqrt{s} \geq M_Z$, is described by analogous transition amplitudes, differing in form only by the insertion of an energy dependent Z boson resonance propagator factor. The Z -pole measurements provide information on a large set of observables. Of particular interest here are the forward-backward asymmetries

$$A_{FB}^f = \frac{(\sigma)_{>} - (\sigma)_{<}}{(\sigma)_{>} + (\sigma)_{<}} \Big|_{e\bar{e} \rightarrow f\bar{f}}$$

which, in the Standard Model, are related to the vector and axial couplings of fermions to the Z boson via :

$$A_{FB}^f = \frac{3}{4} \mathcal{A}^e \mathcal{A}^f \quad \text{where} \quad \mathcal{A}^f = 2g_V^f g_A^f / (g_V^{f2} + g_A^{f2}) \stackrel{\text{tree level}}{=} -T_{3L}^f \quad .$$

The tree level t -channel exchange of a sneutrino (squark) induced by a λ_{ijk} (λ'_{ijk}) coupling affects the forward-backward asymmetries A_{FB}^l (A_{FB}^q) as shown in Fig. 6.5. Note that the

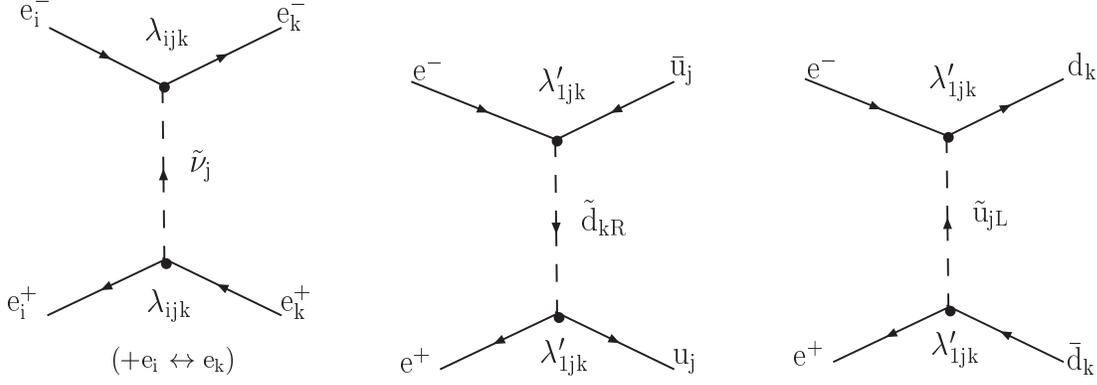


Figure 6.5: \mathcal{R}_p contributions to the forward-backward asymmetries.

s -channel exchange of a sneutrino also affects the Bhabha cross-section, but leaves A_{FB}^e unchanged since the sneutrino decays isotropically in its rest frame. The SM values of A_{FB}^f are modified according to:

$$\begin{aligned}
(A_{FB}^{l_k})_{SM}/A_{FB}^{l_k} &= |1 + r_{1jk}(\tilde{\nu}_j)|^2 & l_k = e : ijk = 121, 131 \\
& & l_k = \mu : ijk = 121, 122, 132, 231 \\
& & l_k = \tau : ijk = 123, 133, 131, 231 \quad (6.38) \\
(A_{FB}^{u_j})_{SM}/A_{FB}^{u_j} &= |1 + r'_{1jk}(\tilde{d}_{kR})|^2 \\
(A_{FB}^{d_k})_{SM}/A_{FB}^{d_k} &= |1 + r'_{1jk}(\tilde{u}_{jL})|^2 .
\end{aligned}$$

Taking from [272] the experimental values for A_{FB}^f , as well as the SM predictions which include radiative corrections, the following 2σ bounds are obtained:

$$\begin{aligned}
\lambda_{ijk} &< 0.37 \tilde{\nu}_{jL} ; & (ijk) = (121), (131) & [A_{FB}^e] \\
\lambda_{ijk} &< 0.25 \tilde{\nu}_{jL} ; & (ijk) = (122), (132), (211), (231) & [A_{FB}^\mu] \\
\lambda_{ijk} &< 0.11 \tilde{\nu}_{jL} ; & (ijk) = (123), (133), (311), (321) & [A_{FB}^\tau] \\
\lambda'_{12k} &< 0.21 \tilde{d}_{kR} & & [A_{FB}^c] \\
\lambda'_{1j2} &< 0.28 \tilde{u}_{jL} & & [A_{FB}^s] \\
\lambda'_{1j3} &< 0.18 \tilde{u}_{jL} & & [A_{FB}^b]
\end{aligned} \quad (6.39)$$

At the one-loop order, \mathcal{R}_p interactions lead to $Z\bar{f}f$ [$f = q, l$] vertex corrections. The diagrams of the dominant \mathcal{R}_p processes contributing at the one-loop order to the leptonic Z decay width Γ_l are shown in Fig. 6.6. The λ' couplings which lead to these contributions also affect the $Z \rightarrow b\bar{b}$ decay width Γ_b , via loop processes propagating internal top and slepton lines. The subsequent change of the hadronic decay width of the Z has thus to be taken into account when calculating the \mathcal{R}_p induced corrections to $R_l = \Gamma_h / \Gamma_l$. Those corrections read [287]:

$$\delta R_l \equiv \frac{R_l}{R_l^{SM}} - 1 = -R_l^{SM} \Delta_l + R_l^{SM} R_b^{SM} \Delta_b$$

where

$$R_b \equiv \Gamma_b / \Gamma_h, \quad \Delta_f \equiv \frac{\Gamma(Z \rightarrow f\bar{f})}{\Gamma_{SM}(Z \rightarrow f\bar{f})} - 1,$$

The comparison with the CERN LEP-I measurements [272] of R_l^Z [$l = e, \mu, \tau$] leads to the following 2σ bounds [271], valid for $m(\tilde{d}_{kR}) = 100$ GeV:

$$\lambda'_{13k} < 0.47, \quad \lambda'_{23k} < 0.45, \quad \lambda'_{33k} < 0.58. \quad (6.40)$$

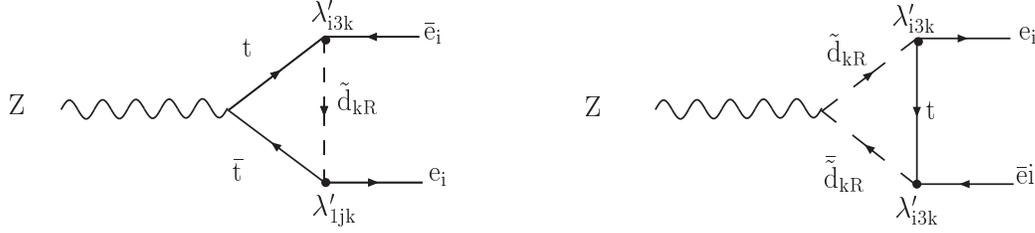


Figure 6.6: \mathcal{R}_p contributions to the leptonic Z decay width. The (subleading) self-energy diagrams are not represented.

The dependence of these bounds on the \tilde{d}_{kR} mass is not trivial and can be found in [287].

The \mathcal{R}_p λ'' interactions affect Γ_h via diagrams similar to those shown in Fig. 6.6, and thus affect R_l and R_b as well [288]. From the measurement of the average leptonic decay width $R_l = 20.795 \pm 0.040$, the following bounds are obtained assuming squark masses of 100 GeV [288]:

$$[\lambda''_{313}, \lambda''_{323}] < 1.46(0.97) \quad , \quad \lambda''_{312} < 1.45(0.96), \quad (6.41)$$

the first (second) number corresponding to the 2σ (1σ) upper bound. Less stringent upper limits on the same λ'' couplings were also obtained in [288] from an old measurement of R_b . These are out-of-date since the measured R_b is now in good agreement with its SM value.

Lebedev et al. [289] have performed a global statistical fit of the one-loop level R -parity violating contributions to the experimental data for the asymmetry parameters A^b , A_{FB}^b gathered at the CERN LEP and Stanford SLC colliders. The pattern of signs from the \mathcal{R}_p corrections is such that certain contributions enter with a sign opposite to the one that would be required by observations. This circumstance lead these authors to conclude that out the whole set of coupling constants λ'_{i31} , λ'_{i32} , λ''_{321} and λ'_{i33} , λ''_{331} was ruled out at the 1σ and 2σ level respectively.

The pair-production of leptons with different flavours at the Z pole provides quadratic bounds on a large subset of the \mathcal{R}_p coupling constants, λ_{ijk} , λ'_{ijk} . Lepton-flavour violating (LFV) decays of the Z , with branching ratios defined by:

$$B_{ii'} \equiv \frac{\Gamma(Z \rightarrow e_i \bar{e}_{i'}) + \Gamma(Z \rightarrow e_{i'} \bar{e}_i)}{\Gamma(Z \rightarrow all)}, \quad [i \neq i'] \quad (6.42)$$

may occur through \mathcal{R}_p induced one-loop processes similar to those shown in Fig. 6.6, whose amplitude is proportional to quadratic products of the relevant \mathcal{R}_p coupling constants. The contribution of such processes induced by $LQ\bar{D}$ operators to the LFV decays of the Z was studied by Anwar Mughal et al. in [290], focusing again on the dominant diagrams involving a top quark in the internal loop. A comparison with the current experimental limits on $B_{e\mu}$, $B_{e\tau}$ and $B_{\mu\tau}$ [272] yields the bounds:

$$\begin{aligned} \sum_k |\lambda'_{13k} \lambda'_{23k}| &< 6.2 \times 10^{-2} \quad [Z \rightarrow e\mu]; & \sum_k |\lambda'_{33k} \lambda'_{13k}| &< 1.5 \times 10^{-1} \quad [Z \rightarrow e\tau]; \\ \sum_k |\lambda'_{23k} \lambda'_{33k}| &< 1.7 \times 10^{-1} \quad [Z \rightarrow \mu\tau] \end{aligned} \quad (6.43)$$

established assuming $m(\tilde{d}_{kR}) = 200$ GeV. The non trivial dependence of these bounds on $m(\tilde{d}_{kR})$ can be found in [290].

A more general study of the LFV Z decays induced by \tilde{R}_p process can be found in [291]. This analysis is not restricted to diagrams involving a top quark in the loop, and λ couplings are also considered. When LFV decays are mediated by λ couplings, it is shown that $B_{JJ'} \approx (|\lambda_{ijJ}\lambda_{ijJ'}^*|/0.01)^2 4. \times 10^{-9}$. Under the hypothesis of a pair of dominant coupling constants, one deduces from the current experimental limits: $|\lambda_{ijJ}\lambda_{ijJ'}^*| < [0.46, 1.1, 1.4]$ for $[(J J') = (12), (23), (13)]$ and $\tilde{m} = 100$ GeV, \tilde{m} being the common mass of the sfermions involved in the contributing loops. LFV decays mediated by λ' interactions are enhanced by an extra colour factor and by the possibility of accommodating an internal top quark in the loops. An approximate estimate reads: $B_{JJ'} \approx (|\lambda'_{jJk}\lambda'_{jJ'k}|/0.01)^2 1.17 \times 10^{-7}$. The comparison with the experimental limits yields the coupling constant bounds: $|\lambda'_{jJk}\lambda'_{jJ'k}| < [3.8 \times 10^{-2}, 9.1 \times 10^{-2}, 1.2 \times 10^{-1}]$, for $[(J J') = (12), (23), (13)]$ and $\tilde{m} = 100$ GeV.

These e^+e^- collider bounds are not yet competitive with bounds obtained from fixed target experiments but they are expected to be improved in the context of future e^+e^- linear colliders. The \tilde{R}_p contributions to Flavour Changing Neutral Currents at e^+e^- colliders for centre of mass energies above the Z boson pole will be discussed in chapter 7.

Atomic Parity Violation and Polarisation Asymmetries

Atomic Parity Violation (APV) has been observed via the $6S \rightarrow 7S$ transitions of ^{133}Cs [292]. In the SM, parity violating transitions between particular atomic levels occur via Z -exchange between the nucleus and the atomic electrons. The underlying four fermion contact interactions, flavour diagonal with respect to the leptons and quarks, are conventionally represented by the effective Lagrangian:

$$\mathcal{L} = \frac{G_F}{\sqrt{2}} \sum_{i=u,d} [C_1(i)(\bar{e}\gamma_\mu\gamma_5 e)(\bar{q}_i\gamma^\mu q_i) + C_2(i)(\bar{e}\gamma_\mu e)(\bar{q}_i\gamma^\mu\gamma_5 q_i)] \quad (6.44)$$

with

$$\begin{aligned} C_1(u) &= 2g_A^e g_V^u = -\frac{1}{2} + \frac{4}{3}x_W, & C_1(d) &= 2g_A^e g_V^d = \frac{1}{2} - \frac{2}{3}x_W \\ C_2(u) &= 2g_V^e g_A^u = -\frac{1}{2} + 2x_W, & C_2(d) &= 2g_V^e g_A^d = \frac{1}{2} - 2x_W, \end{aligned} \quad (6.45)$$

and $x_W = \sin^2 \theta_W$. In the presence of a λ'_{11k} (λ'_{1j1}) coupling, the s -channel exchange of a \tilde{d}_{kR} (\tilde{u}_{jL}) between an electron and a u (d) quark in the nucleus, as shown by the crossed processes depicted in Fig. 6.5b(c), leads to additional parity violating interactions. Moreover, the coefficients C_1 and C_2 are affected by a non vanishing λ_{12k} coupling via its effect on G_F given by equation (6.11). The expression of C_1 and C_2 in the presence of \tilde{R}_p interactions reads as [254]:

$$\begin{aligned} C_1(u) &= \left(-\frac{1}{2} + \frac{4}{3}x_W\right)(1 - r_{12k}(\tilde{e}_{kR})) - r'_{11k}(\tilde{d}_{kR}), \\ C_2(u) &= \left(-\frac{1}{2} + 2x_W\right)(1 - r_{12k}(\tilde{e}_{kR})) - r'_{11k}(\tilde{d}_{kR}), \\ C_1(d) &= \left(\frac{1}{2} - \frac{2}{3}x_W\right)(1 - r_{12k}(\tilde{e}_{kR})) + r'_{1j1}(\tilde{u}_{jL}), \\ C_2(d) &= \left(\frac{1}{2} - 2x_W\right)(1 - r_{12k}(\tilde{e}_{kR})) - r'_{1j1}(\tilde{u}_{jL}). \end{aligned} \quad (6.46)$$

Instead of using the C coefficients directly, one can use the measurement of the weak charge Q_W , defined as $Q_W = -2[(A + Z)C_1(u) + (2A - Z)C_1(d)]$ where Z (A) is the number of

protons (nucleons) in the considered atom, or its difference $\delta Q_W = Q_W - Q_W^{SM}$ to its SM value. In Cs atoms [293]:

$$\delta(Q_W(\text{Cs})) = -2[72.07 r_{12k}(\tilde{e}_{kR}) + 376 r'_{11k}(\tilde{d}_{kR}) - 422 r'_{1j1}(\tilde{u}_{jL})] \quad .$$

Comparison with the experimental measurement :

$$\delta(Q_W(\text{Cs})) = 0.45 \pm 0.48$$

in the single coupling dominance hypothesis leads to the $2 - \sigma$ bounds:

$$|\lambda_{12k}| < 0.05 \tilde{e}_{kR}, \quad |\lambda'_{11k}| < 0.02 \tilde{d}_{kR}, \quad |\lambda'_{1j1}| < 0.03 \tilde{u}_{jL} \quad . \quad (6.47)$$

In Tl atoms, $\delta(Q_W(\text{Tl})) = -2[116.89 r_{12k}(\tilde{e}_{kR}) + 570 r'_{11k}(\tilde{d}_{kR}) - 654 r'_{1j1}(\tilde{q}_{jL})]$. However the resulting bounds on the \mathcal{R}_p couplings are less stringent than the ones given above, due to the large error on the measurement of $\delta(Q_W(\text{Tl}))$.

Closely related to APV measurements in atoms, polarisation asymmetries in elastic and inelastic scattering of longitudinally polarised electrons on proton or nuclear targets can also be used to constrain \mathcal{R}_p interactions [294]. Below, we shall use the summary of experimental results for the parameters $C_{1,2}(q)$ as quoted in [286].

A relevant observable is the asymmetry with respect to the initial lepton longitudinal polarisation for the elastic scattering on scalar $J^P = 0^+$ nuclear targets,

$$\mathcal{A}_{pol} = \frac{d\sigma_R - d\sigma_L}{d\sigma_R + d\sigma_L}; \quad [\mathcal{A}_{pol} = \frac{G_F q^2}{\sqrt{2}\pi\alpha} \frac{3}{2} (C_1(u) + C_1(d))(1 + R(q^2))]. \quad (6.48)$$

The elastic electron scattering $e^- + {}^{12}\text{C} \rightarrow e^- + {}^{12}\text{C}$ is studied at the BATES accelerator. The difference between the experimental measurement and the Standard Model prediction [295, 296] is given by $\delta(C_1(u) + C_1(d)) = (0.137 \pm 0.033) - (0.152 \pm 0.0004) = -0.015 \pm 0.033$. Fitting this to the \mathcal{R}_p contribution yields the coupling constant bounds $\lambda_{12k} < 0.255 \tilde{e}_{kR}$, $\lambda'_{11k} < 0.10 \tilde{d}_{kR}$, and the 1σ level bound $\lambda'_{1j1} < 0.11 \tilde{q}_{jL}$.

The polarisation asymmetry of inelastic electron scattering on deuteron $e + d \rightarrow e' + X$, as measured by the SLAC experiment [297], is described by,

$$\mathcal{A}_{pol} = \frac{3G_F Q^2}{5\sqrt{2}\pi\alpha} [(C_1(u) - \frac{1}{2}C_1(d)) + (C_2(u) - \frac{1}{2}C_2(d)) \frac{1 - (1-y)^2}{1 + (1-y)^2}] \quad [y = \frac{E_e - E'_e}{E_e}]. \quad (6.49)$$

The differences between the experimental values and the Standard Model predictions are, $\delta(2C_1(u) - C_1(d)) = (-0.22 \pm 0.26)$, $\delta(2C_2(u) - C_2(d)) = (-0.77 \pm 1.23)$. Comparing with the \mathcal{R}_p contribution for the first quantity yields the coupling constant bounds $\lambda'_{11k} < 0.29 \tilde{d}_{kR}$, $\lambda'_{1j1} < 0.38 \tilde{q}_{jL}$, and the 1σ level bound, $\lambda_{12k} < 0.20 \tilde{e}_{kR}$. Comparing for the second quantity yields $\lambda_{12k} < 2.0 \times \tilde{e}_{kR}$, $\lambda'_{1j1} < 0.71 \tilde{q}_{jL}$ and at the 1σ level, $\lambda'_{11k} < 0.39 \tilde{d}_{kR}$.

The electron polarisation asymmetry, as measured for the $e_{L,R} + {}^9\text{Be} \rightarrow p + X$ quasi-elastic scattering Mainz accelerator experiment [298], exhibits a discrepancy with respect to the Standard Model prediction, $\mathcal{A}_{Mainz} = 12.7 C_1(u) - 0.65 C_1(d) + 2.19 C_2(u) - 2.03 C_2(d) = (-0.065 \pm 0.19)$. Comparing with the \mathcal{R}_p contribution yields the coupling constant bounds $\lambda'_{11k} < 0.93 \times 10^{-1} \tilde{d}_{kR}$, and at the 1σ level, $\lambda_{12k} < 3.0 \times 10^{-1} \tilde{e}_{kR}$, $\lambda'_{1j1} < 2.4 \times 10^{-1} \tilde{q}_{jL}$. The above results clearly show that the strongest bounds from $\gamma - Z$ interference effects are those emanating from the APV experiments.

6.3.3 Anomalous Magnetic Dipole Moments

The anomalous magnetic dipole ($M1$) moments of the quarks and leptons represent valuable observables that may be accessed in both low and energy experiments. For the light leptons, these observables are determined with high precision thanks to the high sensitivity currently attained by the experimental measurements. Other moments such as the Z boson current anomalous magnetic dipole moments for the τ -lepton $a_\tau(m_Z^2)$ or the b -quark $a_b(m_Z^2)$ are currently accessed in experiments at the leptonic and hadronic colliders.

The discrepancies with respect to the Standard Model expectations for the leptons or quarks, defined as $\delta a_l = a_l^{EXP} - a_l^{SM}$, reflect the corrections arising from the perturbative higher-loop orders electroweak contributions, the virtual hadronic corrections and possibly the Minimal Supersymmetric Standard Model loop corrections. The comparison between theory and experiment is expected to provide a sensitive test for new physics [299]. The electron moment a_e is a basic data for the purpose of extracting the experimental value of the hyperfine constant α . A small finite discrepancy is present for the electron in the difference between the experimental and Standard Model value given by $\delta a_e \equiv a_e^{EXP} - a_e^{SM} = 1. \times 10^{-11}$.

The measurement of the muon anomalous magnetic moment [300] exhibits a finite deviation from the Standard Model prediction, $\delta a_\mu = a_\mu^{EXP} - a_\mu^{SM} = 33.7 (11.2) \times 10^{-10}$, based on e^+e^- data, or $\delta a_\mu = a_\mu^{EXP} - a_\mu^{SM} = 9.4 (10.5) \times 10^{-10}$, based on τ data. The theoretical value $(a_\mu)_{SM}$ includes the contribution from the hadronic radiative effects [301]. The above quoted deviation with respect to the Standard Model is deduced on the basis of calculations of multi-loop diagrams which have not been verified in totality. Recent works by Knecht et al. [302] have resolved the long-standing problem associated with the sign in the muon anomalous magnetic moment [303] for the non-perturbative contribution from the pion-pole term in the light-by-light scattering amplitude. We refer to the review cited in [302] for more details. Although the exact size of the hadronic contributions to a_μ^{SM} remains an unsettled problem, the comparison of the various existing calculations [304] indicates that the corresponding uncertainties do not affect significantly the Standard Model prediction.

An early study by Frank and Hamidian [305] of the \mathcal{R}_p contribution to the leptons anomalous $M1$ moments indicated that the resulting constraints on the \mathcal{R}_p coupling constants were relatively insignificant. The recently reported measurement of the muon anomalous magnetic moment [300] has stimulated two detailed studies of the \mathcal{R}_p effects [306, 307] focused on the muon anomalous $M1$ moment.

The study by Kim et al., [306] is performed within the so-called effective supersymmetry framework. One retains the contributions from the third generation sfermions only, based on the assumption that the first and second generation sfermions decouple as having large masses of order $m_{\tilde{l}} = O(20)$ TeV, [$l = 1, 2$]. Such a radical hypothesis would, of course, relax significantly the various bounds on the \mathcal{R}_p coupling constants with superpartner indices associated to the first two generations. The one-loop diagram contributions to the anomalous $M1$ moment a_{f_j} of a fermion f_j enter in two types depending on whether the required chirality flip between the external fermions takes place on the external lines themselves (giving an external fermion mass overall factor m_{f_j}) or on the internal fermion and sfermion lines (giving an overall factor $m_{f_j} \tilde{m}_{LR}^2/m_{\tilde{f}}^2$). For the muon case, it turns out that the contributions of the first type, with a chirality flip on the external line, are the predominant ones. The bounds inferred by assuming the single coupling constant dominance hypothesis are:

$$[\lambda_{32k}, \lambda_{3j2}, \lambda_{i23}, \lambda_{2j3}] < 0.52 \frac{m_{\tilde{f}}}{100 GeV}. \quad (6.50)$$

Alternatively, if one focuses solely on the coupling constant λ_{322} , based on the observation that this is the least constrained of all the coupling constants involved, then the predicted value of the anomalous moment associated with the \mathcal{R}_p effects,

$$(a_\mu)_{RPV} \simeq 34.9 \times 10^{-10} \left(\frac{100 \text{ GeV}}{\tilde{m}} \right)^2 |\lambda_{322}|^2, \quad (6.51)$$

is seen by comparison with the experimental result to be compatible with the perturbativity bound on the corresponding coupling constant.

A comparison of the \mathcal{R}_p effects on the muon magnetic moment and the neutrino masses is of interest, despite the fact that the one-loop contributions to the neutrino masses are of the type involving chirality flip mass insertion terms for the fermion and sfermion internal lines. Indeed, some correlation still exists between the one-loop contributions in these two cases owing to the identity of the \mathcal{R}_p coupling constant factors. Adhikari and Rajasekaran [307] observe that in order to get \mathcal{R}_p contributions to the muon anomalous magnetic moment and neutrino mass of the size required by the current experiments, $a_\mu = O(10^{-9})$, $m_{\nu_\mu} = O(1)$ eV, one needs to suppress in some way the one-loop contribution to the neutrino mass. This can be achieved by postulating for the chirality flip slepton mass parameters $(\tilde{m}_{LR}^{e2})_{ij}$ either reduced values or a degeneracy with respect to the first two generations, $(\tilde{m}_{LR}^{e2})_{11} \simeq (\tilde{m}_{LR}^{e2})_{22}$. A natural resolution of this issue can be achieved in a model using a discrete symmetry acting on the lepton sector.

6.3.4 CP Violation

The existence of a possible connection between CP violation and R -parity violation has received increased attention in the literature [253, 308, 309, 310, 311, 312, 313, 314, 315, 316, 317]. In this section, we discuss a non-exhaustive set of physical applications which lie at the interface between R -parity violation and CP or T violation. The topics to be addressed include discussions on observables in the neutral $K\bar{K}$ system, the electric dipole moment (EDM) of leptons and quarks, the CP -odd asymmetries in B meson hadronic decay rates and the CP -odd asymmetries in Z boson decay rates into fermion-antifermion pairs. A study of the CP -violation effects in association with sneutrino flavour oscillations was carried out in chapter 5.

General Considerations on CP Violation

As is known, the violation of CP symmetry is revealed in the context of field theories by complex phases present in VEVs of scalar fields, in particles mass parameters or in Yukawa interaction coupling constants which cannot be removed by field redefinitions.

It is conventional to distinguish between soft and hard CP violation, depending on whether the dimensionality of the CP -odd operators in the effective lagrangian is ≤ 3 and ≥ 4 respectively. The spontaneous CP violation case, as characterized by the presence of CP -odd complex phases in scalar fields VEVs resulting from a CP conserving lagrangian, falls naturally within the soft violation category. The distinction between soft and hard CP violations is motivated by the different impact that the quantum and thermal fluctuations effects have in the two cases. The soft CP violation interactions cannot renormalize the hard interactions, unlike the hard CP violation interactions which indeed can renormalize the operators of lower dimensions. The soft CP violation parameters may also be suppressed by thermal fluctuations, eventually leading to a restoration of CP symmetry at high temperatures. By contrast,

the thermal effects do not affect significantly the coupling constant parameters of operators of dimension ≥ 4 , a fact which makes the hard CP violation mechanisms more robust candidates for generating the baryon or lepton asymmetry in the early Universe.

The Standard Model includes two sources of hard CP violation. One is the complex phase in the CKM matrix with three quark generations. The other is the QCD theta-vacuum angle. For supersymmetric models, new sources of soft CP violation appear with the μ term and soft supersymmetry breaking interactions. With the known structure of the constrained MSSM classical action, assuming fully universal soft supersymmetry breaking, the unremovable CP -odd phases are restricted to a pair of phases given by the relative complex phases $\phi_A = \arg(AM_{\frac{1}{2}}^*)$ and $\phi_B = \arg(B\mu^*)$. The experimental constraints give strong individual bounds on these phases i.e. $\phi_{A,B} < O(10^{-3})$. However several other additional phases arise once one relaxes the universality hypothesis for the supersymmetry breaking parameters for the quark and lepton generations or the different gaugino mass parameters. It has been found [318] that in cases where some built-in correlations between the various phases are included, the evaluation of physical observables includes such strong cancellation effects that the experimental bounds relax to values $O(1)$.

With broken R -parity, new sources of CP violation can contribute through complex phases in the parameters μ , μ_i and B , B_i for the bilinear interactions and in the parameters λ_{ijk} , λ'_{ijk} , λ''_{ijk} and A_{ijk} , A'_{ijk} , A''_{ijk} for the trilinear interactions. Each of these coupling constants can carry a complex phase although only the subset of these phases invariant under the fields rephasing is physical. For products of the trilinear \mathcal{R}_p coupling constants only, a CP -odd phase invariant under complex phase redefinitions of the fields can be defined starting from the quartic order. Examples encountered in the calculations of scattering amplitudes for processes involving four fermion fields such as $e^+ + e^- \rightarrow f_J + \bar{f}_{J'}$ are given by: $\arg(\lambda_{i1J}\lambda_{i1J'}^*\lambda_{i'jJ}^*\lambda_{i'jJ'})$, and $\arg(\lambda_{ijJ}\lambda_{ijJ'}^*\lambda_{i'j'J}^*\lambda_{i'j'J'})$.

Although basis-independent studies have been performed for specific cases [26, 319, 320] a full systematic discussion of a basis independent parametrisation of CP violation for the \mathcal{R}_p interactions would be useful in characterizing the natural size of the relevant parameters as can be emphasized from the example described in [321].

Concerning the context of bilinear R -parity violation, a partial study of the parametrisation of CP violation is performed in [322]. For that part of the scalar potential which determines the Higgs bosons VEVs, the CP -odd phase is included through the coupling constant product $\mu^*\mu_i B_i B$. Including the trilinear terms, one characteristic CP violation condition can be identified in terms of the phase in the coupling constant product of λ interactions and regular Yukawa interactions given by: $\Im(\lambda_{nmk}^* \lambda_{ijk} \lambda_{nl}^e \lambda_{il}^{e*} \lambda_{mp}^e \lambda_{jp}^{e*}) \neq 0$. Another interesting conclusion concerning a spontaneous violation of CP in the presence of \mathcal{R}_p interactions is that complex valued sneutrino VEVs can occur in a natural way without fine-tuning of the parameters [322].

Neutral $K\bar{K}$ System

The possibility of embedding a CP -odd complex phase in the \mathcal{R}_p coupling constants has been envisaged at an early stage in a work by Barbieri and Masiero [323] and then further discussed in [359, 371, 112, 324, 325] and references therein. A complex relative phase present in a quadratic product of λ''_{ijk} coupling constants can contribute to the $K_S - K_L$ mass difference.

The most general $\Delta S = 2$ effective lagrangian $\mathcal{L}_{eff}^{\Delta S=2}$ including contributions of charginos and charged Higgs boson neglected in earlier works [323, 371, 112] has been considered in [324]

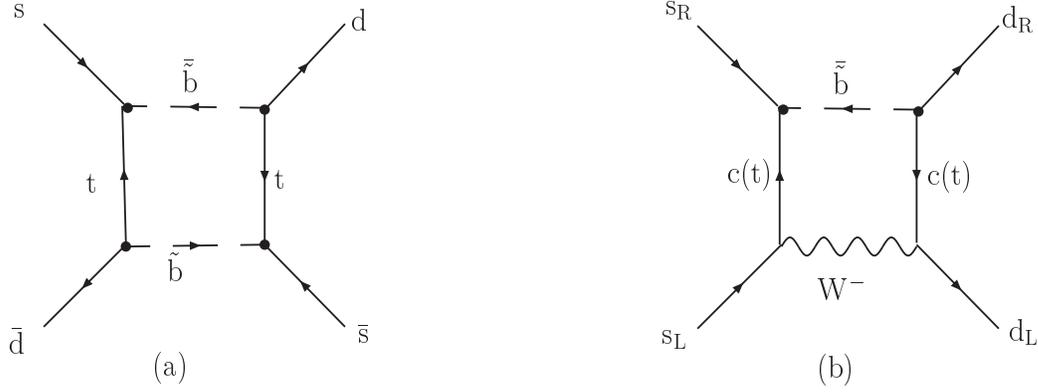


Figure 6.7: Box diagrams leading to $K\bar{K}$ mixing induced by λ'' couplings.

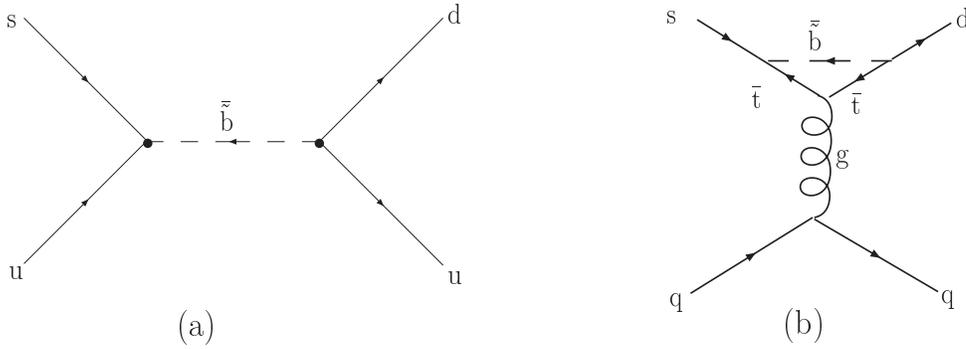


Figure 6.8: Tree level diagram (a) and gluonic penguin one-loop diagram (b) contributing to the direct $\Delta S = 1$ CP violation involving λ'' couplings.

(see also [325]). Its contribution to the $K_S - K_L$ mass difference is related to the matrix element $\langle K^0 | \bar{\mathcal{L}}_{eff}^{\Delta S=2} | \bar{K}^0 \rangle$ and involves the products of $\lambda''_{313} \lambda''_{323}$ couplings (see for example Fig. 6.7) as well as CKM matrix elements⁵. This \tilde{R}_p coupling's contribution to the $K_S - K_L$ mass difference has been calculated in [324] using NLO QCD evolution of Wilson coefficient also included in $\bar{\mathcal{L}}_{eff}^{\Delta S=2}$ [326] as well as lattice calculations for long-distance hadronic processes which cannot be evaluated perturbatively and also contribute to the above matrix element. Requiring that this contribution to the $K_S - K_L$ mass difference is not larger than the experimental value [272]⁶ allows one to set an upper limit [324]:

$$\lambda''_{313} \lambda''_{323}^* < O(0.033) \quad (6.52)$$

by performing a general scan over the parameter space on the minimal supersymmetric extension of the standard model at the weak scale and taking into account the constraints from direct searches for supersymmetric particles.

The λ'' interactions contribute also at the tree level to the direct $\Delta S = 1$ CP violation (see Fig. 6.8(a)), as described by the observable parameter ϵ' . The \tilde{R}_p contribution to ϵ' is described

⁵In [323] the charm contribution and in consequence the $\lambda''_{232} \lambda''_{213}$ products have also been considered where the t-quark in the loop is replaced by a c-quark.

⁶Actually the upper bound derived in [324] comes from the experimental value published in [327] on the $K_S - K_L$ mass difference. However the difference with the published value in [272] being marginal for the present purpose, the conclusion of the analysis presented in [324] on $\lambda''_{232} \lambda''_{213}^*$ is unchanged.

by the relation [323]:

$$\Im(\lambda''_{123}\lambda''_{113}^{\star}) \approx |\epsilon'| 10^1 \tilde{q}^2. \quad (6.53)$$

The gluonic penguin one-loop diagram, see Fig. 6.8(b), provides a competitive contribution to that of the box diagram due to the existence of a logarithmic enhancement factor in the amplitude. The resulting bound reads [323]:

$$\Im(\lambda''_{313}\lambda''_{323}^{\star}) \approx |\epsilon'| 10^{-2} \tilde{q}^2. \quad (6.54)$$

In order to match the currently observed value for $\epsilon' = O(10^{-6})$ one should require values for the quadratic coupling constants $\Im(\lambda''_{123}\lambda''_{113}^{\star})$ (respectively $\Im(\lambda''_{313}\lambda''_{323}^{\star})$) of $O(10^{-5}) \tilde{q}^2$ (respectively $O(10^{-8}) \tilde{q}^2$).

Since different generational configurations of the coupling constants contribute to the CP violation parameters ϵ and ϵ' , one concludes that the \mathcal{R}_p interactions λ'' might be relevant candidates for milliweak type CP violation contributing solely to the indirect CP violation.

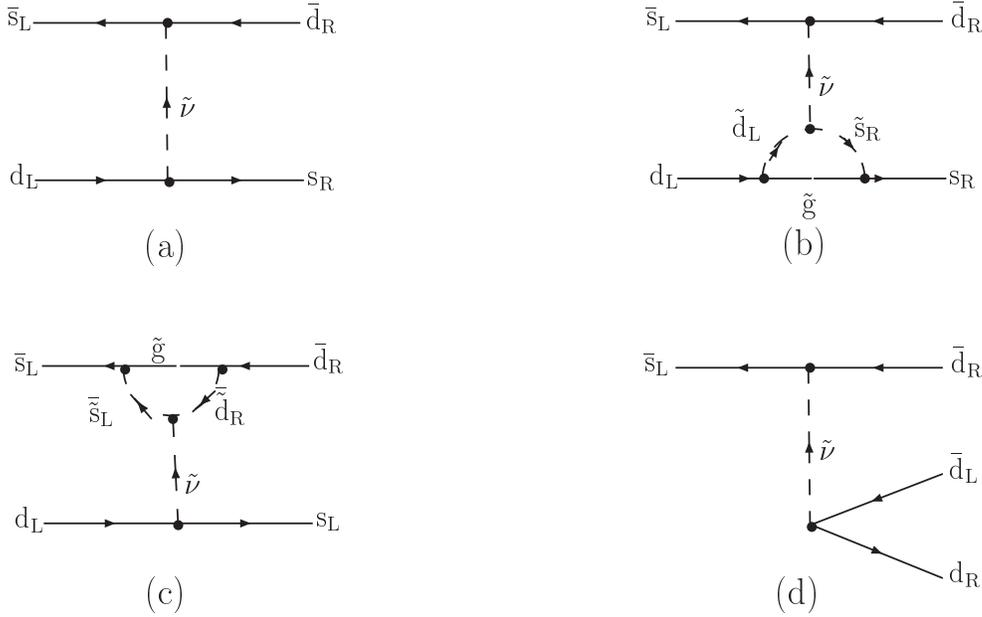


Figure 6.9: Contributions to $\Delta S = 2$ (a, b and c) and $\Delta S = 1$ (d) observables involving λ' couplings.

An interesting proposal [310] is to incorporate the CP -odd phase in the scalar superpartner interactions corresponding to the soft supersymmetry breaking \mathcal{R}_p interactions of the form $V_{soft} = A'_{ijk} \tilde{L}_i \tilde{Q}_j \tilde{D}_k^c + \text{h.c.}$. The contribution to the imaginary part of the $\Delta S = 2$ mass shift is estimated qualitatively as $\epsilon \simeq 10^{-2} \Im(A'_{i21} - A'_{i12})/m_{\tilde{g}}$. The comparison with the experimental value indicates that some cancellation between the above two flavour non-diagonal configurations i.e. A'_{i21} and A'_{i12} , may be required to take place. A contribution to the four quark interaction $\bar{s}_R d_L \bar{d}_R s_L$ arises from a sneutrino exchange penguin type diagram involving a one-loop correction to the $\tilde{\nu} ds$ vertex as shown in Fig. 6.9(b) and 6.9(c). The predicted effect on the direct CP violation $\Delta S = 1$ observable ϵ' , see Fig. 6.9(d), reads [310]:

$$\left| \frac{\epsilon'}{\epsilon} \right| \simeq 10^{-7} \frac{\lambda'_{i11}}{\lambda'_{i12}} > 10^2 \lambda'_{i11} \lambda'_{i21}, \quad (6.55)$$

where the inequality obtained at the second step uses the bounds on the coupling constant products, $\lambda'_{i12} \lambda'_{i21} < 10^{-9} \tilde{\nu}_i^2$.

Asymmetries in Hadron Decay Rates and Polarisation Observables

The polarisation of the muon emitted in the K -meson three-body semileptonic decay $K^+ \rightarrow \pi^0 + \nu + \mu^+$ ($K_{\mu 3}$) or in the radiative decay $K^+ \rightarrow \mu^+ + \nu + \gamma$ ($K_{\mu 2\gamma}$) constitute useful observables for testing T and/or CP violation.

The transverse muon polarization $P_T(K_{\mu 2\gamma})$ can be related ⁷ to $|\Im(\lambda_{2i2}^* \lambda'_{i12})|/m_{\bar{e}_iL}^2$ as shown in [314].

Under various simplifying assumptions [314], rough estimates on upper bounds on $P_T(K_{\mu 2\gamma})$ may be derived from bounds on the branching ratio of $\mu \rightarrow e\gamma$ and from the measured value ⁸ of $BR(K^+ \rightarrow \pi^+ \nu \bar{\nu})$. The $K_{\mu 2\gamma}$ decay has been measured in [329] (see also [330]) and should provide useful handles in constraining these \mathcal{R}_p couplings.

The transverse muon polarization $P_T(K_{\mu 3})$ is $O(10^{-10})$ in the standard model [331]. It can be related to $(\lambda_{232}^* \lambda'_{312})/m_{\bar{\tau}_{iL}}^2$ and $(\lambda_{122}^* \lambda'_{112})/m_{\bar{e}_iL}^2$ as shown in [332] (see also [333, 334]). These contributions from \mathcal{R}_p couplings can be as large as the present experimental limits ⁹. on $P_T(K_{\mu 3})$ [335, 336] (see also [337, 338]).

As discussed in [339] future projects may reach uncertainties approaching the $O(10^{-4})$ level for the measurement of $P_T(K_{\mu 3})$ thus allowing also to test \mathcal{R}_p couplings further.

Z boson partial decay

The Z boson partial decay channels into fermion-antifermion (up-quark, down-quark, charged lepton) pairs of different flavours, $Z \rightarrow f_J + \bar{f}_{J'}$ [$J \neq J'$; $f = u, d, l$], may exhibit potentially observable CP violating decay asymmetries. These are defined by the normalised differences of flavour non-diagonal, spin-independent rates,

$$\mathcal{A}_{JJ'} = \frac{B_{JJ'} - B_{J'J}}{B_{JJ'} + B_{J'J}}, \quad (6.56)$$

where the branching ratios $B_{JJ'}$ are defined in equation (6.42). A finite contribution to the flavour decay asymmetry is rendered possible by the existence of a finite CP -odd complex phase, ψ , embedded in the \mathcal{R}_p coupling constants. The asymmetries [291] are proportional to ratios of the coupling constants of the form:

$$\Im\left(\frac{\lambda_{iJk}^* \lambda'_{iJ'k}}{\lambda_{1Jk}^* \lambda'_{1J'k'}}\right) \propto \sin \psi. \quad (6.57)$$

Should the \mathcal{R}_p coupling constants exhibit generational hierarchies, one could then expect large enhancement or suppression of the asymmetries, depending on the flavour of the emitted fermions. Assuming that the above ratios of \mathcal{R}_p coupling constants products take values of order unity, the resulting asymmetries for the emission of charged leptons, down-quarks and up-quarks are found to be of the order of $\mathcal{A}_{JJ'} \approx (10^{-1} - 10^{-3}) \sin \psi$.

⁷Various expressions for $P_T(K_{\mu 3})$ can be found in [328] in the context of leptoquark models.

⁸At the time of [314] only upper bounds on $BR(K^+ \rightarrow \pi^+ \nu \bar{\nu})$ were known.

⁹The limits used in [332] come from [335] and should be replaced by those published in [336]. However the general conclusion drawn in [332] should not be significantly affected.

Neutron Electric Dipole Moment

The \mathcal{R}_p interactions λ'' may contribute to the neutron electric dipole moment d_n^γ [323] via a quark electric dipole moment described by a two-loop vertex Feynman diagram involving the crossed exchange of W and \tilde{d} internal particle lines as seen in Fig. 6.10. Note that no contributions from the \mathcal{R}_p interactions to the neutron dipole moment can arise at the one-loop order level [340, 341].

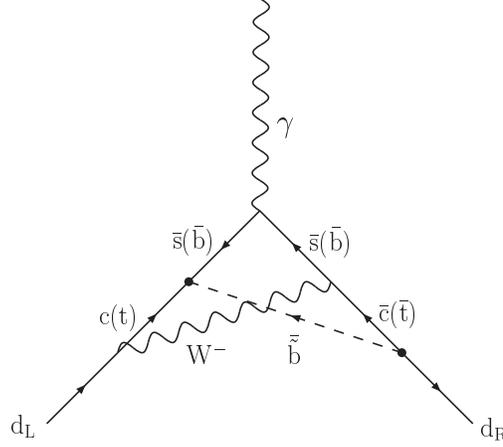


Figure 6.10: Contributions to the neutron electric dipole moment involving λ'' couplings.

The needed suppression to account for a sufficiently small electric dipole moment is provided in part by the light quark mass factors reflecting the chirality flip selection rules of the \mathcal{R}_p couplings. A relative CP -odd complex phase embedded in a pair product of λ'' coupling constants is required in order to obtain a finite contribution to the electric dipole moment. The contribution is maximised by choosing third generation $b - \tilde{b}$ quarks configuration for the internal fermion and sfermion particles. The results derived by Barbieri and Masiero [323] on the basis of the double coupling constant dominance hypothesis read:

$$\Im(\lambda''_{213}\lambda''_{232}^*) \simeq 10^{-2} \left(\frac{d_n^\gamma}{10^{-25} e \times \text{cm}} \right) \tilde{q}^2 \quad (6.58)$$

$$\Im(\lambda''_{312}\lambda''_{332}^*) \simeq 10^{-1} \left(\frac{d_n^\gamma}{10^{-25} e \times \text{cm}} \right) \tilde{q}^2 \quad (6.59)$$

for the internal charm quark and top quark cases, respectively. Using the current experimental bound on the neutron electric dipole moment, $d_n^\gamma < 1.2 \times 10^{-25} e \text{ cm}$ from [342] one obtains a bound for the top quark box diagram contribution only which is $|\Im(\lambda''_{312}\lambda''_{332}^*)| < 0.12\tilde{q}^2$.

The discussion on systematic uncertainties concerning the more recent bound $d_n^\gamma < 6.3 \times 10^{-26} e \cdot \text{cm}$ recently published in [343] has been criticized in [344].

Contributions from products of λ' couplings such as $\Im(\lambda'_{i33}^*\lambda'_{i11})$ are discussed in [345].

New contributions involving both bilinear and trilinear couplings can lead to a neutron electric dipole moment as discussed in [346, 347].

Electron Electric Dipole Moment

Even if one assumes purely real CP conserving \mathcal{R}_p coupling constants, a non-vanishing CP violating contribution could possibly be induced by invoking the existence of other possible sources of complex phases present in the (minimal) Supersymmetric Standard Model. Thus the λ_{ijk} and λ'_{ijk} \mathcal{R}_p couplings may induce one-loop contributions to the electric dipole moment of leptons (and quarks) through an interference with a complex valued CP -odd soft supersymmetry breaking parameters A_{ij}^u and A_{ij}^d associated with the regular Yukawa interactions. A non-vanishing amplitude associated with the Feynman diagram with a pair of sfermion and fermion internal lines requires the presence of a $L - R$ chirality flip mass-mixing insertion \tilde{m}_{LR}^2 for the internal sfermion. Stated equivalently, it requires a mass splitting between the opposite chiralities sfermion eigenstates. The bounds are strongest for the electron electric dipole moment d_e^γ and can lead to several strong individual coupling constant bounds as shown in [305]. A representative subset is tentatively summarized by $\lambda'_{111} < 5.5 \times 10^{-5}$, $\lambda'_{121} < 8.7 \times 10^{-6}$, $\lambda'_{213} < 9.5 \times 10^{-2}$, $\lambda'_{233} < 1.5 \times 10^{-2}$ using $d_e^\gamma = (3 \pm 8) \times 10^{-27} e \text{ cm}$ [378] which could be superseded by the recently [348] measured value $d_e^\gamma = (6.9 \pm 7.4) \times 10^{-28} e \text{ cm}$ i.e. $|d_e^\gamma| = 1.6 \times 10^{-27} e \text{ cm}$

Focusing on the contribution from a complex \mathcal{R}_p coupling constant $\lambda'_{133} = |\lambda'_{133}|e^{i\beta}$, interfering with a complex soft coupling constant $A^q = |A^q|e^{i\alpha_A}$, the current bound on the experimental electron electric dipole moment can admit solutions with large values for both of the above CP -odd phases β and α_A as shown in [349].

However the conclusions drawn from the above two studies [305, 349] have been recently challenged by the observation that no contributions from the \mathcal{R}_p interactions to the electric dipole moment can arise at the one-loop order level [340, 341]. Due to the chirality selection rules, an \tilde{e}_R particle line can never be emitted nor absorbed. For similar reasons, a $\tilde{d}_R - \tilde{d}_L$ mass insertion on the squark line must be accompanied by a neutrino Majorana mass insertion, resulting in a strongly suppressed contribution to the electric dipole moment which exactly vanishes in the zero neutrino mass limit. A one-loop contribution could only be possible through a sneutrino Majorana mass term, $\tilde{m}_{ij}\tilde{\nu}_{iL}\tilde{\nu}_{jL}$ as can be seen in Fig. 6.11.

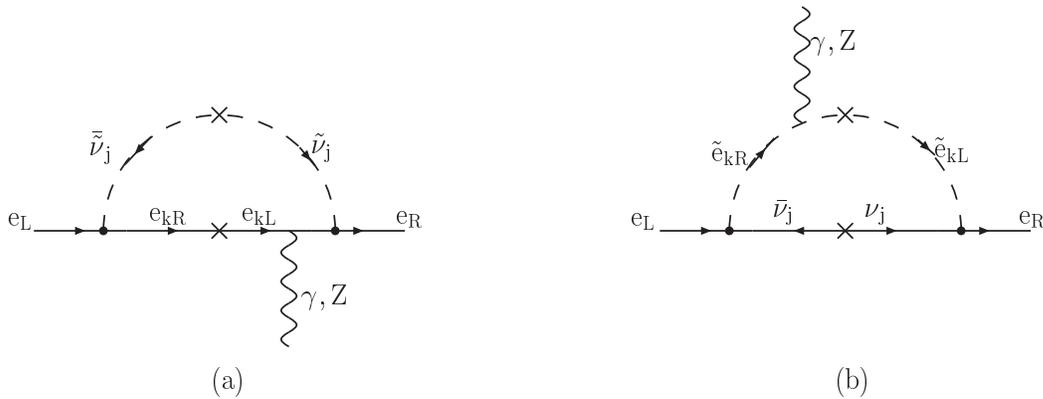


Figure 6.11: One-loop diagrams contribution to the electron dipole moment involving λ couplings.

Similar chirality selection rules would also apply for the analogous chirality flip observables, such as involved in the contributions to the neutrino Majorana mass, the neutrino $M1$ or $E1$ diagonal or off-diagonal moments, or the charged fermions $M1$ transition moments. On the

other hand, $E1$ transition moments for Majorana neutrinos may possibly be initiated by the \mathcal{R}_p interactions at the one-loop order. The above observations figure in [340, 341].

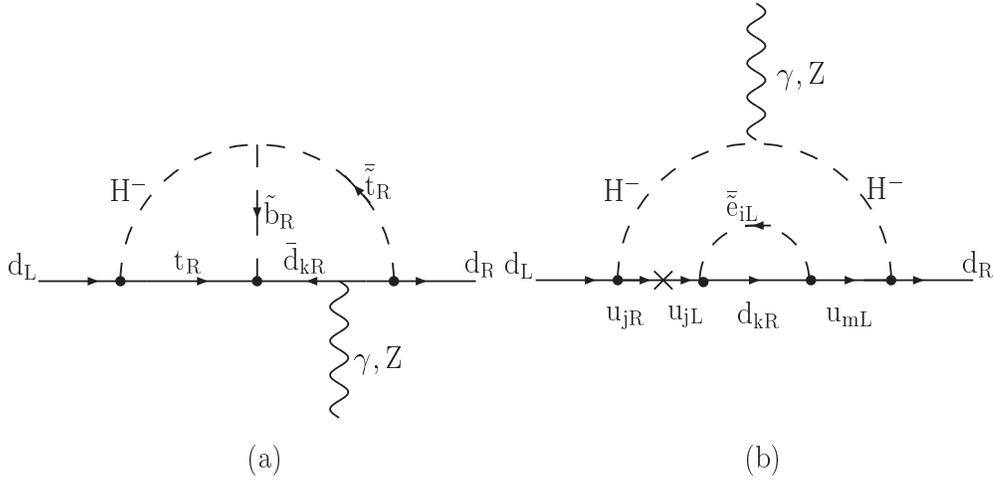


Figure 6.12: Examples of two-loops diagrams contribution to the electric dipole moment of the electron with Higgs and sfermions exchanges λ' couplings (a) and λ and λ'' couplings (b).

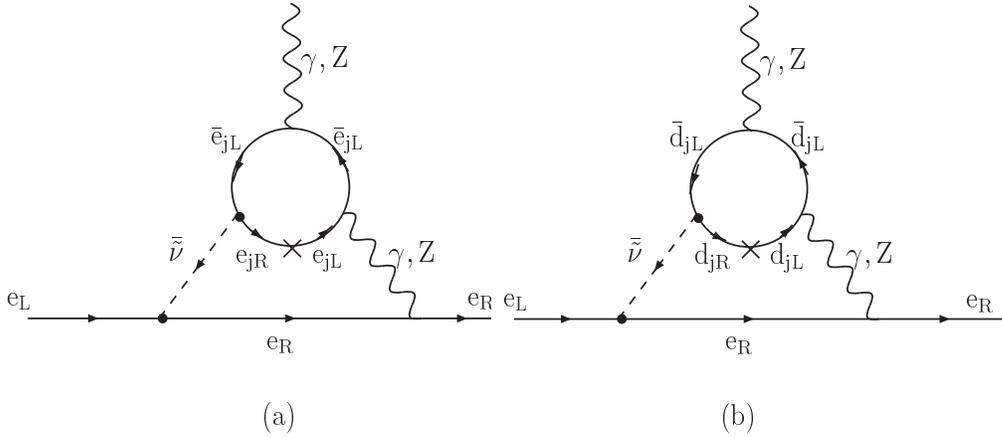


Figure 6.13: Examples of two-loops diagrams contribution to the electric dipole moment of the electron involving λ couplings (a) and λ and λ' couplings (b).

As discussed in [340, 341], at the two-loop order many possible mechanisms can contribute to the electric dipole moment. We have already discussed above the contributions from the λ'' interactions. The two-loop diagrams with overlapping or crossed exchanges of Higgs bosons and sfermions (see Fig. 6.12), or of gauge boson and sfermions (see Fig. 6.13 and Fig. 6.14), yield contributions proportional to quadratic products of the \mathcal{R}_p coupling constants times quadratic products of the CKM matrix elements, entering in appropriately rephased invariant flavour configurations.

New contribution involving both bilinear and trilinear couplings can also lead to electron electric dipole moment as discussed in [346, 347].

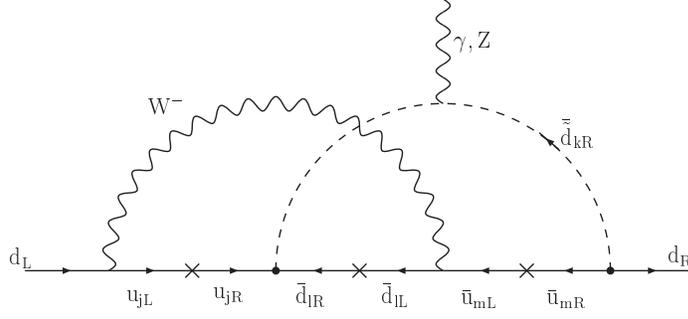


Figure 6.14: Example of two-loop diagram contribution to the electron dipole moment with gauge boson and sfermion exchange involving λ'' couplings.

Atomic Electric Dipole Moment

The electric dipole moment of atoms also present a strong potential interest [350, 351] owing to the high experimental sensitivity that can be attained in the experimental measurements of the electric dipole moment of atoms such as ^{133}Cs or ^{205}Tl . The \mathcal{H}_p contributions to the electron electric dipole moment from the other mechanism described by the two-loop diagram with one fermion closed loop leads to the coupling constant bounds [340, 341, 352] (for $J=1,2,3$):

$$|\Im(\lambda_{1J1}^* \lambda'_{J33})| < 6. \times 10^{-7} \quad (6.60)$$

These bounds should be revisited in view of new experimental results [348].

The \mathcal{H}_p contributions from the two-loop diagram with two crossed sfermionic loops attached to the external line, yield bounds on quartic coupling constant products of the form [341]:

$$\frac{m_l}{m_\tau} |\Im(\lambda_{1mn} \lambda_{jln}^* \lambda_{iml}^* \lambda_{ij1})| < 10^{-6} \quad (6.61)$$

$$\frac{m_l}{m_t} |\Im(\lambda_{1mn} \lambda_{jln}^* \lambda_{iml}^* \lambda_{ij1})| < 3. \times 10^{-6} \quad (6.62)$$

using experimental bounds on the electric dipole moment of both the electron and the neutron.

These bounds on quartic coupling constant products should also be revisited in view of the new experimental result [348] on the electric dipole moment of the electron and the discussion published in [344] on the experimental value of the electric dipole moment of the neutron.

Finally, useful information on the P and T violating $e - N$ interactions as parametrised by the effective Lagrangian:

$$\mathcal{L} = -\frac{G_F}{\sqrt{2}} (C_{Sp} \bar{e} i \gamma_5 e \bar{p} p + i C_{Tp} \bar{e} \sigma_{\alpha\beta} e \bar{p} \tilde{\sigma}^{\alpha\beta} p) + (p \leftrightarrow n), \quad (6.63)$$

with:

$$\tilde{\sigma}_{\alpha\beta} = \frac{1}{2} \epsilon^{\alpha\beta\gamma\delta} \sigma^{\gamma\delta}, \quad (6.64)$$

can be obtained from the experimental limits for the electric dipole moment of atoms such as currently available for the ^{133}Cs or ^{205}Tl atoms [350]. The comparison can result for example in the bound [352] $|\Im(\lambda_{1I1}^* \lambda'_{I11})| < 1.7 \times 10^{-8} \tilde{\nu}_I^2$ ($I=2,3$).

Hadronic B Meson Decay Asymmetries

The formalism for B meson physics as well as CP violation in the B meson system can be found in [272].

The $\Delta b = 1$ non-leptonic decay transition amplitudes arise from tree level diagrams and, when these are forbidden, from one-loop box type and penguin type diagrams associated with the quark subprocess $b \rightarrow d_i \bar{q}' q''$, [$q', q'' = (u, c, d, s)$]. The relevant effective Lagrangian consists of 10 independent operators quartic in the quark fields.

The tree level contribution from the \mathcal{R}_p interactions having the specific form:

$$\mathcal{L} = \sum_i \frac{\lambda'_{ijk} \lambda_{i'j'k'}^*}{m_{\tilde{e}_i L}^2} (\bar{d}_{kR} d_{jL}) (\bar{d}_{j'L} d_{k'R}). \quad (6.65)$$

Assuming the mixing decay amplitudes to consist of the two additive contributions from the Standard Model and \mathcal{R}_p interactions, one can parametrise the off-diagonal elements of the mass matrix M_{12} of the neutral B mesons and the decay amplitude A in terms of real parameters and complex phases r_X and θ_X where X stands either for M (mixing) or D (decay) as:

$$M_{12} = M_{12}^{SM} (1 + r_M e^{i\theta_M}) \quad (6.66)$$

$$A = A_{SM} (1 + r_D e^{i\theta_D}) \quad (6.67)$$

Under the simplifying approximation where the final state CP -even strong interactions phase is the same for all the additive terms in the decay amplitudes, the ratio $\bar{A}/A = e^{-2i\phi_D}$, where \bar{A} is the CP mirror conjugate decay amplitude becomes a pure complex phase, so that one expresses the basic asymmetry parameter as:

$$r_{f(CP)} = e^{-2i(\phi_M + \phi_D)} \quad (6.68)$$

The \mathcal{R}_p corrections may be represented in terms of shifts in the mixing and decay complex phases $\phi_X = \phi_X^{SM} + \delta\phi_X$ (with $X = M, D$) such that:

$$\delta\phi_X = \tan^{-1} \frac{r_X \sin \theta_X}{1 + r_X \cos \theta_X}. \quad (6.69)$$

For illustration, note that in the Standard Model the mixing phase for the B_d system is described by $\phi_M = -\frac{1}{2} \arg(V_{tb}^* V_{td})$, and the decay mode to the final state $f(CP) = J/\Psi \pi^0$ by:

$$r_{f(CP)} = \exp i[\arg(V_{tb}^* V_{td}) + \arg(V_{cs}^* V_{cb}) + \arg(V_{cd}^* V_{cs})] = e^{-2i\beta} \quad (6.70)$$

The decay channels such as $B \rightarrow K^0 \bar{K}^0$, $\phi \pi^0$, ϕK_S are of special interest since their associated quark subprocesses, $\bar{b} \rightarrow \bar{d} \bar{d} \bar{d}$, $\bar{d} \bar{d} \bar{s}$, $\bar{s} \bar{s} \bar{s}$, respectively, are tree level forbidden in the Standard Model ¹⁰.

The \mathcal{R}_p contribution to the mixing parameter reads $r_M \simeq 10^8 \lambda'_{i13} \lambda_{i31}^* \tilde{\nu}^{-2}$ [311]. Predictions for the \mathcal{R}_p contributions to the CP -odd asymmetry parameter r_D in the various decay channels are provided in refs. [309, 311, 312].

¹⁰See for example [272, 353] for experimental results.

Using bounds on quadratic products of the λ' and λ'' coupling constants from experimental constraints in [378], one can observe [309] that the predicted bounds on r_D follow different patterns for the heavy meson decay channels such as $B \rightarrow J/\Psi K_S$, $B \rightarrow D^+ D^-$, in comparison to the light meson decay channels such as $B \rightarrow \phi K_S$, $\phi \pi^0$, $K_S K_S$, the latter generally yielding more favourable signals with $(1 + r_D) \simeq |A_{\mathcal{R}_p}/R_{SM}| \gg 1$. One can also incorporate systematically the mixing effects and updated values for the Wilson coefficients of the operators [312]. The contributions to the asymmetry parameters r_D in the various decays from the λ' interactions are typically of order, $10^{-3} - 10^{-4}$. By contrast, those from the λ'' interactions turn out to arise with a more interesting order of magnitude i.e. $O(1 - 10^{-1})$.

The important decay modes with the final states $f = \phi K_S$ and $J/\Psi K_S$ have been considered in [311]. The Standard Model predicts equal decay phases ϕ_D along with controlled uncertainties for the difference of phases [354]:

$$\Delta\phi_D = |\phi_D(B_d \rightarrow \phi K_S) - \phi_D(B_d \rightarrow J/\Psi K_S)| < O(10^{-1}). \quad (6.71)$$

Anticipating the possibility that the experimental errors may reach a sensitivity at this level of accuracy or higher, an important question is the expected size for the \mathcal{R}_p contributions. These are found to be [311]:

$$\begin{aligned} r_D(B_d \rightarrow \phi K_S) &\simeq 8. \times 10^2 |\lambda'_{i23} \lambda'_{i22} + \lambda'_{i22} \lambda'_{i32}| \left(\frac{m_W}{m_{\tilde{\nu}_i}}\right)^2 \\ r_D(B_d \rightarrow J/\Psi K_S) &\simeq 2. \times 10^2 |\lambda'_{i23} \lambda'_{i22}| \left(\frac{m_W}{m_{\tilde{e}_{iL}}}\right)^2 \end{aligned} \quad (6.72)$$

Using the current bounds on the \mathcal{R}_p coupling constants, especially those coming from $BR(b \rightarrow X_s \nu \bar{\nu})$ [355], yields an encouraging prediction for the above difference of phases, $\Delta\phi_D \simeq O(1)$ [311].

Let us finally note that analogous methods have been developed to extract experimental information for neutral or charged B meson decays into non-pure CP channels. The CP decay rate asymmetries are obtained by forming differences between the decay rates for the CP conjugate transitions, $B^0 \rightarrow f$, $\bar{B}^0 \rightarrow \bar{f}$. Interesting signals from the \mathcal{R}_p contributions are also expected for the charged B meson decays CP asymmetries in the transitions $B^+ \rightarrow f$ and $B^- \rightarrow \bar{f}$ [309] such as, for example, $B_d \rightarrow J/\Psi \rho^0$, $D^\pm \pi^\mp$, $K^+ \pi^-$ or $B_d^+ \rightarrow J/\Psi K^+$, $\pi^+ \pi^0$. The leptonic or semileptonic decay modes of the B mesons also deserve a due consideration.

For the decay mode $B^\pm \rightarrow \pi^\pm K$, the \mathcal{R}_p induced amplitude $A_{\mathcal{R}_p} \propto [\lambda'_{i23} \lambda'_{i12} / \tilde{m}^2] (b\bar{s})(d\bar{d})$ could yield a nearly 100 % contribution to the CP -odd asymmetry much larger than the Standard Model contributions which are expected not to exceed a 40 % effect [317].

The CP violating asymmetries in the decay and polarization observables of hyperon non-leptonic weak decay modes $\Lambda_b \rightarrow p + \pi^-$ are examined in [313].

6.4 Trilinear \mathcal{R}_p Interactions in Flavour Violating Processes and in \mathcal{B} and \mathcal{L} Processes

A very large number of bounds for the trilinear \mathcal{R}_p couplings have been deduced from studies of low and intermediate energy processes. In particular, rare decays involving either hadron flavour

violation or lepton flavour violation (LFV), or both combined, constitute a nearly inexhaustible source of constraints on the trilinear \mathcal{R}_p couplings. Processes that violate lepton number or baryon number also provide strong constraints on trilinear R -parity violation. To review the results obtained in the current literature, we shall organise the discussion into four subsections, where we discuss in succession hadron flavour violating processes, lepton flavour violating processes, lepton number violating processes and baryon number violating processes.

6.4.1 Hadron Flavour Violating Processes

Mixing of Neutral Mesons

The contribution from \mathcal{R}_p coupling to the mass difference and mixing observables for the neutral $B\bar{B}$ meson system (i.e. $[\Delta b = 2]$), has been considered in [112, 356] and further updated in [357, 325].

Sneutrino exchange can contribute to the $B\bar{B}$ mixing as well as $K\bar{K}$ mixing through two λ' couplings via the tree level diagrams shown in Fig. 6.15a,b.

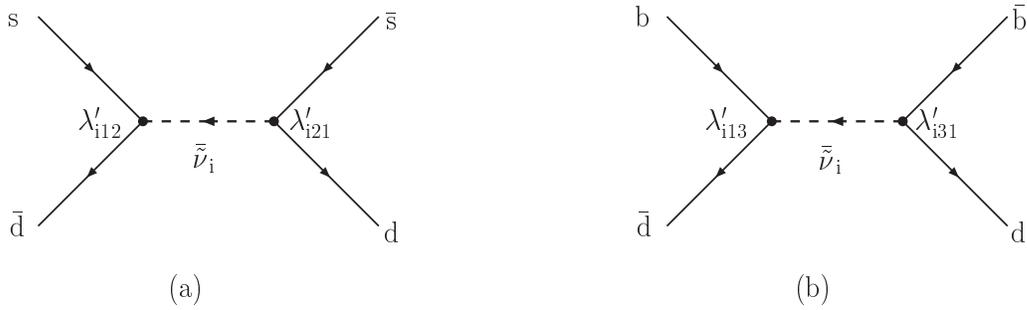


Figure 6.15: \mathcal{R}_p contributions to (a) $K\bar{K}$ and (b) $B\bar{B}$ mixing involving sneutrino in the s -channel.

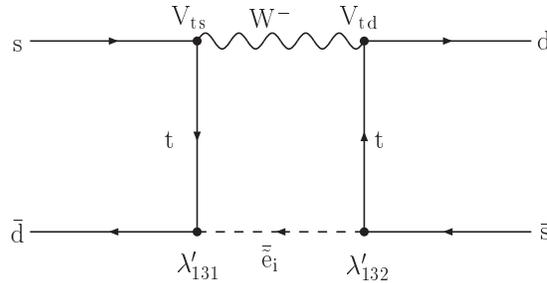


Figure 6.16: Box diagram leading to $K\bar{K}$ mixing induced by λ' couplings.

Individual coupling constant bounds involving the λ' interactions alone, based on the single coupling constant dominance hypothesis in the current basis for quark fields can be obtained [262]. Applying the transformation from current to the mass basis, one may express the transition amplitudes so that only a single \mathcal{R}_p coupling constant appears. The bounds deduced in [262] deserve an update in view of the experimental results published in [272] including the results from the BABAR and BELLE collaborations. These bounds would however depend on

the absolute mixing in the quark sector and would be valid if the relative mixing of the up and down quark sectors was entirely due to the absolute mixing in the down sector. However in this case, no $D\bar{D}$ mixing can be induced by a single \mathcal{R}_p coupling. Alternatively, if the CKM mixing comes only from the mixing in the up quark sector then $D\bar{D}$ mixing can provide a very stringent bound on λ'_{ijk} .

Rare Leptonic Decays of Mesons

The study of rare leptonic decay modes of the K and B mesons offers distinctive probes for new physics beyond the Standard Model [358]. We shall consider in this subsection the leptonic two-body decay channels corresponding to final states with a charged lepton-antilepton pair, $M^0 \rightarrow l_i^- l_j^+$ (with $M^0 = K_L^0, K_S^0, B_d^0$ or B_s^0), as well as charged B meson decays into a charged lepton and a (anti)neutrino, $B^- \rightarrow l^- \bar{\nu}$.

The decays $K^0, B^0 \rightarrow l_i^- l_j^+$ arise via the underlying quark flavour violating subprocess $d_k + \bar{d}_l \rightarrow e_i + \bar{e}_j$ ($k \neq l$). In the Standard Model, the transitions that preserve lepton flavour ($i = j$), such as $K_L \rightarrow \mu^+ \mu^-$ or $B^0 \rightarrow \mu^+ \mu^-$, arise through loop diagrams and are strongly suppressed, while the transitions that violate lepton flavour ($i \neq j$), such as $K_L \rightarrow \mu^+ e^-$, are unobservable due to the smallness of neutrino masses. On the experimental side, the decays $K_L \rightarrow e^+ e^-$ and $K_L \rightarrow \mu^+ \mu^-$ have been measured, while only upper bounds are available on the corresponding K_S decays. In the B meson sector, the experimental upper bounds on the decays $B_{d,s}^0 \rightarrow \mu^+ \mu^-$ and $B_{d,s}^0 \rightarrow e^+ e^-$ are still several orders of magnitude above the Standard Model predictions, while $B_{d,s}^0 \rightarrow \tau^+ \tau^-$ is yet unconstrained.

\mathcal{R}_p interactions contribute to the subprocess $d_k + \bar{d}_l \rightarrow l_i + \bar{l}_j$ via tree-level sneutrino and up squark exchange, as shown in Fig. 6.17. This allows to extract significant bounds on quadratic products of \mathcal{R}_p couplings from rare leptonic meson decays. Specifically, the decay $M^0 \rightarrow l_i^- l_j^+$, where $M^0 = d_k \bar{d}_l$, constrains the following quantities:

$$A_{ij}^{kl} \equiv \sum_{n,p,q} V_{np} V_{qn}^\dagger \frac{\lambda_{ipk}^* \lambda'_{jqk}}{m_{\tilde{u}_{nL}}^2}, \quad B_{ij}^{kl} \equiv \sum_{n,p,q} U_{np}^\dagger U_{qn} \frac{\lambda_{pij}^* \lambda'_{qkl}}{m_{\tilde{\nu}_{nL}}^2}, \quad (6.73)$$

where A_{ij}^{kl} and B_{ij}^{kl} are associated with up squark and sneutrino exchange, respectively. In Eq. (6.73), the couplings λ_{ijk} and λ'_{ijk} are expressed in the mass eigenstate bases of down quarks and charged leptons, which explains the presence of the CKM and MNS mixing angles (see subsection 6.1.2), and the sfermion mass matrices are assumed to be diagonal in the mass eigenstate basis of their fermion partners. In the following, we shall further assume that the masses of the exchanged sfermions are degenerate, i.e. $m_{\tilde{u}_{nL}} \equiv m_{\tilde{u}_L}$ and $m_{\tilde{\nu}_{nL}} \equiv m_{\tilde{\nu}_L}$; then Eq. (6.73) reduces to $A_{ij}^{kl} = \frac{1}{m_{\tilde{u}_L}^2} \sum_p \lambda_{ipk}^* \lambda'_{jpl}$ and $B_{ij}^{kl} = \frac{1}{m_{\tilde{\nu}_L}^2} \sum_p \lambda_{pij}^* \lambda'_{pkl}$.

For mesons that have wave functions of the form $M^{kl} = (d_k \bar{d}_l \pm d_l \bar{d}_k) / \sqrt{2}$, like K_L and K_S in the limit where CP violation is neglected, A_{ij}^{kl} and B_{ij}^{kl} must be replaced by $(A_{ij}^{kl} \pm A_{ij}^{lk}) / \sqrt{2}$ and $(B_{ij}^{kl} \pm B_{ij}^{lk}) / \sqrt{2}$, respectively. One then defines, for the kaon system [359]:

$$A_{ij}^L \equiv \frac{1}{m_{\tilde{u}_L}^2} \sum_p (\lambda_{ip1}^* \lambda'_{jp2} - \lambda_{ip2}^* \lambda'_{jp1}), \quad B_{ij}^L \equiv \frac{1}{m_{\tilde{\nu}_L}^2} \sum_p \lambda_{pij}^* (\lambda'_{p12} - \lambda'_{p21}), \quad (6.74)$$

$$A_{ij}^S \equiv \frac{1}{m_{\tilde{u}_L}^2} \sum_p (\lambda_{ip1}^* \lambda'_{jp2} + \lambda_{ip2}^* \lambda'_{jp1}), \quad B_{ij}^S \equiv \frac{1}{m_{\tilde{\nu}_L}^2} \sum_p \lambda_{pij}^* (\lambda'_{p12} + \lambda'_{p21}), \quad (6.75)$$

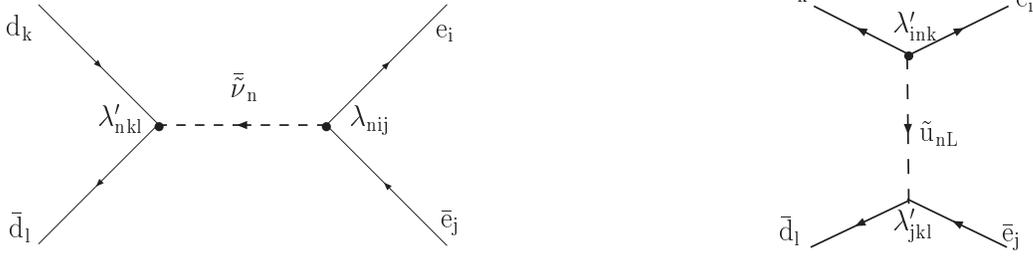


Figure 6.17: \mathcal{R}_p contributions to the process $d_k + \bar{d}_l \rightarrow e_i + \bar{e}_j$.

where A_{ij}^L, B_{ij}^L are relevant for K_L decays, and A_{ij}^S, B_{ij}^S are relevant for K_S decays. Since $A_{ji}^L = -A_{ij}^{L*}$, A_{11}^L and A_{22}^L vanish for real \mathcal{R}_p couplings. As a result, the lepton flavour conserving decays $K_L \rightarrow e^+e^-$ and $K_L \rightarrow \mu^+\mu^-$ only constrain the imaginary part of the products $\lambda_{ip1}^{L*}\lambda'_{ip2}$ ($i = 1, 2$)¹¹. By requiring that the \mathcal{R}_p contribution itself does not exceed the 2σ upper bound on the branching ratios of $K_L \rightarrow e^+e^-$ and $K_L \rightarrow \mu^+\mu^-$, measured to be $(9 \pm 6) \times 10^{-12}$ and $(7.25 \pm 0.16) \times 10^{-9}$ [272], respectively, one obtains the following bounds, which update the ones given in Ref. [359]: $|B_{11}^L| < 1.0 \times 10^{-8} \tilde{\nu}_L^2$, $|B_{22}^L| < 2.2 \times 10^{-7} \tilde{\nu}_L^2$, $|\Im(A_{11}^L)| < 8.1 \times 10^{-5} \tilde{u}_L^2$, $|\Im(A_{22}^L)| < 7.8 \times 10^{-6} \tilde{u}_L^2$. Under the double coupling dominance hypothesis, these bounds yield:

$$\begin{aligned}
|\lambda_{121}^* \lambda'_{212}|, |\lambda_{121}^* \lambda'_{221}| &< 1.0 \times 10^{-8} \tilde{\nu}_L^2 \quad [K_L \rightarrow e^+e^-], \\
|\lambda_{131}^* \lambda'_{312}|, |\lambda_{131}^* \lambda'_{321}| &< 1.0 \times 10^{-8} \tilde{\nu}_L^2 \quad [K_L \rightarrow e^+e^-], \\
|\lambda_{122}^* \lambda'_{112}|, |\lambda_{122}^* \lambda'_{121}| &< 2.2 \times 10^{-7} \tilde{\nu}_L^2 \quad [K_L \rightarrow \mu^+\mu^-], \\
|\lambda_{232}^* \lambda'_{312}|, |\lambda_{232}^* \lambda'_{321}| &< 2.2 \times 10^{-7} \tilde{\nu}_L^2 \quad [K_L \rightarrow \mu^+\mu^-],
\end{aligned} \tag{6.76}$$

$$\begin{aligned}
|\Im(\lambda_{1j1}^* \lambda'_{1j2})| &< 8.1 \times 10^{-5} \tilde{u}_L^2 \quad [K_L \rightarrow e^+e^-], \\
|\Im(\lambda_{2j1}^* \lambda'_{2j2})| &< 7.8 \times 10^{-6} \tilde{u}_L^2 \quad [K_L \rightarrow \mu^+\mu^-].
\end{aligned} \tag{6.77}$$

The bounds associated with the lepton flavour violating decay $K_L \rightarrow e^\pm \mu^\mp$ have been derived in Ref. [359] and updated in Ref. [360] with the 90% CL experimental limit $B(K_L \rightarrow e^\pm \mu^\mp) < 4.7 \times 10^{-12}$ given in Ref. [272]:

$$\begin{aligned}
|\lambda_{122}^* \lambda'_{212}|, |\lambda_{122}^* \lambda'_{221}| &< 6 \times 10^{-9} \tilde{\nu}_L^2, \\
|\lambda_{132}^* \lambda'_{312}|, |\lambda_{132}^* \lambda'_{321}| &< 6 \times 10^{-9} \tilde{\nu}_L^2, \\
|\lambda_{121}^* \lambda'_{112}|, |\lambda_{121}^* \lambda'_{121}| &< 6 \times 10^{-9} \tilde{\nu}_L^2, \\
|\lambda_{231}^* \lambda'_{312}|, |\lambda_{231}^* \lambda'_{321}| &< 6 \times 10^{-9} \tilde{\nu}_L^2, \\
|\lambda_{1j1}^* \lambda'_{2j2}|, |\lambda_{1j2}^* \lambda'_{2j1}| &< 3 \times 10^{-7} \tilde{u}_L^2.
\end{aligned} \tag{6.78}$$

Significantly better bounds are obtained for $\lambda\lambda'$ -type products of couplings; the reason for that is that the contribution of B_{ij}^L to the decay amplitude is enhanced with respect to the contribution of A_{ij}^L by a factor $2m_{K^0}^2/m_l(m_d + m_s)$, where $m_l = m_\mu$ or m_e . In updating the bounds (6.76), we have used the central values of the estimated ranges for m_s and m_s/m_d given in Ref. [272], $m_s = (80 - 155)$ MeV and $m_s/m_d = (17 - 22)$.

¹¹This conclusion remains true when the exchanged sfermions are not degenerate in mass, which is the case considered in Ref. [359]. In this case however, the products $\lambda_{ip1}^{L*}\lambda'_{iq2}$ and $\lambda_{ip2}^{L*}\lambda'_{iq1}$ ($p \neq q$) also contribute to the decays $K_L \rightarrow l_i^+ l_i^-$, but their contribution is suppressed by CKM mixing angles. For the imaginary part of these products, the order of magnitude of the suppression is given by $|V_{pq}|$ (and is therefore rather mild for $\Im(\lambda_{i11}^{L*}\lambda'_{i22})$ and $\Im(\lambda_{i21}^{L*}\lambda'_{i12})$, but the latter is much more constrained by CP violation in the $K\bar{K}$ system, see subsection 6.3.4), while it can be much stronger for the real part. This results in weaker bounds on $\Im(\lambda_{ip1}^{L*}\lambda'_{iq2})$, and especially on $\Re(\lambda_{ip1}^{L*}\lambda'_{iq2})$, than on $\Im(\lambda_{ip1}^{L*}\lambda'_{ip2})$.

The bounds derived from K_S leptonic decays are less stringent than the ones derived from K_L leptonic decays, due to the weaker experimental sensitivity to K_S decays, and we do not list them here. We just mention that, since $A_{ji}^S = A_{ij}^{S*}$, the decays $K_S \rightarrow e^+e^-$ and $K_S \rightarrow \mu^+\mu^-$ provide bounds on the real part of the products $\lambda_{ip1}^{\prime*} \lambda'_{ip2}$ ($i = 1, 2$), while the decays $K_L \rightarrow l_i^+ l_i^-$ only constrain their imaginary part. Stronger bounds on $\Re(\lambda_{ip1}^{\prime*} \lambda'_{ip2})$ can however be derived from $K\bar{K}$ mixing by considering the contribution of box diagrams with an internal W boson, charged Higgs or charged Goldstone boson [356].

The decays $B^0 \rightarrow l_i^- l_j^+$ provide bounds on the coupling products $\lambda_{pij}^* \lambda'_{pkl}$, $\lambda_{pji}^* \lambda'_{plk}$ and $\lambda_{ipk}^* \lambda'_{jpl}$ with $(k, l) = (1, 3), (3, 1)$ (B_d^0 decays) and $(k, l) = (2, 3), (3, 2)$ (B_s^0 decays). Since leptonic B meson decays are less constrained experimentally than leptonic kaon decays, the bounds on coupling products associated with the former are less stringent than those associated with the latter, Eqs. (6.76) – (6.78). Nevertheless leptonic B meson decays provide the best bounds (with some exceptions) on coupling products of the form $\lambda_{pij}^* \lambda'_{pkl}$, with $k = 3$ or $l = 3$. These bounds were derived in Ref. [361] and updated in Refs [360, 362] with the 90% CL experimental limits given in Ref.[272]. We list below the bounds on the $\lambda\lambda'$ -type coupling products given in Ref. [362]:

$$\begin{aligned}
& |\lambda_{i11}^* \lambda'_{i13}|, |\lambda_{i11}^* \lambda'_{i31}| < 1.7 \times 10^{-5} \tilde{\nu}_L^2 [B_d^0 \rightarrow e^+e^-], \\
& |\lambda_{i22}^* \lambda'_{i13}|, |\lambda_{i22}^* \lambda'_{i31}| < 1.5 \times 10^{-5} \tilde{\nu}_L^2 [B_d^0 \rightarrow \mu^+\mu^-], \\
& |\lambda_{i12}^* \lambda'_{i13}|, |\lambda_{i12}^* \lambda'_{i31}|, |\lambda_{i21}^* \lambda'_{i13}|, |\lambda_{i21}^* \lambda'_{i31}| < 2.3 \times 10^{-5} \tilde{\nu}_L^2 [B_d^0 \rightarrow e^\pm \mu^\mp], \\
& |\lambda_{i13}^* \lambda'_{i13}|, |\lambda_{i13}^* \lambda'_{i31}|, |\lambda_{i31}^* \lambda'_{i13}|, |\lambda_{i31}^* \lambda'_{i31}| < 4.9 \times 10^{-4} \tilde{\nu}_L^2 [B_d^0 \rightarrow e^\pm \tau^\mp], \\
& |\lambda_{i23}^* \lambda'_{i13}|, |\lambda_{i23}^* \lambda'_{i31}|, |\lambda_{i32}^* \lambda'_{i13}|, |\lambda_{i32}^* \lambda'_{i31}| < 6.2 \times 10^{-4} \tilde{\nu}_L^2 [B_d^0 \rightarrow \mu^\pm \tau^\mp], \\
& |\lambda_{i11}^* \lambda'_{i23}|, |\lambda_{i11}^* \lambda'_{i32}| < 1.4 \times 10^{-4} \tilde{\nu}_L^2 [B_s^0 \rightarrow e^+e^-], \\
& |\lambda_{i22}^* \lambda'_{i23}|, |\lambda_{i22}^* \lambda'_{i32}| < 2.7 \times 10^{-5} \tilde{\nu}_L^2 [B_s^0 \rightarrow \mu^+\mu^-], \\
& |\lambda_{i12}^* \lambda'_{i23}|, |\lambda_{i12}^* \lambda'_{i32}|, |\lambda_{i21}^* \lambda'_{i23}|, |\lambda_{i21}^* \lambda'_{i32}| < 4.7 \times 10^{-5} \tilde{\nu}_L^2 [B_s^0 \rightarrow e^\pm \mu^\mp].
\end{aligned} \tag{6.79}$$

By contrast, the bounds on $\lambda\lambda'$ -type coupling products associated with rare leptonic decays of B mesons are generally weaker than the products of bounds on individual couplings. We nevertheless list the bounds on the coupling products $\lambda_{ipk}^* \lambda'_{jpl}$ given in Ref. [362] (there is no significant bound associated with the decay modes $B_{d,s}^0 \rightarrow e^+e^-$):

$$\begin{aligned}
& |\lambda_{2j1}^* \lambda'_{2j3}| < 2.1 \times 10^{-3} \tilde{u}_L^2 [B_d^0 \rightarrow \mu^+\mu^-], \\
& |\lambda_{1j1}^* \lambda'_{2j3}|, |\lambda_{1j3}^* \lambda'_{2j1}| < 4.7 \times 10^{-3} \tilde{u}_L^2 [B_d^0 \rightarrow e^\pm \mu^\mp], \\
& |\lambda_{1j1}^* \lambda'_{3j3}|, |\lambda_{1j3}^* \lambda'_{3j1}| < 5.9 \times 10^{-3} \tilde{u}_L^2 [B_d^0 \rightarrow e^\pm \tau^\mp], \\
& |\lambda_{2j1}^* \lambda'_{3j3}|, |\lambda_{2j3}^* \lambda'_{3j1}| < 7.3 \times 10^{-3} \tilde{u}_L^2 [B_d^0 \rightarrow \mu^\pm \tau^\mp], \\
& |\lambda_{2j2}^* \lambda'_{2j3}| < 3.9 \times 10^{-3} \tilde{u}_L^2 [B_s^0 \rightarrow \mu^+\mu^-], \\
& |\lambda_{1j2}^* \lambda'_{2j3}|, |\lambda_{1j3}^* \lambda'_{2j2}| < 9.6 \times 10^{-3} \tilde{u}_L^2 [B_s^0 \rightarrow e^\pm \mu^\mp].
\end{aligned} \tag{6.80}$$

The bounds (6.79) and (6.80) have been derived using $f_{B_d} = f_{B_s} = 200$ MeV; they scale as $(200 \text{ MeV}/f_{B_{d,s}})$. Also $m_b + m_d \approx M_{B_d^0}$ and $m_b + m_s \approx M_{B_s^0}$ have been used for the bounds (6.79).

No dedicated search for the decays $B^0 \rightarrow \tau^+\tau^-$ has yet been carried out explicitly at the existing colliders. However, such decays would manifest themselves at the LEP experiments as $b\bar{b}$ events associated with large missing energy, due to the neutrinos emerging from the τ decays. Such events were studied at LEP to set constraints on the branching ratio for $B^- \rightarrow \tau\bar{\nu}$, and from an analysis of the same data Grossman et al. infer the upper bounds $B(B_d^0 \rightarrow \tau^+\tau^-) < 0.015$ and $B(B_s^0 \rightarrow \tau^+\tau^-) < 0.05$ [363], four orders of magnitude above the Standard Model predictions. These results in the following bounds on the coupling products $\lambda_{i33}^* \lambda'_{ikl}$, with $k = 3$

or $l = 3$ [363]:

$$|\lambda_{i33}^* \lambda'_{i13}|, |\lambda_{i33}^* \lambda'_{i31}| < 6.4 \times 10^{-3} \tilde{\nu}_L^2 \quad [B_d \rightarrow \tau^+ \tau^-], \quad (6.81)$$

$$|\lambda_{i33}^* \lambda'_{i23}|, |\lambda_{i33}^* \lambda'_{i32}| < 1.2 \times 10^{-2} \tilde{\nu}_L^2 \quad [B_s \rightarrow \tau^+ \tau^-]. \quad (6.82)$$

For completeness, we also mention the bounds that have been derived from the non-observation of the lepton flavour violating neutral pion decay $\pi^0 \rightarrow \mu^+ e^-$ in Ref. [360], using the 90% CL experimental upper limit $B(\pi^0 \rightarrow \mu^+ e^-) < 3.8 \times 10^{-10}$ [272]. The following bounds are better than previous bounds:

$$|\lambda_{312}^* \lambda'_{311}|, |\lambda_{321}^* \lambda'_{311}| < 3 \times 10^{-3} \tilde{\nu}_L^2. \quad (6.83)$$

We now consider leptonic decays of charged B mesons, $B^- \rightarrow l^- \bar{\nu}$. In the Standard Model, these decays are suppressed by the CKM angle V_{ub} and by charged lepton masses, and the experimental upper bounds on their branching ratios are still well above the theoretical predictions, except for the decay mode $B^- \rightarrow \tau^- \bar{\nu}$. \mathcal{R}_p interactions contribute to these decays via similar tree-level diagrams to those of Fig. 6.17, with the exchanged sneutrino (resp. up squark) replaced by a charged slepton (resp. down squark). Specifically, the decay $B^- \rightarrow l_i^- \bar{\nu}$ constrains the following quantities [364]:

$$C_{ij} \equiv \sum_{n,p} V_{1p} \frac{\lambda_{ipn}^* \lambda'_{j3n}}{m_{\tilde{d}_{nR}}^2}, \quad D_{ij} \equiv \sum_{n,p} V_{1p} \frac{\lambda_{np3}^* \lambda_{nji}}{m_{\tilde{e}_{nL}}^2}, \quad (6.84)$$

where, as in Eq. (6.73), the couplings λ_{ijk} and λ'_{ijk} are expressed in the mass eigenstate bases of down quarks and charged leptons, and the sfermion mass matrices are assumed to be diagonal. Due to the impossibility of distinguishing experimentally the flavour of the neutrino produced, a single decay mode $B^- \rightarrow l_i^- \bar{\nu}$ constrains the six quantities C_{ij} and D_{ij} , $j = 1, 2, 3$. Then, from a single constraint $|D_{ij}| < \mathcal{B}$, one can derive, under the double coupling dominance hypothesis, the following set of bounds ($n = 1, 2, 3$): $\lambda_{n13}^* \lambda_{nji} < \mathcal{B} \tilde{d}_{nR}^2$, $\lambda_{n23}^* \lambda_{nji} < (\mathcal{B}/V_{us}) \tilde{d}_{nR}^2$ and $\lambda_{n33}^* \lambda_{nji} < (\mathcal{B}/V_{ub}) \tilde{d}_{nR}^2$. A similar statement holds for the bounds on the coupling products $\lambda_{i1n}^* \lambda'_{j3n}$, $\lambda_{i2n}^* \lambda'_{j3n}$, and $\lambda_{i3n}^* \lambda'_{j3n}$ derived from $|C_{ij}| < \mathcal{B}'$.

The bounds on quadratic products of \mathcal{R}_p couplings associated with the 90% CL experimental upper limit on $B(B^- \rightarrow l_i^- \bar{\nu})$ have been derived in Ref. [364]. Ref. [360] obtained weaker bounds from a more careful analysis based on a conservative treatment of the experimental errors. We list below the bounds that are not weaker than bounds associated with other processes or products of individual bounds [360]:

$$\begin{aligned} |\lambda_{i13}^* \lambda_{i31}| &< 6 \times 10^{-4} \tilde{l}_{iL}^2 & [B^- \rightarrow e^- \bar{\nu}], \\ |\lambda_{i13}^* \lambda_{i32}| &< 7 \times 10^{-4} \tilde{l}_{iL}^2 & [B^- \rightarrow \mu^- \bar{\nu}], \\ |\lambda_{313}^* \lambda_{233}| &< 2 \times 10^{-3} \tilde{l}_{3L}^2 & [B^- \rightarrow \tau^- \bar{\nu}], \\ -6 \times 10^{-4} \tilde{l}_{2L}^2 &< \Re(\lambda_{213}^* \lambda_{233}) < 1 \times 10^{-3} \tilde{l}_{2L}^2 & [B^- \rightarrow \tau^- \bar{\nu}]. \end{aligned} \quad (6.85)$$

The bounds on $\lambda' \lambda'$ -type products associated with leptonic decays of charged B mesons are not competitive, since the contribution of C_{ij} to the decay amplitude is suppressed by a factor of m_{l_i}/m_{B^\pm} with respect to the contribution of D_{ij} .

Rare Semileptonic Decays of Mesons

The rare semileptonic FCNC decay $K^+ \rightarrow \pi^+ \nu \bar{\nu}$ is often regarded as a hallmark for tests of the Standard Model and searches for new physics. Indeed, this process is theoretically very clean, since the hadronic matrix element can be extracted from the well-measured decay $K^+ \rightarrow \pi^0 e^+ \nu$, and the long-distance hadronic physics contributions are known to be small [365, 366]. The present experimental value, $B(K^+ \rightarrow \pi^+ \nu \bar{\nu}) = 1.6_{-0.8}^{+1.8} \times 10^{-10}$ [20], is compatible with the SM predictions, but has still large errors.

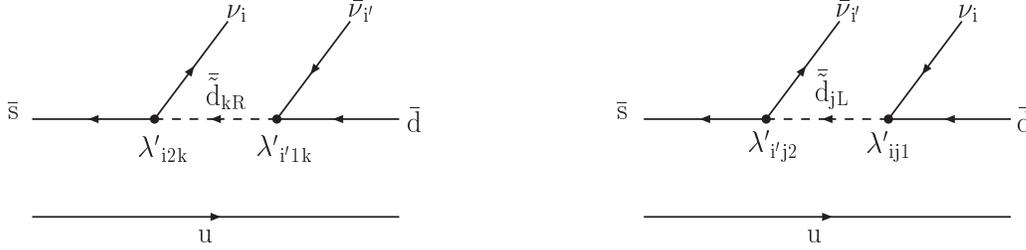


Figure 6.18: \mathcal{R}_p contributions to $K^+ \rightarrow \pi^+ \nu \bar{\nu}$.

The \mathcal{R}_p interactions can contribute to the process $K^+ \rightarrow \pi^+ \nu \bar{\nu}$ through the tree-level diagrams shown in Fig. 6.18, which involve a \tilde{d}_{kR} or a \tilde{d}_{jL} exchange. The dependance of the branching ratio on the \mathcal{R}_p couplings is encapsulated in the auxiliary parameters $\mathcal{E}_{ii'}$ [359]:

$$\mathcal{E}_{ii'} = \sum_k \lambda_{i2k}^* \lambda'_{i'1k} \tilde{d}_{kR}^{-2} - \sum_j \lambda_{ij1}^* \lambda'_{i'j2} \tilde{d}_{jL}^{-2}. \quad (6.86)$$

In Ref. [359], an experimental upper limit was used to put an upper bound on $\sum_{ii'} |\mathcal{E}_{ii'}|^2$, neglecting the Standard Model contribution. A warning is in order concerning this method. Since the present experimental value $B(K^+ \rightarrow \pi^+ \nu \bar{\nu}) = (1.47_{-0.8}^{+1.3}) 10^{-10}$ [367] is close to the expected Standard Model value, it is no longer legitimate to neglect the Standard Model contribution when deriving constraints on \mathcal{R}_p couplings.

Since then a detailed analysis, including all relevant contributions, was performed [368], yielding the upper bound $\sum_{ii'} |\mathcal{E}_{ii'}|^2 < 4.45 \times 10^{-10}$.

One can use the bound on $\sum_{ii'} |\mathcal{E}_{ii'}|^2$ to infer bounds on products of λ' -type couplings. Applying the double coupling dominance hypothesis in the mass eigenstate basis, one obtains [368]:

$$\begin{aligned} |\lambda_{i2k}^* \lambda'_{i'1k}| &< 2.11 \times 10^{-5} \tilde{d}_{kR}^2, \\ |\lambda_{ij1}^* \lambda'_{i'j2}| &< 2.11 \times 10^{-5} \tilde{d}_{jL}^2. \end{aligned} \quad [K^+ \rightarrow \pi^+ \nu \bar{\nu}] \quad (6.87)$$

Bounds on individual couplings may also be obtained if, instead of applying the double coupling dominance hypothesis in the mass eigenstate basis, it is assumed that a single coupling is nonzero in the weak eigenstate basis [262], i.e. $\hat{\lambda}'_{ipq} \neq 0$ in the notation of subsection 6.1.2. Then, upon rotating the down quarks to their mass eigenstate basis, several couplings $\lambda'_{ijk} = (V_L^{dI})_{pj} (V_R^{dT})_{qk} \hat{\lambda}'_{ipq}$ are generated, and one has $\sum_k \lambda_{i2k}^* \lambda'_{i'1k} = \delta_{i'i} (V_L^d)_{2p} (V_L^{d*})_{1p} |\hat{\lambda}'_{ipq}|^2$.

In a similar manner, bounds on the coupling products $\lambda_{i3k}^* \lambda'_{i'2k}$ and $\lambda_{ij2}^* \lambda'_{i'j3}$ can be extracted from the non-observation of the rare semileptonic B meson decay $B \rightarrow X_s \nu \bar{\nu}$ [278]. We have

updated the result of Ref. [278] with the 90% CL experimental upper limit $B(B \rightarrow X_s \nu \bar{\nu}) < 7.7 \times 10^{-4}$ [369], which lies an order of magnitude above the Standard Model prediction:

$$\begin{aligned} |\lambda_{i3k}^{\prime*} \lambda_{i'2k}'| &< 1.5 \times 10^{-3} \tilde{d}_{kR}^2, \\ |\lambda_{ij2}^{\prime*} \lambda_{i'j3}'| &< 1.5 \times 10^{-3} \tilde{d}_{jL}^2. \end{aligned} \quad [B \rightarrow X_s \nu \bar{\nu}] \quad (6.88)$$

Finally, the rare semileptonic decays $B \rightarrow X_s l_i^+ l_j^-$ can also be used to set bounds on $\lambda' \lambda'$ -type and $\lambda \lambda'$ -type coupling products [370].

Rare Hadronic Decays of the B Mesons

The hadronic B meson decays that do not proceed through a $b \rightarrow c$ transition are suppressed in the Standard Model, and offer potentially promising constraints on the \mathcal{R}_p interactions. Unlike the rare leptonic and semileptonic decays discussed before, however, these processes are plagued with large hadronic uncertainties and the bounds on products of \mathcal{R}_p couplings presented below should be considered as indicative.

In Ref. [371], the decays $B^+ \rightarrow \bar{K}^0 K^+$ and $B^+ \rightarrow K^0 \pi^+$ have been used to set bounds on the products of baryon number violating couplings $\lambda_{i23}'' \lambda_{i12}^{\prime*}$ and $\lambda_{i13}'' \lambda_{i12}^{\prime*}$, which contribute to these processes via tree-level exchange of an up squark. We have updated the bound estimates of Ref. [371] by using the 90% CL experimental upper limit $B(B^+ \rightarrow \bar{K}^0 K^+) < 2.4 \times 10^{-6}$ [272] and by requiring that the \mathcal{R}_p contribution to $B^+ \rightarrow K^0 \pi^+$ does not exceed by more than 2σ the measured value of the branching ratio, $B(B^+ \rightarrow K^0 \pi^+) = (1.73_{-0.24}^{+0.27}) \times 10^{-5}$ [272], and found:

$$\begin{aligned} |\lambda_{i23}'' \lambda_{i12}^{\prime*}| &< 1.7 \times 10^{-3} \tilde{u}_{iR}^2 \quad [B^+ \rightarrow \bar{K}^0 K^+], \\ |\lambda_{i13}'' \lambda_{i12}^{\prime*}| &< 6.4 \times 10^{-3} \tilde{u}_{iR}^2 \quad [B^+ \rightarrow K^0 \pi^+]. \end{aligned} \quad (6.89)$$

Ref. [372] improves the results of Ref. [371] by considering a large sample of hadronic decay modes of the B mesons, which receive contributions of the baryon number violating \mathcal{R}_p interactions through tree-level exchange of either a down squark or an up squark. Assuming naive factorization of the hadronic matrix elements, Ref. [372] obtains the following allowed ranges at 90% CL (we give only the stronger constraints):

$$\begin{aligned} -1.1 \times 10^{-3} \tilde{d}_{1R}^2 &< \lambda_{i13}'' \lambda_{i12}'' < 7.8 \times 10^{-4} \tilde{d}_{1R}^2 \quad [B^0 \rightarrow \pi^0 K^{0*} B^+ \rightarrow \pi^0 K^+], \\ -1.2 \times 10^{-3} \tilde{d}_{2R}^2 &< \lambda_{i23}'' \lambda_{i21}'' < 1.4 \times 10^{-3} \tilde{d}_{2R}^2 \quad [B^+ \rightarrow \pi^+ \bar{D}^0, \rho^+ \bar{D}^0; B^0 \rightarrow \bar{D}^0 \pi^0], \\ -1.4 \times 10^{-2} \tilde{d}_{1R}^2 &< \lambda_{i21}'' \lambda_{i12}'' < 2.0 \times 10^{-2} \tilde{d}_{1R}^2 \quad [B^+ \rightarrow D_s^+ \pi^0], \\ -7.9 \times 10^{-4} \tilde{u}_{iR}^2 &< \lambda_{i13}'' \lambda_{i12}'' < 1.2 \times 10^{-3} \tilde{u}_{iR}^2 \quad [B^+ \rightarrow \pi^+ K^0, \pi^0 K^+, \pi^+ K^{0*}], \\ -1.9 \times 10^{-3} \tilde{u}_{iR}^2 &< \lambda_{i23}'' \lambda_{i12}'' < 2.8 \times 10^{-3} \tilde{u}_{iR}^2 \quad [B^0 \rightarrow K^0 \bar{K}^0]. \end{aligned} \quad (6.90)$$

Ref. [373] considers the decay mode $B^- \rightarrow \phi \pi^-$, which, using QCD factorization, they estimate to be suppressed at the level of $B(B^- \rightarrow \phi \pi^-) = (2.0_{-0.1}^{+0.3}) \times 10^{-8}$ in the Standard Model. From the 90% CL upper limit $B(B^- \rightarrow \phi \pi^-) < 1.6 \times 10^{-6}$ [272], they derive the following upper bounds:

$$\begin{aligned} |\lambda_{i23}^{\prime*} \lambda_{i12}'| &< 6 \times 10^{-5} \tilde{u}_{iR}^2, \\ |\lambda_{i32}' \lambda_{i12}^{\prime*}| &< 4 \times 10^{-4} \tilde{\nu}_{iL}^2, \\ |\lambda_{i23}^{\prime*} \lambda_{i21}'| &< 4 \times 10^{-4} \tilde{\nu}_{iL}^2. \end{aligned} \quad [B^- \rightarrow \phi \pi^-] \quad (6.91)$$

FCNC Top Quark Decays

The flavour changing neutral current decays of the top quark, which will be best constrained in future Tevatron experiments at Fermilab and at the CERN LHC, might provide bounds on products of \mathcal{R}_p couplings that are not constrained by other processes. Ref. [374] considered the FCNC top quark decays $t \rightarrow c + V$ ($V = Z, \gamma, g$), for which an experimental sensitivity of $(10^{-5} - 10^{-3})$ is expected, depending on the decay mode. These decays, which are negligible in the Standard Model, are induced at the one-loop level by the \mathcal{R}_p couplings λ'_{ijk} and λ''_{ijk} ; however, given the constraints from other processes on the λ'_{ijk} couplings, only the λ''_{ijk} couplings are likely to give an observable contribution. The corresponding branching ratios are estimated to be, for squark masses $m_{\tilde{d}_{kR}} \lesssim 170$ GeV [374]:

$$B(t \rightarrow c + [Z, \gamma, g]) = [3.6 \times 10^{-5}, 9 \times 10^{-7}, 1.6 \times 10^{-4}] \left| \sum_{j < k} \lambda_{3jk}^{\prime*} \lambda_{2jk}'' \right|^2, \quad (6.92)$$

and scale as $1/m_{\tilde{d}_{kR}}^4$ for larger squark masses. Although modest, the bounds that might be inferred from the expected experimental sensitivities are complementary with the other bounds on the λ''_{ijk} couplings discussed in this chapter.

The Rare Decay $b \rightarrow s\gamma$

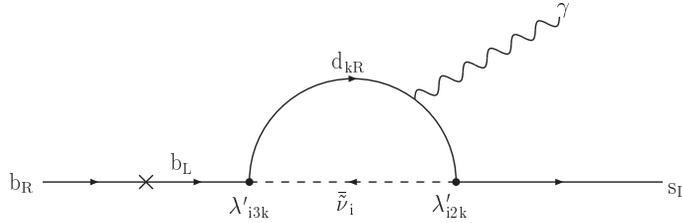


Figure 6.19: Example of the \mathcal{R}_p contributions to the decay $b \rightarrow s\gamma$.

The measured inclusive $b \rightarrow s\gamma$ rate, $B(B \rightarrow X_s\gamma) = (3.3 \pm 0.4) \times 10^{-4}$ [20], is in good agreement with the Standard Model prediction [375, 376, 377]. This constrains new physics contributions, and in particular implies restrictions on the Supersymmetric Standard Model spectrum and on some combinations of \mathcal{R}_p couplings. Ref. [112] considered both the direct contribution of the \mathcal{R}_p interactions, which can mediate $b \rightarrow s\gamma$ through one-loop diagrams such as the one shown in Fig. 6.19, and their indirect contribution through the renormalization group evolution of the soft supersymmetry breaking masses. Indeed, the \mathcal{R}_p couplings enter the renormalization group equations for the supersymmetric parameters, and can generate large flavour violating entries in the squark mass matrices which then induce the decay $b \rightarrow s\gamma$. This indirect contribution can enhance the branching ratio by up to an order of magnitude with respect to the direct contribution, but it is difficult to derive bounds on the \mathcal{R}_p couplings from this effect due to its complicated dependence on the supersymmetric mass spectrum. The direct contribution yields the following upper bounds [112]:

$$\begin{aligned} |\lambda'_{i3k} \lambda_{i2k}^{\prime*}| &< 0.09 (2\tilde{v}_{iL}^{-2} - \tilde{d}_{iR}^{-2})^{-1}, \\ |\lambda_{ij3}^{\prime*} \lambda'_{ij2}| &< 0.035 (\tilde{t}_{iL}^{-2} - \tilde{d}_{jL}^{-2})^{-1}, \\ |\lambda_{i3k}^{\prime*} \lambda_{i2k}''| &< 0.16 \tilde{q}_R^2. \end{aligned} \quad (6.93)$$

Since the experimental value of $B(B \rightarrow X_s \gamma)$ has significantly changed with respect to the one given in Ref. [378] that was used in Ref. [112], these bounds should be considered as indicative. Using more recent data, Ref. [379] derives a weaker bound on the coupling products $\lambda_{33k}^{\prime\prime\star} \lambda_{32k}^{\prime\prime}$. An update of their results, taking into account the reduction of the experimental error, yields the 2σ upper bound:

$$|\lambda_{33k}^{\prime\prime\star} \lambda_{32k}^{\prime\prime}| < 0.35 \tilde{d}_{iR}^2. \quad (6.94)$$

6.4.2 Lepton Flavour Violating Processes

In the Standard Model, lepton flavour violating (LFV) processes occur at a negligible rate due to the smallness of neutrino masses. They are therefore very sensitive probes of new physics, and can be used to place bounds on \tilde{R}_p couplings. In order to disentangle the effect of \tilde{R}_p interactions from the effect of possible flavour non-universalities in the slepton sector, we shall assume in this subsection that the slepton mass matrices are diagonal and proportional to the identity matrix, i.e. $m_{\tilde{l}_{Ri}}^2 \equiv m_{\tilde{l}_R}^2$, $m_{\tilde{l}_{Li}}^2 \equiv m_{\tilde{l}_L}^2$, $m_{\tilde{\nu}_{Li}}^2 \equiv m_{\tilde{\nu}_L}^2$.

Lepton Flavour Violating Radiative Decays of Charged Leptons

The \tilde{R}_p interactions can induce LFV radiative decays of charged leptons, $l_j \rightarrow l_i + \gamma$ ($i \neq j$), through one-loop diagrams analogous to the one shown in Fig. 6.19. The most constrained of these decays, $\mu \rightarrow e\gamma$, yields the following upper bounds on $\lambda\lambda$ and $\lambda'\lambda'$ -type coupling products (the bounds given in Refs. [30] and [380] have been updated in Ref. [381] using the 90% CL experimental upper limit $B(\mu \rightarrow e\gamma) < 1.2 \times 10^{-11}$ [327]):

$$\begin{aligned} |\lambda_{ij2}^* \lambda_{ij1}| &< 8.2 \times 10^{-5} (2\tilde{\nu}_L^{-2} - \tilde{l}_L^{-2})^{-1}, \\ |\lambda_{23k} \lambda_{13k}^*| &< 2.3 \times 10^{-4} (2\tilde{\nu}_L^{-2} - \tilde{l}_R^{-2})^{-1}, \\ |\lambda'_{2jk} \lambda'_{1jk}| &< 7.6 \times 10^{-5} \tilde{d}_{kR}^2 \quad (j = 1, 2). \end{aligned} \quad (6.95)$$

Due to the large top quark mass, the bound on $|\lambda'_{23k} \lambda'_{13k}|$ does not scale as $m_{\tilde{d}_{kR}}^2$. Indeed, updating the bounds of Ref. [380], one obtains:

$$\begin{aligned} |\lambda'_{23k} \lambda'_{13k}| &< 1.3 \times 10^{-3}, 2.0 \times 10^{-3}, 9.9 \times 10^{-3} \quad (k = 1, 2), \\ |\lambda'_{233} \lambda'_{133}| &< 1.7 \times 10^{-3}, 2.0 \times 10^{-3}, 9.9 \times 10^{-3}, \end{aligned} \quad (6.96)$$

for $m_{\tilde{d}_{kR}} = m_{\tilde{l}_L} = 100$ GeV, 300 GeV and 1 TeV, respectively. In Eqs. (6.95) and (6.96), left-right mixing in the squark and charged slepton mass matrices has been neglected. The bounds that can be inferred from $\tau \rightarrow \mu\gamma$ and from $\tau \rightarrow e\gamma$ are much weaker.

Ref. [30] also investigates the indirect contribution of \tilde{R}_p interactions to $\mu \rightarrow e\gamma$ through their effect on the renormalization group evolution of the slepton masses. The indirect contribution often dominates over the direct contribution discussed above; however, due to its complicated dependence on the supersymmetric parameters, it is not possible to derive bounds on \tilde{R}_p couplings from this effect.

Lepton Flavour Violating Decays of μ and τ into three Charged Leptons

The lepton flavour violating decay $l_m^- \rightarrow l_i^- + l_j^- + l_k^+$, where $l_m = \mu$ or τ , can be mediated by tree-level t - and u -channel sneutrino exchange when the involved leptons have nonzero λ -type couplings. The non-observation of these processes yield bounds on products of \mathcal{R}_p couplings of the form $\lambda_{nmi}\lambda_{njk}^*$, $\lambda_{nim}^*\lambda_{nkj}$, $\lambda_{nmj}\lambda_{nik}^*$ and $\lambda_{njm}^*\lambda_{nki}$ [256, 359]. We have updated the bounds of Ref. [359] using the 90% CL experimental upper limits on $B(l_m^- \rightarrow l_i^- + l_j^- + l_k^+)$ given in Ref. [272]:

$$\begin{aligned}
& |\lambda_{321}\lambda_{311}^*|, |\lambda_{i12}^*\lambda_{i11}| < 6.6 \times 10^{-7} \tilde{\nu}_L^2 & [\mu \rightarrow eee], \\
& |\lambda_{231}\lambda_{211}^*|, |\lambda_{i13}^*\lambda_{i11}| < 2.7 \times 10^{-3} \tilde{\nu}_L^2 & [\tau \rightarrow eee], \\
& |\lambda_{231}\lambda_{212}^*|, |\lambda_{313}^*\lambda_{321}| < 2.0 \times 10^{-3} \tilde{\nu}_L^2 & [\tau^- \rightarrow \mu^+ e^- e^-], \\
& |\lambda_{232}\lambda_{211}^*|, |\lambda_{323}^*\lambda_{311}|, |\lambda_{131}\lambda_{121}^*|, |\lambda_{i13}^*\lambda_{i12}| < 2.1 \times 10^{-3} \tilde{\nu}_L^2 & [\tau^- \rightarrow \mu^- e^+ e^-], \\
& |\lambda_{132}\lambda_{121}^*|, |\lambda_{323}^*\lambda_{312}| < 2.0 \times 10^{-3} \tilde{\nu}_L^2 & [\tau^- \rightarrow e^+ \mu^- \mu^-], \\
& |\lambda_{131}\lambda_{122}^*|, |\lambda_{313}^*\lambda_{322}|, |\lambda_{232}\lambda_{212}^*|, |\lambda_{i23}^*\lambda_{i21}| < 2.1 \times 10^{-3} \tilde{\nu}_L^2 & [\tau^- \rightarrow e^- \mu^+ \mu^-], \\
& |\lambda_{132}\lambda_{122}^*|, |\lambda_{i23}^*\lambda_{i22}| < 2.2 \times 10^{-3} \tilde{\nu}_L^2 & [\tau \rightarrow \mu\mu\mu].
\end{aligned} \tag{6.97}$$

The decays $l_m^- \rightarrow l_i^- + l_j^- + l_j^+$ ($k = j$) can also be induced through photon penguin diagrams by the same $\lambda\lambda$ - and $\lambda'\lambda'$ -type coupling products as the radiative decays $l_m \rightarrow l_i\gamma$. In the case of $\mu \rightarrow eee$, the associated bounds are stronger than the ones extracted from the non-observation of $\mu \rightarrow e\gamma$. We list below the bounds given in Ref. [381]:

$$\begin{aligned}
& |\lambda_{232}^*\lambda_{231}| < 4.5 \times 10^{-5}, \quad |\lambda_{232}\lambda_{132}^*| < 7.1 \times 10^{-5}, \quad |\lambda_{233}\lambda_{133}^*| < 1.2 \times 10^{-4}, \\
& |\lambda'_{211}\lambda'_{111}| < 1.3 \times 10^{-4}, \quad |\lambda'_{212}\lambda'_{112}| < 1.4 \times 10^{-4}, \quad |\lambda'_{213}\lambda'_{113}| < 1.6 \times 10^{-4}, \\
& |\lambda'_{221}\lambda'_{121}| < 2.0 \times 10^{-4}, \quad |\lambda'_{222}\lambda'_{122}| < 2.3 \times 10^{-4}, \quad |\lambda'_{223}\lambda'_{123}| < 2.9 \times 10^{-4}.
\end{aligned} \tag{6.98}$$

In Eq. (6.98), the bounds on $\lambda\lambda$ -type (resp. $\lambda'\lambda'$ -type) coupling products have been derived assuming that all slepton (resp. squark) masses are degenerate and equal to $\tilde{m} = 100$ GeV (resp. $\tilde{m} = 300$ GeV) and neglecting left-right mixing in sfermion mass matrices. These bounds do not simply scale as \tilde{m}^2 .

Muon to Electron Conversion in Nuclei

$\mu^- \rightarrow e^-$ conversion in a nucleus can be induced by $\lambda\lambda'$ - and $\lambda'\lambda'$ -type coupling products via the exchange of a sneutrino (resp. a squark) in the t -channel (resp. s - and u -channels) [382]. Experimentally, stringent bounds are set on the rate of $\mu - e$ conversion in a nucleus A relative to the ordinary muon capture, $R_{\mu e} \equiv \Gamma(\mu^- + A \rightarrow e^- + A)/\Gamma(\mu^- \text{ capture in } A)$. Using the 90% CL upper limit $R_{\mu e} < 6.1 \times 10^{-13}$ obtained by the SINDRUM II experiment on a ^{48}Ti target [383], the following bounds are deduced, updating those given in Ref. [382]:

$$\begin{aligned}
& |\lambda'_{i12}\lambda'_{i11}|, |\lambda_{i21}\lambda'_{i11}| < 2.1 \times 10^{-8} \tilde{\nu}_L^2, \\
& |\lambda'_{2j1}\lambda'_{1j1}| < 4.3 \times 10^{-8} \tilde{u}_{jL}^2 \quad (j = 2, 3), \\
& |\lambda'_{21k}\lambda'_{11k}| < 4.5 \times 10^{-8} \tilde{d}_{kR}^2 \quad (k = 2, 3).
\end{aligned} \tag{6.99}$$

The combination $\lambda'_{211}\lambda'_{111}$ can also induce $\mu - e$ conversion in ^{48}Ti , but cancellations may occur between the up squark and the down squark contributions, resulting in a weaker bound, $|\lambda'_{211}\lambda'_{111}| < 4.3 \times 10^{-8} (\tilde{u}_L^{-2} - \frac{70}{74}\tilde{d}_R^{-2})^{-1}$.

\mathcal{R}_p -induced $\mu^- \rightarrow e^-$ conversion in a nucleus can also proceed through photon penguin diagrams [384], in the same way as the LFV decay $\mu \rightarrow eee$. The associated bounds are

stronger than the ones extracted from the non-observation of $\mu \rightarrow e\gamma$ and $\mu \rightarrow eee$, if the latter does not occur at tree level. We list below the bounds given in Ref. [381]:

$$\begin{aligned} |\lambda_{122}^* \lambda_{121}| &< 6.1 \times 10^{-6}, & |\lambda_{132}^* \lambda_{131}| &< 7.6 \times 10^{-6}, & |\lambda_{232}^* \lambda_{231}| &< 8.3 \times 10^{-6}, \\ |\lambda_{231} \lambda_{131}^*| &< 1.1 \times 10^{-5}, & |\lambda_{232} \lambda_{132}^*| &< 1.3 \times 10^{-5}, & |\lambda_{233} \lambda_{133}^*| &< 2.3 \times 10^{-5}, \\ |\lambda'_{222} \lambda'_{122}| &< 4.3 \times 10^{-5}, & |\lambda'_{223} \lambda'_{123}| &< 5.4 \times 10^{-5}. \end{aligned} \quad (6.100)$$

In Eq. (6.100), the bounds on $\lambda\lambda$ -type (resp. $\lambda'\lambda'$ -type) coupling products have been derived assuming that all slepton (resp. squark) masses are degenerate and equal to $\tilde{m} = 100$ GeV (resp. $\tilde{m} = 300$ GeV) and neglecting left-right mixing in sfermion mass matrices. These bounds do not simply scale as \tilde{m}^2 .

Muonium to Antimuonium Conversion

The conversion reaction of a muonium atom into an antimuonium atom, $M(\mu^+e^-) \rightarrow \bar{M}(\mu^-e^+)$, has been initially proposed as a test of a multiplicative lepton number symmetry [385] which would forbid $\Delta L_\mu = \pm 1$ transitions, but would allow for $\Delta L_\mu = \pm 2$ transitions such as $M \rightarrow \bar{M}$. Experimental limits on this process are conventionally expressed in terms of an effective coupling $G_{M\bar{M}}$ defined by [386]:

$$\mathcal{L}_{eff}(M \rightarrow \bar{M}) = \frac{4G_{M\bar{M}}}{\sqrt{2}} (\bar{\mu}_L \gamma^\mu e_L)(\bar{\mu}_L \gamma_\mu e_L) + \text{h.c.} . \quad (6.101)$$

The current 90% CL experimental limit [387] is $G_{M\bar{M}} < 3.0 \times 10^{-3} G_F$. In the presence of R -parity violation, muonium to antimuonium conversion can be mediated by tree-level exchange of a tau sneutrino in the s - or the u -channel as shown in Fig. 6.20. The associated effective

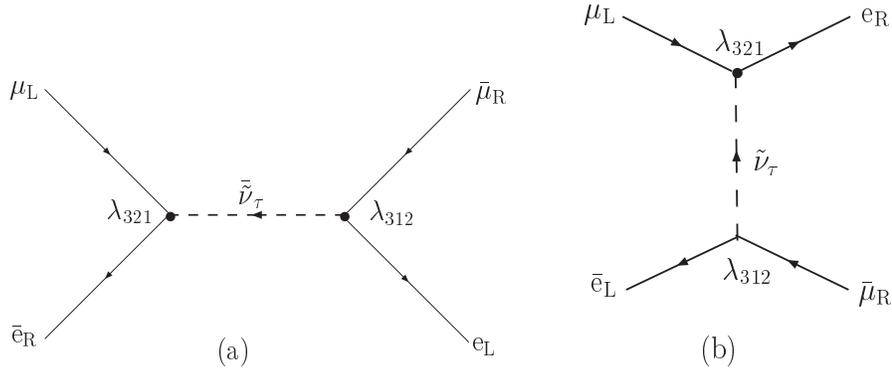


Figure 6.20: R_p contributions to muonium-antimuonium conversion. Similar diagrams involving an incoming μ_R are not shown.

interaction is of the $(V - A)(V + A)$ form (after a Fierz transformation) and is described by an effective coupling $\tilde{G}_{M\bar{M}}$ distinct from the coupling $G_{M\bar{M}}$ defined by Eq. (6.101). Explicitly, one has [382, 388, 389]:

$$\frac{\tilde{G}_{M\bar{M}}}{\sqrt{2}} = \frac{\lambda_{312} \lambda_{321}^*}{8m_{\tilde{\nu}_L}^2}. \quad (6.102)$$

The 90% CL experimental limit on muonium-antimuonium conversion [387], in the case of a $(V - A)(V + A)$ interaction, translates into $\tilde{G}_{M\bar{M}} < 2.0 \times 10^{-3} G_F$. This yields the following upper bound on the coupling product $\lambda_{312} \lambda_{321}^*$, which updates the bound given in Ref. [382]:

$$|\lambda_{312} \lambda_{321}^*| < 1.9 \times 10^{-3} \tilde{\nu}_L^2. \quad (6.103)$$

Lepton Flavour Violating Semileptonic Decays of the τ

The τ -lepton decay modes include a variety of lepton flavour violating processes which yield constraints on several products of \mathcal{R}_p couplings. Of special interest are the two-body decay modes into pseudoscalar and vector mesons, $\tau \rightarrow l + P^0$ and $\tau \rightarrow l + V^0$, with $l = e, \mu$, $P = \pi^0, \eta, K^0$ and $V = \rho^0, \omega, K^{*0}, \phi$. The \mathcal{R}_p interactions contribute to these processes via tree-level sneutrino or squark exchange, induced by $\lambda\lambda'$ -type or $\lambda'\lambda'$ -type coupling pairs, respectively [382]. For sneutrinos or up-type squarks, the corresponding diagrams are the time-reversed of the diagrams shown in Fig. 6.17; the exchange of a down-type squark, which is not shown, corresponds to the subprocess $e_i + \bar{e}_j \rightarrow u_k + \bar{u}_l$.

The sneutrino exchange mediates tau decays into pseudoscalar mesons only; hence the $\lambda\lambda'$ -type coupling products are only constrained by these decays. Using the 90% CL experimental upper limits on $B(\tau \rightarrow l + P^0)$ given in Ref. [272], one obtains the following bounds, which update the bounds of Ref. [382]:

$$\begin{aligned}
|\lambda_{i31}\lambda_{i11}^*|, |\lambda_{i13}^*\lambda'_{i11}| &< 1.6 \times 10^{-3} \tilde{\nu}_{iL}^2 [\tau^- \rightarrow e^- + \eta^0], \\
|\lambda_{i31}\lambda_{i22}^*|, |\lambda_{i13}^*\lambda'_{i22}| &< 1.6 \times 10^{-2} \tilde{\nu}_{iL}^2 [\tau^- \rightarrow e^- + \eta^0], \\
|\lambda_{i31}\lambda_{i12}^*|, |\lambda_{i13}^*\lambda'_{i21}| &< 8.5 \times 10^{-2} \tilde{\nu}_{iL}^2 [\tau^- \rightarrow e^- + K^0], \\
|\lambda_{i32}\lambda_{i11}^*|, |\lambda_{i23}^*\lambda'_{i11}| &< 1.7 \times 10^{-3} \tilde{\nu}_{iL}^2 [\tau^- \rightarrow \mu^- + \eta^0], \\
|\lambda_{i32}\lambda_{i22}^*|, |\lambda_{i23}^*\lambda'_{i22}| &< 1.7 \times 10^{-2} \tilde{\nu}_{iL}^2 [\tau^- \rightarrow \mu^- + \eta^0], \\
|\lambda_{i32}\lambda_{i12}^*|, |\lambda_{i23}^*\lambda'_{i21}| &< 7.6 \times 10^{-2} \tilde{\nu}_{iL}^2 [\tau^- \rightarrow \mu^- + K^0].
\end{aligned} \tag{6.104}$$

$\lambda\lambda'$ -type coupling products induce both decays $\tau \rightarrow l + P^0$ and $\tau \rightarrow l + V^0$, but the latter are more constrained experimentally and therefore provide stronger bounds than the former. Using the 90% CL experimental upper limits on $B(\tau \rightarrow l + V^0)$ given in Ref. [272], one obtains the following bounds, which update the bounds of Ref. [382]:

$$\begin{aligned}
|\lambda'_{3j1}\lambda_{1j1}^*| &< 2.4 \times 10^{-3} \tilde{u}_{jL}^2 [\tau^- \rightarrow e^- + \rho^0], \\
|\lambda'_{3j1}\lambda_{1j2}^*| &< 2.7 \times 10^{-3} \tilde{u}_{jL}^2 [\tau^- \rightarrow e^- + K^{*0}], \\
|\lambda'_{3j1}\lambda_{2j1}^*| &< 4.4 \times 10^{-3} \tilde{u}_{jL}^2 [\tau^- \rightarrow \mu^- + \rho^0], \\
|\lambda'_{3j1}\lambda_{2j2}^*| &< 3.4 \times 10^{-3} \tilde{u}_{jL}^2 [\tau^- \rightarrow \mu^- + K^{*0}], \\
|\lambda'_{31k}\lambda_{11k}^*| &< 2.4 \times 10^{-3} \tilde{d}_{kR}^2 [\tau^- \rightarrow e^- + \rho^0], \\
|\lambda'_{31k}\lambda_{21k}^*| &< 4.4 \times 10^{-3} \tilde{d}_{kR}^2 [\tau^- \rightarrow \mu^- + \rho^0].
\end{aligned} \tag{6.105}$$

6.4.3 Lepton Number Non-Conserving Processes

Neutrinoless Double Beta Decay

Searches for neutrinoless double beta decay ($\beta\beta_{0\nu}$) of nuclei ($(Z, N) \rightarrow (Z+2, N-2) + l_i^- + l_j^-$) are performed using ^{76}Ge , ^{48}Ca , ^{82}Se , ^{100}Mo . They are mainly carried out in underground laboratories and make use of various detection techniques. The current experimental information and some of the promising future prospects are reviewed in Ref. [390].

The nucleon level transition, $n + n \rightarrow p + p + e^- + e^-$ is induced at the quark level by the subprocess $d + d \rightarrow u + u + e + e$. The \mathcal{R}_p operator $L_1 Q_1 D_1^c$ would allow such a transition to occur at the tree level, via processes involving the sequential t -channel exchange of two sfermions and a gaugino, where the sfermion may be a slepton or a squark, \tilde{e}_L or \tilde{u}_L, \tilde{d}_R , and the gaugino, a neutralino or a gluino [391, 392]. Corresponding diagrams are shown in Fig. 6.21. In the limit

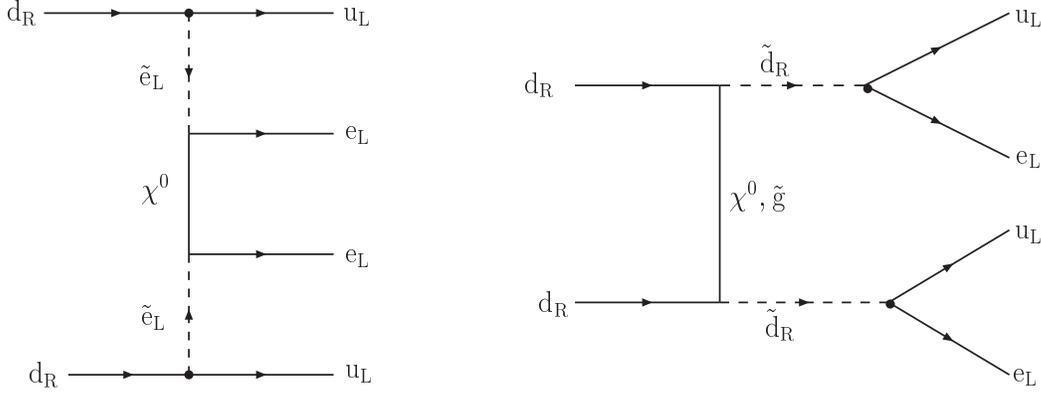


Figure 6.21: Contributions to the neutrinoless double beta decay induced by a λ'_{111} coupling.

of large masses for the exchanged sparticles, these mechanisms can be described in terms of point-like six fermion effective interactions. Relying on such an effective Lagrangian and using an approximate evaluation of the nuclear operator matrix element, an early study by Mohapatra led to the bounds [391]: $|\lambda'_{111}| < 0.48 \times 10^{-9/4} \tilde{f}^2 \tilde{g}^{\frac{1}{2}}$, $|\lambda'_{111}| < 2.8 \times 10^{-9/4} \tilde{f}^2 \tilde{\chi}^{\frac{1}{2}}$. Meanwhile, detailed calculations of the $\beta\beta_{0\nu}$ amplitudes have been performed including all contributing diagrams, and the relevant nuclear matrix elements have been calculated in the proton-neutron Quasiparticle Random Phase Approximation (QRPA) [392]. From the lower limit on the half-life of ^{76}Ge measured by the Heidelberg-Moscow experiment [393]:

$$T_{1/2}^{\beta\beta_{0\nu}}(^{76}\text{Ge}) > 1.1 \times 10^{25} \text{yr}$$

the following bound is obtained in the minimal supergravity framework [394]:

$$|\lambda'_{111}| < 3.3 \times 10^{-4} \tilde{q}^2 \tilde{g}^{\frac{1}{2}}. \quad (6.106)$$

Since the upper bound on λ'_{111} scales with $(T_{1/2}^{\beta\beta_{0\nu}})^{-1/4}$, most recent bounds on the half-life of ^{76}Ge do not significantly improve the above result. Slightly more severe bounds on λ'_{111} have been obtained in Ref. [395] by including the pion-exchange contributions to the \tilde{H}_p induced $\beta\beta_{0\nu}$ decay.

Babu and Mohapatra [396] identified another \tilde{H}_p contribution to $\beta\beta_{0\nu}$, based on the t -channel scalar-vector type exchange of a sfermion and a charged W boson linked together through an intermediate internal neutrino exchange. The corresponding diagram is shown in Fig. 6.22. The amplitude for this process is closely related to that of the familiar SM neutrino exchange, except for the important fact that no chirality flip is required for the intermediate internal neutrino line propagation. The strong suppression factor arising within the Standard Model contribution from the neutrino propagator factor is replaced as, $m_\nu/q^2 \rightarrow 1/g \cdot q = \gamma \cdot q/q^2$, where q is the intermediate neutrino four momentum. The chirality flip penalty is transferred instead to the exchanged down-squark, as seen in Fig. 6.22. The contribution shown in Fig. 6.22 thus disappears in case of a vanishing mixing between \tilde{d}_{kR} and \tilde{d}_{kL} . The bound on $(T_{1/2}^{\beta\beta_{0\nu}})$ leads then to upper limits on the products $\lambda'_{1k1} \lambda'_{11k}$ which scale with $m_{\tilde{d}_{kR}}^4 / (A_k - \mu \tan \beta)$, the denominator determining the left-right mixing in the \tilde{d}_k sector. The resulting bounds for the third, second and first generations, as quoted in Ref. [397], read:

$$\begin{aligned} |\lambda'_{113} \lambda'_{131}| &< 3.8 \times 10^{-8} (\tilde{m}/100 \text{ GeV})^3, \\ |\lambda'_{112} \lambda'_{121}| &< 1.1 \times 10^{-6} (\tilde{m}/100 \text{ GeV})^3, \end{aligned} \quad (6.107)$$

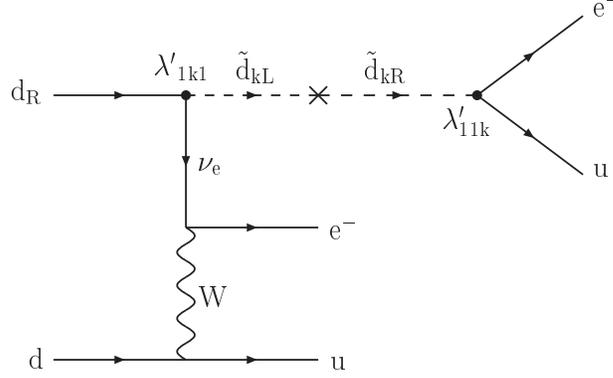


Figure 6.22: Contributions to the neutrinoless double beta decay induced by squark and W exchanges.

assuming the input values for the down squark mass parameters $m_{\tilde{d}_{kR}} \simeq (A_k - \mu \tan \beta) \equiv \tilde{m}$.

A systematic discussion including both the bilinear and trilinear \tilde{R}_p interactions has been given by Faessler et al. in Ref. [398]. It includes a detailed study of the validity of the different approximation schemes in the determination of the relevant nuclear matrix elements. The bilinear \tilde{R}_p terms give rise to several contributions to $\beta\beta_{0\nu}$, either alone or in combination with trilinear \tilde{R}_p interactions. The dominant contribution turns out to be the neutrino exchange diagram controlled by the effective neutrino mass parameter induced by bilinear R -parity violation, $\langle m_\nu \rangle \equiv \sum_i m_{\nu_i} U_{ei}^2 \propto (v_1\mu - v_d\mu_1)^2$. The comparison of their predicted results with the experimental limit for $\beta\beta_{0\nu}$ yields the bounds (assuming a common superpartner mass parameter $\tilde{m} = 100$ GeV and $\tan \beta = 1$):

$$|\mu_1| < 470 \text{ keV}, \quad |\mu_1 \lambda'_{111}| < 100 \text{ eV}, \quad (6.108)$$

$$|v_1| < 840 \text{ keV}, \quad |v_1 \lambda'_{111}| < 55 \text{ eV}. \quad (6.109)$$

Strictly speaking, the bounds (6.108) (resp. the bounds (6.109)) apply in a (H_d, L_i) basis in which $v_i \equiv \langle \tilde{\nu}_i \rangle = 0$ (resp. $\mu_i = 0$).

In Ref. [399], Hirsch studied the contribution of bilinear R -parity violation to $\beta\beta_{0\nu}$ both at the tree-level and at the one-loop level. The consideration of the tree-level contribution led him to exclude values for μ_1 or v_1 in the interval $\mathcal{O}(0.1) - \mathcal{O}(1)$ MeV, in agreement with Faessler et al. [398]. He further observed that even in the case of a perfect alignment between the μ_1 and v_1 parameters (such that $v_1\mu - v_d\mu_1 = 0$, hence bilinear \tilde{R}_p violation does not contribute to $\langle m_\nu \rangle$ at the tree level), there can occur finite contributions to $\langle m_\nu \rangle$ arising at the one-loop level, which leads to the bound $|\mu_1/\mu| < 0.01$.

A lepton number violating process which is closely related to the $\beta\beta_{0\nu}$ reaction concerns the $\mu^+ \rightarrow e^-$ conversion reaction taking place in atomic nuclei via the atomic orbit capture reaction of muons [264], $\mu^+ + (Z, N) \rightarrow e^- + (Z + 2, N - 2)$. The numerical result for the predicted branching fraction, $(B(\mu^+ \rightarrow e^+)/10^{-12}) \simeq |\lambda'_{213}\lambda'_{131}|/2.3 \times 10^{-2}$, as represented by scaling with respect to the current $\mathcal{O}(10^{-12})$ experimental sensitivity, indicates the extent to which future improvement in the measurements of $\mu^+ \rightarrow e^-$ conversion could bring useful information on the \tilde{R}_p interactions.

6.4.4 Baryon Number Non-Conserving Processes

Single Nucleon Decay

Matter instability, as would be implied by a non-conservation of baryon number, is a well-documented subject thanks to the extensive research developed in connection with Grand Unified Theories [8, 400, 401, 402, 403]. The combined contributions of the λ' and λ'' interactions lead to an effective interaction of the form $\mathcal{L} = (\lambda''\lambda'^*/m_{\tilde{d}_R}^2)[(u^c d^c)^\dagger(\nu d) - (u^c d^c)^\dagger(eu)] + h. c.$, which we have written using a two-component Weyl spinor representation for the fermion fields. This effective interaction is obtained by contracting a pair of down-squark fields as $(d^c)^\dagger d^c$, and therefore yields a $(B - L)$ -conserving amplitude. This is illustrated by the the tree-level \tilde{d}_{kR} squark s -channel exchange diagrams shown in Fig. 6.23. The comparison with the experimental

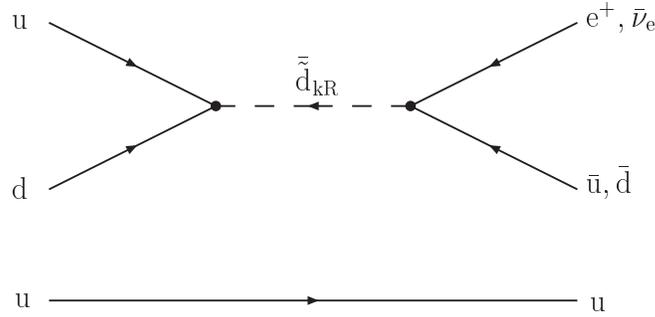


Figure 6.23: \mathcal{B}_p contributions to the proton decay.

limits on nucleon decays yields extremely severe bounds on the \mathcal{B}_p coupling products $\lambda'_{imk}\lambda''_{11k}$ ($i, k = 1, 2, 3, m = 1, 2$). Adapting to the \mathcal{B}_p case the computation of the proton decay rate from dimension-6 operators done in the context of Grand Unified Theories in Ref. [404], and using the experimental lower bounds on partial nucleon lifetimes given in Ref. [20], we obtain:

$$\begin{aligned} |\lambda'_{l1k}\lambda''_{11k}| &\lesssim (2-3) \times 10^{-27} \tilde{d}_{kR}^2 \quad [p \rightarrow \pi^0 l^+], \\ |\lambda'_{31k}\lambda''_{11k}| &\lesssim 7 \times 10^{-27} \tilde{d}_{kR}^2 \quad [n \rightarrow \pi^0 \bar{\nu}], \\ |\lambda'_{i2k}\lambda''_{11k}| &\lesssim 3 \times 10^{-27} \tilde{d}_{kR}^2 \quad [p \rightarrow K^+ \bar{\nu}], \end{aligned} \quad (6.110)$$

which update the estimate given in Ref. [256]. The \tilde{d}_{kR} squark exchange can also occur in the t -channel, yielding a bound on the \mathcal{B}_p coupling products $\lambda'_{l1k}\lambda''_{12k}$ ($l = 1, 2, k = 1, 2, 3$):

$$|\lambda'_{l1k}\lambda''_{12k}| \lesssim (6-7) \times 10^{-27} \tilde{d}_{kR}^2 \quad [p \rightarrow K^0 l^+]. \quad (6.111)$$

One could also alternatively contract the down-squark fields as $d - d^c$ by including a left-right mixing mass insertion term \tilde{m}_{LR}^{d2} , which then yields a $(B + L)$ -conserving amplitude [405]. The bounds derived from the experimental limits on the nucleon decay channels $p \rightarrow K^+ \nu$ and $n \rightarrow \pi^0 \nu$ [20] read ($i, j = 1, 2, 3$):

$$\begin{aligned} |\lambda'_{ij1}\lambda''_{11j}| &\lesssim 7 \times 10^{-27} \tilde{d}_{jL}^2 \left(\frac{m_{\tilde{d}_R}^2}{(\tilde{m}_{LR}^{d2})_{jj}} \right) \quad [n \rightarrow \pi^0 \nu], \\ |\lambda'_{ij2}\lambda''_{11j}| &\lesssim 3 \times 10^{-27} \tilde{d}_{jL}^2 \left(\frac{m_{\tilde{d}_R}^2}{(\tilde{m}_{LR}^{d2})_{jj}} \right) \quad [p \rightarrow K^+ \nu], \\ |\lambda'_{i31}\lambda''_{123}| &\lesssim 3 \times 10^{-27} \tilde{b}_L^2 \left(\frac{m_{\tilde{b}_R}^2}{(\tilde{m}_{LR}^{d2})_{33}} \right) \quad [p \rightarrow K^+ \nu]. \end{aligned} \quad (6.112)$$

These bounds are less stringent than the previous ones due to the presence of the left-right mass term $(\tilde{m}_{LR}^{d2})_{jj} = (A^d - \mu \tan \beta)m_{d_j}$ in the denominator; the best bounds are obtained for $j = 3$ ($\tilde{b}_L - \tilde{b}_R$ exchange). The exchanged scalar field can also be an up-squark, with the insertion of a left-right mass term $(\tilde{m}_{LR}^{u2})_{jj} = (A^u - \mu \cot \beta)m_{u_j}$ [405]. The bounds derived from the experimental limits on the neutron decay modes $n \rightarrow K^+ l^-$ [20] read ($l = 1, 2, j = 1, 2, 3$):

$$|\lambda'_{lj1} \lambda''_{j12}| \lesssim 10^{-26} \tilde{u}_{jL}^2 \left(\frac{m_{u_{jR}}^2}{(\tilde{m}_{LR}^{u2})_{jj}} \right) [n \rightarrow K^+ l]. \quad (6.113)$$

Again the best bounds are obtained for $j = 3$ ($\tilde{t}_L - \tilde{t}_R$ exchange).

The above very stringent bounds concern $\lambda' \lambda''^{(*)}$ products involving dominantly the first two light generation indices. It was observed by Smirnov and Vissani [406] that an appropriate extension of the above analysis to the one-loop level could be used to set strong bounds on coupling products for all possible configurations of the generation indices. The contributions come from one-loop diagrams obtained from the above tree-level diagrams by adding a vertex diagram dressing for the coupling $\nu_i d_{jL} \tilde{d}_{kR}^*$ or for the coupling $u_{i'R} d_{j'R} \tilde{d}_{k'R}$, or a box diagram dressing for both couplings, where the internal lines propagating in the loops are charged or neutral Higgs bosons, winos or sfermions. The loop and flavour mixing suppression factors in the transition amplitudes result in much weaker bounds than Eqs. (6.110)–(6.113). Assuming squark masses around 1 TeV, one obtains the following conservative bound on any product of λ - and λ'' -type couplings [406]:

$$|\lambda'_{ijk} \lambda''_{i'j'k'}| < \mathcal{O}(10^{-9}). \quad (6.114)$$

For squark masses around 100 GeV, this bound would be $\mathcal{O}(10^{-12})$.

Single nucleon decays can also be induced by products of λ -type and λ'' -type couplings, through tree-level diagrams involving the sequential exchange of a squark, a neutralino or chargino, and a slepton, or through one-loop or two-loop diagrams obtained from the dressing of the former tree-level diagrams [371, 407, 408]. Bhattacharyya and Pal [408] consider proton decay mediated by diagrams involving the exchange of a neutralino. Assuming a common superpartner mass $\tilde{m} = 1$ TeV, they obtain the following bounds on the $\lambda \lambda''^{**}$ products involving a coupling λ''_{112} :

$$\begin{aligned} |\lambda_{231} \lambda''_{112}^*|, |\lambda_{132} \lambda''_{112}^*| &\lesssim 10^{-16} [p \rightarrow K^+ e^\pm \mu^\mp \bar{\nu}], \\ |\lambda_{123} \lambda''_{112}^*| &\lesssim 10^{-14} [p \rightarrow K^+ \nu \bar{\nu}], \\ |\lambda_{121} \lambda''_{112}^*|, |\lambda_{131} \lambda''_{112}^*| &\lesssim 10^{-17} [p \rightarrow K^+ \bar{\nu}], \\ |\lambda_{122} \lambda''_{112}^*|, |\lambda_{232} \lambda''_{112}^*| &\lesssim 10^{-20} [p \rightarrow K^+ \bar{\nu}], \\ |\lambda_{133} \lambda''_{112}^*|, |\lambda_{233} \lambda''_{112}^*| &\lesssim 10^{-21} [p \rightarrow K^+ \bar{\nu}]. \end{aligned} \quad (6.115)$$

The bounds obtained from four-body decay modes could actually be relaxed by about two orders of magnitude, due to phase space factors. The constraints on products involving any other λ''_{ijk} coupling are much weaker, since the corresponding vertex must be dressed by a loop with a charged Higgs boson in order to induce proton decay. The resulting bounds read, assuming $m_{H^\pm} = \tilde{m} = 1$ TeV ($(i, j, k) \neq (1, 1, 2)$) [408]:

$$\begin{aligned} |\lambda_{231} \lambda''_{ijk}|, |\lambda_{132} \lambda''_{ijk}| &\lesssim (10^{-7} - 10^{-5}) [p \rightarrow \pi^+(K^+) e^\pm \mu^\mp \bar{\nu}], \\ |\lambda_{123} \lambda''_{ijk}| &\lesssim (10^{-5} - 10^{-3}) [p \rightarrow \pi^+(K^+) \nu \bar{\nu}], \\ |\lambda_{121} \lambda''_{ijk}|, |\lambda_{131} \lambda''_{ijk}| &\lesssim (10^{-8} - 10^{-6}) [p \rightarrow \pi^+(K^+) \bar{\nu}], \\ |\lambda_{122} \lambda''_{ijk}|, |\lambda_{232} \lambda''_{ijk}| &\lesssim (10^{-11} - 10^{-9}) [p \rightarrow \pi^+(K^+) \bar{\nu}], \\ |\lambda_{133} \lambda''_{ijk}|, |\lambda_{233} \lambda''_{ijk}| &\lesssim (10^{-12} - 10^{-10}) [p \rightarrow \pi^+(K^+) \bar{\nu}]. \end{aligned} \quad (6.116)$$

Considering nucleon decay mediated by tree-level diagrams involving a chargino exchange, Carlson et al. [371] find stronger bounds than Eqs (6.116) for the $\lambda\lambda''$ products involving the couplings λ''_{113} , λ''_{123} , λ''_{212} and λ''_{312} :

$$|\lambda_{ijk}\lambda''_{113}| \lesssim 10^{-13}, \quad |\lambda_{ijk}\lambda''_{123}| \lesssim 10^{-12}, \quad |\lambda_{ijk}\lambda''_{212}| \lesssim 10^{-13}, \quad |\lambda_{ijk}\lambda''_{312}| \lesssim 10^{-12}. \quad (6.117)$$

These bounds correspond to $(B + L)$ -conserving decays such as $p \rightarrow l_k^+ \nu_i \nu_j$. The bounds on $\lambda\lambda''$ products involving the other λ''_{ijk} couplings are weaker than Eqs (6.116), since a loop dressing of the corresponding vertex is necessary in order to induce nucleon decay; we therefore do not give them here.

Other independent bounds resulting from the combined effects of the trilinear interactions λ'' and bilinear interactions μ_i are obtained by Bhattacharyya and Pal [409], based on a tree-level mechanism involving the intermediate action of the Yukawa interaction of quarks with the up-type Higgs boson. The relevant effective Lagrangian is $(B + L)$ -conserving and contributes to the proton decay channels $p \rightarrow K^+ \nu$ and $p \rightarrow K^+ \pi^+ l^-$. The bound associated with the channel $p \rightarrow K^+ \nu$ reads ($i = 1, 2, 3$) [409]:

$$|\lambda''_{112} \frac{\mu_i}{\mu}| \lesssim 10^{-23} \tilde{u}_R^2 \quad [p \rightarrow K^+ \nu]. \quad (6.118)$$

At the one-loop level, the same type of Higgs or gaugino dressing as described above can be invoked to deduce analogous bounds involving also the heavy quark generations. The associated mechanism requires the intermediate action of the Yukawa interactions of quarks with Higgs bosons, which results in an extra suppression factor $(\lambda^d)^2$. The associated upper bounds on $\lambda''_{ijn} \mu_{i'}/\mu$, $n = 1, 2$, $(i, j, n) \neq (1, 1, 2)$, vary inside the following range [409]:

$$|\lambda''_{ijn} \frac{\mu_{i'}}{\mu}| \lesssim (10^{-16} - 10^{-12}) \tilde{d}_{nR}^2 \quad [p \rightarrow \pi^+ \nu, p \rightarrow K^+ \nu]. \quad (6.119)$$

We quote below a representative subset of the derived bounds:

$$|\lambda''_{321} \frac{\mu_{i'}}{\mu}| \lesssim 10^{-16} \tilde{d}_R^2, \quad |\lambda''_{331} \frac{\mu_{i'}}{\mu}| \lesssim 10^{-15} \tilde{d}_R^2, \quad |\lambda''_{332} \frac{\mu_{i'}}{\mu}| \lesssim 10^{-16} \tilde{s}_R^2. \quad (6.120)$$

If the production of superpartner particles in single nucleon decays were energetically allowed, additional exotic decay modes could arise from the baryon number violating interactions alone. A familiar example is furnished, for the case of a very light neutralino, $m_{\tilde{\chi}^0} \ll m_p - m_{K^+}$, by the exotic proton decay channel $p \rightarrow \tilde{\chi}^0 K^+$, which can proceed via \tilde{s} tree-level exchange. This decay mode sets the bound $|\lambda''_{112}| \lesssim 10^{-15}$ [410].

For the case of an ultralight gravitino \tilde{G} or axino \tilde{a} [411, 412], as characteristically arises in the low-energy gauge-mediated supersymmetry breaking approach, additional single nucleon decay channels may appear where the \tilde{R}_p interactions initiate processes involving the emission of a light strange meson accompanied by an R -parity odd gravitino or axino. The tree-level \tilde{s} exchange graph for the relevant subprocesses, $ud \rightarrow \tilde{s}\tilde{G}$ and $ud \rightarrow \tilde{s}\tilde{a}$, leads to the bounds [413],

$$|\lambda''_{112}| \lesssim 6 \times 10^{-17} \tilde{s}_R^2 \left(\frac{m_{3/2}}{1 \text{ eV}} \right) \quad [p \rightarrow K^+ \tilde{G}], \quad (6.121)$$

$$|\lambda''_{112}| \lesssim 8 \times 10^{-17} C_q^{-1} \tilde{s}_R^2 \left(\frac{F_a}{10^{10} \text{ GeV}} \right) \quad [p \rightarrow K^+ \tilde{a}], \quad (6.122)$$

applying to the gravitino and axino emission cases, respectively. For the axino case, F_a designates the axionic symmetry breaking mass scale, and the parameter C_q , which describes the

model dependence of the axino couplings to quark and lepton fields, is assigned an order one value or values in the range $C_q^{-1} = \mathcal{O}(10^2 - 10^3)$, depending on the type of axino considered.

Pursuing along the same lines as above with the study of the two-body single nucleon decay modes at the one-loop level, one can derive strong bounds on all couplings λ''_{ijk} . Accounting approximately for the loop and flavour suppression factors associated with the one-loop dressing of the previous tree-level diagrams, Choi et al. obtain bounds in the ranges [414]:

$$|\lambda''_{ijk}| \lesssim (10^{-11} \tilde{m}^3 - 10^{-8} \tilde{m}^2) \left(\frac{m_{3/2}}{1 \text{ eV}} \right), \quad (6.123)$$

$$|\lambda''_{ijk}| \lesssim (10^{-11} \tilde{m}^3 - 10^{-8} \tilde{m}^2) C_q^{-1} \left(\frac{F_a}{10^{10} \text{ GeV}} \right), \quad (6.124)$$

where \tilde{m} denotes a common superpartner mass, for the gravitino and axino emission cases, respectively. A representative subset of these bounds reads:

$$\left[\frac{|\lambda''_{113}|}{\tilde{m}^3}, \frac{|\lambda''_{212}|}{\tilde{m}^2}, \frac{|\lambda''_{323}|}{\tilde{m}^2} \right] \lesssim [2 \times 10^{-11}, 3 \times 10^{-9}, 6 \times 10^{-9}] \left(\frac{m_{3/2}}{1 \text{ eV}} \right), \quad (6.125)$$

$$\left[\frac{|\lambda''_{113}|}{\tilde{m}^3}, \frac{|\lambda''_{212}|}{\tilde{m}^2}, \frac{|\lambda''_{323}|}{\tilde{m}^2} \right] \lesssim [3 \times 10^{-11}, 4 \times 10^{-9}, 8 \times 10^{-9}] C_q^{-1} \left(\frac{F_a}{10^{10} \text{ GeV}} \right), \quad (6.126)$$

for the gravitino and axino emission cases, respectively.

Nucleon-Antinucleon Oscillations and Double Nucleon Decay

The $n \rightarrow \bar{n}$ transition is governed by the effective Lagrangian,

$$\mathcal{L} = -(\bar{n} \bar{n}^c) \begin{pmatrix} m & \delta m \\ \delta m^* & m \end{pmatrix} \begin{pmatrix} n \\ n^c \end{pmatrix}, \quad (6.127)$$

where the inputs needed to determine the mass shift parameter δm , involve the couplings λ'' , the superpartner mass parameters, and the hadronic matrix elements of the relevant $\mathcal{D} = 9$ local operators $d_R d_R d_R u_R q_L q_L$ and $d_R d_R q_L q_L q_L q_L$. While the neutron-antineutron oscillation time, defined approximately by $\tau_{osc} \simeq 1/\delta m$, is strongly hindered by the nuclear interactions, one hopefully anticipates to find observable manifestations of $\Delta B = 2$ baryon number violation under the guise of nuclear two-nucleon disintegration processes, $N + (A-1) \rightarrow \bar{N} + (A-1) \rightarrow X + (A-2)$, where X denotes the possible decay channels for the nucleon-antinucleon pair annihilation reaction $n\bar{n} \rightarrow X$, $n\bar{p} \rightarrow X$ and $p\bar{p} \rightarrow X$, with $X = \pi, 2\pi, 3\pi, 2K, \dots$ [415]. The rôle of the hadronic and nuclear structure effects in the estimation of the dimension-9 operators matrix elements is discussed in Refs. [416, 417, 418].

Two competitive tree-level mechanisms for the \mathcal{R}_p contributions were originally discussed in an initiating study by Zwirner [419]. The dominant process is shown in Fig. 6.24. The bounds inferred by comparison with the experimental limit due to the non-observation of $n\text{-}\bar{n}$ oscillations, using the tentative estimate $|\psi_N(0)|^4 \approx 10^{-4} \text{ GeV}^6$ for the wave function, are rather strong [156, 256, 419]:

$$|\lambda''_{11k}| \lesssim (10^{-8} - 10^{-7}) \frac{10^8 \text{ s}}{\tau_{osc}} \left(\frac{\tilde{m}}{100 \text{ GeV}} \right)^{5/2}. \quad (6.128)$$

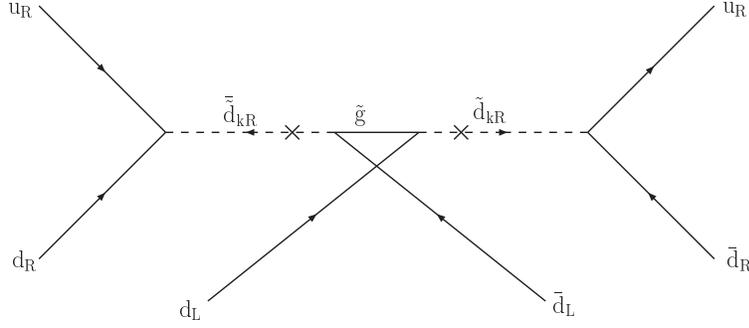


Figure 6.24: R_p contribution to nucleon-antinucleon oscillation.

An alternative estimate reads: $|\lambda''_{11k}| \lesssim (0.3 - 1.7) \times 10^{-10} \tilde{g}^{1/2} \tilde{d}_{kR}^2$. However, these bounds should be taken as indicative only, since an unknown suppression factor from the flavour off-diagonal entries of the left-right mixing squark mass matrix was ignored. The second mechanism discussed by Zwirner [419] is described by an intermediate vertex at which three sfermions, which are emitted by quark lines via λ'' interactions, jointly annihilate via a soft supersymmetry breaking interaction of the type $A''_{ijk} \tilde{u}_i^c \tilde{d}_j^c \tilde{d}_k^c$ [419]. This contribution faces the same problem regarding the unknown input for the interaction trilinear in the squark fields. Being of order λ''^4 , it should be subdominant compared to the above one.

Goity and Sher [100] have challenged the view that n - \bar{n} oscillations do actually constrain the coupling constant λ''_{121} , in view of the uncertain information on the input supersymmetry breaking mass parameters. They argue that one can identify a competitive mechanism, with a fully calculable transition amplitude, which sets a bound on λ''_{131} . This alternative mechanism [100] is based on the sequence of reactions $u_R d_R + d_L \rightarrow \tilde{b}_R^* + d_L \rightarrow \tilde{b}_L^* + d_L \rightarrow \tilde{d}_L + \tilde{b}_L \rightarrow \tilde{d}_L + \tilde{u}_R \tilde{d}_R$, where the intermediate transition $\tilde{b}_L^* + d_L \rightarrow \tilde{d}_L + \tilde{b}_L$ is due to a W boson and gaugino exchange box diagram [100]. The choice of intermediate bottom squarks is the most favourable one in order to maximise factors such as m_d^2/M_W , which arise from the electroweak interactions of d-quarks in the box diagram amplitude. The resulting bound must be evaluated numerically and lies in the wide interval $|\lambda''_{131}| \lesssim (2 \times 10^{-3} - 10^{-1})$, for squark masses varying in the range $m_{\tilde{q}} = (200 - 600)$ GeV. The bound on λ''_{121} is a factor $m_s/m_b \approx 4 \times 10^{-2}$ weaker, $|\lambda''_{121}| \lesssim (5 \times 10^{-2} - 2.5)$, and is of marginal physical interest [100]. Chang and Keung [410] observe that the above mechanism actually includes three other analogous one-loop box diagrams involving the exchange of gaugino- W boson and quark-squark pairs. A single one of these dominates and yields bounds for the associated couplings of the form [410],

$$\begin{aligned} |\lambda''_{321}| &\lesssim [2.1 \times 10^{-3}, 1.5 \times 10^{-2}] \left(\frac{m_s}{200 \text{ MeV}} \right)^{-2}, \\ |\lambda''_{331}| &\lesssim [2.6 \times 10^{-3}, 2 \times 10^{-2}], \end{aligned} \quad (6.129)$$

where the two numbers inside brackets are in correspondence with the two input values used for the squark mass, $m_{\tilde{q}} = [100, 200]$ GeV, and m_s is the strange quark mass.

The generational structure of the λ''_{ijk} couplings imposes non-diagonal flavour configurations for the d^c quarks, which disfavors the strangeness conserving $n \rightarrow \bar{n}$ transition. Based on an observation by Dimopoulos and Hall [156], Barbieri and Masiero [323] propose instead to apply the same mechanism to the $\Delta S = 2$ process $udd \rightarrow u^c s^c s^c$, which contributes to the transition $n \rightarrow \bar{\Xi}$. One avoids in this way the penalty of two flavour off-diagonal left-right mixing squark mass insertions, but the counterpart of this advantage is an energetically suppressed, off-shell $n \rightarrow \bar{\Xi}$ transition. Another hadronic physics aspect in the comparison between the $n \rightarrow \bar{\Xi}$

and $n \rightarrow \bar{n}$ systems resides in their different short distance hadronic interactions. An $n - \bar{\Xi}$ oscillation initiates $\Delta B = \Delta S = 2$ double nucleon decay processes such as $p + p \rightarrow K^+ + K^+$ or $n + n \rightarrow K^0 + K^0$, which could become the predominant channel for a double nucleon induced nuclear decay. Application to the nuclear decay reaction $^{16}\text{O} \rightarrow ^{14}\text{C} + K^+ + K^+$ yields a relationship for the double nucleon decay lifetime, $\tau_{NN} \simeq (10^{-2} \text{ y}) \lambda_{112}''^{-4} (\tilde{q}^4 \tilde{g})^2$, which results in the bound [323]:

$$|\lambda_{121}''| \lesssim 10^{-8.5} \tilde{g}^{\frac{1}{2}} \tilde{q}^2 \left(\frac{\tau_{NN}}{10^{32} \text{ yr}} \right)^{-1/4} \left(\frac{10^{-6} \text{ GeV}^6}{\lesssim \bar{N} |ududs| \Xi \rangle} \right)^{1/2}. \quad (6.130)$$

An alternative treatment of the nuclear decay process is proposed by Goity and Sher [100], where one bypasses the intermediate step of the $n \rightarrow \bar{\Xi}$ transition by dealing directly with the transition $NN \rightarrow KK$. These authors identify a mechanism where the \tilde{R}_p interactions contribute through a Feynman diagram involving the s -channel production of a pair of squarks mediated by the t -channel exchange of a gluino, based on the reaction scheme $(q_i q_j)(q_l q_m) \rightarrow \tilde{q}_k^* \tilde{q}_n^* \rightarrow \bar{q}_k \bar{q}_n$, where (q_i, q_j, q_k) is a permutation of (u_R, d_R, s_R) , and similarly for (q_l, q_m, q_n) . The decay amplitude for the nuclear reaction $^{16}\text{O} \rightarrow ^{14}\text{C} + K^+ + K^+$ is evaluated within an impulse approximation nuclear Fermi gas model for the nuclei, where the nuclear momentum integral contains the folded product of the elementary process cross-section with the nuclear momentum distributions of nucleons. The resulting bound reads [100]:

$$|\lambda_{121}''| \lesssim 10^{-15} \mathcal{R}^{-5/2}, \quad \mathcal{R} \equiv \frac{\tilde{\Lambda}}{(m_{\tilde{g}} m_{\tilde{q}}^4)^{1/5}}, \quad (6.131)$$

where the parameter $\tilde{\Lambda}$ in the overall scale factor parameter \mathcal{R} describes a hadronic scale representing the dimensional analysis estimates of the hadronic and nuclear matrix elements. Varying \mathcal{R} inside the range $(10^{-3} - 10^{-6})$, one finds a bound spanning a wide interval: $|\lambda_{121}''| \lesssim (10^{-7} - 10^0)$. In spite of the strong dependence on the hadronic and nuclear structure inputs, the preferred estimates are quoted in Ref. [100] as $|\lambda_{121}''| \lesssim 10^{-6}$ and $|\lambda_{131}''| \lesssim 10^{-3}$, for the choice of a common superpartner mass $\tilde{m} = 300 \text{ GeV}$.

6.5 General Discussion of Indirect Trilinear Bounds

In this section we shall attempt to assess from a more global perspective the current situation regarding the indirect bounds on the trilinear \tilde{R}_p coupling constants.

6.5.1 Summary of Main Experimental Bounds

We have collected together a sizeable subset of the strongest bounds available in the literature. Table 6.1 displays the results for single coupling constants and Table 6.2 to 6.5 for quadratic coupling constant products. These lists recapitulate bounds already encountered in the preceding sections. The bounds derived from the perturbative unitarity conditions following the discussion of the renormalisation group constraints in chapter 3 have also been included, as well as the bounds inferred from the neutrino mass discussed in chapter 5. Self-evident abbreviations (described in the caption of Table 6.1) are used to identify the associated observable processes from which the bounds are inferred.

	Charged Current	Neutral Current	Other Processes
λ_{12k}	0.05 $\tilde{e}_{kR} [V_{ud}]$ (6.25) 0.07 $\tilde{e}_{kR} [R_{\mu\tau}]$ (6.14)	0.14 $\tilde{e}_{kR} [\nu_\mu e]$ (6.35) 0.13 $\tilde{e}_{k=1L} [\nu_\mu e]$ (6.35) [0.37, 0.25, 0.11] $\tilde{\nu}$ $k = 1, 2, 3 [A_{FB}]$ (6.39) 0.05 $\tilde{e}_{kR} [Q_W(\text{Cs})]$ (6.47) 0.13 $\tilde{e}_{kR} [\nu_\mu q]$ (6.36)	
λ_{13k}	0.07 $\tilde{e}_{kR} [R_\tau]$ (6.17)	[0.37, 0.25, 0.11] $\tilde{\nu}$ $k = 1, 2, 3 [A_{FB}]$ (6.39)	
λ_{23k}	0.07 $\tilde{e}_{kR} [R_\tau]$ (6.17) 0.07 $\tilde{e}_{kR} [R_{\tau\mu}]$ (6.17)	0.11 $\tilde{\tau}_L [\nu_\mu e]$ (6.35) $k = 1$	
λ_{233}			0.90 [RG]
λ_{i22}			$2.7 \times 10^{-2} \tilde{\mu} \tilde{m}^{-\frac{1}{2}} [m_\nu < 1 \text{ eV}]$ ($\tilde{m}_{LR22}^2 = \tilde{m} m_\mu$) (5.11)
λ_{i33}			$1.6 \times 10^{-3} \tilde{\tau} \tilde{m}^{-\frac{1}{2}} [m_\nu < 1 \text{ eV}]$ ($\tilde{m}_{LR33}^2 = \tilde{m} m_\tau$) (5.11)
λ'_{11k}	0.02 $\tilde{d}_{kR} [V_{ud}]$ (6.25) 0.03 $\tilde{d}_{kR} [R_\pi]$ (6.19)	[0.28, 0.18] \tilde{u}_L $k = 2, 3 [A_{FB}]$ (6.39) 0.02 $\tilde{d}_{kR} [Q_W(\text{Cs})]$ (6.47)	
λ'_{111}			$3.3 \times 10^{-4} \tilde{q}^2 \tilde{g}^{\frac{1}{2}} [\beta\beta 0\nu]$ (6.106)
λ'_{12k}	0.44 $\tilde{d}_{kR} [R_{D^+}]$ (6.27) 0.27 $\tilde{d}_{kR} [R_{D^0}]$ (6.27) 0.23 $\tilde{d}_{kR} [R_{D^+}^*]$ (6.27)	0.21 $\tilde{d}_{kR} [A_{FB}]$ (6.39) [0.28, 0.18] \tilde{c}_L $k = 2, 3 [A_{FB}]$ (6.39)	
λ'_{13k}		[0.28, 0.18] \tilde{t}_L $k = 2, 3 [A_{FB}]$ (6.39) 0.47 [Re] (6.40) ($m(\tilde{d}_{kR}) = 100 \text{ GeV}$)	
λ'_{1j1}		0.03 $\tilde{u}_{jL} [Q_W(\text{Cs})]$ (6.47)	
λ'_{2j1}		0.18 $\tilde{d}_{jL} [\nu_\mu q]$ (6.36)	
λ'_{21k}	0.06 $\tilde{d}_{kR} [R_\pi]$ (6.19) 0.08 $\tilde{d}_{kR} [R_{\tau\pi}]$ (6.21)	0.15 $\tilde{d}_{kR} [\nu_\mu q]$ (6.36)	
λ'_{22k}	0.61 $\tilde{d}_{kR} [R_{D^+}]$ (6.27) 0.38 $\tilde{d}_{kR} [R_{D^+}^*]$ (6.27) 0.21 $\tilde{d}_{kR} [R_{D^0}]$ (6.27) 0.65 $\tilde{d}_{kR} [R_{D_s}(\tau\mu)]$ (6.30)		
λ'_{23k}		0.45 [R $_\mu$] (6.40) ($m_{\tilde{d}_{kR}} = 100 \text{ GeV}$)	

	Charged Current	Neutral Current	Other Processes
λ'_{31k}	$0.12 \tilde{d}_{kR} [R_{\tau\pi}]$ (6.21)		
λ'_{32k}	$0.52 \tilde{d}_{kR} [R_{D_s}(\tau\mu)]$ (6.30)		
λ'_{33k}		$0.58 [R_\tau]$ (6.40) ($m_{\tilde{d}_{kR}} = 100 \text{ GeV}$)	
λ'_{333}	$0.32 \tilde{b}_R [B \rightarrow \tau\nu X]$ (6.28)		$1.06 [RG]$
λ'_{i11}			$0.2 \tilde{d}\tilde{m}^{-\frac{1}{2}} [m_\nu < 1 \text{ eV}]$ ($\tilde{m}_{LR11}^{d2} = \tilde{m}m_d$) (5.12)
λ'_{i22}			$10^{-2} \tilde{s}\tilde{m}^{-\frac{1}{2}} [m_\nu < 1 \text{ eV}]$ ($\tilde{m}_{LR22}^{d2} = \tilde{m}m_s$) (5.12)
λ'_{i33}			$4 \times 10^{-4} \tilde{b}\tilde{m}^{-\frac{1}{2}} [m_\nu < 1 \text{ eV}]$ ($\tilde{m}_{LR33}^{d2} = \tilde{m}m_b$) (5.12)
λ''_{11k}			$(10^{-8} - 10^{-7})(10^8 \text{s}/\tau_{osc})\tilde{m}^{5/2}$ $[n\bar{n}]$ (6.128)
λ''_{112}			$10^{-6} [NN]$ ($\tilde{m} = 300 \text{ GeV}$) (6.131) $6 \times 10^{-17} \tilde{s}_R^2 (m_{3/2}/1 \text{ eV})$ $[p \rightarrow K^+\tilde{G}]$ (6.121) $8 \times 10^{-17} C_q^{-1} \tilde{s}_R^2 (F_a/10^{10} \text{ GeV})$ $[p \rightarrow K^+\tilde{a}]$ (6.122)
λ''_{113}			$10^{-3} [NN]$ ($\tilde{m} = 300 \text{ GeV}$) (6.131)
λ''_{123}			$1.25 [RG]$
λ''_{212}			$1.25 [RG]$
λ''_{213}			$1.25 [RG]$
λ''_{223}			$1.25 [RG]$
λ''_{312}		$1.45 [R_l]$ (6.41) ($\tilde{m} = 100 \text{ GeV}$)	$4.28 [RG]$ $2.1 \times 10^{-3} [n\bar{n}]$ (6.129)
λ''_{313}		$1.46 [R_l]$ (6.41) ($\tilde{m} = 100 \text{ GeV}$)	$1.12 [RG]$ $2.6 \times 10^{-3} [n\bar{n}]$ (6.129)
λ''_{323}		$1.46 [R_l]$ (6.41) ($\tilde{m} = 100 \text{ GeV}$)	$1.12 [RG]$
λ''_{ijk}			$(10^{-11} \tilde{m}^3 - 10^{-8} \tilde{m}^2)$ $\times (m_{3/2}/1 \text{ eV}) [p \rightarrow K^+\tilde{G}]$ (6.123) $\times (F_a/10^{10} \text{ GeV}) [p \rightarrow K^+\tilde{a}]$ (6.124)

Table 6.1: Single bounds for the \tilde{R}_p coupling constants at the 2σ level. We use the notation V_{ij} for the CKM matrix, R_l , $R_{l\nu}$, R_D , R_l^Z for various branching fractions or ratios of branching fractions as defined in the text, Q_W for the weak charge, νq , νl for the neutrino elastic scattering on quarks and leptons, m_ν for the neutrino Majorana mass, RG for the renormalisation group, A_{FB} for forward-backward asymmetry, $Q_W(Cs)$ for atomic physics parity violation, $n\bar{n}$ for neutron-antineutron oscillation and NN for two nucleon nuclear decay, $[K\bar{K}]$, for $K^0 - \bar{K}^0$ mixing. The generation indices denoted i, j, k run over the three generations while those denoted l, m, n run over the first two generations. The dependence on the superpartner mass follows the notational convention $\tilde{m}^p = (\frac{\tilde{m}}{100 \text{ GeV}})^p$. Aside from a few cases associated with one-loop effects, we use the reference value $\tilde{m} = 100 \text{ GeV}$. The quoted equation labels refer to equations in the text.

	Lepton Flavour	Hadron Flavour	L and/or B violation
$ \lambda_{ij2}^* \lambda_{ij1} $	$8.2 \times 10^{-5} (\tilde{\nu}_L^2, \tilde{l}_L^2) [\mu \rightarrow e\gamma] (6.95)$		
$ \lambda_{23k} \lambda_{13k}^* $	$2.3 \times 10^{-4} (\tilde{\nu}_L^2, \tilde{l}_R^2) [\mu \rightarrow e\gamma] (6.95)$		
$ \lambda_{312} \lambda_{321}^* $	$1.9 \times 10^{-3} \tilde{\nu}_L^2$ $[\mu^+ e^- \rightarrow \mu^- e^+] (6.103)$		
$ \lambda_{i12}^* \lambda_{i11} $	$6.6 \times 10^{-7} \tilde{\nu}_L^2 [\mu \rightarrow 3e] (6.97)$		
$ \lambda_{321} \lambda_{311}^* $	$6.6 \times 10^{-7} \tilde{\nu}_L^2 [\mu \rightarrow 3e] (6.97)$		
$ \lambda_{i23}^* \lambda_{i22} $	$2.2 \times 10^{-3} \tilde{\nu}_L^2 [\tau \rightarrow 3\mu] (6.97)$		
$ \lambda_{132} \lambda_{122}^* $	$2.2 \times 10^{-3} \tilde{\nu}_L^2 [\tau \rightarrow 3\mu] (6.97)$		
$ \lambda_{i12} \lambda_{j21} $			$0.15 \tilde{l}^2 \tilde{m}^{-1} [m_\nu < 1 \text{ eV}]$
$ \lambda_{i13} \lambda_{j31} $			$8.7 \times 10^{-3} \tilde{l}^2 \tilde{m}^{-1} [m_\nu < 1 \text{ eV}]$
$ \lambda_{i22} \lambda_{j22} $			$7 \times 10^{-4} \tilde{\mu}^2 \tilde{m}^{-1} [m_\nu < 1 \text{ eV}]$
$ \lambda_{i23} \lambda_{j32} $			$4.2 \times 10^{-5} \tilde{l}^2 \tilde{m}^{-1} [m_\nu < 1 \text{ eV}]$
$ \lambda_{i33} \lambda_{j33} $			$2.5 \times 10^{-6} \tilde{\tau}^2 \tilde{m}^{-1} [m_\nu < 1 \text{ eV}]$ $(\tilde{m}_{LR}^2 = \tilde{m} M^e) (5.11)$
$ \lambda_{i12}^* \lambda'_{i11} $	$2.1 \times 10^{-8} \tilde{\nu}_L^2$ $[\mu \rightarrow e (\text{Ti})] (6.99)$		
$ \lambda_{i21} \lambda'_{i11} $	$2.1 \times 10^{-8} \tilde{\nu}_L^2$ $[\mu \rightarrow e (\text{Ti})] (6.99)$		
$ \lambda_{1j1}^* \lambda'_{j33} $	$\mathcal{I} 6 \times 10^{-7} \tilde{\nu}_j^2 [d_e^0] (6.60)$		
$ \lambda_{i31} \lambda'_{i11} $	$1.6 \times 10^{-3} \tilde{\nu}_{iL}^2 [\tau \rightarrow e\eta] (6.104)$		
$ \lambda_{i13}^* \lambda'_{i11} $	$1.6 \times 10^{-3} \tilde{\nu}_{iL}^2 [\tau \rightarrow e\eta] (6.104)$		
$ \lambda_{i32} \lambda'_{i11} $	$1.7 \times 10^{-3} \tilde{\nu}_{iL}^2 [\tau \rightarrow \mu\eta] (6.104)$		
$ \lambda_{i23}^* \lambda'_{i11} $	$1.7 \times 10^{-3} \tilde{\nu}_{iL}^2 [\tau \rightarrow \mu\eta] (6.104)$		

Table 6.2: Quadratic coupling constant product bounds. We use the same conventions as in the preceding table for the single coupling constant bounds. The presence of a symbol \mathcal{I} means that the bound applies to the imaginary part of the coupling constant products.

	Lepton Flavour	Hadron Flavour	L and/or B violation
$ \lambda_{122}^* \lambda'_{112} $		$2.2 \times 10^{-7} \tilde{\nu}_L^2 [K_L \rightarrow \mu^+ \mu^-] (6.76)$	
$ \lambda_{122}^* \lambda'_{121} $		$2.2 \times 10^{-7} \tilde{\nu}_L^2 [K_L \rightarrow \mu^+ \mu^-] (6.76)$	
$ \lambda_{121}^* \lambda'_{212} $		$1.0 \times 10^{-8} \tilde{\nu}_L^2 [K_L \rightarrow e^+ e^-] (6.76)$	
$ \lambda_{121}^* \lambda'_{221} $		$1.0 \times 10^{-8} \tilde{\nu}_L^2 [K_L \rightarrow e^+ e^-] (6.76)$	
$ \lambda_{i12}^* \lambda'_{i12} $		$6 \times 10^{-9} \tilde{\nu}_L^2 [K_L \rightarrow e^\pm \mu^\mp] (6.78)$	
$ \lambda_{i12}^* \lambda'_{i21} $		$6 \times 10^{-9} \tilde{\nu}_L^2 [K_L \rightarrow e^\pm \mu^\mp] (6.78)$	
$ \lambda_{i21}^* \lambda'_{i12} $		$6 \times 10^{-9} \tilde{\nu}_L^2 [K_L \rightarrow e^\pm \mu^\mp] (6.78)$	
$ \lambda_{i21}^* \lambda'_{i21} $		$6 \times 10^{-9} \tilde{\nu}_L^2 [K_L \rightarrow e^\pm \mu^\mp] (6.78)$	
$ \lambda_{i31} \lambda_{i13}^* $		$6 \times 10^{-4} \tilde{l}_{iL}^2 [B^- \rightarrow e^- \bar{\nu}] (6.85)$	
$ \lambda_{i32} \lambda_{i13}^* $		$7 \times 10^{-4} \tilde{l}_{iL}^2 [B^- \rightarrow \mu^- \bar{\nu}] (6.85)$	
$ \lambda_{233} \lambda_{313}^* $		$2 \times 10^{-3} \tilde{l}_{3L}^2 [B^- \rightarrow \tau^- \bar{\nu}] (6.85)$	
$ \lambda_{i11}^* \lambda'_{i13} $		$1.7 \times 10^{-5} \tilde{\nu}_L^2 [B_d^0 \rightarrow e^+ e^-] (6.79)$	
$ \lambda_{i11}^* \lambda'_{i31} $		$1.7 \times 10^{-5} \tilde{\nu}_L^2 [B_d^0 \rightarrow e^+ e^-] (6.79)$	
$ \lambda_{i22}^* \lambda'_{i13} $		$1.5 \times 10^{-5} \tilde{\nu}_L^2 [B_d^0 \rightarrow \mu^+ \mu^-] (6.79)$	
$ \lambda_{i22}^* \lambda'_{i31} $		$1.5 \times 10^{-5} \tilde{\nu}_L^2 [B_d^0 \rightarrow \mu^+ \mu^-] (6.79)$	
$ \lambda_{i12}^* \lambda'_{i13} $		$2.3 \times 10^{-5} \tilde{\nu}_L^2 [B_d^0 \rightarrow e^\pm \mu^\mp] (6.79)$	
$ \lambda_{i12}^* \lambda'_{i31} $		$2.3 \times 10^{-5} \tilde{\nu}_L^2 [B_d^0 \rightarrow e^\pm \mu^\mp] (6.79)$	
$ \lambda_{i21}^* \lambda'_{i13} $		$2.3 \times 10^{-5} \tilde{\nu}_L^2 [B_d^0 \rightarrow e^\pm \mu^\mp] (6.79)$	
$ \lambda_{i21}^* \lambda'_{i31} $		$2.3 \times 10^{-5} \tilde{\nu}_L^2 [B_d^0 \rightarrow e^\pm \mu^\mp] (6.79)$	
$ \lambda_{231} \lambda_{112}^{''*} $			$10^{-16} [p \rightarrow K^+ e^\pm \mu^\mp \bar{\nu}]$
$ \lambda_{132} \lambda_{112}^{''*} $			$10^{-16} [p \rightarrow K^+ e^\pm \mu^\mp \bar{\nu}]$
$ \lambda_{123} \lambda_{112}^{''*} $			$10^{-14} [p \rightarrow K^+ \nu \bar{\nu}]$
$ \lambda_{i11} \lambda_{112}^{''*} $			$10^{-17} [p \rightarrow K^+ \bar{\nu}]$
$ \lambda_{i22} \lambda_{112}^{''*} $			$10^{-20} [p \rightarrow K^+ \bar{\nu}]$
$ \lambda_{i33} \lambda_{112}^{''*} $			$10^{-21} [p \rightarrow K^+ \bar{\nu}]$
			$(\tilde{m} = 1 \text{ TeV}) (6.115)$
$ \lambda_{ijj} \lambda_{i'j'k'}^{''*} $			$(10^{-12} - 10^{-6}) [p \rightarrow \pi^+ (K^+) \bar{\nu}]$
			$(m_{h^+} = \tilde{m} = 1 \text{ TeV}) (6.116)$
$ \lambda_{ijk} \lambda_{113}'' $			$10^{-13} [p \rightarrow l^+ \nu \nu] (6.117)$
$ \lambda_{ijk} \lambda_{123}'' $			$10^{-12} [p \rightarrow l^+ \nu \nu] (6.117)$
$ \lambda_{ijk} \lambda_{212}'' $			$10^{-13} [p \rightarrow l^+ \nu \nu] (6.117)$
$ \lambda_{ijk} \lambda_{312}'' $			$10^{-12} [p \rightarrow l^+ \nu \nu] (6.117)$

Table 6.3: Quadratic coupling constant product bounds. We use the same conventions as in the preceding table.

	Lepton Flavour	Hadron Flavour	L and/or B violation
$ \lambda'_{i21}\lambda'_{i12} $		$4.5 \times 10^{-9} \tilde{\nu}_{iL}^2 [K\bar{K}]$	
$ \lambda'_{i31}\lambda'_{i22} $		$1. \times 10^{-4} [K\bar{K}] (\tilde{m} = 100 \text{ GeV})$	
$ \lambda'_{i31}\lambda'_{i32} $		$7.7 \times 10^{-4} [K\bar{K}] (\tilde{m} = 100 \text{ GeV})$	
$ \lambda'_{i2k}\lambda'_{i'1k} $		$2.11 \times 10^{-5} \tilde{d}_{kR}^2 [K^+ \rightarrow \pi^+ \nu \bar{\nu}] (6.87)$	
$ \lambda'_{ij1}\lambda'_{i'j2} $		$2.11 \times 10^{-5} \tilde{d}_{jL}^2 [K^+ \rightarrow \pi^+ \nu \bar{\nu}] (6.87)$	
$ \lambda'_{i31}\lambda'_{i13} $		$3.3 \times 10^{-8} \tilde{\nu}_{iL}^2 [B\bar{B}]$	
$ \lambda'_{i31}\lambda'_{i33} $		$1.3 \times 10^{-3} [B\bar{B}]$	
$ \lambda'_{i3k}\lambda'_{i'2k} $		$1.5 \times 10^{-3} \tilde{d}_{kR}^2 [B \rightarrow X_s \nu \bar{\nu}] (6.88)$	
$ \lambda'_{ij2}\lambda'_{i'j3} $		$1.5 \times 10^{-3} \tilde{d}_{jL}^2 [B \rightarrow X_s \nu \bar{\nu}] (6.88)$	
$ \lambda'_{2mk}\lambda'_{1mk} $	$7.6 \times 10^{-5} \tilde{d}_{kR}^2 [\mu \rightarrow e\gamma] (6.95)$		
$ \lambda'_{23k}\lambda'_{13k} $	$2.0 \times 10^{-3} [\mu \rightarrow e\gamma] (6.96)$ $(m_{\tilde{d}_{kR}} = m_{\tilde{t}_L} = 300 \text{ GeV})$		
$ \lambda'_{1j1}\lambda'_{1j2} $		$\mathcal{I} 8.1 \times 10^{-5} \tilde{u}_L^2 [K_L \rightarrow e^+ e^-] (6.77)$	
$ \lambda'_{2j1}\lambda'_{2j2} $		$\mathcal{I} 7.8 \times 10^{-6} \tilde{u}_L^2 [K_L \rightarrow \mu^+ \mu^-] (6.77)$	
$ \lambda'_{1j1}\lambda'_{2j2} $		$3 \times 10^{-7} \tilde{u}_L^2 [K_L \rightarrow e^\pm \mu^\mp] (6.78)$	
$ \lambda'_{1j2}\lambda'_{2j1} $		$3 \times 10^{-7} \tilde{u}_L^2 [K_L \rightarrow e^\pm \mu^\mp] (6.78)$	
$ \lambda'_{2j1}\lambda'_{2j3} $		$2.1 \times 10^{-3} \tilde{u}_L^2 [B_d^0 \rightarrow \mu^+ \mu^-] (6.80)$	
$ \lambda'_{1j1}\lambda'_{2j3} $		$4.7 \times 10^{-3} \tilde{u}_L^2 [B_d^0 \rightarrow e^\pm \mu^\mp] (6.80)$	
$ \lambda'_{1j3}\lambda'_{2j1} $		$4.7 \times 10^{-3} \tilde{u}_L^2 [B_d^0 \rightarrow e^\pm \mu^\mp] (6.80)$	
$ \lambda'_{2j1}\lambda'_{1j1} $	$4.3 \times 10^{-8} \tilde{u}_{jL}^2 [\mu \rightarrow e (\text{Ti})] (6.99)$		
$ \lambda'_{3j1}\lambda'_{1j1} $	$2.4 \times 10^{-3} \tilde{u}_{jL}^2 [\tau \rightarrow e\rho] (6.105)$		
$ \lambda'_{11k}\lambda'_{12k} $		$5.3 \times 10^{-3} \tilde{d}_{kR}^2 [\Lambda \rightarrow pl^- \bar{\nu}_l] (6.31)$	
$ \lambda'_{21k}\lambda'_{11k} $	$4.5 \times 10^{-8} \tilde{d}_{kR}^2 [\mu \rightarrow e (\text{Ti})] (6.99)$		
$ \lambda'_{31k}\lambda'_{11k} $	$2.4 \times 10^{-3} \tilde{d}_{kR}^2 [\tau \rightarrow e\rho] (6.105)$		

Table 6.4: Quadratic coupling constant product bounds. We use the same conventions as in the preceding table.

	Lepton Flavour	Hadron Flavour	L and/or B violation
$ \lambda'_{113}\lambda'_{131} $			$3.8 \times 10^{-8} [\beta\beta 0\nu]$ (6.107)
$ \lambda'_{112}\lambda'_{121} $			$1.1 \times 10^{-6} [\beta\beta 0\nu]$ (6.107)
$ \lambda'_{i3k}\lambda'_{i2k} $		$0.09 (\tilde{\nu}_{iL}^2, \tilde{d}_{iR}^2) [B \rightarrow K\gamma]$ (6.93)	
$ \lambda'_{ij3}\lambda'_{ij2} $		$0.035 (\tilde{e}_{iL}^2, \tilde{d}_{jL}^2) [B \rightarrow K\gamma]$ (6.93)	
$ \lambda'_{i11}\lambda'_{j11} $			$5 \times 10^{-2} \tilde{d}^2 \tilde{m}^{-1} [m_\nu < 1 \text{ eV}]$
$ \lambda'_{i12}\lambda'_{j21} $			$3 \times 10^{-3} \tilde{q}^2 \tilde{m}^{-1} [m_\nu < 1 \text{ eV}]$
$ \lambda'_{i13}\lambda'_{j31} $			$8 \times 10^{-5} \tilde{q}^2 \tilde{m}^{-1} [m_\nu < 1 \text{ eV}]$
$ \lambda'_{i22}\lambda'_{j22} $			$2 \times 10^{-4} \tilde{s}^2 \tilde{m}^{-1} [m_\nu < 1 \text{ eV}]$
$ \lambda'_{i23}\lambda'_{j32} $			$5 \times 10^{-6} \tilde{q}^2 \tilde{m}^{-1} [m_\nu < 1 \text{ eV}]$
$ \lambda'_{i33}\lambda'_{j33} $			$10^{-7} \tilde{b}^2 \tilde{m}^{-1} [m_\nu < 1 \text{ eV}]$ $(\tilde{m}_{LR}^{d2} = \tilde{m} M^d)$ (5.12)
$ \lambda'_{l1k}\lambda''_{11k} $			$(2-3) \times 10^{-27} \tilde{d}_{kR}^2 [p \rightarrow \pi^0 l^+]$ (6.110)
$ \lambda'_{31k}\lambda''_{11k} $			$7 \times 10^{-27} \tilde{d}_{kR}^2 [n \rightarrow \pi^0 \bar{\nu}]$ (6.110)
$ \lambda'_{i2k}\lambda''_{11k} $			$3 \times 10^{-27} \tilde{d}_{kR}^2 [p \rightarrow K^+ \bar{\nu}]$ (6.110)
$ \lambda'_{l1k}\lambda''_{12k} $			$(6-7) \times 10^{-27} \tilde{d}_{kR}^2 [p \rightarrow K^0 l^+]$ (6.111)
$ \lambda'_{ij1}\lambda''_{11j} $			$7 \times 10^{-26} \tilde{d}_{jL}^2 (m_{\tilde{d}_{jR}}^2 / (\tilde{m}_{LR}^{d2})_{jj})$
$ \lambda'_{ij2}\lambda''_{11j} $			$3 \times 10^{-27} \tilde{d}_{jL}^2 (m_{\tilde{d}_{jR}}^2 / (\tilde{m}_{LR}^{d2})_{jj})$
$ \lambda'_{i31}\lambda''_{123} $			$3 \times 10^{-27} \tilde{b}_L^2 (m_{\tilde{b}_R}^2 / (\tilde{m}_{LR}^{d2})_{33})$ $[n \rightarrow \pi^0 \nu, p \rightarrow K^+ \nu]$ (6.112)
$ \lambda'_{lj1}\lambda''_{j12} $			$10^{-26} \tilde{u}_{jL}^2 (m_{\tilde{u}_{jR}}^2 / (\tilde{m}_{LR}^{u2})_{jj})$ $[n \rightarrow K^+ l]$ (6.113)
$ \lambda'_{ijk}\lambda''_{i'j'k'} $			$10^{-9} [p \rightarrow X \bar{\nu} (X\nu)]$ $(\tilde{m} = 1 \text{ TeV})$ (6.114)
$ \lambda''_{232}\lambda''_{231} $		$\text{Min}[6. \times 10^{-4} \tilde{c}, 2. \times 10^{-4} \tilde{c}^2]$ $[K \bar{K}]$	
$ \lambda''_{332}\lambda''_{331} $		$\text{Min}[6. \times 10^{-4} \tilde{t}, 3. \times 10^{-4} \tilde{t}^2]$ $[K \bar{K}]$	
$ \lambda''_{i13}\lambda''_{i12} $		$6.4 \times 10^{-3} \tilde{u}_{iR}^2 [B^+ \rightarrow K^0 \pi^+]$ (6.89)	
$ \lambda''_{i23}\lambda''_{i12} $		$6 \times 10^{-5} \tilde{u}_{iR}^2 [B^- \rightarrow \phi \pi^-]$ (6.91)	
$ \lambda''_{213}\lambda''_{232} $		$\mathcal{I} 10^{-2} \tilde{q}^2 [d_n^\gamma]$ (6.58)	
$ \lambda''_{312}\lambda''_{332} $		$\mathcal{I} 10^{-1} \tilde{q}^2 [d_n^\gamma]$ (6.59)	
$ \lambda''_{i3k}\lambda''_{i2k} $		$0.16 \tilde{q}_R^2 [B \rightarrow K\gamma]$ (6.93)	

Table 6.5: Quadratic coupling constant product bounds. We use the same conventions as in the preceding table.

It appears clearly from the tables that the low energy phenomenology is a rich and valuable source of information on the \mathcal{R}_p interactions. The most robust cases include the single nucleon decay channels, neutrinoless double beta decay, double nucleon decay, the neutral K , B meson mixings and rare leptonic or semileptonic decays, the lepton number and/or flavour violating decays of leptons. The strongest single coupling constant bounds arise, in order of decreasing strength, from the baryon number violating processes of $n - \bar{n}$ oscillation and NN decay, from neutrinoless double beta decay, neutrino masses, semileptonic decays of K mesons, and from neutral current (APV) and charged current lepton universality. For the quadratic coupling constant bounds, a similar classification ordered with respect to decreasing strength, places baryon number violating processes in first position, followed by K and B meson mixing, $\mu \rightarrow e$ conversion, leptonic or semileptonic decays of K and B mesons, neutrinoless double beta decay, three-body lepton decays, and neutrino masses.

The consideration of the loop level contributions is a very effective way to deduce complementary bounds on coupling constants involving the heavier generations of quarks and leptons. For instance, the single nucleon stability bounds $|\lambda'_{ijk}\lambda''_{j'k'}| < \mathcal{O}(10^{-9})$, which are valid for all the generation indices, have far-reaching implications. Should a single lepton number violating coupling constant λ'_{ijk} be sizeable, then one would conclude a strong suppression of the full set of baryon number violating $\lambda''_{j'k'}$ coupling constants. An analogous converse statement would hold for all the λ'_{ijk} if a single $\lambda''_{j'k'}$ were sizeable.

6.5.2 Observations on the Bound Robustness and Validity

Before discussing the impact on supersymmetric model building of the indirect bounds, we start with some general preliminary observations aimed at appreciating their potential usefulness.

6.5.2 a) Natural Order of Magnitude for \mathcal{R}_p Couplings

First, it is important to ask what might be considered as natural values for the dimensionless R -parity violating trilinear interactions coupling constants. (For convenience, we shall denote these collectively as $\hat{\lambda}_{ijk}$.) In the absence of any symmetry, the anticipated natural values are $\mathcal{O}(1)$ or $\mathcal{O}(g)$. If one assumed instead a hierarchical structure with respect to the quarks and leptons generations, analogous to that exhibited by the regular R -parity conserving Yukawa interactions, an educated guess could be, for instance, $\hat{\lambda}_{ijk} = \mathcal{O}((m_i m_j m_k / v^3)^{1/3})$, where m_j denote the q, l masses. A variety of alternative forms for the generation dependence are suggested by considerations based on the physics of discrete symmetries or grand unified and string theories. Just on the basis of the existing experimental constraints, one can check that the individual coupling constant bounds, as given in Table 6.1 fall in an interval of values $\mathcal{O}(10^{-1}) - \mathcal{O}(10^{-2})$ which interpolates between the above two extreme estimates.

6.5.2 b) Impact of the SUSY Masses on the Bounds

A second observation concerns the dependence of the indirect bounds with respect to the superpartner mass parameters. Our reference value for the supersymmetry breaking mass parameter is set uniformly at $\tilde{m} = 100$ GeV, apart from a very few exceptions. The tree level mechanisms have, of course, a transparent dependence on the superpartners masses, such that the single or quadratic coupling constant bounds scale linearly or quadratically with \tilde{m} . Several tree level dominated observables involve a single superpartner species, which then allows us to identify the relevant sfermion by indicating explicitly its particle name. The bounds associated with one-loop effects have, in general, a weaker mass dependence over the mass interval,

$\tilde{m} = 100 - 500$ GeV. With increasing values of the superpartner masses, both the tree and loop level bounds gradually get weaker. In fact, if the supersymmetry breaking mass scale happened to reach the $\mathcal{O}(1)$ TeV extrem limit for the Standard Model naturalness, a large number of the existing individual indirect bounds would become useless. For the so-called "More Minimal Supersymmetric Standard Model" [420] where the third generation squarks or sleptons constitute the lightest scalar superpartners and the first and second generation sfermion masses are raised up to the TeV scale, one would be led to strongly weakened bounds for the first two generations of sfermions. Several quadratic bounds would still remain of interest, especially those associated with a simultaneous B and L number violation, due to the extreme severity of the nucleon stability bounds.

There are two other important exceptions to the suppression effect of the bounds from large sfermions masses. The first concerns the process independent bounds derived from the renormalisation group considerations, as was discussed in chapter 3. Because the perturbative unitarity or quasi-fixed points bounds originate from indirect effects associated with the resummation of large logarithms, they are practically insensitive to the value of the supersymmetry breaking scale as long as this does not extend beyond the TeV decade. The second exception concerns the class of observables governed by dimension nine operators, such as the amplitudes for the $\beta\beta_{0\nu}$ or $n - \bar{n}$ processes, where several contributions from different intermediate states, associated with sfermions and gauginos, compete with one another. The destructive interference of these contributions renders the inferred bounds sensitive to the supersymmetry breaking mass spectrum as a whole.

6.5.2 c) Validity of the Assumption of one or two Dominant Couplings

A third observation concerns the validity of the single or double coupling constant dominance hypotheses. When applied to the \mathcal{R}_p interactions, the dominance hypotheses rest on the premise that some hierarchy exists either between the B and L number violations or between the different quark and lepton generations. The conclusions from certain studies might be altered if the dominance hypotheses were not justified or if certain unexpected finely tuned cancellations were at work. One could imagine, for example, that a subset of the coupling constants exhibited generational degeneracies that would induce cancellations between the contributions of different component interactions part of the predominant subset. An indirect evidence for a possible correlation between different coupling constants is furnished by the observation that the strongest constraints arise for quadratic products rather than the individual coupling constant bounds. This is clearly not surprising since the latter entail less demanding model-dependent assumptions.

An examination of Table 6.1 reveals that a few amongst the charge current and neutral current single coupling constant bounds are immune to invalidating cancellation effects. Examples of robust bounds comprise for the charged current interactions, those deduced from the renormalised observable parameters G_μ and M_W , and for the neutral current interactions, those deduced from the forward-backward asymmetry parameter A_{FB} , and the auxiliary parameter, $C_2(d)$. Partly responsible for this state of affairs is the use of ratios of rates or branching fractions. While the comparison with experimental data for such ratios removes the dependence on some poorly known hadronic matrix elements parameters, this has the drawback of introducing cancelling contributions. As a result, these ratios obtain corrections from different \mathcal{R}_p interactions which often combine together destructively, with opposite signs. The quadratic coupling constant bounds are exposed to a much lesser extent to cancellations since they are often derived for observables where the contributions from different sets of coupling constants add up incoherently.

6.5.2 d) Bound Robustness in Regards to Model Dependence

As a final remark we should emphasise that not all coupling constant bounds are to be treated indiscriminately. One must exercise a critical eye on the model-dependent assumptions. It is important to keep track of the superpartner generation index in light of the possibility of a large splitting between the sfermion generations. The generational structure of the sfermion chirality-flip mass matrices \tilde{m}_{LR}^2 is a crucial input for the one-loop contributions to the neutrinos Majorana masses or the $n - \bar{n}$ oscillation amplitude. Deviations from a generation universality yield large off-diagonal contributions $(\tilde{m}_{LR}^2)_{ij}$ which could modify the ensuing predictions.

6.5.3 Phenomenological Implications of Bounds

What implications on theoretical models beyond the Standard Model can be drawn from the existing bounds? As discussed in chapitre 3, works have been done on model building using renormalization group equations (RGE) to get bounds at the M_{GUT} scale [95]. One might ask whether the results hint at any of the known alternatives, especially the gauged horizontal continuous or discrete symmetries. The existence of some correlations with the flavour symmetries is clearly suggested. Indeed, it is generally the case that the coupling constants in the first and second generations are more constrained, although this might just reflect the lack of direct experimental data for the heavy flavoured hadrons or leptons. The fact that the strongest bounds are for products $\lambda'\lambda''$ and $\lambda\lambda''$ hints at an incompatibility between simultaneous B and L number violations. Separate B or L number violation, as described by interactions governed by the coupling constant products $\lambda\lambda$, $\lambda\lambda'$, $\lambda'\lambda'$ or $\lambda''\lambda''$, may also be disfavoured but in a way which depends on flavour, the first and second generations being those most strongly constrained. Ready solutions to prevent a coexistence of B and L number non-conservation are offered by the B and L parities or the corresponding generalised discrete symmetries versions.

The existence of a strong hierarchical structure in the \mathcal{R}_p coupling constants does not exclude the presence of certain unexpected degeneracies with respect to the quarks and leptons generations, as would be implied by the presence of unbroken discrete symmetries. To establish this possibility one would need global studies of the \mathcal{R}_p interactions effects encompassing a large body of experimental data. One way to infer robust bounds in cases where one suspects cancellation effects to be at work, is by choosing suitable observables which depend selectively on fixed products of the coupling constants. Such an example was encountered with the \mathcal{R}_p induced contributions to the non $V - A$ charged current interactions (see section 6.3.1). Another attractive idea would be to fit a selected subset of the \mathcal{R}_p interactions coupling constants to a correspondingly selected subset of experimental constraints. While global studies along these lines are routinely performed in the context of the contact interactions physics [286] or the mirror fermions physics [421] their application to the \mathcal{R}_p physics appears problematical in view of the proliferation of the coupling constants. Interesting partially global studies of the \mathcal{R}_p interactions have been recently reported in the literature regarding fits to the APV observables [422] or the Z boson partial decay width observables [289]. The recent accumulated experimental information on the neutrino oscillations has also allowed to implement in part such a program by envisaging global fits to the data for the neutrino Majorana masses based on the \mathcal{R}_p contributions. Even if these studies must appeal to some assistance from theory, through certain specialised assumptions on the generational structure of the sfermion mass parameters, they have yielded a wealth of useful, although model-dependent, information on the \mathcal{R}_p interactions. Of course, one should keep in mind the alternative options to explain the neutrino physics experimental data, which include in fact the \mathcal{R}_p mechanism of flavour changing neutral current neutrino interactions with quarkonic and leptonic matter.

The model-independent studies devoted to the four fermions contact interactions may be of some use in establishing the existence of possible cancellation effects amongst different \mathcal{R}_p interactions. Special attention, motivated by searches of compositeness [423, 424, 425], has been devoted in recent years to the flavour diagonal contact interactions. Along with the low energy neutral and charged current interactions (neutrino or (polarised) electron elastic and inelastic scattering data) the current fits [286, 426] include the high energy data for the Drell-Yan dilepton production and large p_T jet production at the Fermilab Tevatron collider, the dijet production (e.g., $e^-e^+ \rightarrow s\bar{s}$) at the CERN LEP collider, and the deep inelastic electron and positron scattering at the HERA collider at DESY. Based on the initial studies [423], one generally restricts the consideration to the dominant $\mathcal{D} = 6$ Lorentz vector interactions, using an effective Lagrangian of the general form,

$$\mathcal{L}_{NC} = \sum_{[(i,j)=(L,R);q=(u,d)]} \frac{4\pi\eta_{ij}^q}{\Lambda_{ij}^{q^2}} \bar{e}_i \gamma_\mu e_i \bar{q}_j \gamma_\mu q_j, \quad (6.132)$$

where a sum over the fermions flavour and chirality is understood and $\eta^q = \pm 1$ stand for a sign phase. One may express the relationship between the different scale parameters, denoted generically by Λ , and the \mathcal{R}_p interactions coupling constants by the order of magnitude relation, $\hat{\lambda}^2/\tilde{m}^2 \approx 4\pi/\Lambda^2$. More quantitatively, an identification with the neutral current interactions, for instance, yields [427],

$$C_1(q) = \frac{\sqrt{2}\pi}{G_F} \left(\frac{\eta_{RL}^q}{\Lambda_{RL}^{q^2}} - \frac{\eta_{LL}^q}{\Lambda_{LL}^{q^2}} - \frac{\eta_{LR}^q}{\Lambda_{LR}^{q^2}} + \frac{\eta_{RR}^q}{\Lambda_{RR}^{q^2}} \right).$$

An important observation here is that the high energy collider experimental data favour low values of the energy scales. Some currently quoted experimental bounds are, $\Lambda_{[LR,RL]}^{[-,+d]} > [1.4, 1.6]$ TeV, from the dijet production data [428], $\Lambda_{[LR,RL]}^{[+,+u]} > [2.5, 2.5]$ TeV from the Drell-Yan production data [429] and $\Lambda \approx 1$ TeV from the anomalous deep inelastic scattering events data [277, 430, 431]. In contrast to these results, it appears that the low energy experimental data consistently favours larger values of the energy scales. This is most explicit in the Cesium atom APV data, where assuming that no cancellations occur between the different terms in $C_1(q)$, leads to the strong bound, $\Lambda > 10$ TeV. More quantitatively, the simultaneous fits of the flavour diagonal $eeqq$ contact interactions to both low and high energy experimental data, as completed by incorporation of the HERA high Q^2 data [286], infer large values of the scale parameters with a non-trivial trend of relative signs between the different interactions. Quoting from [286] one finds the fitted values:

$$\Lambda_{LL}^{-eu} = 12.4 \begin{pmatrix} +50.6 \\ -34.8 \end{pmatrix} \text{ TeV}, \quad \Lambda_{LR}^{+eu} = 3.82 \begin{pmatrix} +0.93 \\ -1.62 \end{pmatrix} \text{ TeV}, \quad \Lambda_{RL}^{+eu} = 5.75 \begin{pmatrix} +5.06 \\ -6.88 \end{pmatrix} \text{ TeV}.$$

These quantitative analyses indicate that cancellation effects are taking place at low energies between the contributions from different interactions. Such cancellations would clearly pass unnoticed within analyses based on a single coupling constant dominance hypothesis. Tentative explanations have been sought in terms of a short distance parity conserving interaction [427], implying the relations $\frac{\eta_{iL}^q}{(\Lambda_{iL}^q)^2} = -\frac{\eta_{iR}^q}{(\Lambda_{iR}^q)^2}$, or an extended global flavour symmetry group [432]. Applied to the \mathcal{R}_p interactions, the implications would be in the existence of degeneracies amongst the subset of relevant \mathcal{R}_p coupling constants.

The Lorentz vector component of the charged current (CC) electron-quark four fermions contact interactions appears also to lead to similar conclusions. The fits to the leptonic or

hadronic colliders data based on the conventional parametrisation of the effective Lagrangian,

$$\mathcal{L}_{CC} = \frac{4\pi\eta}{\Lambda_{CC}^2} \bar{e}_L \gamma_\mu \nu_L \bar{u}_L \gamma_\mu d'_L$$

yield the typical bounds, $\Lambda_{CC}^- > 1.5$ TeV. The recent deep inelastic scattering events observed at HERA also favour low scales, $\Lambda_{CC} = (0.8 - 1)$ TeV [277, 431]. By contrast, the fits to the low energy experimental data associated with the leptons universality or for meson decays favour larger scales [431], $\Lambda_{CC} \approx (10. - 30.)$ TeV. A recent study of the non $V - A$ charged current interactions, based on the high precision measurements of the muon decay rate differential distributions, also predicts strong bounds for the scales [433], $\Lambda_{CC}^{\pm ll} > [7.5, 10.2]$ TeV, for the four lepton interactions and $\Lambda_{CC}^{\pm lq} > [5.8, 10.1]$ TeV for the two lepton two quark interactions.

Chapter 7

PHENOMENOLOGY AND SEARCHES AT COLLIDERS

7.1 Introduction

The search for \mathcal{R}_p supersymmetry processes has been a major analysis activity at high energy colliders over the past decade, and is likely to remain so at existing and future colliders unless the idea of supersymmetry itself somehow becomes falsified.

We have seen in chapters 1 and 2 that on the theory side, \mathcal{R}_p is (and will) remain a central issue since gauge invariance and renormalizability do not ensure lepton- and baryon-number conservation in supersymmetric extensions of the Standard Model. A consequence is that a general superpotential allows for trilinear terms corresponding to \mathcal{R}_p fermion-fermion-sfermion interactions involving λ , λ' or λ'' Yukawa couplings. It moreover possibly allows for additional *explicit* (bilinear) or *spontaneous* sources of lepton-number violation.

The presence of \mathcal{R}_p interactions could have important consequences on the phenomenology relevant for supersymmetry searches at high energy colliders. This is because \mathcal{R}_p entails a fundamental instability of supersymmetric matter, thus opening up new decay channels for sparticles. Especially crucial in this respect will be the fate of the lightest supersymmetric particle (LSP). Even for relatively weak \mathcal{R}_p interaction strengths, the decay of the LSP will lead to event topologies departing considerably from the characteristic "missing momentum" signal of R_p conserving theories. But \mathcal{R}_p could be more than a mere observational complication. It could also enlarge the discovery reach for supersymmetry itself as it allows for the creation or exchange of single sparticles.

In this chapter, essential ingredients of the phenomenology and search strategies for \mathcal{R}_p physics at colliders are presented. Extensive references to related detailed studies for specific supersymmetry models are provided. Existing experimental constraints established at LEP e^+e^- , HERA ep and Tevatron $p\bar{p}$ colliders are reviewed and discovery prospects in future collider experiments are discussed. The analyses and prospective studies in the literature have generally been carried in the context of a given existing or future collider project. The Table 7.1 gives a list of the machine parameters considered in the studies reviewed in this chapter.

Collider	Beams	\sqrt{s}	$\int \mathcal{L} dt$	Years
LEP 1	e^+e^-	M_Z	$\sim 160 \text{ pb}^{-1} \otimes 4$	1989-95
LEP 2	e^+e^-	$> 2 \times M_W$	$\sim 620 \text{ pb}^{-1} \otimes 4$	1996-00
HERA Ia	e^-p	300 GeV	$\mathcal{O}(1 \text{ pb}^{-1}) \otimes 2$	1992-93
HERA Ib	$e^\pm p$	$\lesssim 320 \text{ GeV}$	$\mathcal{O}(100 \text{ pb}^{-1}) \otimes 2$	1994-00
Tevatron Run Ia	$p\bar{p}$	1.8 TeV	$\mathcal{O}(10 \text{ pb}^{-1})$	1987-89
Tevatron Run Ib	$p\bar{p}$	1.8 TeV	$\mathcal{O}(100 \text{ pb}^{-1}) \otimes 2$	1992-96
HERA II	$e_{L,R}^\pm p$	$\sim 320 \text{ GeV}$	$\sim 1 \text{ fb}^{-1} \otimes 2$	≥ 2002
Tevatron Run II	$p\bar{p}$	$\sim 2.0 \text{ TeV}$	$1 - 10 \text{ fb}^{-1} \otimes 2$	≥ 2002
LHC	pp	14.0 TeV	$10 - 100 \text{ fb}^{-1} \otimes 2$	$\gtrsim 2007$
Future LC	e^+e^-	$\sim 0.5 - 1.0 \text{ TeV}$	50 fb^{-1}	... NLC [434]
		$\sim 0.5 - 1.0 \text{ TeV}$	500 fb^{-1}	... TESLA [435]
Future μC	$\mu^+\mu^-$	$\sim 0.35 - 0.5 \text{ TeV}$	10 fb^{-1}	... FMC [436]
		$\sim 1.0 - 3.0 \text{ TeV}$	1000 fb^{-1}	... NMC [436]

Table 7.1: Main contemporary and future collider facilities which are considered in the search analyses and prospective studies described in this chapter. The facilities are listed together with the nature of the colliding beams, the available centre-of-mass energies \sqrt{s} , and the integrated luminosities $\int \mathcal{L} dt$ accumulated (or the range of $\int \mathcal{L} dt$ expected) per experiment. The multiplicative factors after the \otimes sign denotes the number of multi-purpose collider experiments operating (or expected to be operating) simultaneously around each collider.

7.2 Interaction Strength and Search Strategies

The way supersymmetry could become manifest at colliders crucially depends both on the structure and parameters of the model followed by Nature and on the a priori unknown magnitudes (individual and relative) of the new \mathcal{R}_p couplings. The weakest \mathcal{R}_p coupling values are likely to be felt mostly through the decay of sparticles otherwise pair produced via gauge couplings. The strongest \mathcal{R}_p coupling values could contribute to direct or indirect single sparticle production. The best search strategy at a given collider will ultimately depend on the specific signal and background environment.

In the absence of definite theoretical predictions for the values of the 45 independent trilinear Yukawa couplings Λ (λ_{ijk} , λ'_{ijk} and λ''_{ijk}), and facing the formidable task of testing $2^{45} - 1$ possible non-vanishing coupling combinations, it is necessary in practice to assume a strong hierarchy among the couplings. For the "hierarchy" between different types of couplings this is an arbitrary choice since λ , λ' and λ'' appear fundamentally independent. Empirically, it can be partially justified by the fact that indirect bounds are particularly stringent on non-vanishing coupling products involving a \mathcal{L} and a \mathcal{B} coupling as was seen in section 6.4.4. For example, the lower limit on the proton lifetime translates [406] into very stringent bounds on the $\lambda' \times \lambda'' < \mathcal{O}(10^{-9})$ applicable to all possible flavour combinations. Restrictions on combinations of couplings of a given type can be legitimized by analogy with the strong hierarchy of the Higgs Yukawa couplings structure in the Standard Model [255, 261]. It may also be empirically justified by the fact that indirect bounds (chapter 6) are generally more stringent on the product of two different couplings than on the square of individual λ , λ' or λ'' couplings.

Thus, a reasonable simplifying assumption for the search strategy at colliders is to postulate the existence of a single (dominant) \mathcal{R}_p coupling. Most of the prospective studies on \mathcal{R}_p and

actual search analyses at colliders rely on this assumption, i.e. that only one \mathcal{R}_p coupling exists which can connect sleptons or squarks to ordinary fermions. By doing so, it is in addition assumed implicitly or explicitly (through some mixing angles [255] connecting the squark current and mass basis) that flavour mixing relating various couplings (see section 2.1.4) is suppressed.

Having chosen (somehow) a single dominant coupling Λ , the next question is that of the range of coupling values relevant for collider physics. As to what concerns lower bounds, cosmology considerations do not provide much help. As discussed in section 4.1.1, a lightest supersymmetric particle (LSP) can no more be considered as a cold dark matter candidate in presence of a single non-vanishing \mathcal{R}_p Yukawa coupling with values even as small as $\mathcal{O}(10^{-20})$. Strengthened lower bounds of $[\lambda, \lambda', \lambda''] > \mathcal{O}(10^{-12})$ are obtained from the argument (section 4.1.1) that an unstable LSP ought to decay fast enough in order not to disrupt nucleosynthesis. But even these still lie many orders of magnitude below the sensitivity reach of collider experiments. For Λ coupling values below $\mathcal{O}(10^{-8} - 10^{-6})$ (depending in detail on model parameters), the lifetime of the LSP is so large that it is likely to completely escape detection in a typical $\mathcal{O}(10)$ m diameter collider experiment. An immediate consequence is that for a wide range of coupling values, the phenomenology at colliders would appear indistinguishable from that of \mathcal{R}_p conserving theories. Only a discovery that the LSP turns out to be coloured or charged, a fact forbidden by cosmological constraints for a stable LSP, could be an indirect hint of the existence of \mathcal{R}_p interactions beyond the collider realm. Otherwise, there exist no known direct observational tests for such *very long-lived* LSPs [259]. This inaccessible coupling range will not be discussed further in this chapter.

In case a non-vanishing \mathcal{R}_p coupling does exist with a magnitude leading to distinct phenomenology at colliders, the optimal search strategy will then depend on the absolute coupling value and the relative strength of the \mathcal{R}_p and gauge interactions, as well of course on the nature of the supersymmetric model considered (sparticle spectrum and parameter space depending on the supersymmetry breaking mechanism, etc.). Sparticle direct and indirect \mathcal{R}_p decay topologies will be discussed on general grounds in section 7.3. Anticipating this discussion, a direct sensitivity to a *long-lived* LSP might be provided by the observation of displaced vertices in an intermediate range of coupling values up to $\mathcal{O}(10^{-5} - 10^{-4})$.

For even larger Λ values, the presence of \mathcal{R}_p supersymmetry could become trivially manifest through the decay of *short-lived* sparticles pair produced via gauge couplings. A possible search strategy in such cases consists of neglecting \mathcal{R}_p contributions at production (in non-resonant processes). This is valid provided that the \mathcal{R}_p interaction strength remains sufficiently small compared to electromagnetic or weak interaction strengths, i.e. for Λ values typically below $\mathcal{O}(10^{-2} - 10^{-1})$. Such a strategy has been thoroughly explored at existing colliders to study how the experimental constraints on basic model parameters in specific supersymmetry models be affected by the presence of \mathcal{R}_p interactions. This and the question of whether and how different types of couplings could be distinguished at colliders in such a scenario will be discussed in section 7.4.

In a similar range of (or for larger) coupling values, \mathcal{R}_p could manifest itself most strikingly at colliders via single resonant or non-resonant production of supersymmetric particles. Single sparticle production involving \mathcal{R}_p couplings and how it allows the extension of the discovery mass reach for supersymmetric matter at a given collider is discussed in section 7.5.

Coupling values corresponding to interactions stronger than the electromagnetic interaction might still be allowed for sufficiently large masses. For masses beyond the kinematic reach of a given collider, \mathcal{R}_p could contribute to observable processes through virtual sparticle exchange. This is discussed in section 7.6.

Realistic search strategies at colliders must take into account the upper bounds on the Λ couplings derived from indirect processes. As was seen in chapter 6, these bounds all become weaker with increasing scalar masses but each possibly with a specific functional mass-dependence and each depending on a specific type of scalar [259].

Ultimately, the question of whether or not a given \mathcal{R}_p process is truly allowed by existing constraints must be answered at each point of the parameter space of a given supersymmetry model. A review of the huge number of publications dealing with specific aspects of \mathcal{R}_p in specific supersymmetry models would clearly be beyond the scope of this chapter. In the following, essential aspects of the phenomenology will be discussed and references to detailed studies provided.

7.3 Decay of Sparticles Involving \mathcal{R}_p Couplings

In the scenario with \mathcal{R}_p due to the trilinear terms, the supersymmetric particles are allowed to decay into standard particles through one \mathcal{R}_p coupling. For sparticles other than the LSP, these \mathcal{R}_p -decays will in general compete with "cascade decays" initiated by standard gauge couplings. The review of possibly allowed direct and cascade \mathcal{R}_p -decays for sfermions and gauginos-higgsinos is presented in this section. This will later on allow us to easily characterize the essential event topologies expected in \mathcal{R}_p -SUSY searches. Direct decays are discussed in subsections 7.3.1 and 7.3.2. Indirect cascade decays are discussed in subsection 7.3.3. For completeness, decays involving bilinear interactions are discussed in 7.3.4.

7.3.1 Direct \mathcal{R}_p Decays of Sfermions

The $LL\bar{E}$, $LQ\bar{D}$, or $\bar{U}\bar{D}\bar{D}$ couplings allow for a \mathcal{R}_p direct decay into two standard fermions of, respectively, sleptons, sleptons and squarks, or squarks. The allowed decays become evident when considering the Lagrangian for the trilinear Yukawa interactions written in expended notations in Eq. (2.7) to Eq. (2.9) and discussed in more details in Appendix B. For convenience the corresponding list of decay channels is given in Table 7.2. The \mathcal{R}_p decay of a sfermion of a particular family will be possible only for specific indices i, j, k of the relevant Yukawa coupling.

The partial widths of $\tilde{\nu}_i$'s when decaying via $\lambda_{ijk}LL\bar{E}$ or $\lambda'_{ijk}LQ\bar{D}$ are given (neglecting lepton and quark masses) by [437]:

$$\Gamma(\tilde{\nu}_i \rightarrow \ell_j^+ \ell_k^-) = \frac{1}{16\pi} \lambda_{ijk}^2 m_{\tilde{\nu}_i}, \quad (7.1)$$

$$\Gamma(\tilde{\nu}_i \rightarrow \bar{d}_j d_k) = \frac{3}{16\pi} \lambda'_{ijk}{}^2 m_{\tilde{\nu}_i}, \quad (7.2)$$

where the factor 3 between relations 7.1 and 7.2 is a colour factor. For sneutrinos undergoing direct decays, the mean decay length L in centimetres can then be numerically estimated from:

$$L(\text{cm}) = 10^{-12} (\beta\gamma) \left(\frac{1\text{GeV}}{m_{\tilde{\nu}_i}} \right) \frac{1}{\lambda_{ijk}^2, 3\lambda'_{ijk}{}^2}. \quad (7.3)$$

Supersymmetric particles	Couplings		
	λ_{ijk}	λ'_{ijk}	λ''_{ijk}
$\tilde{\nu}_{i,L}$	$\ell_{j,L}^+ \ell_{k,R}^-$	$d_{j,L} d_{k,R}$	
$\tilde{\ell}_{i,L}$	$\bar{\nu}_{j,L} \ell_{k,R}^-$	$\bar{u}_{j,L} d_{k,R}$	
$\tilde{\nu}_{j,L}$	$\ell_{i,L}^+ \ell_{k,R}^-$		
$\tilde{\ell}_{j,L}$	$\bar{\nu}_{i,L} \ell_{k,R}^-$		
$\tilde{\ell}_{k,R}$	$\nu_{i,L} \ell_{j,L}^-, \ell_{i,L}^- \nu_{j,L}$		
$\tilde{u}_{i,R}$			$d_{j,R} d_{k,R}$
$\tilde{u}_{j,L}$		$\ell_{i,L}^+ d_{k,R}$	
$\tilde{d}_{j,L}$		$\bar{\nu}_{i,L} d_{k,R}$	
$\tilde{d}_{j,R}$			$\bar{u}_{i,R} \bar{d}_{k,R}$
$\tilde{d}_{k,R}$		$\nu_{i,L} d_{j,L}, \ell_{i,L}^- u_{j,L}$	$\bar{u}_{i,R} \bar{d}_{j,R}$

Table 7.2: Direct decays of sleptons and squarks via trilinear \mathcal{R}_p operators $\lambda_{ijk} L_i L_j \bar{E}_k$, $\lambda'_{ijk} L_i Q_j \bar{D}_k$ and $\lambda''_{ijk} \bar{U}_i \bar{D}_j \bar{D}_k$.

Similar formulae hold for charged sleptons in absence of mixing.

In the case of squarks or sleptons of the third generation, a possible mixing between supersymmetric partners of left- and right-handed fermions has to be taken into account. For instance, the width of the lightest stop \tilde{t}_1 writes [438]:

$$\Gamma(\tilde{t}_1 \rightarrow \ell_i^+ d_k) = \frac{1}{16\pi} \lambda'_{ijk}{}^2 \cos^2(\theta_t) m_{\tilde{t}_1}, \quad (7.4)$$

where θ_t is the mixing angle of top squarks. The case of the stop is somewhat special. The typical decay time of a 100 GeV stop via a \mathcal{R}_p decay mode is roughly 3×10^{-23} s for a coupling value of 10^{-1} , and 3×10^{-21} s for a coupling value of 10^{-2} . So the stop \mathcal{R}_p decay time is of the same order or even greater than its hadronization time which from the strong interaction is $\mathcal{O}(10^{-23})$ s. Thus, the stop may hadronize before it decays.

7.3.2 Direct \mathcal{R}_p Decays of Gauginos-Higgsinos

In a direct \mathcal{R}_p decay, the neutralino (chargino) decays into a fermion and a virtual sfermion with this virtual sfermion subsequently decaying to standard fermions via a \mathcal{R}_p coupling. Thus, direct \mathcal{R}_p decays of gauginos-higgsinos are characterized by three fermions in the final state with the fermion type depending on the dominant coupling. The possible decays are listed in Table. 7.3. The corresponding diagrams are shown for the $L_i L_j E_k^c$ interactions in Figs. 7.1 and 7.2.

A collection of general expressions for three-body decays and matrix elements entering in the calculation of partial widths can be found in appendix C. In the case of a pure photino neutralino decaying with λ_{ijk} , the expression for the partial width simplifies [34] to

$$\Gamma = \lambda_{ijk}{}^2 \frac{\alpha}{128\pi^2} \frac{m_{\tilde{\chi}_1^0}^5}{m_{\tilde{f}}^4} \quad (7.5)$$

with $m_{\tilde{f}}$ the mass of the virtual slepton in the decay. Further details can be found in Ref. [439].

Supersymmetric particles	Couplings		
	λ_{ijk}	λ'_{ijk}	λ''_{ijk}
$\tilde{\chi}^0$	$\ell_i^+ \bar{\nu}_j \ell_k^-, \ell_i^- \nu_j \ell_k^+, \bar{\nu}_i \ell_j^+ \ell_k^-, \nu_i \ell_j^- \ell_k^+$	$\ell_i^+ \bar{u}_j d_k, \ell_i^- u_j \bar{d}_k, \bar{\nu}_i \bar{d}_j d_k, \nu_i d_j \bar{d}_k$	$\bar{u}_i d_j d_k, u_i d_j \bar{d}_k$
$\tilde{\chi}^+$	$\ell_i^+ \ell_j^+ \ell_k^-, \ell_i^+ \bar{\nu}_j \nu_k, \bar{\nu}_i \ell_j^+ \nu_k, \nu_i \nu_j \ell_k^+$	$\ell_i^+ \bar{d}_j d_k, \ell_i^+ \bar{u}_j u_k, \bar{\nu}_i \bar{d}_j u_k, \nu_i u_j \bar{d}_k$	$u_i d_j u_k, u_i u_j \bar{d}_k, \bar{d}_i \bar{d}_j \bar{d}_k$

Table 7.3: Direct decays of neutralinos and charginos with trilinear \mathcal{R}_p operators $\lambda_{ijk} L_i L_j \bar{E}_k$, $\lambda'_{ijk} L_i Q_j \bar{D}_k$ and $\lambda''_{ijk} \bar{U}_i \bar{D}_j \bar{D}_k$.

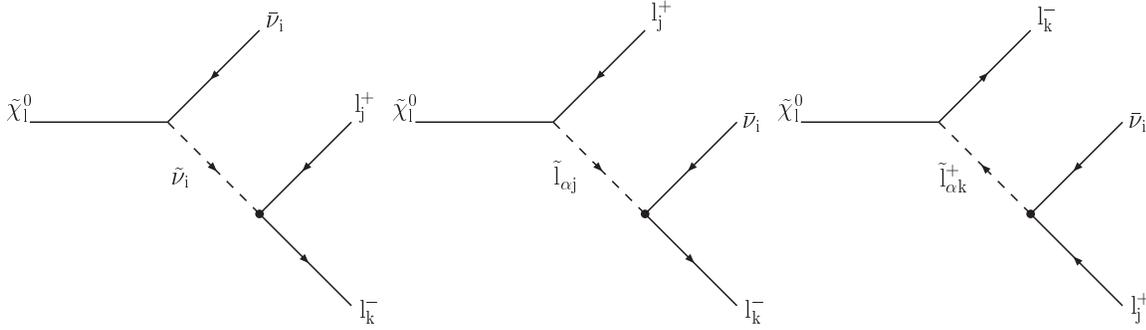


Figure 7.1: Diagrams for the direct decays of the neutralino $\tilde{\chi}_l^0$ via the coupling λ_{ijk} of the \mathcal{R}_p trilinear $L_i L_j E_k^c$ interaction. The index $l = 1 \dots 4$ determines the mass eigenstate of the neutralino. The indices $i, j, k = 1, 2, 3$ correspond to the generation. Gauge invariance forbids $i = j$. The index $\alpha = 1, 2$ gives the slepton mass eigenstate (i.e. the chirality of the SM lepton partner in absence of mixing).

In practice, the LSP lifetime is a crucial observable when discussing the final state topology to be expected for supersymmetric events. The experimental sensitivity of collider experiments is often optimal if the LSP has a negligible lifetime so that the production and decay vertices coincide. Otherwise the LSP decay vertex is displaced. If the lifetime is sufficiently large, the LSP decays may occur outside the detector, giving rise to final states characteristic of R_p conserving models.

The mean decay length L in centimetres for the lightest neutralino can be numerically estimated [255] from:

$$L(\text{cm}) = 0.3(\beta\gamma) \left(\frac{m_{\tilde{f}}}{100 \text{ GeV}} \right)^4 \left(\frac{1 \text{ GeV}}{m_{\tilde{\chi}_1^0}} \right)^5 \left[\frac{1}{\lambda_{ijk}^2}, \frac{3}{\lambda'_{ijk}{}^2}, \frac{3}{\lambda''_{ijk}{}^2} \right]. \quad (7.6)$$

Figure 7.3 illustrates the behaviour of the LSP lifetime as presented in M_2 versus μ planes for different values of $\tan \beta$ and m_0 , and considering a dominant λ_{133} coupling. A translation in terms of L as a function of $m_{\tilde{\chi}_1^0}$ for a fixed $m_{\tilde{f}}$ is shown in Fig. 7.4. Measurements of \mathcal{R}_p coupling values can be performed through displaced vertex associated to the \mathcal{R}_p decay of the LSP.

The sensitivities on the \mathcal{R}_p couplings obtained via a displaced vertex depend of course on the specific detector geometry and performances. Let us estimate the largest values of the \mathcal{R}_p coupling constants that can be measured via the displaced vertex analysis. The LSP is assumed

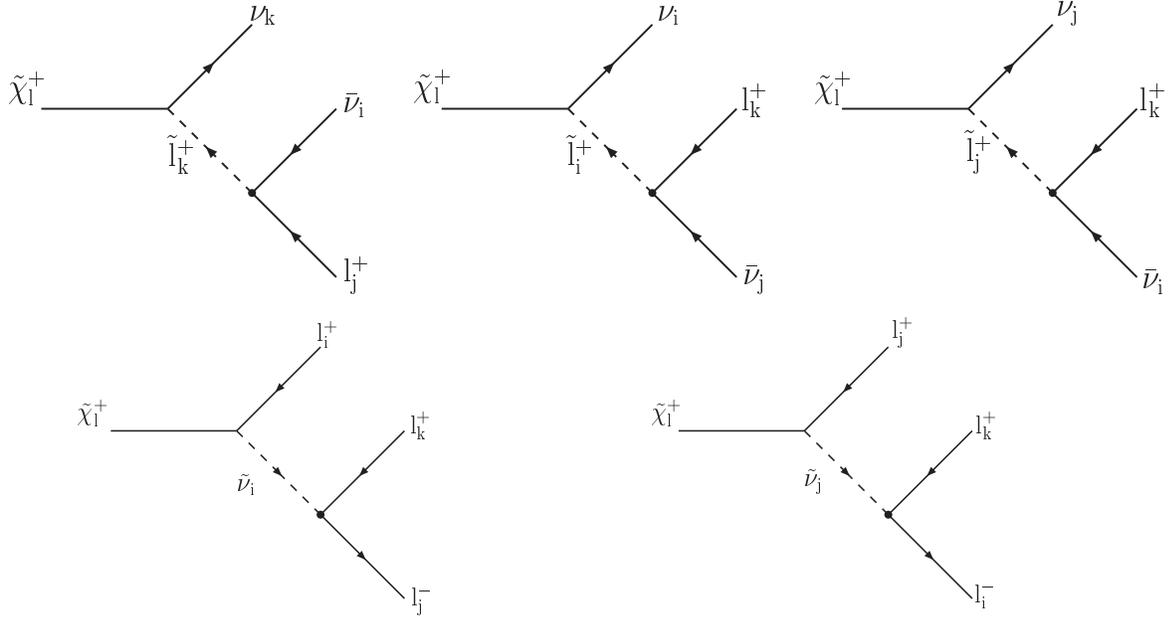


Figure 7.2: Diagrams for the direct decays of the chargino $\tilde{\chi}_l^+$ via the coupling λ_{ijk} of the R_p trilinear $L_i L_j E_k^c$ interaction. The index $l = 1 \dots 4$ determines the mass eigenstate of the neutralino. The indices $i, j, k = 1, 2, 3$ correspond to the generation. Gauge invariance forbids $i = j$. The index $\alpha = 1, 2$ gives the slepton mass eigenstate (i.e. the chirality of the SM lepton partner in absence of mixing).

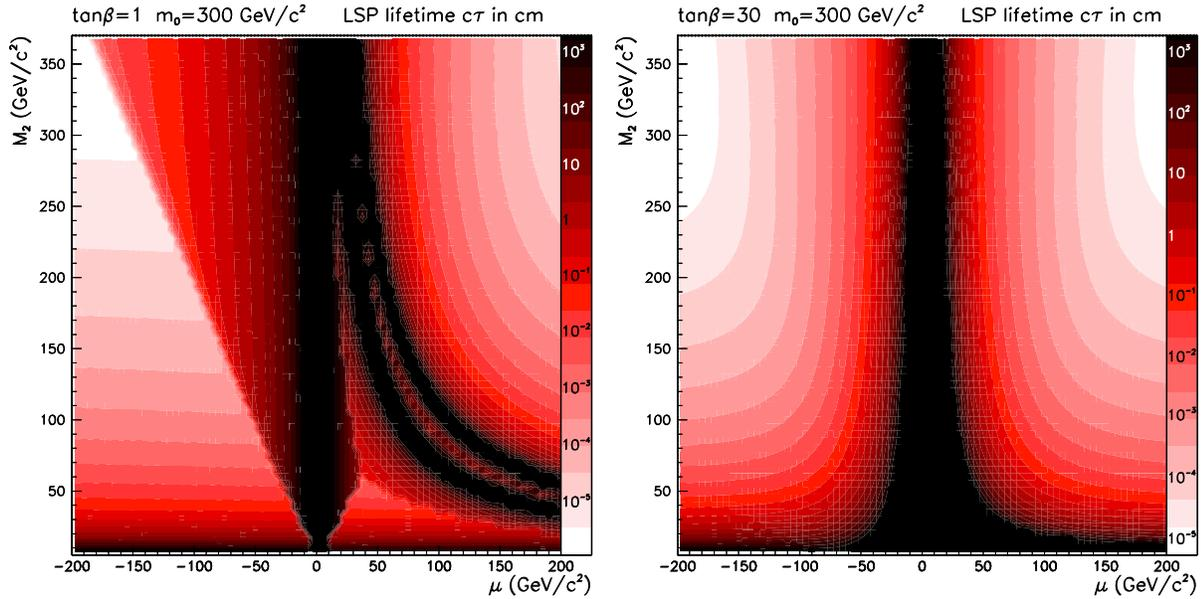


Figure 7.3: LSP lifetime for different values of the MSSM parameters, and with a dominant λ_{133} coupling; For this illustration, the coupling has been set to $\lambda_{133} = 0.004$.

to be the lightest neutralino ($\tilde{\chi}_1^0$). Since a displaced vertex analysis is an experimental challenge at hadron colliders, the performance typically achievable at a future e^+e^- linear collider is considered here. Assuming that the minimum distance between two vertices necessary to

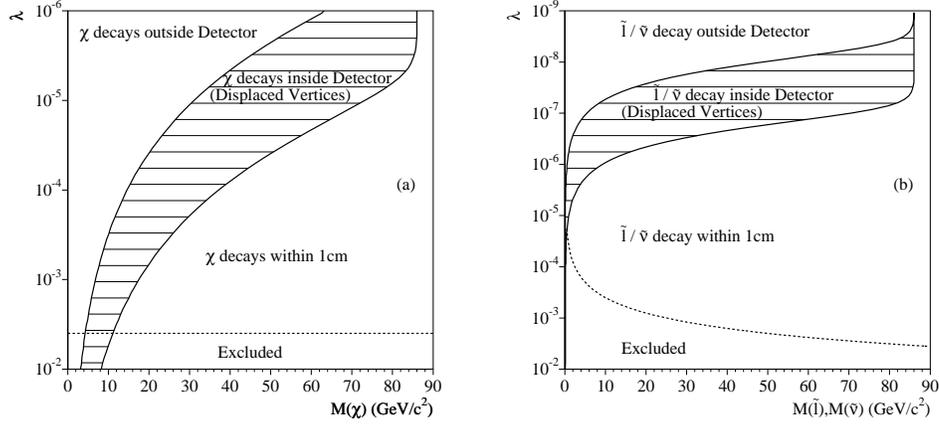


Figure 7.4: Regions in the λ versus sparticle mass plane where the sparticle has a mean decay length of $L < 1$ cm, $1 < L < 3m$ (displaced vertices), and $L > 3m$ (decay outside a typical HEP detector) for a) $\tilde{\chi}_1^0$ assuming $m_{\tilde{f}} = 100$ GeV and b) sleptons and sneutrinos. The dashed lines show an indirect limit on λ_{133} [440].

distinguish them experimentally is of order $\mathcal{O}(2 \times 10^{-5})m$, it can be seen from Eq. (7.6) that the \tilde{R}_p couplings can be measured up to the values,

$$\Lambda < 1.2 \times 10^{-4} \gamma^{1/2} \left(\frac{m_{\tilde{f}}}{100 \text{ GeV}} \right)^2 \left(\frac{100 \text{ GeV}}{m_{\tilde{\chi}_1^0}} \right)^{5/2}. \quad (7.7)$$

where $\Lambda = \lambda, \lambda'/\sqrt{3}$ or $\lambda''/\sqrt{3}$, and γ is the Lorentz boost factor.

There is a gap between these values and the sensitivity of low-energy experiments which requires typically \tilde{R}_p coupling values in the range $\Lambda \sim \mathcal{O}(10^{-1} - 10^{-2})$ for superpartners masses of 100 GeV. However, the domain above the values of Eq. (7.7) can be tested through the study of the single production of supersymmetric particles as will be discussed in section 7.5. Indeed, the cross-sections of such reactions are directly proportional to a power of the relevant \tilde{R}_p coupling constant(s), which allows the determination of the values of the \tilde{R}_p couplings. Therefore, there exists a complementarity between the displaced vertex analysis and the study of singly produced sparticles, since these two methods allow to investigate different ranges of values of the \tilde{R}_p coupling constants.

7.3.3 Cascade Decays Initiated by Gauge Couplings

In an indirect decay, the supersymmetric particle first decays through a R_p conserving vertex (i.e. through gauge couplings) to an on-shell supersymmetric particle, thus initiating a cascade which continues till reaching the LSP. The LSP then decays as described above via one \tilde{R}_p coupling.

The sfermions may for example decay indirectly (i.e. undergo first a gauge decay) into a fermion plus a $\tilde{\chi}_1^0$ if the lightest neutralino $\tilde{\chi}_1^0$ is the LSP, as shown for example in the case of sleptons in Fig. 7.5a and b. The $\tilde{\chi}_1^0$ will subsequently undergo a \tilde{R}_p decay via one of the trilinear couplings. In the squark sector, such decays have mainly been considered for the stop and sbottom in actual searches at colliders as they possess a mass eigenstate which can be

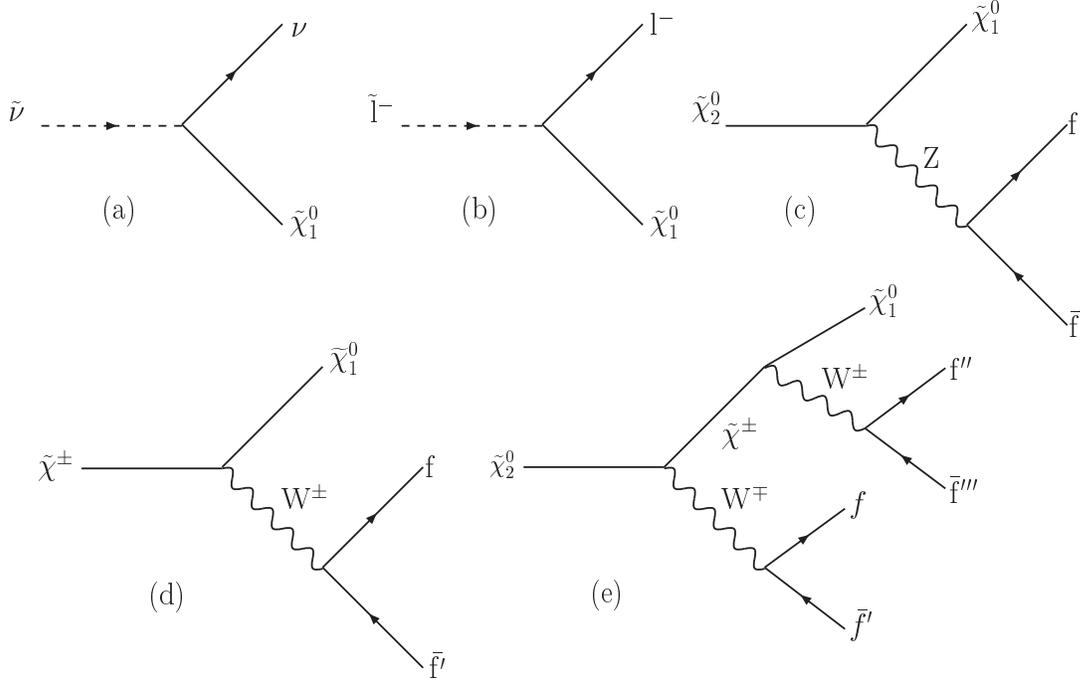


Figure 7.5: Slepton (a, b) and gauginos (c, d, e) indirect decay diagrams.

among the lightest for squarks. If the lightest stop mass eigenstate \tilde{t}_1 is not the LSP but the lightest charged supersymmetric particle, the cascade will be initiated through a decay to $\tilde{t}_1 \rightarrow c\tilde{\chi}_1^0$. If $m_{\tilde{t}_1} > m_{\tilde{\chi}^\pm} + m_b$ then the decay $\tilde{t}_1 \rightarrow b\tilde{\chi}_1^\pm$ is possible. In the case of the sbottom, the indirect decay $\tilde{b}_1 \rightarrow b\tilde{\chi}_1^0$ is generally treated as the dominant one.

In the gaugino-higgsino sector, the heavy neutralino and chargino mass eigenstates can decay, depending on their mass difference with the $\tilde{\chi}_1^0$, either directly into three standard fermions, or indirectly to $\tilde{\chi}_1^0$ via a virtual Z or W , as illustrated in Fig. 7.5c, d and e.

Assuming a small value for the \tilde{R}_p coupling, the indirect decay mode will generally dominate as soon as there is enough phase space available between “mother” and “daughter” sparticles. For searches at existing colliders this happens when the mass difference between these two sparticles is larger than about 5 to 10 GeV. As an example, the Fig. 7.6 shows the \tilde{R}_p decay branching fraction of the $\tilde{\tau}_R$ via the λ_{133} coupling as a function of the stau mass, for different values of the neutralino mass. If the slepton is lighter than the neutralino, only the \tilde{R}_p mode is opened. As soon as the indirect decay mode is possible, it dominates.

Nevertheless, there exist regions of the SUSY parameter space where the R_p conserving decay (initiating the cascade) suffers from a “dynamic” suppression. This is the case for example if the field component of the two lightest neutralinos is mainly the photino, in which case the indirect decay $\tilde{\chi}_2^0 \rightarrow \tilde{\chi}_1^0 Z^*$ is suppressed. In these regions, even if the sparticle is not the LSP it will decay through a direct \tilde{R}_p mode.

It should be emphasized here that the indirect decays lead to final state topologies which differ strongly from direct \tilde{R}_p decays. For example, the direct decay of a neutralino via a $LL\bar{E}$ coupling leads to a purely leptonic final state, while the indirect decay adds (mainly) jets to such final state. The allowed indirect decays and their branching ratios depend on the parameters values for the specific supersymmetry model (e.g. MSSM, mSUGRA, ...) as well as on the value of the \tilde{R}_p coupling considered.

Detailed strategies for practical searches at colliders will be discussed starting in section 7.4.

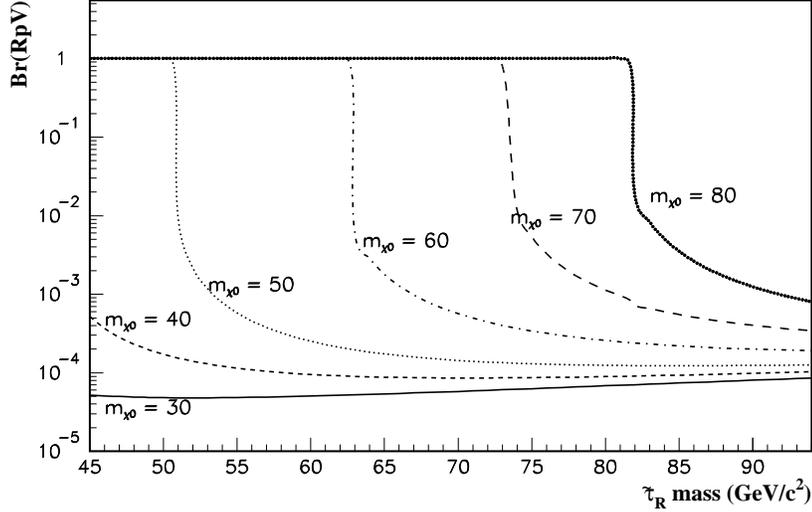


Figure 7.6: Branching ratio of the \tilde{R}_p decay $\tilde{\tau}_R \rightarrow ee, e\tau, \tau\tau + \cancel{E}$ as a function of the mass of the $\tilde{\tau}_R$ and for different values of the neutralino mass.

7.3.4 Decays Through Mixing Involving Bilinear Interactions

For completeness, the effects of the $\mu_i L_i H_u$ bilinear terms in the superpotential which violate lepton-number conservation must be discussed in the context of collider physics. The theoretical motivations for the appearance of such terms in the superpotential of supersymmetric models were discussed in detail in chapter 2. They appear for instance as a consequence of non-zero right handed sneutrino vacuum expectation values in models with spontaneous R -parity violation, or in models with explicitly broken R -parity.

As discussed in section 2.3, there are strong constraints on the bilinear \tilde{R}_p parameters from the neutrino sector. For this reason, the μ_i are often considered to be suppressed [259] and thus neglected in collider analyses, with the notable exception of the LSP decays, where the LSP is not necessarily a neutralino in this context. Indeed, values of the μ_i suggested by the solar and atmospheric neutrino experiments can lead to observable decays of the LSP at colliders, with correlations between the neutrino mixing angles and the branching ratios into different lepton flavours [50, 51, 52, 54, 231] (see section 5.2.2).

However, exotic scenarios with non-negligible μ_i parameters have been considered, in particular in the context of spontaneous R -parity violation [63, 64, 65]. Although these scenarios are disfavoured by neutrino oscillation data, we mention for completeness the expected effect of e.g. a non-negligible μ_3 . Such a term introduces a tau component in the chargino mass eigenstate. As a consequence, the tree level decay $Z \rightarrow \tilde{\chi}^- \tau^+$ becomes for instance possible. In the top sector, bilinear terms could rise to additional decay modes for top-quarks and stop-squarks such as $t \rightarrow \tilde{\tau}_1^+ + b$ or $\tilde{t}_1 \rightarrow \tau^+ + b$. Most of these new decay modes result, through cascade decays, in final states with two τ 's and two b-quarks plus the possibility of additional jets and leptons. B-tagging and τ identification are therefore important tools for the analysis. Note that the $\tilde{t} \rightarrow \tau + b$ decay could also occur via a trilinear λ'_{333} coupling.

Spontaneous R -parity violation has been studied in the context of a single tau-lepton-number-violating bilinear term at the Tevatron $p\bar{p}$ collider in Ref. [441] and the $\tilde{t} \rightarrow \tau + b$ decay was

found to be competitive with the decay in $c\tilde{\chi}_1^0$ for a discovery of the \tilde{t} . For the LHC pp collider, the possibility to observe spontaneous R -parity violation through multilepton and same sign dilepton signatures in gluino pair-production has been considered in Ref. [442].

7.4 \mathcal{R}_p Phenomenology from Pair Produced Sparticles

In this section, we are interested in the way the collider phenomenology for Supersymmetric models is affected by the presence of an individual \mathcal{R}_p coupling with a value $\Lambda^2 \ll 4\pi\alpha$ such that \mathcal{R}_p contributions can be neglected at production.

In such a configuration, a first question of interest for searches at colliders is whether or not the nature of a specific non-vanishing \mathcal{R}_p coupling can be identified (within a range of allowed values) starting from the characteristics of the observed final states. Assuming that the presence of specific \mathcal{R}_p interactions is eventually established, a next important question is to understand whether and how the sensitivity to the fundamental parameters of a given supersymmetric theory is affected.

7.4.1 Gaugino-Higgsino Pair Production

7.4.1 a) Production and final states

Gaugino-higgsino pair production via standard gauge couplings at colliders has been thoroughly studied in the literature and a detailed review is clearly outside the scope of this paper. Here, only the key ingredients shall be summarized. Otherwise we concentrate on the phenomenology associated with the presence of \mathcal{R}_p interactions.

At l^+l^- lepton colliders, the neutralinos are produced by pairs via s -channel Z exchange (provided they have a higgsino component), or via t -channel \tilde{l}^\pm exchange (provided they have a gaugino component). The charginos are produced by pairs in the s -channel via γ or Z exchange, or in the t -channel via sneutrino ($\tilde{\nu}_l$) exchange if the charginos have a gaugino component. Of course, the t -channel contributions are suppressed for high slepton masses.

In the case of neutralinos, the t -channel exchange contributes to an enhancement which can be significant for slepton masses typically below $\sqrt{s_{ll}}/2$ (i.e. $m_{\tilde{e}} \lesssim 100$ GeV in the case of selectron exchange at LEP 2 e^+e^- collider). In contrast, the chargino pair production cross-section can decrease due to destructive interference between the s - and t -channel amplitudes (i.e. between \tilde{e} and $\tilde{\nu}_e$ exchange at a e^+e^- collider) if the \tilde{l}^\pm and $\tilde{\nu}_l$ masses are comparable.

As an example, one can consider pair production in the framework of the MSSM, assuming in addition that scalars have a common mass m_0 at the GUT scale. In such a case m_0 determines the slepton masses at EW scale and the relevant MSSM parameters are M_2 , μ , $\tan\beta$ and m_0 . In such a framework the production cross-sections are generally found to be large. If the dominant component of neutralinos and charginos is the higgsino ($|\mu| \ll M_2$) the production cross-sections are also insensitive to slepton masses. Over a wide range of MSSM parameter values, the pair production cross-sections at LEP 2 for $\sqrt{s_{ee}} \simeq 200$ GeV is found to vary typically from 0.1 to 10 pb. Investigations of gaugino pair production in a similar constrained MSSM framework and in presence of \mathcal{R}_p have been performed for the case of a future 500 GeV e^+e^- collider in Ref. [443].

At $p\bar{p}$ and pp hadron colliders, the main production process which has been studied for neutralinos and charginos is the associated production $q\bar{q}' \rightarrow \tilde{\chi}^\pm \tilde{\chi}^0$. In R_p -conserving theories like the MSSM or mSUGRA, measurable rates are expected mainly in the case of $\tilde{\chi}_1^\pm \tilde{\chi}_2^0$ and only for certain regions of the parameter space. In presence of \mathcal{R}_p interactions of course, the process $q\bar{q}' \rightarrow \tilde{\chi}_1^\pm \tilde{\chi}_1^0$ involving the lowest $\tilde{\chi}^0$ mass eigenstate could also become observable. In addition, \mathcal{R}_p could allow for pair production of neutralinos and charginos in $q\bar{q} \rightarrow \gamma, Z$ annihilation processes to become observable. The production cross-sections would then depend on the gaugino and higgsino components as discussed above for l^+l^- annihilation.

The final states resulting from the decay of pair-produced neutralinos or charginos are listed in Table 7.4 for the three different couplings $LL\bar{E}$, $LQ\bar{D}$ and $\bar{U}\bar{D}\bar{D}$.

gauginos	decay mode	$LL\bar{E}$	$LQ\bar{D}$	$\bar{U}\bar{D}\bar{D}$
$\tilde{\chi}_1^0 \tilde{\chi}_1^0$	direct	$4l + \cancel{E}$	$1l + 4j + \cancel{E}$ $2l + 4j$ $4j + \cancel{E}$	$6j$
$\tilde{\chi}_1^+ \tilde{\chi}_1^-$	direct	$2l + \cancel{E}$ $4l + \cancel{E}$ $6l$	$1l + 4j + \cancel{E}$ $2l + 4j$ $4j + \cancel{E}$	$6j$
$\tilde{\chi}_2^0 \tilde{\chi}_1^0$	indirect	$4l + \cancel{E}$ $4l + 2j + \cancel{E}$ $6l + \cancel{E}$	$1l + 4j + \cancel{E}$ $1l + 6j + \cancel{E}$ $2l + 4j + \cancel{E}$ $2l + 6j$ $3l + 4j + \cancel{E}$ $4l + 4j$ $6l + \cancel{E}$	$8j$ $6j + 2l$ $6j + \cancel{E}$
$\tilde{\chi}_1^+ \tilde{\chi}_1^-$	indirect	$4l + 4j + \cancel{E}$ $5l + 2j + \cancel{E}$ $6l + \cancel{E}$	$1l + 6j + \cancel{E}$ $1l + 8j + \cancel{E}$ $2l + 4j + \cancel{E}$ $2l + 6j + \cancel{E}$ $2l + 8j$ $3l + 4j + \cancel{E}$ $3l + 6j + \cancel{E}$ $4l + 4j + \cancel{E}$ $8j + \cancel{E}$	$10j$ $8j + 1l + \cancel{E}$ $6j + 2l + \cancel{E}$

Table 7.4: Neutralino and chargino pair production final states in case of \mathcal{R}_p decays. The notations l , \cancel{E} and j correspond respectively to charged lepton, missing energy from at least one neutrino and jet final states.

At first approximation, with $\lambda \neq 0$ the final states are characterized by multi-lepton (charged leptons and escaping neutrinos) event topologies. In contrast, with $\lambda' \neq 0$, the final states are likely to contain multi-jets and several more or less isolated leptons. One exception concerns here slepton pair production which could lead to four jet final states. Finally $\lambda'' \neq 0$, leads to final states with very high jet multiplicities. Thus, the existence of either a non-vanishing λ ($LL\bar{E}$), λ' ($LQ\bar{D}$), or λ'' ($\bar{U}\bar{D}\bar{D}$) can indeed be readily distinguished.

Of course such a simple picture applies essentially in the framework of MSSM or mSUGRA models where the $\tilde{\chi}_1^0$ is likely to be the lightest supersymmetric particle. It moreover has to be modulated in the presence of indirect (cascade) decays. For instance indirect gaugino decays when involving an intermediate Z^* or W^* might lead to final states containing jets for $LL\bar{E}$ interactions or, symmetrically, containing leptons and neutrinos for $\bar{U}\bar{D}\bar{D}$ interactions.

7.4.1 b) Searches for Gaugino Pair Production at e^+e^- Colliders

It is interesting to review what has been learned from studies by the experiments at the LEP collider. The analyses have been performed assuming "short lived" sparticles such that the \tilde{R}_p decays occur close enough to the production vertex and are not observable. In practice this implies a LSP flight path of less than $\mathcal{O}(1)$ cm. Considering the upper limits on the λ_{ijk} derived from low energy measurements (chapter 6), and according to Eq. 7.6, the analyses are thus insensitive to a light $\tilde{\chi}$ of mass $M_{\chi_{LSP}} \leq 10$ GeV (due first to the term $m_{\tilde{\chi}}^{-5}$ and second to the term $(\beta\gamma)$ which becomes important). When studying $\tilde{\chi}$ decays, for typical masses considered, the LEP analyses have a lower limit in sensitivity on the λ coupling of the order of 10^{-4} to 10^{-5} .

In most of the \tilde{R}_p analyses, the main background contributions come from the four-fermion processes and $f\bar{f}\gamma$ events. A discussion of such SM background contributions can be found in Ref. [444]. The $f\bar{f}\gamma$ cross-section decreases with the increase of the centre-of-mass energy; on the other hand, the cross-sections of the four-fermion processes increase; in particular beyond the W^+W^- and the ZZ thresholds, these processes contribute significantly to the background, and lead to final states very similar to several \tilde{R}_p signal event topologies.

The $LL\bar{E}$ searches at LEP were mainly multi-lepton analyses, with the missing energy in the final states most often coming from neutrinos. However, the indirect decay topologies may also contain hadronic jets (indirect decay of gauginos, see Table 7.4). The number of charged leptons in the final state varied between 4 and 6 except for direct decays of charginos with two neutrinos which lead to 2 charged leptons in the final state. Therefore, the crucial step in the selection of the signal events was the electron, muon or tau identification. Electrons and muons are typically identified by well isolated charged tracks in combination with either dE/dx measurements and deposits in the electromagnetic calorimeters (e) or information from hadron calorimeters and muon chambers (μ , τ) of the experiments. Tau decays may also be identified through isolated thin hadronic jets. In case of W or tau jets, signal selection has been performed with the additional discrimination provided by topological variables like the y_{cut} jet resolution variable. The two-lepton final states are difficult to separate from the SM background mainly coming from $f\bar{f}\gamma$ and $\gamma\gamma$ events and have been considered in the analyses. The other multi-lepton final states on the other hand, provided almost background free analyses with efficiencies typically between 20 and 60 %. The decays producing taus in the final states were found to have lower efficiencies and rejection power. The analyses designed for signals produced with a dominant λ_{133} can be applied to signals produced with other λ_{ijk} , and the efficiencies are either of the same order or higher. Therefore, the weakest limits which have been derived are those resulting from analyses performed assuming a dominant λ_{133} coupling [445].

For the $LQ\bar{D}$ searches at LEP, the analyses of gaugino decays all included hadronic activity in the final state (at least 4 hadronic jets, see Table 7.4) such that topological variables like jet resolution and thrust were used to select events in combination with missing energy and/or one or two identified leptons. For the topologies with missing energy the polar angle of the missing momentum has also been used to select candidate events. The analysis of gaugino decays via the couplings λ'_{i3k} and λ'_{ij3} also benefits from the presence of b-quarks, and thereby from possible background reduction via b-tagging. The topologies of the indirect chargino

decays depend heavily on the mass difference between chargino and neutralino, which is a free parameter in the model. Sensitivity to a large range of topologies is hence needed in order to completely cover all possible $LQ\bar{D}$ scenarios. Several of the gaugino final state topologies closely resemble those of \tilde{R}_p sfermion decays and the same event selection may therefore be used to cover these channels too, e.g. sneutrino and slepton decays. The SM background consists mainly of four-fermion events decaying either to hadronic or semileptonic final states. Signal efficiencies typically range from over 50% down to a few %, depending on topology and selection criteria. The worst efficiency is generally obtained for decays into taus and light quarks. The couplings generating these final states (e.g. λ'_{311}) are therefore used to evaluate conservative constraints on the production cross-sections. The excluded $LQ\bar{D}$ gaugino cross-sections at a 95% confidence level are typically of the order of 0.5 pb [446].

For the LEP searches in the case of a single dominant $\bar{U}\bar{D}\bar{D}$ coupling, the gauginos decay into mainly hadronic final states, however, the indirect gaugino decays may also include leptons and missing energy, depending on the decay mode of the W . As seen from Table 7.4, the number of jets expected in the final states varies between six and ten. The selection of candidate events typically depends on topological variables like jet resolution, thrust and jet angles, thereby rejecting the major part of the SM $f\bar{f}\gamma$, W^+W^- and ZZ background events. The absence of neutrinos and missing energy in the fully hadronic final states also enables direct reconstruction of the gaugino masses. The mass reconstruction consists of assigning each reconstructed jet to its parent gaugino and thereafter applying a kinematic fitting algorithm. These algorithms are also used to reconstruct the mass of the W bosons produced at LEP 2 and impose constraints on conserved energy and momenta in combination with equal masses of the pair produced gauginos. The indirect chargino decays, again, strongly depend on the mass difference between chargino and neutralino, thereby making it difficult to use the same event selection to cover all possible scenarios. Decays into light quarks (λ''_{112} and λ''_{122} couplings) generally have lower efficiencies and are therefore used to derive conservative cross-section limits at a 95% confidence level (CL) [445].

Since none of the \tilde{R}_p gaugino searches at LEP 2 show any excess of data above the Standard Model expectations, the results are interpreted in terms of exclusions of the MSSM parameters. The gaugino pair production cross-sections are, as previously discussed, mainly determined by the MSSM parameters μ , M_2 , m_0 and $\tan\beta$. The excluded gaugino cross-section at a 95% CL for each experimental search channel is therefore compared to the production cross-section provided by the MSSM for each set of these four parameters. Hereby an exclusion of experimentally disproved combinations of the parameters is obtained for each of the performed search channels. This exclusion is then typically presented as contours in the μ , M_2 plane for different fixed values of $\tan\beta$ and m_0 [446, 445, 447, 448]. The LEP 1 excluded region of the (μ, M_2) contours is obtained from the Z line-shape measurement. Examples of such (μ, M_2) exclusion contours are shown in Figures 7.7, 7.8 and 7.9. The dominant contribution to the exclusion contours comes from the chargino pair production analyses in any \tilde{R}_p couplings. The neutralino pair production analysis becomes relevant in case of low $\tan\beta$, low m_0 , small M_2 and negative μ values (Fig. 7.9) which means when the chargino pair production cross-section is suppressed by destructive interferences between s - and t -channels.

From the exclusion plots in the (μ, M_2) plane the extraction of the minimum gaugino masses which is not excluded for the investigated range of parameters within the MSSM is performed. These limits on the lightest chargino and neutralino are obtained for high m_0 value which corresponds to the disappearance of neutralino pair production contribution. The mass of the lightest non-excluded gaugino is naturally shifted when $\tan\beta$ is changed. In Fig. 7.10, the lightest non-

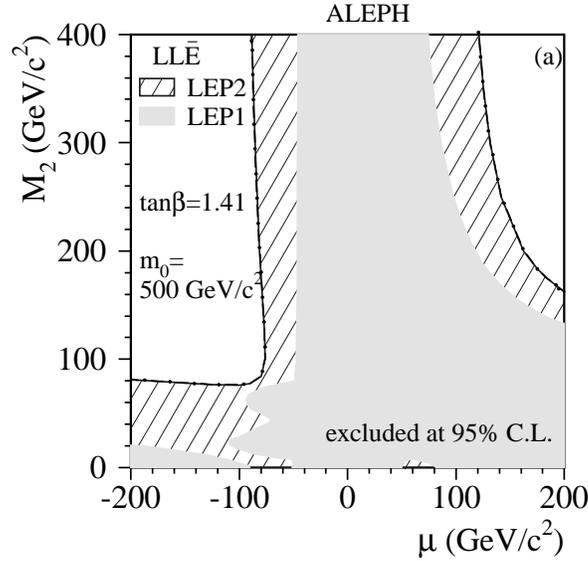


Figure 7.7: Regions in the (μ, M_2) plane excluded at 95% CL at $\tan\beta= 1.41$ and $m_0 = 500$ GeV for $LL\bar{E}$ coupling [446]. The dotted line is the kinematic limit for pair production of the lightest chargino.

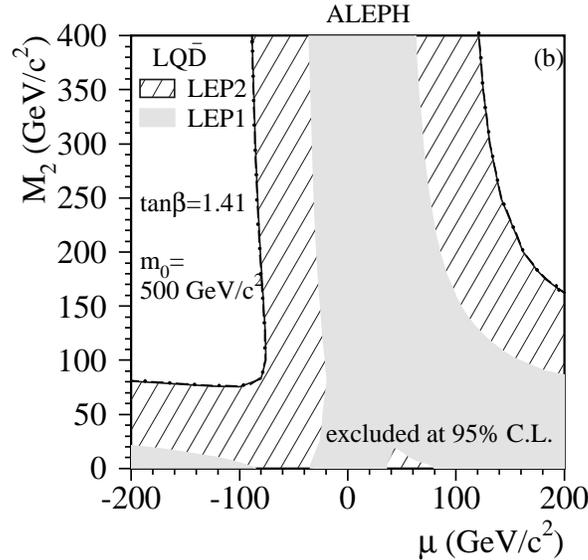


Figure 7.8: Regions in the (μ, M_2) plane excluded at 95% CL for $\tan\beta= 1.41$ and $m_0 = 500$ GeV in the case of the dominant $LQ\bar{D}$ coupling [446]. The black line is the kinematic limit for pair production of the lightest chargino.

excluded neutralino mass as a function of $\tan\beta$ for the $LL\bar{E}$ searches in DELPHI is shown. It has been checked that this result is independent of m_0 values.

In this context, one of the most important results in the searches for supersymmetry obtained with data taken up to a centre-of-mass energy of 208 GeV at LEP 2 by the four LEP experiments is that the lightest chargino mass is excluded at 95% CL up to 103 GeV and the lightest neutralino mass is excluded at 95% CL up to 39 GeV in the framework of the MSSM with R_p assuming that the $\tilde{\chi}_1^0$ decays in the detector. These results are formally only valid in

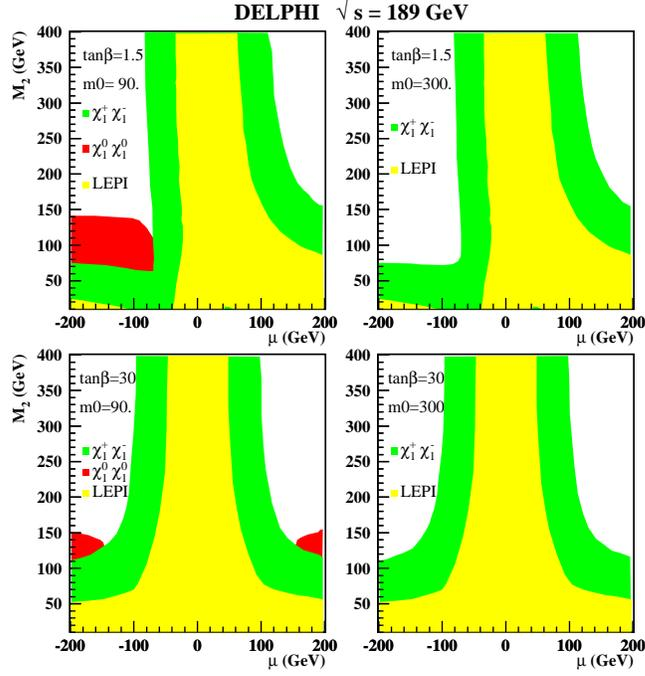


Figure 7.9: Regions in the (μ, M_2) plane excluded at 95% CL for $\tan\beta = 1.5, 30$ and $m_0 = 90, 300$ GeV in the case of a dominant $\bar{U}\bar{D}\bar{D}$ coupling [445].

the scanned MSSM parameter space, i.e. for $1 \leq \tan\beta \leq 35$, $m_0 \leq 500$ GeV, $|\mu| \leq 200$ GeV, $M_2 \leq 500$ GeV, and for any coupling value from 10^{-4} up to the existing limits.

We hinted above of situations where indirect (cascade) decays could play a significant role. This could be the case for instance at future lepton colliders where centre-of-mass energies far beyond the current lower mass limits on the LSP are being contemplated. In view of the constraints established at LEP 2, the possibility of opening up large production of heavier neu-

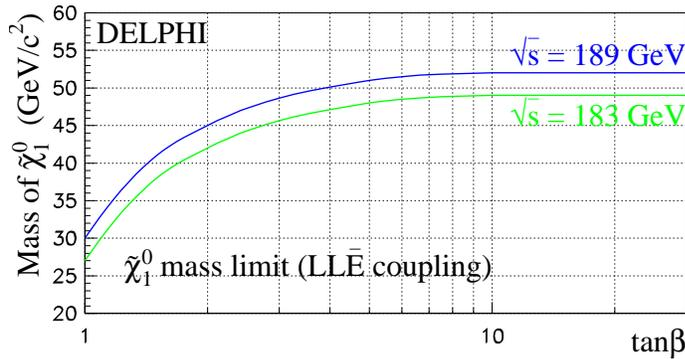


Figure 7.10: The lightest non-excluded neutralino mass as a function of $\tan\beta$ at 95% CL. This limit is independent of the choice of m_0 in the explored range and of the generation indices i, j, k of the λ_{ijk} coupling [445] and it assumes that the $\tilde{\chi}_1^0$ is in the detector.

tralinos and charginos at a future 500 GeV e^+e^- linear collider (LC) has been studied in Ref. [443] assuming that the lightest neutralino is the LSP and in presence of \mathcal{R}_p . The study showed in this case (for a representative but finite number of points in the constrained MSSM parameter space) that only the production modes involving the $\tilde{\chi}_1^0, \tilde{\chi}_2^0, \tilde{\chi}_1^\pm$ need to be considered. The $\tilde{\chi}_3^0, \tilde{\chi}_4^0$, and $\tilde{\chi}_2^\pm$ being almost always beyond the reach of a 500 GeV machine. As a consequence, the analysis would remain relatively simple, with a limited amount of cascade decays to take into account. Moreover, for a large part of the parameter space, the $\tilde{\chi}_2^0$ is nearly degenerate with the lighter chargino, and then, the number of decay chains to be considered is further reduced. The signals produced by $L\bar{L}\bar{E}, LQ\bar{D}, \bar{U}\bar{D}\bar{D}$ operators have been studied in Ref. [443] and retain the basic characteristics listed above. For $L\bar{L}\bar{E}$ the dominating signal remains an excess of multi-lepton final states, with possibly substantial missing energy. For $LQ\bar{D}$ the final states contain again leptons and jets. In this case, an algorithm to reconstruct the LSP and higher neutralino masses enables to identify the signal as due to supersymmetry with specific \mathcal{R}_p operators. The existence of like-sign dilepton final states, originating from the Majorana nature of neutralinos, appears to be a very promising signal practically free of true Standard Model background sources. For $\bar{U}\bar{D}\bar{D}$ the final states consist again of multiple jets which are more difficult to disentangle from a large number of Standard Model background sources. Mass reconstruction nevertheless appears promising here also to allow to identify the signal as due to supersymmetry with specific \mathcal{R}_p operators.

7.4.1 c) Searches for Gaugino Pair Production at Hadron Colliders

Cascade decays involving trilinear \mathcal{R}_p couplings could also play a major rôle at future hadron colliders.

Outstanding multi-lepton event signatures are expected in the presence of a λ Yukawa coupling. The case of gaugino pair production with a trilepton signature has been investigated for the $D\emptyset$ experiment at the Tevatron collider in Ref. [449], in the framework of mSUGRA.

$D\emptyset$ [450] also considered the dimuon and four-jets channel occurring after $\tilde{\chi}_1^0$ decay via the λ'_{2jk} coupling ($j = 1, 2; k = 1, 2, 3$) where the $\tilde{\chi}_1^0$ can be produced either directly in pair or through cascade decays from squarks or gluinos. Gluinos masses below 224 GeV (for all squark masses and for $\tan\beta = 2$) are excluded. For equal masses of squarks and gluinos the mass limit is 265 GeV.

The λ'' coupling implies multi-jet final states for sparticle decays which severely challenges the sensitivity at $p\bar{p}$ and pp colliders.

However the 1-lepton and various dileptons and multi-lepton event topologies that result from simultaneous production of all sparticles at the Tevatron assuming the LSP decays via baryon number violating operators have been studied in [451] giving reaches on the gluino mass from 150 GeV up to 360 GeV depending on the specific topology.

The study of the decay chain $\tilde{q}_L \rightarrow \tilde{\chi}_2^0 q \rightarrow \tilde{l}_R l q \rightarrow \tilde{\chi}_1^0 l l q$ followed by the decay of the $\tilde{\chi}_1^0$ into three quarks assuming a non-zero λ''_{212} at the LHC has been performed in [452]. This study shows that even in the choice of a non-zero λ''_{212} , which is considered as the hardest choice, the $\tilde{\chi}_2^0, \tilde{\chi}_2^0$ and \tilde{q}_L can be detected and their masses measured and that the mass of the \tilde{l}_R can be obtained in much of the parameter space.

7.4.2 Sfermion Pair Production

7.4.2 a) Production and final states

As for the gaugino-higgsino production discussed above, we shall concentrate in this section on the phenomenology associated with the presence of \mathcal{R}_p interactions. But we shall first briefly review the key ingredients for sfermion pair production via standard gauge couplings at colliders.

The sfermion mass eigenstates, \tilde{f}_1 and \tilde{f}_2 ($f: q$ or ℓ , \tilde{f}_1 lighter than \tilde{f}_2), are obtained from the two supersymmetric scalar partners \tilde{f}_L and \tilde{f}_R of the corresponding left and right-handed fermion [453, 454]:

$$\begin{aligned}\tilde{f}_1 &= \tilde{f}_L \cos\theta_{\tilde{f}} + \tilde{f}_R \sin\theta_{\tilde{f}} \\ \tilde{f}_2 &= -\tilde{f}_L \sin\theta_{\tilde{f}} + \tilde{f}_R \cos\theta_{\tilde{f}}\end{aligned}$$

where $\theta_{\tilde{f}}$ is the mixing angle with $0 \leq \theta_{\tilde{f}} \leq \pi$. According to the equations which give the sfermion masses (see for example in [455]), the left-handed sfermions are most often heavier than their right-handed counterparts. The \tilde{f}_L - \tilde{f}_R mixing is related to the off-diagonal terms of the scalar squared-mass matrix. It is proportional to the fermion mass, and is small compared to the diagonal terms, with the possible exception of the third family sfermion [456]. The lightest squark is then probably the lighter stop \tilde{t}_1 . This is due not only to the mixing effect but also to the effect of the large top Yukawa coupling; both tend to decrease the mass of \tilde{t}_1 [457]. The lightest charged slepton is probably the $\tilde{\tau}_1$. For small values of $\tan\beta$, $\tilde{\tau}_1$ is predominantly a $\tilde{\tau}_R$, and it is not so much lighter than \tilde{e}_R and $\tilde{\mu}_R$.

Sleptons and squarks can be pair produced in e^+e^- collisions via the ordinary gauge couplings of supersymmetry with conserved R -parity provided that their masses are kinematically accessible. They can be produced via s -channel Z or γ exchange with a cross-section depending on the sfermion mass. The $\tilde{\nu}_e$ (\tilde{e}) can also be produced via the exchange of a chargino (neutralino) in the t -channel, provided that the gaugino component of the chargino (neutralino) is the dominant one. The t -channel contributes if the chargino (neutralino) mass is sufficiently low, and then the cross-section depends also on the $\tilde{\chi}^\pm$ ($\tilde{\chi}^0$) mass and field composition and thereby on the relevant parameters of the supersymmetric model. The coupling between the squarks and the Z boson depends on the mixing angle $\theta_{\tilde{q}}$, and it is minimal for a particular angle value. For example in the case of the stop, the decoupling between the $\theta_{\tilde{t}}$ and the Z is maximal for $\theta_{\tilde{t}} = 0.98$ rad such that the stop pair production cross-section is minimal.

In general, both direct and indirect decays of sfermions can be studied in sparticle pair production at colliders. The direct decay of a sfermion via a given \mathcal{R}_p coupling involves specific standard fermions and can be (e.g. when involving the top quark) kinematically closed. The final states resulting from the decay of pair-produced sleptons or squarks are listed in Table 7.5 and 7.6 for the three different couplings λ ($LL\bar{E}$), λ' ($LQ\bar{D}$), or λ'' ($\bar{U}\bar{D}\bar{D}$).

When considering sfermion pair production and the decays of Table 7.5 and 7.6 relevant for e^+e^- colliders, it should be noticed that in general the indirect decays into a chargino will not be considered. This is because the chargino search itself provides a mass limit close to the kinematic limit. There is no phase space left for the production of (e.g.) two sleptons followed by decays involving charginos. This explains why for instance at LEP, the most general sfermion indirect decay studied has been the decay into the lightest neutralino considered as the LSP ($\tilde{\nu} \rightarrow \nu \tilde{\chi}_1^0$, $\tilde{\ell} \rightarrow \ell \tilde{\chi}_1^0$, $\tilde{q} \rightarrow q' \tilde{\chi}_1^0$). The final states are then composed of two fermions plus the decay products of the \mathcal{R}_p decay of the neutralino pair (see Table 7.6).

7.4.2 b) Slepton Searches at lepton colliders

sfermions	$LL\bar{E}$	$LQ\bar{D}$	UDD
$\tilde{\nu}\tilde{\nu}$	4ℓ	$4j$	not possible
$\ell_R^+\ell_R^-$	$\ell\ell' + \cancel{E}$	not possible	not possible
$\ell_L^+\ell_L^-$	$2\ell + \cancel{E}$	$4j$	not possible
$\tilde{u}_L\tilde{u}_L, \tilde{d}_R\tilde{d}_R$	not possible	$2\ell + 2j$	$4j$
$\tilde{d}_R\tilde{d}_R$		$1\ell + 2j + \cancel{E}$	
$\tilde{d}_L\tilde{d}_L, \tilde{d}_R\tilde{d}_R$		$2j + \cancel{E}$	

Table 7.5: Sfermion pair production final states in case of direct R_p decays. The notations ℓ , \cancel{E} and j correspond respectively to charged lepton, missing energy from at least one neutrino and jet final states.

sfermions	$LL\bar{E}$	$LQ\bar{D}$	UDD
$\tilde{\nu}\tilde{\nu}$	$4\ell + \cancel{E}$	$2\ell + 4j + \cancel{E}$ $2\ell + 4j + \cancel{E}$ $4j + \cancel{E}$	$6j + \cancel{E}$
$\ell^+\ell^-$	$6\ell + \cancel{E}$	$4\ell + 4j$ $3\ell + 4j + \cancel{E}$ $2\ell + 4j + \cancel{E}$	$2\ell + 6j$
$\tilde{q}\tilde{q}$	$4\ell + 2j + \cancel{E}$	$2\ell + 6j$ $\ell + 6j + \cancel{E}$ $6j + \cancel{E}$	$8j$

Table 7.6: Sfermion pair production final states in case of indirect decays when the LSP is the lightest neutralino. The notations ℓ , \cancel{E} and j correspond respectively to charged lepton, missing energy from at least one neutrino and jet final states.

Here again one can profit from what has been learned from actual studies by the experiments at LEP collider where both productions of sneutrino and charged slepton pairs have been searched for.

Early discussions on several R -parity-violating processes at e^+e^- colliders including charged slepton pairs can be found in [458, 459].

Lets first consider the case of sneutrino pair production. In the presence of $LL\bar{E}$ interactions, searches for four charged lepton final states are performed. The six possible configurations are listed in Table 7.7. Event topologies containing muons and electrons allow for a high selectivity by applying conditions on two lepton invariant masses. The highest efficiencies are obtained when there are at least two muons in the final states, and the lowest when there are taus. In the latter case, a certain amount of energy is missing in the final state, due to the neutrinos produced in the tau decays. Then, most often, two extreme cases in the coupling choice are studied: the first one considering that the λ_{122} or λ_{232} is dominant, leading to the most efficient analyses, the second considering that the λ_{133} or λ_{233} is dominant, leading to the least efficient analyses. With these two analysis types, all the possible final states are probed.

In the presence of $LQ\bar{D}$ interactions, searches for four jets final states are performed. Here also, the absence of missing energy in the final state offers the possibility to reconstruct the sneutrino mass. Depending on the generation indices, 0, 2, and 4 jets can contain a b-quark (Table 7.8). With the possibility to tag the jets generated by b-quarks, the analyses are very efficient.

final states	processes and couplings		
	$\tilde{\nu}_e \tilde{\nu}_e$	$\tilde{\nu}_\mu \tilde{\nu}_\mu$	$\tilde{\nu}_\tau \tilde{\nu}_\tau$
eeee		λ_{121}	λ_{131}
ee $\mu\mu$	λ_{121}	λ_{122}	$\lambda_{132}, \lambda_{231}$
ee $\tau\tau$	λ_{131}	$\lambda_{123}, \lambda_{231}$	λ_{133}
$\mu\mu\mu\mu$	λ_{122}		λ_{232}
$\mu\mu\tau\tau$	$\lambda_{123}, \lambda_{132}$	λ_{232}	λ_{233}
$\tau\tau\tau\tau$	λ_{133}	λ_{233}	

Table 7.7: Four lepton final states produced by the direct decay via a $LL\bar{E}$ term of a sneutrino pair.

final states	processes and couplings		
	$\tilde{\nu}_e \tilde{\nu}_e$	$\tilde{\nu}_\mu \tilde{\nu}_\mu$	$\tilde{\nu}_\tau \tilde{\nu}_\tau$
4 q (no b-quarks)	$\lambda'_{1jk, j, k \neq 3}$	$\lambda'_{2jk, j, k \neq 3}$	$\lambda'_{3jk, j, k \neq 3}$
2 q 2 b	$\lambda'_{1j3, j \neq 3}, \lambda'_{13k, k \neq 3}$	$\lambda'_{2j3, j \neq 3}, \lambda'_{23k, k \neq 3}$	$\lambda'_{3j3, j \neq 3}, \lambda'_{33k, k \neq 3}$
4 b	λ'_{133}	λ'_{233}	λ'_{333}

Table 7.8: Four jet final states produced by the direct decay via a $LQ\bar{D}$ term of a sneutrino pair.

The LEP experiments have presented results on the lower limit on the sneutrino electron mass derived by searching for the direct decay of sneutrinos in the data collected in 1999 and 2000 up to a centre-of-mass energy of 208 GeV. With a $LL\bar{E}$ ($LQ\bar{D}$) coupling, the most conservative lower limits are 98 (91) GeV [446, 445, 448]. For the derivation of limits, efficiencies are determined as function of the sneutrino mass. In case of $\tilde{\nu}_e$, due to the possible t -channel contribution, they are considered for a specific set of MSSM parameters, generally for $\mu = -200$ GeV, $M_2 = 100$ GeV. When the contribution of the t -channel becomes negligible, the $\tilde{\nu}_e \tilde{\nu}_e$ production cross-section is similar to the $\tilde{\nu}_\mu \tilde{\nu}_\mu$ or $\tilde{\nu}_\tau \tilde{\nu}_\tau$ ones. Taking into account the number of expected events from the Standard Model processes, the number of observed events, and the analysis efficiencies, upper limits at 95% of confidence level on the sneutrino cross-section are obtained as function of the sneutrino mass. Comparing these upper limits to the expected MSSM cross-section, limits on the sneutrino mass have been derived, as illustrated in Fig 7.11. The limits obtained are much stronger than those existing in the hypothesis of R -parity conservation, in which the sneutrino pair production is invisible.

Right-handed charged sleptons are mainly studied, because their production cross-section, for a given slepton mass, is lower than for the left-handed ones, therefore leading to more conservative results. The direct decay of a pair of charged sleptons lead to two charged leptons and some missing energy. This low multiplicity final state is difficult to analyse due to the high background of low multiplicity processes. With a dominant λ_{ijk} coupling constant, only the pair produced $\tilde{\ell}_{kR}$ and $\tilde{\ell}_{iL}$ or $\tilde{\ell}_{jL}$ are allowed to directly decay. The decay of $\tilde{\ell}_{kR}^+ \tilde{\ell}_{kR}^-$ gives $l_i l_i, l_i l_j, l_j l_j + \cancel{E}$, and since $i \neq j$ two lepton flavours are mixed in the final state (see Table 7.9). It is not the case in the direct decay of the supersymmetric partners of the left-handed charged leptons, for which there is only one lepton flavour in the $2\ell + \cancel{E}$ final state (Table 7.10). In case of selectrons, the $\tilde{e}_L \tilde{e}_R$ production is possible in the t -channel; direct decay of both selectrons is possible only via λ_{121} (ee, $e\mu + \cancel{E}$ final state) or via λ_{131} (ee, $e\tau + \cancel{E}$ final state).

Similarly to the sneutrino decay, the search for final states containing mainly taus is the

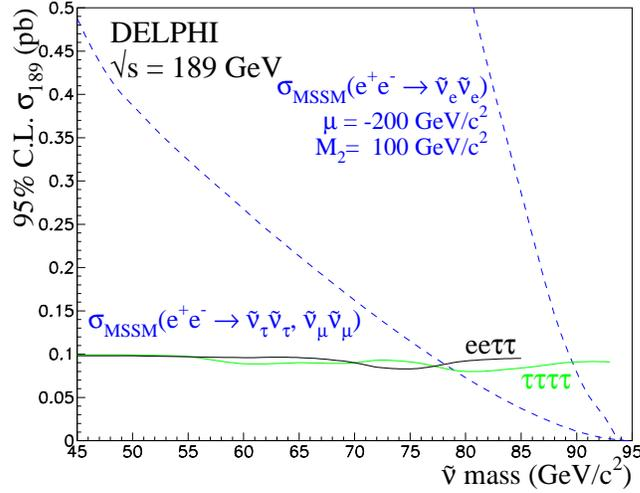


Figure 7.11: Sneutrino direct decay searches with $LL\bar{E}$ coupling: limit on the $\tilde{\nu}\tilde{\nu}$ production cross-section as a function of the mass for two different final states. The MSSM cross-sections are reported in order to derive a limit on the sneutrino mass in the case of direct \tilde{H}_p decay. The dashed lower curve corresponds to both $\tilde{\nu}_\mu\tilde{\nu}_\mu$ and $\tilde{\nu}_\tau\tilde{\nu}_\tau$ cross-sections, which depend only on the sneutrino mass. The dashed upper curve on the plot is the $\tilde{\nu}_e\tilde{\nu}_e$ cross-section obtained for $\mu = -200$ GeV and $M_2 = 100$ GeV, the corresponding chargino mass lies between 90 and 120 GeV [445].

final states	processes and couplings		
	$\tilde{e}_R\tilde{e}_R$	$\tilde{\mu}_R\tilde{\mu}_R$	$\tilde{\tau}_R\tilde{\tau}_R$
$ee, e\mu, \mu\mu + \cancel{E}$	λ_{121}	λ_{122}	λ_{123}
$ee, e\tau, \tau\tau + \cancel{E}$	λ_{131}	λ_{132}	λ_{133}
$\mu\mu, \mu\tau, \tau\tau + \cancel{E}$	λ_{231}	λ_{232}	λ_{233}

Table 7.9: Final states produced by the direct decay via a $LL\bar{E}$ term of a pair of supersymmetric partners of the right-handed leptons.

least efficient one. An upper limit on the cross-section is obtained as a function of the slepton mass. Comparing this upper limit to the expected MSSM cross-section, limits on the slepton mass is deduced. In case of selectron production, the limit depends also on the chosen MSSM parameters, since the neutralino exchange in the t -channel may also contribute to the cross-section. From the data collected at LEP 2, the ALEPH experiment derived a lower limit of 96 GeV on the $\tilde{\mu}_R$ [446], and OPAL obtained a limit of 74 GeV for the same slepton mass [448],

final states	processes and couplings		
	$\tilde{e}_L\tilde{e}_L$	$\tilde{\mu}_L\tilde{\mu}_L$	$\tilde{\tau}_L\tilde{\tau}_L$
$ee + \cancel{E}$	$\lambda_{121,131}$	$\lambda_{121,231}$	$\lambda_{131,231}$
$\mu\mu + \cancel{E}$	$\lambda_{122,132}$	$\lambda_{122,232}$	$\lambda_{132,232}$
$\tau\tau + \cancel{E}$	$\lambda_{123,133}$	$\lambda_{123,233}$	$\lambda_{133,233}$

Table 7.10: Two lepton with missing energy final states produced by the direct decay via a $LL\bar{E}$ term of a pair of supersymmetric partners of left-handed charged leptons.

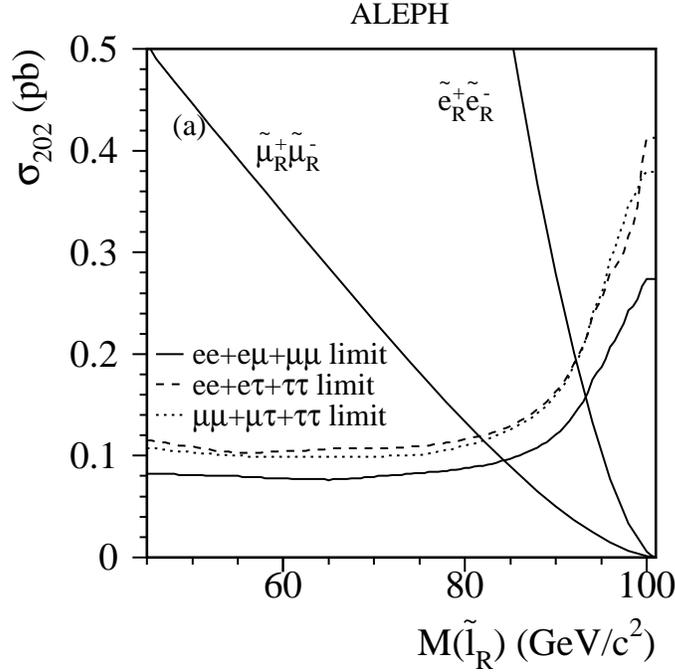


Figure 7.12: Charged slepton direct decay searches with $LL\bar{E}$ couplings: the 95% CL exclusion cross-sections for sleptons. The MSSM cross-section for pair production of right-handed selectrons and smuons are superimposed [446].

when a $LL\bar{E}$ coupling is considered to be dominant.

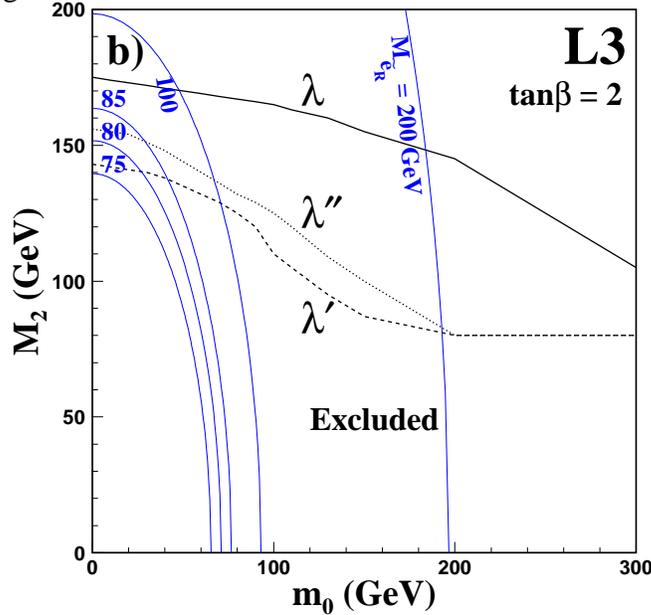


Figure 7.13: Exclusion contours in the m_0 - M_2 plane, for $\tan\beta = 2$, at 95% CL. The lines represent the isomasses of the supersymmetric partner of the right-handed electron (labelled with the corresponding value in GeV). The solid and dotted curves show the 95% CL lower limits on M_2 as a function of m_0 from which the limits on the scalar electron mass were derived [447].

From exclusion contours in the μ - M_2 plane, determined with the MSSM interpretation of the gaugino pair production results, after the analysis of the data collected up to 189 GeV, the

L3 experiment sets indirect lower limit on the scalar lepton masses [447]. Figure 7.13 shows how the lower limits on the mass of the supersymmetric partner of the right-handed electron are derived, taking into account the limits on M_2 as a function of m_0 .

Contrary to the direct decays, the slepton indirect decays can be studied in any choice of the dominant coupling. As previously said, mainly the indirect decay into a neutralino (LSP) is searched for:

- indirect decay $\tilde{\nu} \rightarrow \nu \tilde{\chi}_1^0$, $\tilde{\chi}_1^0 \tilde{R}_p$ decay via any coupling,
- indirect decay $\tilde{\ell} \rightarrow \ell \tilde{\chi}_1^0$, $\tilde{\chi}_1^0 \tilde{R}_p$ decay via any coupling.

Then the final state depends on the slepton type (and flavour in case of charged sleptons), and mainly on the $\tilde{\chi}_1^0$ LSP decay. The efficiencies are determined in a $m_{\tilde{\chi}}$ versus $m_{\tilde{\nu}}$ ($m_{\tilde{\ell}}$) plane as well as the upper limit on the cross-section, which is compared to the MSSM cross-section, in order to exclude domains in the same $m_{\tilde{\chi}}$ versus $m_{\tilde{\nu}}$ ($m_{\tilde{\ell}}$) plane (see Fig. 7.14). The limit on the neutralino mass is used to set the limit on the sneutrino (slepton) mass in case of indirect decay. The results obtained on data collected in 1998, 1999 and 2000 [446, 445, 447, 448] are summarized in Table 7.11.

experiments	ALEPH	DELPHI	L3	OPAL	
DATA	1998-2000	1998-2000	1998-2000	1998-2000	
$\tilde{\nu}_{\mu,\tau}$	LLE	89	85	78	81
	$LQ\bar{D}$	78			
	$\bar{U}\bar{D}\bar{D}$	65		70	
\tilde{e}_R	LLE	96	95	79	99
	$LQ\bar{D}$	93			92
	$\bar{U}\bar{D}\bar{D}$	94	92	96	
$\tilde{\mu}_R$	LLE	96	90	87	94
	$LQ\bar{D}$	90			87
	$\bar{U}\bar{D}\bar{D}$	85	87	86	
$\tilde{\tau}_R$	LLE	95		86	92
	$LQ\bar{D}$	76			
	$\bar{U}\bar{D}\bar{D}$	70		75	

Table 7.11: 95% CL lower limits (in GeV) on the slepton mass, considering the slepton indirect decay in lepton and lightest neutralino only.

The pair production of right selectrons followed by their decay in the presence of R -parity-violating couplings has been investigated for a 500 GeV e^-e^- linear collider (with possibly highly polarized beams) in Ref. [460].

At such a collider, a very strong suppression of the Standard Model background is expected and this could be further reduced by exploiting specific beam polarizations. The conservation of electric charge and lepton number actually forbid the pair production of most of supersymmetric particles at a e^-e^- collider: only selectrons can be produced via the t -channel exchange of a neutralino. The pair production of selectrons has been studied in the hypothesis of R -parity violation. In case of LLE operator, the decay of the pair produced right selectrons will lead to final state consisting in $e^-e^- + 4\ell^\pm + E_{miss}$, where the flavour of ℓ^\pm depend on the particular

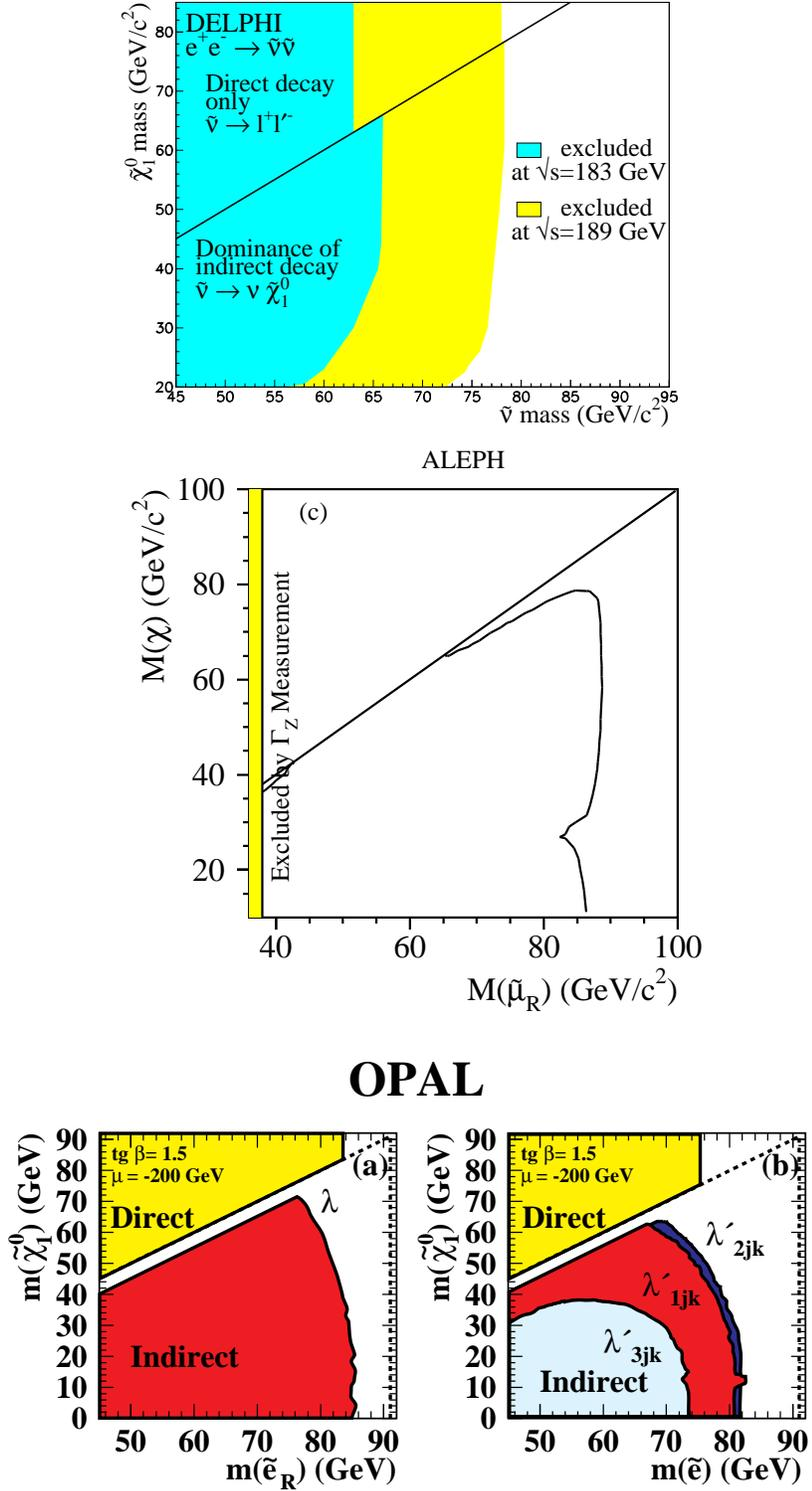


Figure 7.14: Top: Search for sneutrino decaying via a dominant $LL\bar{E}$ coupling in DELPHI; excluded region at 95% CL in $m_{\tilde{\nu}}$, $m_{\tilde{\chi}^0_1}$ plane by $\tilde{\nu}$ pair production for direct and indirect decays. The dark grey area shows the part excluded by the searches at $\sqrt{s} = 183$ GeV, the light grey area the one excluded by the searches at $\sqrt{s} = 189$ GeV. Middle: Search for smuon decaying via a dominant $\bar{U}D\bar{D}$ coupling in ALEPH; excluded region at 95% CL in $m_{\tilde{\chi}^0_1}$, $m_{\tilde{\mu}_R}$ plane. Bottom: Search for selectron decaying indirectly via a dominant $LL\bar{E}$ (left) and $LQ\bar{D}$ (right) coupling in OPAL; MSSM exclusion region for selectron pair production in the $(m_{\tilde{\chi}^0_1}, m_{\tilde{e}})$ plane at 95% CL.

type of coupling. This kind of final state is free from Standard Model background and permit an easy detection at a 500 GeV e^-e^- collider. In case of a dominant $LQ\bar{D}$ operator, the final state consists of charged leptons, multiple jets and/or missing energy, and in addition, the Majorana nature of the LSP gives rise to like-sign dilepton signal, with almost no background from Standard Model. In case of a dominant $\bar{U}\bar{D}\bar{D}$ operator, the final state consists of multiple jets associated to like-sign dielectrons. In both $LQ\bar{D}$ and $\bar{U}\bar{D}\bar{D}$ cases, it might be possible to give an estimate for the LSP mass from invariant mass reconstruction.

7.4.2 c) Squark Searches at lepton colliders

\mathcal{R}_p decays of pair-produced squarks have been searched for in e^+e^- collisions at LEP 2. Special emphasis has been given to the \tilde{t} and \tilde{b} as they could possibly be the lightest squarks.

For squarks of the third generation, the $\tilde{f}_L-\tilde{f}_R$ mixing cannot be neglected. Hence a mixing angle must be taken into account for the pair production cross-section. This parameter will consequently enter as a free parameter when deriving experimental squark mass limits.

The results obtained at LEP 2 for the searches of both squark direct and indirect decays are reviewed in the following.

For small couplings ($< O(10^{-1})$) the \tilde{t} hadronises into colourless bound states before decaying (see section 7.3.1), producing additional hadronic activity in the decay. Another consequence of the small width of the \tilde{t} indirect decay ($\tilde{t} \rightarrow c\tilde{\chi}_1^0$) is that, unusually, the direct decay dominates over the indirect decay for a large range of coupling values ($> O(10^{-5})$). On the contrary the indirect decay of the \tilde{b} ($\tilde{b} \rightarrow b\tilde{\chi}_1^0$) dominates whenever kinematically possible.

As no quark superfield enters in the $LL\bar{E}$ term of the \mathcal{R}_p superpotential, there is no direct two-body decay of squark via a λ coupling. The $LQ\bar{D}$ and $\bar{U}\bar{D}\bar{D}$ terms can be responsible for squark direct decays. In the first case, the final states consist of two jets and charged lepton(s) and/or missing energy: the three possibilities are listed in Table 7.6. In the stop pair production searches, only the channels with two charged leptons were considered. Highest efficiencies are obtained for final states containing electrons (λ'_{13k}) or muons (λ'_{23k}); final states with two taus (λ'_{33k}) are more problematic and consequently have lower efficiency and lead to weakest limits. Using the efficiencies determined for different stop masses, an upper limit on the stop pair production cross-section can be set at 95% CL as a function of the stop mass. Then, considering the cross-section for the stop pair production (e.g. in the framework of the MSSM) and in case of no mixing and maximal decoupling to the Z boson, a lower limit on the stop mass can be derived. In the tau channel, a stop mass lower than 96 GeV has been excluded by OPAL [448] for any mixing angle using the data recorded in 1999 and 2000. At a centre-of mass energy from 189 to 209 GeV, considering also the tau channel, but in a no mixing scenario, stop masses lower than 97 GeV are excluded by ALEPH [446].

Via a $\bar{U}\bar{D}\bar{D}$ term, the stop decays directly into two down quarks and the sbottom into an up and a down quark. The signature for the pair production of squarks is therefore four hadronic jets. Selections for these types of topologies rely mainly on reconstructing the mass of the decaying squark by forcing the event to four jets and forming the invariant masses between pairs of jets. For couplings involving a b-quark in the final state “b-tagging” algorithms based on requiring large impact parameter tracks are also helpful to separate signal from the large background coming from two-quark and four-quark Standard Model processes. In “flavour blind” searches, the cross-section limits degraded in the range of W mass. For direct decay via a $\bar{U}\bar{D}\bar{D}$ interaction (λ'' coupling), stop masses lower than 77 GeV have been excluded by OPAL [448] for any mixing angle using the data recorded in 1999 and 2000.

Assuming that the lightest neutralino $\tilde{\chi}_1^0$ is the LSP, the squark indirect decay into a quark and a neutralino with the subsequent \tilde{R}_p decay of the neutralino, has been studied. As any squark field can couple to the $\tilde{\chi}_1^0$, there are no restrictions related to the squark “chirality”. Final states for each coupling consist of the corresponding fermions from the neutralino pair decay plus two jets.

In case of $LL\bar{E}$ coupling, the relevant final states are two hadronic jets + 4 leptons + missing energy. Six jets are expected with a $LQ\bar{D}$ coupling, together with two charged leptons and no missing energy or 0-1 lepton + missing energy. Pure hadronic final states consisting of eight jets are expected in case of $\bar{U}\bar{D}\bar{D}$ couplings.

Using the efficiencies determined in the $(m_{\tilde{t}}, m_{\tilde{\chi}_1^0})$ plane, upper limit on the stop pair production cross-section can be derived as a function of the stop and neutralino masses (taking $\mu = -200$ GeV and $\tan\beta = 1.5$). Considering the MSSM cross-section for the stop pair production in case of no mixing and in case of a maximal decoupling to the Z boson exclusion contours were derived in the $m_{\tilde{t}}, m_{\tilde{\chi}_1^0}$ plane. By combining the exclusion contours with the result on the neutralino mass limit, a lower bound on stop mass can be derived.

From the analysis of the events collected at a centre-of-mass energy from 189 GeV to 209 GeV, in the hypothesis of a dominant $LL\bar{E}$ coupling, a left-handed stop lighter than 91 GeV at 95% CL has been excluded by ALEPH [446]. ALEPH, DELPHI and L3 have performed the search for stop and sbottom indirect decays in the hypothesis of a dominant $\bar{U}\bar{D}\bar{D}$ coupling. Using the limit on the neutralino mass (32 GeV) from the gaugino searches, DELPHI set lower bounds on the squark masses with $m_{\tilde{q}} - m_{\tilde{\chi}_1^0} > 5$ GeV (Fig. 7.15). The lower mass limit on the stop (sbottom) is 87 GeV (78 GeV) in case of no mixing, and 77 GeV in case of maximal Z-decoupling. The study of indirect decay of left-handed stop and sbottom by ALEPH lead to exclude stop and sbottom lighter than 71 GeV at 95% CL (Fig. 7.15).

In view of the limitations posed on centre-of-mass energies and luminosities by e^+e^- collider technologies, the case of a high energy $\mu^+\mu^-$ collider using storage rings has been considered. The phenomenology of supersymmetry with \tilde{R}_p at a $\mu^+\mu^-$ collider resembles very much to the one at a e^+e^- collider. R -parity violation can manifest itself via either a) pair-production of supersymmetric particles followed by \tilde{R}_p decays or b) resonant and non-resonant production of a single supersymmetric particle or finally c) virtual effects in four fermions processes. The case (a) is discussed below. The cases (b) and (c) will be discussed in sections 7.5 to 7.6.

The discussion of pair-production of supersymmetric particles followed by \tilde{R}_p decays for $\mu^+\mu^-$ colliders is analogous in most of the aspects to the one for e^+e^- colliders and can be found in 7.3. However, unlike e^+e^- colliders, a particular feature of $\mu^+\mu^-$ colliders stems from the possible s -channel production of the CP -even (h^0 and H^0) or CP -odd (A^0) Higgs bosons of e.g. the MSSM. The Higgs boson produced would then decay into a pair of supersymmetric particles in processes like $h^0(H^0, A^0) \rightarrow \tilde{\chi}^+\tilde{\chi}^-, \tilde{\chi}^o\tilde{\chi}^o, \tilde{u}^c\tilde{u}, \tilde{d}^c\tilde{d}, \tilde{l}^c\tilde{l}$, etc, where \tilde{u} and \tilde{d} denote generically up-type down-type squarks respectively. The supersymmetric particles themselves would then undergo \tilde{R}_p decays according to Table 7.2 and 7.3. The analysis of these specific pair production of supersymmetric particles is governed by the analysis of the Higgs bosons decay widths with respect to the parameters of the minimal supersymmetric extension of the Standard Model into consideration [461]. The results of this analysis have then to be merged with the more familiar analysis of pair production of supersymmetric particles from ordinary processes arising from $\mu^+\mu^-$ annihilation (either γ and Z in the s -channel or sfermions or gauginos in the t -channel) as in the case of e^+e^- annihilation.

Additional Higgs bosons decays may also come into consideration such as $H^\pm \rightarrow W^\pm h^0$, $A^0 \rightarrow Zh^0$, $H^0 \rightarrow h^0 h^0$ and $H^0 \rightarrow A^0 A^0$ which may lead to the production of a pair of

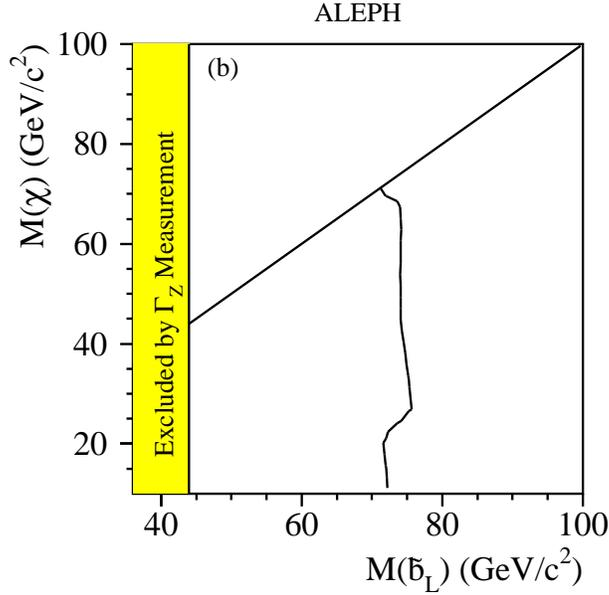
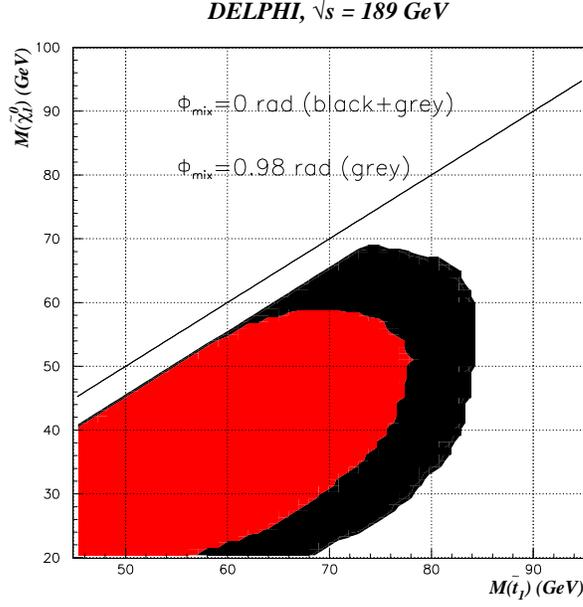


Figure 7.15: Top: Search for stop decaying indirectly via a dominant $\bar{U}\bar{D}\bar{D}$ operator in DELPHI; excluded region at 95% CL in $m_{\tilde{\chi}_0}$ versus $m_{\tilde{b}_L}$ plane; the largest excluded area corresponds to the case of no mixing and the smallest one to the case with the mixing angle which gives a minimum cross-section. Bottom: Search for left-handed sbottom decaying indirectly via a dominant $\bar{U}\bar{D}\bar{D}$ operator in ALEPH; the 95% CL exclusion cross-sections is shown in the $m_{\tilde{\chi}_0}$ versus $m_{\tilde{b}_L}$ plane.

supersymmetric particles in association with a gauge boson or to the production of four supersymmetric particles and thus to more complicated signature when \tilde{R}_p decays are switched on. We refer the reader to [461] for the calculation of the cross-section $\mu^+\mu^- \rightarrow higgs$ as well as the Higgs bosons total width.

7.4.2 d) Sfermion and Gluino Pair Production at Hadron Colliders

Following the observation of an excess of high Q^2 events at HERA experiments [462, 463], the CDF collaboration examined two scenarii with $\lambda'_{121} \neq 0$ using 107 pb^{-1} of data [464]:

$$p\bar{p} \rightarrow \tilde{g}\tilde{g} \rightarrow (c\tilde{c}_L)(c\tilde{c}_L) \rightarrow c(e^\pm d)c(e^\pm d) \quad (7.8)$$

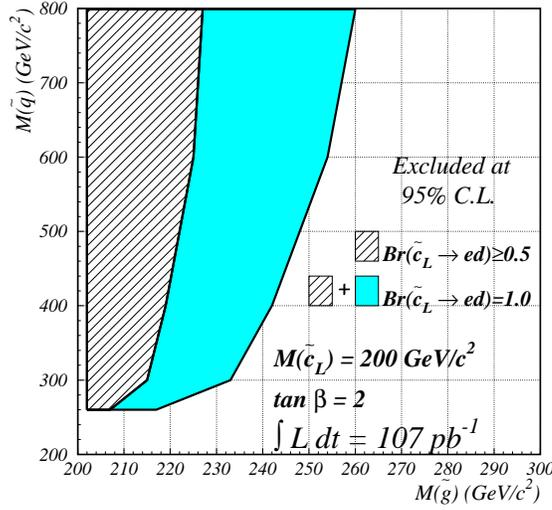


Figure 7.16: Exclusion region in the plane $m_{\tilde{g}}-m_{\tilde{q}}$ for the charm squark analysis of the CDF collaboration.

and

$$p\bar{p} \rightarrow \tilde{q}\tilde{q} \rightarrow (q\tilde{\chi}_1^0)(\bar{q}\tilde{\chi}_1^0) \rightarrow q(dce^\pm)\bar{q}(dce^\pm). \quad (7.9)$$

For process (7.8) assumptions made were $m_{\tilde{q}} > m_{\tilde{g}} > m_{\tilde{c}_L} = 200$ GeV, where degenerate mass for all up-type squarks (except \tilde{c}_L) and all right-handed down-type squarks is denoted by $m_{\tilde{q}}$. The masses of all left-handed down-type squarks were obtained by using the HERA motivated relations given in [465]. For analysing process (7.9) assumptions made were $m_{\tilde{\chi}_1^\pm} > m_{\tilde{q}} > m_{\tilde{\chi}_0}$ and $m_{\tilde{\chi}_1^\pm} \simeq 2m_{\tilde{\chi}_0}$. Five degenerate squarks and the stop were treated separately. In the case of the process involving stop to ensure 100 % branching ratio for the decay $\tilde{t}_1 \rightarrow c\tilde{\chi}_1^0$ when $m_{\tilde{t}_1} < m_t$, an additional condition that $m_{\tilde{\chi}_1^\pm} > m_{\tilde{t}_1} - m_b$ was imposed.

The Majorana nature of gluino and neutralino implies processes (7.8) and (7.9) each yield like sign dilepton and opposite sign dilepton with equal probability. Since the like-sign dilepton signature has very little SM background, for both processes (7.8) and (7.9) CDF searched for events with like sign dileptons and at least two jets.

Analysis of 107 pb^{-1} data yields no event with an expected contribution of 0.3 ± 0.3 events from backgrounds. Exclusion contours obtained for process (7.8) are shown in Fig. 7.16 in the $m_{\tilde{g}}-m_{\tilde{q}}$ plane for different assumptions for the $Br(\tilde{c}_L \rightarrow ed)$. The region below $m_{\tilde{q}} \leq 260$ GeV is not excluded because in this region \tilde{b}_L becomes lighter than \tilde{c}_L , hence suppressing the decay $\tilde{g} \rightarrow c\tilde{c}_L$. Figure 7.17 (bottom) shows the 95% CL upper limit on the cross-section times branching ratios (obtained for process (7.9)) along with the NLO prediction [466] for the cross-section, as a function of squark masses. 95% CL lower limits are given for two different masses of the lightest neutralino.

A lower limit on the degenerate squark mass was found to be in the range of 200–260 GeV depending on the mass of the lightest neutralino and gluino (range of gluino mass considered was 200–1000 GeV). Figure 7.17 (top) shows also a similar plot in the case of the stop. The mass of the stop was excluded below 135(120) GeV for a heavy (light) neutralino. The analysis for process (7.9) has been performed for the Tevatron Run II in [467]: it shows that squark masses up to 380 GeV should be tested. Finally, one point to note here is that, although the

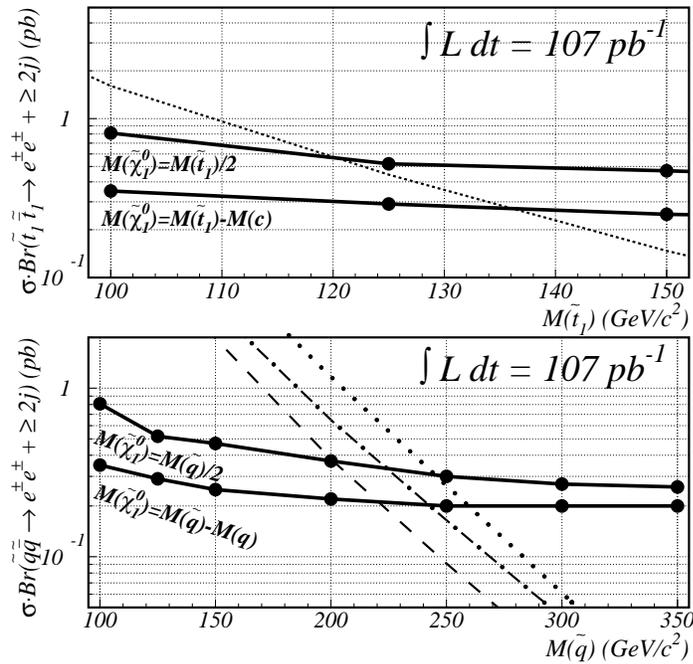


Figure 7.17: Bottom) upper limits on the cross-section times branching ratio for the production of 5 degenerate squark flavours decaying to electrons and jets via neutralinos (solid lines). Also shown is the theoretical prediction for $\sigma \cdot Br$ for three values of the gluino mass: 200 GeV (dotted line), 500 GeV (dot-dashed line), and 1 TeV (dashed line). Top) upper limits on the cross-section times branching ratio for stop pair production decaying to electrons and jets via neutralinos (solid lines). The dashed curve is the theoretical prediction.

analysis for process (7.9) assumed only one \mathcal{R}_p coupling λ'_{121} to be non-zero, as the analysis does not depend on the quark flavours, the results are equally valid for any λ'_{1jk} ($j=1, 2$ and $k=1, 2, 3$) couplings.

$D\emptyset$ [468] considered squark pair production leading in \mathcal{R}_p -SUGRA to like-sign dielectron events accompanied by jets, and has ruled out $M_{\tilde{q}} < 243$ GeV (95 % CL) when assuming five degenerate squark flavours. The $D\emptyset$ analysis covers all λ'_{1jk} couplings. From a similar analysis by CDF [469] but restricted to $\lambda'_{121} \neq 0$, one can infer that a cross-section five times smaller would lead to a $M_{\tilde{q}}$ limit of $\simeq 150$ GeV depending on the gluino and $\tilde{\chi}_0$ masses.

CDF also considered separately [469, 464] the pair production of a light stop \tilde{t}_1 assuming a decay into $c\tilde{\chi}_1^0$ and excluded $M_{\tilde{t}} < 135$ GeV. To translate this constraint in one relevant for $\lambda'_{13k} \neq 0$, it should be noted that in this latter case, \mathcal{R}_p -decays of the \tilde{t} would dominate over loop decays into $c\tilde{\chi}_1^0$. Moreover, \mathcal{R}_p -decays would themselves be negligible compared to $\tilde{t} \rightarrow b\tilde{\chi}_1^+$ decays as soon as this becomes allowed, i.e. if $M(\tilde{t}_1) > M(\tilde{\chi}_1^+)$ and if the \tilde{t}_1 eigenstate possesses a sizeable admixture of \tilde{t}_L . The subsequent decays of the $\tilde{\chi}_1^+$ would then lead to final states similar to those studied by CDF for $\tilde{t}_1 \rightarrow c\tilde{\chi}_1^0$. Thus, 130 – 150 GeV appears to be reasonable rough estimate of the Tevatron sensitivity to a light \tilde{t} for $\lambda'_{13k} \neq 0$. In summary, Tevatron and HERA sensitivities are competitive in \mathcal{R}_p -SUSY models with five degenerate squarks, but models predicting a light \tilde{t} are better constrained at HERA provided that λ'_{13j} is not too small.

In the above mentioned search by the $D\emptyset$ experiment [450] in the dimuon plus four-jets channel (occurring after $\tilde{\chi}_1^0$ decay via the λ' coupling, see section 7.4.1), it was seen that squark masses below 240 GeV (for all gluino masses and for $\tan\beta = 2$) are excluded. For equal masses of squarks and gluinos the mass limit is 265 GeV

In contrast with the above studies of the λ' coupling constants which were based on the analysis of a given superpartner pair production, the $D\emptyset$ Collaboration has performed a study of the λ'_{1jk} and λ'_{2jk} ($j=1, 2$ and $k=1, 2, 3$) couplings based on the Monte Carlo simulation of all the superpartner pair productions [467, 470]. In this work, it was assumed that the LSP is the lightest neutralino. The exclusion plot obtained in [467, 470] in the case of a single dominant \mathcal{R}_p coupling of type λ'_{1jk} is presented in Fig.7.18. In this case, the studied final state is composed of 2 e^\pm and at least 4 jets. We observe in Fig.7.18 that the $D\emptyset$ Collaboration is expected to search for squarks of mass up to 575 GeV and gluinos of mass up to 520 GeV. In the case of a single dominant \mathcal{R}_p coupling of type λ'_{2jk} , it was shown in [467, 470] that the analysis of the dimuon plus four jets signature leads to the expectation that squarks of mass up to 640 GeV and gluinos of mass up to 560 GeV will be tested by the $D\emptyset$ Collaboration during the Tevatron Run II.

7.4.3 Effects of Bilinear \mathcal{R}_p Interactions

Search for spontaneous \mathcal{R}_p violation has been performed at LEP 2 by the DELPHI experiment [471].

This search is based on the model described in Refs. [63, 64], in which \mathcal{R}_p breaking is parametrized by effective bilinear terms $\mu_i L_i H_u$ (see section 2.4 for a theoretical review of this model). The most important phenomenological implication of the model is the existence of a massless Majoron J which is the LSP. Therefore the Majoron enters in the chargino and neutralino decays and the branching ratios of these new processes depend on an effective bilinear term parameter denoted by ϵ in Refs. [63, 64, 471]. In the case where the ϵ parameter is sufficiently high, roughly for $\epsilon > 10$ GeV the chargino decay is fully dominated by the Majoron

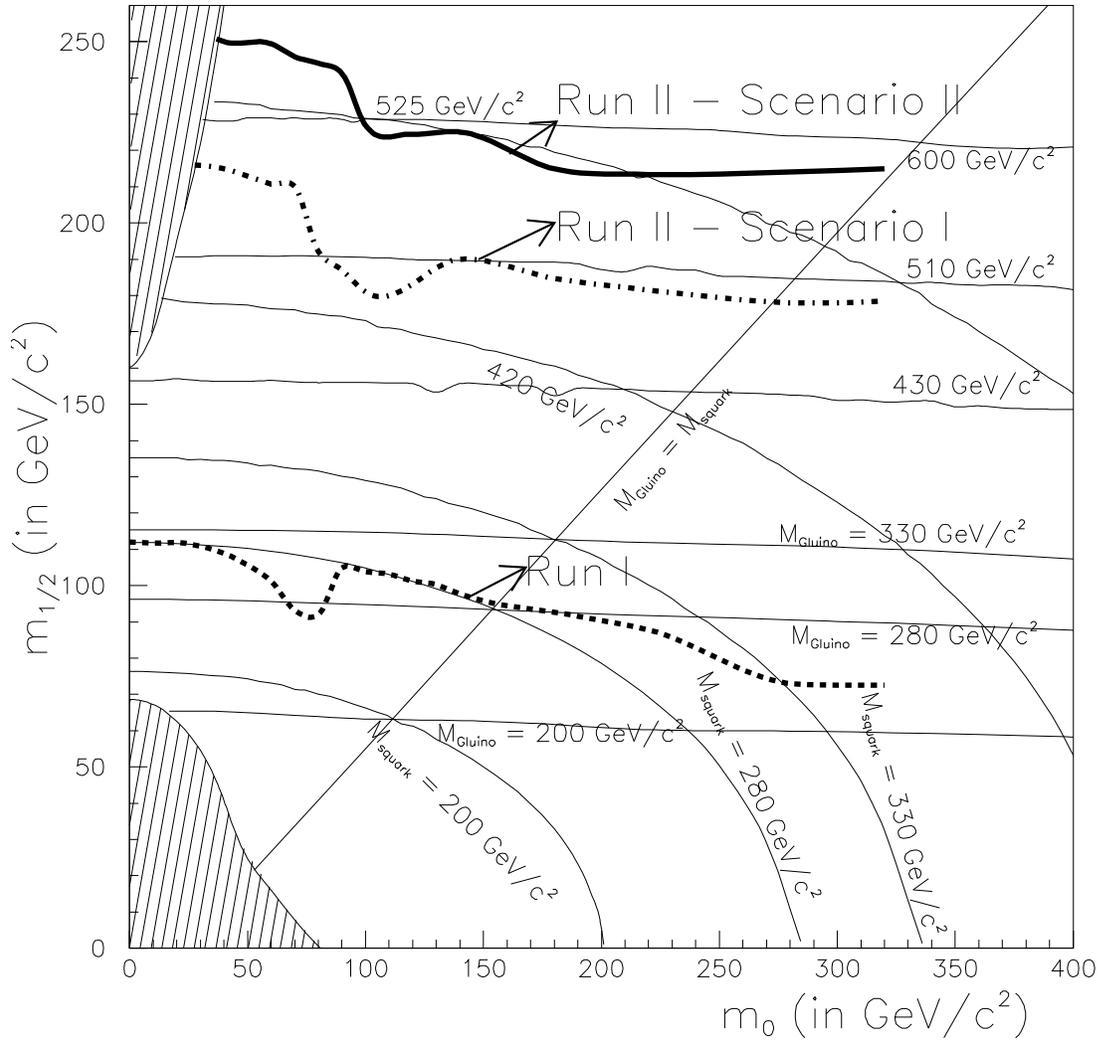


Figure 7.18: *Estimated exclusion contour for Tevatron Run I and II, within the mSUGRA framework, in the $(m_0, m_{1/2})$ plane for $\tan \beta = 2$, $A_0 = 0$ and $\mu < 0$, from the dielectron and four jets channel. Scenario I corresponds to a background of $36 \pm 4 \pm 6$ events (direct scaling from Run I) while scenario II uses the background of $15 \pm 1.5 \pm 1.5$ events (scaling, but with improvements in the detector taken into account).*

channel: $\tilde{\chi}^\pm \rightarrow \tau^\pm J$. Therefore, the experimental signature of the chargino pair production in this scenario is two acoplanar taus and missing momentum from the undetected Majorons. One should note, however, that such values of the ϵ parameter are incompatible with the cosmological bound on stable neutrino masses, and can arise only in the context of exotic scenarios with a heavy decaying neutrino ($m_\nu \sim 1$ MeV).

The search for spontaneous \mathcal{R}_p violation in DELPHI was performed in the MSSM framework [471]. An upper limit at 95% CL on the chargino production cross-section of 0.3 pb and on the chargino mass of 94 GeV (close to the kinematic limit for 1998 data) has been obtained.

Before closing the discussion on the possible effects of bilinear \mathcal{R}_p interactions at lepton colliders, it is interesting to come back to the case of resonant higgs production at $\mu^+\mu^-$ colliders discussed above in the presence of trilinear \mathcal{R}_p interactions. The effects of bilinear terms from spontaneously broken R -parity would lead to invisible signature when $h^0 \rightarrow JJ$ where J stands for the Majoron. Furthermore, possible signatures with missing energies, when for example $\mu^+\mu^- \rightarrow H^0 \rightarrow h^0 h^0$, followed by $h^0 \rightarrow JJ$ for one of the h^0 and by $h^0 \rightarrow \tilde{\chi}_1^+ \tilde{\chi}_1^-$ for the other h^0 , with the subsequent decay $\tilde{\chi}_1^+ \rightarrow \tau^+ J$, deserve further studies.

Effects of bilinear \mathcal{R}_p interactions could be observed already at existing hadron colliders. Current data from Tevatron Run I are already sensitive to these decays and effectively limits the total branching ratio of top decays in different channels than $t \rightarrow W^+ b$ to approximately 25%. The Tevatron Run II data will enhance the sensitivity for alternative top decays to branching ratios of $10^{-3} - 10^{-2}$ depending on the decay mode. If the stop is lighter than the lightest chargino it may decay dominantly through $\tilde{t}_1 \rightarrow \tau^+ + b$. By interpreting the stop as a third generation leptoquark, the exclusion obtained from leptoquark searches can in this case be applied [472, 473]. This leads to an exclusion of scalar-stop masses below 80 – 100 GeV from the Run I data. Here too, the Run II data will improve the sensitivity to a wider region of the SUSY parameter space.

7.5 Single Sparticle Production

New \mathcal{R}_p trilinear interactions enter directly in sparticle production and decays via basic tree diagrams as was illustrated in Fig. 2.1. The corresponding complete interaction Lagrangian is discussed in detail in section 2.1 and appendix B. The most striking feature of \mathcal{R}_p is to allow for single production of supersymmetric particles. For given centre-of-mass collider energies, this extends the discovery mass reach for supersymmetric matter beyond that of superpartner pair production in R -parity conserving models.

A list of the s -channel processes allowed at lowest order in e^+e^- , ep and $p\bar{p}$ collisions is given in Table 7.12. The L -violating (\mathcal{L}) term $LL\bar{E}$ couples sleptons and leptons (Fig. 2.1a). It allows for resonant production of $\tilde{\nu}$ at l^+l^- colliders and for the direct \mathcal{R}_p -decay of sleptons $\tilde{l}^\pm \rightarrow l'^\pm \nu$ and $\tilde{\nu} \rightarrow l^+l'^-$. The \mathcal{L} term $LQ\bar{D}$ couples squarks to lepton-quark pairs (Fig. 2.1b) and sleptons to quark pairs. It allows for resonant production of \tilde{q} at ep colliders and $\tilde{\nu}$ or \tilde{l}^\pm at pp colliders. Direct \mathcal{R}_p -decay of squarks via $\tilde{q} \rightarrow lq'; \nu q''$ or sleptons via \tilde{l}^\pm or $\tilde{\nu} \rightarrow qq'$ are made possible. The B -violating (\mathcal{B}) term $\bar{U}\bar{D}\bar{D}$ couples squarks to quark pairs (Fig. 2.1c). It allows for resonant production of \tilde{q} at pp colliders and direct \mathcal{R}_p -decay of squarks via $\tilde{q} \rightarrow q'q''$.

Moreover, as seen in sections 7.3.1 and 7.3.2, there is a gap between the constraints obtained via the detection of the displaced vertex and the low-energy experimental constraints on

Resonant Production of Sfermions at Colliders (lowest-order processes)			
Collider	Coupling	Sfermion Type	Elementary Process
e^+e^-	λ_{1j1}	$\tilde{\nu}_\mu, \tilde{\nu}_\tau$	$l_i^+ l_k^- \rightarrow \tilde{\nu}_j \quad i = k = 1, j = 2, 3$
$pp, p\bar{p}$	λ'_{ijk}	$\tilde{\nu}_e, \tilde{\nu}_\mu, \tilde{\nu}_\tau$	$d_k \bar{d}_j \rightarrow \tilde{\nu}_i \quad i, j, k = 1, \dots, 3$
	λ''_{ijk}	$\tilde{e}, \tilde{\mu}, \tilde{\tau}$	$u_j \bar{d}_k \rightarrow \tilde{l}_{iL} \quad i, k = 1, \dots, 3, j = 1, \dots, 2$
		$\tilde{d}, \tilde{s}, \tilde{b}$	$\bar{u}_i \bar{d}_j \rightarrow \tilde{d}_k \quad i, j, k = 1, \dots, 3, j \neq k$
ep	λ'_{1jk}	$\tilde{d}_R, \tilde{s}_R, \tilde{b}_R$	$l_1^- u_j \rightarrow \tilde{d}_{kR} \quad j = 1, 2$
	λ'_{1jk}	$\tilde{u}_L, \tilde{c}_L, \tilde{t}_L$	$l_1^+ d_k \rightarrow \tilde{u}_{jL} \quad i, j, k = 1, \dots, 3$

Table 7.12: Sfermions s -channel resonant production at colliders. Charge conjugate processes (not listed here) are also possible. Real $\tilde{\nu}$ production at an e^+e^- collider can only proceed via λ_{121} or λ_{131} . In $e\gamma$ collisions all λ_{ijk} couplings where i, j or k is equal to one can be probed. The $e\gamma$ collision mode opens new possibilities, such as the single production of the $\tilde{\nu}_e$ via λ_{i11} or the single slepton production. Single squark production is also possible via a λ'_{1jk} coupling. Real \tilde{q} production at an ep collider is possible via any of the nine λ'_{1jk} couplings.

the \mathcal{R}_p couplings. This domain can be tested through the study of the single production of supersymmetric particles. Indeed, the cross-sections of such reactions are directly proportional to a power of the relevant \mathcal{R}_p coupling constant(s), which allows to determine the values of the \mathcal{R}_p couplings. Therefore, there exists a complementarity between the displaced vertex analysis and the study of singly produced sparticles, since these two methods allow to investigate different ranges of values of the \mathcal{R}_p coupling constants.

For values beyond $\mathcal{O}(10^{-4})$, single sparticle production will allow in favorable cases to determine or constrain specific λ, λ' or λ'' couplings as will be discussed in more details in sections 7.5.1 and 7.5.2. Otherwise, the presence of such a large \mathcal{R}_p coupling will become trivially manifest through the decay of pair produced sparticles.

7.5.1 Single Sparticle Production at Leptonic Colliders

At leptonic colliders resonant (as well as non-resonant) production of single supersymmetric particles involve the λ_{ijk} couplings.

Early discussions on several R_p -violating processes at e^+e^- colliders including single supersymmetric particles production can be found in [458, 459].

At a e^+e^- leptonic colliders, the sneutrinos $\tilde{\nu}_\mu$ and $\tilde{\nu}_\tau$ can be produced at resonance through the couplings λ_{211} and λ_{311} , respectively. The sneutrino may then decay either via an \mathcal{R}_p interaction [261], for example through λ_{ijk} as, $\tilde{\nu}^i \rightarrow \bar{l}_j l_k$, or via gauge interaction as, $\tilde{\nu}_L^i \rightarrow \tilde{\chi}_a^+ l^i$, or, $\tilde{\nu}_L^i \rightarrow \tilde{\chi}_a^0 \nu_L^i$. The sneutrino partial width is given in Eq. (7.1) for the leptonic decay channel and is given in the following equation for the gauge decay channel [254]:

$$\Gamma(\tilde{\nu}_L^i \rightarrow \tilde{\chi}_a^+ l^i, \tilde{\chi}_a^0 \nu_L^i) = \frac{Cg^2}{16\pi} m_{\tilde{\nu}_L^i} \left(1 - \frac{m_{\tilde{\chi}_a^+}^2}{m_{\tilde{\nu}_L^i}^2}\right)^2, \quad (7.10)$$

where $C = |V_{a1}|^2$ for the decay into chargino and $C = |N_{a2}|^2$, for the neutralino case, with V_{a1} and N_{a2} the mixing matrix elements written in the notations of [25]. For reasonable values of λ_{ijk} (≤ 0.1) and most of the region of the supersymmetric parameter space, the decay modes of Eq. (7.10) are dominant, if kinematically accessible [474, 254]. In the SUGRA parameter space, if $m_{\tilde{\nu}_L^i} > 80$ GeV, with $M_2 = 80$ GeV, $\mu = 150$ GeV and $\tan \beta = 2$, the total sneutrino width is higher than 100 MeV which is comparable to or greater than the typical expected experimental resolutions. The cross-section formula, for the sneutrino production in the s -channel, is the following [254],

$$\sigma(e^+e^- \rightarrow \tilde{\nu}_L^i \rightarrow X) = \frac{4\pi s}{m_{\tilde{\nu}_L^i}^2} \frac{\Gamma(\tilde{\nu}_L^i \rightarrow e^+e^-)\Gamma(\tilde{\nu}_L^i \rightarrow X)}{(s - m_{\tilde{\nu}_L^i}^2)^2 + m_{\tilde{\nu}_L^i}^2 \Gamma_{\tilde{\nu}_L^i}^2}, \quad (7.11)$$

where $\Gamma(\tilde{\nu}_L^i \rightarrow X)$ generally denotes the partial width for the sneutrino decay into the final state X . At sneutrino resonance, Eq. (7.11) takes the form,

$$\sigma(e^+e^- \rightarrow \tilde{\nu}_L^i \rightarrow X) = \frac{4\pi}{m_{\tilde{\nu}_L^i}^2} B(\tilde{\nu}_L^i \rightarrow e^+e^-)B(\tilde{\nu}_L^i \rightarrow X), \quad (7.12)$$

where $B(\tilde{\nu}_L^i \rightarrow X)$ generally denotes the branching ratio for sneutrino decay into a final state X .

Diagrams for the single particle production at leptonic colliders are shown in Fig. 7.19.

The case of resonant production of single supersymmetric particles at $\mu^+\mu^-$ colliders resembles very much the one of e^+e^- colliders described above. The relevant decay widths and cross-section formulae are obtained respectively from Eq. 7.10, 7.11 and 7.12 by replacing e^+ and e^- by μ^+ and μ^- .

The gauge decays of a resonantly produced sneutrino at leptonic colliders lead to single chargino or neutralino production, or to the production of a lighter slepton in association with an electroweak gauge boson when this is kinematically allowed. Away from the sneutrino resonance, other diagrams contribute to the single production of sparticles. The t -channel exchange of a slepton can lead to single chargino or neutralino production, and the t - or u -channel exchange of a lepton allows for single slepton production.

Single chargino and neutralino productions both receive contributions from the resonant sneutrino production at e^+e^- colliders (see Fig. 7.19a and b). The single production of a chargino, $e^+e^- \rightarrow \tilde{\chi}_a^\pm l_j^\mp$ (via λ_{1j1}), receives a contribution from the s -channel exchange of a $\tilde{\nu}_{jL}$ sneutrino and another one from the exchange of a $\tilde{\nu}_{eL}$ sneutrino in the t -channel (see Fig. 7.19a). The single neutralino production, $e^+e^- \rightarrow \tilde{\chi}_a^0 \nu_j$ (via λ_{1j1}), occurs through the s -channel $\tilde{\nu}_{jL}$ sneutrino exchange and also via the exchange of a \tilde{e}_L slepton in the t -channel or a \tilde{e}_R slepton in the u -channel (see Fig. 7.19b). The single $\tilde{\chi}_1^\pm$ ($\tilde{\chi}_1^0$) production rate is reduced in the higgsino dominated region $|\mu| \ll M_1, M_2$ where the $\tilde{\chi}_1^\pm$ ($\tilde{\chi}_1^0$) is dominated by its higgsino component, compared to the wino dominated domain $|\mu| \gg M_1, M_2$ in which the $\tilde{\chi}_1^\pm$ ($\tilde{\chi}_1^0$) is mainly composed by the higgsino [475]. In addition, the single $\tilde{\chi}_1^\pm$ ($\tilde{\chi}_1^0$) production cross-section depends weakly on the sign of the μ parameter at large values of $\tan \beta$. However, as

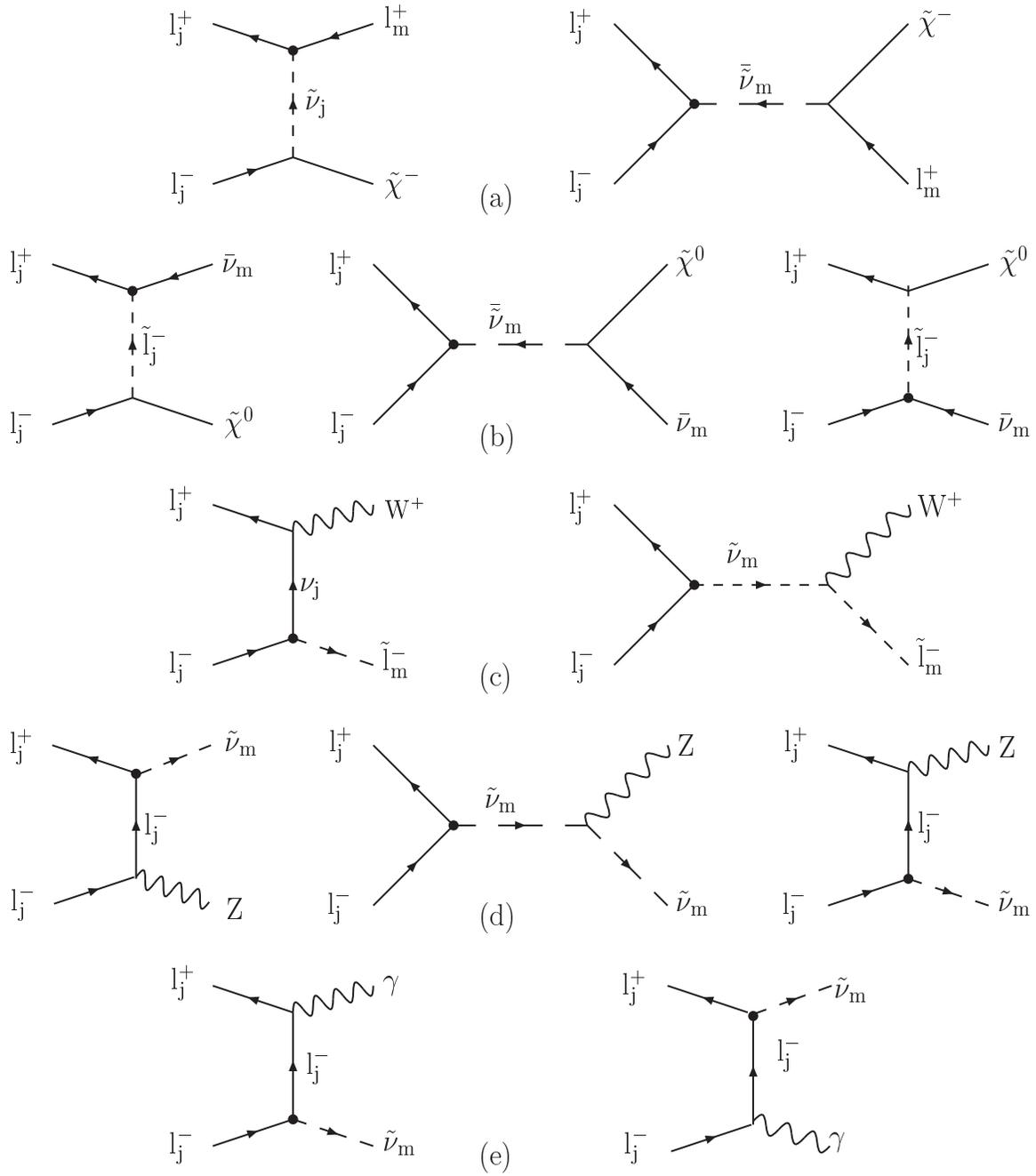


Figure 7.19: Diagrams for the single production processes at leptonic colliders, namely, $l_j^+ l_j^- \rightarrow \tilde{\chi}^- l_m^+$ (a), $l_j^+ l_j^- \rightarrow \tilde{\chi}^0 \tilde{\nu}_m$ (b), $l_j^+ l_j^- \rightarrow \tilde{l}_m^- W^+$ (c), $l_j^+ l_j^- \rightarrow \tilde{\nu}_m L Z$ (d) and $l_j^+ l_j^- \rightarrow \tilde{\nu}_m L \gamma$ (e). The circled vertex corresponds to the \tilde{R}_p interaction, with the coupling constant λ_{mjj} , and the arrows indicate the flow of the lepton number.

$\tan \beta$ decreases the rates increase (decrease) for $sign(\mu) > 0$ (< 0). This evolution of the rates with the $\tan \beta$ and $sign(\mu)$ parameters is explained by the evolution of the $\tilde{\chi}_1^\pm$ and $\tilde{\chi}_1^0$ masses in the supersymmetric parameter space [475].

For $\lambda_{1j1} = 0.05$, $50 \text{ GeV} < m_0 < 150 \text{ GeV}$ and $50 \text{ GeV} < M_2 < 200 \text{ GeV}$ in a SUGRA parameter space, the off-pole values of the cross-sections are typically [475] of the order of 100 fb (10 fb) for the single chargino production and of 10 fb (1 fb) for the single neutralino production at $\sqrt{s} = 200 \text{ GeV}$ (500 GeV) (see Fig. 7.20).

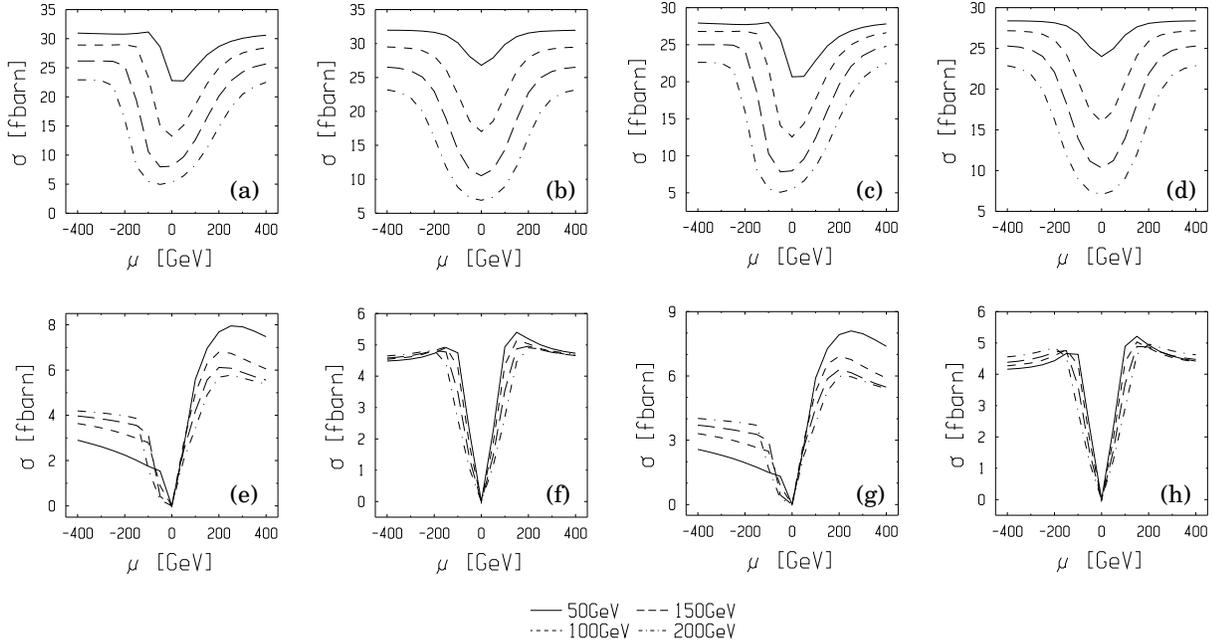


Figure 7.20: The integrated cross-sections [475] for the processes (a,b,c and d) $e^+e^- \rightarrow \tilde{\chi}_1^- l_j^+$ and (e,f,g and h) $e^+e^- \rightarrow \tilde{\chi}_1^0 \bar{\nu}_j$, at a centre-of-mass energy of 500 GeV, are shown as a function of μ for discrete choices of the remaining parameters: (a,e) $\tan \beta = 2$, $m_0 = 50 \text{ GeV}$, (b,f) $\tan \beta = 50$, $m_0 = 50 \text{ GeV}$, (c,g) $\tan \beta = 2$, $m_0 = 150 \text{ GeV}$, and (d,h) $\tan \beta = 50$, $m_0 = 50 \text{ GeV}$, with $\lambda_{1j1} = 0.05$. The windows conventions are such that $\tan \beta = 2, 50$ horizontally and $m_0 = 50, 150 \text{ GeV}$ vertically. The different curves refer to the value of M_2 of 50 GeV (continuous line), 100 GeV (dot-dashed line), 150 GeV (dotted line), as indicated at the bottom of the figure.

At the sneutrino resonance, the cross-sections of the single gaugino production are important: using Eq. (7.12), the rate for the neutralino production in association with a neutrino is of the order of $3 \cdot 10^3$ in units of the QED point cross-section, $R = \sigma_{pt} = 4\pi\alpha^2/3s$, for $M_2 = 200 \text{ GeV}$, $\mu = 80 \text{ GeV}$, $\tan \beta = 2$ and $\lambda_{1j1} = 0.1$ at $\sqrt{s} = m_{\tilde{\nu}_L^j} = 120 \text{ GeV}$ [254]. The cross-section for the single chargino production reaches $2 \cdot 10^{-1} \text{ pb}$ at $\sqrt{s} = m_{\tilde{\nu}_L^j} = 500 \text{ GeV}$, for $\lambda_{1j1} = 0.01$ and $m_{\tilde{\chi}^\pm} = 490 \text{ GeV}$ [458, 476]. The Initial State Radiation (ISR) lowers the single gaugino production cross-section at the $\tilde{\nu}$ pole but increases greatly the single gaugino production rate in the domain $m_{gaugino} < m_{\tilde{\nu}} < \sqrt{s}$. This ISR effect can be observed in Fig. 7.21 which shows the single charginos and neutralinos productions cross-sections as a function of the centre-of-mass energy for a given MSSM point [474].

The experimental searches of the single chargino and neutralino productions have been performed at the LEP collider at various centre-of-mass energies [477, 478, 479]. The off-pole effects of the single gaugino productions rates are at the limit of observability at the LEP collider

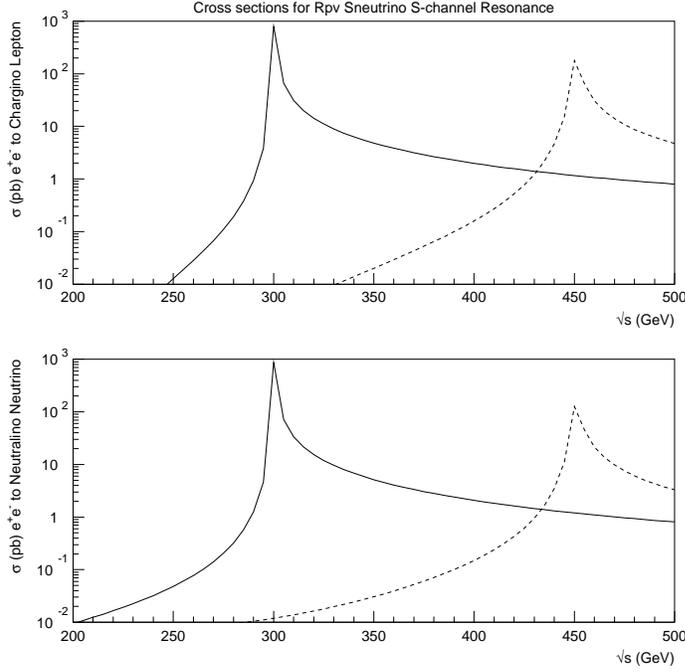


Figure 7.21: Cross sections of the single charginos and neutralinos productions as a function of the centre-of-mass energy for $m_{\tilde{\nu}} = 300$ GeV (full curves) and $m_{\tilde{\nu}} = 450$ GeV (dashed curves) with $m_{\tilde{e}} = 1$ TeV, $M_2 = 250$ GeV, $\mu = -200$ GeV, $\tan\beta = 2$ and $\lambda_{1j1} = 0.1$. The rates values are calculated by including the ISR effect and by summing over the productions of the different $\tilde{\chi}_i^\pm$ and $\tilde{\chi}_j^0$ eigenstates which can all be produced for this MSSM point.

even with the integrated luminosity of LEP 2. Therefore, the experimental analyses of the single gaugino productions have excluded values of the λ_{1j1} couplings smaller than the low-energy bounds only at the sneutrino resonance point $\sqrt{s} = m_{\tilde{\nu}}$ and, due to the ISR effect, in a range of typically $\Delta m_{\tilde{\nu}} \sim 50$ GeV around the $\tilde{\nu}$ pole. Finally, for the various sneutrino resonances, the sensitivities on the λ_{1j1} couplings which have been derived from the LEP data reach values of order 10^{-3} . The experimental analyses of the single chargino and neutralino productions will be continued at the future linear collider. Using its polarisation capability as well as the specific kinematics of the single chargino production allows to reduce the expected background from pair productions of supersymmetric particles. As an example, this background reduction allows to improve the sensitivity to the λ_{121} coupling obtained from the $\tilde{\chi}_1^\pm \mu^\mp$ production study at linear colliders [435] for $\sqrt{s} = 500$ GeV and $\mathcal{L} = 500$ fb $^{-1}$ which then amounts to values of the order of 10^{-4} at the sneutrino resonance and can improve the low-energy constraint over a range of $\Delta m_{\tilde{\nu}} \approx 500$ GeV around the $\tilde{\nu}$ pole [480]. Due to the high luminosities reached at linear colliders, the off-resonance contributions to the cross-section play an important role in the single $\tilde{\chi}_1^\pm$ production analysis.

The slepton and the sneutrino can also be singly produced via the coupling λ_{1j1} in the (non-resonant) reactions $e^+e^- \rightarrow \tilde{l}_{jL}^\mp W^\pm$, $e^+e^- \rightarrow \tilde{\nu}_L^j Z^0$ and $e^+e^- \rightarrow \tilde{\nu}_L^j \gamma$. Those reactions receive contributions from the exchange of a charged or neutral lepton of the first generation in the t - or u -channel (see Fig. 7.19). The single productions of a sneutrino accompanied by a Z or a W boson also occur through the exchange in the s -channel of a $\tilde{\nu}_L^j$ sneutrino which can not be produced on-shell. When kinematically allowed, these processes have some rates of order

100 fb at $\sqrt{s} = 200$ GeV and 10 fb at $\sqrt{s} = 500$ GeV, for $\lambda_{1j1} = 0.05$ and various masses of the scalar supersymmetric particles [475].

The production of single gaugino and the non-resonant production of single slepton (either charged or neutral) similar to those in Fig 7.21 are relevant at $\mu^+\mu^-$ colliders. The only difference stems from the initial state particles which, being muons instead of electrons, allows to test different λ couplings as given in Table 7.13.

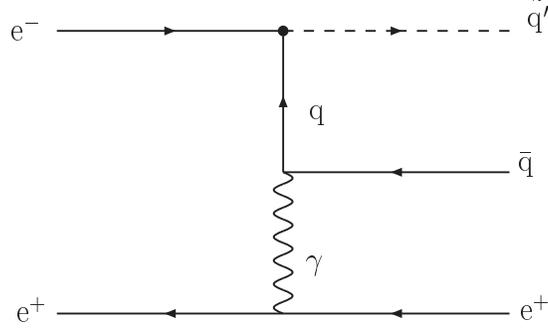
e^+e^- colliders				$\mu^+\mu^-$ colliders			
coupling	final state	exchange	channel	coupling	final state	exchange	channel
λ_{121}	$\tilde{\chi}_a^\pm \mu^\mp$	$\tilde{\nu}_e$	t	λ_{212}	$\tilde{\chi}_a^\pm e^\mp$	$\tilde{\nu}_\mu$	t
	$\tilde{\chi}_a^\pm \mu^\mp$	$\tilde{\nu}_\mu$	s		$\tilde{\chi}_a^\pm e^\mp$	$\tilde{\nu}_e$	s
	$\tilde{\chi}_b^0 \nu_\mu$	\tilde{e}	t+u		$\tilde{\chi}_b^0 \nu_e$	$\tilde{\mu}$	t+u
	$\tilde{\chi}_b^0 \nu_\mu$	\tilde{e}	s		$\tilde{\chi}_b^0 \nu_e$	$\tilde{\mu}$	s
	$\tilde{\mu}^\pm W^\mp$	ν_e	t		$\tilde{e}^\pm W^\mp$	ν_μ	t
	$\tilde{\mu}^\pm W^\mp$	$\tilde{\nu}_\mu$	s		$\tilde{e}^\pm W^\mp$	$\tilde{\nu}_e$	s
	$\tilde{\nu}_\mu Z$	e	t+u		$\tilde{\nu}_e Z$	μ	t+u
	$\tilde{\nu}_\mu Z$	$\tilde{\nu}_\mu$	s		$\tilde{\nu}_e Z$	$\tilde{\nu}_e$	s
	$\tilde{\nu}_\mu \gamma$	e	t+u		$\tilde{\nu}_e \gamma$	μ	t+u
λ_{131}	$\tilde{\chi}_a^\pm \tau^\mp$	$\tilde{\nu}_e$	t	λ_{232}	$\tilde{\chi}_a^\pm \tau^\mp$	$\tilde{\nu}_\mu$	t
	$\tilde{\chi}_a^\pm \tau^\mp$	$\tilde{\nu}_\tau$	s		$\tilde{\chi}_a^\pm \tau^\mp$	$\tilde{\nu}_\tau$	s
	$\tilde{\chi}_b^0 \nu_\tau$	\tilde{e}	t+u		$\tilde{\chi}_b^0 \nu_\tau$	$\tilde{\mu}$	t+u
	$\tilde{\chi}_b^0 \nu_\tau$	$\tilde{\tau}$	s		$\tilde{\chi}_b^0 \nu_\tau$	$\tilde{\tau}$	s
	$\tilde{\tau}^\pm W^\mp$	ν_e	t		$\tilde{\tau}^\pm W^\mp$	ν_μ	t
	$\tilde{\tau}^\pm W^\mp$	$\tilde{\nu}_\tau$	s		$\tilde{\tau}^\pm W^\mp$	$\tilde{\nu}_\tau$	s
	$\tilde{\nu}_\tau Z$	e	t+u		$\tilde{\nu}_\tau Z$	μ	t+u
	$\tilde{\nu}_\tau Z$	$\tilde{\nu}_\tau$	s		$\tilde{\nu}_\tau Z$	$\tilde{\nu}_\tau$	s
	$\tilde{\nu}_\tau \gamma$	e	t+u		$\tilde{\nu}_\tau \gamma$	μ	t+u

Table 7.13: Resonant and non-resonant single production of gauginos and sleptons at e^+e^- colliders and $\mu^+\mu^-$ colliders. The indices a and b run as follow $a = 1, 2$ and $b = 1, 4$. The $\tilde{\chi}_a^\pm$ and the $\tilde{\chi}_b^0$ can further cascade decay through ordinary gauge decays till either the $\tilde{\chi}_1^\pm$ or the $\tilde{\chi}_1^0$ is reached. The $\tilde{\chi}_1^\pm$ can either decay into $W^\pm \tilde{\chi}_1^\pm$ or via virtual sfermion exchange and then with the λ coupling involved in the single production. The $\tilde{\chi}_1^0$ can also further decay with the λ coupling involved in the single production. The sleptons can also decay either directly via the λ coupling involved in their single production or into leptons and gauginos followed by the gauginos decay via the same λ coupling. The multilepton final state can then be deduced using Table 7.2 and Table 7.3.

Leptonic colliders allows also for lepton-photon collisions in which sleptons and squarks can also be singly produced thus opening additional perspectives for \mathcal{R}_p coupling studies. For example [481] the processes $e^\pm \gamma \rightarrow l^\pm \tilde{\nu}, \tilde{l}^\pm \nu$, involving an on-shell photon radiated from one of the colliding leptons, allow to probe the $\lambda_{122}, \lambda_{123}, \lambda_{132}, \lambda_{133}$ and λ_{231} \mathcal{R}_p couplings which are otherwise not involved in the single sparticle productions from e^+e^- reactions.

The slepton or sneutrino production occurs either via the exchange of a charged lepton in the s -channel or the exchange of a charged slepton or lepton in the t -channel. Since the t -channel

Figure 7.22: Example diagram for single squark production in electron-photon collisions.



is dominant and $m_{\tilde{\tau}} \gg m_t$, the slepton production is about two order of magnitude less than the sneutrino production which is $\sigma(e^+e^- \rightarrow \tilde{\nu}_j e \tau) = 300 \text{ fb}$ at $\sqrt{s} = 500 \text{ GeV}$.

In lepton-photon collisions, single squark production occurs via λ' couplings as shown for example in Fig. 7.22 for $e\gamma$ collisions. When the produced squark directly decays via λ' into a lepton and a quark the final state consists of one hard mono-jet with one well isolated energetic electron, and eventually a soft jet in the forward region of the detector in the case where the initial electron which scatters the quasi real photon escapes detection.

7.5.2 Single Sparticle Production at Lepton-Hadron Colliders

An lp collider provides both leptonic and baryonic quantum numbers in the initial state and is thus ideally suited for \mathcal{R}_p SUSY searches involving λ'_{ijk} . Among the twenty-seven possible λ'_{ijk} couplings, each of the nine couplings with $i = 1$ can lead to direct squark resonant production through e - q fusion at an ep collider such as HERA. The phenomenology of such processes was first investigated theoretically in Refs. [482, 483, 484, 485]. Search strategies taking into account in general the indirect \mathcal{R}_p squark decay modes were discussed in Refs. [485, 486, 487].

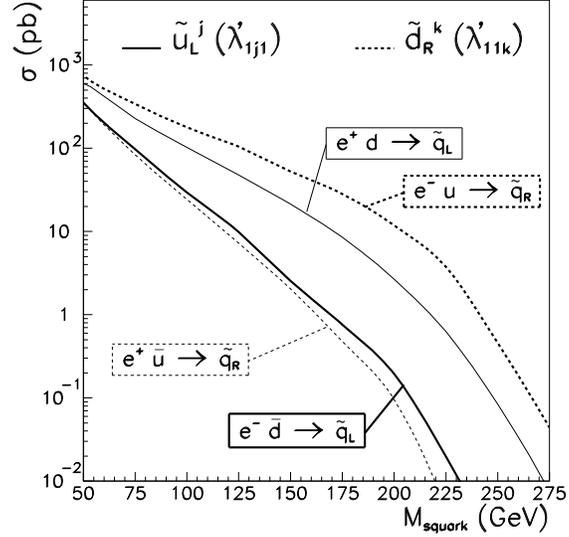
The production processes are listed in Table 7.14 in the case of an incident e^+ beam.

λ'_{1jk}	production process	
111	$e^+ + \bar{u} \rightarrow \tilde{d}_R$	$e^+ + d \rightarrow \tilde{u}_L$
112	$e^+ + \bar{u} \rightarrow \tilde{s}_R$	$e^+ + s \rightarrow \tilde{u}_L$
113	$e^+ + \bar{u} \rightarrow \tilde{b}_R$	$e^+ + b \rightarrow \tilde{u}_L$
121	$e^+ + \bar{c} \rightarrow \tilde{d}_R$	$e^+ + d \rightarrow \tilde{c}_L$
122	$e^+ + \bar{c} \rightarrow \tilde{s}_R$	$e^+ + s \rightarrow \tilde{c}_L$
123	$e^+ + \bar{c} \rightarrow \tilde{b}_R$	$e^+ + b \rightarrow \tilde{c}_L$
131	$e^+ + \bar{t} \rightarrow \tilde{d}_R$	$e^+ + d \rightarrow \tilde{t}_L$
132	$e^+ + \bar{t} \rightarrow \tilde{s}_R$	$e^+ + s \rightarrow \tilde{t}_L$
133	$e^+ + \bar{t} \rightarrow \tilde{b}_R$	$e^+ + b \rightarrow \tilde{t}_L$

Table 7.14: Direct resonant production of squarks at an ep collider via a \mathcal{R}_p λ'_{1jk} coupling. The processes are listed for an incident e^+ beam. Charge conjugate processes are accessible for an incident e^- beam.

In e^+p collisions, the production of \tilde{u}_L^j squarks of the j^{th} generation via λ'_{1j1} is especially interesting as it involves a valence d quark of the incident proton. In contrast, for e^-p collisions where charge conjugate processes are accessible, the λ'_{11k} couplings become of special interest

Figure 7.23: Squark production cross-sections in $e^\pm p$ collisions calculated [487] for a coupling $\lambda' = 0.1$ and a collider centre-of-mass energy of $\sqrt{s_{ep}} = 300$ GeV.

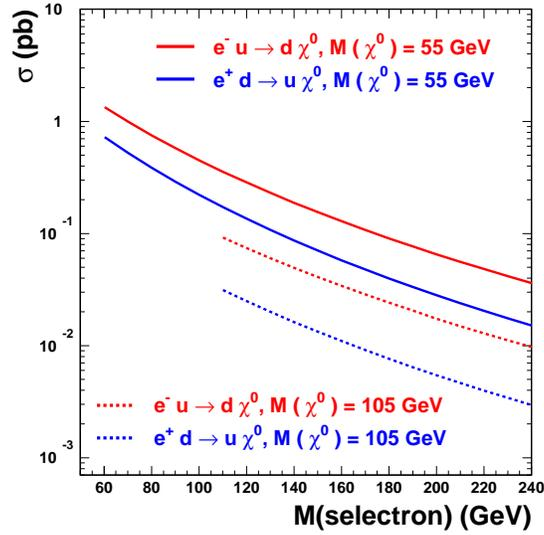


as they allow for the production, involving a valence u quark, of \tilde{d}_R^k squarks of the k^{th} generation. As an illustration, the Fig. 7.23 shows the production cross-sections in $e^\pm p$ collisions for the “up”-like squarks \tilde{u}_L^j via λ'_{1j1} ($j = 1 \dots 3$) compared to that for the “down”-like squarks \tilde{d}_R^k via λ'_{11k} ($k = 1 \dots 3$). The cross-sections are calculated [487] for coupling values of $\lambda' = 0.1$ and for an available centre-of-mass energy of $\sqrt{s_{ep}}$ of 300 GeV characteristic of the HERA collider. By gauge symmetry, only \tilde{u}_L -like or \tilde{d}_R -like squarks (or their charge conjugates) can be produced in ep collisions. Since superpartners of left- and right-handed fermions may have different allowed or dominant decay modes, the dichotomy between the resonant production of \tilde{u}_L -like squarks in e^+p collisions and that of \tilde{d}_R -like squarks in e^-p collisions implies that the detailed analysis will differ between e^- and e^+ incident beams.

In the case of a direct \tilde{R}_p decay through a λ' coupling, the squarks which have been resonantly produced in ep collisions behave as leptoquarks [488]. The \tilde{u}_L may couple to an $e^+ + d$ pair via a Yukawa coupling λ'_{111} in a way similar to the coupling of the first generation $\tilde{S}_{1/2,L}$ leptoquark of charge $|Q_{em}| = 2/3$. Via the same coupling, the \tilde{d}_R couples to $e^- + u$ or $\nu_e + d$ pairs, thus behaving like the first-generation $S_{0,L}$ leptoquark of charge $|Q_{em}| = 1/3$. As a general consequence, it is possible to translate constraints on the λ couplings of leptoquarks into constraints on the λ'_{1jk} couplings of squarks in R_p -violating supersymmetry. For real squark production, this translation is limited to coupling values $\lambda' \gtrsim \sqrt{4\pi\alpha}$. For smaller values, the branching ratio into leptoquark-like final states rapidly drops as squarks will prefer indirect \tilde{R}_p decays. Such a re-interpretation of leptoquark constraints from early HERA data has been performed in Refs. [489, 490, 491]. For virtual squark exchange in the case where $M_{\tilde{q}} \gg \sqrt{s_{ep}}$, constraints can be established via four-fermion leptoquark-like contact interaction analysis as will be discussed in section 7.6.1.

In the case of indirect \tilde{R}_p decays, the squarks in a first stage decay through gauge couplings into a quark and a gaugino-higgsino ($\tilde{\chi}^0, \tilde{\chi}^\pm$) or, if $M_{\tilde{g}} \ll M_{\tilde{q}}$, into a quark and a gluino. Such squark decays involving \tilde{R}_p couplings were discussed in detail in section 7.3. Here again, at an ep collider, the dichotomy between the production of \tilde{u}_L and \tilde{d}_R will have important phenomenological consequences. While the \tilde{u}_L might decay via $\tilde{u}_L \rightarrow u\tilde{\chi}_l^0$ or $\tilde{\chi}_m^+$, the \tilde{d}_R mainly decays via $\tilde{d}_R \rightarrow d\tilde{\chi}_l^0$, the \tilde{b}_R decay into a chargino being also possible via the higgsino component of the latter.

Figure 7.24: Cross-sections for $\tilde{\chi}^0$ production in $e^\pm p$ collisions from t -channel selectron exchange calculated [492] for a coupling $\lambda'_{1j1} = 0.5$ and for collider centre-of-mass energy of $\sqrt{s_{ep}} = 300$ GeV.



Depending on the mixing parameters in the neutralino and chargino sectors, the dominating event topologies to be expected might depend on whether the collider is running in e^+p or in e^-p mode. Decays of $\tilde{\chi}^0$ and $\tilde{\chi}^+$ mass eigenstates were discussed in detail in section 7.3.

Detailed discussion on the event topologies expected at an ep collider for single squark production in the presence of \tilde{R}_p couplings can be found in Refs. [485, 486, 487].

Real or virtual squark exchange in the s -channel contributes to the single production of neutralinos or charginos. These can also be singly produced via \tilde{R}_p interactions in lowest order processes involving sleptons or sneutrinos. The $\tilde{\chi}^0$ can be produced via t -channel slepton exchange or via u -channel squark exchange. The $\tilde{\chi}^+$ can be produced via t -channel sneutrino exchange.

The Fig. 7.24 shows the neutralino production cross-sections in $e^\pm p$ collisions expected for a coupling value $\lambda'_{1jk} = 0.5$ and for an available centre-of-mass energy of $\sqrt{s_{ep}}$ of 300 GeV characteristic of the HERA collider. The cross-sections are calculated [492] for selectron exchange only in the framework of the MSSM augmented by a single non-vanishing λ' coupling, for two values of $M_{\tilde{\chi}^0}$ and for $\tan\beta = 1$. Such cross-sections could be expected in case $M_{\tilde{e}} \ll M_{\tilde{q}}$. When both s -channel \tilde{q} exchange and t -channel \tilde{e} contribute, the interference between these cannot be neglected. For example at HERA II, constructive interference between squark and selectron exchange processes could contribute [492] up to 20% of the total $\tilde{\chi}^0$ production

Searches for single squark production have been performed at HERA_I under the hypothesis of a single dominant λ'_{1jk} coupling. The constraints obtained [493, 494, 495] by the H1 experiment are shown in Fig. 7.25. Similar results were obtained [496] by the ZEUS experiment. All possible event topologies (multijets and lepton and/or missing energy) resulting from the direct or indirect sparticle decays involving such coupling have been considered in the analysis. The HERA_I results are compared to the best existing indirect bounds [259] from low-energy experiments. The λ'_{111} coupling is seen to be very severely constrained by the non-observation of neutrinoless double-beta decay. The most stringent low-energy constraints on λ'_{121} and λ'_{131} come from atomic-parity violation measurements. From these HERA I results, it can be inferred that HERA II could offer a sensitivity reach beyond the domain excluded by indirect constraints for 2nd and 3rd generation squarks.

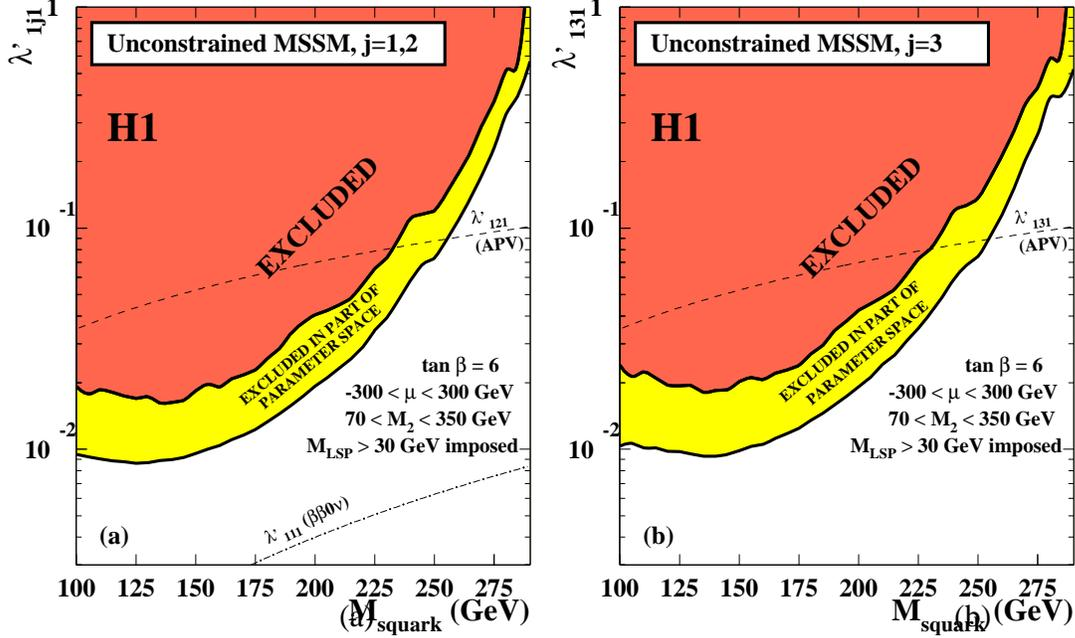


Figure 7.25: Upper Limits (95% CL) on a) the coupling λ'_{1j1} with $j = 1, 2$ and b) λ'_{131} as a function of the squark mass for $\tan \beta = 6$ in the unconstrained MSSM. The limits are obtained from a scan of the μ and M_2 parameters within $-300 < \mu < 300$ GeV and $70 < M_2 < 350$ GeV and imposing that the lightest sparticle (LSP) has a mass M_{LSP} above 30 GeV. The dark shaded area is excluded for any parameter values. The light shaded area is excluded for some parameters values. The dashed-dotted curve is the indirect upper bound [259] on λ'_{111} derived from constraints on neutrinoless double-beta decays [497, 498]. The dashed curves are the indirect upper bounds [259] on λ'_{1j1} derived from constraints on atomic-parity violation [499].

The HERA results analysed in the framework of \tilde{R}_p mSUGRA are shown in Fig. 7.26 and compared to complementary \tilde{R}_p SUSY searches made at LEP 2 and Tevatron Run I colliders. The searches were performed here also under the hypothesis of a single dominant λ'_{1jk} coupling. The results are presented as excluded domains in the parameter space of the model. The constraints from the $D\emptyset$ [468] experiment at the Tevatron were obtained from a search for \tilde{q} pair production through gauge couplings. The $D\emptyset$ analysis profits in this framework from an approximate mass degeneracy implicitly extended to five \tilde{q} flavours ($\tilde{d}, \tilde{u}, \tilde{s}, \tilde{c}, \tilde{b}$) and both (partners) chiralities (\tilde{q}_L, \tilde{q}_R). The \tilde{R}_p couplings are assumed to be significantly smaller than the gauge couplings, so that direct \tilde{R}_p decays are suppressed and each squark rather decays back into a quark and the LSP through gauge couplings. The only effect of the \tilde{R}_p couplings is then to make the LSP unstable. The $D\emptyset$ analysis is further restricted to \tilde{R}_p coupling values $\gtrsim 10^{-3}$ to guarantee a negligible decay length of the LSP. In the domains considered, the LSP is almost always the lightest neutralino $\tilde{\chi}_1^0$. The $\tilde{\chi}_1^0$ decays via λ'_{1jk} into a first-generation lepton (e or ν_e) and two quarks. The analysis is restricted to $j = 1, 2$ and $k = 1, 2, 3$ and, in practice, the $D\emptyset$ selection of event candidates requires like-sign di-electrons accompanied by multiple jets. The constraints from the L3 experiment at LEP were obtained from a search for pair production through gauge couplings of neutralinos ($e^+e^- \rightarrow \tilde{\chi}_m^0 \tilde{\chi}_n^0$ with $m = 1, 2$ and $n = 1, \dots, 4$), charginos ($e^+e^- \rightarrow \tilde{\chi}_1^+ \tilde{\chi}_1^-$) and scalar leptons ($e^+e^- \rightarrow \tilde{l}_R^+ \tilde{l}_R^-, \tilde{\nu} \tilde{\nu}$). The \tilde{R}_p couplings contribute here again in opening new decay modes for the sparticles. A negligible decay length of the sparticles through these decay modes is ensured by restricting the analysis to coupling values $\gtrsim 10^{-5}$. All possible event topologies (multijets and lepton and/or missing energy) resulting from the direct or indirect sparticle decays involving the λ'_{ijk} couplings have been considered in

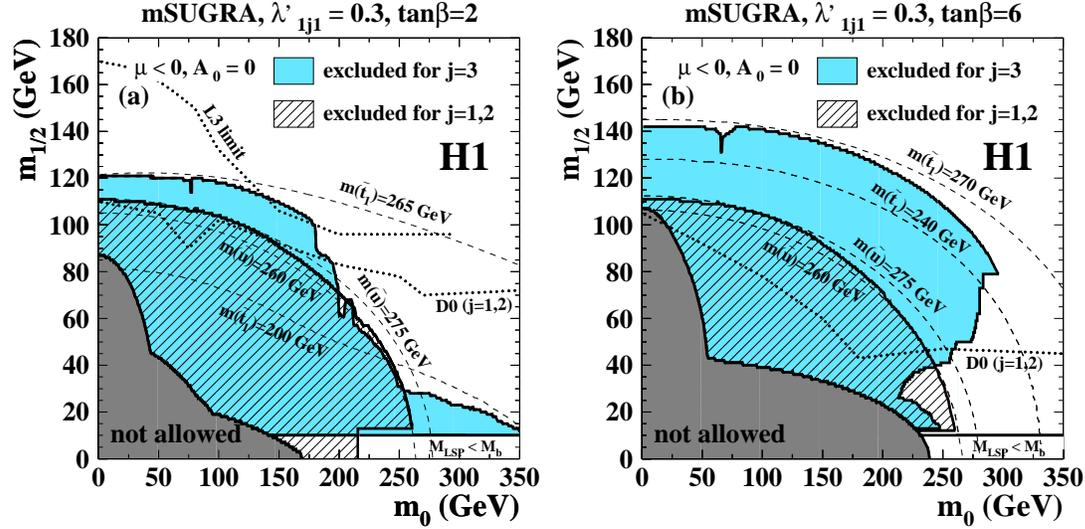


Figure 7.26: Constraints on squark production via λ'_{1j1} in R_p -violating SUSY in the parameter space of Minimal Supergravity. Excluded domains obtained by the H1 [495] (shaded area) and D0 (dotted curves) experiments are shown for a) $\tan \beta = 2$ and b) $\tan \beta = 6$. In a) the limit obtained by the L3 experiment at LEP 2 is also shown as the upper dotted curve. Contours of constant values for the light stop mass are drawn as dashed curves. The shaded region marked “not allowed” corresponds to points in the parameter space where the radiative electroweak symmetry breaking does not occur (or which lead to unphysical Higgs or sfermion masses). Also marked as “not allowed” in this particular analysis are cases where the LSP is the sneutrino.

the L3 analysis.

For the set of mSUGRA parameters with $\tan \beta = 2$, the Tevatron experiment excludes squarks with masses $M_{\tilde{q}} < 243$ GeV (95 % CL) for any value of $M_{\tilde{g}}$ and a finite value ($\gtrsim 10^{-3}$) of λ'_{1jk} with $j = 1, 2$ and $k = 1, 2, 3$. The sensitivity decreases for the parameter set with a larger value of $\tan \beta$ due in part to a decrease of the photino component of the LSP, which implies a decrease of the branching fraction of the LSP into electrons, and in part to a softening of the final-state particles for lighter charginos and neutralinos. The best sensitivity at $\tan \beta = 2$ is offered by LEP for any of the λ'_{ijk} couplings. HERA offers a best complementary sensitivity to the coupling λ'_{131} which allows for resonant stop production via positron-quark fusion $e^+d \rightarrow \tilde{t}_1$. The HERA constraints (shown here for a coupling of electromagnetic strength, i.e. $\lambda'_{131} = 0.3$) extend beyond LEP and Tevatron constraints towards larger $\tan \beta$.

7.5.3 Single Sparticle Production at Hadron-Hadron Colliders

The SUSY particles can be produced as resonances at hadron colliders through the \tilde{R}_p interactions. This is particularly attractive as hadron colliders allow to probe for resonances over a wide mass range given the continuous energy distribution of the colliding partons. If a single \tilde{R}_p coupling is dominant, the resonant SUSY particle may decay through the same coupling involved in its production, giving a two quark final state at the partonic level. However, it is also possible that the decay of the resonant SUSY particle is mainly due to gauge interactions, giving rise to a cascade decay. A review focusing on Tevatron Run-II can be found in [467].

• Single sparticle production via λ'

First, a resonant sneutrino can be produced in $d\bar{d}$ annihilations through the constant λ'_{ijk} . The associated formula can be written as follows [500]:

$$\sigma(d_k\bar{d}_j \rightarrow \tilde{\nu}^i \rightarrow X_1X_2) = \frac{4}{9} \frac{\hat{s}}{m_{\tilde{\nu}^i}^2} \frac{\pi\Gamma_{d_k\bar{d}_j}\Gamma_f}{(\hat{s} - m_{\tilde{\nu}^i}^2)^2 + m_{\tilde{\nu}^i}^2\Gamma_{\tilde{\nu}^i}^2}, \quad (7.13)$$

where $\Gamma_{d_k\bar{d}_j}$, and Γ_f are the partial width of the channels, $\tilde{\nu}^i \rightarrow d_k\bar{d}_j$, and, $\tilde{\nu}^i \rightarrow X_1X_2$, respectively, $\Gamma_{\tilde{\nu}^i}$ is the total width of the sneutrino, $m_{\tilde{\nu}^i}$ is the sneutrino mass and \hat{s} is the square of the parton centre-of-mass energy. The factor $1/9$ in front is from matching the initial colours, and $\Gamma_{d_k\bar{d}_j}$ is given by,

$$\Gamma_{d_k\bar{d}_j} = \frac{3}{4}\alpha_{\lambda'_{ijk}} m_{\tilde{\nu}^i}, \quad (7.14)$$

where $\alpha_{\lambda'_{ijk}} = \lambda'^2_{ijk}/4\pi$. To compute the rate at a $p\bar{p}$ collider, the usual formalism of the parton model of hadrons can be used [501]:

$$\sigma(p\bar{p} \rightarrow \tilde{\nu}^i \rightarrow X_1X_2) = \sum_{j,k} \int_{\tau_0}^1 \frac{d\tau}{\tau} \left(\frac{1}{s} \frac{dL_{jk}}{d\tau} \right) \hat{s} \sigma(d_k\bar{d}_j \rightarrow \tilde{\nu}^i \rightarrow X_1X_2), \quad (7.15)$$

where s is the centre-of-mass energy squared, τ_0 is given by $\tau_0 = (M_{X_1} + M_{X_2})^2/s$ and τ is defined by $\tau = \hat{s}/s = x_1x_2$, x_1, x_2 denoting the longitudinal momentum fractions of the initial partons j and k , respectively. The quantity $dL_{jk}/d\tau$ is the parton luminosity defined by,

$$\frac{dL_{jk}}{d\tau} = \int_{\tau}^1 \frac{dx_1}{x_1} [f_j^h(x_1)f_k^p(\tau/x_1) + f_j^p(x_1)f_k^h(\tau/x_1)], \quad (7.16)$$

where the parton distribution $f_j^h(x_1)$ denotes the probability of finding a parton j with momentum fraction x_1 inside a hadron h , and generally depends on the Bjorken variable, Q^2 , the square of the characteristic energy scale of the process under consideration. In order to see the effects of the parton distributions on the resonant sneutrino production, some values of the rates are given in the following [502]: For instance, with an initial state $d\bar{d}$ for the hard process, the cross-section value is $\sigma(p\bar{p} \rightarrow \tilde{\nu}^i) = 8.5$ nb for a sneutrino mass of 100 GeV and a coupling, $\lambda'_{i11} = 1$ at $\sqrt{s} = 2$ TeV. For identical values of the parameters and of the centre-of-mass energy, the cross-section is $\sigma(p\bar{p} \rightarrow \tilde{\nu}^i) = 4$ nb with an initial state, $d\bar{s}$, and $\sigma(p\bar{p} \rightarrow \tilde{\nu}^i) = 0.8$ nb with an initial state, $d\bar{b}$. The charged slepton can also be produced as a resonance at hadron colliders from an initial state $u_j\bar{d}_k$ and via the constant λ'_{ijk} . The cross-section value is $\sigma(p\bar{p} \rightarrow \tilde{l}_L^i) = 2$ nb for $m_{\tilde{l}_L^i} = 100$ GeV, $\sqrt{s} = 2$ TeV and $\lambda'_{i11} = 1$ ([502, 503]).

The single production of SUSY particles via λ' occurring through *two-to-two*-body processes, offers the opportunity to study the parameter space of the \mathcal{R}_p models with a quite high sensitivity at hadron colliders.

In Fig. 7.27, all the single superpartner productions which occur via λ'_{ijk} through *two-to-two*-body processes at hadron colliders and receive a contribution from a resonant SUSY particle production are presented [504]. The spin summed amplitudes of those reactions including the higgsino contributions have been calculated in [504]. In a SUGRA model, the rates of the reactions presented in Fig. 7.27 depend mainly on the m_0 and M_2 parameters.

In Fig. 7.28, the variations of the $\sigma(p\bar{p} \rightarrow \tilde{\chi}_{1,2}^+\mu^-)$ cross-sections with m_0 for fixed values of M_2, μ and $\tan\beta$ and various \mathcal{R}_p couplings of the type λ'_{2jk} at Tevatron Run II in a SUGRA

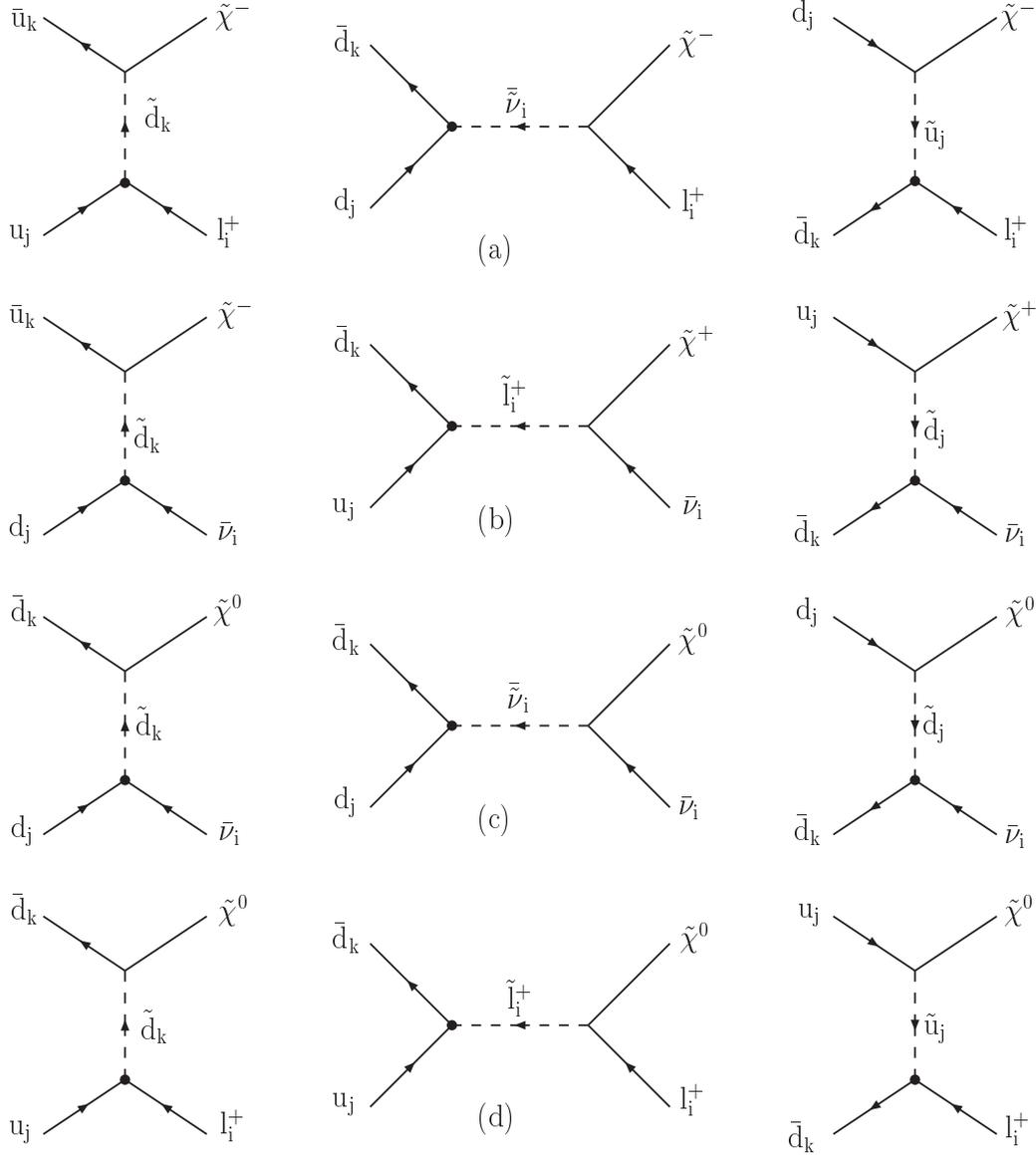


Figure 7.27: Diagrams for the four single superpartner production reactions involving λ'_{ijk} at hadron colliders which receive a contribution from a resonant supersymmetric particle production. The λ'_{ijk} coupling constant is symbolised by a small circle and the arrows indicate the flow of the lepton or baryon number.

model are shown [504]. The \mathcal{R}_p couplings giving the highest cross-sections have been considered. The $\sigma(p\bar{p} \rightarrow \tilde{\chi}_{1,2}^+ \mu^-)$ rates decrease when m_0 increases since then the sneutrino becomes heavier and more energetic initial partons are required in order to produce the resonant sneutrino. A decrease of the cross-sections also occurs at small values of m_0 , the reason being that when m_0 approaches M_2 the $\tilde{\nu}$ mass is getting closer to the $\tilde{\chi}^\pm$ masses so that the phase space factors associated to the decays $\tilde{\nu}_\mu \rightarrow \chi_{1,2}^\pm \mu^\mp$ decrease. The differences between the $\tilde{\chi}_1^+ \mu^-$ production rates occurring via the various λ'_{2jk} couplings are explained by the different partonic luminosities. Indeed, as shown in Fig. 7.27 the hard process associated to the $\tilde{\chi}_1^+ \mu^-$ production occurring through the λ'_{2jk} coupling constant has a partonic initial state $\bar{q}_j q_k$. The $\tilde{\chi}_1^+ \mu^-$ production via the λ'_{211} coupling has first generation quarks in the initial state which provide the maximum partonic luminosity.

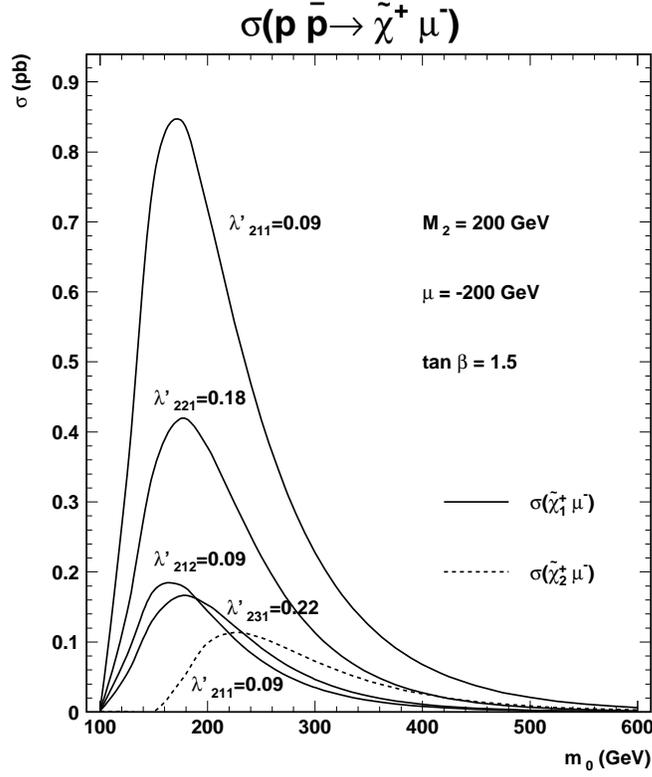


Figure 7.28: Cross-sections (in pb) of the single chargino productions $p\bar{p} \rightarrow \tilde{\chi}_{1,2}^+ \mu^-$ as a function of the m_0 parameter (in GeV). The centre-of-mass energy is taken at $\sqrt{s} = 2$ TeV and the considered set of parameters is: $\lambda'_{211} = 0.09$, $M_2 = 200$ GeV, $\tan \beta = 1.5$ and $\mu = -200$ GeV. The rates for the $\tilde{\chi}_1^+$ production via the \tilde{R}_p couplings $\lambda'_{212} = 0.09$, $\lambda'_{221} = 0.18$ and $\lambda'_{231} = 0.22$ are also given. The chosen values of the \tilde{R}_p couplings correspond to the low-energy limits for a squark mass of 100 GeV [258].

In Fig. 7.29, the variations of the rates of the reactions $p\bar{p} \rightarrow \tilde{\chi}_1^- \nu$, $p\bar{p} \rightarrow \tilde{\chi}_{1,2}^0 \mu^-$ and $p\bar{p} \rightarrow \tilde{\chi}_1^0 \nu$ with the m_0 parameter in a SUGRA model are shown [504]. From this figure one can see that the single neutralino productions do not decrease at small m_0 values in contrast with the single chargino productions (see also Fig. 7.28). This is due to the fact that in SUGRA scenarios the $\tilde{\chi}_1^0$ and \tilde{l}_L ($\tilde{l}_L = \tilde{l}_L^\pm, \tilde{\nu}_L$) masses are never close enough to induce a significant decrease of the phase space factor associated to the decay $\tilde{l}_L \rightarrow \tilde{\chi}_1^0 l$ ($l = l^\pm, \nu$). By analysing Fig. 7.28 and Fig. 7.29, one can also see that the $\tilde{\chi}^- \nu$ ($\tilde{\chi}^0 \mu^-$) production rate is larger than the $\tilde{\chi}^+ \mu^-$ ($\tilde{\chi}^0 \nu$) production rate. The explanation is that in $p\bar{p}$ collisions the initial states of the resonant charged slepton production $u_j \bar{d}_k, \bar{u}_j d_k$ have higher partonic luminosities than the initial states of the resonant sneutrino production $d_j \bar{d}_k, \bar{d}_j d_k$.

The neutralino production in association with a charged lepton via λ' (see Fig. 7.27d) is an interesting case at Tevatron [502]. The topology of the events consists of an isolated lepton in one hemisphere balanced by a lepton plus two jets in the other hemisphere, coming from the neutralino decay via λ' . The Standard Model background arising from the production of two jets plus a Z^0 , decaying into two leptons, has a cross-section of order 10^{-3} nb [501], and can be greatly reduced by excluding lepton pairs with an invariant mass equal to the Z^0 mass. The other source of Standard Model background, which is the Drell-Yan mechanism into 2 leptons accompanied by 2 jets, is suppressed by a factor, $10^{-6}/\alpha_\lambda$. Moreover, the signal can be enhanced by looking at the invariant mass of the 2 jets and the lepton in the same hemisphere,

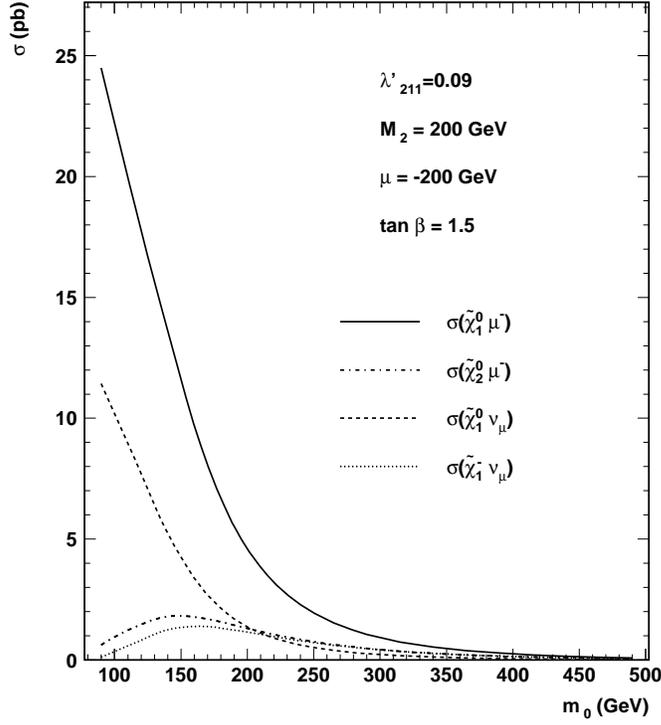


Figure 7.29: Cross-sections (in pb) of the $\tilde{\chi}_1^- \nu$, $\tilde{\chi}_{1,2}^0 \mu^-$ and $\tilde{\chi}_1^0 \nu$ productions at Tevatron Run II as a function of the m_0 parameter (in GeV). The centre-of-mass energy is taken at $\sqrt{s} = 2$ TeV and the considered set of parameters is: $\lambda'_{211} = 0.09$, $M_2 = 200$ GeV, $\tan \beta = 1.5$ and $\mu = -200$ GeV.

which should peak around the neutralino mass.

The single production via λ' of the neutralino together with a charged lepton can also generate clean signatures free from large Standard Model background, containing two like-sign charged leptons [255, 467, 505, 506, 507, 504, 508, 509]. As a matter of fact, the neutralino has a decay channel into a lepton and two jets through the coupling λ'_{ijk} and due to its Majorana nature, the neutralino decays to the charge conjugate final states with equal probability: $\Gamma(\tilde{\chi}^0 \rightarrow l_i u_j \bar{d}_k) = \Gamma(\tilde{\chi}^0 \rightarrow \bar{l}_i \bar{u}_j d_k)$. Therefore, the lepton coming from the production can have the same sign than the one coming from the neutralino decay. Since λ'_{111} has a strong indirect bound, it is interesting to consider the coupling constant λ'_{211} , which corresponds to the dimuons production with an initial state $u\bar{d}$ or $\bar{u}d$ (see Fig. 7.27d) composed of first generation quarks. The analysis of the like sign di-taus signature generated by the $\tilde{\chi}^0 \tau^\pm$ production through the λ'_{311} coupling (see Fig. 7.27d) suffers from a reduction of the selection efficiency due to the tau-lepton decay. Besides, the study of the $\tilde{\chi}_1^0 \mu^\pm$ production via λ'_{211} in a scenario where the $\tilde{\chi}_1^0$ is the LSP is particularly attractive since then the $\tilde{\chi}_1^0$ can only undergo \tilde{R}_p decays. It was found that in a SUGRA model, such a study can probe values of the λ'_{211} coupling at the 5σ discovery level down to $2 \cdot 10^{-3}$ (10^{-2}) for a muon-slepton mass of $m_{\tilde{\mu}_L} = 100$ GeV ($m_{\tilde{\mu}_L} = 300$ GeV) with $M_2 = 100$ GeV, $2 < \tan \beta < 10$ and $|\mu| < 10^3$ GeV at Tevatron Run II assuming a luminosity of $\mathcal{L} = 2 fb^{-1}$ [467, 505], and down to $2 \cdot 10^{-3}$ (10^{-2}) for $m_{\tilde{\mu}_L} = 223$ GeV ($m_{\tilde{\mu}_L} = 540$ GeV) with $m_{1/2} = 300$ GeV, $A = 300$ GeV, $\tan \beta = 2$ and $sign(\mu) > 0$ at the LHC assuming a luminosity of $\mathcal{L} = 10 fb^{-1}$ [506, 507]. It was also shown in [504], by using a detector response simulation, that the study of the single LSP production at Tevatron Run II $p\bar{p} \rightarrow \tilde{\chi}_1^0 \mu^\pm$ would al-

λ'_{211}	λ'_{212}	λ'_{213}	λ'_{221}	λ'_{222}	λ'_{223}	λ'_{231}	λ'_{232}	λ'_{233}
0.01	0.02	0.02	0.02	0.03	0.05	0.03	0.06	0.09

Table 7.15: Sensitivities on the λ'_{2jk} coupling constants for $\tan\beta=1.5$, $M_1 = 100$ GeV, $M_2 = 200$ GeV, $\mu = -500$ GeV, $m_{\tilde{q}} = m_{\tilde{t}} = 300$ GeV and $m_{\tilde{\nu}} = 400$ GeV, assuming an integrated luminosity of $\mathcal{L} = 30fb^{-1}$.

low to probe $m_{1/2}$ values up to ~ 850 GeV and m_0 values up to ~ 550 GeV at the 5σ discovery level, in a SUGRA scenario where $sign(\mu) < 0$, $A = 0$, $\tan\beta = 1.5$, $\lambda'_{211} = 0.05$ and assuming a luminosity of $\mathcal{L} = 2fb^{-1}$. In the case where one considers the Standard Model background combined with the background generated by the superpartner pair production [509], the single $\tilde{\chi}_1^0$ production study based on the like sign dilepton signature analysis still allows to test large ranges of the SUGRA parameter space at Tevatron Run II or LHC, for λ'_{211} values of the same order of its present limit.

Besides, the like sign dilepton signature analysis based on the $\tilde{\chi}_1^0\mu^\pm$ production (see Fig. 7.27d) allows the $\tilde{\chi}_1^0$ and $\tilde{\mu}_L^\pm$ mass reconstructions since the decay chain $\tilde{\mu}_L^\pm \rightarrow \tilde{\chi}_1^0\mu^\pm$, $\tilde{\chi}_1^0 \rightarrow \mu^\pm ud$ can be fully reconstructed [504, 509]. Based on the like sign dilepton signature analysis, the $\tilde{\chi}_1^0$ ($\tilde{\mu}_L^\pm$) mass can be measured with a statistical error of $\sim 11(20)$ GeV at the Tevatron Run II [504].

The single $\tilde{\chi}_1^\pm$ production in association with a charged lepton (see Fig. 7.27a) is another interesting reaction at hadron colliders. In a scenario where $\tilde{\chi}_1^0$ is the LSP and $m_{\tilde{\nu}}, m_{\tilde{t}}, m_{\tilde{q}} > m_{\tilde{\chi}_1^\pm}$, this single production receives a contribution from the resonant sneutrino production and the singly produced chargino decays into quarks and leptons with branching ratios respectively of $B(\tilde{\chi}_1^\pm \rightarrow \tilde{\chi}_1^0 d_p u_{p'}) \approx 70\%$ ($p = 1, 2, 3; p' = 1, 2$) and $B(\tilde{\chi}_1^\pm \rightarrow \tilde{\chi}_1^0 l_p^\pm \nu_p) \approx 30\%$ due to the colour factor. The neutralino decays via λ'_{ijk} either into a lepton as, $\tilde{\chi}_1^0 \rightarrow l_i u_j \bar{d}_k, \bar{l}_i \bar{u}_j d_k$, or into a neutrino as, $\tilde{\chi}_1^0 \rightarrow \nu_i d_j \bar{d}_k, \bar{\nu}_i \bar{d}_j d_k$. Hence, if both the $\tilde{\chi}_1^\pm$ and $\tilde{\chi}_1^0$ decay into charged leptons, the $\tilde{\chi}_1^\pm l_i^\mp$ production can lead to the three charged leptons signature which has a small Standard Model background at hadron colliders [510, 507, 504, 508, 511]. The study of the three leptons signature generated by the $\tilde{\chi}_1^\pm\mu^\mp$ production via the λ'_{211} coupling constant is particularly interesting for the same reasons as above. The sensitivity to the λ'_{211} coupling obtained from this study at Tevatron Run II would reach a maximum value of ~ 0.04 for $m_0 \approx 200$ GeV in a SUGRA model with $M_2 = 200$ GeV, $sign(\mu) < 0$, $A = 0$ and $\tan\beta = 1.5$, assuming a luminosity of $\mathcal{L} = 2fb^{-1}$ [504]. The sensitivities on the λ'_{2jk} couplings that can be obtained from the tripleton analysis based on the $\tilde{\chi}_1^\pm\mu^\mp$ production at the LHC for a given set of MSSM parameters are shown in Table 7.15 [510]. For each of the λ'_{2jk} couplings the sensitivity has been obtained assuming that the considered coupling was the single dominant one. The difference between the various results presented in this table is due to the fact that each λ'_{2jk} coupling involves a specific initial state (see Fig. 7.27a) with its own parton density. Besides, all the sensitivities shown in Table 7.15 improve greatly the present low-energy constraints. The tripleton analysis based on the $\tilde{\chi}_1^\pm e^\mp$ ($\tilde{\chi}_1^\pm \tau^\mp$) production would allow to test the λ'_{1jk} (λ'_{3jk}) couplings constants. While the sensitivities obtained on the λ'_{1jk} couplings are expected to be of the same order of those presented in Table 7.15, the sensitivities on the λ'_{3jk} couplings should be weaker due to the tau-lepton decay. The results presented in Table 7.15 illustrate the fact that even if some studies on the single superpartner production via λ' at hadron colliders (see Fig. 7.27) only concern the λ'_{211} coupling constant, the analysis of a given single superpartner production at Tevatron or LHC allows to probe many λ'_{ijk} coupling constants down to values smaller than the corresponding limits from low-energy data.

Besides, the three leptons final state study based on the $\tilde{\chi}_1^\pm\mu^\mp$ production (see Fig. 7.27a)

allows to reconstruct the $\tilde{\chi}_1^0$, $\tilde{\chi}_1^\pm$ and $\tilde{\nu}$ masses [510, 507, 504, 508, 511]. Indeed, the decay chain $\tilde{\nu}_i \rightarrow \tilde{\chi}_1^\pm l_i^\mp$, $\tilde{\chi}_1^\pm \rightarrow \tilde{\chi}_1^0 l_p^\pm \nu_p$, $\tilde{\chi}_1^0 \rightarrow l_i^\pm u_j d_k$ can be fully reconstructed since the produced charged leptons can be identified thanks to their flavours and signs. Based on the tripleton signature analysis, the $\tilde{\chi}_1^0$ mass can be measured with a statistical error of ~ 9 GeV at the Tevatron Run II [508, 504] and of ~ 100 MeV at the LHC [511, 507, 510]. Furthermore, the width of the Gaussian shape of the invariant mass distribution associated to the $\tilde{\chi}_1^\pm$ ($\tilde{\nu}$) mass is of ~ 6 GeV (~ 10 GeV) at the LHC for the MSSM point defined by $M_1 = 75$ GeV, $M_2 = 150$ GeV, $\mu = -200$ GeV, $m_{\tilde{f}} = 300$ GeV and $A = 0$ [511, 507, 510].

Let us make a general remark concerning the superpartner mass reconstructions based on the single superpartner production studies at hadron colliders. The combinatorial background associated to these mass reconstructions is smaller than in the mass reconstructions analyses based on the supersymmetric particle pair production since in the single superpartner production studies only one cascade decay must be reconstructed.

At hadron colliders, some supersymmetric particles can also be singly produced through *two-to-two*-body processes which generally do not receive contribution from resonant superpartner production [504]. Some single productions of squark (slepton) in association with a gauge boson can occur through the exchange of a quark in the t -channel or a squark (slepton) in the s -channel via λ'' (λ'). From an initial state g q , a squark (slepton) can also be singly produced together with a quark (lepton) with a coupling constant λ'' (λ') via the exchange of a quark or a squark in the t -channel, and of a quark in the s -channel. Finally, a gluino can be produced in association with a lepton (quark) through a coupling constant λ' (λ'') via the exchange of a squark in the t -channel (and in the s -channel).

Let us enumerate the single scalar particle and gluino productions occurring via the *two-to-two*-body processes which involve the λ'_{ijk} coupling constants [504] (one must also add the charge conjugate processes):

- The gluino production $\bar{u}_j d_k \rightarrow \tilde{g} l_i$ via the exchange of a \tilde{u}_{jL} (\tilde{d}_{kR}) squark in the t -(u -) channel.
- The squark production $\bar{d}_j g \rightarrow \tilde{d}_{kR}^* \nu_i$ via the exchange of a \tilde{d}_{kR} squark (d_j quark) in the t -(s -) channel.
- The squark production $\bar{u}_j g \rightarrow \tilde{d}_{kR}^* l_i$ via the exchange of a \tilde{d}_{kR} squark (u_j quark) in the t -(s -) channel.
- The squark production $d_k g \rightarrow \tilde{d}_{jL} \nu_i$ via the exchange of a \tilde{d}_{jL} squark (d_k quark) in the t -(s -) channel.
- The squark production $d_k g \rightarrow \tilde{u}_{jL} l_i$ via the exchange of a \tilde{u}_{jL} squark (d_k quark) in the t -(s -) channel.
- The sneutrino production $\bar{d}_j d_k \rightarrow Z \tilde{\nu}_{iL}$ via the exchange of a d_k or d_j quark ($\tilde{\nu}_{iL}$ sneutrino) in the t -(s -) channel.
- The charged slepton production $\bar{u}_j d_k \rightarrow Z \tilde{l}_{iL}$ via the exchange of a d_k or u_j quark (\tilde{l}_{iL} slepton) in the t -(s -) channel.
- The sneutrino production $\bar{u}_j d_k \rightarrow W^- \tilde{\nu}_{iL}$ via the exchange of a d_j quark (\tilde{l}_{iL} slepton) in the t -(s -) channel.

- The charged slepton production $\bar{d}_j d_k \rightarrow W^+ \tilde{l}_{iL}$ via the exchange of a u_j quark ($\tilde{\nu}_{iL}$ sneutrino) in the t -(s -) channel.

One must also add to this list the $gd_k \rightarrow t\tilde{l}_i$ reaction which occurs via the λ'_{i3k} coupling through the exchange of a d_k quark in the s -channel and a top quark in the t -channel [512].

Among these single productions only the $\bar{u}_j d_k \rightarrow W^- \tilde{\nu}_{iL}$ and $\bar{d}_j d_k \rightarrow W^+ \tilde{l}_{iL}$ reactions can receive a contribution from a resonant sparticle production. However, in most of the SUSY models, as for example the supergravity or the gauge mediated models, the mass difference between the so called left-handed charged slepton and the left-handed sneutrino is due to the D-terms so that it is fixed by the relation $m_{\tilde{l}_L^\pm}^2 - m_{\tilde{\nu}_L}^2 = \cos 2\beta M_W^2$ [513] and thus it does not exceed the W boson mass. In scenarios with large $\tan \beta$ values, a scalar particle of the third generation produced as a resonance can generally decay into the W boson due to the large mixing in the third family sfermions sector. For instance, in the SUGRA model with a large $\tan \beta$ a tau-sneutrino produced as a resonance in $d_k \bar{d}_j \rightarrow \tilde{\nu}_\tau$ through λ'_{3jk} can decay as $\tilde{\nu}_\tau \rightarrow W^\pm \tilde{\tau}_1^\mp$, $\tilde{\tau}_1^\mp$ being the lightest stau.

Similarly, the single scalar particle and gluino productions occurring via the *two-to-two*-body processes which involve the λ''_{ijk} coupling constants cannot receive a contribution from a resonant scalar particle production for low $\tan \beta$. Indeed, the only reactions among these *two-to-two*-body processes which can receive such a contribution are of the type $qq \rightarrow \tilde{q} \rightarrow \tilde{q}W$. In this type of reaction, the squark produced in the s -channel, is produced via λ''_{ijk} and is thus either a Right squark \tilde{q}_R , which does not couple to the W boson, or the squarks $\tilde{t}_{1,2}$, $\tilde{b}_{1,2}$. However, the single gluino productions occurring via the *two-to-two*-body processes which involve the λ''_{ijk} coupling constants can receive a contribution from a resonant scalar particle production.

Therefore, the single scalar particle and gluino productions occurring via the *two-to-two*-body processes are generally non resonant single superpartner productions, as already mentioned at the beginning of this section. These non resonant single superpartner productions have typically smaller cross-sections than the reactions receiving a contribution from a resonant superpartner production. For instance, with $m_{\tilde{q}} = 250$ GeV, the cross-section $\sigma(p\bar{p} \rightarrow \tilde{u}_L \mu)$ is of order $\sim 10^{-3} pb$ at a centre-of-mass energy of $\sqrt{s} = 2$ TeV, assuming an \tilde{R}_p coupling of $\lambda'_{211} = 0.09$ [504]. However, the non resonant single productions can lead to interesting signatures. For instance, the production, $q\bar{q} \rightarrow \tilde{f}W$ leads to the final state $2l + 2j + W$ for a non vanishing \tilde{R}_p coupling constant λ' and to the signature $4j + W$ for a λ'' [255]. Furthermore, the non resonant single productions are interesting as their cross-section involves only few SUSY parameters, namely one or two scalar superpartner(s) mass(es) and one \tilde{R}_p coupling constant.

The $D\emptyset$ collaboration searched for single slepton production through the λ'_{211} coupling in the two muons and two hadron jets channel [514]. In the absence of any evidence for an excess of events with respect to expectation from Standard Model processes, bounds on supergravity parameters $m_{1/2}$, m_0 have been set. Sneutrinos and smuons masses up to 280 GeV have been excluded.

• Single sparticle production via λ''

The B -violating couplings λ''_{ijk} allows for resonant production of squarks at hadron colliders. Either a squark \tilde{u}_i or \tilde{d}_k can be produced at the resonance from an initial state, $\bar{d}_j \bar{d}_k$ or $\bar{u}_i \bar{d}_j$, respectively. For $m_{\tilde{d}_R^k} = 100$ GeV, $\sqrt{s} = 2$ TeV and $\lambda''_{11k} = 1$, the rate of the down squark production at the Tevatron is $\sigma(p\bar{p} \rightarrow \tilde{d}_R^k) = 25$ nb [502].

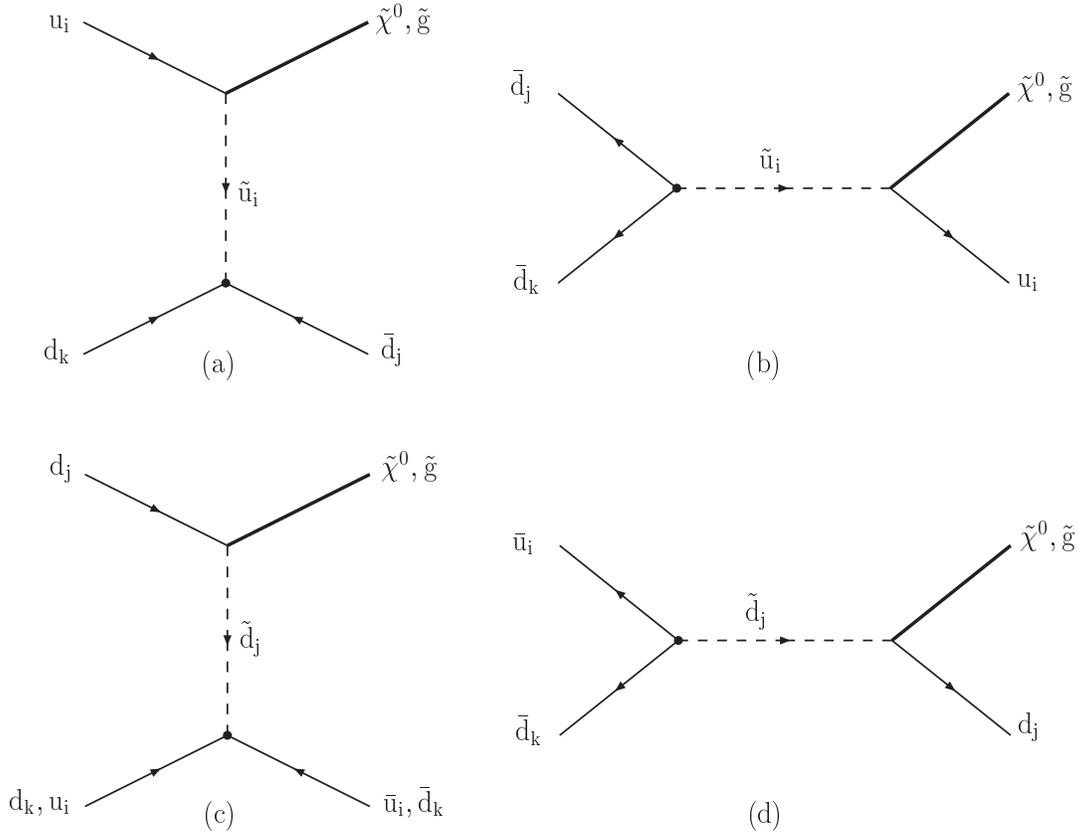


Figure 7.30: Diagrams for the single neutralino production reactions involving λ''_{ijk} at hadron colliders. The λ''_{ijk} coupling constant is symbolised by a small circle and the arrows indicate the flow of the baryon number.

For $m_{\tilde{t}_1} = 600$ GeV, $\sqrt{s} = 2$ TeV and $\lambda''_{323} = 0.1$, the rate of the resonant stop production is $\sigma(p\bar{p} \rightarrow \tilde{t}_1) = 10^{-3}$ picobarns [515]. Note that this rate is higher than the stop pair production rate at the same centre-of-mass energy and for the same stop mass, which is of order $\sigma(p\bar{p} \rightarrow \tilde{t}_1\tilde{t}_1) = 10^{-6}$ picobarns.

The single superpartner production can also occur as a *two-to-two*-body process, through an R_p coupling λ'' and an ordinary gauge interaction vertex: In baryon-number-violating models, any gaugino (including gluino) can be produced in association with a quark, in quark-quark scattering, by the exchange of a squark in the *s*-, *t*- or *u*-channel.

For example, let us consider the photino and gluino production [502]: The rate values in the *t*- and *u*-channel are, $\sigma(p\bar{p} \rightarrow \tilde{\gamma}q) = 2 \cdot 10^{-2}$ nb, and, $\sigma(p\bar{p} \rightarrow \tilde{g}q) = 3 \cdot 10^{-1}$ nb, for, $m_{\tilde{q}} = m_{\tilde{g}} = m_{\tilde{\gamma}} = 100$ GeV, $\sqrt{s} = 2$ TeV and $\lambda''_{111} = 1$. The photino or gluino which is produced will then decay into three jets via the λ'' coupling, resulting in a four jets final state. The corresponding QCD background is strong: It is estimated to be about 10 nb for $\sqrt{s} = 2$ TeV [516]. Of course, the ratio signal over background can be enhanced considerably by looking at the mass distribution of the jets: the QCD 4 jets are produced relatively uncorrelated, while the trijet mass distribution of the signal should peak around the gaugino mass. However, one of the three jets may be too soft to be measured or jet coalescence may occur, especially for small values of the gaugino mass. The study of this example bring us to the conclusion that,

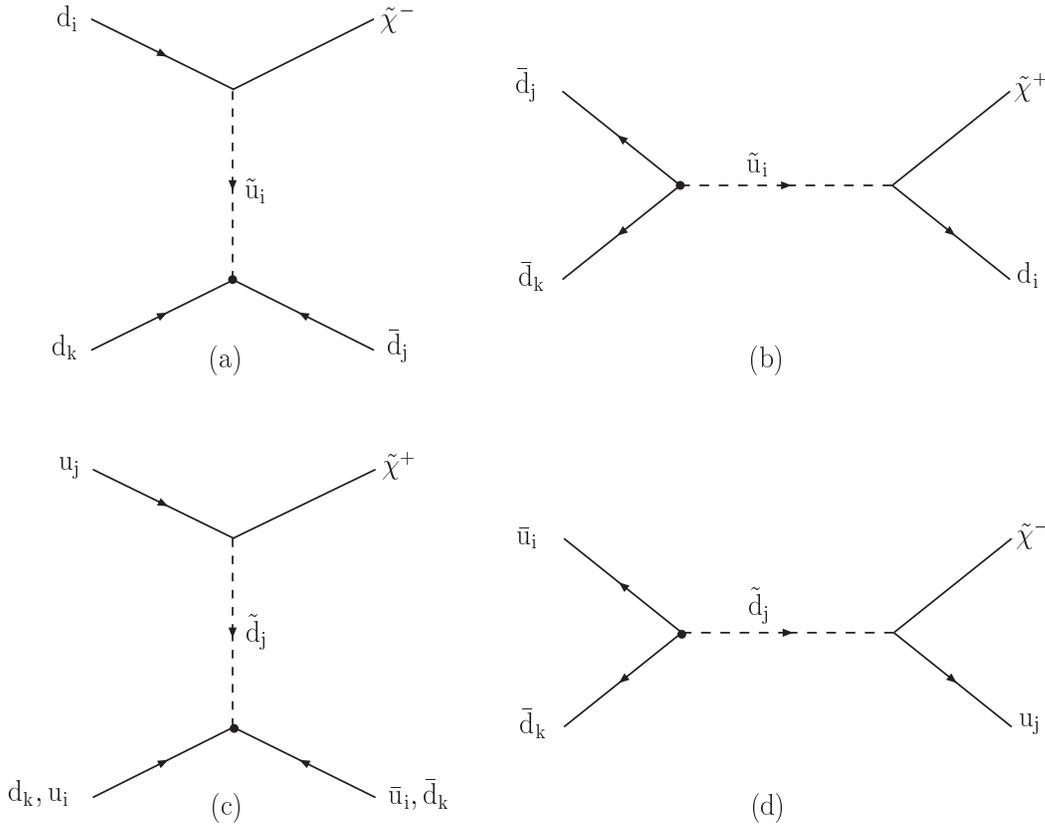


Figure 7.31: Diagrams for the single chargino production reactions involving λ''_{ijk} at hadron colliders. The λ''_{ijk} coupling constant is symbolised by a small circle and the arrows indicate the flow of the baryon number.

due to high QCD background, the analysis of the single production via λ'' remains difficult.

Nevertheless, there are some specific cases where the final state can be clear and free from a large background. For instance, a $\tilde{\chi}_1^+$ chargino can be produced via λ''_{3jk} through the resonant production of a top squark as $\bar{d}_j \bar{d}_k \rightarrow \tilde{t}_1 \rightarrow b \tilde{\chi}_1^+$, \tilde{t}_1 being the lightest top squark, and then decay into the lightest neutralino plus leptons as $\tilde{\chi}_1^+ \rightarrow \bar{l}_i \nu_i \tilde{\chi}_1^0$ [515, 467]. Due to the stop resonance, this reaction can reach high rate values. The cascade decay demands the mass hierarchy, $m_{\tilde{t}_1} > m_{\tilde{\chi}_1^+} > m_{\tilde{\chi}_1^0}$, to be respected, and by consequence is not allowed in all regions of the supergravity parameter space. Assuming λ''_{3jk} to be the single dominant \mathcal{R}_p coupling constant and the $\tilde{\chi}_1^0 = LSP$ to be lighter than the top quark, the $\tilde{\chi}_1^0$ should then be treated as a stable particle. Then, the signal for our process would be very clear since it would consist of a tagged b-quark jet, a lepton and missing transverse energy. The Standard Model background for such a signature comes from the single top quark production, via $W g$ fusion, and the production of a W gauge boson in association with $b\bar{b}$, $c\bar{c}$ or a jet faking a b-quark jet. Experimental studies lead to the conclusion that values of $\lambda'' > 0.03 - 0.2$ and $\lambda'' > 0.01 - 0.03$ can be excluded at the 95% confidence level for, $180 \text{ GeV} < m_{\tilde{t}_1} < 285 \text{ GeV}$, at the Tevatron Run I ($\sqrt{s} = 1.8 \text{ TeV}$ and $\int \mathcal{L} dt = 110 \text{ pb}^{-1}$) and for, $180 \text{ GeV} < m_{\tilde{t}_1} < 325 \text{ GeV}$, at the Run II of the Tevatron ($\sqrt{s} = 2 \text{ TeV}$ and $\int \mathcal{L} dt = 2 \text{ fb}^{-1}$), respectively. This result is based on the leading-order CTEQ-4L parton distribution functions [517] and holds for the normalisation, $\lambda'' = \lambda''_{312} = \lambda''_{313} = \lambda''_{323}$, and for the point of a minimal supergravity model,

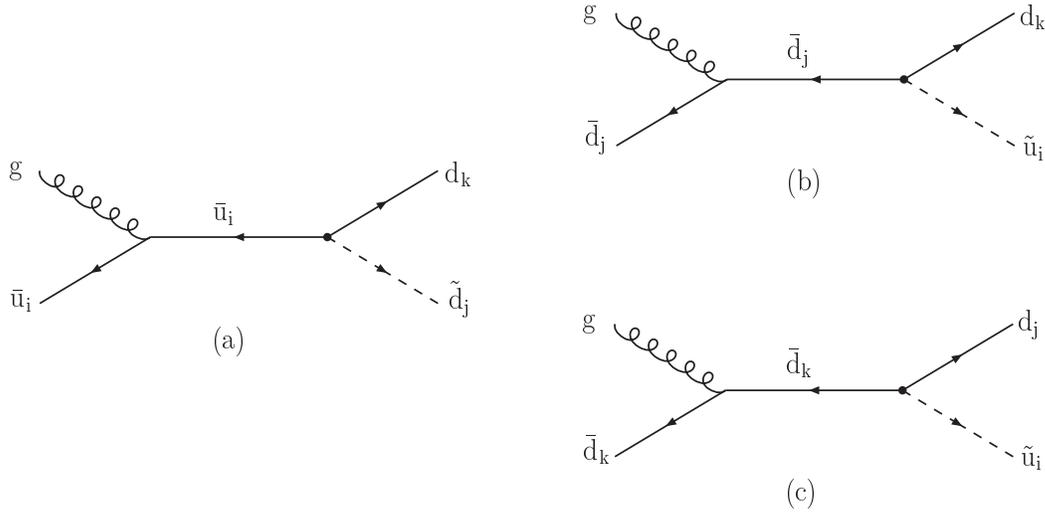


Figure 7.32: Diagrams for the resonant production of squarks involving λ''_{ijk} at hadron colliders. The λ''_{ijk} coupling constant is symbolised by a small circle and the arrows indicate the flow of the baryon number.

$m_{1/2} = 150$ GeV, $A_0 = -300$ GeV and $\tan \beta = 4$. The constraints obtained on λ'' are stronger than the present low energy bounds.

Another particularly interesting reaction has been studied in [518]: the single gluino production $\bar{d}_j \bar{d}_k \rightarrow t \tilde{g}$ which can receive a contribution from the resonant stop production via the λ''_{3jk} coupling. In certain regions of the mSUGRA parameter space, this single gluino production can reach rates at LHC of order $10^2 fb$ (for $\lambda''_{3jk} = 10^{-1}$) thanks to the contribution coming from the resonant \tilde{t}_2 production, \tilde{t}_2 being the heavier top squark. The interesting point is that in these mSUGRA domains the branching ratios of the decays $\tilde{g} \rightarrow t b \tilde{\chi}_1^\pm$ and $\tilde{g} \rightarrow t \bar{t} \tilde{\chi}_1^0$ reach also significant values thanks to the exchange of the virtual \tilde{t}_1 (the lighter top squark) which is the lighter squark and has a mixing angle near $\pi/2$. By consequence, the process $pp \rightarrow t \tilde{g}$ ($\bar{t} \tilde{g}$) can simultaneously have large cross section values at LHC and produce in a significant way a clear signature containing 3 b quarks, at least 2 charged leptons and some missing energy (due to the top quark decay $t \rightarrow b l \nu$). Since the background associated to this final state can be greatly reduced thanks to the large b -tagging efficiency available at the LHC ($\sim 50\%$), the study of the reaction $pp \rightarrow t \tilde{g}$ ($\bar{t} \tilde{g}$) should provide an effective test of the λ''_{3jk} coupling constant.

7.6 Virtual Effects involving \mathcal{R}_p Couplings

In a scenario where none of the supersymmetric particles can be directly produced at colliders with a significant cross-section, because of very high masses or unfavorable couplings with the Standard Model particles, the effects induced by \mathcal{R}_p could turn out to be felt only in indirect processes involving virtual sparticle exchange.

In contrast to single sparticle production for which a \mathcal{R}_p coupling only enter at one vertex when calculating total production rates, \mathcal{R}_p contributions (via additional sparticle exchange) to

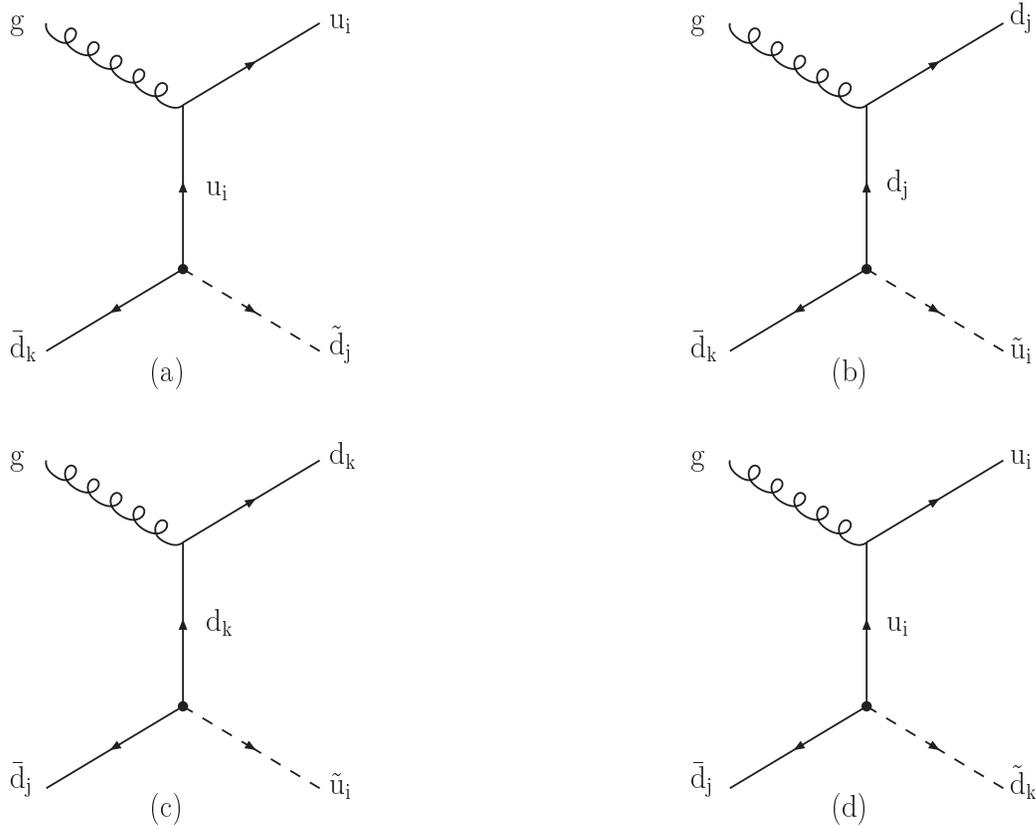


Figure 7.33: Diagrams for the non-resonant production of squarks involving λ''_{ijk} at hadron colliders. The λ''_{ijk} coupling constant is symbolised by a small circle and the arrows indicate the flow of the baryon number.

Standard Model processes are suppressed in proportion to the square of the Yukawa coupling. These processes generally imply high statistics inclusive measurements as in the case of fermion pair production and effective four-fermion contact interactions discussed in section 7.6.1.

7.6.1 Fermion Pair Production

For sparticle masses far above the kinematical reach of a given collider, \mathcal{R}_p interactions could manifest themselves through effective four-fermion contact interactions interfering with Standard Model fermion pair production processes.

At leptonic colliders dilepton production can occur in the presence of a unique (or largely dominant) \mathcal{R}_p coupling. The resonant sneutrino $\tilde{\nu}_\mu$ or $\tilde{\nu}_\tau$ production via λ_{121} or λ_{131} respectively followed by a decay through the same coupling constant (i.e. $\tilde{\nu}^i \rightarrow \bar{l}_j l_k$ via λ_{ijk}) would lead to a spectacular signature such as an excess of events Bhabha scattering events [261]. For example the cross-section of Bhabha scattering including the $\tilde{\nu}_{(\mu,\tau)}$ sneutrino s -channel exchange and the interference terms reaches 3 pb at $\sqrt{s} = m_{\tilde{\nu}_{(\mu,\tau)}} = 200$ GeV [519, 520, 521] for $\Gamma_{\tilde{\nu}_{(\mu,\tau)}} = 1$ GeV and $\lambda_{1(2,3)1} = 0.1$.

Table 7.16 shows the accessible λ couplings at e^+e^- and $\mu^+\mu^-$ colliders and fermion pair production to which a single dominant λ coupling can contribute. Except few exceptions, e^+e^-

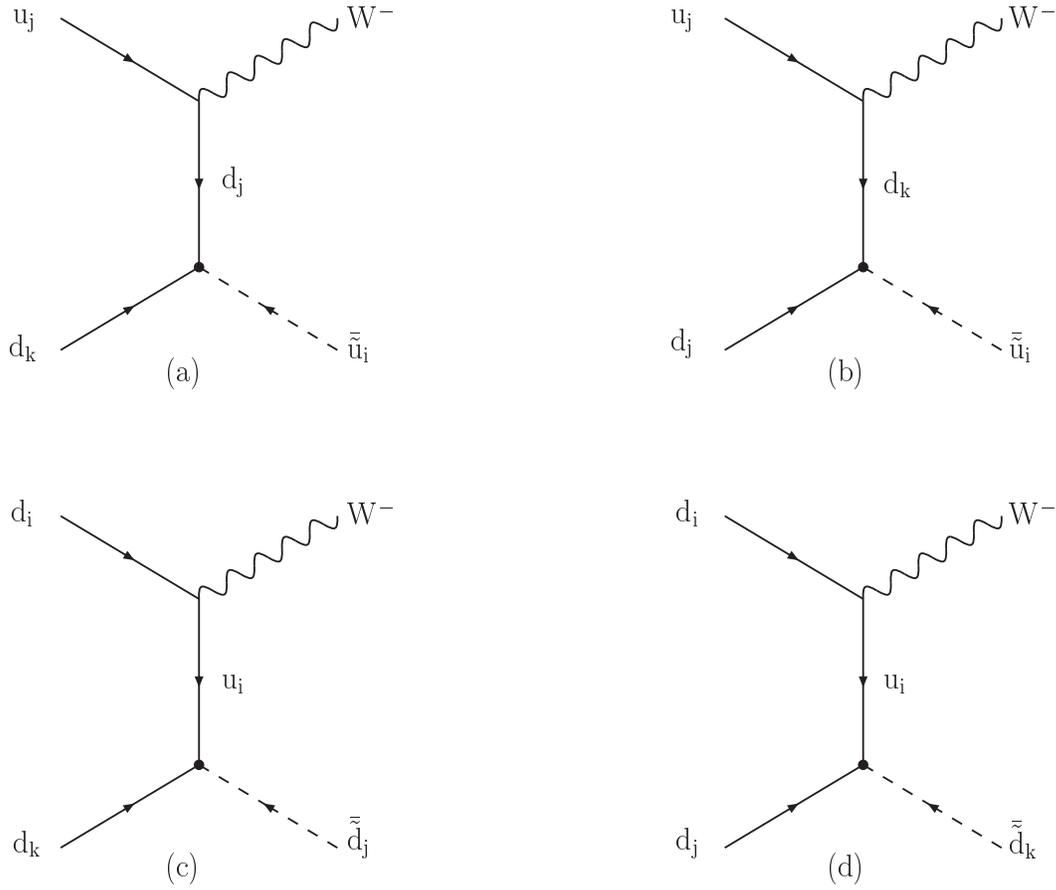


Figure 7.34: Diagrams for the associated $\bar{q} - W$ production involving λ''_{ijk} at hadron colliders. The λ''_{ijk} coupling constant is symbolised by a small circle and the arrows indicate the flow of the baryon number.

and $\mu^+\mu^-$ colliders allow to access the same λ couplings. The difference in center-of mass energies and luminosities between these two types of leptonic colliders will determine the explorable domain of these couplings.

The observation of an excess of high Q^2 events at HERA experiments [462, 463] and its interpretation in terms of \bar{R}_p interactions has been followed by numerous discussions on dilepton production at LEP [519, 520, 521, 522, 523, 524] which are beyond the scope of this review.

Di-jets production can also occur at leptonic colliders in the presence of a unique λ' coupling through the exchange of a squark in the t -channel. The $b\bar{b}$ and $c\bar{c}$ production via λ'_{1k3} and λ'_{12k} respectively are of particular interest due to the possibility of tagging bottom, charm or light quarks (u,d,s) at the experiment level [525]. Table 7.17 shows the accessible λ' couplings at e^+e^- and $\mu^+\mu^-$ colliders and fermion pair production to which a single dominant λ' coupling can contribute. In contrast to the case of λ couplings, e^+e^- and $\mu^+\mu^-$ colliders access completely different sets of λ' couplings. More specifically, in the case of λ' couplings, fermion pair production allows to explore only λ'_{1jk} at e^+e^- colliders and λ'_{2jk} at $\mu^+\mu^-$ colliders.

Preliminary studies have been performed in [252] focusing on the study of $\mu^+\mu^- \rightarrow \mu^+\mu^-$ via $\tilde{\nu}_\tau$ involving the λ_{232} coupling and $\mu^+\mu^- \rightarrow b\bar{b}$ via $\tilde{\nu}_\tau$ involving the product $\lambda_{232}\lambda'_{333}$.

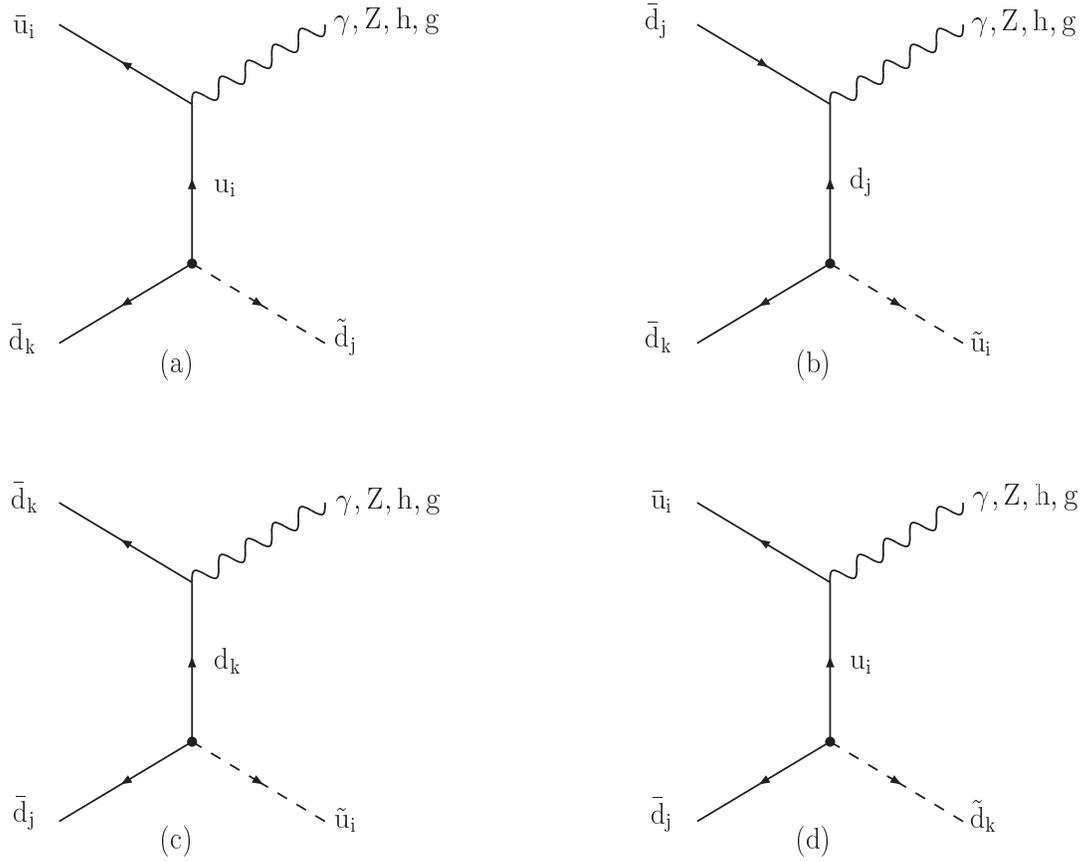


Figure 7.35: Diagrams for the associated $\tilde{q} - \gamma$, ($-Z$, $-h$ and $-g$) production involving λ''_{ijk} at hadron colliders. The λ''_{ijk} coupling constant is symbolised by a small circle and the arrows indicate the flow of the baryon number.

In this case it has been found that once the mass of the $\tilde{\nu}_\tau$ is known from earlier stage of a e^+e^- collider or the $\mu^+\mu^-$ collider and once fixing the center-of-mass energy at $\tilde{\nu}_\tau$ resonance or around the resonance with the $\mu^+\mu^-$ collider, one can explore λ_{232} down to 10^{-4} with an integrated luminosity of 3 fb^{-1} and a beam energy resolution of 0.1 %.

Further preliminary studies have been performed in [526].

At hadron colliders R_p reactions can induce contributions to Standard Model di-jets or dileptons production processes. First, the jets pair production receives contributions from reactions involving either λ' or λ'' coupling constants. As a matter of fact, a pair of quarks can be produced through the λ'' couplings with an initial state ud or $\bar{u}\bar{d}$ (dd or $\bar{d}\bar{d}$) by the exchange of a \tilde{d} (\tilde{u}) squark in the s -channel, and also with an initial state $w\bar{u}$ or $d\bar{d}$ ($u\bar{d}$ or $\bar{u}d$) by the exchange of a \tilde{u} or \tilde{d} (\tilde{d}) squark in the t -channel. If the s -channel exchanged particle is produced on shell the resonant diagram is of course dominant with respect to the t -channel diagram. The dijet channel can also be generated via the λ' couplings from an initial state $u\bar{d}$, $\bar{u}d$ or $d\bar{d}$ through the exchange of a \tilde{l} or $\tilde{\nu}$ slepton (respectively) in the s -channel.

If the dominant mechanism for either the slepton or the squark decay leads to two jets, the resonant production of such a scalar particle would result in a bump in the two-jet invariant mass distribution [261, 502] which would be a very clean signature. However the dijet production

	e^+e^- colliders			$\mu^+\mu^-$ colliders		
coupling	final state	exchange	channel	final state	exchange	channel
λ_{121}	e^+e^-	$\tilde{\nu}_\mu$	s	e^+e^-	$\tilde{\nu}_e$	t
	$\mu^+\mu^-$	$\tilde{\nu}_e$	t	-	-	-
λ_{122}	$\mu^+\mu^-$	$\tilde{\nu}_\mu$	t	e^+e^-	$\tilde{\nu}_\mu$	t
	-	-	-	$\mu^+\mu^-$	$\tilde{\nu}_e$	s+t
λ_{123}	$\tau^+\tau^-$	$\tilde{\nu}_\mu$	t	$\tau^+\tau^-$	$\tilde{\nu}_e$	t
λ_{131}	$\tau^+\tau^-$	$\tilde{\nu}_e$	t	-	-	-
	e^+e^-	$\tilde{\nu}_\tau$	s	-	-	-
λ_{132}	$\mu^+\mu^-$	$\tilde{\nu}_\tau$	t	e^+e^-	$\tilde{\nu}_\tau$	t
	-	-	-	$\tau^+\tau^-$	$\tilde{\nu}_e$	t
λ_{133}	$\tau^+\tau^-$	$\tilde{\nu}_\tau$	t	-	-	-
λ_{231}	$\tau^+\tau^-$	$\tilde{\nu}_\mu$	t	e^+e^-	$\tilde{\nu}_\tau$	t
	$\mu^+\mu^-$	$\tilde{\nu}_\tau$	t	-	-	-
λ_{232}	-	-	-	$\mu^+\mu^-$	$\tilde{\nu}_\tau$	s+t
	-	-	-	$\tau^+\tau^-$	$\tilde{\nu}_\mu$	t
λ_{233}	-	-	-	$\tau^+\tau^-$	$\tilde{\nu}_\tau$	t

Table 7.16: Accessible λ couplings at e^+e^- and $\mu^+\mu^-$ colliders and fermion pair production to which a single dominant coupling can contribute.

through $\tilde{\mathcal{R}}_p$ coupling constants will be hard to study at LHC unless the narrow resonances are copiously produced given the severe expected QCD background [255, 527]. This was discussed in more details above in section 7.5.

Top quark pair production appears to be a particular case of fermion pair production at hadron colliders because if kinematically allowed new decay channels such as $t \rightarrow d\tilde{d}_R$ and $t \rightarrow d\tilde{l}_L$ can open up. The amplitudes for top quark pair production involve diagrams with an initial state $d_k\bar{d}_k$ with either a \tilde{l}_L^i slepton exchange (via λ'_{i3k}) or a \tilde{d}_R^i squark exchange. The supersymmetric parameter space region allowed at a 95% confidence level by the D0 and CDF data [528] on $t\bar{t}$ production cross-section have also been obtained in [529] and are shown in Fig. 7.36 in the plane $\lambda'_{i31}/m_{\tilde{l}_L^i}$ and in Fig. 7.37 in the plane $\lambda''_{31i}/m_{\tilde{d}_R^i}$. Furthermore, $\tilde{\mathcal{R}}_p$ interactions being chiral, one expects the two top quarks to be polarized thus providing an additional handle to probe the details of $\tilde{\mathcal{R}}_p$ couplings [530] since the polarization of the top quark pairs is very small in the Standard Model.

More complicated decay chains of the top quark such as the double cascade decays $t \rightarrow \tilde{l}_i^+ d_k, \tilde{l}_i^+ \rightarrow \tilde{\chi}^0 + e_i, \tilde{\chi}^0 \rightarrow \nu_i b\bar{d}_k + \bar{\nu}_i \bar{b}d_k$ where the top quark and neutralino $\tilde{\mathcal{R}}_p$ decay processes are both controlled by the coupling constants λ'_{i3k} can lead to two potentially observable effects in the leptonic events namely a deviation from lepton universality and (for $k = 3$) an excess of b quark hadron events. A study based on the comparison of the ratio of branching fractions for single e to single μ events $B(t\bar{t} \rightarrow (e + jets))/B(t\bar{t} \rightarrow \mu + jets)$ to the experimental ratio of events $N(e + jets)/N(\mu + jets) = 1 \binom{+a}{-b}$ from the one charged lepton and two b -quark jets final state of the CDF top quark sample of Tevatron Run I gives the bound [262] $\lambda'_{13n} < 0.41, [n = 1, 2]$.

Another method of analysis based on an identification of this ratio with the ratio of the experimental to theoretical total production cross sections yields $\lambda'_{13n} < 0.48$. An analysis of the hadron b quarks events yields [262] $\lambda'_{133} < 0.41$.

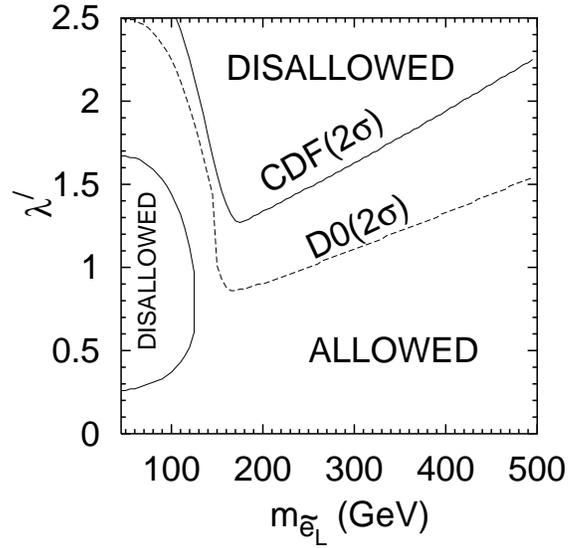


Figure 7.36: Allowed regions in the plane of λ'_{i3k} and the mass of the left slepton in a lepton-number-violating scenario. Solid (dashed) lines correspond to the $2\text{-}\sigma$ bounds from the CDF (D0) collaborations.

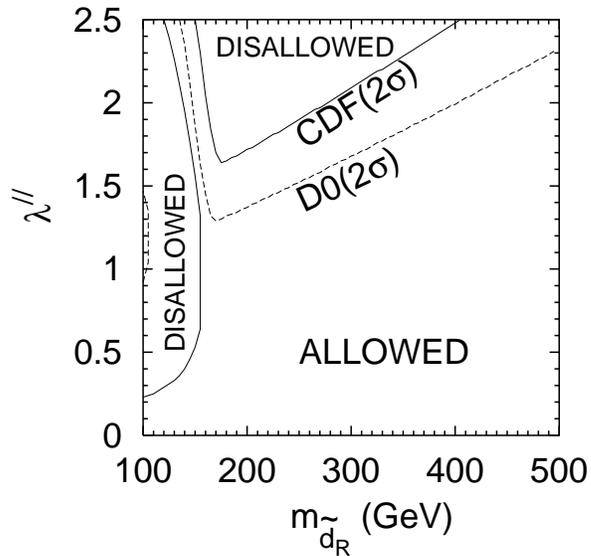


Figure 7.37: Allowed regions in the plane of λ''_{3ki} and the mass of the right d -squark in a baryon-number-violating scenario. Solid (dashed) lines correspond to the $2\text{-}\sigma$ bounds from the CDF (D0) collaborations.

	e^+e^- colliders			$\mu^+\mu^-$ colliders		
coupling	final state	exchange	channel	final state	exchange	channel
λ'_{111}	$d\bar{d}$	\tilde{u}_L	t	-	-	-
λ'_{111}	$u\bar{u}$	\tilde{d}_R	t	-	-	-
λ'_{112}	$s\bar{s}$	\tilde{u}_L	t	-	-	-
λ'_{112}	$u\bar{u}$	\tilde{s}_R	t	-	-	-
λ'_{113}	$b\bar{b}$	\tilde{u}_L	t	-	-	-
λ'_{113}	$u\bar{y}$	\tilde{b}_R	t	-	-	-
λ'_{121}	$d\bar{d}$	\tilde{c}_L	t	-	-	-
λ'_{121}	$c\bar{c}$	\tilde{d}_R	t	-	-	-
λ'_{122}	$s\bar{s}$	\tilde{c}_L	t	-	-	-
λ'_{122}	$c\bar{c}$	\tilde{s}_R	t	-	-	-
λ'_{123}	$b\bar{b}$	\tilde{c}_L	t	-	-	-
λ'_{123}	$c\bar{c}$	\tilde{b}_R	t	-	-	-
λ'_{131}	$d\bar{d}$	\tilde{t}_L	t	-	-	-
λ'_{131}	$t\bar{t}$	\tilde{d}_R	t	-	-	-
λ'_{132}	$s\bar{s}$	\tilde{t}_L	t	-	-	-
λ'_{132}	$t\bar{t}$	\tilde{s}_R	t	-	-	-
λ'_{133}	$b\bar{b}$	\tilde{t}_L	t	-	-	-
λ'_{133}	$t\bar{t}$	\tilde{b}_R	t	-	-	-
λ'_{211}	-	-	-	$d\bar{d}$	\tilde{u}_L	t
λ'_{211}	-	-	-	$u\bar{u}$	\tilde{d}_R	t
λ'_{212}	-	-	-	$s\bar{s}$	\tilde{u}_L	t
λ'_{212}	-	-	-	$u\bar{u}$	\tilde{s}_R	t
λ'_{213}	-	-	-	$b\bar{b}$	\tilde{u}_L	t
λ'_{213}	-	-	-	$u\bar{y}$	\tilde{b}_R	t
λ'_{221}	-	-	-	$d\bar{d}$	\tilde{c}_L	t
λ'_{221}	-	-	-	$c\bar{c}$	\tilde{d}_R	t
λ'_{222}	-	-	-	$s\bar{s}$	\tilde{c}_L	t
λ'_{222}	-	-	-	$c\bar{c}$	\tilde{s}_R	t
λ'_{223}	-	-	-	$b\bar{b}$	\tilde{c}_L	t
λ'_{223}	-	-	-	$c\bar{c}$	\tilde{b}_R	t
λ'_{231}	-	-	-	$d\bar{d}$	\tilde{t}_L	t
λ'_{231}	-	-	-	$t\bar{t}$	\tilde{d}_R	t
λ'_{232}	-	-	-	$s\bar{s}$	\tilde{t}_L	t
λ'_{232}	-	-	-	$t\bar{t}$	\tilde{s}_R	t
λ'_{233}	-	-	-	$b\bar{b}$	\tilde{t}_L	t
λ'_{233}	-	-	-	$t\bar{t}$	\tilde{b}_R	t
λ'_{3jk}	-	-	-	-	-	-

Table 7.17: Accessible λ' couplings at e^+e^- and $\mu^+\mu^-$ colliders and fermion pair production processes to which a single dominant coupling can contribute.

Alternatively [104] the top quark R_p decay channel $t \rightarrow b\bar{\tau}^+$ initiated by the λ'_{333} coupling leads to signature which can not be confused with the Standard Model decay channel and can compete with it. This induces a reduction of the observed Standard Model $t\bar{t}$ event rates. The

correction factor reads:

$$R_B \simeq 1.12 \lambda'_{333} \left(1 - \frac{m_{\tilde{\tau}_L}^2}{m_t^2}\right)^{-2} \quad (7.17)$$

Similarly the hadron two-body decay channels $t \rightarrow \bar{d}_j + \bar{d}_{kR}$ with λ'' couplings have an impact on the $t\bar{t}$ events through a modification in the fraction of hadron top quark decays. Performing a similar analysis to the one above for the \tilde{R}_p decay modes $t \rightarrow \bar{b}\tilde{s}$ initiated by the λ''_{323} coupling where the $t\bar{t}$ pairs cascade down to a 5 jets final state leads to an induced reduction factor on the multiple jet signal of $(1 + 0.16\lambda''_{323})$. Aside from ruling out the associated \tilde{R}_p coupling constants, one can evade a conflict with the experimental observations by closing the relevant decay channels by assuming stau or squark masses larger than 150 GeV.

Before closing this subsection on fermion pair production one has to keep in mind that allowing for more than one dominant \tilde{R}_p coupling leads to further possibilities for fermion pair production at both leptonic and hadron colliders.

At leptonic colliders, dilepton production involving two dominant λ_{ijk} couplings such as for example $e^+e^- \rightarrow \mu^+\mu^-$ involving λ_{131} and λ_{232} with s -channel $\tilde{\nu}_\tau$ exchange or $e^+e^- \rightarrow \tau^+\tau^-$ involving λ_{131} and λ_{232} with a s -channel $\tilde{\nu}_\mu$ exchange have been considered [519, 523]. Di-jet production can also occur in processes involving λ_{ijk} and λ'_{ijk} couplings with s -channel $\tilde{\nu}$ exchange. For example $e^+e^- \rightarrow b\bar{b}$ involving λ_{131} and λ'_{333} or $e^+e^- \rightarrow d\bar{d}$ involving λ_{131} and λ'_{311} both with s -channel $\tilde{\nu}_\tau$ exchange have been discussed in [477, 503]. Since the angular distribution of the d and \bar{d} jets is nearly isotropic on the sneutrino resonance, the strong forward-backward asymmetry in the Standard Model continuum, $A_{FB}(b) \approx 0.65$ at $\sqrt{s} = 200$ GeV, is reduced to ≈ 0.03 on top of the sneutrino resonance [503].

Studies involving products of λ coupling, products of λ' and products of λ with λ' couplings at $\mu^+\mu^-$ colliders have been performed in [526].

At hadron colliders the third generation slepton resonant production i.e. $\tilde{\nu}_\tau$ tau-sneutrino (neutral current) and $\tilde{\tau}$ stau (charged current) involving weakly constrained $\lambda'_{311}\lambda_{3jk}$ coupling constants thus leading to lepton pair production, have been considered in [531] for both the Tevatron and LHC colliders. The reach in terms of the slepton mass ranges from 800 GeV at the Tevatron Run II to 4 TeV at the LHC for sizeable values of $X = \lambda'_{311}\lambda_{3jk}B_l$, B_l being the leptonic branching ratio, from $X \approx 10^{-3}$ down to $X = 10^{-(5-8)}$ the latter for small slepton masses of the order of hundred GeV. In the particular case of e^+e^- production, existing Tevatron data [532] from the CDF detector on the e^+e^- production have been exploited in [503] to derive the following bounds on the product $\lambda'_{311}\lambda_{311}$ (with some theoretical uncertainties coming from the knowledge of K factor for slepton production):

$$(\lambda'_{311}\lambda_{311})^{1/2} < 0.08 \Gamma_{\tilde{\nu}_\tau}^{1/4} \quad (7.18)$$

for sneutrino masses in the range 120 – 250 GeV where $\Gamma_{\tilde{\nu}_\tau}$ denotes the sneutrino width in units of GeV. The particular cases of $\mu^+\mu^-$ and $\tau^+\tau^-$ productions have been considered in [315] based on the total cross-section studies above a given threshold on the dilepton invariant mass in order to get rid of the background from the s -channel Z resonance contribution.

Futhermore, the distinction between a scalar or a new gauge boson resonance can be performed [531] by testing the lepton universality and by measuring the forward-backward asymmetry which is expected to be zero in the case of a resonant scalar production and non zero in the case of a new gauge boson resonance as well as the leptonic charge asymmetry defined as:

$$A(\eta) = \frac{\frac{dN_+}{d\eta} - \frac{dN_-}{d\eta}}{\frac{dN_+}{d\eta} + \frac{dN_-}{d\eta}} \quad (7.19)$$

where N_{\pm} are the number of positively/negatively charged leptons of a given rapidity η . The presence of the slepton tends to drive the leptonic charge asymmetry to smaller absolute values while a new W' gauge boson substantially increases the magnitude of this asymmetry. At the Tevatron Run II, the minimum value of the product $\lambda\lambda'$ for which the asymmetry differs significantly from the Standard Model expectation is 0.1, for a luminosity of 2 fb^{-1} , assuming $m_{\tilde{l}} = 750 \text{ GeV}$ and $\Gamma_{\tilde{l}}/m_{\tilde{l}} = 0.004$.

7.6.2 \mathcal{R}_p Contributions to FCNC

In the Standard Model flavour changing neutral current effects arise through loop diagrams. They are strongly suppressed [533, 534, 535] because of the CKM matrix unitarity and the quark mass degeneracy (except the top quark) relative to the Z boson mass. In several supersymmetric extensions of the Standard Model like the MSSM the large flavour changing neutral current effects are expected to be reduced by assuming either a degeneracy of the soft supersymmetry breaking scalars masses or an alignment of the fermion and scalar superpartners mass matrices [536]. In addition flavour changing decay rates such as $Z \rightarrow q_J \bar{q}_{J'}$ through triangle diagrams involving squarks and gluinos have been found to be small with respect the Standard Model predictions [537, 538].

The \mathcal{R}_p interaction, because of its non-trivial flavour structure, opens up the possibility of observable flavour changing effects at the tree level.

The \mathcal{R}_p interactions contributions to the Z boson flavour off-diagonal decays branching ratios were discussed in Section 6.3.2.

At colliders, these flavour changing \mathcal{R}_p processes occur through the exchange of a supersymmetric scalar particle in the s - or t -channel and lead to fermion pair productions $f_J f_{J'}$ with $J \neq J'$.

Furthermore, in minimal supersymmetric extension of the Standard Model without degeneracies for sleptons masses, flavour changing effects can be induced in the supersymmetric particle pair production involving \mathcal{R}_p interactions.

At leptonic colliders, with centre-of-mass energies above the Z boson pole, single top quark production such as $l_i^+ l_i^- \rightarrow t \bar{c}, \bar{t} c$ occurring via the exchange of a \tilde{d}_{kR} squark in the t -channel through the \mathcal{R}_p couplings λ'_{i2k} and λ'_{i3k} offers a clean opportunity to observe one of these tree level flavour changing neutral current effects [539, 540, 541, 542, 543]. Indeed single top quark production occurring at the one loop level in the Standard Model [533, 534, 535] is suppressed with respect to $b\bar{s}$ production since it does not receive large contributions from heavy fermions in the loop. Moreover the MSSM contribution has been shown to be small compared to the Standard Model one [537, 538]. The cross-section of $e^+e^- \rightarrow t\bar{c} + \bar{t}c$ is shown in Fig. 7.38 from [540] for $\lambda'_{12k}\lambda'_{13k} = 0.01$ which is the order of magnitude of the low-energy constraint on this product of \mathcal{R}_p couplings for $m_{\tilde{f}} = 100 \text{ GeV}$.

The reaction $e^+e^- \rightarrow t\bar{c} + \bar{t}c$ receives also contributions at one loop level from the λ'' interactions [542, 540] in which a \tilde{d}_R squark is involved with the λ''_{2jk} and λ''_{3jk} coupling constants. In particular the combination $\lambda''_{223} \lambda''_{323}$ with a low energy constraint of $\lambda''_{223} \lambda''_{323} < 0.625$ which is less stringent than the constraints of the other $\lambda''_{2jk} \lambda''_{3jk}$ combinations can lead to cross-sections as big as 1 fb for $m_{\tilde{d}_{kR}} = 100 \text{ GeV}$.

The $t\bar{c}/\bar{t}c$ production can also occur at one loop level via photon-photon reactions $e^+e^- \rightarrow \gamma\gamma \rightarrow t\bar{c} + \bar{t}c$ which involve the products of \mathcal{R}_p couplings $\lambda'_{i2k}\lambda'_{i3k}$ when \tilde{l}_{iL} sleptons or \tilde{d}_{kR}

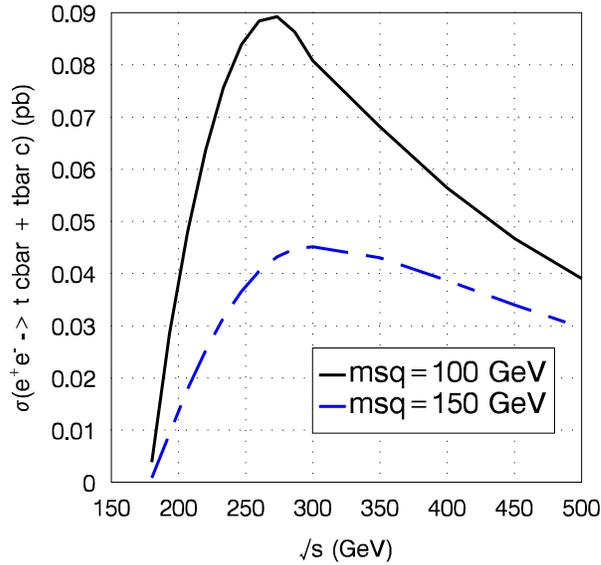


Figure 7.38: Cross section of the reaction $e^+e^- \rightarrow t\bar{c} + \bar{t}c$ as a function of the centre-of-mass energy for $\lambda'_{12k}\lambda'_{13k} = 0.01$. The solid line corresponds to $m_{\tilde{d}_{kR}} = 100$ GeV and the dashed line to $m_{\tilde{d}_{kR}} = 150$ GeV.

squarks are exchanged in the loop and the products $\lambda''_{2jk}\lambda''_{3jk}$ when \tilde{d}_R squarks run in the loop. Again the combinations $\lambda'_{323}\lambda'_{333}$ ($\lambda''_{223}\lambda''_{323}$) which have less stringent low-energy constraints than the other $\lambda'_{i2k}\lambda'_{i3k}$ ($\lambda''_{2jk}\lambda''_{3jk}$) combinations lead to cross-sections which are about an order of magnitude below the cross-sections of Fig. 7.38 from tree level diagrams involving $\lambda'_{12k}\lambda'_{13k}$. A combination of the results from the e^+e^- and $\gamma\gamma$ collisions would allow to distinguish between the λ' and λ'' effects on the $t\bar{c}/\bar{t}c$ production.

On the experimental side the $t\bar{c}$ or $\bar{t}c$ production can lead to $bcl\nu$ final state. The background from Standard Model processes such as $e^+e^- \rightarrow W^+W^- \rightarrow bcl\nu$ can then be significantly reduced by observing that the c-quark has a fixed energy given by [541]:

$$E(c) = (s + m_t^2 - m_c^2)/2\sqrt{s}. \quad (7.20)$$

Searches for $t\bar{c}$ or $\bar{t}c$ production have been performed at LEP_{II} along these lines. However they have not yet allowed to put a more stringent constraint on $\lambda'_{12k}\lambda'_{13k}$ than those coming from low energy. Searches for $t\bar{c}$ or $\bar{t}c$ production will be performed at the futur linear collider. The study of the final state $bcl\nu$ would allow to probe values of the product $\lambda'_{12k}\lambda'_{13k}$ down to ~ 0.1 for $m_{\tilde{d}_{kR}} = 1$ TeV at a linear collider with a centre-of-mass energy of $\sqrt{s} = 500$ GeV and a luminosity of $\mathcal{L} = 100fb^{-1}$ [541].

The $t\bar{c}$ or $\bar{t}c$ production can occur at $\mu^+\mu^-$ colliders as well. The cross-section for such a production is shown in Fig. 7.39 from [540] for $\lambda'_{223}\lambda'_{233} = 0.065$ which is equal to its low-energy limit for $m_{\tilde{f}} = 100$ GeV. An additionnal motivation for this choice of \tilde{R}_p couplings is provided by the observation that among the possible $\lambda'_{22k}\lambda'_{23k}$ combinations the $\lambda'_{223}\lambda'_{233}$ one has the less stringent low-energy constraint.

Finally flavour changing effects in sfermion pair production can be investigated in high precision measurements planned to be performed for example at future leptonic linear colliders [544]. The \tilde{R}_p interactions can generate such effects through the exchange of a neutrino

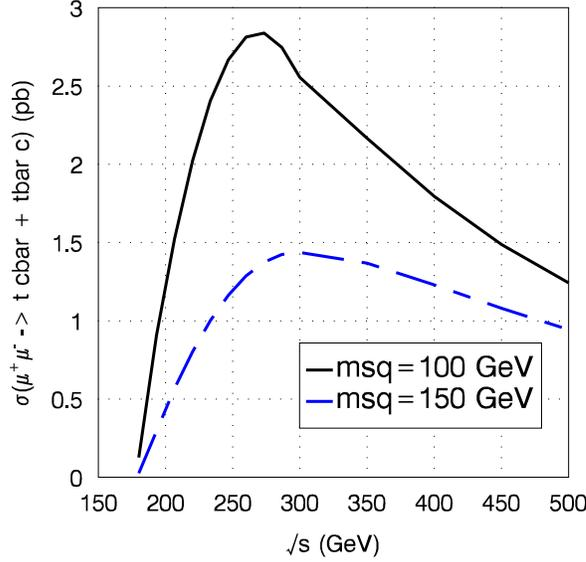


Figure 7.39: Cross section of the reaction $\mu^+ \mu^- \rightarrow t \bar{c} + \bar{t} c$ as a function of the centre-of-mass energy for $\lambda'_{223} \lambda'_{233} = 0.065$. The solid line corresponds to $m_{\tilde{d}_{kR}} = 100$ GeV and the dashed line to $m_{\tilde{d}_{kR}} = 150$ GeV.

in the t -channel in slepton pair production $e^+ e^- \rightarrow \tilde{l}_J \tilde{l}_{J'}^*$ ($J \neq J'$). The flavour non-diagonal rates vary in the range $\sigma_{JJ'} \approx (\frac{\Lambda}{0.1})^4 (2 - 20)$ fb [545] with $\Lambda = \lambda, \lambda'$ for sleptons masses $m_{\tilde{l}} < 400$ GeV as one covers centre-of-mass energy regions from the Z boson pole up to the TeV region. Due to the strong dependence on the \tilde{R}_p couplings, the flavour non-diagonal rates reach smaller values than the rates obtained in the flavour oscillations approach [546] which range between 250(100) and 0.1(0.01) fb for $\sqrt{s} = 190(500)$ GeV.

At hadron colliders flavour changing lepton pair productions $l_j l_{j'}$ as well as quark pair productions $q_j q_{j'}$ ($j \neq j'$) are both expected to be challenging to search for since the environment in terms of background is not as clean as the environment at leptonic colliders.

For example flavour changing lepton pair productions occur from an initial state $d_j \bar{d}_k$ ($d_k \bar{d}_k$) through the exchange of a $\tilde{\nu}_L^i$ sneutrino (\tilde{u}_L^j squark) in the s -channel (t -channel) via the couplings product $\lambda'_{ijk} \lambda_{iJJ'}$ ($\lambda'_{Jjk} \lambda'_{J'jk}$), or, from an initial state $u_j \bar{u}_j$ through the exchange of a \tilde{d}_R^k squark in the t -channel via the couplings product $\lambda'_{Jjk} \lambda'_{J'jk}$. More specific studies on flavour changing lepton pair productions remain to be done.

More striking signatures of \tilde{R}_p induced flavour changing neutral current effects could be observed in rare decays of the top quark as discussed in section 6.4.1.

Finally the possibility of single top quark production via squark and slepton exchanges to probe several combinations of \tilde{R}_p couplings at hadron colliders has been studied in [547, 548, 549, 550]. Initial state partons such as $u \bar{d}$ are particularly relevant for $p\bar{p}$ colliders such as the Tevatron while the $u \bar{d}$ initial state system is more relevant for pp colliders such as the LHC.

The single top quark production $u_i \bar{d}_j \rightarrow t \bar{b}$ can occur via the exchange of a \tilde{d}_R^k squark in the t -channel, through the product of couplings $\lambda''_{i3k} \lambda''_{3jk}$. The choice of the initial state of the reaction $u_i \bar{d}_j \rightarrow t \bar{b}$ fixes the flavour indices of the coupling constants product $\lambda''_{i3k} \lambda''_{3jk}$ because of

$m_{\tilde{s}_R}$ in GeV	100	200	300	400	500	600	700	800
$\lambda''_{132} \lambda''_{312}$	0.01	0.02	0.03	0.04	0.06	0.08	0.1	0.13

Table 7.18: Sensitivities on the product $\lambda''_{132} \lambda''_{312}$ for various $m_{\tilde{s}_R}$ at the upgraded Tevatron from the process $u_1 \bar{d}_1 \rightarrow \tilde{s}_R \rightarrow t \bar{b}$ from [548].

the antisymmetry of the generation indices of the coupling constants λ'' . Furthermore, because of the low energy constraints and the low parton luminosities, the only product of interest is $\lambda''_{132} \lambda''_{312}$. Assuming the observability criteria $\Delta\sigma/\sigma_0 > 20\%$ where $\Delta\sigma$ is the \mathcal{R}_p cross-section and σ_0 is the Standard Model cross-section, Table 7.18 from [548] shows the sensitivities on $\lambda''_{132} \lambda''_{312}$ at the upgraded Tevatron for various $m_{\tilde{s}_R}$.

The single top quark production $u_j \bar{d}_k \rightarrow t \bar{b}$ can also occur through the exchange of a \tilde{l}_L^i slepton in the s -channel via the couplings product $\lambda'_{ijk} \lambda'_{i33}$. The dominant process $u \bar{d} \rightarrow \tilde{l}_L^i \rightarrow t \bar{b}$ which involves the sum of couplings $\lambda'_{111} \lambda'_{133} + \lambda'_{211} \lambda'_{233} + \lambda'_{311} \lambda'_{333}$ has been considered in [549]. According to [549] values of λ' couplings below the low energy bounds can be probed if the slepton mass lies in the range $200 \text{ GeV} < m_{\tilde{l}_L} < 340 \text{ GeV}$ for the upgraded Tevatron and in the range $200 \text{ GeV} < m_{\tilde{l}_L} < 400 \text{ GeV}$ for the LHC. Although larger parton momenta are allowed at the LHC the result is not really improved at LHC because of the relative suppression of the \bar{d} quark structure function compared to the d quark one.

Turning to the case of $u_i d_j$ initial state partons, the single top quark production can also occur through the exchange of a \tilde{d}_R^k squark in the s -channel via the couplings product $\lambda''_{ijk} \lambda''_{33k}$. Table 7.19 gives an example of the cross-section obtained from different initial parton states at the LHC. Sensitivities on the coupling product $\lambda''_{212} \lambda''_{332}$ at the upgraded Tevatron and at the

Initial partons	cd	cs	ub	cb	
Exchanged particle	\tilde{s}	\tilde{d}	\tilde{s}	\tilde{d}	\tilde{s}
Couplings	$\lambda''_{212} \lambda''_{332}$	$\lambda''_{212} \lambda''_{331}$	$\lambda''_{132} \lambda''_{332}$	$\lambda''_{231} \lambda''_{331}$	$\lambda''_{232} \lambda''_{332}$
Cross-section in pb	3.98	1.45	5.01	0.659	

Table 7.19: Cross section in pb of the reaction $u_i d_j \rightarrow \tilde{d}_R^k \rightarrow t b$ at LHC for a squark of mass of 600 GeV assuming and $\lambda''_{ijk} = 0.1$ and $\Gamma_{R_p}(\tilde{q}) = 0.5 \text{ GeV}$ where $\Gamma_{R_p}(\tilde{q})$ is the width of the exchanged squark due to R -parity conserving decay.

LHC have been obtained in [549]. A more detailed simulation has been performed in [550] and the sensitivities on the coupling product $\lambda''_{212} \lambda''_{332}$ are shown in Fig. 7.40. The reaction $u_j d_k \rightarrow t b$ receives also a contribution from the exchange of a \tilde{l}_{iL}^\pm slepton in the u -channel via the λ'_{ij3} and λ'_{i3k} couplings [550].

Supersymmetric particle masses reconstruction have been also performed within the framework of single top production in [550].

To summarize, the studies of single top quark production at hadron colliders [547, 548, 549, 550] tend to indicate that the LHC is better at probing the B -violating couplings λ'' whereas the Tevatron and the LHC have a similar sensitivity to λ' couplings. Furthermore, this is the only framework in which the constraints on λ'' from physics at colliders are comparable or better than the low energy bounds on the λ'' coupling constants.

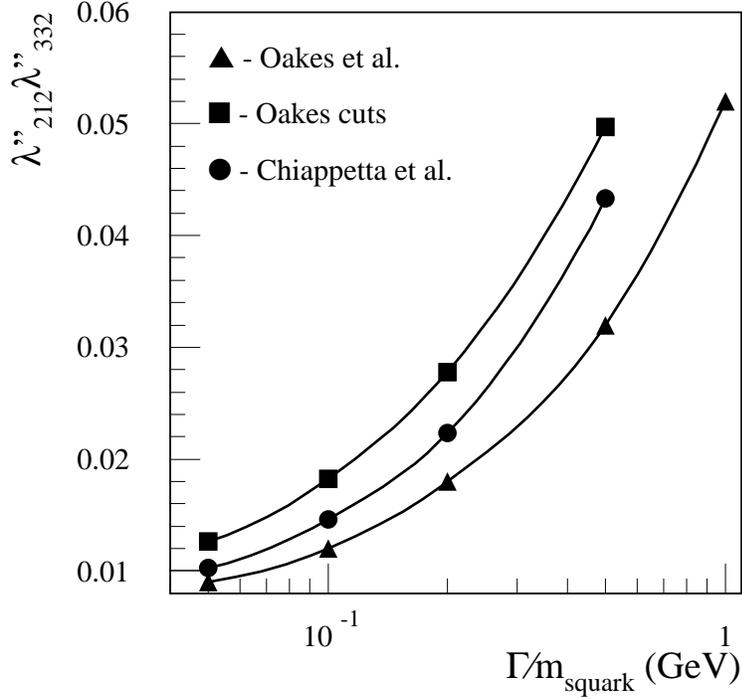


Figure 7.40: Sensitivity limits on the $\lambda''_{212}\lambda''_{332}$ Yukawa couplings obtained from the analysis of the reaction $cd \rightarrow \tilde{s}^* \rightarrow tb$ at the LHC after 1 year with low luminosity for $m_{\tilde{s}} = 300$ GeV, found in [550] (circles) and in [549] (triangles). The squares indicate the results obtained in [550] by applying the simplified cuts used in [549].

7.6.3 \tilde{R}_p Contributions to CP Violation

As already discussed in section 6.3.4 the \tilde{R}_p coupling constants can have a complex phase and hence be by themselves an independent source of CP violation motivating many studies on low energy \tilde{R}_p physics. These can still lead to new tests of CP violation in combination with the other possible source of complex phase in supersymmetric extensions of the Standard Model such as the MSSM even if one assumes that the \tilde{R}_p interactions are CP conserving. For instance the \tilde{R}_p couplings can bring a dependence on the CKM matrix elements due to the fermion mass matrix transformation from current basis to mass basis.

A study of CP violation effects in association with sneutrino flavour oscillations has been carried out in section 5.5. The CP violation effects from \tilde{R}_p couplings in the $K^0\bar{K}^0$ system and in hadrons decays asymmetries has been discussed in section 6.3.4. The CP asymmetries at the Z boson pole has been discussed in section 6.3.4.

At colliders, CP violation effects from \tilde{R}_p couplings can also be further studied from fermion pair productions either flavour changing or non flavour changing. These effects are either controlled by interference terms between tree and loop amplitudes in the case of CP asymmetries or directly considered from tree level processes.

Furthermore, if both non-degeneracies and mixing angles between all slepton flavours and if the CP odd phase do not vanish, CP violation asymmetries can also be observable in supersymmetric particles pair production. The R -parity odd interactions can provide an alternative

mechanism for explaining CP violation asymmetries in such productions through possible ψ CP odd phase incorporated in the relevant dimensionless coupling constant.

At leptonic colliders the effects of \mathcal{R}_p interactions on the CP asymmetries in the processes $l^+l^- \rightarrow f_J\bar{f}_{J'}$, with $J \neq J'$, were calculated in [542]. The \mathcal{R}_p contributions to these CP asymmetries are controlled by interference terms between tree and loop level amplitudes. The discussion of loop amplitudes was restricted to the photon and Z boson vertex corrections. The off Z boson pole asymmetries is given by:

$$\mathcal{A}_{JJ'} = \frac{\sigma_{JJ'} - \sigma_{J'J}}{\sigma_{JJ'} + \sigma_{J'J}}, \quad (7.21)$$

where $\sigma_{JJ'} = \sigma(l^+l^- \rightarrow f_J\bar{f}_{J'})$. Defining ψ as the CP odd phase, these asymmetries lie at $\mathcal{A}_{JJ'} \approx (10^{-2} - 10^{-3}) \sin \psi$ for leptons and quarks irrespective of whether one deals with light or heavy flavours.

The CP asymmetries $\mathcal{A}_{JJ'}$ depend on a ratio of different \mathcal{R}_p coupling constants and are therefore less sensitive to the absolute magnitude of these couplings than the flavour changing rates $\sigma_{JJ'}$ which involve higher power of the \mathcal{R}_p constants. The particular dependence of the CP asymmetries on the couplings is of the form $Im(\lambda\lambda^*\lambda\lambda^*)/\lambda^4$ and may thus lead to strong enhancement or suppression factors depending on the largely unknown flavour hierarchical structure of the involved Yukawa couplings. For example the study of single top production $l^+l^- \rightarrow t\bar{c}$ with $t \rightarrow bW \rightarrow bl\nu$ allows to learn about CP violation in the quark sector. In this reaction the CP violation can be probed through the asymmetry defined in Eq. (7.21) or via the following flavour off-diagonal CP asymmetry [541]:

$$\mathcal{A}_{+-} = \frac{\frac{d\sigma^+}{dE_l} - \frac{d\sigma^-}{dE_l}}{\frac{d\sigma^+}{dE_l} + \frac{d\sigma^-}{dE_l}}, \quad (7.22)$$

where $\sigma^+ = \sigma(l^+l^- \rightarrow t\bar{c} \rightarrow b\bar{c}l\nu)$, $\sigma^- = \sigma(l^+l^- \rightarrow \bar{t}c \rightarrow \bar{b}cl\bar{\nu})$ and E_l is the energy of the produced charged lepton. The values of this CP asymmetry \mathcal{A}_{+-} range typically in $\mathcal{A}_{+-} \approx (10^{-2} - 10^{-3}) \sin \psi$ for $E_l < 300$ GeV [541]. These $\mathcal{A}_{JJ'}$ and \mathcal{A}_{+-} CP asymmetries can be enhanced up to $\sim 10^{-1} \sin \psi$ if the \mathcal{R}_p coupling constants exhibit large hierarchies with respect to the generations.

Turning now briefly to CP violation asymmetries in supersymmetric particles pair production, as in the case of flavour changing fermion pair production, the \mathcal{R}_p contributions to these CP asymmetries in scalar particles pair production are controlled by interference terms between tree and loop level amplitudes. For example the flavour non-diagonal CP asymmetries $\mathcal{A}_{JJ'}$ for the slepton pair production, $e^+e^- \rightarrow \tilde{l}_J\tilde{l}_{J'}^*$ ($J \neq J'$) are predicted to be $\mathcal{A}_{JJ'} \approx (10^{-2} - 10^{-3}) \sin \psi$ [545].

Finally, the \mathcal{R}_p interactions can give rise to CP violation effects at tree level in the non flavour changing reaction $e^+e^- \rightarrow \tau^+\tau^-$ via the observation of the double spin correlations of the produced tau-leptons pair.

This possibility studied in [253] stands out as an very interesting issue by itself since previous studies of CP -violating effects in the process $e^+e^- \rightarrow \tau^+\tau^-$ which can happen for instance in models with multi-Higgs doublet or in leptoquark, Majorana $\tilde{\nu}$ or supersymmetry models, all occur at one loop level.

Here the CP asymmetries are generated from the exchange of a resonant $\tilde{\nu}_\mu$ sneutrino in the s -channel via the real coupling λ_{121} and the complex coupling λ_{323} if a $\tilde{\nu}_\mu - \tilde{\bar{\nu}}_\mu$ mixing exists.

This sneutrino mixing can generate both CP -even and CP -odd spin asymmetries which are forbidden in the Standard Model and that can be measured for τ leptons at leptonic colliders. The observation of such asymmetries would provide explicit information about three different aspects of new physics: $\tilde{\nu}_\mu - \tilde{\bar{\nu}}_\mu$ mixing, CP violation and \tilde{R}_p . The sneutrino-antisneutrino mixing phenomena which have been gaining some interest recently [250, 184, 551] is interesting since it is closely related to the generation of neutrino masses [250, 184]. The polarisation asymmetries from double spin correlations of the produced tau-leptons pair provide a feasible alternative for establishing the mass splitting between the CP even $\tilde{\nu}_\pm^\mu$ and CP odd $\tilde{\nu}_\pm^\mu$ muon-sneutrino mass eigenstates [253]. These polarisation asymmetries depend on the relative values of the real part, a , and the imaginary part, b , of the complex coupling constant λ_{323} . At the next linear collider with $\sqrt{s} = 500$ GeV [253], with the simultaneous measurement of the CP conserving and CP -violating asymmetries, the whole range $0 \leq \frac{b}{a+b} \leq 1$ can be probed to at least 3σ in the $m_{\tilde{\nu}_\mu}$ mass range of 20 GeV around resonance i.e. $\sqrt{s} - 10$ GeV $< m_{\tilde{\nu}_\mu} < \sqrt{s} + 10$ GeV even for a small mass splitting of 1 GeV.

At hadron colliders, in analogy to the case of the leptonic colliders, the resonant production of a sneutrino gives also rise to the possibility of having CP violation effects at tree level [315].

If the τ spins can be measured, CP violation effects in the polarisation asymmetries of the hard process $d_j \bar{d}_k \rightarrow \tilde{\nu}_\mu \rightarrow \tau^+ \tau^-$ can be observed at the Tevatron. The \tilde{R}_p coupling constant λ'_{2jk} which enters this subprocess is chosen real, while λ_{233} is taken complex in order to generate CP asymmetries. However, at hadron colliders, spin asymmetries deserves a careful discussion. The spin asymmetries change sign around $\sqrt{s} \approx m_{\tilde{\nu}_\pm^\mu}$ so that one has to integrate over \sqrt{s} of the initial parton system. In consequence the spin asymmetries seem too small to be measurable. Nevertheless a two-step measurement helps in overcoming this problem. In a first step one has to determine the mass of the resonant sneutrino by measuring the $\tau\tau$ invariant mass distribution and in a second step one has to integrate the absolute values of the polarization asymmetries [315].

At the Tevatron Run IIA (IIB) with $\mathcal{L} = 2 \text{ fb}^{-1}$ (30 fb^{-1}), taking their low energy bounds as the values of λ'_{2jk} and $|\lambda_{233}|$ and including all j, k combinations in $d_j \bar{d}_k$ fusion, the CP conserving and CP -violating asymmetries may be detected with a sensitivity above 3σ over the mass range $155 \text{ GeV} < m_{\tilde{\nu}_\pm^\mu} < 400 \text{ GeV}$ ($155 \text{ GeV} < m_{\tilde{\nu}_\pm^\mu} < 300 \text{ GeV}$) if $\Delta m_{\tilde{\nu}_\mu} = \Gamma_{\tilde{\nu}_\mu}$ ($\Delta m_{\tilde{\nu}_\mu} = \Gamma_{\tilde{\nu}_\mu}/10$) where $\Gamma_{\tilde{\nu}_\mu}$ is the sneutrino width.

Moreover the entire range $0 \leq \frac{b}{a+b} \leq 1$ can be practically covered for $m_{\tilde{\nu}_\pm^\mu} = 200$ GeV at the Tevatron with at least 3σ standard deviations for $\Delta m_{\tilde{\nu}_\mu} = \Gamma_{\tilde{\nu}_\mu}$ ($\Delta m_{\tilde{\nu}_\mu} = \Gamma_{\tilde{\nu}_\mu}/4$).

These results show that in contrast to the case of leptonic colliders [253], the CP odd and CP even spin asymmetries can be observed over a wide $\tilde{\nu}_\mu$ sneutrino mass range of about 300 GeV.

Chapter 8

CONCLUSIONS AND PROSPECTS

After the great successes of spontaneously broken gauge theories and of the Standard Model, supersymmetric theories of particles and interactions constitute one of the best motivated frameworks for the discussion of new physics beyond the Standard Model. The reasons are profound and fundamental – although none is definitely conclusive, especially in view of the fact that the new R -odd superpartners have escaped, for a long time now, all experimental efforts to disclose their existence.

Among the reasons to consider supersymmetry is our desire to see bosons and fermions play similar rôles, although this is against all immediate evidence, known bosons and fermions having very different properties! Indeed the supersymmetry algebra did not allow us to relate directly known bosons with known fermions, and we had to invent, instead, a whole new zoo of “supersymmetric particles”, squarks and sleptons, gluinos, charginos and neutralinos, etc., so as to allow us to view the world as possibly supersymmetric. These objects are, precisely, the new R -odd particles. Not only do we have to “double everything” – which was once considered as evidence against supersymmetry – but in the usual framework of spontaneously broken gauge theories additional Higgses should also be introduced, with their associated higgsinos! And the whole construction assumes the existence of new self-conjugate Majorana fermions, often considered as ugly beasts, only Dirac fermions being known in Nature! Is all this too high a price to pay? Only the future – and experiments – will tell.

But what can such supersymmetric theories do for us? Plenty of things, many of them well-known, according to different arguments all based on the nice and attractive features of supersymmetric theories. There are also, unfortunately, less nice features, as the reader who went through detailed discussions of the many possible supersymmetry-breaking terms in R -parity conserving and R -parity-violating theories will certainly have noticed.

Among the attractive features is the fact that, in supersymmetric theories – which are closely related with gravitation – the Higgs potential is largely determined by the supersymmetry. The quartic Higgs boson self-coupling (λ in the Standard Model), or rather self-couplings (for two Higgs doublets), instead of being arbitrary, are now fixed by g^2 and $g^2 + g'^2$, a fact at the origin of many relations involving massive gauge bosons and Higgs bosons. The new particles introduced also allow for an appropriate high-energy convergence of the three $SU(3)$, $SU(2)$ and $U(1)$ gauge couplings, whose values get unified, as it would be the case in a grand-unified theory. Supersymmetric theories also have improved convergence properties at the quantum level, leading to hopes of solving or alleviating the hierarchy problems associated with the extreme smallness of the cosmological constant Λ , or the smallness of m_W and m_Z compared

to the GUT or Planck scales (although these hints towards solutions would still have to survive supersymmetry-breaking). Supersymmetry usually also appears as a necessary ingredient in the construction of consistent string (and brane) theories – and, even without having to consider strings and branes at all, shows us the way towards new spacetime dimensions...

The fundamental motivations for supersymmetric theories are and remain strong, even if we still don't know which particular model, within the general class of supersymmetric theories of weak, electromagnetic and strong interactions, should effectively be chosen. While the allowed parameter space of the popular Minimal version of the Supersymmetric Standard Model has now very seriously shrunk, we have known from the beginning that other ingredients (such as an extra singlet superfield coupled to the two Higgs doublets H_d and H_u) could naturally be present, with no special reason to stick to the “MSSM”. In addition, we still have very little insight on how supersymmetry should be broken. In the absence of a really satisfactory, consistent and predicting mechanism, one generally chooses the option of parametrizing the various possible supersymmetry-breaking terms. Even soft terms are numerous, and this led to the introduction of a large number of arbitrary parameters in supersymmetric theories, as the price to pay for our ignorance.

Yes, but what about R -parity, the subject of this review? As discussed in chapter 1, one of the initial difficulty with supersymmetry was the absence of Majorana fermions in Nature, all known fermions appearing as Dirac particles carrying additive quantum numbers, baryon number B and lepton number L , both very well conserved. When trying to implement supersymmetry we had to cope with the fact that these conserved B and L appear as carried by fundamental fermions only – quarks and leptons – not by bosons! Still an additive R -quantum number might tentatively have been interpreted as a lepton number, if we could have used supersymmetry to relate the photon with a neutrino. However, once supersymmetry transforms the photon into a “photino”, the gluons with gluinos, quarks with squarks, etc., this R -number, if it survives at all (under the form of a discrete R -parity character), must be given a different interpretation. While the ordinary particles of the Standard Model are R -even, their superpartners, including the various squarks and sleptons, are R -odd – with $R_p = (-1)^R$. But we may have introduced the wolf inside the sheepfold since B and L get now carried, not only by fundamental fermions (which would make it easy to understand their conservation), but also by fundamental bosons, the new (R -odd) squarks and sleptons! If these are not well behaved we shall certainly face severe problems with B and L non-conservation.

Good behavior is, as we saw, closely connected with R -parity, even if R -parity may ultimately turn out not to be exactly conserved. Indeed R -parity conservation, or possibly non-conservation, is related with B and L conservation laws, as easily seen by reexpressing R -parity as $(-1)^{2S} (-1)^{3B+L}$. A conserved R -parity would prevent unwanted direct exchanges of spin-0 squarks and sleptons between ordinary particles. It would, also, prevent neutrinos from mixing with the photino or, more generally, the various neutralinos, etc..

With no R -parity at all, i.e. if R -parity is not even an approximate symmetry of the superpotential and of the supersymmetry-breaking terms (or in the absence of analogous symmetries that would play a similar rôle in excluding unwanted interactions), supersymmetric theories are not phenomenologically viable, since they would lead, in general, to much too large B - and/or L -violating processes – e.g. a much too fast proton decay, or too large neutrino masses.

R -parity, on the other hand, naturally excludes unwanted B - and/or L -violating terms from the superpotential, and from the supersymmetry-breaking terms. It leads to the famous “missing-energy” signature of supersymmetric theories at colliders, and to the stability of the Lightest Supersymmetric Particle, the LSP, generally thought to be the lightest neutralino. It then provides

us, for free, with a stable weakly-interacting non-baryonic Dark Matter candidate. Quite remarkably, such a candidate is naturally present for structural reasons, without being introduced “by hand” for the sole purpose of obtaining Dark Matter.

R -parity may well be viewed as having a very fundamental origin, in relation with the reflection symmetry $\theta \rightarrow -\theta$ in superspace, or with the existence of extra dimensions which may be responsible for supersymmetry breaking by dimensional reduction. It is, on the other hand, often criticized by tenants of an opposite attitude, explaining that they don’t see anything fundamental in this symmetry. And that all possible terms compatible with gauge symmetries should therefore be included in the superpotential; and also added in the Lagrangian density, as supersymmetry-breaking terms.

This certainly leads, in general, to a complete disaster, which necessitates the reintroduction of R -parity or R -parity-like symmetries, at least for parts of the Lagrangian density or as approximate symmetries. Actually some other symmetries (coming e.g. from higher energy ...) could mimic the effects of an R -symmetry or R -parity in excluding a certain number of terms from the superpotential and the supersymmetry-breaking terms, while still allowing others, possibly with small or even extremely small coefficients. This makes it worthwhile to study possible violations of R -parity, within supersymmetric theories. And to discuss in a systematic way the constraints existing on the possible \mathcal{R}_p terms, taking into account all data, originating from astrophysics and cosmology as well as from accelerator experiments.

It is clear that R -parity violations are certainly allowed, but only provided they are sufficiently well hidden and therefore not too large ! From the cosmological point of view the most drastic – and in general regretted – consequence of R -parity violation is that the LSP should normally be unstable, and must then in general be abandoned as a favorite Dark Matter candidate (unless of course its lifetime were extremely long, at least of the order of the age of the universe). If the LSP is really unstable, however, one has to make sure that the \mathcal{R}_p interactions responsible for its decay are sizeable enough for this decay to occur before nucleosynthesis. In this case, the LSP is no longer constrained to be electrically neutral and uncolored. \mathcal{R}_p interactions, which would also violate the B and/or L symmetries, may allow for new baryogenesis scenarios. Conversely, one has to make sure that these new \mathcal{R}_p interactions are sufficiently small so as not to erase the baryon asymmetry needed to understand the origin of matter in our universe.

The most flagrant penalties for too much \mathcal{R}_p are, as we have discussed, too large B - and/or L -violating processes, leading for example to a too short lifetime for the proton, or too large masses for the neutrinos. But neutrinos are now known to have small masses anyway, and it is tempting to speculate that these very small neutrino masses may have something to do with a very small mixing between the neutrino and neutralino sectors, that would be induced in \mathcal{R}_p theories, in the presence of L -violating interactions.

Small neutrino masses, as well as neutrino oscillations from one flavour to another, could then be viewed as originating from the effect of large neutralino masses, transmitted to the neutrino sector through (sufficiently small) \mathcal{R}_p interactions. This certainly constitutes an appealing alternative to the familiar see-saw mechanism, as a framework in which to discuss the properties of neutrinos, masses and oscillations, as well as possible magnetic moments. It may be in fact closely related to the general question of the origin of the mixing between the three quark and lepton families. The question of R -parity conservation, or non-conservation (or of how it might turn out to be slightly violated), may then simply appear as one of the aspects of a much more general “flavour problem”. This is indeed quite crucial, but also not easy to solve!

Ongoing experiments such as MiniBoone at FERMILAB, possible future experimentation close to a nuclear reactor à la CHOOZ and future long baseline projects as the US NUMI, CERN to Gran Sasso in Europe and T2K in Japan are expected to give highly valuable informations on neutrino oscillations. Exploiting the β -decay of tritium as in the futur KATRIN spectrometer in Germany and using the search for $0\nu\beta\beta$ decay as planned by the NEMO3 and the GENIUS experiments will also bring fundamental informations for the understanding of neutrino mass spectrum. On the longer term, projects involving very high intensity neutrino beams like beta-beams and megaton Cerenkov detectors are expected to further help determine the parameters of the neutrino sector and hopefully bring some information on CP violation in this sector. These data will be exploited in order to solve at least a part of this “flavour problem”.

Supersymmetric particles have been searched for intensively in a large variety of accelerator experiments, most notably at e^+e^- , e^+p and $p\bar{p}$ colliders – both under the assumptions of a conserved, or violated, R -parity. No direct experimental sign of supersymmetry has been found yet, and it is known, from LEP, HERA and Tevatron experiments, that superpartners should be heavier than about 100 GeV at least, excepted may be for some of the neutral ones, both in R_p -conserving and R_p -violating theories.

Furthermore, sets of bounds for the parameters of \mathcal{R}_p interactions have been discussed, both from the indirect searches for such interactions, and from the direct production of the new particles – either isolated or in pairs – in a situation of R -parity violation. The most characteristic signature of supersymmetry is then no longer the missing energy-momentum carried away by the two unobserved LSP's. These bounds have been obtained and discussed, either as bounds on every single \mathcal{R}_p coupling constant considered isolately, or as bounds on products of two such \mathcal{R}_p coupling constants.

A large number of the many \mathcal{R}_p coupling constants and parameters still remain unconstrained. Imaginative efforts to find new processes that might fill in the remaining gaps in the information will require a concerted effort between theory and experiment. One needs to identify processes, allowing for significant contributions from the \mathcal{R}_p interactions, where a high experimental sensitivity, also taking into account the uncertainties in the Standard Model predictions, is attainable. Several measurements aiming at detecting rare processes are expected to be performed soon and should further extend the search for \mathcal{R}_p effects. Just to cite a few, the searches for $\mu \rightarrow e$ conversion either with the $\mu \rightarrow e\gamma$ decay as chased by the MEG experiment at PSI or with $\mu N \rightarrow eN$ conversion processes as considered by the MECO project at BNL are expected to gain 2 to 3 orders of magnitude in sensitivity with respect to their predecessors (the MEGA and SINDRUM2 experiments at PSI). Other promising examples are offered by B meson and τ lepton rare decay processes. If some coupling constants happen to be of the order of 10^{-1} , this could be enough to lead to observable effects at high energy colliders.

The prospects on the long term are encouraging. Thanks to the ongoing experiments such as BABAR at SLAC and BELLE at KEK, both aiming at very high B meson production statistics corresponding to several hundreds fb^{-1} of integrated luminosity, experimental measurements of rare (“forbidden”) decay processes are expected to gain several orders of magnitude in sensitivity. This kind of gain is also expected for planned projects such as CKM at FERMILAB, CLEO upgrades at Cornell, KOPIO at BNL and JHF at Tokai for high intensity kaon beams, as well as detectors such as LHCb at CERN and BTeV at FERMILAB, dedicated to B physics. In parallel the CDF and $D\bar{0}$ experiments at Tevatron Run II at FERMILAB are expected to gain 2 to 3 orders of magnitude in sensitivity for B physics with respect to Run I thus providing further tests for \mathcal{R}_p interactions. As for more direct searches both CDF and $D\bar{0}$ are expected to extend their searches for supersymmetry with \mathcal{R}_p effects in both the single supersymmetric

particle production mode and the more conventional pair production mode followed by \tilde{R}_p decays. Factors of 10 – 100 improvements in accuracy are also anticipated for high precision measurements of magnetic or electric dipole moments as, for example, the $10^{-28} e \cdot \text{cm}$ region for the electric dipole moment of the neutron (to be explored with the spallation ultra-cold neutron source (SUNS) at PSI). Some progress is expected thanks to the high energy leptonic colliders for high precision Z boson physics observables, especially with the possibility of the high luminosity option of a future linear electron collider running at the Z boson resonance. Our theoretical understanding of supersymmetry and of physics beyond the Standard Model is likely to deepen in the meantime. On a different front it is likely, also, that we shall learn more about the properties of the Dark Matter and possibly its nature.

Ultimately if supersymmetry is indeed a symmetry of Nature along the lines presented here, there is no substitute for a direct observation of the superpartners. The best hope is that superpartners could show up directly, in a few years from now, at the LHC pp collider at CERN, revealing directly the presence of supersymmetry as a fundamental symmetry of the world of particles and interactions. One would then expect a wealth of new results, on the mass spectrum of the new particles as well as on their production and decay properties, which should all be more precisely measured at a future linear electron collider. These data should be crucial to help us understand the actual mechanism which breaks supersymmetry, and to discover whether R -parity is conserved or not. And, in the last case, how and how much it turns out to be violated. In particular the instability of the LSP associated with \tilde{R}_p could be observable, especially if \tilde{R}_p interactions were effectively responsible for neutrino masses. Beyond the possible discovery of supersymmetry, the knowledge about the conservation or possible violations of R -parity is expected to be essential for the understanding of several fundamental problems in particle physics, and cosmology.

Acknowledgements

This review emerged from common efforts initiated in the framework of the *R*-Parity Working Group of the French *Groupement de Recherche en Supersymétrie* (GDR). We wish to thank P. Binétruy who headed the GDR for his continuous support. We are grateful to all members of the *R*-Parity Working Group for useful discussions. We wish to acknowledge in particular the contributions at early stages of this review work of F. Brochu, P. Coyle, D. Fouchez, P. Jonsson, F. Ledroit-Guillon, A. Mirea, E. Nagy, R. Nicolaidou, N. Parua and G. Sajot.

We also wish to thank the *Institut National de Physique Nucléaire et de Physique des Particules* (IN2P3), the *Centre National de la Recherche Scientifique* (CNRS) and the *Commissariat à l'Énergie Atomique* (CEA) for their support.

Appendix A

Notations and Conventions

In the following, the notations and conventions used throughout this review are presented.

The three $SU(3)_C \times SU(2)_L \times U(1)_Y$ gauge couplings of the Standard Model are denoted by g_3 , g and g' respectively and the electroweak mixing angle by θ_W . We use the metric $(+, -, -, -)$.

The superpartners of matter, Higgs and gauge fields in the Supersymmetric Standard Model are denoted as follows:

- Scalar partners of left-handed quark fields $\begin{pmatrix} u_{iL} \\ d_{iL} \end{pmatrix}$ (squarks) by $\tilde{Q}_i = \begin{pmatrix} \tilde{u}_{iL} \\ \tilde{d}_{iL} \end{pmatrix}$, and scalar partners of right-handed quark fields u_{iR} , d_{iR} by \tilde{u}_{iR} , \tilde{d}_{iR} ($i = 1, 2, 3$ is a family index). Similarly, the superpartners of the left-handed lepton fields $\begin{pmatrix} \nu_{iL} \\ l_{iL} \end{pmatrix}$ (sleptons) are denoted by $\tilde{L}_i = \begin{pmatrix} \tilde{\nu}_{iL} \\ \tilde{l}_{iL} \end{pmatrix}$, and those of the right-handed leptons l_{iR} by \tilde{l}_{iR} . The corresponding superfields are denoted with capital letters $Q_i = \begin{pmatrix} U_i \\ D_i \end{pmatrix}$, $L_i = \begin{pmatrix} N_i \\ E_i \end{pmatrix}$, U_i^c , D_i^c , E_i^c . Since we use left-handed chiral superfields only, right-handed fermion fields and their scalar partners are described by the corresponding CP conjugate fields (for example the scalar and fermion components of U_i^c are $\tilde{u}_i^c \equiv (\tilde{u}_{iR})^*$ and $u_i^c \equiv C(\overline{u_{iR}})^T$, respectively).

- The two Higgs doublets of the Supersymmetric Standard Model are denoted by $h_d = \begin{pmatrix} h_d^0 \\ h_d^- \end{pmatrix}$ and $h_u = \begin{pmatrix} h_u^+ \\ h_u^0 \end{pmatrix}$, the corresponding Weyl fermions (higgsinos) by \tilde{h}_d and \tilde{h}_u , and the corresponding superfields by H_d and H_u . The Higgs VEVs are $\langle h_d^0 \rangle = v_d/\sqrt{2}$ and $\langle h_u^0 \rangle = v_u/\sqrt{2}$ (we adopt the normalization $\phi = (a+ib)/\sqrt{2}$ for complex scalar fields), and the ratio of VEVs is $\tan \beta = v_u/v_d$. The five physical Higgs states of the Minimal Supersymmetric Standard Model, in which no other superfield than the ones mentioned here are introduced, include two neutral scalars (CP -even) denoted by h (for the lightest one) and H , a charged Higgs boson H^\pm and a pseudoscalar (CP -odd) Higgs boson A .

- The Majorana fermion partners of the gluons (gluinos) are denoted by \tilde{g}^a ($a = 1 \dots 8$); similarly, the superpartners of the $SU(2)_L \times U(1)_Y$ gauge bosons are gaugino fields denoted by \tilde{W}^i ($i = 1, 2, 3$) and \tilde{B} . Alternatively, one can define the fermionic partners of the photon, Z and W^\pm gauge fields: two Majorana spinors $\tilde{\gamma} \equiv \sin \theta_W \tilde{W}^3 + \cos \theta_W \tilde{B}$ and $\tilde{Z} \equiv \cos \theta_W \tilde{W}^3 - \sin \theta_W \tilde{B}$, and a Dirac spinor $\tilde{W}^\pm \equiv (\tilde{W}^1 \mp i\tilde{W}^2)/\sqrt{2}$. The mass eigenstates of the higgsino-gaugino system, the neutralinos and the charginos, are denoted by $\tilde{\chi}_l^0$ ($l = 1 \dots 4$) and $\tilde{\chi}_{l'}^\pm$ ($l' = 1, 2$), respectively.

The chiral superfields are normalized so that the lowest term in the $\theta, \bar{\theta}$ expansion of the left-handed chiral superfield Φ associated with the complex scalar field $\phi = (a + ib)/\sqrt{2}$ is $\Phi|_{\theta=\bar{\theta}=0} = (a + ib)/\sqrt{2}$. We adopt the following convention for the contraction of two $SU(2)_L$ doublets Φ and Ψ : $\Phi\Psi \equiv \epsilon_{ab}\Phi^a\Psi^b = \Phi^1\Psi^2 - \Phi^2\Psi^1$, where $a, b = 1, 2$ are $SU(2)_L$ indices, $\epsilon_{ab} = -\epsilon_{ba}$ is the totally antisymmetric tensor (with $\epsilon_{12} = +1$), and Φ^1 (resp. Φ^2) denotes the $T_3 = +\frac{1}{2}$ (resp. $T_3 = -\frac{1}{2}$) component of Φ .

The discussion of R -parity violation does not depend, in general, of the particular version of the Supersymmetric Standard Model considered. In the following, we nevertheless specialize for clarity on the minimal supersymmetric extension of the Standard Model (MSSM). With the above notations, the renormalizable superpotential of the MSSM reads

$$W_{MSSM} = \mu H_u H_d + \lambda_{ij}^e H_d L_i E_j^c + \lambda_{ij}^d H_d Q_i D_j^c - \lambda_{ij}^u H_u Q_i U_j^c, \quad (\text{A.1})$$

where μ is the supersymmetric Higgs mass parameter, and $\lambda_{ij}^{u,d,e}$ denote the quark and charged lepton Yukawa coupling matrices. In Eq. (A.1), like in most equations of this review, a summation over the generation indices $i, j = 1, 2, 3$, and over gauge indices is understood. In the absence of R -parity, the following \mathcal{R}_p terms may also be added to the superpotential (A.1) :

$$W_{\mathcal{R}_p} = \mu_i H_u L_i + \frac{1}{2} \lambda_{ijk} L_i L_j E_k^c + \lambda'_{ijk} L_i Q_j D_k^c + \frac{1}{2} \lambda''_{ijk} U_i^c D_j^c D_k^c. \quad (\text{A.2})$$

The supersymmetric mass parameters μ_i as well as the trilinear couplings λ_{ijk} and λ'_{ijk} violate lepton-number conservation law, while the couplings λ''_{ijk} violate baryon-number conservation law. Gauge invariance enforces antisymmetry of the λ_{ijk} (λ''_{ijk}) couplings in their first (last) two indices: $\lambda_{ijk} = -\lambda_{jik}$ ($\lambda''_{ijk} = -\lambda''_{ikj}$). To avoid unwanted factors of 2 in scattering amplitudes, a factor 1/2 has been introduced in the definition of the λ_{ijk} and λ'_{ijk} couplings in Eq. (A.2). It should be noted that some authors omit these factors but restrict the sum over generation indices to $i < j$ (resp. $j < k$) in the $\lambda_{ijk} L_i L_j E_k^c$ (resp. $\lambda''_{ijk} U_i^c D_j^c D_k^c$) terms; this alternative writing is equivalent to our definition (A.2).

The Supersymmetric Standard Model makes use of a large number of parameters describing our ignorance about the mechanism which breaks supersymmetry. As is customary, we consider the most general terms that break supersymmetry in a soft way, i.e. without reintroducing quadratic divergences. In the MSSM, these ‘‘soft supersymmetry-breaking parameters’’ consist of the following:

- The mass parameters M_1, M_2 and M_3 for the $U(1)_Y, SU(2)_L$ and $SU(3)_C$ gauginos.
- 3×3 hermitian mass matrices for each type of squarks and sleptons, both left- and right-handed: $m_{\tilde{Q}}^2, m_{\tilde{u}^c}^2, m_{\tilde{d}^c}^2, m_{\tilde{L}}^2, m_{\tilde{e}^c}^2$. We shall sometimes use the alternative notation \tilde{m}_{ij} for $(m_{\tilde{L}}^2)_{ij}$. When R -parity is broken, there may also be Higgs-slepton mixing soft masses $\tilde{m}_{\tilde{d}i}^2$.
- The ‘‘analytic’’ (i.e. involving only the scalar components of chiral superfields, and not their complex conjugates) trilinear scalar couplings A , with the same structure as the Yukawa couplings λ . For example, the up-quark-type Yukawa couplings $\lambda_{ij}^u H_u Q_i U_j^c$ have associated trilinear soft terms $A_{ij}^u h_u \tilde{Q}_i \tilde{u}_j^c$. When R -parity is explicitly broken, there are also trilinear couplings A_{ijk}, A'_{ijk} and A''_{ijk} corresponding to the \mathcal{R}_p superpotential couplings $\lambda_{ijk}, \lambda'_{ijk}$ and λ''_{ijk} , with the same symmetry properties. The A parameters have mass dimension 1.
- The soft mass parameters \tilde{m}_d^2 and \tilde{m}_u^2 for the two Higgs doublets h_d and h_u , and a bilinear analytic mass term $B h_u h_d$, corresponding to the supersymmetric Higgs mass term $\mu H_u H_d$ in

the superpotential. There are also \mathcal{R}_p bilinear soft terms $B_i h_u \tilde{L}_i$ corresponding to the \mathcal{R}_p mass terms $\mu_i H_u L_i$ in the superpotential. The B parameters have mass dimension 2.

The soft supersymmetry-breaking terms in the Lagrangian density of the MSSM are then given by

$$\begin{aligned}
-\mathcal{L}_{\mathcal{R}_p}^{soft} &= (m_{\tilde{Q}}^2)_{ij} \tilde{Q}_i^\dagger \tilde{Q}_j + (m_{\tilde{u}^c}^2)_{ij} \tilde{u}_i^{c\dagger} \tilde{u}_j^c + (m_{\tilde{d}^c}^2)_{ij} \tilde{d}_i^{c\dagger} \tilde{d}_j^c + (m_{\tilde{L}}^2)_{ij} \tilde{L}_i^\dagger \tilde{L}_j + (m_{\tilde{l}^c}^2)_{ij} \tilde{l}_i^{c\dagger} \tilde{l}_j^c \\
&+ \left(A_{ij}^e h_d \tilde{L}_i \tilde{l}_j^c + A_{ij}^d h_d \tilde{Q}_i \tilde{d}_j^c - A_{ij}^u h_u \tilde{Q}_i \tilde{u}_j^c + \text{h.c.} \right) \\
&+ \tilde{m}_d^2 h_d^\dagger h_d + \tilde{m}_u^2 h_u^\dagger h_u + (B h_u h_d + \text{h.c.}) \\
&+ \frac{1}{2} M_1 \tilde{B} \tilde{B} + \frac{1}{2} M_2 \tilde{W}^3 \tilde{W}^3 + M_2 \tilde{W}^+ \tilde{W}^+ + \frac{1}{2} M_3 \tilde{g}^a \tilde{g}^a, \tag{A.3}
\end{aligned}$$

where we have written the gaugino soft mass terms in a four-component notation, with Majorana spinors \tilde{B} , \tilde{W}^3 , \tilde{g}^a and a charged Dirac spinor \tilde{W}^+ . In the absence of R -parity, additional soft supersymmetry-breaking terms may also be introduced in the Lagrangian density, as given by:

$$\begin{aligned}
-\mathcal{L}_{\mathcal{R}_p}^{soft} &= V_{\mathcal{R}_p}^{soft} = \frac{1}{2} A_{ijk} \tilde{L}_i \tilde{L}_j \tilde{l}_k^c + A'_{ijk} \tilde{L}_i \tilde{Q}_j \tilde{d}_k^c + \frac{1}{2} A''_{ijk} \tilde{u}_i^c \tilde{d}_j^c \tilde{d}_k^c \\
&+ B_i h_u \tilde{L}_i + \tilde{m}_{di}^2 h_d^\dagger \tilde{L}_i + \text{h.c.} . \tag{A.4}
\end{aligned}$$

Appendix B

Yukawa-like \mathcal{R}_p Interactions Associated with the Trilinear \mathcal{R}_p Superpotential

In the following, the Yukawa-like (fermion-fermion-scalar) \mathcal{R}_p interactions associated with the trilinear \mathcal{R}_p superpotential couplings of Eq. (A.2) are derived.. The latter also give rise to \mathcal{R}_p conserving scalar interactions that are quartic in the squark and slepton fields. However these have no significant phenomenological effects on the low-energy physics for heavy superpartners, so we do not discuss them here (see section 2.1.2).

Let us first derive explicitly the couplings trilinear in the fields generated by the part of the superpotential (A.2) given by

$$W_{L_i L_j E_k^c} = \frac{1}{2} \lambda_{ijk} L_i L_j E_k^c. \quad (\text{B.1})$$

The trilinear couplings coming from $W_{L_i L_j E_k^c}$ are obtained by differentiating $W_{L_i L_j E_k^c}$, expressed in term of the scalar components z of the superfields, over all the scalar fields:

$$\mathcal{L}_{L_i L_j E_k^c} = -\frac{1}{2} \sum_{\alpha, \beta} \frac{\partial^2 W_{L_i L_j E_k^c}(z)}{\partial z_\alpha \partial z_\beta} \psi_\alpha \psi_\beta - \frac{1}{2} \sum_{\alpha, \beta} \frac{\partial^2 W_{L_i L_j E_k^c}^*(z)}{\partial z_\alpha^* \partial z_\beta^*} \bar{\psi}_\alpha \bar{\psi}_\beta, \quad (\text{B.2})$$

where the two-component spinors ψ are the superpartners of the scalar fields z . The two-component spinors ψ and $\bar{\psi}$ belong respectively to the $(1/2, 0)$ and $(0, 1/2)$ representations of the Lorentz group. Eq.(B.1) and Eq.(B.2) lead together to,

$$\begin{aligned} \mathcal{L}_{L_i L_j E_k^c} = & - \frac{1}{2} \sum_{\alpha, \beta} \frac{\partial^2 \left[\frac{1}{2} \lambda_{ijk} \left(\tilde{\nu}_{iL} \tilde{l}_{jL} - \tilde{l}_{iL} \tilde{\nu}_{jL} \right) \tilde{l}_{kR}^c \right]}{\partial z_\alpha \partial z_\beta} \psi_\alpha \psi_\beta \\ & - \frac{1}{2} \sum_{\alpha, \beta} \frac{\partial^2 \left[\frac{1}{2} \lambda_{ijk}^* \left(\tilde{\nu}_{iL}^* \tilde{l}_{jL}^* - \tilde{l}_{iL}^* \tilde{\nu}_{jL}^* \right) \tilde{l}_{kR}^{c*} \right]}{\partial z_\alpha^* \partial z_\beta^*} \bar{\psi}_\alpha \bar{\psi}_\beta, \end{aligned} \quad (\text{B.3})$$

where $\tilde{\nu}$ and \tilde{l} denote the sneutrinos and charged sleptons, respectively, the superscripts c denote the charge conjugate fields and the superscripts $*$ the complex conjugate fields. The ‘R’ and ‘L’ chirality indices for the scalar fields distinguish independent fields corresponding to superpartners of right- and left-handed fermions, respectively. The Lagrangian density (B.3) is equivalent to

$$\mathcal{L}_{L_i L_j E_k^c} = - \frac{1}{2} \lambda_{ijk} \left(\chi_{\nu_i} \chi_{l_j} \tilde{l}_{kR}^c + \chi_{\nu_i} \eta_{l_k} \tilde{l}_{jL} + \chi_{l_j} \eta_{l_k} \tilde{\nu}_{iL} - (i \leftrightarrow j) \right)$$

$$- \frac{1}{2} \lambda_{ijk}^* \left(\bar{\chi}_{\nu_i} \bar{\chi}_{l_j} \tilde{l}_{kR}^{c*} + \bar{\chi}_{\nu_i} \bar{\eta}_{l_k} \tilde{l}_{jL}^* + \bar{\chi}_{l_j} \bar{\eta}_{l_k} \tilde{\nu}_{iL}^* - (i \leftrightarrow j) \right). \quad (\text{B.4})$$

In our notations, the two-component spinors χ_l (χ_ν) and η_l (η_ν) associated with the charged lepton (neutrino) are related to the four-component Dirac spinors describing the charged leptons l (neutrinos ν) and antileptons l^c (antineutrinos ν^c) by

$$l = \begin{pmatrix} \chi_l \\ \bar{\eta}_l \end{pmatrix}, \quad l^c = \begin{pmatrix} \eta_l \\ \bar{\chi}_l \end{pmatrix}, \quad \nu = \begin{pmatrix} \chi_\nu \\ \bar{\eta}_\nu \end{pmatrix}, \quad \nu^c = \begin{pmatrix} \eta_\nu \\ \bar{\chi}_\nu \end{pmatrix}. \quad (\text{B.5})$$

The products of two-component spinors ψ and $\bar{\psi}$ and the products of four-component Dirac spinors Ψ and $\bar{\Psi} = \Psi^\dagger \gamma_0$ are related through the equations,

$$\bar{\Psi}_1 P_L \Psi_2 = \eta_1 \chi_2, \quad \bar{\Psi}_2 P_R \Psi_1 = \bar{\eta}_1 \bar{\chi}_2, \quad (\text{B.6})$$

where P_L and P_R are respectively the left and right chirality projectors. By applying the relations (B.6), one can express the Lagrangian density (B.4) in terms of the four-component Dirac spinors:

$$\mathcal{L}_{L_i L_j E_k^c} = -\frac{1}{2} \lambda_{ijk} \left(\tilde{\nu}_{iL} \bar{l}_{kR} l_{jL} + \tilde{l}_{jL} \bar{l}_{kR} \nu_{iL} + \tilde{l}_{kR}^* \bar{\nu}_{iR}^c l_{jL} - (i \leftrightarrow j) \right) + \text{h.c.}, \quad (\text{B.7})$$

where for instance $\bar{\nu}_{iR}^c = \overline{(\nu_i^c)_R}$.

Similarly, the couplings trilinear in the fields generated by the superpotential terms $W_{L_i Q_j D_k^c} = \lambda'_{ijk} L_i Q_j D_k^c$ and $W_{U_i^c D_j^c D_k^c} = \frac{1}{2} \lambda''_{ijk} U_i^c D_j^c D_k^c$ are found to be

$$\mathcal{L}_{L_i Q_j D_k^c} = -\lambda'_{ijk} \left(\tilde{\nu}_{iL} \bar{d}_{kR} d_{jL} + \tilde{d}_{jL} \bar{d}_{kR} \nu_{iL} + \tilde{d}_{kR}^* \bar{\nu}_{iR}^c d_{jL} - \tilde{l}_{iL} \bar{d}_{kR} u_{jL} - \tilde{u}_{jL} \bar{d}_{kR} l_{iL} - \tilde{d}_{kR}^* \bar{l}_{iR}^c u_{jL} \right) + \text{h.c.}, \quad (\text{B.8})$$

and

$$\mathcal{L}_{U_i^c D_j^c D_k^c} = -\frac{1}{2} \lambda''_{ijk} \left(\tilde{u}_{iR}^* \bar{d}_{jR} d_{kL}^c + \tilde{d}_{jR}^* \bar{u}_{iR} d_{kL}^c + \tilde{d}_{kR}^* \bar{u}_{iR} d_{jL}^c \right) + \text{h.c.}, \quad (\text{B.9})$$

respectively.

Appendix C

Production and Decay Formulae

In the following, some useful formulas relevant for R -parity violation searches at colliders are listed. This section is based to a large extent on appendix B of [552]. The formulas for the decays are organized here by particle families.

Mixing

The mixing for the first two generations of sleptons and squarks is expected to be small to a good accuracy due to the small fermion masses in the off-diagonal elements of the mass matrices. On the other hand, a large mixing between the left and right handed stops is expected because of the large top-quark mass.

For the current eigenstates $\tilde{q}_{L,R}^i$ and the mass eigenstates $\tilde{q}_{1,2}^i$ the mixing matrix is

$$\begin{pmatrix} \tilde{q}_L^i \\ \tilde{q}_R^i \end{pmatrix} = \begin{pmatrix} \cos \theta_q^i & \sin \theta_q^i \\ -\sin \theta_q^i & \sin \theta_q^i \end{pmatrix} \begin{pmatrix} \tilde{q}_1^i \\ \tilde{q}_2^i \end{pmatrix}. \quad (\text{C.1})$$

It will be denoted as Q_{jk}^i where $i = u, d, s, c, b, t$ is the quark flavour index. The slepton mixing matrix is similar and will be denoted as L_{jk}^i , where $i = e^-, \nu_e, \mu^-, \nu_\mu, \tau^-, \nu_\tau$ is the lepton flavour index. Sfermion mixing between generations will be neglected.

Two body decays

The two-body decay rate corresponding to an averaged matrix element $\overline{M}(A \rightarrow B + C)$ with no angular dependence is:

$$\Gamma(A \rightarrow B + C) = \frac{|\overline{M}(A \rightarrow B + C)|^2}{16\pi m_A^3} \sqrt{[m_A^2 - (m_B + m_C)^2][m_A^2 - (m_B - m_C)^2]}. \quad (\text{C.2})$$

Three body decays

The partial width is given by

$$\Gamma(A \rightarrow 1 + 2 + 3) = \frac{1}{(2\pi)^3} \frac{1}{32m_A^3} \int_{(m_{12}^2)_{min}}^{(m_{12}^2)_{max}} d m_{12}^2 \int_{(m_{23}^2)_{min}}^{(m_{23}^2)_{max}} d m_{23}^2 |\overline{M}|^2, \quad (\text{C.3})$$

where $m_{12}^2 \equiv (p_1 + p_2)^2 = m_A^2 + m_3^2 - 2m_A E_3$ and p_1, p_2 are the 4-momenta of particles 1 and 2 respectively, while E_3 is the energy of particle 3 in the rest frame of particle A . m_{23} is defined in a similar way. Therefore we obtain $(m_{12}^2)_{max} = (m_A - m_3)^2$, $(m_{12}^2)_{min} = (m_1 + m_2)^2$,

$$\begin{aligned} (m_{23}^2)_{max} &= (E_2 + E_3)^2 - \left(\sqrt{E_2^2 - m_2^2} - \sqrt{E_3^2 - m_3^2} \right)^2, \\ (m_{23}^2)_{min} &= (E_2 + E_3)^2 - \left(\sqrt{E_2^2 - m_2^2} + \sqrt{E_3^2 - m_3^2} \right)^2. \end{aligned}$$

$E_2 = (m_{12}^2 - m_1^2 + m_2^2)/2m_{12}$ and $E_3 = (m_A^2 - m_{12}^2 - m_3^2)/2m_{12}$ are now the energies of particles 2 and 3 in the rest frame of the reduced variable m_{12} .

C.1 Sfermions

Two-body R -parity-violating decays of sfermions are given by (C.2) with the following matrix elements (averaged over spin and colour). α is the mass eigenstate of the sfermion if there is mixing. i, j, k are the generation indices.

For sneutrinos we have:

$$\begin{aligned} |\overline{M}(\tilde{\nu}_j \rightarrow \ell_i^+ \ell_k^-)|^2 &= |\lambda_{ijk}|^2 (m_{\tilde{\nu}}^2 - m_{\ell_i}^2 - m_{\ell_k}^2), \\ |\overline{M}(\tilde{\nu}_i \rightarrow \bar{d}_j d_k)|^2 &= N_c |\lambda_{ijk}'|^2 (m_{\tilde{\nu}}^2 - m_{d_j}^2 - m_{d_k}^2), \end{aligned} \quad (\text{C.4})$$

for sleptons:

$$\begin{aligned} |\overline{M}(\tilde{e}_{j\alpha}^- \rightarrow \bar{\nu}_i \ell_k^-)|^2 &= |\lambda_{ijk}|^2 |L_{1\alpha}^{2j-1}|^2 (m_{\tilde{e}}^2 - m_{\ell_k}^2), \\ |\overline{M}(\tilde{e}_{k\alpha}^- \rightarrow \nu_i \ell_j^-)|^2 &= |\lambda_{ijk}|^2 |L_{2\alpha}^{2k-1}|^2 (m_{\tilde{e}}^2 - m_{\ell_j}^2), \\ |\overline{M}(\tilde{e}_{i\alpha}^- \rightarrow \bar{u}_j d_k)|^2 &= N_c |\lambda_{ijk}'|^2 |L_{1\alpha}^{2i-1}|^2 (m_{\tilde{e}}^2 - m_{u_j}^2 - m_{d_k}^2), \end{aligned} \quad (\text{C.5})$$

for squarks:

$$\begin{aligned} |\overline{M}(\tilde{u}_{j\alpha} \rightarrow e_i^+ d_k)|^2 &= |\lambda_{ijk}'|^2 |Q_{1\alpha}^{2j}|^2 (m_{\tilde{u}}^2 - m_{e_i}^2 - m_{d_k}^2), \\ |\overline{M}(\tilde{u}_{i\alpha} \rightarrow \bar{d}_j \bar{d}_k)|^2 &= (N_c - 1)! |\lambda_{ijk}''|^2 |Q_{2\alpha}^{2i}|^2 (m_{\tilde{u}}^2 - m_{d_j}^2 - m_{d_k}^2), \\ |\overline{M}(\tilde{d}_{j\alpha} \rightarrow \bar{\nu}_i d_k)|^2 &= |\lambda_{ijk}'|^2 |Q_{1\alpha}^{2j-1}|^2 (m_{\tilde{d}}^2 - m_{d_k}^2), \\ |\overline{M}(\tilde{d}_{k\alpha} \rightarrow \nu_i d_j)|^2 &= |\lambda_{ijk}'|^2 |Q_{2\alpha}^{2k-1}|^2 (m_{\tilde{d}}^2 - m_{d_j}^2), \\ |\overline{M}(\tilde{d}_{k\alpha} \rightarrow e_i^- u_j)|^2 &= |\lambda_{ijk}'|^2 |Q_{2\alpha}^{2k-1}|^2 (m_{\tilde{d}}^2 - m_{e_i}^2 - m_{u_j}^2), \\ |\overline{M}(\tilde{d}_{k\alpha} \rightarrow \bar{u}_i \bar{d}_j)|^2 &= (N_c - 1)! |\lambda_{ijk}''|^2 |Q_{2\alpha}^{2k-1}|^2 (m_{\tilde{d}}^2 - m_{u_i}^2 - m_{d_j}^2), \end{aligned} \quad (\text{C.6})$$

where N_c is the number of colours.

Stops

A large mixing between the left and right handed stops is expected because of the large top-quark mass. We show here explicitly the effect of the mixing given in general terms above. The mass eigenstates are [438]

$$\begin{pmatrix} \tilde{t}_1 \\ \tilde{t}_2 \end{pmatrix} = \begin{pmatrix} \tilde{t}_L \cos \theta_t - \tilde{t}_R \sin \theta_t \\ \tilde{t}_L \sin \theta_t + \tilde{t}_R \cos \theta_t \end{pmatrix}, \quad (\text{C.7})$$

where θ_t denotes the mixing angle of the stops:

$$\sin 2\theta_t = \frac{2a_t m_t}{\sqrt{(m_{\tilde{t}_L}^2 - m_{\tilde{t}_R}^2)^2 + 4a_t^2 m_t^2}}, \quad (\text{C.8})$$

$$\cos 2\theta_t = \frac{m_{\tilde{t}_L}^2 - m_{\tilde{t}_R}^2}{\sqrt{(m_{\tilde{t}_L}^2 - m_{\tilde{t}_R}^2)^2 + 4a_t^2 m_t^2}}. \quad (\text{C.9})$$

The $m_{\tilde{t}_{L,R}}$ and a_f are the SUSY mass parameters and m_t is the top-quark mass. The mass eigenvalues are given by:

$$\begin{aligned} m_{\tilde{t}_1}^2 &= \frac{1}{2} \left\{ m_{\tilde{t}_L}^2 + m_{\tilde{t}_R}^2 - \left[(m_{\tilde{t}_L}^2 - m_{\tilde{t}_R}^2)^2 + (2a_t m_t)^2 \right]^{1/2} \right\}, \\ m_{\tilde{t}_2}^2 &= \frac{1}{2} \left\{ m_{\tilde{t}_L}^2 + m_{\tilde{t}_R}^2 + \left[(m_{\tilde{t}_L}^2 - m_{\tilde{t}_R}^2)^2 + (2a_t m_t)^2 \right]^{1/2} \right\}. \end{aligned} \quad (\text{C.10})$$

The partial width of the lightest stop \tilde{t}_1 for the corresponding R_p -violating decay is:

$$\Gamma(\tilde{t}_1 \rightarrow \ell_i^+ d_k) = \frac{1}{16\pi} \lambda'_{ijk}{}^2 \cos^2(\theta_t) m_{\tilde{t}_1}, \quad (\text{C.11})$$

if the masses in the final state are neglected. Depending on the mass of the stop this decay mode may be competitive with respect to the R -parity conserving ones $\tilde{t}_1 \rightarrow t \tilde{\chi}^0$ and $\tilde{t}_1 \rightarrow b \tilde{\chi}^+$.

The sneutrinos may also decay via gauge interactions as $\tilde{\nu}_L^i \rightarrow \tilde{\chi}_a^+ l^i$ or $\tilde{\nu}_L^i \rightarrow \tilde{\chi}_a^0 \nu_L^i$. The partial width is [254]:

$$\Gamma(\tilde{\nu}_L^i \rightarrow \tilde{\chi}_a^+ l^i, \tilde{\chi}_a^0 \nu_L^i) = \frac{C g^2}{16\pi} m_{\tilde{\nu}_L^i} \left(1 - \frac{m_{\tilde{\chi}_a^+}^2}{m_{\tilde{\nu}_L^i}^2}\right)^2, \quad (\text{C.12})$$

where $C = |V_{a1}|^2$ for the decay into chargino and $C = |N_{a2}|^2$, for the neutralino case, with V_{a1} and N_{a2} the mixing matrix elements.

The cross section for the sneutrino production in the s -channel at e^+e^- colliders, is

$$\sigma(e^+e^- \rightarrow \tilde{\nu}_L^i \rightarrow X) = \frac{4\pi s}{m_{\tilde{\nu}_L^i}^2} \frac{\Gamma(\tilde{\nu}_L^i \rightarrow e^+e^-)\Gamma(\tilde{\nu}_L^i \rightarrow X)}{(s - m_{\tilde{\nu}_L^i}^2)^2 + m_{\tilde{\nu}_L^i}^2 \Gamma_{\tilde{\nu}_L^i}^2}, \quad (\text{C.13})$$

where $\Gamma(X)$ generally denotes the partial width for the sneutrino decay into the final state X . At sneutrino resonance, Eq.(C.13) takes the form,

$$\sigma(e^+e^- \rightarrow \tilde{\nu}_L^i \rightarrow X) = \frac{4\pi}{m_{\tilde{\nu}_L^i}^2} B(\tilde{\nu}_L^i \rightarrow e^+e^-) B(\tilde{\nu}_L^i \rightarrow X), \quad (\text{C.14})$$

where $B(X)$ denotes the partial width for sneutrino decay into a final state X .

The $\tilde{\nu}$ production $d\bar{d}$ annihilations through λ'_{ijk} is [500]:

$$\sigma(d_k\bar{d}_j \rightarrow \tilde{\nu}^i \rightarrow X_1X_2) = \frac{4}{9} \frac{\pi\Gamma_{d_k\bar{d}_j}\Gamma_f}{(\hat{s} - m_{\tilde{\nu}^i}^2)^2 + m_{\tilde{\nu}^i}^2\Gamma_{\tilde{\nu}^i}^2}, \quad (\text{C.15})$$

where $\Gamma_{d_k\bar{d}_j}$ and Γ_f are, respectively, the partial widths of the channels $\tilde{\nu}^i \rightarrow d_k\bar{d}_j$ and $\tilde{\nu}^i \rightarrow X_1X_2$, $\Gamma_{\tilde{\nu}^i}$ is the total width of the sneutrino, $m_{\tilde{\nu}^i}$ is the sneutrino mass and \hat{s} is the square of the parton energy in the centre of mass reference frame. A factor 1/3 originates from the matching of the color indices in the initial state. $\Gamma_{d_k\bar{d}_j}$ is given by

$$\Gamma_{d_k\bar{d}_j} = \frac{3}{4}\alpha_{\lambda'_{ijk}} m_{\tilde{\nu}^i}, \quad (\text{C.16})$$

where $\alpha_{\lambda'_{ijk}} = \lambda'^2_{ijk}/4\pi$.

C.2 Neutralinos

The three-body partial width of the neutralino can be calculated using the matrix elements given in the following together with the width formula (C.3). The spin and colour averaged matrix elements are given in terms of the following functions:

$$\begin{aligned} R(\tilde{a}, m_{bc}^2) &\equiv \frac{1}{(m_{bc}^2 - M_{\tilde{a}}^2)^2 + \Gamma_{\tilde{a}}^2 M_{\tilde{a}}^2}, \\ S(\tilde{a}, \tilde{b}, m_{cd}^2, m_{ef}^2) &\equiv R(\tilde{a}, m_{cd}^2)R(\tilde{b}, m_{ef}^2) \\ &\quad [(m_{cd}^2 - M_{\tilde{a}}^2)(m_{ef}^2 - M_{\tilde{b}}^2) + \Gamma_{\tilde{a}}\Gamma_{\tilde{b}}M_{\tilde{a}}M_{\tilde{b}}], \end{aligned} \quad (\text{C.17})$$

where $m_{bc}^2 = (p_b + p_c)^2$, and $M_{\tilde{a}}$, $\Gamma_{\tilde{a}}$ are the mass and the decay width of the sfermion \tilde{a} .

$$\begin{aligned} \Psi(\tilde{a}, 1, 2, 3) &\equiv R(\tilde{a}, m_{12}^2) (m_{12}^2 - m_1^2 - m_2^2) \\ &\quad [(a^2(\tilde{a}) + b^2(\tilde{a})) (m_A^2 + m_3^2 - m_{12}^2) + 4a(\tilde{a})b(\tilde{a})m_3m_A], \\ \Upsilon(\tilde{a}, 1, 2, 3) &\equiv S(\tilde{a}_1, \tilde{a}_2, m_{12}^2, m_{12}^2) (m_{12}^2 - m_1^2 - m_2^2) \\ &\quad [(a(\tilde{a}_1)a(\tilde{a}_2) + b(\tilde{a}_1)b(\tilde{a}_2)) (m_A^2 + m_3^2 - m_{12}^2) \\ &\quad + 2(a(\tilde{a}_1)b(\tilde{a}_2) + a(\tilde{a}_2)b(\tilde{a}_1)) m_3m_A], \\ \Phi(\tilde{a}, \tilde{b}, 1, 2, 3) &\equiv S(\tilde{a}, \tilde{b}, m_{12}^2, m_{23}^2) \left[m_1m_3a(\tilde{a})a(\tilde{b}) (m_{12}^2 + m_{23}^2 - m_1^2 - m_3^2) \right. \\ &\quad + m_1m_Ab(\tilde{a})a(\tilde{b}) (m_{23}^2 - m_2^2 - m_3^2) \\ &\quad + m_3m_Aa(\tilde{a})b(\tilde{b}) (m_{12}^2 - m_1^2 - m_2^2) \\ &\quad \left. + b(\tilde{a})b(\tilde{b}) (m_{12}^2m_{23}^2 - m_1^2m_3^2 - m_A^2m_2^2) \right], \end{aligned} \quad (\text{C.18})$$

where m_A is the mass of the neutralino, \tilde{a}_1 and \tilde{a}_2 are the mass eigenstates of the SUSY particle. The functions a and b are gaugino-sfermion-fermion coupling constants. For the neutralino decay the couplings a and b are as follows:

$$a(\tilde{\nu}_i) = 0, \quad b(\tilde{\nu}_i) = \frac{gN'_{l2}}{2\cos\theta_W}, \quad (\text{C.19})$$

$$\begin{aligned}
a(\tilde{\ell}_{i\alpha}) &= m_{\ell_i} \frac{gN_{l3}}{2M_W \cos \beta} L_{1\alpha}^{2i-1} + L_{2\alpha}^{2i-1} \left(eN'_{l1} - \frac{g \sin^2 \theta_W N'_{l2}}{\cos} \right), \\
b(\tilde{\ell}_{i\alpha}) &= m_{\ell_i} \frac{gN_{l3}}{2M_W \cos \beta} L_{2\alpha}^{2i-1} - L_{1\alpha}^{2i-1} \left(eN'_{l1} + \frac{gN'_{l2} \left(\frac{1}{2} - \sin^2 \theta_W \right)}{\cos \theta_W} \right), \quad (C.20)
\end{aligned}$$

$$\begin{aligned}
a(\tilde{d}_{i\alpha}) &= m_{d_i} \frac{gN_{l3}}{2M_W \cos \beta} Q_{1\alpha}^{2i-1} - Q_{2\alpha}^{2i-1} \left(ee_d N'_{l1} - \frac{ge_d \sin^2 \theta_W N'_{l2}}{\cos \theta_W} \right), \\
b(\tilde{d}_{i\alpha}) &= m_{d_i} \frac{gN_{l3}}{2M_W \cos \beta} Q_{2\alpha}^{2i-1} + Q_{1\alpha}^{2i-1} \left(ee_d N'_{l1} - \frac{gN'_{l2} \left(\frac{1}{2} + e_d \sin^2 \theta_W \right)}{\cos \theta_W} \right), \quad (C.21)
\end{aligned}$$

$$\begin{aligned}
a(\tilde{u}_{i\alpha}) &= m_{u_j} \frac{gN_{l4}}{2M_W \sin \beta} Q_{1\alpha}^{2j} - Q_{2\alpha}^{2j} \left(ee_u N'_{l1} - \frac{ge_u \sin^2 \theta_W N'_{l2}}{\cos \theta_W} \right), \\
b(\tilde{u}_{i\alpha}) &= m_{u_i} \frac{gN_{l4}}{2M_W \sin \beta} Q_{2\alpha}^{2i} + Q_{1\alpha}^{2i} \left(ee_u N'_{l1} + \frac{gN'_{l2} \left(\frac{1}{2} - e_u \sin^2 \theta_W \right)}{\cos \theta_W} \right). \quad (C.22)
\end{aligned}$$

In terms of these functions and couplings, the averaged matrix elements for three-body neutralino decays can be written:

$$\begin{aligned}
|\overline{M}(\tilde{\chi}_l^0 \rightarrow \tilde{\nu}_i \ell_j^+ \ell_k^-)|^2 &= \\
&\lambda_{ijk}^2 \left[\Psi(\tilde{\nu}_i, \ell_j, \ell_k, \nu_i) + \sum_{\alpha=1,2} |L_{1\alpha}^{2j-1}|^2 \Psi(\tilde{\ell}_{j\alpha}, \nu_i, \ell_k, \ell_j) \right. \\
&+ \sum_{\alpha=1,2} |L_{2\alpha}^{2k-1}|^2 \Psi(\tilde{\ell}_{k\alpha}^*, \nu_i, \ell_j, \ell_k) \\
&+ 2L_{11}^{2j-1} L_{12}^{2j-1} \Upsilon(\tilde{\ell}_j, \nu_i, \ell_k, \ell_j) + 2L_{21}^{2k-1} L_{22}^{2k-1} \Upsilon(\tilde{\ell}_k^*, \nu_i, \ell_j, \ell_k) \\
&- \sum_{\alpha=1,2} 2L_{1\alpha}^{2j-1} \Phi(\tilde{\ell}_{j\alpha}, \tilde{\nu}_i, \nu_i, \ell_k, \ell_j) - \sum_{\alpha=1,2} 2L_{2\alpha}^{2k-1} \Phi(\tilde{\ell}_{k\alpha}^*, \tilde{\nu}_i, \nu_i, \ell_j, \ell_k) \\
&\left. - \sum_{\alpha,\beta=1,2} 2L_{1\alpha}^{2j-1} L_{2\beta}^{2k-1} \Phi(\tilde{\ell}_{k\beta}^*, \tilde{\ell}_{j\alpha}, \ell_j, \nu_i, \ell_k) \right], \quad (C.23)
\end{aligned}$$

$$\begin{aligned}
|\overline{M}(\tilde{\chi}_l^0 \rightarrow \tilde{\nu}_i \bar{d}_j d_k)|^2 &= \\
&\lambda_{ijk}{}^{\prime 2} N_c \left[\Psi(\tilde{\nu}_i, d_j, d_k, \nu_i) + \sum_{\alpha=1,2} |Q_{1\alpha}^{2j-1}|^2 \Psi(\tilde{d}_{j\alpha}, \nu_i, d_k, d_j) \right. \\
&+ \sum_{\alpha=1,2} |Q_{2\alpha}^{2k-1}|^2 \Psi(\tilde{d}_{k\alpha}^*, \nu_i, d_j, d_k) \\
&+ 2Q_{11}^{2j-1} Q_{12}^{2j-1} \Upsilon(\tilde{d}_j, \nu_i, d_k, d_j) + 2Q_{21}^{2k-1} Q_{22}^{2k-1} \Upsilon(\tilde{d}_k^*, \nu_i, d_j, d_k) \\
&- \sum_{\alpha=1,2} 2Q_{1\alpha}^{2j-1} \Phi(\tilde{d}_{j\alpha}, \tilde{\nu}_i, \nu_i, d_k, d_j) - \sum_{\alpha=1,2} 2Q_{2\alpha}^{2k-1} \Phi(\tilde{d}_{k\alpha}^*, \tilde{\nu}_i, \nu_i, d_j, d_k) \\
&\left. - \sum_{\alpha,\beta=1,2} 2Q_{1\alpha}^{2j-1} Q_{2\beta}^{2k-1} \Phi(\tilde{d}_{k\beta}^*, \tilde{d}_{j\alpha}, d_j, \nu_i, d_k) \right], \quad (C.24)
\end{aligned}$$

$$\begin{aligned}
|\overline{M}(\tilde{\chi}_l^0 \rightarrow \ell_i^+ \bar{u}_j d_k)|^2 = & \\
& \lambda_{ijk}{}^2 N_c \left[\sum_{\alpha=1,2} |L_{1\alpha}^{2i-1}|^2 \Psi(\tilde{\ell}_{i\alpha}, u_j, d_k, \ell_i) + \sum_{\alpha=1,2} |Q_{1\alpha}^{2j}|^2 \Psi(\tilde{u}_{j\alpha}, \ell_i, d_k, u_j) \right. \\
& + \sum_{\alpha=1,2} |Q_{2\alpha}^{2k-1}|^2 \Psi(\tilde{d}_{k\alpha}^*, \ell_i, u_j, d_k) + 2L_{11}^{2i-1} L_{12}^{2i-1} \Upsilon(\tilde{\ell}_i, u_j, d_k, \ell_i) \\
& + 2Q_{11}^{2j} Q_{12}^{2j} \Upsilon(\tilde{u}_j, \ell_i, d_k, u_j) + 2Q_{21}^{2k-1} Q_{22}^{2k-1} \Upsilon(\tilde{d}_k^*, \ell_i, u_j, d_k) \\
& - \sum_{\alpha,\beta=1,2} 2L_{1\alpha}^{2i-1} Q_{1\beta}^{2j} \Phi(\tilde{u}_{j\beta}, \tilde{\ell}_{i\alpha}, \ell_i, d_k, u_j) \\
& - \sum_{\alpha,\beta=1,2} 2L_{1\alpha}^{2i-1} Q_{2\beta}^{2k-1} \Phi(\tilde{d}_{k\beta}^*, \tilde{\ell}_{i\alpha}, \ell_i, u_j, d_k) \\
& \left. - \sum_{\alpha,\beta=1,2} 2Q_{1\alpha}^{2j} Q_{2\beta}^{2k-1} \Phi(\tilde{d}_{k\beta}^*, \tilde{u}_{j\alpha}, u_j, \ell_i, d_k) \right], \tag{C.25}
\end{aligned}$$

$$\begin{aligned}
|\overline{M}(\tilde{\chi}_l^0 \rightarrow \bar{u}_i \bar{d}_j \bar{d}_k)|^2 = & \\
& \lambda_{ijk}{}^2 N_c! \left[\sum_{\alpha=1,2} |Q_{2\alpha}^{2i}|^2 \Psi(\tilde{u}_{i\alpha}^*, d_j, d_k, u_i) + \sum_{\alpha=1,2} |Q_{2\alpha}^{2j-1}|^2 \Psi(\tilde{d}_{j\alpha}^*, u_i, d_k, d_j) \right. \\
& + \sum_{\alpha=1,2} |Q_{2\alpha}^{2k-1}|^2 \Psi(\tilde{d}_{k\alpha}^*, u_i, d_j, d_k) + 2Q_{21}^{2i} Q_{22}^{2i} \Upsilon(\tilde{u}_i^*, d_j, d_k, u_i) \\
& + 2Q_{21}^{2j-1} Q_{22}^{2j-1} \Upsilon(\tilde{d}_j^*, u_i, d_k, d_j) + 2Q_{21}^{2k-1} Q_{22}^{2k-1} \Upsilon(\tilde{d}_k^*, u_i, d_j, d_k) \\
& - \sum_{\alpha,\beta=1,2} 2Q_{2\alpha}^{2i-1} Q_{2\beta}^{2j-1} \Phi(\tilde{d}_{j\beta}^*, \tilde{u}_{i\alpha}^*, u_i, d_k, d_j) \\
& - \sum_{\alpha,\beta=1,2} 2Q_{2\alpha}^{2i-1} Q_{2\beta}^{2k-1} \Phi(\tilde{d}_{k\beta}^*, \tilde{u}_{i\alpha}^*, u_i, d_j, d_k) \\
& \left. - \sum_{\alpha,\beta=1,2} 2Q_{2\alpha}^{2j-1} Q_{2\beta}^{2k-1} \Phi(\tilde{d}_{k\beta}^*, \tilde{d}_{j\alpha}^*, d_j, u_i, d_k) \right]. \tag{C.26}
\end{aligned}$$

C.3 Charginos

Three-body decays of the chargino are obtained in terms of the same functions (C.17,C.18) given in the previous section (C.2), but the coefficients a and b for the couplings are as follows:

$$\begin{aligned}
a(\tilde{\ell}_{i\alpha}) &= 0 & b(\tilde{\ell}_{i\alpha}) &= L_{1\alpha}^{2i-1} U_{l1} - \frac{U_{l2} L_{2\alpha}^{2i-1} m_{e_i}}{\sqrt{2} M_W \cos \beta} \\
a(\tilde{\nu}_i) &= \frac{U_{l2} m_{e_i}}{\sqrt{2} M_W \cos \beta} & b(\tilde{\nu}_i) &= V_{l1}^* \\
a(\tilde{u}_{i\alpha}) &= -\frac{m_{d_i} U_{l2} Q_{1\alpha}^{2i}}{\sqrt{2} M_W \cos \beta} & b(\tilde{u}_{i\alpha}) &= V_{l1}^* Q_{1\alpha}^{2i} - \frac{m_{u_i} V_{l2}^* Q_{2\alpha}^{2i}}{\sqrt{2} M_W \sin \beta} \\
a(\tilde{d}_{i\alpha}) &= -\frac{m_{u_i} V_{l2}^* Q_{1\alpha}^{2i-1}}{\sqrt{2} M_W \sin \beta} & b(\tilde{d}_{i\alpha}) &= Q_{1\alpha}^{2i-1} U_{l1} - \frac{U_{l2} Q_{2\alpha}^{2i-1} m_{d_i}}{\sqrt{2} M_W \cos \beta}. \tag{C.27}
\end{aligned}$$

The averaged matrix elements are:

$$|\overline{M}(\tilde{\chi}_l^+ \rightarrow \bar{\nu}_i \ell_j^+ \nu_k)|^2 = \frac{g^2 \lambda_{ijk}{}^2}{2} \left[\sum_{\alpha=1,2} |L_{2\alpha}^{2k-1}|^2 \Psi(\tilde{\ell}_{k\alpha}^*, \nu_i, \ell_j, \nu_k) + 2L_{21}^{2k-1} L_{22}^{2k-1} \Upsilon(\tilde{\ell}_k^*, \nu_i, \ell_j, \nu_k) \right], \quad (\text{C.28})$$

$$\begin{aligned} |\overline{M}(\tilde{\chi}_l^+ \rightarrow \nu_i \nu_j \ell_k^+)|^2 = & \frac{g^2 \lambda_{ijk}{}^2}{2} \left[\sum_{\alpha=1,2} |L_{1\alpha}^{2i-1}|^2 \Psi(\tilde{\ell}_{i\alpha}, \nu_j, \ell_k, \nu_i) + \sum_{\alpha=1,2} |L_{1\alpha}^{2j-1}|^2 \Psi(\tilde{\ell}_{j\alpha}, \nu_i, \ell_k, \nu_j) \right. \\ & 2L_{11}^{2i-1} L_{12}^{2i-1} \Upsilon(\tilde{\ell}_i, \nu_j, \ell_k, \nu_i) + 2L_{11}^{2j-1} L_{12}^{2j-1} \Upsilon(\tilde{\ell}_j, \nu_i, \ell_k, \nu_j) \\ & \left. + \sum_{\alpha,\beta=1,2} L_{1\alpha}^{2i-1} L_{1\beta}^{2j-1} \Phi(\tilde{\ell}_{j\beta}, \tilde{\ell}_{i\alpha}, \nu_i, \ell_k, \nu_j) \right], \quad (\text{C.29}) \end{aligned}$$

$$|\overline{M}(\tilde{\chi}_l^+ \rightarrow \ell_i^+ \ell_j^+ \ell_k^-)|^2 = \frac{g^2 \lambda_{ijk}{}^2}{2} [\Psi(\tilde{\nu}_i, \ell_j, \ell_k, \ell_i) + \Psi(\tilde{\nu}_j, \ell_i, \ell_k, \ell_j) + 2\Phi(\tilde{\nu}_j, \tilde{\nu}_i, \ell_i, \ell_k, \ell_j)], \quad (\text{C.30})$$

$$|\overline{M}(\tilde{\chi}_l^+ \rightarrow \bar{\nu}_i \bar{d}_j u_k)|^2 = \frac{g^2 \lambda_{ijk}{}^2 N_c}{2} \left[\sum_{\alpha=1,2} |Q_{2\alpha}^{2k-1}|^2 \Psi(\tilde{d}_{k\alpha}^*, \nu_i, d_j, u_k) + 2Q_{21}^{2k-1} Q_{22}^{2k-1} \Upsilon(\tilde{d}_k^*, \nu_i, d_j, u_k) \right] \quad (\text{C.31})$$

$$|\overline{M}(\tilde{\chi}_l^+ \rightarrow \ell_i^+ \bar{u}_j u_k)|^2 = \frac{g^2 \lambda_{ijk}{}^2 N_c}{2} \left[\sum_{\alpha=1,2} |Q_{2\alpha}^{2k-1}|^2 \Psi(\tilde{d}_{k\alpha}^*, \ell_i, u_j, u_k) + 2Q_{21}^{2k-1} Q_{22}^{2k-1} \Upsilon(\tilde{d}_k^*, \ell_i, u_j, u_k) \right] \quad (\text{C.32})$$

$$\begin{aligned} |\overline{M}(\tilde{\chi}_l^+ \rightarrow \ell_i^+ \bar{d}_j d_k)|^2 = & \frac{g^2 \lambda_{ijk}{}^2 N_c}{2} \left[\Psi(\tilde{\nu}_i, d_j, d_k, \ell_i) + \sum_{\alpha=1,2} |Q_{1\alpha}^{2j}|^2 \Psi(\tilde{u}_{j\alpha}, \ell_i, d_k, d_j) \right. \\ & \left. + 2Q_{11}^{2j} Q_{12}^{2j} \Upsilon(\tilde{u}_j, \ell_i, d_k, d_j) + 2 \sum_{\alpha=1,2} Q_{1\alpha}^{2j} \Phi(\tilde{u}_{j\alpha}, \tilde{\nu}_i, \ell_i, d_k, d_j) \right], \quad (\text{C.33}) \end{aligned}$$

$$\begin{aligned} |\overline{M}(\tilde{\chi}_l^+ \rightarrow \nu_i u_j \bar{d}_k)|^2 = & \frac{g^2 \lambda_{ijk}{}^2 N_c}{2} \left[\sum_{\alpha=1,2} |L_{1\alpha}^{2i-1}|^2 \Psi(\tilde{\ell}_{i\alpha}, u_j, d_k, \nu_i) + \sum_{\alpha=1,2} |Q_{1\alpha}^{2j-1}|^2 \Psi(\tilde{d}_{j\alpha}, \nu_i, d_k, u_j) \right. \\ & + 2L_{11}^{2i-1} L_{12}^{2i-1} \Upsilon(\tilde{\ell}_i, u_j, d_k, \nu_i) + 2Q_{11}^{2j-1} Q_{12}^{2j-1} \Upsilon(\tilde{d}_j, \nu_i, d_k, u_j) \\ & \left. + 2 \sum_{\alpha,\beta=1,2} L_{1\alpha}^{2i-1} Q_{1\beta}^{2j-1} \Phi(\tilde{d}_{j\beta}, \tilde{\ell}_{i\alpha}, \nu_i, d_k, u_j) \right], \quad (\text{C.34}) \end{aligned}$$

$$\begin{aligned}
|\overline{M}(\tilde{\chi}_l^+ \rightarrow u_i u_j d_k)|^2 = & \\
& \frac{g^2 N_c!}{2(1 + \delta_{ij})} \left[\lambda_{jik}''^2 \sum_{\alpha=1,2} |Q_{2\alpha}^{2i-1}|^2 \Psi(\tilde{d}_{i\alpha}^*, u_j, d_k, u_i) + \lambda_{ijk}''^2 \sum_{\alpha=1,2} |Q_{2\alpha}^{2j-1}|^2 \Psi(\tilde{d}_{j\alpha}^*, u_i, d_k, u_j) \right. \\
& + 2\lambda_{jik}''^2 Q_{21}^{2i-1} Q_{22}^{2i-1} \Upsilon(\tilde{d}_i^*, u_j, d_k, u_i) + 2\lambda_{ijk}''^2 Q_{21}^{2j-1} Q_{22}^{2j-1} \Upsilon(\tilde{d}_j^*, u_i, d_k, u_j) \\
& \left. + 2\lambda_{ijk}'' \lambda_{jik}'' \sum_{\alpha,\beta=1,2} Q_{2\alpha}^{2i-1} Q_{2\beta}^{2j-1} \Phi(\tilde{d}_{j\beta}^*, \tilde{d}_{i\alpha}^*, u_i, d_k, u_j) \right], \tag{C.35}
\end{aligned}$$

$$\begin{aligned}
|\overline{M}(\tilde{\chi}_l^+ \rightarrow \bar{d}_i \bar{d}_j \bar{d}_k)|^2 = & \\
& \frac{g^2 N_c!}{2(1 + \delta_{ij} + \delta_{jk} + \delta_{ik})} \left[\lambda_{ijk}''^2 \sum_{\alpha=1,2} |Q_{2\alpha}^{2i}|^2 \Psi(\tilde{u}_{i\alpha}^*, d_j, d_k, d_i) \right. \\
& + \lambda_{jki}''^2 \sum_{\alpha=1,2} |Q_{2\alpha}^{2j}|^2 \Psi(\tilde{u}_{j\alpha}^*, d_i, d_k, d_j) \\
& + \lambda_{kij}''^2 \sum_{\alpha=1,2} |Q_{2\alpha}^{2k}|^2 \Psi(\tilde{u}_{k\alpha}^*, d_i, d_j, d_k) + 2\lambda_{ijk}''^2 Q_{21}^{2i} Q_{22}^{2i} \Upsilon(\tilde{u}_i^*, d_j, d_k, d_i) \\
& + 2\lambda_{jki}''^2 Q_{21}^{2j} Q_{22}^{2j} \Upsilon(\tilde{u}_j^*, d_i, d_k, d_j) + 2\lambda_{kij}''^2 Q_{21}^{2k} Q_{22}^{2k} \Upsilon(\tilde{u}_{k\alpha}^*, d_i, d_j, d_k) \\
& - 2\lambda_{ijk}'' \lambda_{jki}'' \sum_{\alpha,\beta=1,2} Q_{2\alpha}^{2i} Q_{2\beta}^{2j} \Phi(\tilde{u}_{j\beta}^*, \tilde{u}_{i\alpha}^*, d_i, d_k, d_j) \\
& - 2\lambda_{ijk}'' \lambda_{kij}'' \sum_{\alpha,\beta=1,2} Q_{2\alpha}^{2i} Q_{2\beta}^{2k} \Phi(\tilde{u}_{k\beta}^*, \tilde{u}_{i\alpha}^*, d_i, d_j, d_k) \\
& \left. - 2\lambda_{jki}'' \lambda_{kij}'' \sum_{\alpha,\beta=1,2} Q_{2\alpha}^{2j} Q_{2\beta}^{2k} \Phi(\tilde{u}_{k\beta}^*, \tilde{u}_{j\alpha}^*, d_j, d_i, d_k) \right]. \tag{C.36}
\end{aligned}$$

Bibliography

- [1] P. Fayet, Nucl. Phys. **B90** (1975) 104.
- [2] P. Fayet, Phys. Lett. **B64** (1976) 159; Phys. Lett. **B69** (1977) 489.
- [3] P. Fayet, Phys. Lett. **B70** (1977) 461.
- [4] P. Fayet, in *New Frontiers in High-Energy Physics*, Proc. Orbis Scientiae, Coral Gables (Florida, USA), 1978, eds. A. Perlmutter and L.F. Scott (Plenum, N.Y., 1978) p. 413.
- [5] G.R. Farrar and P. Fayet, Phys. Lett. **B76** (1978) 575.
- [6] G.R. Farrar and P. Fayet, Phys. Lett. **B79** (1978) 442.
- [7] P. Fayet, Phys. Lett. **B78** (1978) 417.
- [8] S. Weinberg, Phys. Rev. **D26** (1982) 287.
- [9] Yu A. Gol'fand and E.P. Likhtman, ZhETF Pis. Red. **C13** (1971) 452 (Sov. Phys. JETP Lett. **C13** (1971) 323).
- [10] D.V. Volkov and V.P. Akulov, Phys. Lett. **B46** (1973) 109.
- [11] J. Wess and B. Zumino, Nucl. Phys. **B70** (1974) 39; Phys. Lett. **B49** (1974) 52.
- [12] S. Ferrara, D.Z. Freedman and P. van Nieuwenhuizen, Phys. Rev. **D13** (1976) 3214; S. Deser and B. Zumino, Phys. Lett. **B62** (1976) 335; for reviews see P. Van Nieuwenhuizen, Phys. Rep. **68** (1981) 189 or H.P. Nilles, Phys. Rep. **110** (1984) 1 and references therein.
- [13] P. Fayet and J. Iliopoulos, Phys. Lett. **B51** (1974) 461; P. Fayet, Phys. Lett. **B58** (1975) 67; L. O'Raifeartaigh, Nucl. Phys. **B96** (1975) 331.
- [14] E. Cremmer *et al.*, Phys. Lett. **B147** (1979) 105.
- [15] P. Fayet, Phys. Lett. **B175** (1986) 471.
- [16] P. Fayet, Nucl. Phys. **B78** (1974) 14.
- [17] A. Salam and J. Strathdee, Nucl. Phys. **B87** (1975) 85.
- [18] P. Fayet, in *History of original ideas and basic discoveries in Particle Physics*, eds. H. Newman and T. Ypsilantis, Proc. Erice Conf. (1994), *NATO Series B* **352**, 639 (Plenum, N.Y., 1996).
- [19] L. Girardello and M.T. Grisaru, Nucl. Phys. **B194** (1982) 65.

- [20] S. Eidelman *et al.*, *Review of Particle Physics*, Phys. Lett. **B592** (2004) 1.
- [21] P. Fayet, in *Minneapolis 2000, 30 years of supersymmetry*, Nucl. Phys. Proc. Suppl. **101** (2001) 81.
- [22] P. Fayet, Phys. Lett. **B159** (121) 1985; Nucl. Phys. **B263** (649) 1986; Proc. 2nd Nobel Symp. on El. Part. Physics (Marstrand, Sweden, 1986), Phys. Scripta **T15** (1987) 46.
- [23] N. Sakai and T. Yanagida, Nucl. Phys. **B197** (1982) 533.
- [24] L.J. Hall and M. Suzuki, Nucl. Phys. **B231** (1984) 419.
- [25] H.E. Haber and G.L. Kane, Phys. Rep. **117** (1985) 175.
- [26] S. Davidson and J. Ellis, Phys. Lett. **B390** (1997) 210; Phys. Rev. **D56** (1997) 4182.
- [27] S. Davidson, Phys. Lett. **B439** (1998) 63.
- [28] J. Ferrandis, Phys. Rev. **D60** (1999) 095012.
- [29] H.K. Dreiner and M. Thormeier, Phys. Rev. **D69** (2004) 053002.
- [30] B. de Carlos and P.L. White, Phys. Rev. **D54** (1996) 3427.
- [31] E. Nardi, Phys. Rev. **D55** (1997) 5772.
- [32] H. Dreiner and H. Pois, “Two Loop Supersymmetric Renormalization Group Equations Including R -parity Violation and Aspects of Unification”, (1995) *unpublished*; eprint hep-ph/9511444.
- [33] I.H. Lee, Phys. Lett. **B138** (1984) 121; Nucl. Phys. **B246** (1984) 120.
- [34] S. Dawson, Nucl. Phys. **B261** (1985) 297.
- [35] T. Banks, Y. Grossman, E. Nardi and Y. Nir, Phys. Rev. **D52** (1995) 5319.
- [36] M. Bisset, O.C.W. Kong, C. Macesanu, and L.H. Orr, Phys. Lett. **B430** (1998) 274.
- [37] P. Binétruy, E. Dudas, S. Lavignac and C. Savoy, Phys. Lett. **B422** (1998) 171.
- [38] Y. Grossman and H.E. Haber, Phys. Rev. **D59** (1999) 093008.
- [39] R. Hempfling, Nucl. Phys. **B478** (1996) 3.
- [40] H.-P. Nilles and N. Polonsky, Nucl. Phys. **B484** (1997) 33.
- [41] F. de Campos, M.A. Garcia-Jareño, A.S. Joshipura, J. Rosiek, and J.W.F. Valle, Nucl. Phys. **B451** (1995) 3.
- [42] M.A. Diaz, J.C. Romao and J.W.F. Valle, Nucl. Phys. **B524** (1998) 23.
- [43] C.-H. Chang and T.-F. Feng, Eur. Phys. J **12** (2000) 137.
- [44] S. Davidson, M. Losada and N. Rius, Nucl. Phys. **B587** (2000) 118.
- [45] O.C.W. Kong, “On the Formulation of the Generic Supersymmetric Standard Model”, (May 2002) 27pp., eprint hep-ph/0205205.

- [46] C.L. Bennett *et al.*, *Astrophys. J. Suppl.* **148** (2003) 1; D.N. Spergel *et al.*, *Astrophys. J. Suppl.* **148** (2003) 175.
- [47] M. Colless *et al.*, *Mon. Not. Roy. Astron. Soc.* **328** (2001) 1039.
- [48] J.C. Romao *et al.*, *Nucl. Phys.* **B482** (1996) 3; A.G. Akeroyd, M.A. Diaz and J.W.F. Valle, *Phys. Lett.* **B441** (1998) 224.
- [49] M.C. Gonzalez-Garcia, J.C. Romao and J.W.F. Valle, *Nucl. Phys.* **B391** (1993) 100; A. Bartl *et al.*, *Nucl. Phys.* **B502** (1997) 19
- [50] B. Mukhopadhyaya, S. Roy, and F. Vissani, *Phys. Lett.* **B443** (1998) 191; A. Datta, B. Mukhopadhyaya, and F. Vissani, *Phys. Lett.* **B492** (2000) 324.
- [51] W. Porod, M Hirsch, J.C. Romao and J.W.F. Valle, *Phys. Rev.* **D63** (2001) 115004.
- [52] M Hirsch and W. Porod, *Phys. Rev.* **D68** (2003) 115007.
- [53] S. Roy and B. Mukhopadhyaya, *Phys. Rev.* **D55** (1997) 7020.
- [54] M Hirsch, W. Porod, J.C. Romao and J.W.F. Valle, *Phys. Rev.* **D66** (2002) 095006.
- [55] C.S. Aulakh and R.N. Mohapatra, *Phys. Lett.* **B119** (1982) 136.
- [56] J. Ellis, G. Gelmini, C. Jarlskog, G.G. Ross and J.W.F. Valle, *Phys. Lett.* **B150** (1985) 142.
- [57] G. Ross and J. Valle, *Phys. Lett.* **B151** (1985) 375.
- [58] Y. Chikashige, R.N. Mohapatra, and R. Peccei, *Phys. Lett.* **B98** (1981) 265.
- [59] G.B. Gelmini and M. Roncadelli, *Phys. Lett.* **B99** (1981) 41.
- [60] H. Georgi, S.L. Glashow and S. Nussinov, *Nucl. Phys.* **B193** (1981) 297; M. Fukugita, S. Watamura and M. Yoshimura, *Phys. Rev. Lett.* **48** (1982) 1522.
- [61] D. Comelli, A. Masiero, M. Pietroni and A. Riotto, *Phys. Lett.* **B324** (1994) 397.
- [62] J.W.F. Valle, *Phys. Lett.* **B196** (1987) 157; M.C. Gonzalez-Garcia and J.W.F. Valle, *Nucl. Phys.* **B355** (1991) 330.
- [63] A. Masiero and J.W.F. Valle, *Phys. Lett.* **B251** (1990) 273.
- [64] J.C. Romao, C.A. Santos and J.W.F. Valle, *Phys. Lett.* **B288** (1992) 311.
- [65] G.F. Giudice, A. Masiero, M. Pietroni and A. Riotto, *Nucl. Phys.* **B396** (1993) 243; M. Shiraishi, I. Umemura and K. Yamamoto, *Phys. Lett.* **B313** (1993) 89.
- [66] J.C. Romao, A. Ioannissyan and J.W.F. Valle, *Phys. Rev.* **D55** (1997) 427.
- [67] A.S. Joshipura and S.D. Rindani, *Phys. Rev. Lett.* **69** (1992) 3269; J.C. Romao, F. de Campos and J.W.F. Valle, *Phys. Lett.* **B292** (1992) 329; A.S. Joshipura and J.W.F. Valle, *Nucl. Phys.* **B397** (1993) 105.
- [68] J.C. Romao and J.W.F. Valle, *Nucl. Phys.* **B381** (1992) 87; A.D. Dolgov, S. Pastor, J.C. Romao and J.W.F. Valle, *Nucl. Phys.* **B496** (1997) 24.

- [69] M.C. Gonzalez-Garcia and Y. Nir, Phys. Lett. **B232** (1990) 383; P. Noguera and J.C. Roñao, Phys. Lett. **B234** (1990) 371.
- [70] F. de Campos, O.J.P. Eboli, M.A. Garcia-Jareno, and J.W.F. Valle, Nucl. Phys. **B546** (1999) 33.
- [71] F. Borzumati, Y. Grossman, E. Nardi and Y. Nir, Phys. Lett. **B384** (1996) 123.
- [72] V. Ben-Hamo and Y. Nir, Phys. Lett. **B339** (1994) 77.
- [73] P. Binétruy, S. Lavignac and P. Ramond, Nucl. Phys. **B477** (1996) 353.
- [74] J. Ellis, S. Lola, and G.G. Ross, Nucl. Phys. **B526** (1998) 115.
- [75] G. Bhattacharyya, Phys. Rev. **D57** (1998) 3944.
- [76] C.D. Froggatt and H.B. Nielsen, Nucl. Phys. **B147** (1979) 277; L.E. Ibáñez and G.G. Ross, Phys. Lett. **B332** (1994) 100; P. Binétruy and P. Ramond, Phys. Lett. **B350** (1995) 49; V. Jain and R. Shrock, Phys. Lett. **B352** (1995) 83; E. Dudas, S. Pokorski and C. Savoy, Phys. Lett. **B356** (1995) 43.
- [77] E. Dudas and S. Lavignac, note GDR-Supersymétrie GDR-S-010 (LPTHE, Orsay, May 1998).
- [78] G. Giudice and A. Masiero, Phys. Lett. **B206** (1988) 480.
- [79] H. Murayama and D.B. Kaplan, Phys. Lett. **B336** (1994) 221.
- [80] N. Irges, S. Lavignac and P. Ramond, Phys. Rev. **D58** (1998) 035003.
- [81] A.Y. Smirnov and F. Vissani, Nucl. Phys. **B460** (1996) 37.
- [82] D. Brahm and L.J. Hall, Phys. Rev. **D40** (1989) 2449.
- [83] K. Tamvakis, Phys. Lett. **B383** (1996) 307; Phys. Lett. **B382** (1996) 251.
- [84] R. Barbieri, A. Strumia and Z. Berezhiani, Phys. Lett. **B407** (1997) 250.
- [85] G.F. Giudice and R. Rattazzi, Phys. Lett. **B406** (1997) 321.
- [86] R.N. Mohapatra, "Supersymmetric Grand Unification", Proceedings of the TASI '97 School on Supersymmetry, Supergravity and Supercolliders (Ed. J.A. Bagger), Boulder, USA (2 - 27 June 1997) 601-657.
- [87] L.E. Ibáñez and G.G. Ross, Nucl. Phys. **B368** (1992) 3.
- [88] B. C. Allanach, A. Dedes and H. K. Dreiner, Phys. Rev. **D69** (2004) 115002.
- [89] L. Krauss and F. Wilczek, Phys. Rev. Lett. **62** (1989) 1221; T. Banks, Nucl. Phys. **B323** (1989) 90; G. Gilbert, Nucl. Phys. **B328** (1989) 159; M. Alford, J. March-Russell and F. Wilczek, Nucl. Phys. **B337** (1990) 695.
- [90] L.E. Ibáñez and G.G. Ross, Phys. Lett. **B260** (1991) 291.
- [91] M.B. Green and J.H. Schwarz, Phys. Lett. **B149** (1984) 117.

- [92] L.E. Ibáñez, Phys. Lett. **B303** (1993) 55.
- [93] W. J. Marciano, “Low-Energy Phenomenology, Proton Decay, And Grand Unification”, in *Syracuse 1987, Proceedings of the 8th Workshop on Grand Unification*, ed. K.C. Wali, World Scientific, pp. 185-199; U. Amaldi *et al.*, Phys. Rev. **D36** (1987) 1385; J. Ellis, S. Kelley and D. V. Nanopoulos, Phys. Lett. **B249** (1990) 441; U. Amaldi, W. de Boer and H. Furstenau, Phys. Lett. **B260** (1991) 447.
- [94] C. Jarlskog, Z. Phys. **C29** (491) 1985.
- [95] B. C. Allanach, A. Dedes and H. K. Dreiner, Phys. Rev. **D60** (1999) 056002; Phys. Rev. **D60** (1999) 075014.
- [96] S. P. Martin and M. T. Vaughn, Phys. Rev. **D50** (1994) 2282.
- [97] J. E. Bjorkman and D. R. Jones, Nucl. Phys. **B259** (1985) 533.
- [98] M.A. Diaz, J. Ferrandis, J.C. Romão, and J.W.F. Valle, Phys. Lett. **B453** (1999) 263.
- [99] B. Brahmachari and P. Roy, Phys. Rev. **D50** (1994) R39; (*Erratum* Phys. Rev. **D51** (1995) 3974).
- [100] J.L. Goity and M. Sher, Phys. Lett. **B346** (1995) 69; Phys. Lett. **B385** (1996) 500 (E).
- [101] B. Pendleton and G.G. Ross, Phys. Lett. **B98** (1981) 291.
- [102] C.T. Hill, Phys. Rev. **D24** (691) 1981.
- [103] G. Auberson and G. Moulataka, Eur. Phys. J **12** (331) 2000; D. Kazakov and G. Moulataka, Nucl. Phys. **B577** (121) 2000; Y. Mambrini, G. Moulataka and M. Rausch de Traubenberg, Nucl. Phys. **B609** (83) 2001.
- [104] V. Barger, M.S. Berger, R.J.N. Phillips and T. Wöhrmann, Phys. Rev. **D53** (1996) 6407.
- [105] V. Barger, M. S. Berger, W.Y. Keung, R.J.N. Phillips and T. Wöhrmann, Nucl. Phys. (**Proc. Suppl.**) **52B** (1997) 69.
- [106] J. Mc Curry, PhD Thesis, Oxford University, 1993 ; H. Dreiner and H. Pois, eprint hep-ph/9511444.
- [107] B.C. Allanach and S.F. King, Phys. Lett. **B407** (1997) 124.
- [108] S. A. Abel and B. Allanach, Phys. Lett. **B415** (1997) 371.
- [109] I. Jack and D.R.T. Jones, Phys. Lett. **B443** ((1998) 17.
- [110] B. Ananthanarayanan and P.N. Pandita, Phys. Lett. **B454** (1999) 84; P.N. Pandita and P.F. Paulraj, Phys. Lett. **B462** (1999) 294.
- [111] B. Ananthanarayanan and P.N. Pandita, Phys. Rev. **D62** (036009) 2000, *Erratum-ibid.* Phys. Rev. **D63** (099901) 2001, *ibid.* Phys. Rev. **D63** (076008) 2001; P.N. Pandita, Phys. Rev. **D64** (056002) 2001; see however Y. Mambrini and G. Moulataka, Phys. Rev. **D65** (058901) 2002; B. Ananthanarayanan and P.N. Pandita, Phys. Rev. **D65** (058902) 2002; Y. Mambrini and G. Moulataka, Phys. Rev. **D65** (115011) 2002 for discussion and comments on the validity of the approximations used in computing the fixed points.

- [112] B. de Carlos and P.L. White, Phys. Rev. **D55** (1997) 4222.
- [113] J. R. Ellis, J. S. Hagelin, D. V. Nanopoulos, K. A. Olive and M. Srednicki, Nucl. Phys. **B238** (1984) 453.
- [114] S. Wolfram, Phys. Lett. **B82** (1979) 65.
- [115] C. B. Dover, T. K. Gaisser and G. Steigman, Phys. Rev. Lett. **42** (1979) 1117; D. A. Dicus and V. L. Teplitz, Phys. Rev. Lett. **44** (1980) 218.
- [116] M.L. Perl *et al.*, Int. J. Mod. Phys. **A16** (2001) 2137.
- [117] P. F. Smith and J. R. J. Bennett, Nucl. Phys. **B149** (1979) 525.
- [118] T. K. Hemmick *et al.*, Phys. Rev. **D41** (1990) 2074.
- [119] P. F. Smith *et al.*, Nucl. Phys. **B206** (1982) 333.
- [120] P. Verkerk *et al.*, Phys. Rev. Lett. **68** (1992) 1116.
- [121] S. P. Ahlen *et al.*, Phys. Lett. **B195** (1987) 603; D. O. Caldwell *et al.*, Phys. Rev. Lett. **61** (1988) 510; M. Beck *et al.*, Phys. Lett. **B336** (1994) 141.
- [122] T. Falk, K. A. Olive and M. Srednicki, Phys. Lett. **B339** (1994) 248.
- [123] R.D. Peccei and H.R. Quinn, Phys. Rev. Lett. **38** (1977) 1440; R.D. Peccei and H.R. Quinn, Phys. Rev. **D16** (1977) 1791.
- [124] L. Covi, J. E. Kim and L. Roszkowski, Phys. Rev. Lett. **82** (1999) 4180; L. Covi, H. B. Kim, J. E. Kim and L. Roszkowski, J. Hi. Ener. Phys. **05** (2001) 033.
- [125] D. Lindley, Astrophys. J. **294** (1985) 1.
- [126] J.E. Kim, B. Kyae, and J.D. Park, "Cosmological Light Element Bound on R -parity Violating Parameters", Seoul National University preprint SNUTP-98-071A (October 1998) 20pp.
- [127] E.A. Baltz and P. Gondolo, Phys. Rev. **D57** (1998) 7601.
- [128] V. Berezhinsky, A. Masiero, and J.W.F. Valle, Phys. Lett. **B266** (1991) 382.
- [129] V. Berezhinsky, A.S. Joshipura, and J.W.F. Valle, Phys. Rev. **D57** (1998) 147.
- [130] S. Weinberg, Phys. Rev. Lett. **48** (1982) 1303.
- [131] P. Fayet, Proc. XVIIth Renc. de Moriond, Les Arcs, France (1982), Vol. 1, page 483.
- [132] H. Pagels and J.R. Primack, Phys. Rev. Lett. **48** (1982) 223.
- [133] P. Fayet, Phys. Lett. **B86** (1979) 272.
- [134] P. Fayet, Proc. XVIth Renc. de Moriond, Les Arcs, France (1981), Vol. 1, page 347.
- [135] M. Y. Khlopov and A. D. Linde, Phys. Lett. **B138** (1984) 265.
- [136] J. R. Ellis, J. E. Kim and D. V. Nanopoulos, Phys. Lett. **B145** (1984) 181.

- [137] T. Moroi, H. Murayama and M. Yamaguchi, Phys. Lett. **B303** (1993) 289.
- [138] R. H. Cyburt, J. R. Ellis, B. D. Fields and K. A. Olive, Phys. Rev. **D67** (2003) 103521.
- [139] A. D. Linde, *Particle Physics And Inflationary Cosmology*, Harwood (1990).
- [140] D. H. Lyth and A. Riotto, Phys. Rep. **314** (1999) 1.
- [141] G.R. Farrar and S. Weinberg, Phys. Rev. **D27** (1983) 2732.
- [142] F. Takayama and M. Yamaguchi, Phys. Lett. **B485** (2000) 388.
- [143] G. Moreau and M. Chemtob, Phys. Rev. **D65** (2002) 024033.
- [144] S. Dimopoulos, R. Esmailzadeh, L.J. Hall, and G.D. Starkman, Astrophysics J. **330** (1988) 545.
- [145] L.J. Hall, 1987 TASI Lectures, eds. R. Slansky and G. West (World Scientific, Singapore, 1988).
- [146] K. Jedamzik, Phys. Rev. Lett. **84** (2000) 3248.
- [147] S. Sarkar, “Measuring the baryon content of the universe: BBN vs CMB”, invited talk at 14th Rencontres de Blois: Matter - Anti-matter Asymmetry, Château de Blois, France, 17-22 Jun 2002; eprint astro-ph/0205116.
- [148] A. D. Sakharov, Sov. Phys. JETP Lett. **C5** (1967) 24.
- [149] N. S. Manton, Phys. Rev. **D28** (1983) 2019.
- [150] F. R. Klinkhamer and N. S. Manton, Phys. Rev. **D30** (1984) 2212.
- [151] V. A. Kuzmin, V. A. Rubakov and M. E. Shaposhnikov, Phys. Lett. **B155** (1985) 36.
- [152] G. R. Farrar and M. E. Shaposhnikov, Phys. Rev. **D50** (1994) 774; M. B. Gavela, P. Hernandez, J. Orloff and O. Pene, Mod. Phys. Lett. **A9** (1994) 795.
- [153] M. Quiros, Nucl. Phys. Proc. Suppl. **101** (2001) 401.
- [154] M. Fukugita and T. Yanagida, Phys. Lett. **B174** (1986) 45.
- [155] I. Affleck and M. Dine, Nucl. Phys. **B249** (1985) 361.
- [156] S. Dimopoulos and L.J. Hall, Phys. Lett. **B196** (1987) 135.
- [157] J. Cline and S. Raby, Phys. Rev. **D43** (1991) 1781; R.J. Scherrer, J. Cline, S. Raby, and D. Seckel, Phys. Rev. **D44** (1991) 3760.
- [158] S. Mollerach and E. Roulet, Phys. Lett. **B281** (1992) 303.
- [159] R. Adhikari and U. Sarkar, Phys. Lett. **B427** (1998) 59.
- [160] T. Hambye, Nucl. Phys. **B633** (2002) 171.
- [161] A. Masiero and A. Riotto, Phys. Lett. **B289** (1992) 73.
- [162] U. Sarkar and R. Adhikari, Phys. Rev. **D55** (1997) 3836.

- [163] T. Hambye, E. Ma and U. Sarkar, Phys. Rev. **D62** (2000) 015010; T. Hambye, E. Ma and U. Sarkar, Nucl. Phys. **B590** (2000) 429.
- [164] S.Y. Khlebnikov and M.E. Shaposhnikov, Nucl. Phys. **B308** (1988) 885; Phys. Lett. **B387** (1996) 817.
- [165] J.A. Harvey and M.S. Turner, Phys. Rev. **D42** (1990) 3344.
- [166] A. Bouquet and P. Salati, Nucl. Phys. **B284** (1987) 557.
- [167] B.A. Campbell, S. Davidson J. Ellis, and K.A. Olive, Phys. Lett. **B256** (1991) 457.
- [168] W. Fischler, G. Giudice, R.S. Leigh, and S. Paban, Phys. Lett. **B258** (1991) 45.
- [169] B.A. Campbell, S. Davidson, J. Ellis, and K.A. Olive, Astropart. Phys. **1** (1992) 77.
- [170] H. Dreiner and G.G. Ross, Nucl. Phys. **B410** (1993) 188.
- [171] T. Inui, T. Ichihura, Y. Mimura, and N. Sakai, Phys. Lett. **B325** (1994) 392.
- [172] S. Davidson, "Cosmological constraints on $B - L$ violation", in *Trento 1998, Lepton and baryon number violation*, pp. 394-414; eprint hep-ph/9808427.
- [173] B.A. Campbell, S. Davidson, J. Ellis, and K.A. Olive, Phys. Lett. **B297** (1992) 118.
- [174] J. M. Cline, K. Kainulainen and K. A. Olive, Phys. Rev. **D49** (1994) 6394.
- [175] S. Davidson and R. Hempfling, Phys. Lett. **B391** (1997) 287.
- [176] M. Gell-Mann, P. Ramond, and R. Slansky in Sanibel Talk, CALT-68-709, February 1979, and in *Supergravity* (North Holland, Amsterdam 1979). T. Yanagida, *Proceedings of the Workshop on Unified Theory and Baryon Number of the Universe*, KEK, Japan, 1979.
- [177] A. Zee, Phys. Lett. **B93** (1980) 389.
- [178] K.S. Babu, Phys. Lett. **B203** (1988) 132.
- [179] B. Pontecorvo, ZhETF **33** (1957) 549 (Sov. Phys. JETP **6** (1957) 429); *idem* ZhETF **34** (1958) 247 (Sov. Phys. JETP **7** (1958) 172).
- [180] Z. Maki, M. Nakagawa and S. Sakata, Prog. Theor. Phys. **28** (870) 1962.
- [181] A.S. Joshipura and M. Nowakowski, Phys. Rev. **D51** (1995) 2421.
- [182] K.S. Babu and R.N. Mohapatra, Phys. Rev. Lett. **64** (1990) 1705.
- [183] G. Bhattacharyya, H.V. Klapdor-Kleingrothaus and H. Paes, Phys. Lett. **B463** (1999) 77.
- [184] Y. Grossman and H. Haber, Phys. Rev. Lett. **78** (1997) 3438; Y. Grossman, Proc. of the Workshop Beyond the Desert 1997, Tegernsee, Germany, (8-14 June 1997) 254-264.
- [185] D.E. Kaplan and A.E. Nelson, J. Hi. Ener. Phys. **01** (2000) 033.
- [186] E.J. Chun and S.K. Kang, Phys. Rev. **D61** (2000) 075012.

- [187] K. Cheung and O.C.W. Kong, Phys. Rev. **D61** (2000) 113012.
- [188] O. C. Kong, J. Hi. Ener. Phys. **09** (2000) 037.
- [189] M. Hirsch, M. A. Diaz, W. Porod, J. C. Romao and J. W. Valle, Phys. Rev. **D62** (2000) 113008 [*Erratum-ibid.* Phys. Rev. **D65** (2002) 119901].
- [190] S. Davidson and M. Losada, J. Hi. Ener. Phys. **05** (2000) 021.
- [191] S. Davidson and M. Losada, Phys. Rev. **D65** (2002) 075025.
- [192] S. K. Kang and O. C. W. Kong, Phys. Rev. **D69** (2004) 013004.
- [193] Y. Grossman and S. Rakshit, Phys. Rev. **D69** (2004) 093002.
- [194] Y. Fukuda *et al.* [Super-Kamiokande Collaboration], Phys. Lett. **BB433** (1998) 9; *ibid*, Phys. Lett. **B436** (1998) 33; *ibid*, Phys. Lett. **B467** (1999) 185; *idem*, Phys. Rev. Lett. **82** (1999) 2644.
- [195] W. W. Allison *et al.* [Soudan-2 Collaboration], Phys. Lett. **B449** (1999) 137; D. A. Petyt [on behalf Soudan-2 Collaboration], Nucl. Phys. **B110 (Proc. Suppl.)** (349) 2002.
- [196] M. Ambrosio *et al.* [MACRO Collaboration], Phys. Lett. **B517** (2001) 59.
- [197] M. H. Ahn *et al.* [K2K Collaboration], Phys. Rev. Lett. **90** (2003) 041801.
- [198] M. C. Gonzalez-Garcia and C. Pena-Garay, Phys. Rev. **D68** (2003) 093003.
- [199] B. T. Cleveland *et al.*, Astrophys. J. **496** (1998) 505.
- [200] W. Hampel *et al.* [GALLEX Collaboration], Phys. Lett. **B447** (1999) 127; M. Altmann *et al.* [GNOCollaboration], Phys. Lett. **B490** (2000) 16; J. N. Abdurashitov *et al.* [SAGECollaboration], J. Exp. Theor. Phys. **95** (2002) 181.
- [201] Y. Fukuda *et al.* [Kamiokande Collaboration], Phys. Rev. Lett. **77** (1996) 1683.
- [202] S. Fukuda *et al.* [Super-Kamiokande Collaboration], Phys. Lett. **B539** (2002) 179.
- [203] Q. R. Ahmad *et al.* [SNO Collaboration], Phys. Rev. Lett. **87** (2001) 071301; *ibid*, Phys. Rev. Lett. **89** (2002) 011301.
- [204] K. Eguchi *et al.* [KamLAND Collaboration], Phys. Rev. Lett. **90** (2003) 021802.
- [205] M.C. Gonzalez-Garcia, M. Maltoni, C. Pena-Garay and J.W. Valle, Phys. Rev. **D63** (2001) 033005.
- [206] L. Wolfenstein, Phys. Rev. **D17** (1978) 2369
- [207] S.P. Mikheev and A.Y. Smirnov, Sov. J. Nucl. Phys. **42** (1985) 913 [*Yad. Fiz.* **42** (1985) 1441].
- [208] G.L. Fogli, E. Lisi, A. Marrone, D. Montanino, A. Palazzo and A.M. Rotunno, Phys. Rev. **D67** (2003) 073002.
- [209] M. Maltoni, T. Schwetz and J. W. Valle, Phys. Rev. **D67** (2003) 093003.

- [210] J.N. Bahcall, M.C. Gonzalez-Garcia and C. Pena-Garay, *J. Hi. Ener. Phys.* **02** (2003) 009.
- [211] P. C. de Holanda and A. Y. Smirnov, *JCAP* **0302** (2003) 001.
- [212] M. Apollonio *et al.* [CHOOZ Collaboration], *Phys. Lett.* **B466** (1999) 415.
- [213] C. Athanassopoulos *et al.* [LSND Collaboration], *Phys. Rev. Lett.* **81** (1998) 1774; A. Aguilar *et al.* [LSND Collaboration], *Phys. Rev.* **D64** (112007) 2001.
- [214] L. Baudis *et al.*, *Phys. Rev. Lett.* **83** (1999) 41.
- [215] M. Drees, S. Pakvasa, X. Tata, and T. der Veldhuis, *Phys. Rev.* **D57** (1998) 5335.
- [216] V. D. Barger, T. Han, S. Hesselbach and D. Marfatia, *Phys. Lett.* **B538** (346) 2002.
- [217] A.S. Joshipura and S.K. Vempati, *Phys. Rev.* **D60** (1999) 111303.
- [218] A.S. Joshipura, R.D. Vaidya and S.K. Vempati, *Phys. Rev.* **D65** (2002) 053018.
- [219] Y. Koide and A. Ghosal, eprint hep-ph/0203113.
- [220] F. Borzumati and J. S. Lee, *Phys. Rev.* **D66** (2002) 115012.
- [221] K. Choi, K. Hwang and E.J. Chun, *Phys. Rev.* **D60** (1999) 031301.
- [222] E.J. Chun, S.K. Kang, C.W. Kim, and U.W. Lee, *Nucl. Phys.* **B544** (1999) 89.
- [223] O.C.W. Kong, *Mod. Phys. Lett.* **A14** (1999) 903.
- [224] S.Y. Choi, E.J. Chun, S.K. Kang, and J. S. Lee, *Phys. Rev.* **D60** (1999) 075002
- [225] O. Haug, J.D. Vergados, A. Faessler and S. Kovalenko, *Nucl. Phys.* **B565** (2000) 38.
- [226] A.S. Joshipura and S.K. Vempati, *Phys. Rev.* **D60** (1999) 095009.
- [227] F. Takayama and M. Yamaguchi, *Phys. Lett.* **B476** (2000) 116.
- [228] A. S. Joshipura, R. D. Vaidya and S. K. Vempati, *Nucl. Phys.* **B639** (2002) 290.
- [229] E. J. Chun, D. W. Jung and J. D. Park, *Phys. Lett.* **B557** (2003) 233.
- [230] M. A. Diaz, M. Hirsch, W. Porod, J. C. Romao and J. W. F. Valle, *Phys. Rev.* **D68** (2003) 013009.
- [231] D. Restrepo, W. Porod and J.W.F. Valle, *Phys. Rev.* **D64** (2001) 055011.
- [232] J.M. Mira, E. Nardi, D.A. Restrepo and J.W.F. Valle, *Phys. Lett.* **B492** (2000) 81.
- [233] A. Abada, S. Davidson and M. Losada, *Phys. Rev.* **D65** (2002) 075010.
- [234] B.W. Lee and R.E. Shrock, *Phys. Rev.* **D16** (1977) 1444.
- [235] W.J. Marciano and A.I. Sanda, *Phys. Lett.* **B67** (1977) 303.
- [236] E.K. Akhmedov, *Phys. Lett.* **B213** (1988) 64.
- [237] C. Lim and W.J. Marciano, *Phys. Rev.* **D37** (1988) 1368.

- [238] O.G. Miranda, T.I. Rashba, A.I. Rez and J.W.F. Valle, Phys. Rev. Lett. **93** (2004) 051304.
- [239] R. Barbieri, M.M. Guzzo, A. Masiero, and D. Tommasini, Phys. Lett. **B252** (1990) 251.
- [240] M.B. Voloshin, Yad. Fiz. **48**, 804 (1988) [Sov. J. Nucl. Phys. **48**, 512 (1988)].
- [241] K.S. Babu and R.N. Mohapatra, Phys. Rev. Lett. **63** (1990) 228.
- [242] E. Roulet, Phys. Rev. **D44** (1991) 935.
- [243] M.M. Guzzo, A. Masiero and S.T. Petcov, Phys. Lett. **B260** (1991) 154.
- [244] S. Bergmann, Y. Grossman and D.M. Pierce, Phys. Rev. **D61** (2000) 053005.
- [245] S. Bergmann, M.M. Guzzo, P.C. de Holanda, P.I. Krastev and H. Nunokawa, Phys. Rev. **D62** (2000) 073001.
- [246] A.M. Gago, M.M. Guzzo, P.C. de Holanda, H. Nunokawa, O.L. Peres, V. Pleitez and R. Zukanovich Funchal, Phys. Rev. **D65** (2002) 073012.
- [247] M. Guzzo, P.C. de Holanda, M. Maltoni, H. Nunokawa, M. A. Tortola and J. W. Valle, Nucl. Phys. **B629** (2002) 479.
- [248] R. Adhikari, A. Sil and A. Raychaudhuri, Eur. Phys. J **25** (2002) 125.
- [249] H.K. Dreiner and G. Moreau, Phys. Rev. **D67** (055005) 2003.
- [250] M. Hirsch, H.V. Klapdor-Kleingrothaus, and S. G. Kovalenko, Phys. Lett. **B398** (1997) 311.
- [251] M. Hirsch, H.V. Klapdor-Kleingrothaus, and S.G. Kovalenko, Phys. Rev. **D57** (1997) 1947.
- [252] J.L. Feng, J.F. Gunion and T. Han, Phys. Rev. **D58** (1998) 071701.
- [253] S. Bar-Shalom, G. Eilam and A. Soni, Phys. Rev. Lett. **80** (1998) 4629.
- [254] V. Barger, G.F. Giudice, and T. Han, Phys. Rev. **D40** (1989) 2987.
- [255] H. Dreiner and G.G. Ross, Nucl. Phys. **B365** (1991) 597.
- [256] I. Hinchliffe and T. Kaeding, Phys. Rev. **D47** (1993) 279.
- [257] R.N. Mohapatra, Prog. Part. Nucl. Phys. **31**, 39 (1993).
- [258] G. Bhattacharyya, talk given at Workshop on Physics Beyond the Standard Model: Beyond the Desert: Accelerator and Nonaccelerator Approaches, Tegernsee, Germany, 8-14 June 1997, eprint hep-ph/9709395.
- [259] H.K. Dreiner, "An Introduction to Explicit R -parity Violation", in *Perspectives on supersymmetry*, (World Scientific 1998, Ed. G.L. Kane) 462-479.
- [260] B. C. Allanach, A. Dedes and H. K. Dreiner, Phys. Rev. **D60** (1999) 075014.
- [261] S. Dimopoulos and L.J. Hall, Phys. Lett. **B207** (1988) 210.

- [262] K. Agashe and M. Graesser, Phys. Rev. **D54** (1996) 4445.
- [263] G.G. Ross, “Grand unified theories”, Benjamin-Cummings, Menlo Park, CA, 1985; H.-P. Nilles, Phys. Rep. **110** (1984) 1.
- [264] R.N. Mohapatra and P.B Pal, “Massive neutrinos in physics and astrophysics”, World Scientific, Singapore, 1991.
- [265] V.D. Barger and R.J.N. Phillips, “Collider Physics”, Addison-Wesley Publishing Company, New York, 1987.
- [266] V. Barger, W.Y. Keung, and S. Pakvasa, Phys. Rev. **D25** (1982) 907.
- [267] G. Raffelt and A. Weiss, Phys. Rev. **D51** (1995) 1495.
- [268] P. Langacker, “Precision tests of standard model of electroweak interactions”, ed. P. Langacker (World Scientific, Singapore, 1996) p. 881.
- [269] P. Langacker and J. Erler, Review of Particle Physics, Eur. Phys. J **3** (1998) 90.
- [270] U. Amaldi *et al.*, Phys. Rev. **D36** (1987) 1385; G. Costa *et al.*, Nucl. Phys. **B297** (1988) 244; P. Langacker and D. London, Phys. Rev. **D38** (1988) 886 and references therein.
- [271] F. Ledroit and G. Sajot, Rapport GDR-Supersymétrie, GDR-S-008 (ISN, Grenoble, 1998).
- [272] K. Hagiwara *et al.* [Particle Data Group Collaboration], Review of Particle Physics, Phys. Rev. **D66** (2002) 010001.
- [273] W. Fetscher and H.-J. Gerber, “Precision tests of standard model of electroweak interactions”, ed. P. Langacker (World Scientific, Singapore, 1996) p. 655.
- [274] K. Cheung and R.-J. Zhang, Phys. Lett. **B427** (1998) 73.
- [275] M. Herz, “Bounds on leptoquark and supersymmetric, R -parity violating interactions from meson decays.” (PhD thesis, in German), hep-ph/0301079.
- [276] G. Bhattacharyya and D. Choudhury, Mod. Phys. Lett. **A10** (1995) 1699.
- [277] G. Altarelli, G. F. Giudice, and M. L. Mangano, Nucl. Phys. **B506** (1997) 29.
- [278] Y. Grossman, Z. Ligeti, and E. Nardi, Nucl. Phys. **B465** (1996) 369 [Erratum-ibid. **480** (1996) 753].
- [279] J. Erler, J. Feng, and N. Polonsky, Phys. Rev. Lett. **78** (1997) 3063.
- [280] F. Tahir, M. Sadiq, M. Anwar Mughal, and K. Ahmed, Phys. Lett. **B439** (1998) 316.
- [281] J. Panman, in “Precision tests of standard model of electroweak interactions”, ed. P. Langacker (World Scientific, Singapore, 1996) p. 504.
- [282] F. Perrier, “Precision tests of standard model of electroweak interactions”, ed. P. Langacker (World Scientific, Singapore, 1996) p. 383.
- [283] A.K. Mann, in “Precision tests of standard model of electroweak interactions”, ed. P. Langacker (World Scientific, Singapore, 1996) p. 491.

- [284] P. Vilain *et al.* [CHARM II Collaboration], Phys. Lett. **B335** (1994) 246.
- [285] K.S.M. Mc Farland *et al.* [CCFR Collaboration], Eur. Phys. J **1** (1998) 509.
- [286] V. Barger, K. Cheung, K. Hagiwara, and D. Zeppenfeld, Phys. Rev. **D57** (1998) 391.
- [287] G. Bhattacharyya, J. Ellis, and K. Sridhar, Mod. Phys. Lett. **A10** (1995) 1583.
- [288] G. Bhattacharyya, D. Choudhury, and K. Sridhar, Phys. Lett. **B355** (1995) 193.
- [289] O. Lebedev, W. Loinaz and T. Takeuchi, Phys. Rev. **D62** (015003) 2000.
- [290] M. Anwar Mughal, M. Sadiq, and K. Ahmed, Phys. Lett. **B417** (1998) 87.
- [291] M. Chemtob and G. Moreau, Phys. Rev. **D59** (1999) 116012.
- [292] C.S. Wood *et al.*, Science, **275**, (1997) 1759.
- [293] J. L. Rosner, Phys. Rev. D **65** (2002) 073026; J. S. M. Ginges and V. V. Flambaum, Phys. Rept. **397** (2004) 63.
- [294] W. Marciano, “Precision tests of standard model of electroweak interactions”, ed. P. Langacker (World Scientific, Singapore, 1996) p. 170.
- [295] P.A. Souder *et al.*, Phys. Rev. Lett. **65** (1990) 694; M. Musolf and T. Donnelly, Z. Phys. **C57** (1993) 559.
- [296] P.A. Souder, in “Precision tests of standard model of electroweak interactions”, ed. P. Langacker (World Scientific, Singapore, 1996) p. 599.
- [297] C.Y. Prescott *et al.*, Phys. Lett. **B84** (1979) 524.
- [298] W. Heil *et al.*, Nucl. Phys. **B327** (1989) 1.
- [299] W. Marciano, Susy '97 Nucl. Phys. (**Proc. Suppl.**) **62B** (1998) 457.
- [300] H. N. Brown *et al.* [Muon g-2 Collaboration], Phys. Rev. Lett. **86** (2001) 2227; G. W. Bennett *et al.* [Muon g-2 Collaboration], Phys. Rev. Lett. **89** (2002) 101804 [Erratum-ibid. **89** (2002) 129903].
- [301] M. Davier and A. Höcker, Phys. Lett. **B435** (1998) 427; M. Davier, S. Eidelman, A. Hocker and Z. Zhang, Eur. Phys. J **27** (2003) 497.
- [302] M. Knecht and A. Nyffeler, Phys. Rev. **D65** (2002) 073034; M. Knecht, A. Nyffeler, M. Perrottet, and E. de Rafael, Phys. Rev. Lett. **88** (2002) 071802; for a detailed review see <http://parthe.lpthe.jussieu.fr/poincare/textes/octobre2002/Knecht.ps>.
- [303] M. Hayakawa and T. Kinoshita, hep-ph/0112102.
- [304] W.J. Marciano and B. Lee Roberts, “Status of the Hadronic Contribution to the Muon (g-2) Value”, (2001) *unpublished*; eprint hep-ph/0105056.
- [305] M. Frank and H. Hamidian, J. Phys. **G24**, 2203 (1998).
- [306] J. E. Kim, B. Kyae and H. M. Lee, Phys. Lett. **B520** (2001) 298.

- [307] R. Adhikari and G. Rajasekaran, “Anomalous Magnetic Moment of Muon and L Violating Supersymmetric Models”, (2001) *unpublished*; eprint hep-ph/0107279.
- [308] Y. Grossman and M.P. Worah, Phys. Lett. **B395** (1997) 241.
- [309] D.E. Kaplan, “Violating R -parity at the b Factory”, (1997) *unpublished*; eprint hep-ph/9703347.
- [310] S. Abel, Phys. Lett. **B410** (1997) 173.
- [311] D. Guetta, Phys. Rev. **D58** (116008) 1998.
- [312] Ji-Ho Jang and Jae Sik Lee, KAIST-TH 98/12, eprint hep-ph/9808406.
- [313] R. Mohanta, Phys. Rev. **D63** (2001) 056006
- [314] C.H. Chen, C.Q. Geng and C. C. Lih, Phys. Rev. **D56** (1997) 6856.
- [315] S. Bar-Shalom, G. Eilam and A. Soni, Phys. Rev. **D59** (1999) 055012.
- [316] T. Handoko and J. Hashida, Phys. Rev. **D58** (1998) 094008.
- [317] G. Bhattacharyya, A. Datta, Phys. Rev. Lett. **83** (1999) 2300.
- [318] M. Bhrlík, G.J. Good, and G.L. Kane, Phys. Rev. **D59** (1999) 115004.
- [319] S. Davidson and J. Ellis, Phys. Rev. **D56** (1997) 4182.
- [320] Y. Grossman and H. Haber, Phys. Rev. **D56** (2001) 075011.
- [321] K. Huitu, K. Puolamäki and D.X. Zhang, Phys. Lett. **B446** (1999) 285.
- [322] A.S. Joshipura and M. Nowakowski, Phys. Rev. **D51** (1995) 5271.
- [323] R. Barbieri and A. Masiero, Nucl. Phys. **B267** (1986) 679.
- [324] P. Slavich, Nucl. Phys. **B595** (2001) 33.
- [325] A. Kundu and J.P. Saha, Phys. Rev. **D70** (2004) 096002.
- [326] M. Ciuchini *et al.*, J. Hi. Ener. Phys. **10** (1998) 008.
- [327] D. E. Groom *et al.* [Particle Data Group Collaboration], Review of Particle Physics, Eur. Phys. J **15** (2000) 1.
- [328] G. Bélanger and C.Q. Geng, Phys. Rev. **D44** (1991) 2789.
- [329] M.A. Aliev *et al.*, PLB55420034.
- [330] S.C. Adler *et al.*, Phys. Rev. Lett. **85** (2000) 2256.
- [331] E. Golowich and G. Valencia, Phys. Rev. **D40** (1989) 112.
- [332] P. Herczeg, Beyond the Desert 1999, Accelerator, Nonaccelerator and Space Approaches, Ringberg Castle, Tegernsee, Germany, 1999. Editors H.V. Klapdor-Kleingrothaus and I.V. Krivosheina.

- [333] M. Fabbrichesi and F. Vissani, Phys. Rev. **D55** (1997) 5334.
- [334] G.H. Wu and J.N. Ng, Phys. Lett. **B392** (1997) 93.
- [335] M. Abe *et al.*, Phys. Rev. Lett. **83** (1999) 4253.
- [336] M. Abe *et al.*, Nucl. Phys. **A721** (2003) 445.
- [337] V.V. Anisimovsky *et al.*, hep-ex/0304027.
- [338] S.R. Blatt *et al.*, Phys. Rev. **D27** (1983) 1056.
- [339] M.V. Diwan and H. Ma, Int. J. Mod. Phys. **A1716** (2001) 2449.
- [340] R.M. Godbole, S. Pakvasa, S.D. Rindani, and X. Tata, Phys. Rev. **D61** (2000) 113003.
- [341] S. A. Abel, A. Dedes and H. K. Dreiner, J. Hi. Ener. Phys. **05** (2000) 013.
- [342] K.F. Smith *et al.*, Phys. Lett. **B234** (1990) 191.
- [343] P.G. Harris *et al.*, Phys. Rev. Lett. **82** (1999) 904.
- [344] S.K. Lamoreaux and R. Golub, Phys. Rev. **D61** (2000) 051301.
- [345] D. Chang *et al.*, Phys. Rev. **D62** (2000) 095002.
- [346] K. Choi, E.J. Chun and K. Hwang, Phys. Rev. **D63** (2001) 013002.
- [347] Y.Y. Keum and O.C.W. Kong, Phys. Rev. Lett. **86** (2001) 393.
- [348] B.C. Regan *et al.*, Phys. Rev. Lett. **88** (2002) 071805.
- [349] R. Adhikari and G. Omanovic, Phys. Rev. **D59** (1999) 073003.
- [350] I.B. Khriplovich and S.K. Lamoreaux, “CP-violation without strangeness”, Springer Verlag, Berlin, 1997.
- [351] W. Bernreuther and M. Suzuki, Rev. Mod. Phys. **63** (1991) 313.
- [352] P. Herczeg, Phys. Rev. **D61** (2000) 095010.
- [353] J.R. Fry, XXI International Symposium on Lepton and Photon interactions at High Energies, Fermilab, Batavia, Illinois USA, 2003.
- [354] Y. Grossman, G. Isidori and M.P. Worah, Phys. Rev. **D58** (1998) 057504.
- [355] R. Barate *et al.*, Eur. Phys. J **19** (2001) 213.
- [356] G. Bhattacharyya and A. Raychaudhuri, Phys. Rev. **D57** (1998) 3837.
- [357] J.P. Saha and A. Kundu, Phys. Rev. **D69** (2004) 016004.
- [358] L. Littenberg and G. Valencia, in S. Eidelman *et al.*, *Review of Particle Physics*, Phys. Lett. **B592** (2004) 1.
- [359] D. Choudhury and P. Roy, Phys. Lett. **B378** (1996) 153.
- [360] H. K. Dreiner, G. Polesello and M. Thormeier, Phys. Rev. **D65** (2002) 115006.

- [361] J.-H. Jang, J.K. Kim, and J.S. Lee, Phys. Rev. **D55** (1997) 7296.
- [362] J. P. Saha and A. Kundu, Phys. Rev. **D66** (2002) 054021.
- [363] Y. Grossman, Z. Ligeti, and E. Nardi, Phys. Rev. **D55** (1997) 2768.
- [364] S. Baek and Y. G. Kim, Phys. Rev. **D60** (1999) 077701.
- [365] L. Littenberg and G. Valencia, Ann. Rev. Nucl. Part. Phys. **43**, 729 (1993).
- [366] I.I. Bigi and F. Gabbiani, Nucl. Phys. **B367** (1991) 3.
- [367] S. C. Adler *et al.* [E787 Collaboration], Phys. Rev. Lett. **79** (1997) 2204; S. Adler *et al.* [E787 Collaboration], Phys. Rev. **D70** (2004) 037102; V. V. Anisimovsky *et al.* [E949 Collaboration], Phys. Rev. Lett. **93** (2004) 031801.
- [368] A. Deandrea, J. Welzel and M. Oertel, J. Hi. Ener. Phys. **0410** (2004) 038.
- [369] H. Kroba [on behalf of ALEPH Collaboration], Proceedings of the 28th International Conference on High Energy Physics, July 1996, Warsaw, Poland, eds. Z. Ajduk and A.K. Wroblewski, World Scientific, Singapore (1997).
- [370] J.-H. Jang, Y.G. Kim, and J.S. Lee, Phys. Rev. **D58** (1998) 035006.
- [371] C.E. Carlson, P. Roy, and M. Sher, Phys. Lett. **B357** (1995) 99.
- [372] D. Chakraverty and D. Choudhury, Phys. Rev. **D63** (2001) 112002.
- [373] S. Bar-Shalom, G. Eilam and Y-D Yang, Phys. Rev. **D67** (2003) 014007.
- [374] J.M. Yang, B.-L. Young, and X. Zhang, Phys. Rev. **D58** (1998) 055001.
- [375] K. Chetyrkin, M. Misiak and M. Münz, Phys. Lett. **B400** (1997) 206 [Erratum-ibid. **425** (1998) 414].
- [376] A.J. Buras, A. Kwiatkowski and N. Pott, Phys. Lett. **B414** (1997) 157 [Erratum-ibid. **434** (1998) 459].
- [377] A.L. Kagan and M. Neubert, Eur. Phys. J **C7** (1999) 5.
- [378] R. M. Barnett *et al.* [Particle Data Group Collaboration], Review of Particle Physics, Phys. Rev. **D54** (1996) 1.
- [379] D. Chakraverty and D. Choudhury, Phys. Rev. **D63** (2001) 075009.
- [380] M. Chaichian and K. Huitu, Phys. Lett. **B384** (1996) 157.
- [381] A. de Gouvêa, S. Lola and K. Tobe, Phys. Rev. **D63** (2001) 035004.
- [382] J.E. Kim, P. Ko, and D.-G. Lee, Phys. Rev. **D56** (1997) 100.
- [383] P. Wintz [on behalf of SINDRUM II Collaboration], Proceedings of the 14th International Conference on Particles and Nuclei (PANIC96), Williamsburg, USA (22-28 May 1996), (World Scientific 1997, Eds. C.E. Carlson and J.J. Domingo) 458.
- [384] K. Huitu, J. Maalampi, M. Raidal, and A. Santamaria, Phys. Lett. **B430** (1998) 355.

- [385] G. Feinberg and S. Weinberg, Phys. Rev. **123** (1961) 1439.
- [386] G. Feinberg and S. Weinberg, Phys. Rev. Lett. **6** (1961) 381.
- [387] L. Willmann *et al.*, Phys. Rev. Lett. **82** (1999) 49.
- [388] A. Halprin and A. Masiero, Phys. Rev. **D48** (1993) 2987.
- [389] R.N. Mohapatra, Z. Physik, **C56**, S117 (1992).
- [390] S.R. Elliott and J. Engel, J. Phys. **G30** (2004) R183.
- [391] R.N. Mohapatra, Phys. Rev. **D34** (1986) 3457.
- [392] M. Hirsch, H.V. Klapdor-Kleingrothaus, and S. G. Kovalenko, Phys. Rev. Lett. **75** (1995) 17; Phys. Rev. **D53** (1996) 1329; Susy '96 Nucl. Phys. (**Proc. Suppl.**)**52A** (1997) 257.
- [393] L. Baudis *et al.*, Phys. Lett. **B407** (1997) 219.
- [394] M. Hirsch and H.V. Klapdor-Kleingrothaus, Susy '97 Nucl. Phys. (**Proc. Suppl.**)**62B** (1998) 224.
- [395] A. Faessler, S. Kovalenko, F. Simkovic and J. Schwieger, Phys. Rev. Lett. **78** (1997) 183.
- [396] K.S. Babu and R. N. Mohapatra, Phys. Rev. Lett. **75** (1995) 2276.
- [397] H. Pas, M. Hirsch and H.V. Klapdor-Kleingrothaus, Phys. Lett. **B459** (1999) 450.
- [398] A. Faessler, S. Kovalenko, and F. Simkovic, Phys. Rev. **D58** (1998) 055004.
- [399] M. Hirsch, Nucl. Phys. **B** ((Proc. Suppl.) 81) 2000249.
- [400] P. Langacker, Phys. Rep. **72** (1981) 185.
- [401] A. Masiero, Int. School for Advanced studies, Grand unification with and without supersymmetry and cosmological implications (World Scientific, Singapore, 1984).
- [402] S. Weinberg, Phys. Rev. Lett. **43** (1979) 1566.
- [403] S. Weinberg, Phys. Rev. **D22** (1980) 1694.
- [404] J. Hisano, "Proton decay in the supersymmetric grand unified models", in "Fujiyoshida 2000, Neutrino oscillations and their origin"(February 2000), p. 93-102, eprint hep-ph/0004266.
- [405] F. Vissani, Phys. Rev. **D52** (1995) 4245.
- [406] A. Yu. Smirnov and F. Vissani, Phys. Lett. **B380** (1996) 317.
- [407] H.N. Long and P.B. Pal, Mod. Phys. Lett. **A13** (1998) 2355.
- [408] G. Bhattacharyya and P.B. Pal, Phys. Rev. **D59** (1999) 097701.
- [409] G. Bhattacharyya and P.B. Pal, Phys. Lett. **B439** (1998) 81.

- [410] D. Chang and W.-K. Keung, Phys. Lett. **B389** (1996) 294.
- [411] J.E. Kim, Phys. Rep. **150** (1987) 1; H.-Y. Cheng, Phys. Rep. **158** (1988) 1.
- [412] K. Rajagopal, M.S. Turner, and F. Wilczek, Nucl. Phys. **B358** (1991) 447.
- [413] E.J. Choi, E.J. Chun, and J.S. Lee *et al.*, Phys. Rev. **D55** (1997) R3924.
- [414] E.J. Choi, K. Hwang, and J.S. Lee *et al.*, Phys. Lett. **B428** (1998) 129.
- [415] R.N. Mohapatra and R.E. Marshak, Phys. Lett. **B94** (0) 1980183; V.A. Kuzmin, Zh. Eksp. Teor. Fiz. **13**, 335 (1970) ; R.N. Mohapatra and G. Senjanovic, Phys. Rev. Lett. **49** (1982) 7.
- [416] J. Pasupathy, Phys. Lett. **B114** (1982) 172.
- [417] C.B. Dover, A. Gal, and J.-M. Richard, Phys. Rev. **D27** (1983) 1090; Phys. Rev. **C31** (1985) 1423; Riazuddin, Phys. Rev. **D25** (1982) 885.
- [418] W.M. Alberico, A. de Pace, and M. Pignone, Nucl. Phys. **A523** (1991) 488.
- [419] F. Zwirner, Phys. Lett. **B132** (1983) 103.
- [420] A. Cohen, D.B. Kaplan and A. Nelson Phys. Lett. **B388** (1996) 588.
- [421] D. London, "Precision tests of standard model of electroweak interactions", ed. P. Langacker (World Scientific, Singapore, 1996) p. 951.
- [422] V. Barger and K. Cheung, Phys. Lett. **B480** (2000) 149.
- [423] O. Shanker, Nucl. Phys. **B204** (1982) 375; M.V. Voloshin, Phys. Lett. **B283** (1992) 120.
- [424] E.J. Eichten, K.D. Lane, and M.E. Peskin, Phys. Rev. Lett. **50** (1983) 811.
- [425] K. Hagiwara and K. Hikasa, Review of particle physics, Particle Data Group, Eur. Phys. J **15** (2000) 852.
- [426] A. F. Zarnecki, Eur. Phys. J **11** (1999) 539.
- [427] K. S. Babu, C. Kolda, J. March-Russell, and F. Wilczek, Phys. Lett. **B402** (1997) 367.
- [428] R. Barate *et al.* [ALEPH Collaboration], Eur. Phys. J **12** (2000) 183; P. Abreu *et al.* [DELPHI Collaboration], Phys. Lett. **B485** (2000) 45; M. Acciari *et al.* [L3 Collaboration], Phys. Lett. **B489** (2000) 81; G. Abbiendi *et al.* [OPAL Collaboration], Eur. Phys. J **13** (2000) 553.
- [429] CDF Collab., F. Abe *et al.*, Phys. Rev. Lett. **77** (1996) 5336.
- [430] C. Adloff *et al.* [H1 Collaboration], Z. Phys. **C74** (1997) 191; J. Breitweg *et al.* [ZEUS Collaboration], Z. Phys. **C74** (1997) 207; E. Elsen, Intl. Europhysics Conf. (Jerusalem, August 1997).
- [431] G. Altarelli, Susy '97 Nucl. Phys. (**Proc. Suppl.**)**62B** (1998) 3.
- [432] A. Nelson, Phys. Rev. Lett. **78** (1997) 4159.

- [433] K. Hagiwara and S. Matsumoto, Phys. Lett. **B424** (1998) 362.
- [434] “Next Linear Collider (NLC) test accelerator: Conceptual Design Report”, SLAC-0411 (August 1993) 121pp.; “Physics and Experiments with Future Linear e^+e^- Colliders”, (Eds. A. Para and H.E. Fisk), Fermilab and AIP conference proceedings (2001) 974pp..
- [435] “Conceptual Design Report of a 500 GeV e^+e^- Linear Collider with Integrated X-ray Laser Facility”, (Eds. R. Brinkmann, G. Materlik, J. Rossbach and A. Wagner), DESY 1997-048 (May 1997) 1183pp.; “TESLA Technical Design Report, Part 3. Physics at an e^+e^- linear collider”, (ECFA/DESY LC Physics Working Group), DESY-2001-011 (March 2001) 192pp..
- [436] R. Palmer *et al.* [on behalf of Muon Collider Collaboration], “Muon Collider Overview: Progress and Future Plans”, Proc. of the “6th European Particle Accelerator Conference” (EPAC 98), Stockholm, Sweden (June 1998) 838-840;
M. Alsharoa *et al.* [on behalf of Muon Collider and Neutrino Factory Collaboration], “Status of Neutrino Factory and Muon Collider Research ...”, preprint FERMILAB-PUB-02-149-E (July 2002) 103pp. [unpublished].
- [437] Breaking hep-ph/9507426 V. Barger, W.Y. Keung, R.J.N. Phillips, Phys. Lett. **B364** (1995) 27; *Erratum* Phys. Lett. **B377** (1996) 486.
- [438] T. Kon, T. Kobayashi, S. Kitamura, Phys. Lett. **B333** (1994) 263.
- [439] E.A. Baltz, P. Gondolo; Phys. Rev. **D57** (1998) 2969.
- [440] R. Barate *et al.* [ALEPH Collaboration], Eur. Phys. J **4** (1998) 433.
- [441] F. de Campos *et al.*, in *Searching for R-parity Violation at Run-II of the Tevatron* ed. H. Dreiner.
- [442] A. Bartl *et al.*, Nucl. Phys. **B502** (19) 1997.
- [443] D. K. Ghosh, R. M. Godbole, S. Raychaudhuri, “Signals for R -parity violating Supersymmetry at a 500 GeV e^+e^- Collider”, Tata Institute of Fundamental Research preprint TIFR-TH/99-12 (April 1999) 42pp.
- [444] Physics at LEP2, CERN Yellow Report 96-01, vol.1, p.207.
- [445] P. Abreu *et al.* [DELPHI Collaboration], Eur. Phys. J **13** (2000) 591; *idem*, Phys. Lett. **B487** (2000) 36; *idem*, Phys. Lett. **B500** (2001) 22; *idem*, *Preprint CERN*, CERN-EP/03-092.
- [446] D. Buskulic *et al.* [ALEPH Collaboration], Phys. Lett. **B349** (1995) 238; *idem*, Phys. Lett. **B384** (1996) 461; *idem*, Eur. Phys. J **7** (1999) 383; *idem*, Eur. Phys. J **13** (2000) 29; A. Heister *et al.*, Eur. Phys. J **31** (2003) 1.
- [447] M. Acciarri *et al.* [L3 Collaboration], Phys. Lett. **B414** (1997) 373; *idem*, Phys. Lett. **B459** (1999) 354; *idem*, Eur. Phys. J **19** (2001) 397; *idem*, Phys. Lett. **B524** (2002) 65.

- [448] P.D. Acton *et al.* [OPAL Collaboration], Phys. Lett. **B313** (1993) 333;*idem*, G. Abbiendi *et al.*, Eur. Phys. J **11** (1999) 619;*idem*, G. Abbiendi *et al.*, Eur. Phys. J **13** (2000) 553;*idem*, Eur. Phys. J **12** (2000) 1;*idem*, Eur. Phys. J **33** (2004) 149.
- [449] B. Abbott *et al.* [$D\bar{0}$ Collaboration], Phys. Rev. **D62** (2000) 071701.
- [450] V.M. Abazov *et al.* [$D\bar{0}$ Collaboration], Phys. Rev. Lett. **89** (2002) 171801.
- [451] H. Baer *et al.*, PRD5319966241.
- [452] B.C. Allanach *et al.*, J. Hi. Ener. Phys. **03** (2001) 048.
- [453] J. Ellis and S. Rudaz, Phys. Lett. **B128** (1983) 248
- [454] A. Bartl *et al.*, Z. Phys. **C76** (1997) 549
- [455] S. P. Martin, “A Supersymmetry Primer”, in *Perspectives on Supersymmetry*, (World Scientific 1998, Ed. G.L. Kane) 1-98.
- [456] M. Drees, “An introduction to supersymmetry” Lectures given at Inauguration Conference of the Asia Pacific Center for Theoretical Physics (APCTP), Seoul, Korea, 4-19 Jun 1996; eprint hep-ph/9611409
- [457] M. Drees and S.P. Martin, “Implications of SUSY model building”, in “Electroweak symmetry breaking and new physics at the TeV scale” (Eds. T.L. Barklow *et al.*), (March 1995) p.146-215.
- [458] H. Dreiner and S. Lola, “ R -parity Violation”, Proc. of the workshop “ e^+e^- Collisions at 500 GeV: The Physics Potential” (Ed. P.M. Zerwas), Munich-Annecy-Hamburg (1991) p.707-710; Proc. of the workshop “ e^+e^- Collisions at TeV Energies: (Ed. P.M. Zerwas), Annecy-Gran Sasso-Hamburg (1995) p.435-441.
- [459] L. Roszkowski, Invited talk at 2nd International Workshop on Physics and Experiments with Linear e^+e^- Colliders, Waikoloa, HI, 26-30 Apr 1993. Published in Waikoloa Linear Collid.1993:0854-859, hep-ph/9309208.
- [460] D. K. Ghosh and S. Roy, Phys. Rev. **D63** (2001) 055005.
- [461] J.F. Gunion, H.E. Haber, G. Kane, S. Dawson, The Higgs Hunter’s Guide, Addison-Wesley Publishing Company; V. Barger, M.S. Berger, J.F. Gunion, T. Han, Higgs Boson Physics in the s -channel at $\mu^+\mu^-$ Colliders, Phys. Rep. **286** (1997) 1.
- [462] C. Adloff *et al.*, Z. Phys. **C74** (1997) 191.
- [463] J. Breitweg *et al.*, Z. Phys. **C74** (1997) 207.
- [464] F. Abe *et al.*[CDF Collaboration], Phys. Rev. Lett. **83** (1999) 2133.
- [465] D. Choudhury *et al.*, Phys. Lett. **B401** (1997) 54.
- [466] W. Beenakker *et al.*, Phys. Rev. Lett. **74** (1995) 2905.

- [467] B. Allanach *et al.*, “Searching for R -Parity Violation at RUN II of the TeVatron”, Workshop on Supersymmetry / Higgs: Summary Meeting, Batavia, IL, 19-21 Nov 1998, edited by H. Dreiner, eprint hep-ph/9906224.
- [468] B. Abbott *et al.* [$D\bar{0}$ Collaboration], Phys. Rev. Lett. **83** (1999) 4476.
- [469] M. Chertok [on behalf of $D\bar{0}$ and CDF Collaborations], Proc. XXXIIIrd Renc. de Moriond, QCD and High Energy Hadronic Interactions, Les Arcs, France, (March 21-28, 1998) 6pp.
- [470] S. Banerjee *et al.*, Contribution to Physics at Run II: QCD and Weak Boson Physics Workshop, Batavia, IL, 4-6 Mar 1999, edited by G. Landsberg, eprint hep-ph/9904397.
- [471] P. Abreu *et al.* [DELPHI Collaboration], Phys. Lett. **B502** (2001) 24.
- [472] B. Abbott *et al.* [$D\bar{0}$ Collaboration], Phys. Rev. Lett. **79** (1997) 4321;*idem* Phys. Rev. Lett. **80** (1998) 2051.
- [473] F. Abe *et al.* [CDF Collaboration], Phys. Rev. Lett. **79** (1997) 4327.
- [474] S. Lola, Presented at the 2nd ECFA/DESY study on Linear Colliders, Frascati, November 1998, LC note LC-TH-1999-021, hep-ph/9912217.
- [475] M. Chemtob and G. Moreau, Phys. Rev. **D59** (1999) 055003.
- [476] G.F. Giudice *et al.*, “Searches for New Physics”, Proc. of the workshop “Physics at LEP2”, Geneva, Switzerland (November 1995) p.463-524;
E. Accomando *et al.*, Phys. Rep. **299** (1998) 1.
- [477] Y. Arnoud *et al.* [on behalf of DELPHI Collaboration], submitted to HEP’97 (Abstract Number 589), DELPHI 97-119 CONF 101 (1997).
- [478] F. Ledroit-Guillon and R. López-Fernández [on behalf of DELPHI Collaboration], DELPHI 98-165 PHYS 805 (1998).
- [479] R. Barate *et al.* [ALEPH Collaboration], Eur. Phys. J **19** (2001) 415; A. Heister *et al.* [ALEPH Collaboration], Eur. Phys. J **25** (2002) 1.
- [480] G. Moreau, Theoretical Linear Collider note LC-TH-2000-040, eprint hep-ph/0009140; Ph.D. Thesis, University of Paris VII-Denis Diderot, 2000, eprint hep-ph/0012156.
- [481] B.C. Allanach, H. Dreiner, P. Morawitz and M.D. Williams, Phys. Lett. **B420** (1998) 307
- [482] J. Butterworth and H. Dreiner, “Finding Supersymmetry with R -parity Violation”, Proc. of the workshop “Physics at HERA” (Eds. W. Buchmüller and G. Ingelman), DESY Hamburg Germany (October 1991) p.1079-1087.
- [483] T. Kon, T. Kobayashi and K. Nakamura, “Scalar Top Production at HERA”, Proc. of the workshop “Physics at HERA” (Eds. W. Buchmüller and G. Ingelman), DESY Hamburg, Germany (October 1991) p.1099-1093.
- [484] T. Kon and T. Kobayashi, Phys. Lett. **B270** (1991) 81.

- [485] J. Butterworth and H. Dreiner, Nucl. Phys. **B397** (1993) 3.
- [486] E. Perez, Y. Sirois and H. Dreiner, “*R*-parity Violating Supersymmetry at HERA”, Proc. of the workshop “Future Physics at HERA” (Eds. G. Ingelman, A. DeRoeck and R. Klanner) Hambourg, Germany (1995-96) p.295-311.
- [487] E. Perez and Y. Sirois, “Searches for *R*-parity Violating Supersymmetry at HERA”, Proc. of the Workshop “Dark Matter in Astro- and Particle Physics”, (Eds. H.V. Klapdor-Kleingrothaus and Y. Ramachers), Heidelberg, Germany (September 1996) p.615-639.
- [488] W. Buchmüller, R. Rückl, and D. Wyler, Phys. Lett. **B191** (1987) 442;erratum in Phys. Lett. **B448** (1999) 320.
- [489] T. Ahmed *et al.* [H1 Collaboration], Z. Phys. **C64** (1994) 545.
- [490] C. Adloff *et al.* [H1 Collaboration], Eur. Phys. J **11** (1999) 447;*ibid* (Erratum) Eur. Phys. J **14** (1999) 553;
- [491] J. Breitweg *et al.* [ZEUS Collaboration], Eur. Phys. J **16** (2000) 253;
- [492] E. Perez, “Supersymmetry in *ep* Collisions”, Contribution to the Workshop “Tools for SUSY 99”, Lyon, France (April 1999), unpublished.
- [493] S. Aid *et al.* [H1 Collaboration], Z. Phys. **C71** (1996) 211.
- [494] C. Adloff *et al.* [H1 Collaboration], Eur. Phys. J **20** (2001) 639.
- [495] A. Aktas *et al.* [H1 Collaboration], Eur. Phys. J **36** (2004) 425.
- [496] J. Breitweg *et al.* [ZEUS Collaboration], Contributed paper #1042 to the XXXth Int. Conf. on High Energy Physics (ICHEP 2000) 27pp.
- [497] M. Hirsch, H.V. Klapdor-Kleingrothaus, and S.G. Kovalenko, Phys. Lett. **B352** (1995) 1.
- [498] A. Balysh *et al.*, Phys. Lett. **B356** (1995) 450.
- [499] P. Langacker, Phys. Lett. **B256** (1991) 277.
- [500] C. Quigg, *Gauge Interactions of the Strong, Weak, and Electromagnetic Interactions* (Benjamin-Cummings, Reading, Mass., 1983).
- [501] E. Eichten, I. Hinchliffe, K. Lane, and C. Quigg, Rev. Mod. Phys. **56** (1984) 579.
- [502] S. Dimopoulos *et al.*, Phys. Rev. **D41** (1990) 2099.
- [503] J. Kalinowski, R. Rückl, H. Spiesberger and P. M. Zerwas, Phys. Lett. **B414** (1997) 297;J. Kalinowski, Proceedings of “*Beyond the Desert 97 – Accelerator and Non-Accelerator Approaches*”, Ringberg Castle, Germany, June 1997, eprint hep-ph/9708490.
- [504] F. Déliot, G. Moreau and C. Royon, Eur. Phys. J **19** (2001) 155.
- [505] H. Dreiner, P. Richardson and M. H. Seymour, eprint hep-ph/9903419, to be published in the Physics at Run II Workshop: Supersymmetry/Higgs, ed. H. Dreiner.

- [506] H. Dreiner, P. Richardson and M. H. Seymour, Proceedings of the Workshop “Physics at TeV Colliders”, Les Houches, France 8-18 June 1999, eprint hep-ph/0001224.
- [507] S. Abdullin *et al.*, Report of the SUSY working group of the 1999 Les Houches Workshop “Physics at TeV Colliders”, Les Houches, France 8-18 June 1999, eprint hep-ph/0005142.
- [508] F. Déliot *et al.*, Phys. Lett. **B475** (184) 2000.
- [509] H. Dreiner, P. Richardson and M. H. Seymour, Phys. Rev. **D63** (055008) 2001.
- [510] G. Moreau, E. Perez and G. Polesello, Nucl. Phys. **B604** (3) 2001.
- [511] G. Moreau, E. Perez and G. Polesello, Proceedings of the Workshop “Physics at TeV Colliders”, Les Houches, France 8-18 June 1999, eprint hep-ph/0002130.
- [512] F. Borzumati, J.L. Kneur and N. Polonsky, Phys. Rev. **D60** (1999) 115011.
- [513] L.E. Ibañez and G.G. Ross, “Electroweak Breaking in Supersymmetric Models”, in *Perspectives in Higgs Physics* (World Scientific 1993, Ed. G. Kane) 229-275.
- [514] V.M. Abazov *et al.* [$D\bar{0}$ Collaboration], Phys. Rev. Lett. **89** (2002) 261801.
- [515] E.L. Berger, B. W. Harris and Z. Sullivan, Phys. Rev. Lett. **83** (1999) 4472.
- [516] E. N. Argyres, C. G. Papadopoulos and S.D.P. Vlassopoulos, Phys. Lett. **B202** (1988) 425.
- [517] H. Lai *et al.* [CTEQ Collaboration], Phys. Rev. **D55** (1997) 1280.
- [518] M. Chaichian, K. Huitu and Z.-H. Yu, Phys. Lett. **B490** (87) 2000.
- [519] J. Kalinowski, R. Rückl, H. Spiesberger and P. M. Zerwas, Phys. Lett. **B406** (1997) 314.
- [520] J. Kalinowski, Acta Phys. Polon. **B28**, 2423 (1997).
- [521] J. Kalinowski, R. Rückl, H. Spiesberger and P. M. Zerwas, Z. Phys. **C74** (1997) 595.
- [522] D. Choudhury, Phys. Lett. **B376** (1996) 201.
- [523] P. J. Holt and P. B. Renton [on behalf of DELPHI Collaboration], submitted to HEP’97 (Abstract Number 467), DELPHI 97-116 CONF 98 (1997), CERN-EP/99-05.
- [524] G. Abbiendi *et al.* [OPAL Collaboration], Eur. Phys. J **6** (1999) 1.
- [525] F. Richard, Preprint DELPHI 97-46 PHYS 698 (1997).
- [526] D. Choudhury, S. Raychaudhuri, eprint hep-ph/9807373.
- [527] P. Binétruy *et al.*, ECFA Large Hadron Collider (LHC) Workshop, Aachen, 1990, Vol. II.
- [528] P. Tipton, Talk presented at the Int. Conf. on High Energy Physics, Warsaw (July 1996).
- [529] D. K. Ghosh, S. Raychaudhuri and K. Sridhar, Phys. Lett. **B396** (1997) 177.
- [530] K. Hikasa, J. M. Yang and B. Young, Phys. Rev. **D60** (1999) 114041.

- [531] J. L. Hewett and T. G. Rizzo, Proc. of 29th Int. Conf. on High-Energy Physics (ICHEP 98), Vancouver, Canada (23-29 July) 1998, vol. 2 p.1698.
- [532] F. Abe *et al.*, Phys. Rev. Lett. **79** (1997) 2198.
- [533] A. Axelrod, Nucl. Phys. **B209** (1982) 349.
- [534] M. Clements *et al.*, Phys. Rev. **D27** (1983) 570.
- [535] V. Ganapathi *et al.*, Phys. Rev. **D27** (1983) 579.
- [536] P. Binetruy, Nucl. Phys. **B62A-C (Proc. Suppl.)** (1998) 152.
- [537] M. J. Duncan, Phys. Rev. **D31** (1985) 1139.
- [538] B. Mukhopadhyaya and A. Raychaudhuri, Phys. Rev. **D39** (1989) 280.
- [539] U. Mahanta and A. Ghosal, Phys. Rev. **D57** (1998) 1735.
- [540] Y. Zeng-Hui, H. Pietschmann, M. Wen-Gan, H. Liang and J. Yi, eprint hep-ph/9910323.
- [541] M. Chemtob and G. Moreau, Phys. Rev. **D61** (2000) 116004.
- [542] M. Chemtob and G. Moreau, Phys. Rev. **D59** (1999) 116012.
- [543] Y. Zeng-Hui, H. Pietschmann, M. Wen-Gan, Han Liang and J. Yi, Eur. Phys. J **16** (2000) 541.
- [544] J. A. Bagger, Nucl. Phys. **(Proc. Suppl.)62B** (1998) 23.
- [545] M. Chemtob and G. Moreau, Phys. Lett. **B448** (1999) 57.
- [546] N. Arkani-Hamed, H. C. Cheng, J. L. Feng, L. J. Hall, Phys. Rev. Lett. **77** (1996) 1937.
- [547] T. Stelzer and S. Willenbrock, Phys. Lett. **B357** (1995) 125.
- [548] A. Datta, J. M. Yang, B.-L. Young and X. Zhang, Phys. Rev. **D56** (1997) 3107.
- [549] R. J. Oakes, K. Whisnant, J. M. Yang, B.-L. Young and X. Zhang, Phys. Rev. **D57** (1998) 534.
- [550] P. Chiappetta, A. Deandrea, E. Nagy, S. Negroni, G. Polesello and J.M. Virey, Phys. Rev. **D61** (2000) 115008.
- [551] L. Hall, T. Moroi and H. Murayama, Phys. Lett. **B424** (1998) 305.
- [552] H. Dreiner, P. Richardson and M. H. Seymour, J. Hi. Ener. Phys. **04** (2000) 008.